MECHANISTIC STUDIES OF UNUSUAL MORITA-BAYLIS-HILLMAN REACTIONS

THESIS

Submitted in fulfilment of the requirements
for the degree of

DOCTOR OF PHILOSOPHY

of

RHODES UNIVERSITY

By

DUBEKILE NYONI

BSc. Hons. (Midlands State University, Zimbabwe), MSc. (Rhodes University)

December 2011

ABSTRACT

This study has focussed on the application of synthetic, kinetic and exploratory theoretical methods in elucidating the reaction mechanisms of four Morita-Baylis-Hillman (MBH) type reactions, *viz,* i) the reactions of the disulfide 2,2'-dithiodibenzaldehyde with various activated alkenes in the presence of DBU and Ph_3P, ii) the reactions of chromone-3-carbaldehydes with MVK, iii) the reactions of chromone-2-carbaldehydes with acrylonitrile and iv) with methyl acrylate. Attention has also been given to the origin of the observed regioselectivity in Michaelis-Arbuzov reactions of 3-(halomethyl)coumarins.

Cleavage of the sulfur-sulfur bond of aryl and heteroaryl disulfides by the nitrogen nucleophile DBU has been demonstrated, and a dramatic increase in the rate of tandem MBH and disulfide cleavage reactions of 2,2'-dithiodibenzaldehyde with the activated alkenes, MVK, EVK, acrylonitrile, methyl acrylate and *tert*-butyl acrylate has been achieved through the use of the dual organo-catalyst system, $DBU-Ph_3P$ – an improvement accompanied by an increase in the yields of the isolated products. Detailed NMR-based kinetic studies have been conducted on the DBU-catalysed reactions of 2,2'-dithiodibenzaldehyde with MVK and methyl acrylate, and a theoretical kinetic model has been developed and complementary computational studies using Gaussian 03, at the DFT-B3LYP/6-31G(d) level of theory have provided valuable insights into the mechanism of these complex transformations.

Reactions of chromone-3-carbaldehydes with MVK to afford chromone dimers and tricyclic products have been repeated, and a novel, intermediate MBH adduct has been isolated. The mechanisms of the competing pathways have been elucidated by DFT calculations and the development of a detailed theoretical kinetic model has ensued.

Unusual transformations in MBH-type reactions of chromone-2-carbaldehydes with acrylonitrile and methyl acrylate have been explored and the structures of the unexpected products have been established using 1- and 2-D NMR, HRMS and X-ray crystallographic techniques.

Attention has also been given to the synthesis of 3-(halomethyl)coumarins *via* the MBH reaction, and their subsequent Michaelis-Arbuzov reactions with triethyl phosphite. An exploratory study of the kinetics of the phosphonation reaction has been undertaken and the regio-selectivity of nucleophilic attack at the 4- and 1'-positions in the 3-chloro- and 3-

(iodomethyl)coumarins has been investigated by calculating Mulliken charges, LUMO surfaces and Fukui condensed local softness functions.

ACKNOWLEDGEMENTS

LIST OF ABBREVIATIONS

AIBN	Azobisisobutyronitrile
B3LYP	Becke's three parameter and the Lee, Yang and Parr correlation functional
CDI	1,1'-carbonyldiimidazole
COSY	Correlation spectroscopy (^{1}H-^{1}H)
DABCO	1,4-Diazabicyclo[2.2.2]octane
DBU	1,8-Diazabicyclo[5.4.0]undec-7-ene
DFT	Density functional theory
DIBAL-H	Diisobutylaluminium hydride
DIPT	Diisopropyltrytamine
DMAC	Dimethylacetamide
DMAP	4-Dimethylaminopyridine
DMF	Dimethylformamide
DMS	Dimethylsulphide
DPPB	Diphenylphosphinobutane
EtOAc	Ethyl acetate
EtOH	Ethanol
ESI-MS/MS	tandem Electron spray ionisation mass spectrometry
EVK	Ethyl vinyl ketone
3-HQ	3-Hydroxyquinuclidine
HMBC	Heteronuclear multiple bond coherence (^{1}H-^{13}C)
HOMO	Highest occupied molecular orbital
HSQC	Heteronuclear single quantum coherence (^{1}H-^{13}C)
i-PrOH	Isopropanol
IEF-PCM	Polarisable continuum model with integral equation formatism variant

KIE	Kinetic isotope effects
LUMO	Lowest unoccupied molecular orbital
MBH	Morita-Baylis-Hillman
MeOH	Methanol
MP2	Møller-Plesset perturbation theory
MVK	Methyl vinyl ketone
NBS	*N*-Bromosuccinimide
NOESY	Nuclear Overhauser effect spectroscopy
PCC	Pyridinium chlorochromate
TBHP	*tert*-Butyl hydroperoxide
THF	Tetrahydrofuran
TMB	1,3,5-Trimethoxybenzene
TMPDA	*N,N,N,N'*-Tetramethyl-1,3-propanediamine
ZPE	zero-point energy
ZPEC	zero-point energy correction

CONTENTS

1. INTRODUCTION

1.1 The Morita-Baylis-Hillman reaction

The Morita-Baylis-Hillman (MBH) reaction involves the coupling of electron deficient alkenes, such as α,β-unsaturated ketones, with sp^2 hybridised carbon electrophiles, such as aldehydes, ketones and aldimines, catalysed by nucleophilic amines or phosphines as illustrated in Scheme 1.

EWG = electron withdrawing group
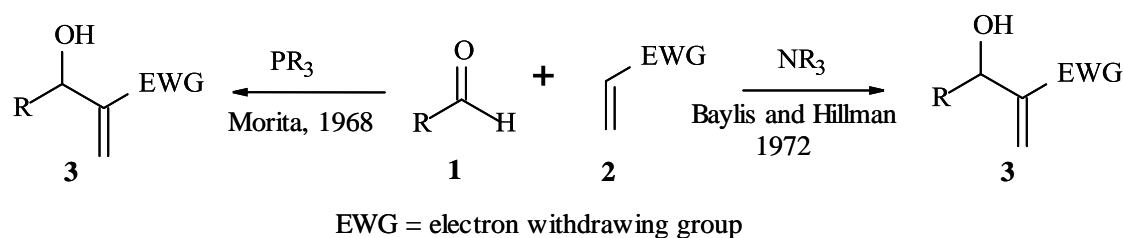
Scheme 1. The MBH reaction

In 1968, Morita[1] described a novel reaction between various aldehydes and acrylic compounds catalysed by a tertiary phosphine and yielding the vinylic compounds **3** (Scheme 1). Baylis and Hillman in 1972[2] reported a similar reaction between acetaldehyde and ethyl acrylate or acrylonitrile in the presence of catalytic amounts of Lewis bases such as 1,4-diazabicyclo[2.2.2]octane (DABCO) to obtain similar products to those which Morita had obtained earlier.

R^1 = Alkyl or aryl
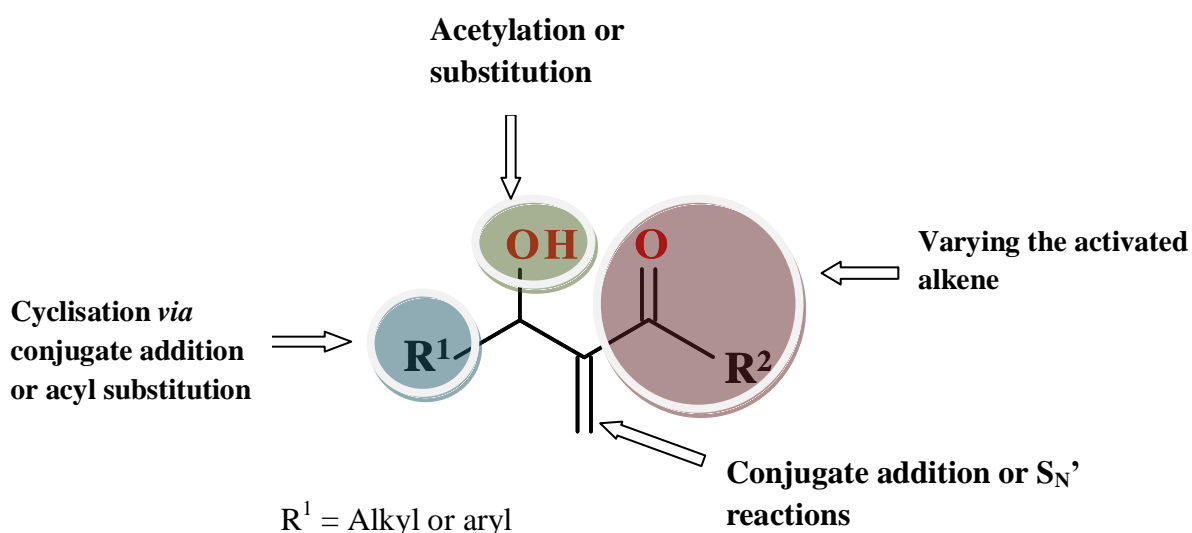
Figure 1. Various opportunities for transforming the MBH adduct.

The transformation, now known as the Baylis-Hillman (BH) or Morita-Baylis-Hillman (MBH) reaction, has become a very important carbon-carbon bond-forming reaction, giving rise to highly functionalised allylic alcohols **3**, as evidenced by the numerous reviews and papers on its applications.[3-24] MBH adducts have proved to be valuable intermediates in the construction of benzannulated heterocyclic compounds of biological importance. Figure 1 shows the various functionalities on the MBH product that can be exploited synthetically. The formation of a new chiral center in the MBH product allows it to be used in asymmetric transformations. Through the introduction of a chiral source into any of the three components involved in the MBH reaction (activated alkene, carbon electrophile or catalyst), asymmetric transformations of the MBH product can be realised. A number of research groups have explored the asymmetric version of the MBH reaction.[3,4,16,25-28] Hayashi *et al.*[29] used a chiral diamine **5**, as catalyst in a MBH reaction between substituted benzaldehydes and MVK, and obtained moderate to high enantioselectivities (Scheme 2).
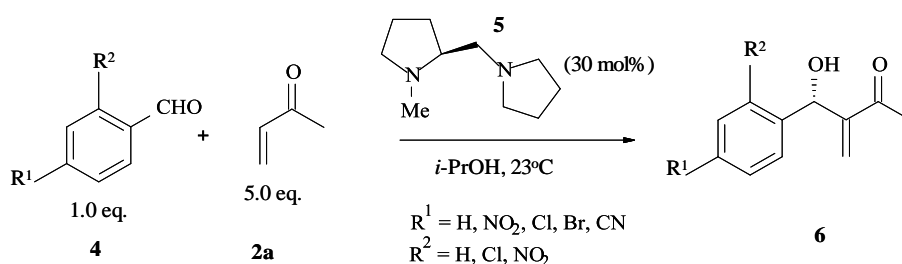
Scheme 2.

Bauer and Tarasiuk[25] introduced a chiral electrophile in their MBH reactions with cyclic ketones using a Me_2S-$TiCl_4$ catalytic system (Scheme 3), and observed high enantioselectivities of $> 95\%$.
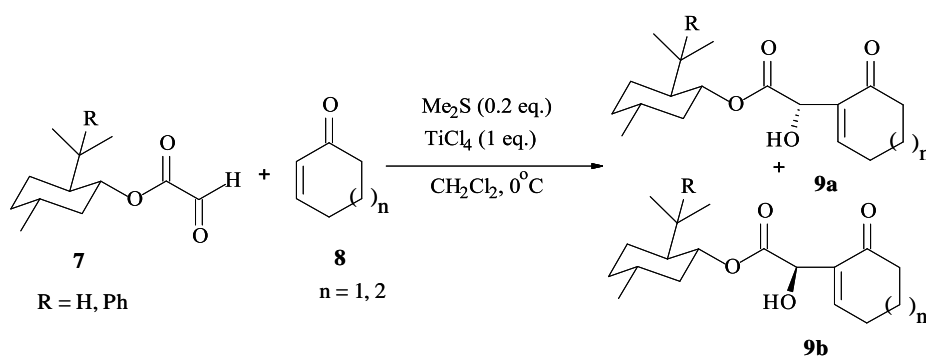
Scheme 3.

Another way of achieving stereocontrol in MBH reactions is through the use of chiral activated alkenes. Leahy and co-workers[4] used (+)-*N*-propenylbomane-2,10-sultam **10**, commonly known as "Oppolzer's Sultam", in MBH reactions with various aldehydes in the presence of DABCO, and obtained the dioxanone products **13** in enantiomeric excess greater than 99%. The 1,3-dioxan-4-one products were readily converted into α-methylene-β-hydroxy esters **14**.
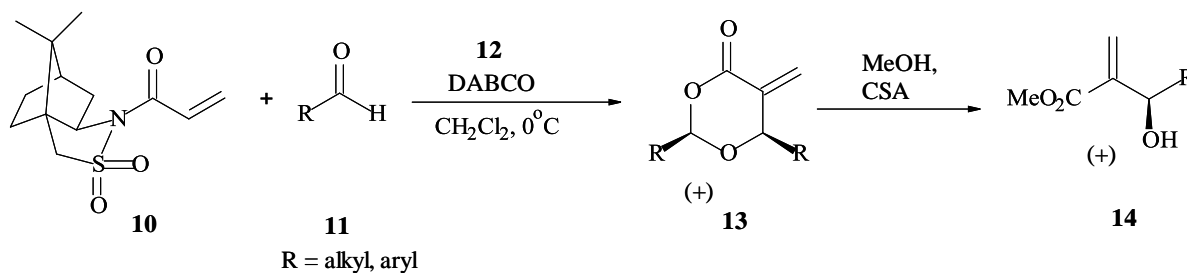
Scheme 4.

1.1.1 Mechanistic Studies of the Morita-Baylis-Hillman reaction

1.1.1.1 Experimental studies

The mechanism for the MBH reactions outlined in Scheme 5, was proposed by Hill and Isaacs[30] on the basis of pressure and kinetic isotope effects (KIE) studies. The reaction is initiated by conjugate addition of the tertiary amine **12** (or phosphine catalyst) to the activated alkene **2b** generating the zwitterionic intermediate **16**. The zwitterion **16** then reacts with the aldehyde **15** in an aldol type reaction to give a second zwitterionic intermediate **17** which then undergoes proton transfer followed by E2 or $E1_{CB}$ elimination of the catalyst to yield the MBH product **20**. The second step, involving reaction of the carbon electrophile **15** with the zwitterion **16**, was considered to be the rate determining step (RDS).
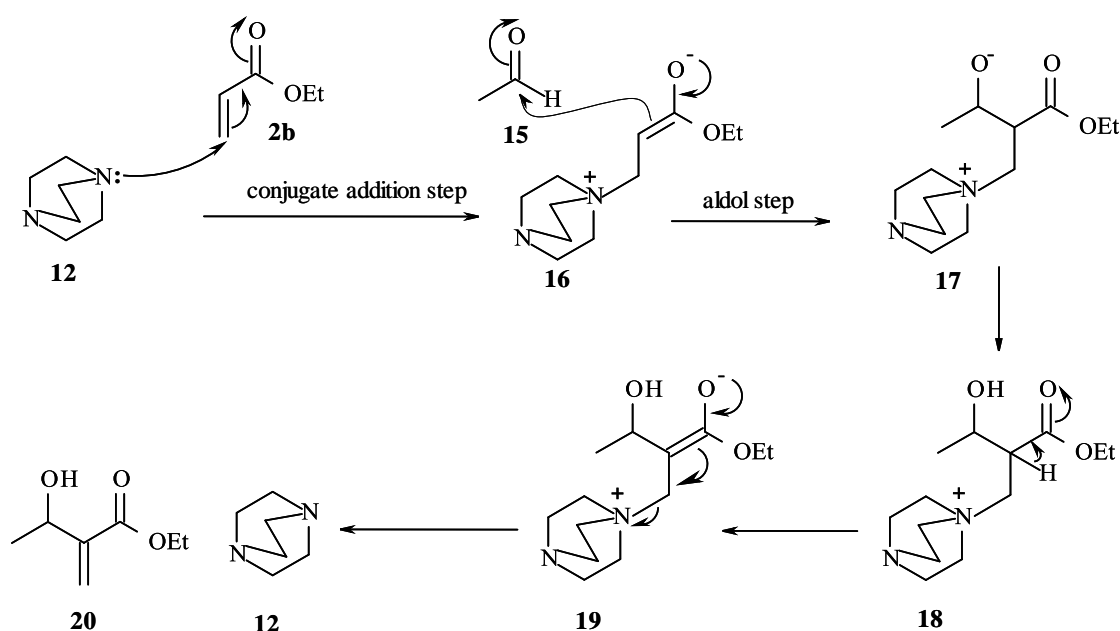
Scheme 5. Hill and Isaacs[30] proposed mechanism of the MBH reaction, exemplified by the reaction between acetaldehyde and ethyl acrylate with DABCO as catalyst.

Evidence for the catalytic role of DABCO in the MBH reaction was provided by an experimental study by Drewes *et al.*[31] They reacted methyl acrylate **2c** with 2-hydroxybenzaldehyde **21** in CH_2Cl_2 at 0^oC in the presence of DABCO and isolated the coumarin salt, **22**, the structure of which was confirmed by X-ray crystallography.
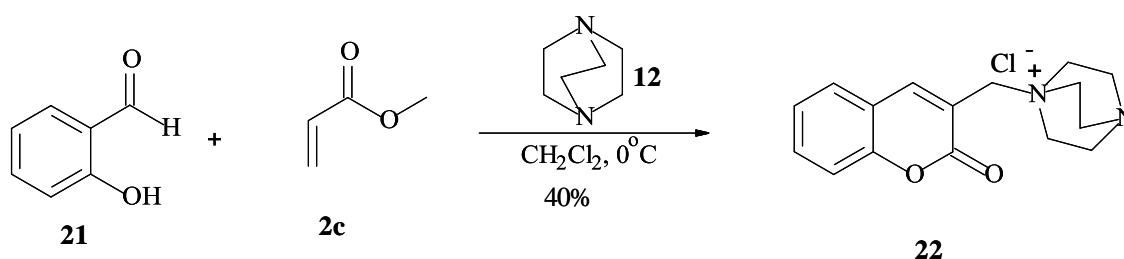
Scheme 6

In our own research group, Bode and Kaye[32] carried out the first NMR-based kinetic-mechanistic study of the MBH reaction and their results were consistent with the mechanism proposed in Scheme 5. They reacted pyridine carbaldehydes **24** with acrylate esters **2** in the presence of DABCO as shown in Scheme 7. The experimental results showed the mechanism to follow third-order kinetics (Equation 1) or pseudo second-order on the assumption that the concentration of the amine remains constant (Equation 2).

$$\text{Rate} = k_{obs}[\text{aldehyde}] \, [\text{alkene}] \, [3^o \text{ amine}] \qquad (1)$$

$$\text{Rate} = k_a[\text{aldehyde}] \, [\text{alkene}] \qquad (2)$$

$$\text{where } k_a = k_{obs}[3^o \text{ amine}]$$

$$\text{Rate} = k_2 K_1[\text{aldehyde}] \, [\text{alkene}] \, [3^o \text{ amine}] \qquad (3)$$

These experimental studies gave no insight into the details of the final step involving elimination of the catalyst, but it became increasingly evident that an $E1_{CB}$ process was more likely[33] – a view presented in the treatment of the reaction in an important new textbook.[34]

X= N, CH
Y= H, OH
R^1= pyridine-4-carbaldehyde,
   pyridine-2-carbaldehyde
R^2= Me, Et, Pr^i
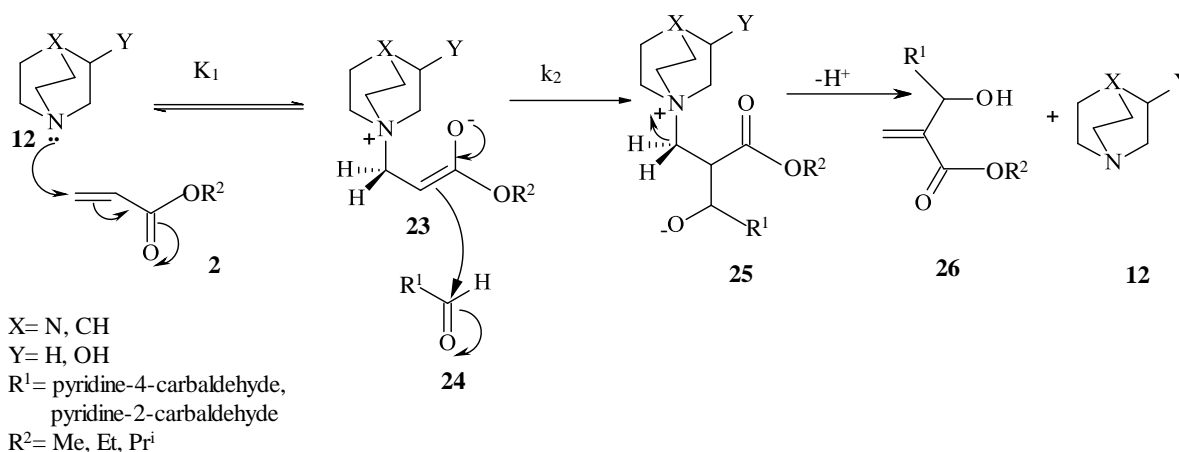
Scheme 7

For some time, little further attention appeared to be given to the mechanism of this important reaction. In recent years, however, a number of contributions have been published. Coelho and co-workers[35] used electrospray ionisation mass and tandem mass spectrometry (ESI-MS/MS) to intercept and identify the putative intermediates in the proposed MBH mechanism outlined in Scheme 5. In an approach which had not been used previously to study the MBH reaction, they examined reactions of the two aldehydes **27** and **28** with methyl acrylate and DABCO in MeOH at room temperature (Scheme 8). Figure 2 shows their results, which provided further evidence of the generally accepted mechanism of the MBH reaction, by demonstrating the formation of species corresponding to compounds **16** and **19** (Scheme 5).
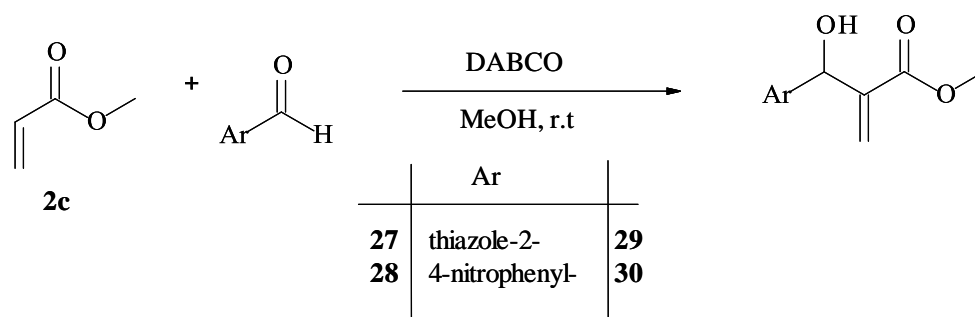
Scheme 8
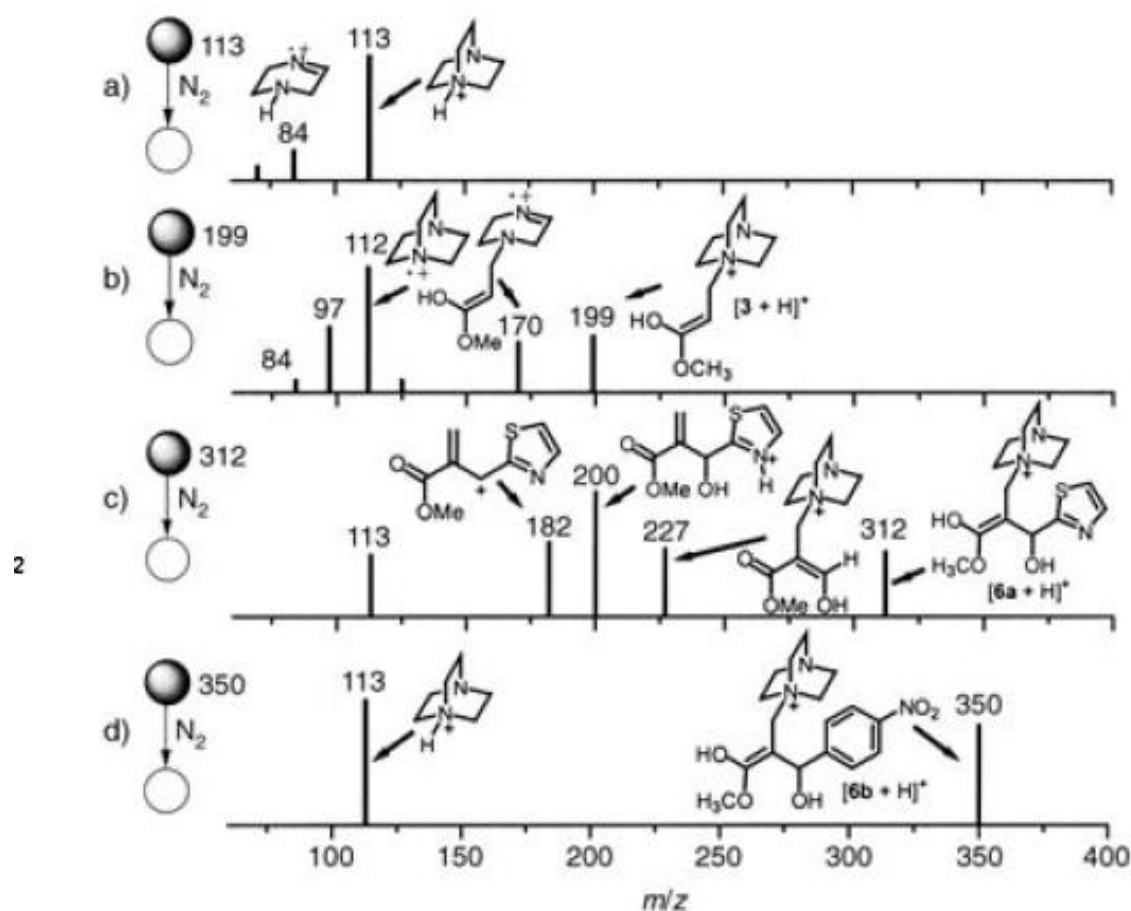
Figure 2. ESI(+)-MS/MS spectra of the intercepted MBH intermediates and protonated DABCO, from the reactions between thiazole-2-carbaldehyde **27** and 4-nitrobenzaldehyde **28** with methyl acrylate and using DABCO as catalyst.[35] Reproduced with permission.

McQuade and co-workers[36,37] proposed a new mechanism for the MBH reaction, in which the fundamental difference related to the final phase of the reaction, *viz.*, elimination of the catalyst. In their proposed mechanism, outlined in Scheme 9, the rate-determining step is second-order in aldehyde and first-order in both catalyst (DABCO) and acrylate, giving

fourth-order kinetics overall. The mechanistic proposals stem from kinetic isotope effects (KIE) experiments with isotopically labelled α-deuterio-*p*-nitrobenzaldehyde and methyl α-^{2}H acrylate in two separate experiments. In terms of their proposal, the reaction is initiated by nucleophilic attack of DABCO on the acrylate **2c** to give the zwitterion **31**, followed by addition of the zwitterion **31** to the aldehyde **28** to give a second zwitterion **32** as initially proposed by Hill and Isaacs[30] and supported by Bode and Kaye.[32] However , a second equivalent of the aldehyde then reacts with the zwitterion **32** to give the hemiacetal **33**, which then undergoes rate-limiting deprotonation through the transition state **34** to give intermediate **35**, which breaks down to afford the MBH product **3**.
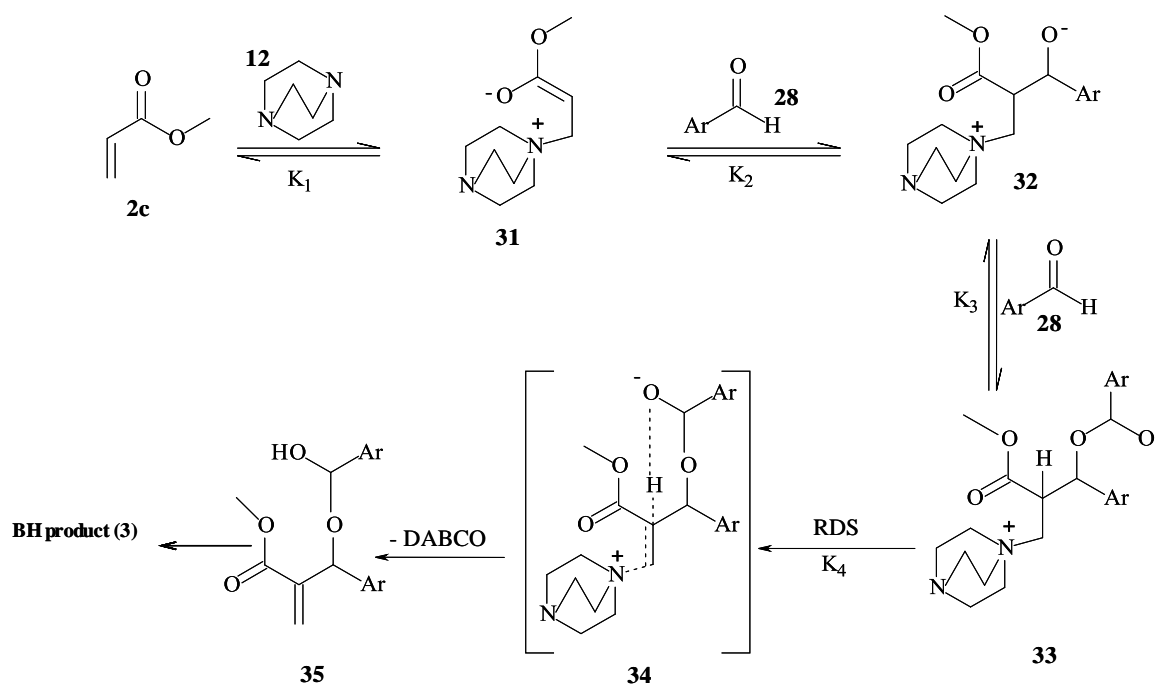
Scheme 9. The mechanism of the MBH reaction, proposed by McQuade[36,37] in which Rate = $K_{obs}[\mathbf{28}]^2[\mathbf{12}][\mathbf{2c}]$

^{1}H NMR studies and simulated kinetic models of the reaction between ethyl acrylate and benzaldehyde catalysed by quinuclidine, provided Aggarwal and co-workers[38] with a different insight into the mechanism of the MBH reaction. Their findings showed the proton-transfer step (step iii, Scheme 10) to be rate-determining as observed by McQuade.[36,37] However, in the absence of protic solvents or proton donors, autocatalysis of the reaction occurred. This observation implied that the proton-transfer step was rate-determining during the inital stages of the reaction, but once sufficient product had built up, step ii, which is the aldol reaction of the aldehyde **38** with the enolate **37**, became the rate-determining step.
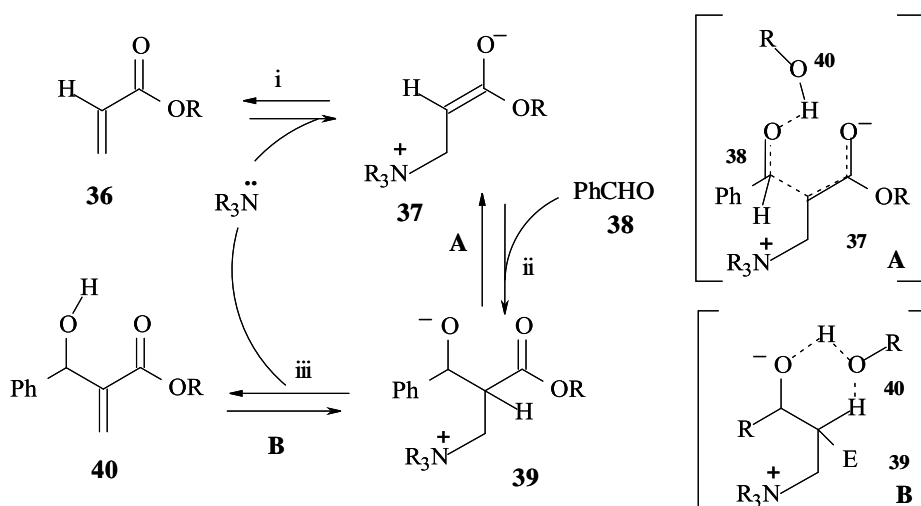
Scheme 10. The mechanism of the autocatalytic MBH reaction through transition states **A** or **B** as proposed by Aggarwal and co-workers.[38]

Based on the proposals by McQuade[36,37] and Aggarwal,[38] that the proton-transfer step is rate-determining (Scheme 11), Eberlin and co-workers[39] performed complementary investigations on the MBH reaction using ESI-MS/MS techniques with the aim of intercepting and characterising the intermediates implicated in the key rate-determining proton-transfer step.
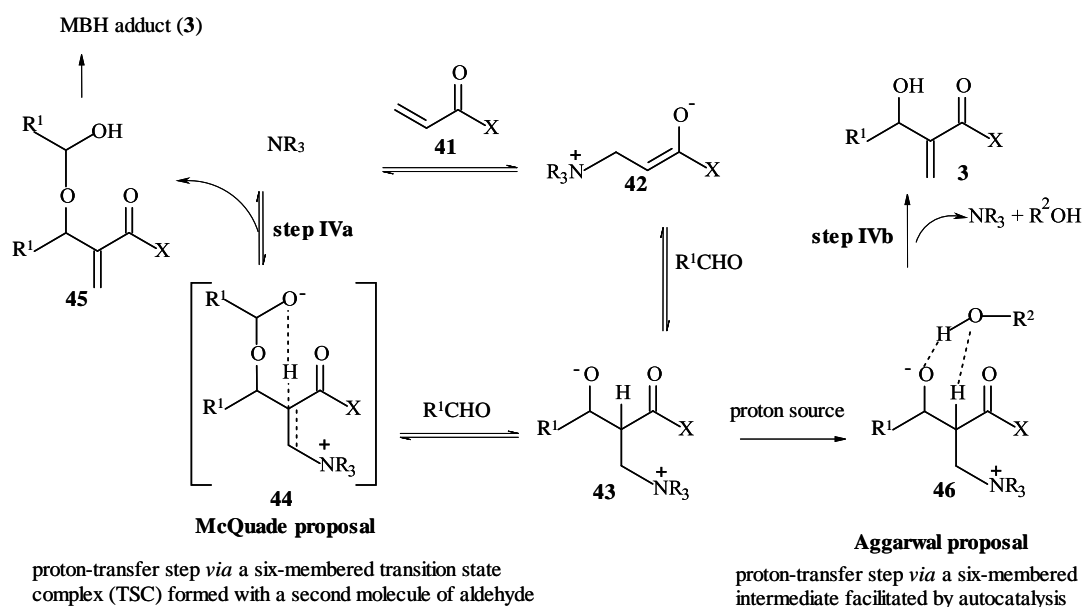
Scheme 11. McQuade's and Aggarwal's proton-transfer step proposals.[36,37,38]

They monitored the DABCO-catalysed reaction of methyl acrylate with excess benzaldehyde without solvent and were able to intercept the intermediate of type **44** proposed by McQuade[36,37] (Figure 3). When the MBH reaction was studied using the same experimental protocol, but adding β-naphthol (to act as a proton source), they intercepted an intermediate of type **46** (Scheme 11), supporting Aggarwal's proposal that a proton source participates in the final elimination step (Figure 3).
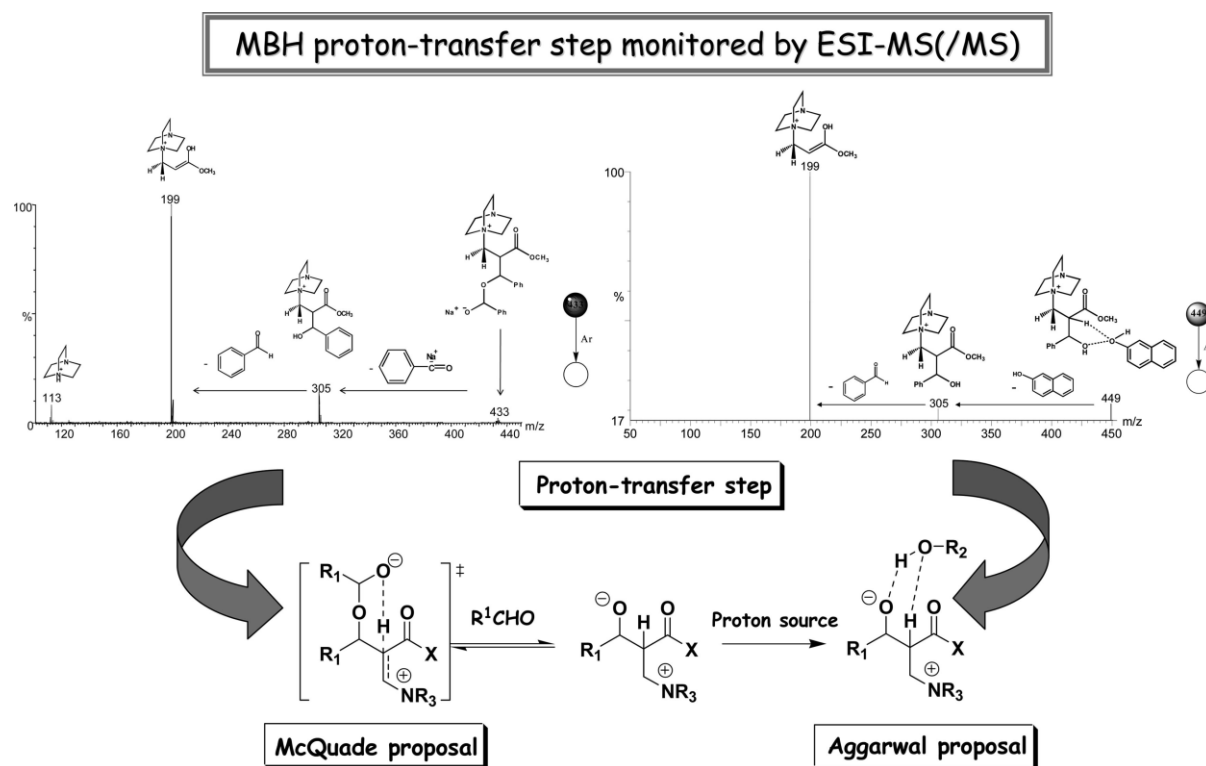
Figure 3. ESI-MS(/MS) of the intercepted ions of type **44** (McQuade)[36,37] and **46** (Aggarwal)[38] shown in Scheme 11. Reproduced with permission.[39]

1.1.1.2: Theoretical studies

The application of computational methods in solving chemical problems has grown considerably over recent decades. Several theoretical methods can be used to determine the total energy when predicting molecular structures, and these methods fall into two main categories: Molecular Mechanics, based on classical mechanics; and Quantum Mechanics methods such as semi-empirical, Hartree-Fock (HF) and density functional theory (DFT) calculations.

Hybrid functionals, which combine density functional with Hartree-Fock methods are also being used. An example is the use of DFT, together with Becke's three-parameter functional

(B3) and the Lee, Yang and Parr (LYP) correlation functional − commonly known as B3LYP. These methods permit frequency calculation, geometry optimisation and the determination of electronic structure, the exploration of potential energy surfaces, electron and charge distributions, the identification of transition-state complexes and, hence rate constants for chemical reactions.

The application of theoretical methods to understanding the mechanism of the MBH has received considerable attention in the past few years. In 2006, Xu[40] presented what is probably the first theoretical report on the mechanism of the MBH reaction. The theoretical models used in the report were based on the reaction of acetaldehyde and acrylonitrile in dichloromethane, with PMe$_3$ as catalyst (Figure 4). Geometry optimisation of the intermediates and transition states was achieved at the DFT B3LYP/ 6-311+G(d) level, with (IEF-PCM) solvent correction using the Gaussian 03 programme package. Based on the results, Xu predicted the proton-transfer step to be rate-determining but accepted that, under certain conditions, the aldol reaction (step II) could be rate-determining (Figure 4).
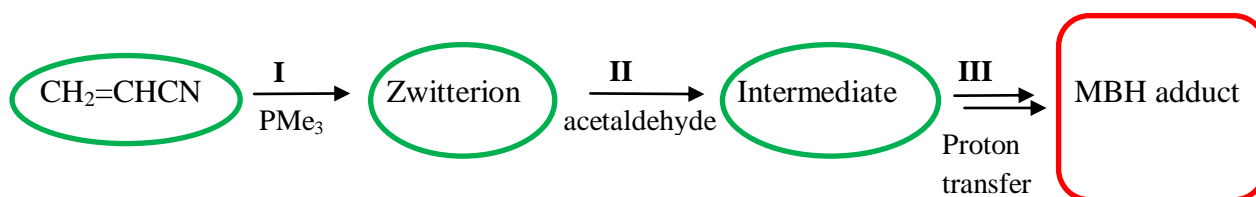
Figure 4. Sequence of steps and reactants used by Xu.[40]

In a subsequent study, Roy and Sunoj[41] studied a model system, in which acrolein was reacted with formaldehyde in the presence of NMe$_3$ in order to establish the reaction profile. Once established, the reaction profile was then applied to a real system in which MVK was reacted with benzaldehyde and DABCO as catalyst. The CBS-4M, MP2/6-31+G* and mPW1K/6-31+G* levels of theories were used in the calculations and solvation effects were accounted for by use of the continuum dielectric method included in the polarisable continuum model (IEF-PCM). The activation barrier for C-C bond formation in the reaction between the initial zwitterion and benzaldehyde was found to be 20.2 kcal/mol lower than that for the proton transfer step, providing further evidence that the latter step is rate-determining.

Aggarwal *et al.*[42] carried out a computational investigation of the MBH reaction based on earlier suggestions[38] that the proton-transfer step was rate-determining. The earlier report,[38] however, did not give details on the exact nature of the rate-determining step or the mechanism of the proton-transfer step in either the presence or absence of alcohol. The computational approach permitted these issues to be addressed. Their study focused on the reaction between methyl acrylate and benzaldehyde catalysed by a tertiary amine in both the presence and absence of alcohol. The MBH reaction has been shown to be accelerated by the presence of hydrogen-bond donors,[36,37,43] and this study provided theoretical evidence supporting these experimental observations. A lower energy pathway, involving concerted proton-transfer catalysed by one molecule of methanol or of product (autocatalysis), was found. The intermediates **int1** and **int2** were stabilised by hydrogen bonding with MeOH, making their formation more thermodynamically favoured than when aprotic solvents are used. Moreover in the absence of alcohol, the calculated energy barrier for the rate determining step was found to be high (28.7 kcal/mol) − a result which accounted for the observed low reaction rates in most MBH reactions. The overall results of the study by Aggarwal *et. al.*[42] are summarised in the potential energy diagram in Figure 5.
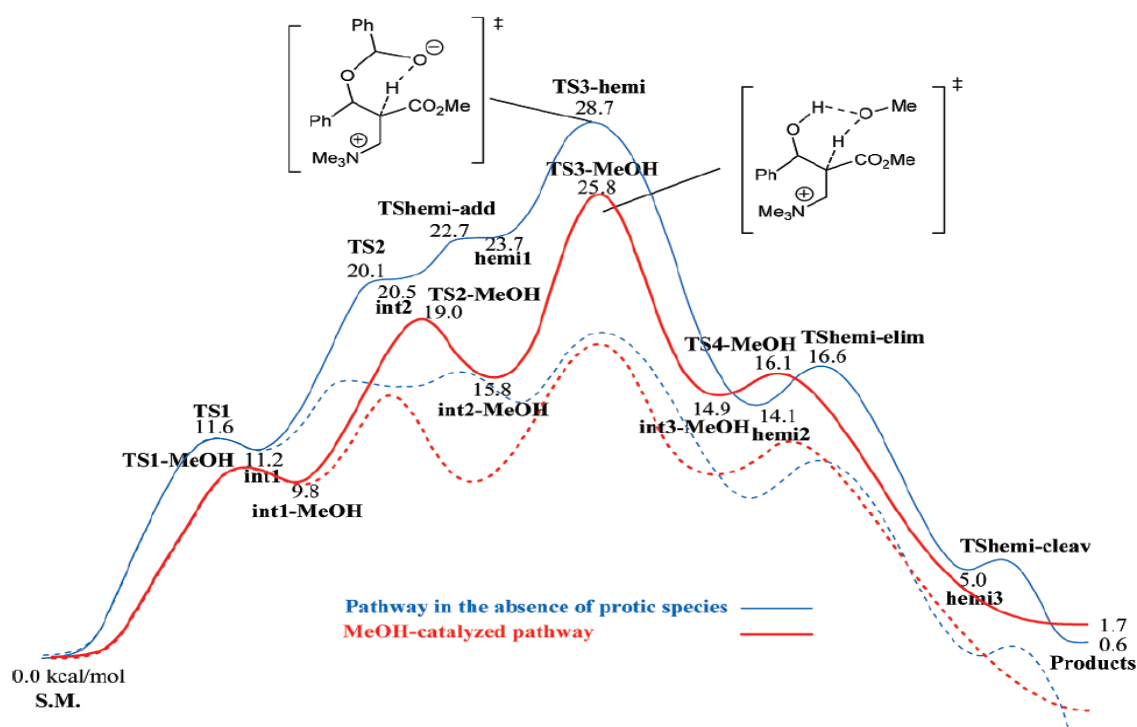
Figure 5. Calculated potential energy surface (kcal/mol) for the MBH reaction in the absence (blue) and in the presence (red) of alcohol, at the B3LYP/6-31+G** (THF)//B3LYP/6-31+G*(THF) level of theory. The dotted curves correspond to qualitative energy profiles taking into account the estimated errors in the B3LYP method.[42] Reproduced with permisson.

Based on experimental evidence by Aggarwal,[38] Amarante *et al.*[44] investigated the MBH reaction of formaldehyde **47** and acrolein **2d** in the presence of trimethylamine as catalyst and MeOH as solvent to give the MBH product **48** (Scheme 12).
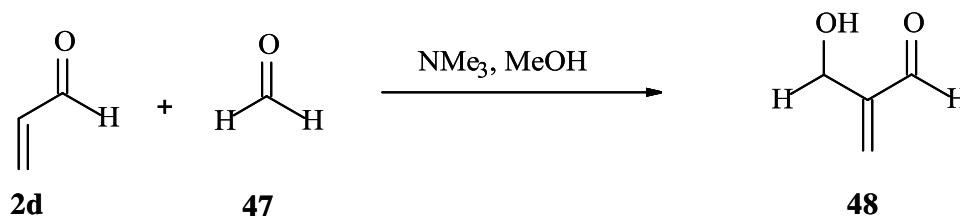
Scheme 12

Their results clearly showed that the proton transfer step is the rate-determining step and that MeOH is important as it acts as a proton shuttle between the carbon and oxygen centres, as Robiette *et al.*[42] had proposed earlier. However, in non-protic solvents the reaction appeared to follow a different pathway involving a hemiacetal species as proposed by McQuade and co-workers.[36,37]

1.1.2 Improvements in the Morita-Baylis-Hillman reaction

The MBH reaction, although very atom economical, often suffers from very poor reaction rates, thus limiting its practicability. Some MBH reactions can take up to a month to reach acceptable levels of completion. Several factors such as temperature,[16,28,45,46] pressure,[47,48] solvent[38,49-54] and the nature of the substrate and catalyst,[32,49,50,55-70] have been found to contribute to the rate of this reaction. Through manipulation of these different factors many research groups, including our own, have been able to accelerate the reaction.

1.1.2.1 Nature of the substrate

Pyridinecarbaldehydes were found to be more reactive than benzaldehydes[32] and using these substrates, Bode and Kaye were able to follow the reaction on a convenient time-scale. Moreover, they showed that increasing the electron-releasing inductive effect of the *O*-alkyl substituent in the acrylate ester (R = Me < Et < Pr') decreased the rate, due, they suggested, to the consequent decrease in the electrophilicity of the activated alkene. Caubere and co-workers[70] also showed that the nature of the *O*-alkyl group played a significant role in the reactivity of acrylic esters. Aryl acrylates are less reactive compared to alkyl acrylates, while increasing the length of the alkyl group also appears to decrease the reactivity. MVK has been shown to react much faster than methyl acrylate,[71,72] while cyclic ketones have been shown to be less reactive.[59,73]

1.1.2.2 Solvent effects

The MBH reaction has been reported to be accelerated in aqueous media.[43,51,54,58,74,75] Homogeneous solvent systems, such as mixtures of MeOH and H_2O have also been reported to lead to higher reaction yields.[43] Aqueous THF has been used with great success in reactions involving cycloalkenones which have been shown to react quite slowly or not at all in MBH reactions conducted in $CHCl_3$.[59,72] The use of protic solvents for this reaction is now well established and the significant rate accelerations which have been observed, have been attributed to hydrogen bonding, and to a lesser extent, hydrophobic effects.[56,44] Caumul and Hailes[76] suggested that use of an aqueous acidic medium changed the catalytic cycle and the intermediates involved, compared to reaction under non-acidic conditions, as outlined in Scheme 13. Thus, use of acidified media leads to protonation of the acrylate ester **2c** (*via* deprotonation of the trialkyammonium ion **49**) and enhances the subsequent conjugate addition of the neutral amine catalyst. The enol **50** then undergoes addition to the protonated aldehyde **51** and, finally, deprotonation and elimination of the amine catalyst from intermediate **52** gives the MBH adduct **53**.
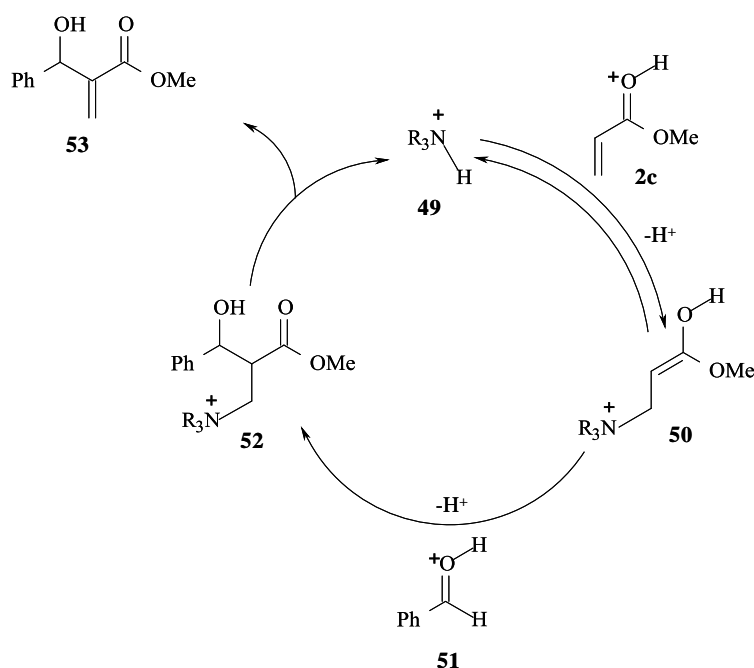
Scheme 13. MBH reaction between benzaldehyde and methyl acrylate under aqueous acidic conditions.[76]

Aggarwal[56] has observed metal- and ligand-accelerated catalysis of the MBH reaction, reporting that, while conventional Lewis acids reduced reaction rates, group III and

lanthanide triflates increased rates. They found the best salts to be La(OTf)$_3$ and Sm(OTf)$_3$; these gave rate accelerations (k_{rel}) of approximately 4.7 and 4.9, respectively, in reactions between *tert*-butyl acrylate and benzaldehyde using stoichiometric amounts of DABCO. MBH reactions under neat conditions have in some cases been reported to give better yields and increased reaction rates compared to those involving solvent[77,78] – not surprisingly, perhaps, given the consequent increase in reactant concentrations.

Intrestingly, the MBH reaction has a very high negative volume of activation (-70 cm^3/mol), shown from early work by Hill and Isaacs,[30] and can therefore be accelerated by increasing the pressure. This enables application of the reaction to β-substituted electron-poor alkenes which only react under high pressure. The use of β-substituted alkenes **54** leads to the formation of *E/Z*-isomers, and van Rozendaal *et al.*[48] have sought to explore the effect of solvent, pressure and catalyst on the *E/Z*-ratio of the resulting MBH adducts (Scheme 14).
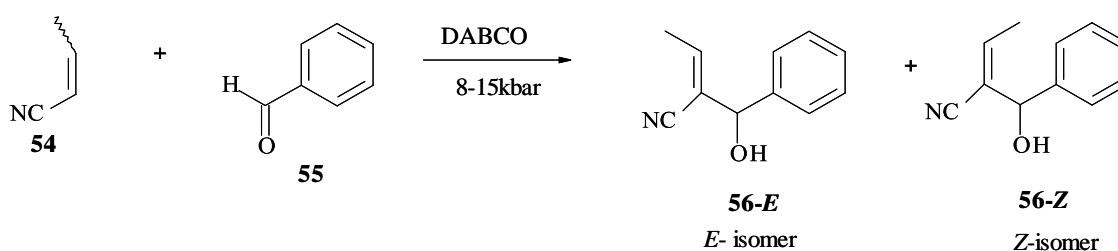
Scheme 14

At atmospheric pressure under neat conditions, as well as in solvents such as THF and CHCl$_3$, they found the *E/Z*-ratio to be close to 1; in more polar solvents, such as MeOH and acetonitrile, the *E*-isomer was formed in excess. Under neat conditions and in aprotic solvents the yield of the *E*-isomer increases with increasing pressure. In CHCl$_3$ at 15 kbar pressure, the *E*-isomer is formed in 96% excess, whereas in polar protic solvents, like MeOH, no pressure dependence was observed. When the tertiary amine catalyst was varied, it was found that decreasing the basicity of the amine led to an increase in the *E*-isomer; for DABCO the *E/Z*-ratio was found to be 1. These results were rationalised mechanistically, as outlined in Scheme 15, in terms of the influence of pressure on internal rotation of critical intermediates in the final elimination process (E2 or E1$_{CB}$).
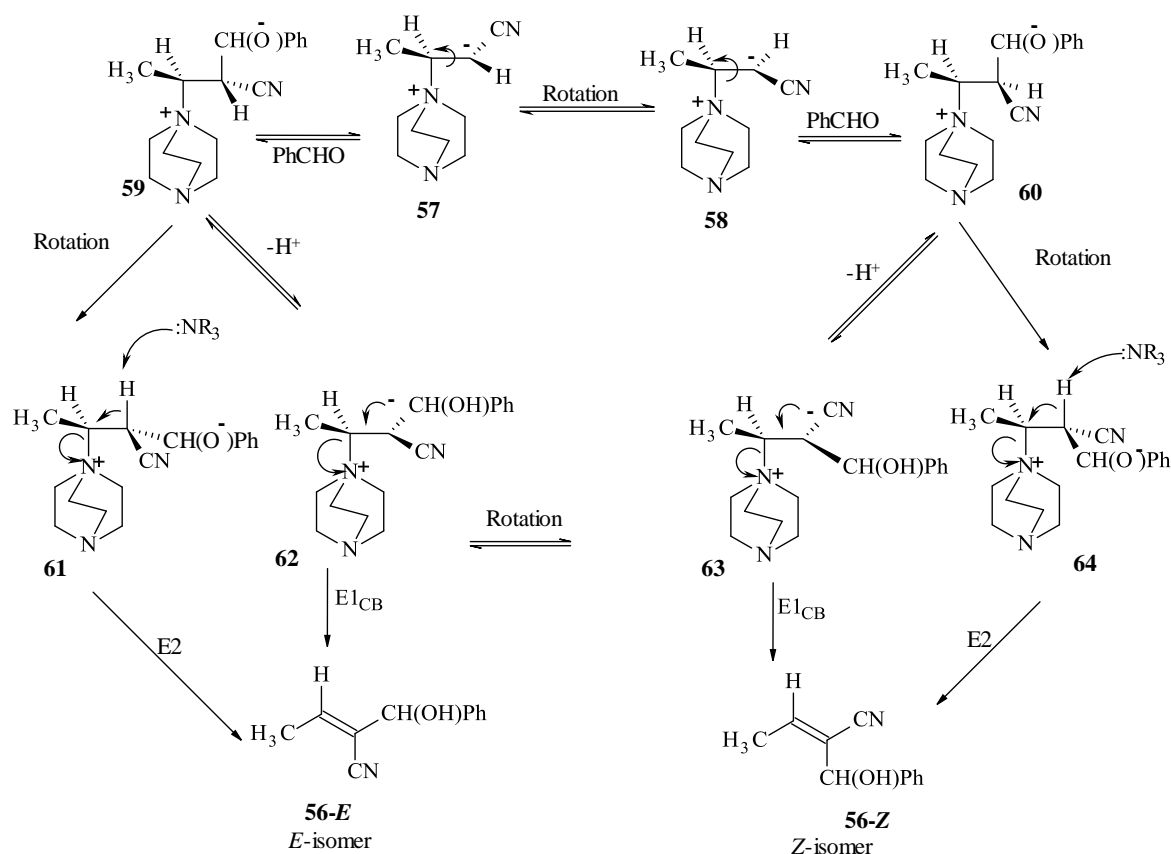
Scheme 15

1.1.2.3 Catalyst effects

Baylis and Hillman[2] reported DABCO as their catalyst of choice and, subsequently, most researchers have initially used DABCO as the catalyst for these reactions. However, because of the slow reaction rates with some substrates, researchers began to explore alternative nucleophilic catalysts which might give better yields and increase reaction rates. Other tertiary amines, such as 1,8-diazabicyclo[5.4.0]undec-7-ene (DBU),[6,50,55,61] *N,N,N',N'*-tetramethyl-1,3-propanediamine (TMPDA),[50,59] imidazole,[50,58] 4-(dimethyl-amino)pyridine (DMAP),[18,43,58] tetramethylguanidine (TMG)[61] and hexamethylenetetramine (HMT),[43] and 3-hydroxyquinuclidine (3-HQ)[79,80] and phosphines, such as Ph_3P and various trialkylphosphines, have found application in the MBH reaction.[45,55,67,68,81,82] DMAP, TMPDA and imidazole have been used in reactions involving cyclic ketones, which are generally less reactive than the acyclic ketones[59,73] while, in some cases, different catalysts have resulted in the formation of different products altogether (Scheme 16).[55] Thus, reactions of the α-keto esters **65** with **2**-cyclopentenone **66** in the presence of diphenylmethylphosphine (PPh_2Me), gave the corresponding MBH products **68** in moderate to excellent yields. On the

other hand, use of DBU in the same reaction gave the aldol product **70** as the *syn*-conformer, exclusively.
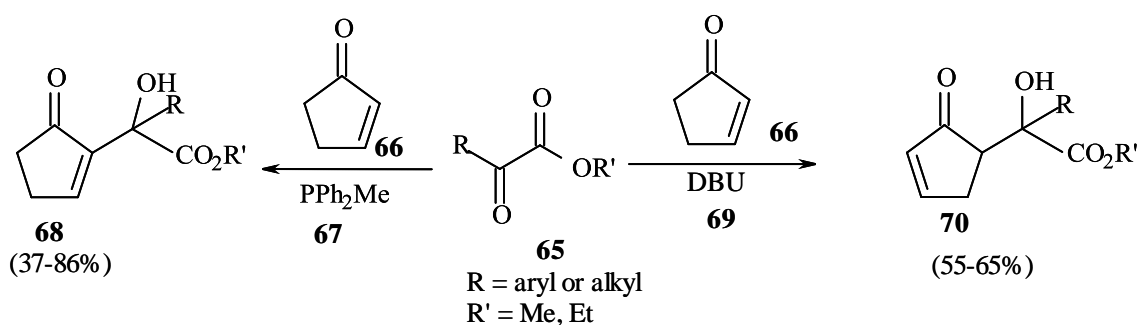
Scheme 16

DABCO has also been used, together with scandium and lanthanide triflates, as co-catalysts,[56] while Connon and Maher[57] have demonstrated that the use of bis-aryl ureas with DABCO, as a co-organocatalyst, increased the efficiency of the reaction. More recently, Legros and co-workers[83] combined DABCO with a perfluoroalkyl halide $R_{fn}X$ to form a recyclable fluorous organocatalyst **71** shown in Figure 6, which catalysed MBH reactions in moderate to excellent yields.
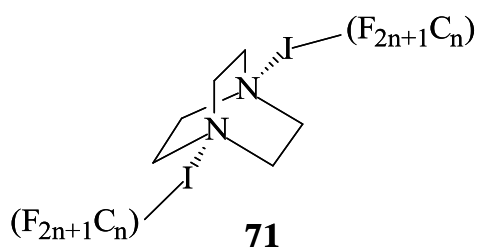
Figure 6. Recyclable fluorous organocatalyst.[83]

1.1.3 Synthetic applications of Morita-Baylis-Hillman adducts

The versatile nature of the MBH adducts allows them to be transformed into a wide range of products. In a review on the MBH reaction, Basavaiah *et al.*[16] outlined some of the transformations (Figure 7), in which MBH adducts could be manipulated to produce different products, both cyclic and acyclic, depending on the nature of the aldehyde or alkene. Applications of the reaction have continued to increase.
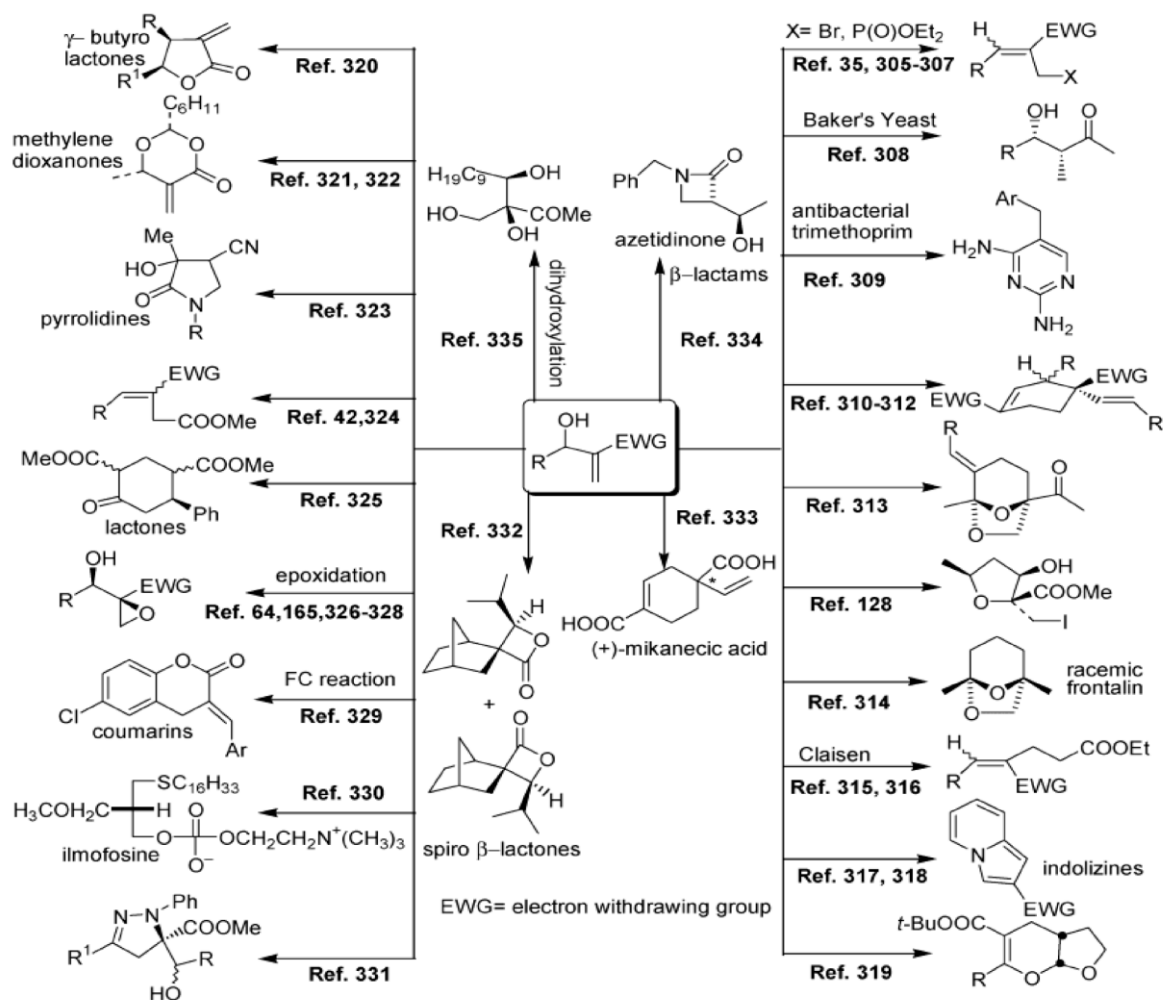
Figure 7. Range of heterocyclic products derived from MBH adducts. Reference numbers refer to the numbering by Basavaiah.[16] Reproduced with permission.

Heterocyclic systems are commonly found in nature and have been shown to possess a wide range of medicinal properties, and the MBH reaction affords access to numerous benzannulated heterocyclic systems. In our group, the MBH reaction has been used to develop novel syntheses of chromenes,[5,84] coumarins,[84-88] thiochromenes,[6,72] indolizines,[23,32]

quinoline derivatives[11,14,] as well as the unexpected chromone derivatives,[79,80] as shown in Figure 8. Other groups have also synthesised heterocyclic systems from MBH adducts.[89-95] The common heteroatoms found in these systems include oxygen, nitrogen and sulphur, with some of the products containing more than one heteroatom.
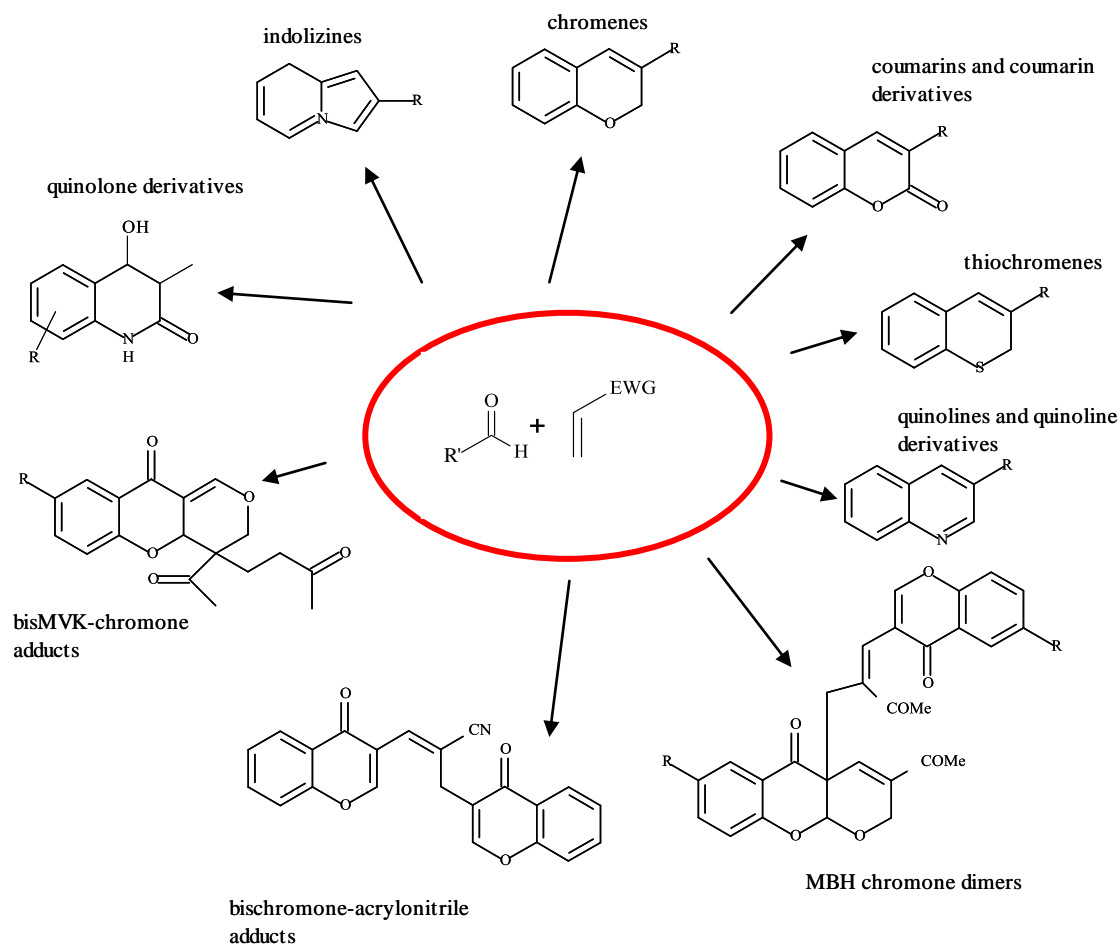
Figure 8. Applications of MBH methodology in the construction of benzannulated heterocyclics, developed in our group.

1.1.3.1 Oxygen-containing heterocycles derived from MBH adducts

Chromenes and coumarins, have been accessed *via* the MBH reaction of substituted 2-hydroxybenzaldehydes. Earlier work in our group[5,84] led to the isolation of both chromenes and coumarins as mixtures following spontaneous cyclisation of MBH adducts *via* the two cyclisation pathways shown in Scheme 17. Path **I** involves cyclisation *via* conjugate addition to the vinylic carbon leading to the formation of chromenes, while path **II** involves nucleophilic acyl substitution at the carbonyl carbon of the ester group to give coumarin

derivatives. The use of vinyl ketones was subsequently shown to afford chromenes selectively by inhibiting the nucleophilic acyl substitution pathway.[5]
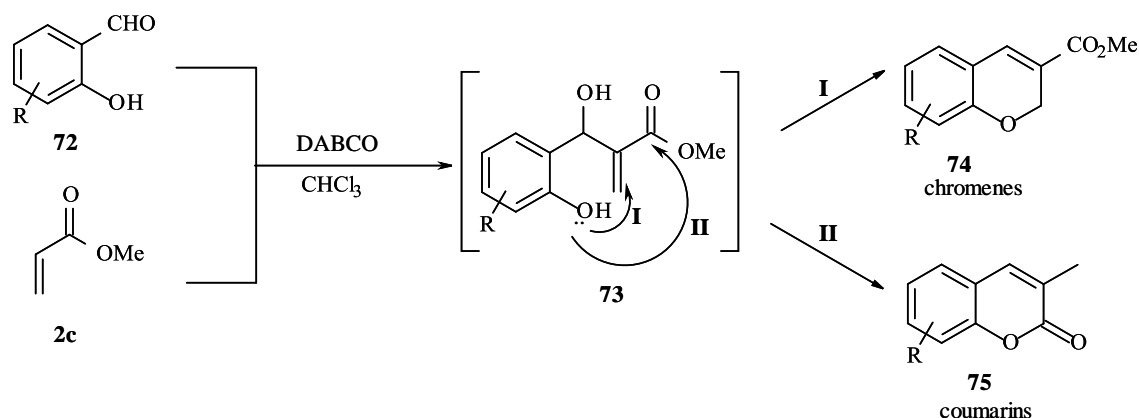
Scheme 17. Possible cyclisation pathways of MBH adducts.

Selective formation of coumarins was achieved by Musa,[19,85] using both protected and unprotected salicylaldehydes. The protected salicylaldehydes (Scheme 18), were obtained by benzylating the phenolic hydroxyl group to give ethers of type **77**, which were then reacted with methyl acrylate in MBH reactions. Treatment of the MBH products **78**, with the nitrogen nucleophiles, piperidine or benzylamine, afforded the conjugate addition products **79**. Hydrogenolysis, in the presence of a 10% Pd-C catalyst, allowed deprotection of the phenolic oxygen, permiting cyclisation *via* acyl substitution to afford the 3-(aminomethyl)- coumarins **80**. Halogen acids were used in an alternative approach to effect deprotection and cyclisation to the 3-halomethyl analogues **81** and **82** in a single step.

Use of *tert*-butyl acrylate in this MBH reaction, provided another route to the synthesis of 3-(halomethyl)coumarins (Scheme 19), obviating the need for the protection-deprotection steps. Treatment of the *tert*-butyl acrylate-derived MBH adducts with HCl in acetic acid under reflux gave the 3-(chloromethyl)coumarins in very good yield. When the adducts were refluxed in acetic acid alone, however, a mixture of chromenes and coumarins were obtained.

Further work in this area,[86-88] aimed at developing potential dual-action HIV-1 protease and reverse-transcriptase inhibitors, has resulted in modification of the 3-(chloromethyl)coumarins **82**, by nucleophilic substitution reactions, using nitrogen nucleophiles such as benzylamine and propargylamine as shown in Scheme 20.
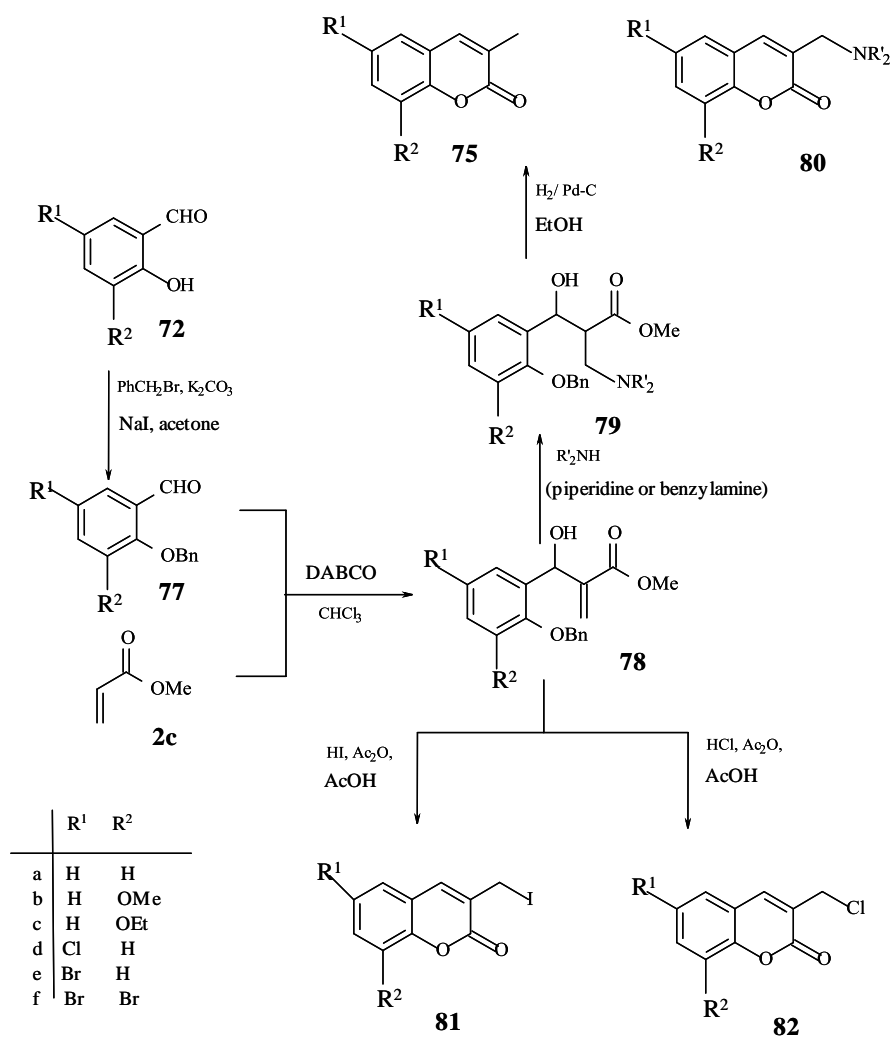
Scheme 18. Synthesis of coumarin derivatives *via* benzyl ether-protected salicylaldehydes.[19,85]
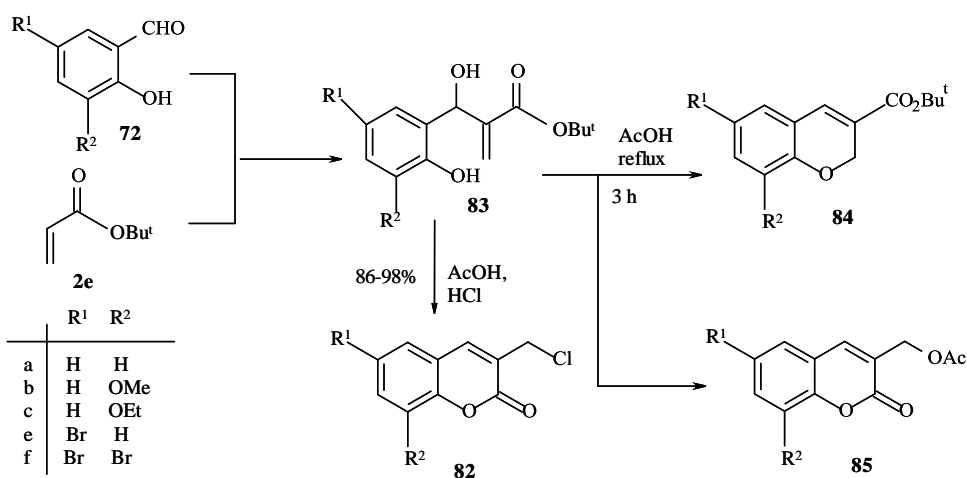
Scheme 19. Synthesis of coumarin derivatives *via* unprotected salicylaldehydes, using *tert*-butyl acrylate as the activated alkene.[85]
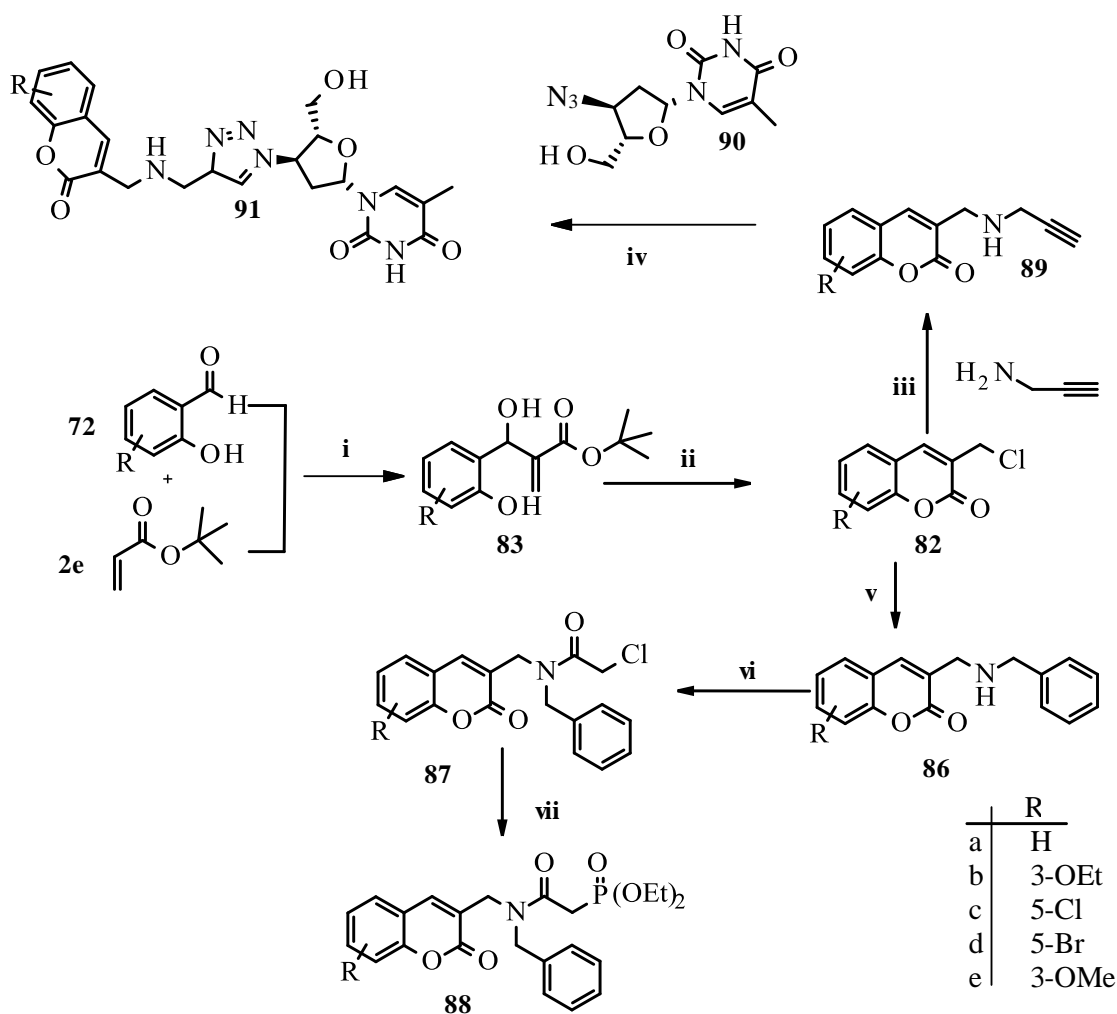
Scheme 20. Reagents and conditions: i) DABCO, CHCl$_3$; ii) HCl, Ac$_2$O, reflux; iii) propargylamine, THF; iv) sodium ascorbate, Cu$_2$SO$_4$.5H$_2$O-THF; v) PhCH$_2$NH$_2$, THF; vi) ClCH$_2$COCl, THF, reflux; vii) P(OEt)$_3$, N$_2$, reflux.[86-88]

Lee and co-workers[89] have synthesised methyl 7*H*-dibenzo[*b*,*g*]oxocin-6-carboxylates **98** from MBH adducts of 2-phenoxybenzaldehydes. As shown in Scheme 21, MBH reactions of the phenoxybenzaldehydes **94** with methyl acrylate in the presence of DABCO and triethanolamine gave the corresponding MBH products **95** in high yield. Treatment of the MBH adducts with NBS gave the MBH allyl bromides **96,** Friedel-Crafts cyclisation of which, using aluminium chloride in dichloromethane, afforded the tricyclic products **98** in moderate to high yields.
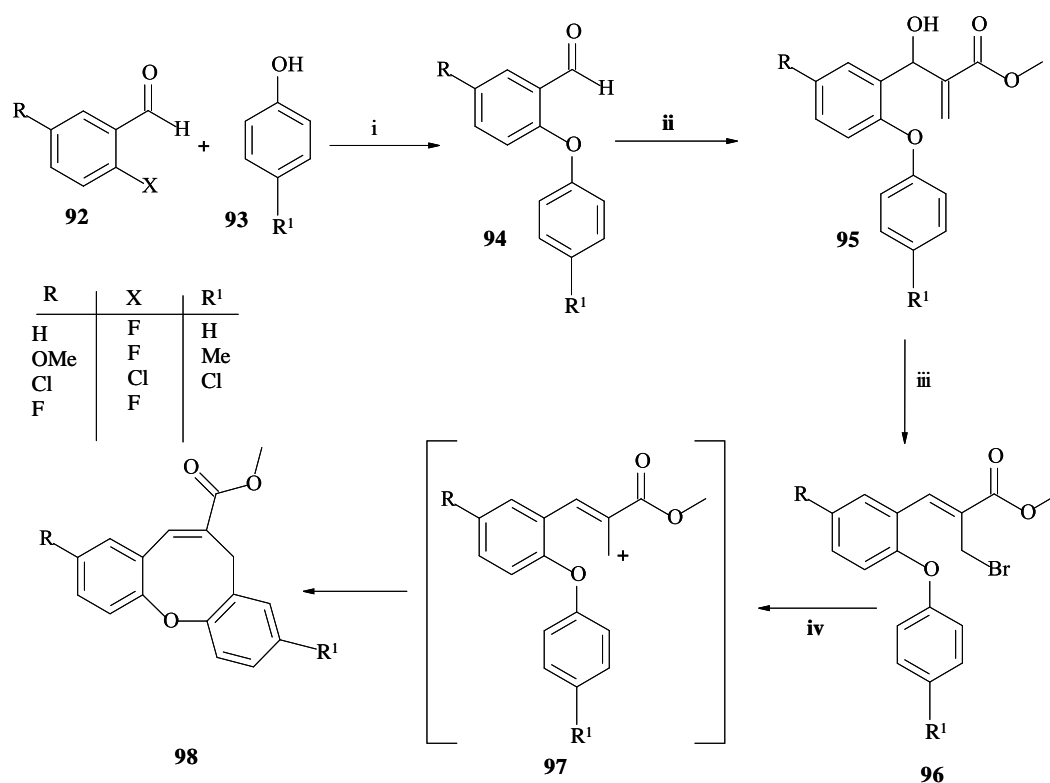
Scheme 21. Reagents and conditions: i) K_2CO_3, DMAC, 170 ^{o}C, 3-5 h; ii) $H_2C=CHCO_2Me$, $(HOCH_2CH_2)_3N$, DABCO, r.t, 9-63 h; iii) NBS, DMS, CH_2Cl_2, 0 ^{o}C- r.t, 6-12 h; iv) $AlCl_3$, CH_2Cl_2, reflux, 10 min-2 h.[89]

In a series of consecutive steps, involving radical cyclisation, halolactonisation and decarboxylation, Gowrisanker *et al.*[90] managed to synthesise the 3,4-disubstituted 2,5-dihydrofurans **104** and **105** from MBH adducts **99** (Scheme 22). Introducing a tosylamide moiety at the vinylic methylene centre of the MBH adducts, enabled extension of this methodology to the synthesis of *N*-tosyl-2,5-dihdropyrrole derivatives **107**. Furanones have been reported as potential anti-inflammatory agents and, using the multi-step sequence illustrated in Scheme 23, Amarante *et al.*[91] synthesised biologically active furanones **114**, enantioselectively from a MBH adduct.

Scheme 22. *Reagents and conditions*: i) Propargyl alcohol, H_2SO_4 (cat.), CH_2Cl_2, r.t., 6 h.; ii) a. AIBN (cat.), Bu_3SnH(1.5 eq), neat, 80 ^{o}C, 20 min., b. dil HCl (cat.), Et_2O, r.t., 20 min.; iii) LiOH (1.5 eq), aq THF, r.t., 4 h.; iv) I_2 (3 eq), $NaHCO_3$, THF, r.t., 4 h.; v) NBS (3 eq), $NaHCO_3$, THF, r.t., 4 h.[90]

Scheme 23. *Reagents and conditions*: i) CH_3Li, CuI, -20 to -40 ^{o}C, 10 h.; ii) DIBAL-H, CH_2Cl_2, -78 ^{o}C, 2 h.; iii) (-) -DIPT, $Ti(O^iPr)_4$, TBHP, CH_2Cl_2, -40 to -20 ^{o}C.; iv) a. MsCl, Et_3N, CH_2Cl_2, 0 ^{o}C, 10 min., b. $LiAlH_4$, THF, 0 ^{o}C, 30 min.; v) 20 mol% $Pd(OAc)_2$, bathocuproine (20 mol%),H_2O, O_2, 100 ^{o}C, 30 h.; vi) DPC, DMAP, 2-isopropoxy acetic acid, DCE.; vii) $CF_3CO_2^iPr$, DBU, CH_3CN, reflux 10 h.[91]

Jayashankaran *et al.*[92] explored [3+2] cycloaddition reactions using the MBH adducts **115** as dipolarophiles, and obtained spiropyrrolidines regio-and stereoselectively. They reacted sarcosine **116** with ninhydrin **117** generating azamethine ylides *in situ*, which reacted with the MBH adducts to give compounds **119** as shown in Scheme 24. Isatin and acenaphthaquinone were also used in place of ninhydrin to give the corresponding cycloaddition products **118**. When the reaction was repeated in a different solvent, methanol, polycyclic products **120** were isolated, containing both oxygen and nitrogen as heteroatoms. Their formation was attributed to hemiactal cyclisation of the initial products **118**. Structures were confirmed by spectroscopic analysis and X-ray crystallography.
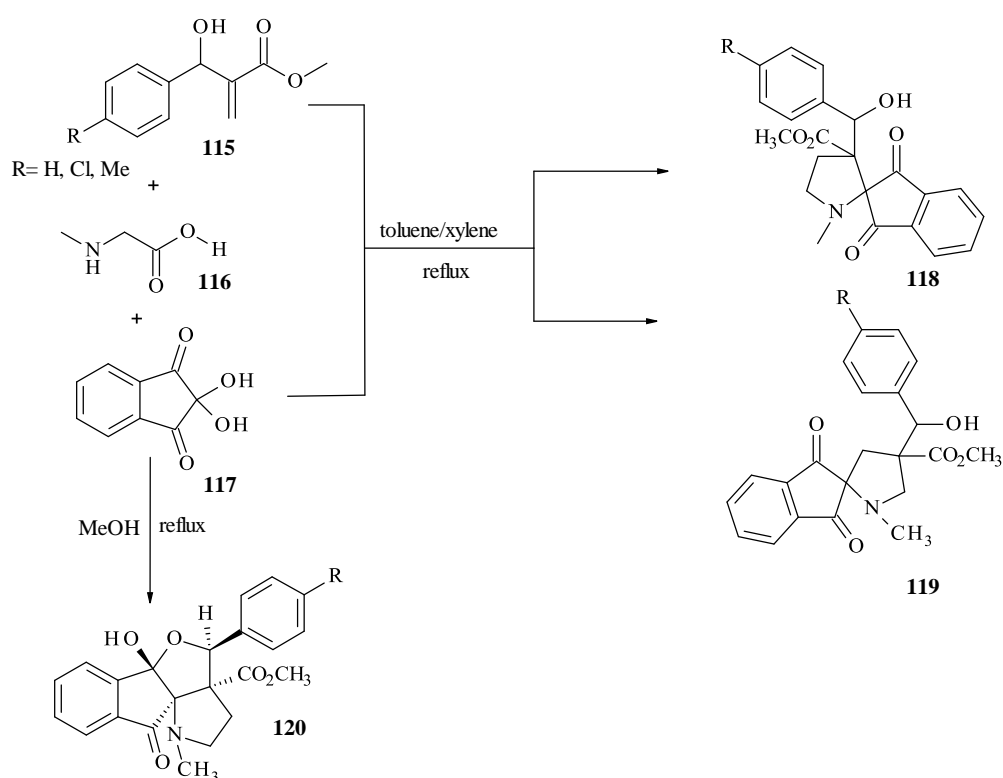
Scheme 24.[92]

In a similar approach, Bakthadoss and co-workers[93] as well as Ramesh *et al.*,[94] synthesised oxygen-nitrogen fused heterocycles from MBH allylic bromides **121**. Bakthadoss and co-workers[93] used K_2CO_3 in acetonitrile to form the intermediates **122**, while Ramesh *et al.*[94] used K_2CO_3 in acetone; both methods gave the intermediates **122** in excellent yields. In an intramolecular [3+2] cycloaddition reaction, the intermediates **122** were converted to the heterocyclic products **124** with high diastereoselectivity (Scheme 25).

Scheme 25.

R= H, 4-Me, 4-Et, 4-^{i}Pr, 4-F, 2-Cl, 3-Cl, 4-Cl
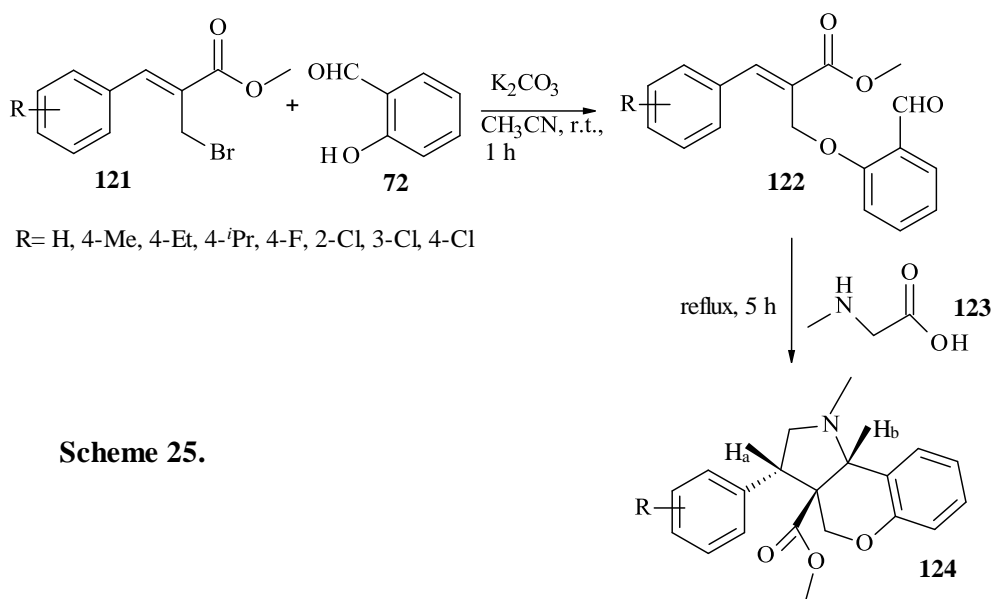
Basavaiah and Rao[95] synthesised tetracyclic indolizine-fused chromones **128** starting from 6-substituted chromones **125** as activated alkenes in MBH reactions with various pyridine-carbaldehydes **126** in the presence of trimethylamine. Treatment of the corresponding MBH adducts with acetic anhydride under reflux gave the tetracyclic products in the case of R^1 being the pyrid-2-yl group.
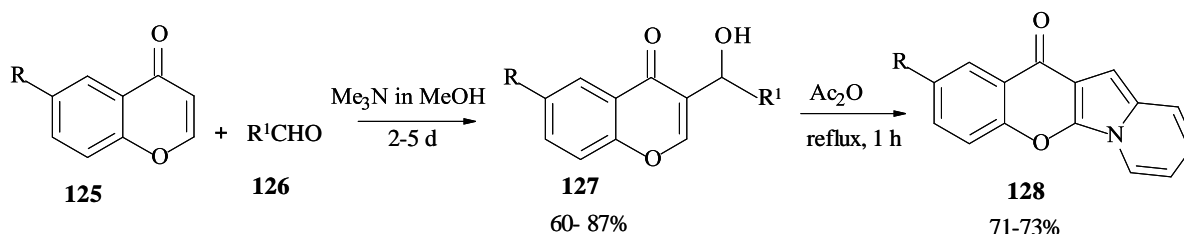
R=CH$_3$: R^1 = pyrid-2-yl, pyrid-3-yl, pyrid-4-yl,
           fur-2-yl,

R= H: R^1 = pyrid-2-yl, pyrid-3-yl, pyrid-4-yl, fur-2-yl,
           thiophen-2-yl, 2-nitrophenyl, 4-nitrophenyl

Scheme 26.[95]

In a similar approach, Kaye and co-workers[96] synthesised tetra- and penta-cyclic indolizine-fused-chromones, from MBH products. Various chromones were reacted with three aldehydes, *viz.*, pyridine-2-carbaldehyde, 6-methylpyridine-2-carbaldehyde and quinoline-2-carbaldehyde in MBH reactions in the presence of TMPDA in a THF-H$_2$O mixture (1:1).[96] Refluxing the MBH products in acetic anhydride as previously reported by Basavaiah[95] gave the desired products. Microwave synthesis at this step gave higher yields and cleaner products, in shorter reaction times.
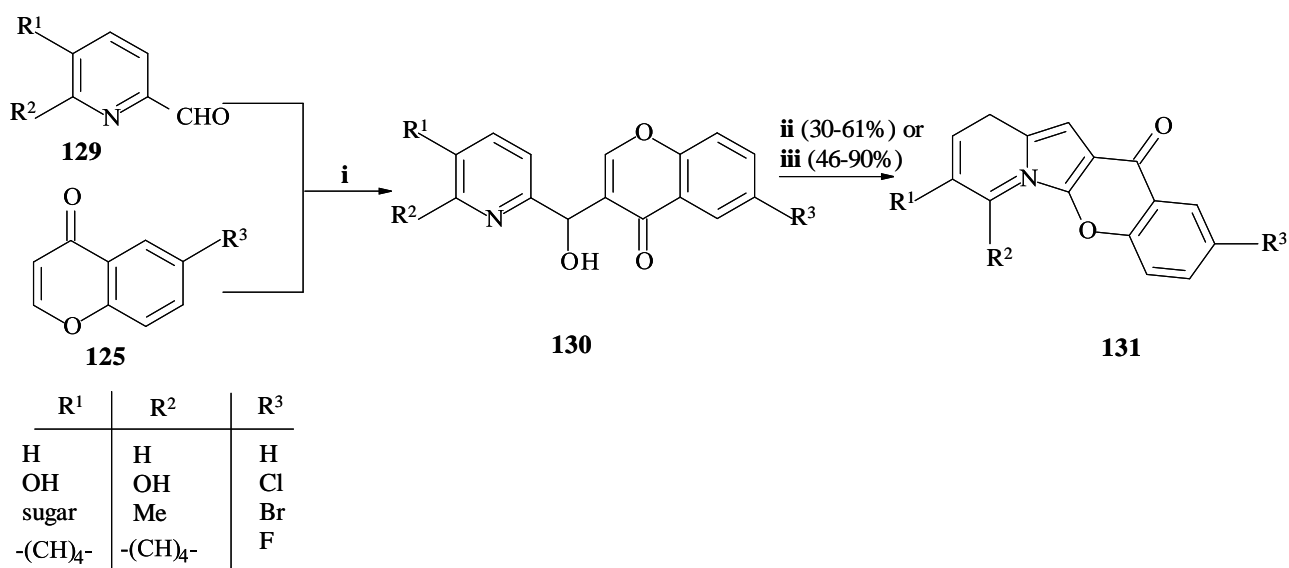
Scheme 27. *Reagents and conditions*: i) TMPDA, THF-H_2O, r.t.; ii) Ac_2O, reflux, 2 h.; iii) Ac_2O, microwave, 5 min.[96]

1.1.3.2 Nitrogen-containing heterocyles derived from MBH adducts

Many research groups have reported the synthesis of nitrogen-containing heterocycles from MBH adducts, and a recent review has been published.[97] The synthesis of quinolines and quinoline derivatives *via* the MBH reaction was pioneered in our group[14] and extended by others. Substituted 2-nitrobenzaldehydes were reacted with various activated alkenes in MBH reactions to give the MBH adducts **132**, illustrated in Scheme 28. Cyclisation of the MBH adducts **132** can follow either conjugate addition (path **I**) to give the quinoline derivatives **134**, or path **II**, which depending on the nature of the activated alkene, may involve either nucleophilic addition to give quinolines **136** and quinoline *N*-oxides **137**, or nucleophilic acyl substitution to give the 2-quinolone derivatives **139**, **140** and **141** (Scheme 28).

Basavaiah *et al.*[12] went on to react various 2-nitrobenzaldehydes with chromones as activated alkenes and obtained the corresponding MBH adducts **142** in good yields. Treatment of the adducts with iron powder in acetic acid under reflux was expected to give the tetracyclic products **144** and **145**, but instead they isolated compound **146** in 61% yield. (Scheme 29).

Scheme 28.[14]

	R¹	R²	R³	R⁴
a	H	H	H	H
b	H	H	Cl	H
c	H	H	OH	H
d	OMe	H	H	H
e	H	H	H	Cl
f	H	OMe	OMe	H
g	H	-OCH₂O-		H
h	H	NO₂	H	H

Scheme 29.[12]
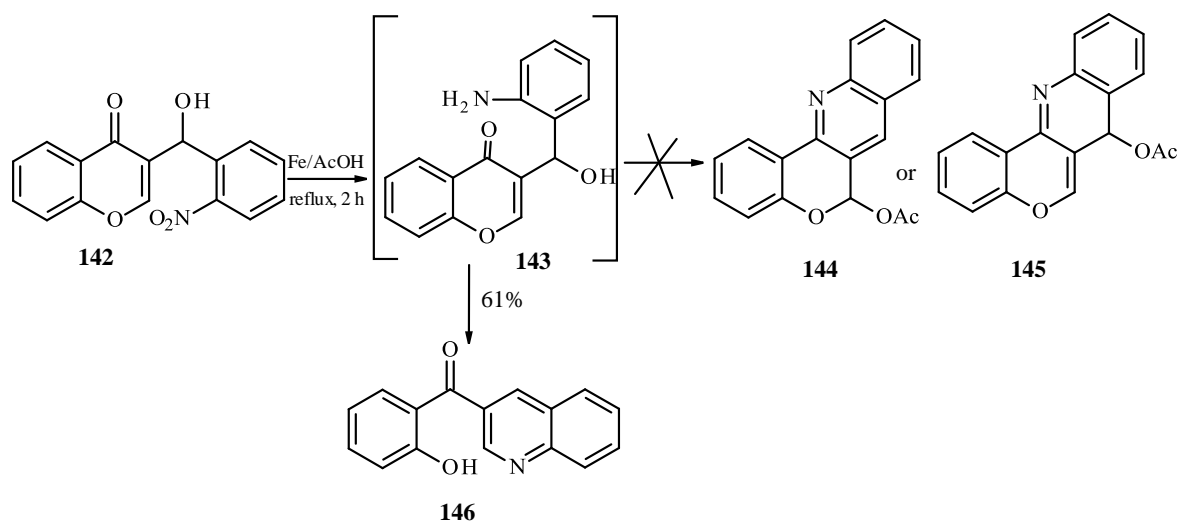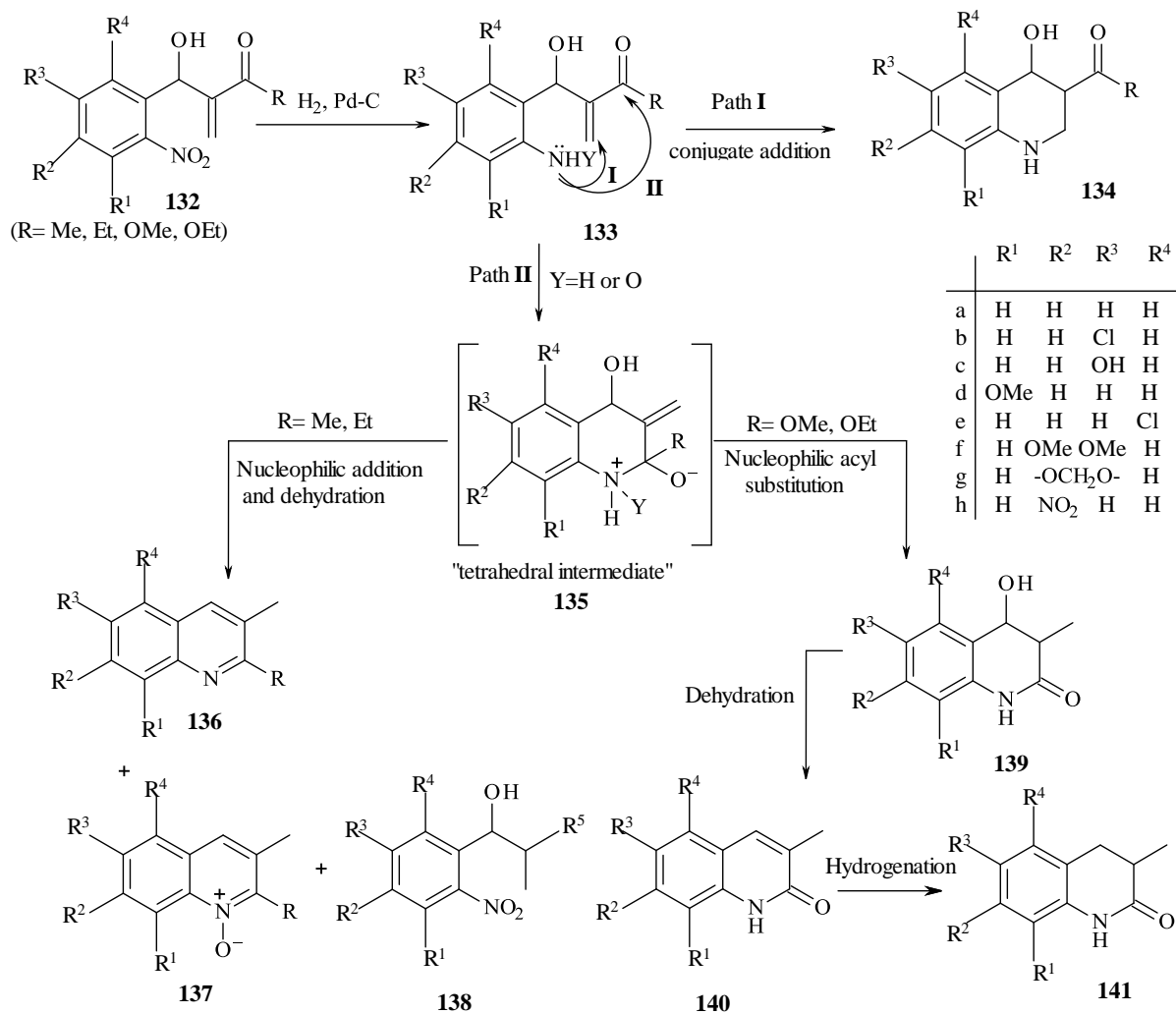
Kim and co-workers[98-101] have contributed significantly to the synthesis of quinoline derivatives from MBH adducts. They have reported the preparation of 4-hydroxy-3-(ethoxycarbonyl)quinoline *N*-oxide derivatives from 2-nitrobenzaldehydes.[98] In a different approach outlined in Scheme 30,[99] they synthesised 1,2-dihydroquinoline-3-carboxylic acid esters **150** from the *N*-tosylimines MBH adducts **147**.
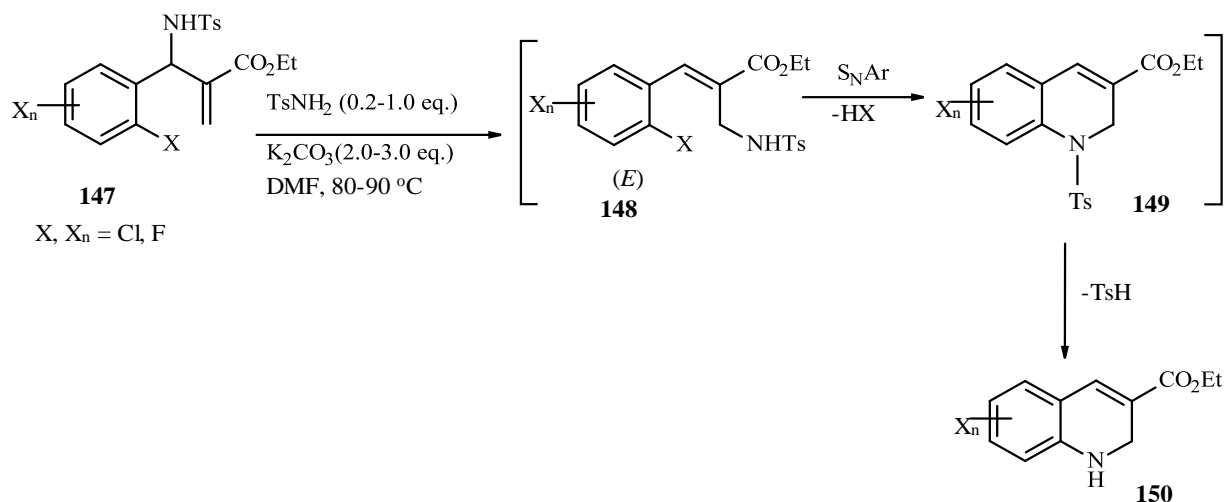
Scheme 30.[99]

In a similar approach, starting from MBH acetates, Kim and co-workers[100] were able to form *N*-substituted 1,4-dihydroquinolines **154** in moderate to good yields (Scheme 31). MBH acetates also gave access to indenoquinolones.[101] Refluxing the MBH acetates with aniline gave the intermediate **155**. Reaction of this intermediate with polyphosphoric acid (PPA) at 120 ^{o}C gave the indenoquinolines **156** and **157**, as well as compound **160** (Scheme 32).

Scheme 31.[100]

Scheme 32.[101]

1,3-Dipolar cycloaddition reactions have been used by Singh *et al.*[102] to access spiro-fused quinolones **165** in good yields from MBH adducts **162** as shown in Scheme 33.
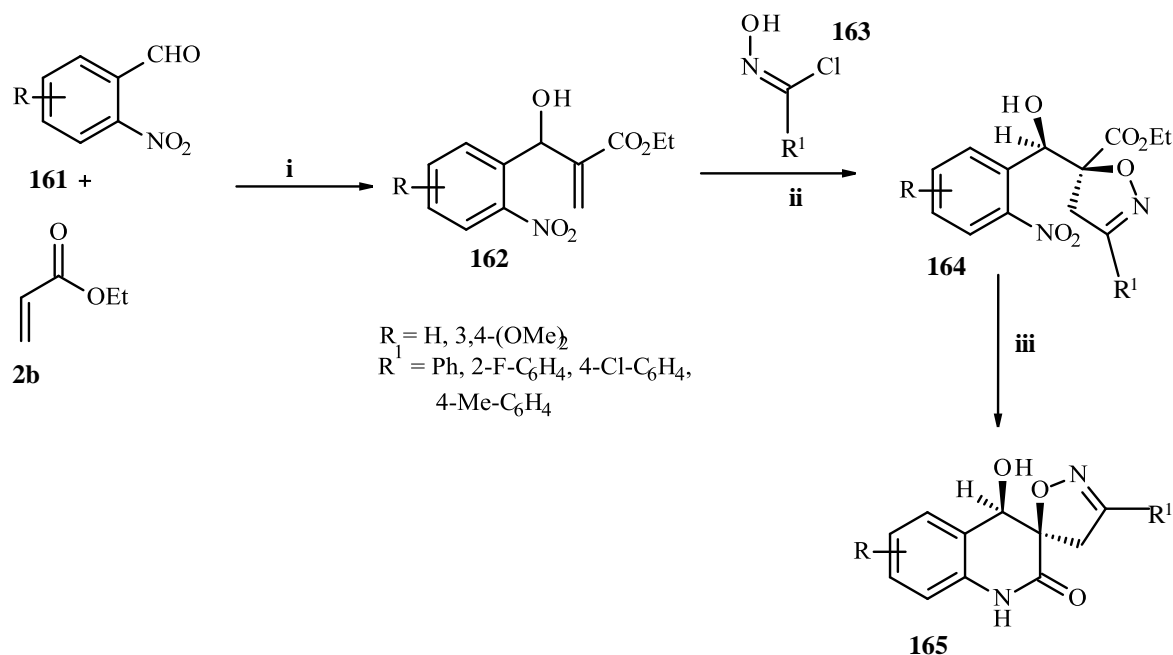
Scheme 33. Reagents and conditions: i) DABCO, neat, r.t., 10-24 h; ii) Et$_3$N, anhydrous Et$_2$O, -78 ^{o}C to r.t., 3 h; iii) In/HCl, 70 ^{o}C, THF/H$_2$O (3:2), 5-7 min.[102]

In other work pioneered in our group,[23,32,103,104,105] the MBH reaction has provided access to indolizines, another class of heterocycles containing nitrogen. Pyridine-2-carbaldehydes **166** were reacted with acrylate esters **2c** in the presence of DABCO or 3-HQ to give the corresponding MBH adducts **167.** Heating the adducts at 120 ^{o}C for 30 min gave the cyclised indolizine-2-carboxylate esters **170**. Acetylation of the MBH adducts at 100 ^{o}C for 30 min. gave the expected MBH acetates, and a rather interesting and unexpected quinoline derivative **169c** in 6 % yield. The MBH acetates were subsequently converted to the indolizine-2-carboxylate esters. Saponification, followed by neutralisation of the carboxylate esters converted them to the corresponding carboxylic acid derivatives **171**. With the aim of synthesising potential HIV-1 protease inhibitors, the indolizine-2-carboxylic acids were then coupled with amino compounds **172a-h**, using carbonyl diimidazole (CDI) in dry DMF, to give the novel *N*-substituted indolizine-2-carboxamides **173**.[106,107]
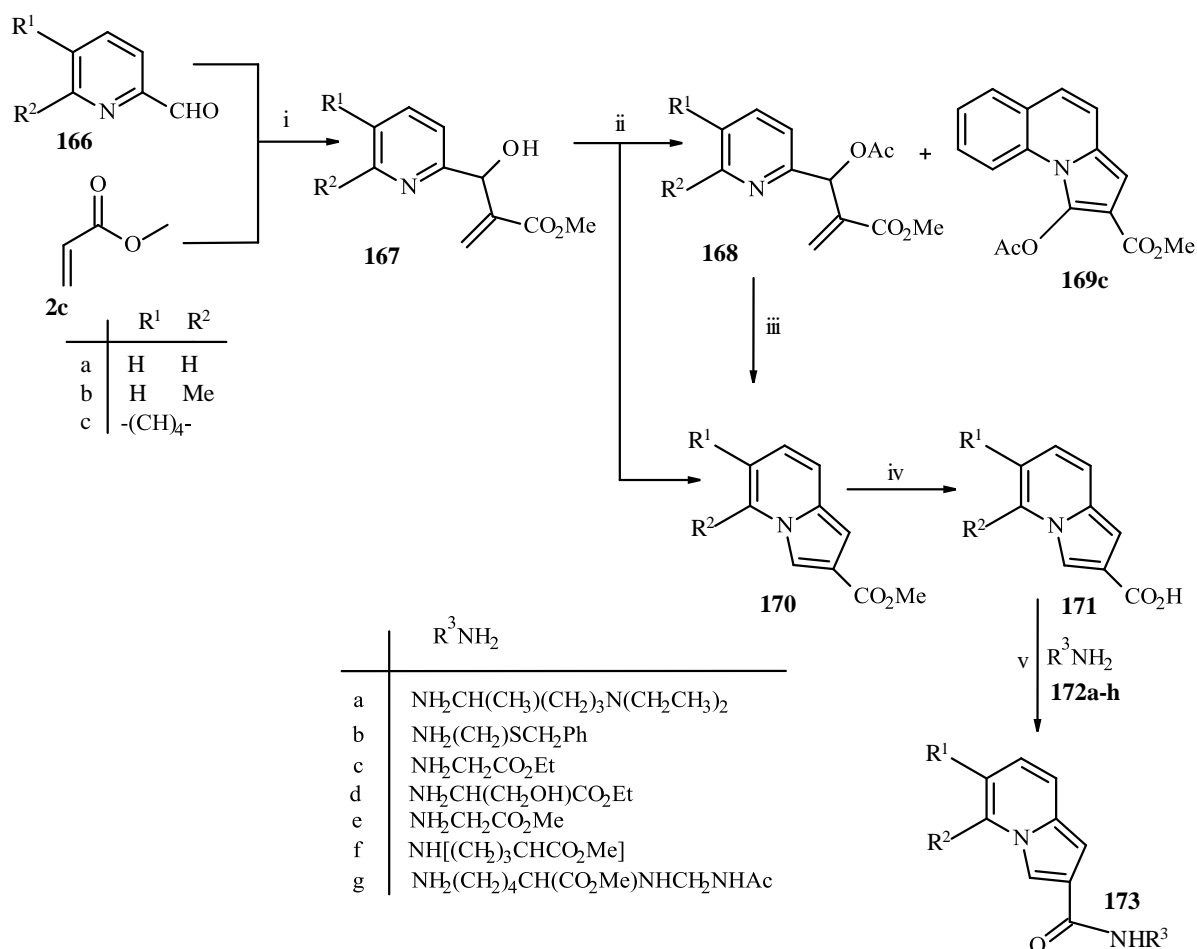
Scheme 34. Reagents and conditions: i) DABCO or 3-HQ, CHCl$_3$; ii) Ac$_2$O, 100 ^{o}C, 30 min; iii) 120 ^{o}C, 1h; iv) KOH, EtOH, reflux, 16 h, then dil. HCl; v) CDI, DMF, 40 ^{o}C, then amino compounds (as hydrochloride or acetate salt with pyridine), r.t., overnight.

Kim and co-workers[108,109] have synthesised indoles in very good yield from enamides of MBH adducts[108] as well as from MBH acetates,[109] and Scheme 35 illustrates the approach using MBH acetates. The required intermediates **176**, were synthesised by reacting the MBH acetates **174** with indole derivatives **175** in the presence of KOH in DMF at 0 ^{o}C. The isomers obtained were separated quite easily, with the *E*-isomer being the major product. Treatment of the intermediate products with palladium acetate, effected an intramolecular palladium-catalysed annulation to give the seven-membered cyclic products **177**. Compounds which had methyl groups on the indolizine ring formed eight-membered derivatives **178** due to aryl-aryl bond formation.
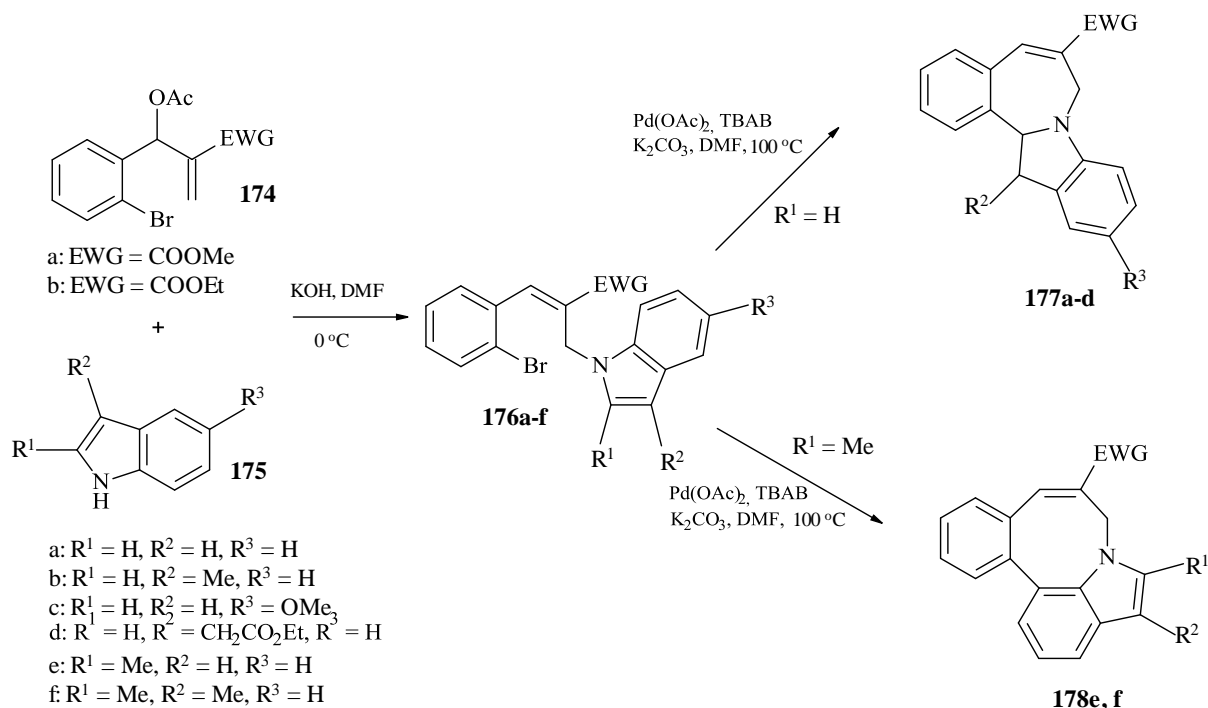
Scheme 35.[109]

The same group has also synthesised poly-substituted pyrroles from MBH adducts *via* the [3+1+*N*] annulations shown in Scheme 36.[110] Bromination of the MBH adducts **179** gave the allyl bromides **180**, which were reacted with aldehydes in an indium-mediated Barbier reaction to form compounds **181**. Oxidation of these compounds with pyridinium chlorochromate (PCC) gave the α-methylene-γ-keto esters **182** in 90% yield. Reaction of these compounds with various amines gave the products **186** in 50% yield as well as the corresponding amide derivatives **187** in 5% yield, *via* the intermediates **183**-**185**.
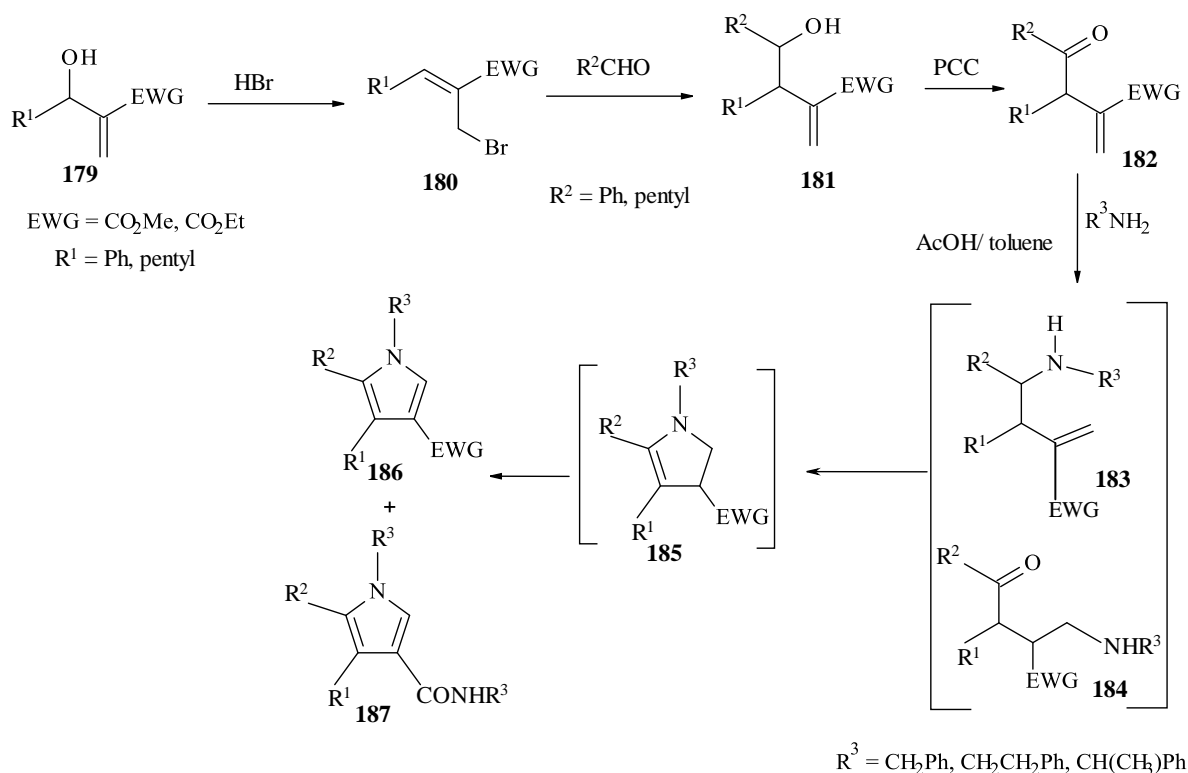
Scheme 36.[110]

More recently, using a one-pot methodology and also starting from MBH acetates, Cao *et al.*[111] synthesised seven-membered lactams *via* amination followed by palladium-catalysed intramolecular cyclo-carbonylation. The MBH acetates **174** were treated with various amines **188** in the presence of the Pd catalyst and carbon monoxide in basic medium to give the lactams **189** (Scheme 37).
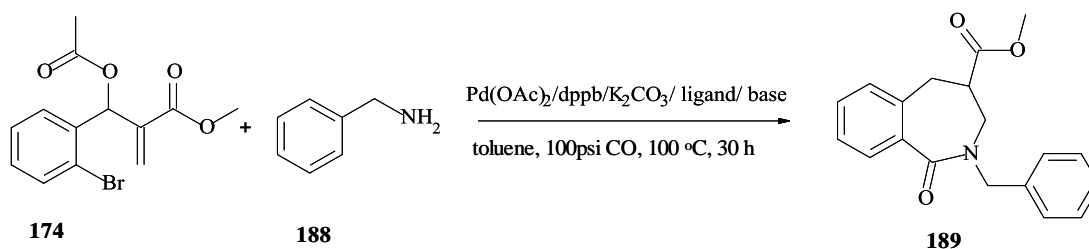
Scheme 37.[111]

A glycosidase inhibitor has been synthesised from an MBH adduct in a stereoselective reaction by Galeazzi *et al.*,[112] as illustrated in Scheme 38. The MBH adduct **190** was converted to the diastereomeric 3-hydroxypyrrolidin-2-ones **191** and **192**, by reaction with the chiral amine, (*S*)-phenylethylamine, in a conjugate addition reaction. An equimolar mixture of the two diastereomers was isolated. Both compounds **191** and **192** were converted to the desired product **196** in a series of steps, using different synthetic routes. The synthetic pathway illustrated, was used for converting diastereomer **192**.
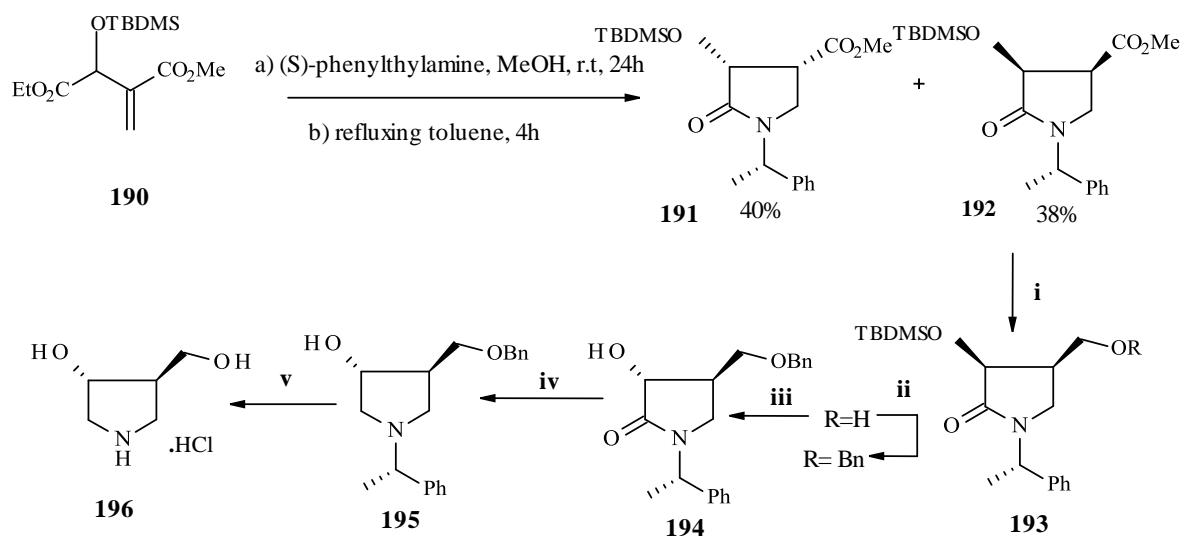
Scheme 38. Reagents and conditions: i) LiAlH$_4$, THF, 0 ^{o}C, 80 %. ; ii) *n*-BuLi, THF, 0 ^{o}C, 5 min, then BnBr, refluxing THF, 80 %. ; iii) KOH, refluxing MeOH-H$_2$O, 30 h, 58 %.; iv) LiAlH$_4$, refluxing THF. ; v) a. 20% Pd(OH)$_2$, on C, H$_2$; b. 3*M* HCl, 94 %.

Recently Basavaiah *et al.*[113] synthesised Himanimide A, from the MBH adducts **198**. Himanimides are a class of bioactive compounds which have been isolated from the bacterial strain *serpula himantoides*. They reacted the α-keto ester **197** with acrylonitrile **2f** to obtain the MBH adduct **198** (Scheme 39). Refluxing the adduct in benzene in the presence of methanesulfonic acid gave the 3,4-disubstituted maleimide **199**. Further derivatisation gave the target compound, Himanimide A **200** .
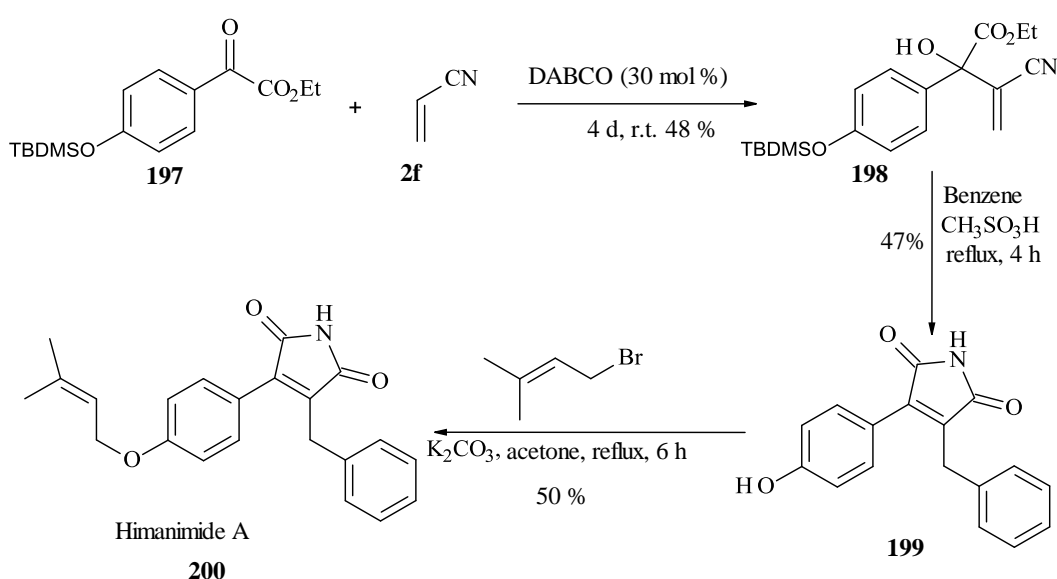
Scheme 39. [113]

1.1.3.3 Sulfur-containing heterocyles derived from MBH adducts

The MBH reaction has also found application in the synthesis of sulfur-containing heterocyles. In 2001, Kaye and Nocanda[6,114] reported a one-pot synthesis of 3-substituted 2*H*-1-benzothiopyrans using the MBH reaction. They reacted the disulfide, 2,2'-dithiodibenzaldehyde **201**, with various acyclic activated alkenes **2a-c, f-i** in the presence of DBU, and obtained the thiochromenes **202a-c, f-i** in moderate yields. Interestingly the cleavage of the disulfide link and cyclisation to the corresponding thiochromenes occurred *in situ*. When this methodology was extended to the use of cyclic ketones **203**, no product was observed but, when the catalyst was changed to TMPDA in a THF-H$_2$O mixture, the tricyclic derivatives **204** were isolated.[72] TMPDA has been shown to facilitate MBH reactions involving cyclic enones, which are generally less reactive than the acyclic enones.
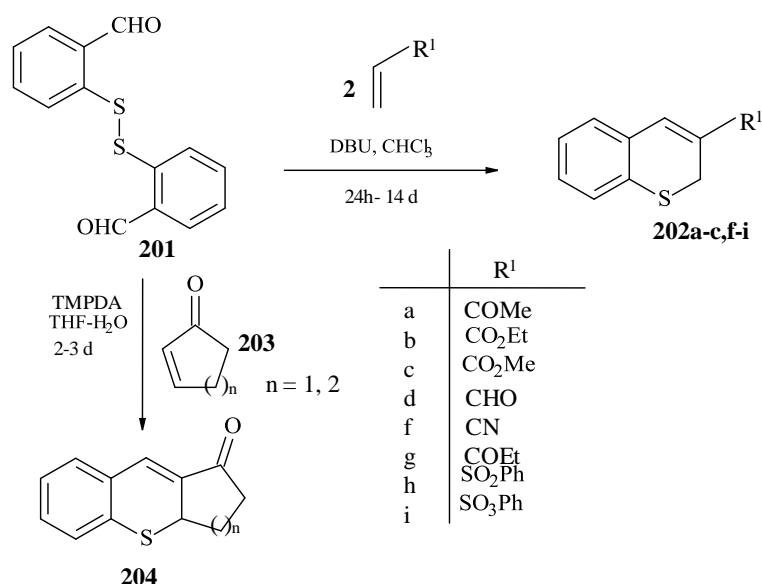
Scheme 40.[6,72,114]

In a recent report, Zhong and co-workers[115] synthesised tetra-fused heterocyclic systems containing both nitrogen and sulphur atoms (Scheme 41). Their methodology involved initial reaction of substituted 2-chloroquinoline-3-carbaldehydes **205** with 4-isopropylbenzenethiol **206** in the presence of sodium hydride in DMSO at 90 °C for 2 h, in a nucleophilic aromatic substitution reaction (S$_N$Ar) to obtain the 2-arylthioquinoline-3-carbaldehydes **207**. MBH reactions of these aldehydes with activated alkenes in the presence of either DABCO or DMAP gave the corresponding adducts **208**. Intramolecular Friedel-Crafts cyclisation of the MBH adducts gave the tetracyclic products **209** and, in some cases, the eight-membered fused ring systems **210**.
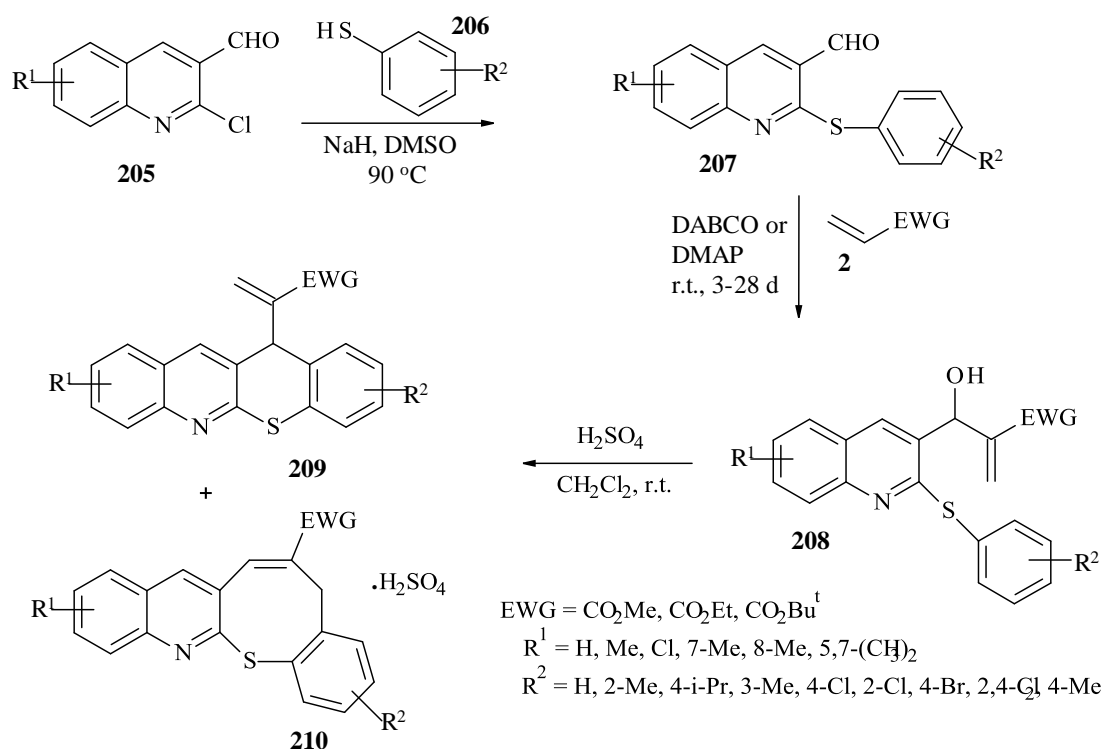
Scheme 41.[115]

Heck coupling of aza-MBH products has been used to access constrained heterocyclic systems. Vasudevan *et al.*[116] synthesised such systems by reacting suitably substituted sulfonamides **211** with benzaldehydes **212** and methyl acrylate **2c** in the presence of titanium isopropoxide, 2-hydroxyquinuclidine and molecular sieves in *i*-PrOH as solvent to give the aza-MBH adducts **213** (Scheme 42). Heck coupling of these adducts using a palladium catalyst system with Et_3N as base in THF, afforded the cyclised products **214** in moderate to good yields.

Scheme 42.[116]
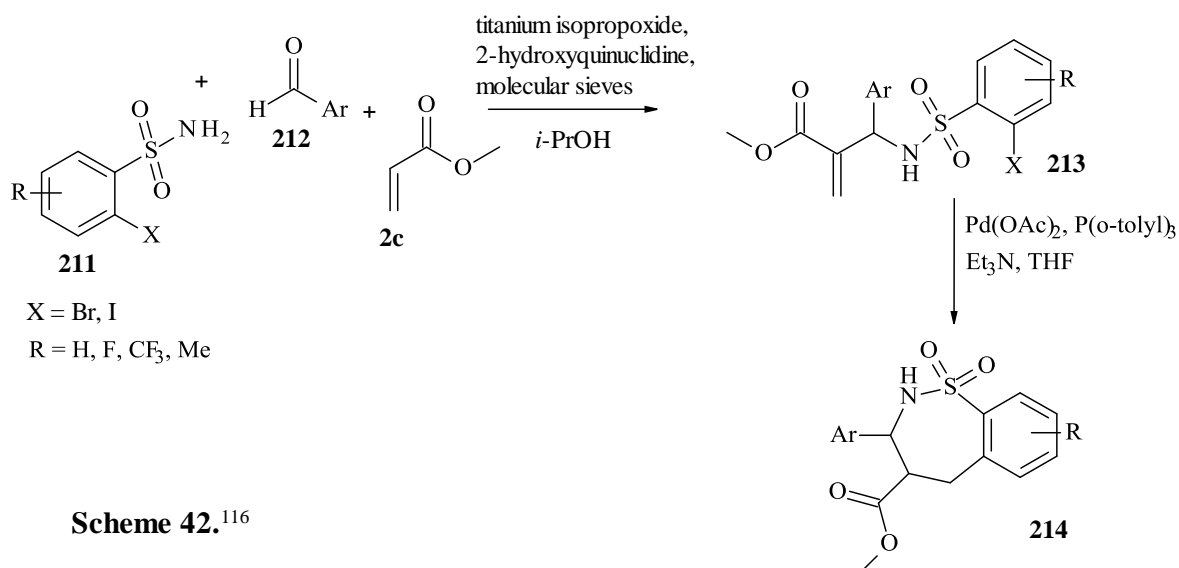
1.2 Previous work in the group and aims of the present investigation

1.2.1 Previous work done in the group relevant to the present study.

As indicated already, our research group has been involved in exploring various applications of MBH methodology. Questions concerning the mechanistic implications of some of these reactions have provided the basis for the present investigation.

1.2.1.1 The MBH synthesis of thiochromenes

Access to the 2*H-1*-benzothiopyran unit was achieved by reaction of the disulfide dialdehyde **201** with various activated acylic and cyclic alkenes in the presence of either DBU or TMPDA in MBH reactions as mentioned earlier.[6,72,114] The thiochromenes **202** were accessed in a single step as shown in Scheme 43. It was expected that the reaction would afford the MBH adduct **215**, which would then require reductive cleavage of the sulfur-sulfur bond to give the mercapto-MBH intermediate **216**. Cyclisation of this adduct *via* intramolecular conjugate addition was then expected to give the hydroxythiochromene **217**, dehydration of which would lead to the desired thiochromenes **202**.[6] The results, however indicated that sulfur-sulfur bond cleavage as well as cyclisation and dehydration had occurred *in situ* under the conditions employed. It was apparent that this reaction needed to be explored further in order to understand the actual mechanism involved in the reported transformations.
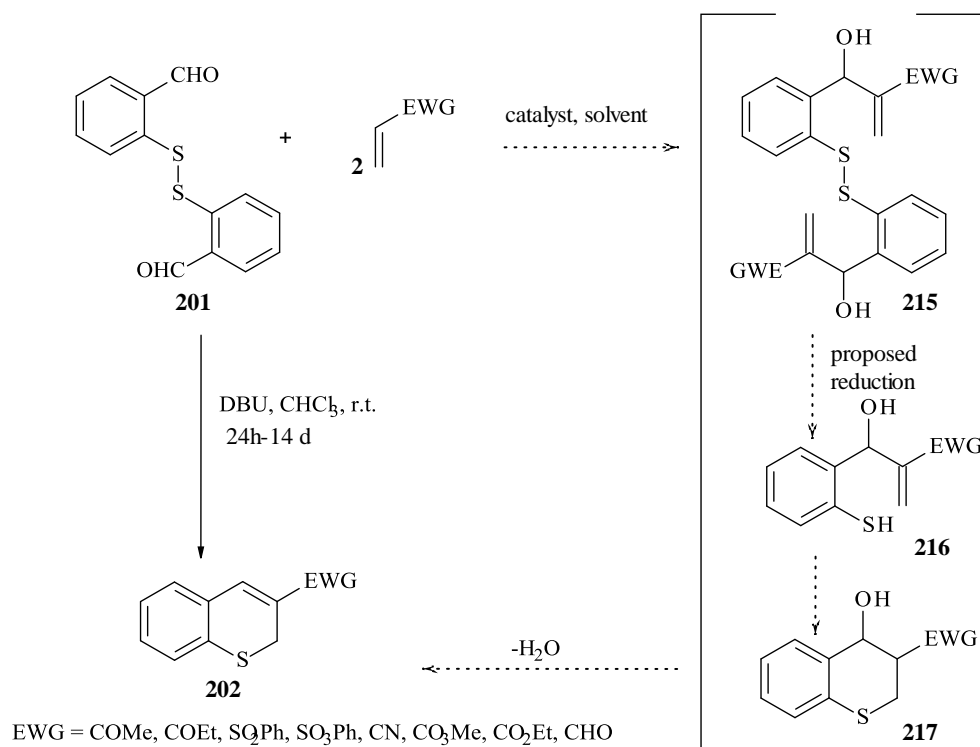
Scheme 43.

1.2.1.2 MBH reaction of substituted chromone-3-carbaldehydes with MVK

When substituted chromone-3-carbaldehydes **218** were reacted with MVK **2a** in the presence of 3-HQ, the expected MBH adducts **219** were not isolated but, instead, the novel bis-MVK chromone dimers **220** and tricyclic products **221** were obtained (Scheme 44).[80] Somewhat different chromone dimers had been isolated previously[79,80,117,118,119,120] in DABCO-catalysed reactions of chromone-3-carbaldehydes with methyl acrylate or acrylonitrile. Formation of the dimers has been presumed to proceed *via* formation of the MBH products **219**, which have been isolated in rather low yields when DABCO is used as catalyst.[80] When 3-HQ was used, however, none of the expected MBH adducts were observed, unless the concentration of MVK was increased.
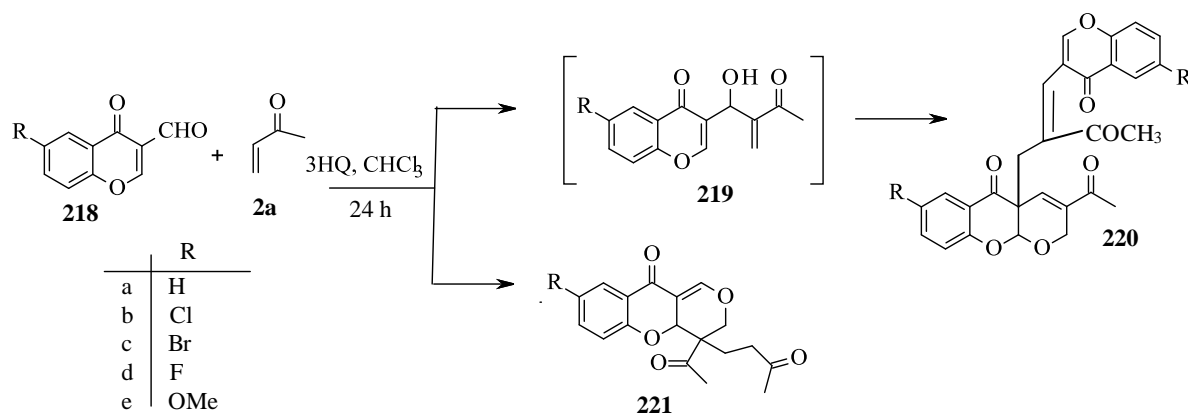
Scheme 44.

1.2.1.3 MBH reaction of chromone-2-carbaldehydes and acrylonitrile.

In another interesting MBH reaction, in this case between chromone-2-carbaldehydes **222** and acrylonitrile **2e**[79] in the presence of 3-HQ, the expected MBH adducts **223** were also not obtained. Instead, products which were tentatively identified as azetidene derivatives **224**, based on the spectroscopic data, were isolated (Scheme 45). Azetidenes are generally difficult to prepare and their apparent access using the MBH methodology was particularly interesting. The mechanistic sequence involved in such a transformation clearly required elucidation.
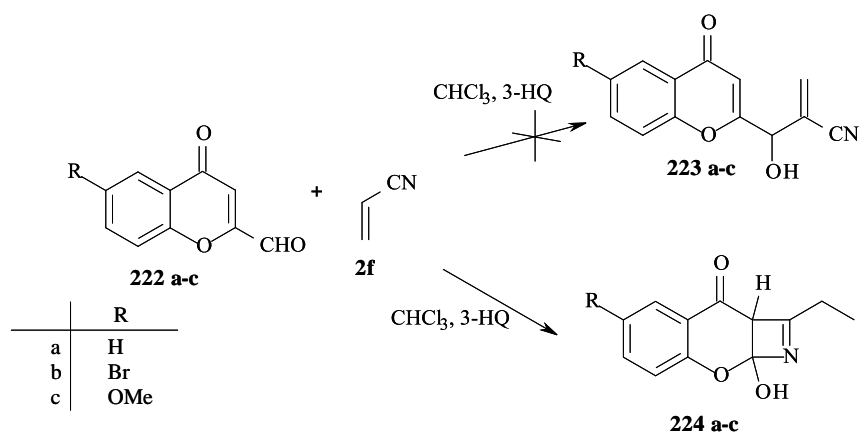
Scheme 45.

1.2.1.4 Reaction of 6-methoxychromone-2-carbaldehyde and methyl acrylate in the presence of 3-hydroxyquinuclidine.

When 6-methoxychromone-2-carbaldehyde **222c** was reacted with methyl acrylate in the presence of 3-HQ, compound **226** was isolated instead of the expected MBH product **225** (Scheme 46). The observed result required further elucidation in order to ascertain the mechanism involved.
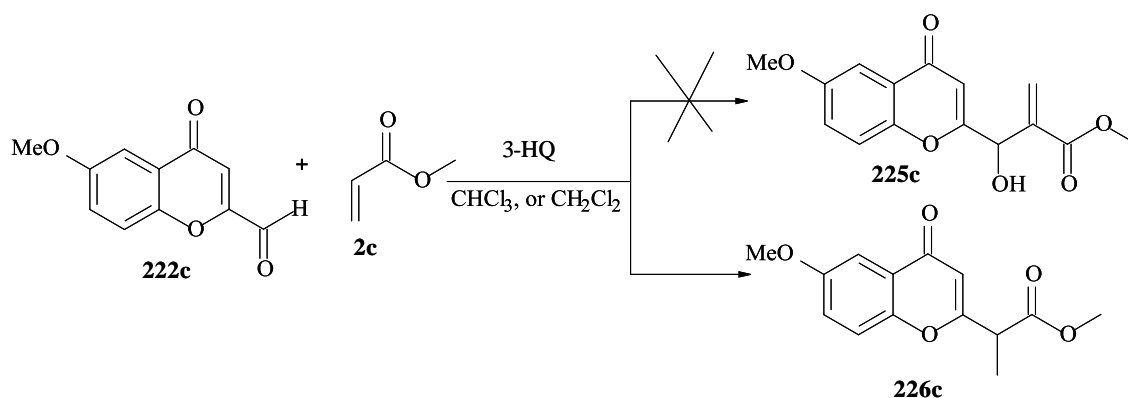
Scheme 46.

1.2.1.5 The Arbuzov reaction of 3-halomethylcoumarins derived from MBH adducts

Access to 3-halomethylcoumarins was provided by cyclisation of MBH adducts derived from 2-hydroxybenzaldehydes as mentioned earlier (Section 1.1.3.1). The Michaelis-Arbuzov reaction of the 3-halomethylcoumarins **81** and **82** was expected to give the direct nucleophilic substitution (S_N) products **228** − which was the case when the 3-(iodomethyl)coumarins **81** were used. However, when the 3-(chloromethyl)coumarins **82** were treated with triethylphosphite under reflux for 4 h, the 4-phosphonated (S_N') products **227** were isolated. When the same reaction was repeated under nitrogen, both the expected 1'-phosphonated (S_N) products **230** and the 4-phosphonated (S_N') products **227** were isolated in yields of up to 67 % and 16 % respectively (Scheme 47). The electronegativities of the halide atoms was suggested as the reasons for the different reactivities of compounds **81** and **82** in these Michaelis-Arbuzov reactions.[86,121]
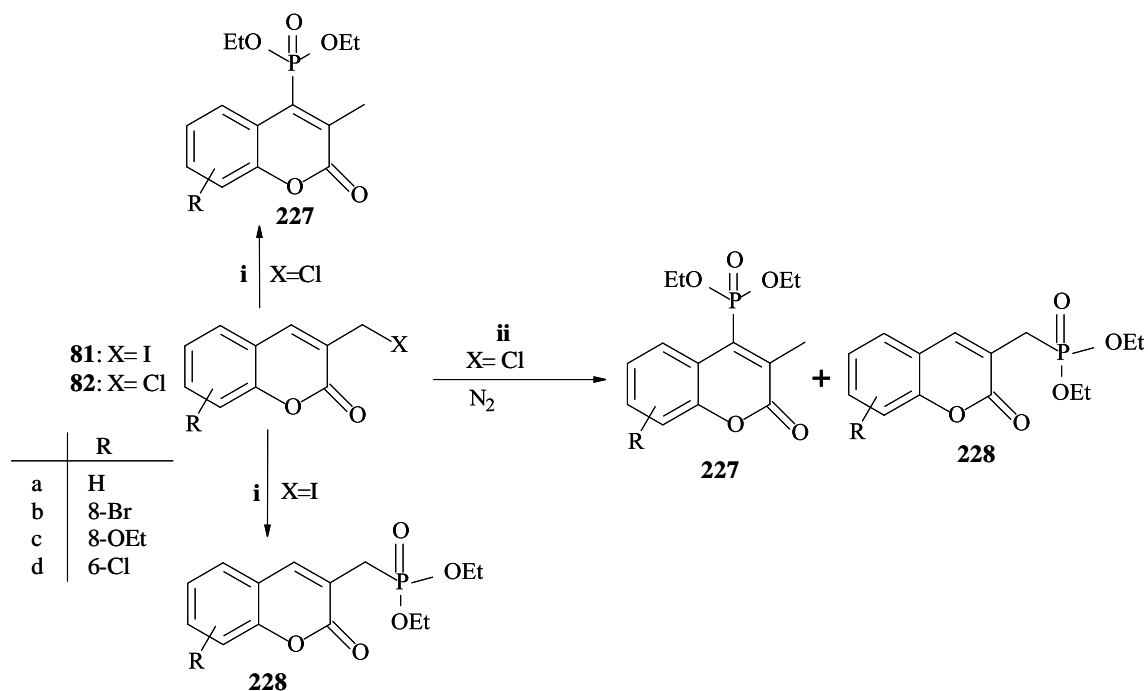
Scheme 47. Reagents and conditions: i) 2 eq. P(OEt)$_3$, reflux, 4 h; ii) 2 eq. P(OEt)$_3$, N$_2$, reflux, 4 h.

1.2.2 Aims of the present investigation

As indicated in the previous sections, our group has achieved access to a range of heterocyclic systems using MBH methodology. In some cases unexpected and rather unusual products have been isolated raising mechanistic questions with regard to their formation. Elucidation of reaction mechanisms forms an essential part of modern organic chemistry and can often lead to the optimisation of yields and the control of chemo- and stereoselectivity in certain transformations. The application of experimental kinetic and theoretical methods in addressing mechanistic questions relating to the reactions outlined in Section, 1.2.1, has been the focus of the present study. More specifically, attention has been given to explore the following transformations:

1. The MBH reaction of 2,2'-dithiodibenzaldehyde with various activated alkenes to afford 2*H*-1-benzothiopyrans, with particular emphasis on :- i) the capacity of the catalyst DBU to cleave various disulfides; ii) the use of different catalytic systems; and iii) experimental, kinetic and theoretical studies to establish the reaction mechanism.

2. The MBH reaction of chromone-3-carbaldehydes with MVK by repeating the synthesis of substituted chromone-3-carbaldehydes and their reactions with MVK and undertaking kinetic and theoretical studies to establish the mechanism.

3. The surprisingly different MBH reactions of chromone-2-carbaldehydes with acrylonitrile and methyl acrylate by:- i) synthesising substituted chromone-2-carbaldehydes and repeating their reactions with acrylonitrile and methyl acrylate; ii) confirming the identity of the different products produced in these reactions; and iii) undertaking experimental, kinetic and theoretical studies to determine the mechanisms of both reactions.

4. The Arbuzov reaction of 3-(halomethyl)coumarins to determine the apparent halogen-mediated regioselectivity. This was expected to involve:- i) synthesis of MBH-derived 3-(chloromethyl)- and 3-(iodomethyl)coumarins; ii) kinetic studies of the Arbuzov reaction between the 3-halomethyl coumarins and triethylphosphite; and iii) a theoretical study of the proposed mechanism.

2. RESULTS and DISCUSSION

Understanding reaction pathways enables one to explore possible alternatives in terms of substrates as well as reaction conditions, more so in drug design, where economically viable reaction pathways in the synthesis of drugs may contribute to the affordability of the final product. Mechanisms of chemical reactions can often be predicted prior to the actual experiment; however, in some cases, reactions may give rise to unexpected and often unusual products. In such cases, based on the nature of the product, there is a need to explore the mechanism/s involved. This discussion will focus on the application of synthetic, kinetic and theoretical methods to solving the mechanisms of four interesting MBH-type reactions *viz.*; i) the reaction of the disulfide 2,2'-dithiodibenzaldehyde with various activated alkenes; ii) the reaction of chromone-3-carbaldehydes with MVK; iii) the reactions of chromone-2-carbaldehydes with acrylonitrile and; iv) reactions of chromone-2-carbaldehydes with methyl acrylate. Attention will also be given to a preliminary investigation of the mechanism of a post-MBH reaction, involving MBH-derived 3-(halomethyl)coumarins, and triethylphosphite in an Arbuzov reaction.

2.1 The synthesis of 2*H*-1-benzothiopyrans

The 2*H*-1-benzothiopyran unit occurs in a variety of plants, and has been shown to exhibit interesting biological properties, such as anti-inflammatory, anti-bacterial, anti-cancer and pain relief.[122-126] Some compounds containing the benzothiopyran moiety have been tested and applied as drugs.[122-126] Their synthesis commonly involves a series of steps starting with the condensation of thiophenols with acrylic acid derivatives, followed by reduction and dehydration.[127] Alternative approaches have also been reported.[128-135] In our own group the MBH reaction has provided access to thiochromenes *via* the 1,8-diazabicylo[5.4.0]undec-7-ene (DBU)-catalysed reaction of 2,2'-dithiodibenzaldehyde **201** with activated alkenes.[6] In this reaction, disulfide bond cleavage occurs *in situ* in the absence of any added reductant, and in order to understand the mechanism, some of these reactions were repeated and monitored to obtain the necessary kinetic data. The disulfide, 2,2'-dithiodibenzaldehyde **201**, the required precursor, was synthesised *via* a two-step sequence (Scheme 48), starting with the reduction of 2-mercaptobenzoic acid **229** to the alcohol **230** as reported by Arnoldi and Carrughi,[129] followed by controlled oxidation using pyridinium chlorochromate (PCC) as reported by Kasmai and Mischke,[136] to give the disulfide 2,2'-dithiodibenzaldehyde.
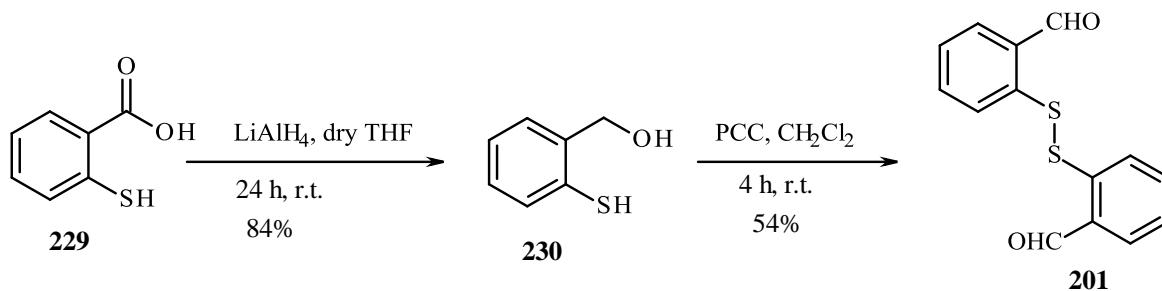
Scheme 48.

The above transformation is illustrated in Figure. 9. The stacked ^{1}H NMR plots show the mercapto proton in the starting material resonating *ca.* 4.7 ppm, while in the mercapto benzyl alcohol, it resonates at 3.67 ppm and the methylene protons in the alcohol resonate as a singlet at 4.72 ppm. Formation of the aldehyde is quite evident with the appearance of an aldehyde signal at 10.20 ppm, while the mercapto signal is absent due to the formation of the disulfide.
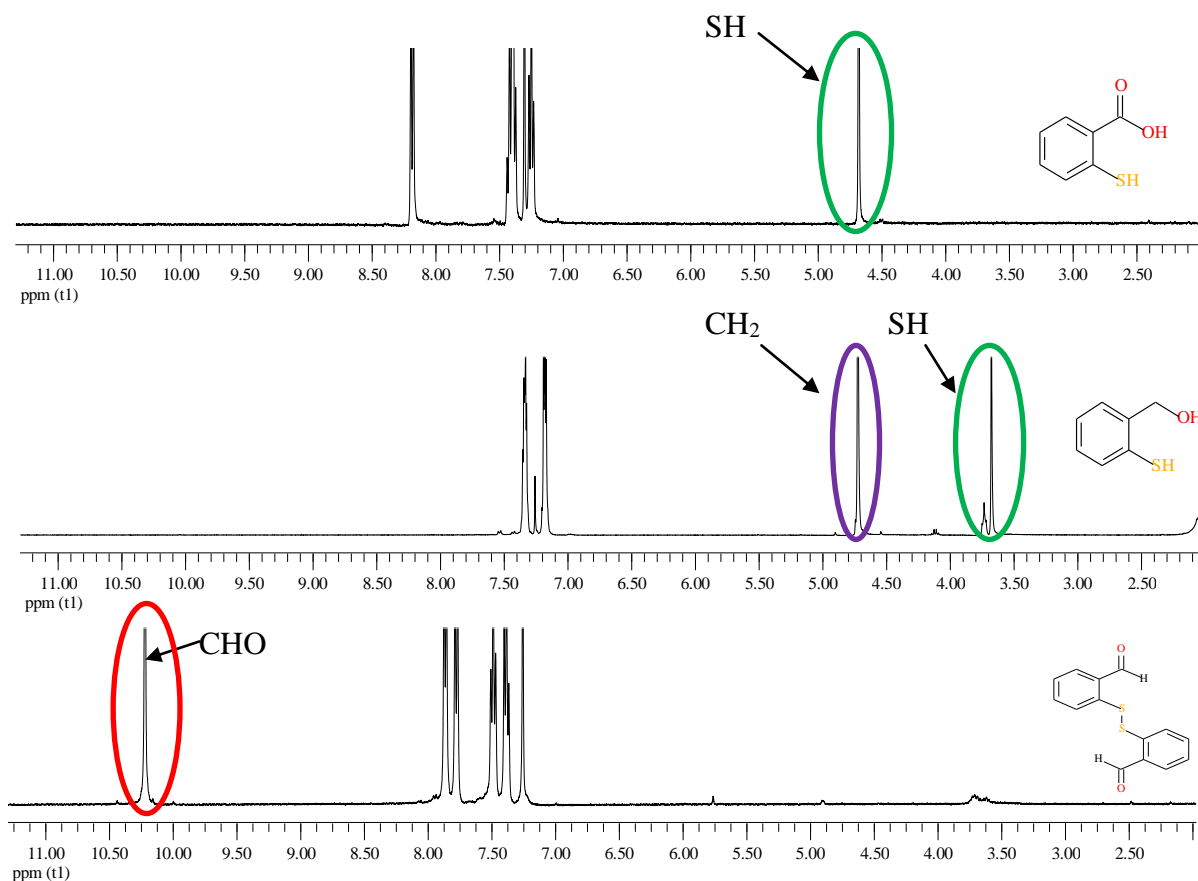
Figure 9. Stacked ^{1}H NMR plots showing synthesis of the disulfide, 2,2'-dithiodibenzaldehyde **201**.

2.1.1 The Morita-Baylis-Hillman reactions of 2,2'-dithiodibenzaldehyde

In this study, the DBU-catalysed MBH reactions of 2,2'-dithiodibenzaldehyde **201** with methyl vinyl ketone (MVK), ethyl vinyl ketone (EVK), acrylonitrile and methyl acrylate were replicated and a further reaction, using *tert*-butyl acrylate, a substrate not used in the previous study,[6] was also undertaken (Scheme 49). The thiochromenes were obtained in moderate yields (40-67%). Figure 10 shows the ^{1}H NMR spectrum of the *ter*t-butyl ester derivative **202d**. The *t*-butyl protons resonate as a singlet at 1.54 ppm, while the methylene proton signal appears at 3.68 ppm. The ^{13}C NMR spectrum (Figure 11) accounts for all the expected signals, with the methylene carbon resonating at 24.0 ppm, the *t*-butyl methyl carbons at 28.1 ppm and the carbonyl carbon further downfield at 165.0 ppm. When the methodology was extended to the use of the cyclic ketones, 2-cyclohexenone and 2-cyclopentenone (substrates not used in the initial report[6]), no products were observed. However, following the method reported by Kim and co-workers,[59] the reaction of 2,2'-dithiodibenzaldehyde with cyclic ketones was repeated using TMPDA as catalyst in place of DBU and aqueous THF in place of chloroform. Under these conditions the tricyclic derivatives **204a,b** were again obtained[72] (Scheme 49).
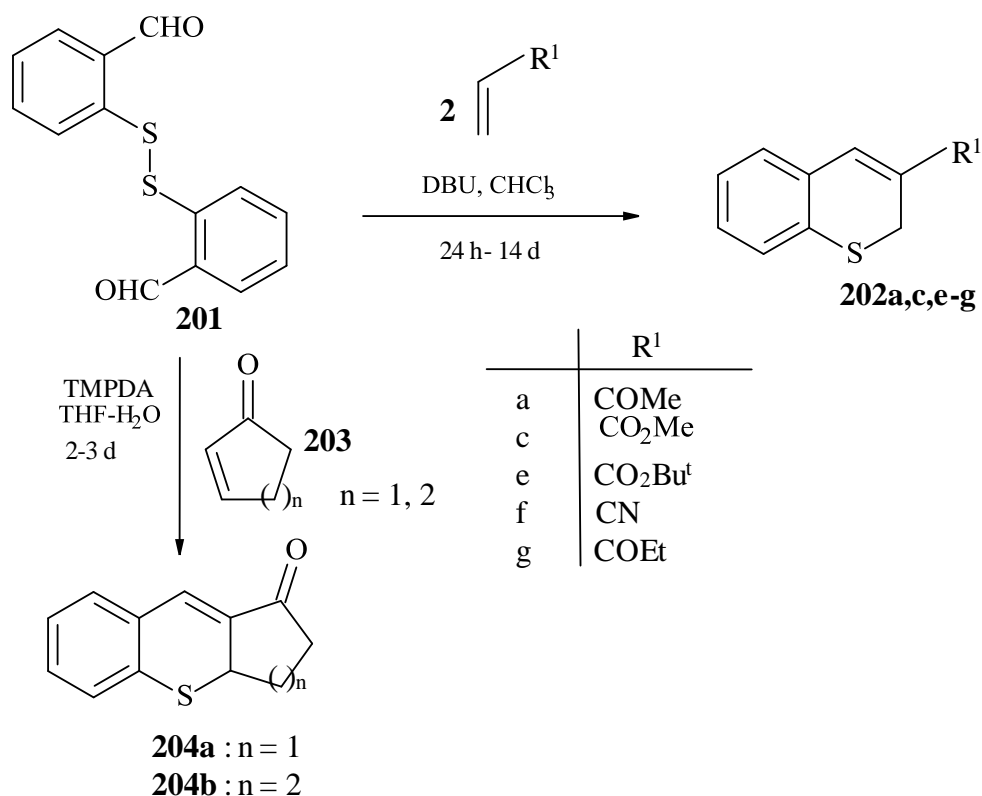
Scheme 49.
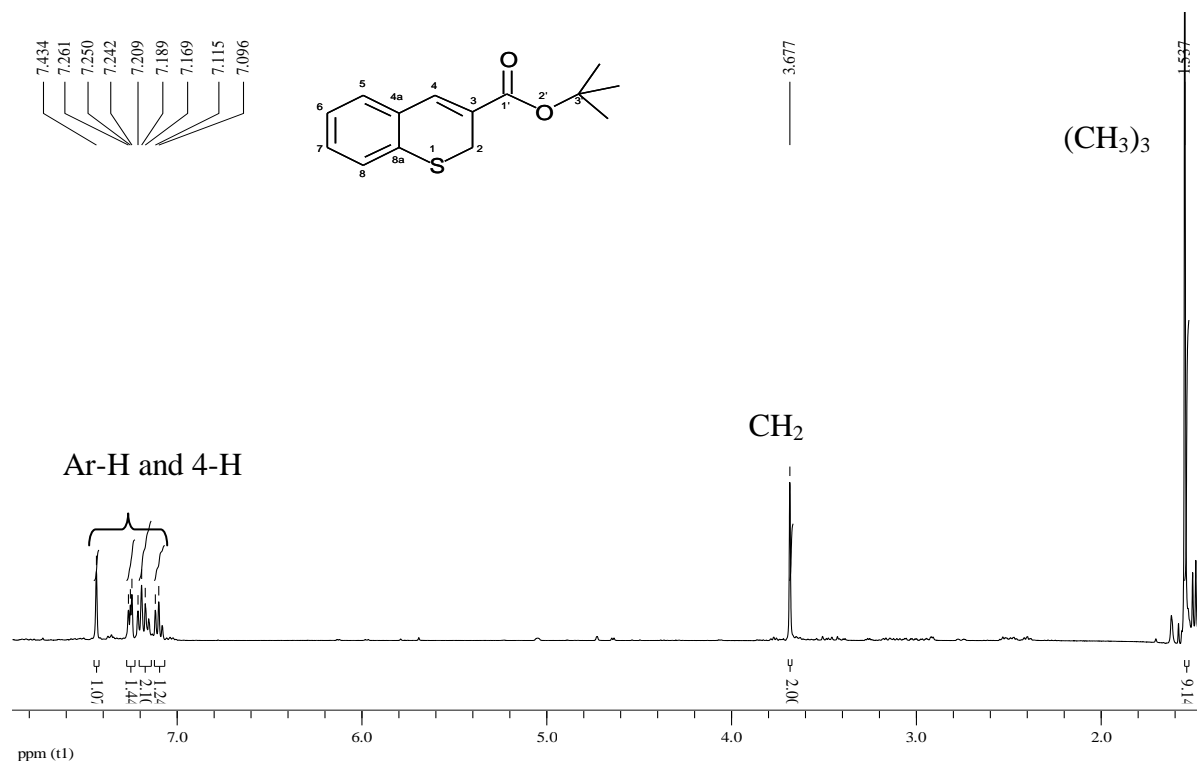
Figure 10. 400 MHz ^{1}H NMR spectrum of *tert*-butyl 2*H*-1-thiochromene-3-carboxylate **202e** in CDCl$_3$.
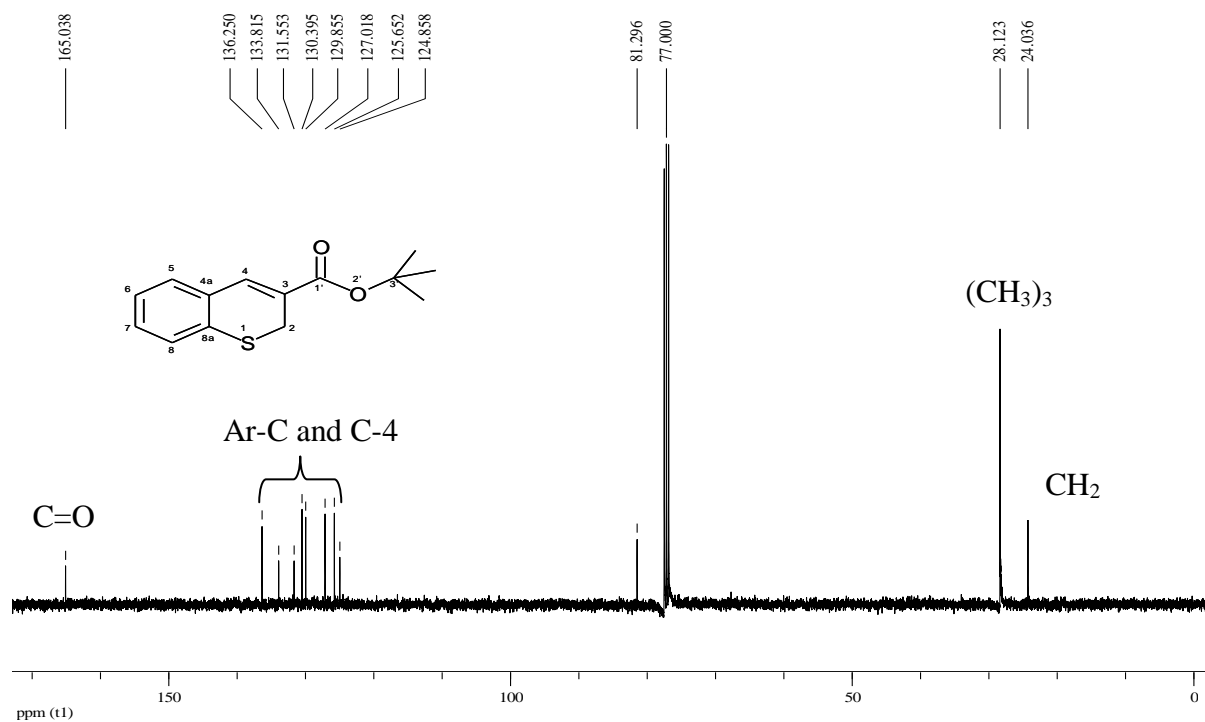
Figure 11. 100 MHz ^{13}C NMR spectrum of *tert*-butyl 2*H*-1-thiochromene-3-carboxylate **202e** in CDCl$_3$.

46

2.1.2 Unusual Catalytic effects in the MBH synthesis of 2*H*-1-benzothiopyrans

In the initial report by Kaye and Nocanda,[6] a mechanism was proposed which accounted for the observed *in situ* reduction of the sulfur-sulfur bond. In this mechanism, outlined in Scheme 50, it was proposed that the bis-MBH adduct **215** would be formed initially, followed by reduction and dehydration to the thiochromenes **202**. Isolation of the thiochromenes **202** suggested the capacity of DBU to reduce the disulfides, prompting further research directed at exploring DBU's capacity to reduce disulfides to mercaptans, and elucidating the mechanism of the overall transformation.
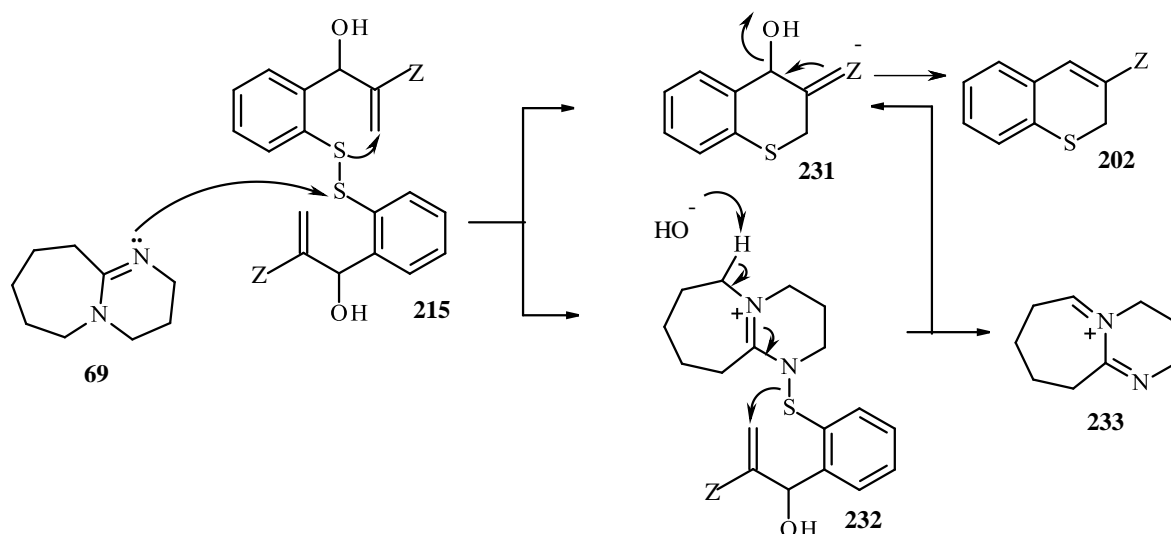
Scheme 50. Putative mechanism to account for the formation of the thiochromenes.[6]

In order to investigate the potential of DBU to serve as a disulfide reducing agent, solutions of six disulfides, including 2,2'-dithiodibenzaldehyde **201**, in chloroform, were treated with DBU in the same molar ratios and under the same reaction conditions used in the previously reported MBH reactions, but without any activated alkene. Three disulfides, which did not contain a carboxylic acid moiety, gave the expected mercaptans, but the carboxylic acid derivatives afforded crystalline products, preliminary NMR analysis of which suggested possible trapping of the putative oxidised DBU cation **233** (Scheme 50). X-ray crystallography of the product obtained using the dicarboxylic acid **237**, however, confirmed the formation of the corresponding DBU-disulfide salts (**242-244**) (Scheme 51). The salts contained a protonated 1,8-diazabicyclo(5.4.0)undecene cation and the disulfide mono-carboxylate anion (Figure 12). Figures 13 and 14 show the ^{1}H- and ^{13}C NMR spectra of the mono-DBU-disulfide salt **243**.
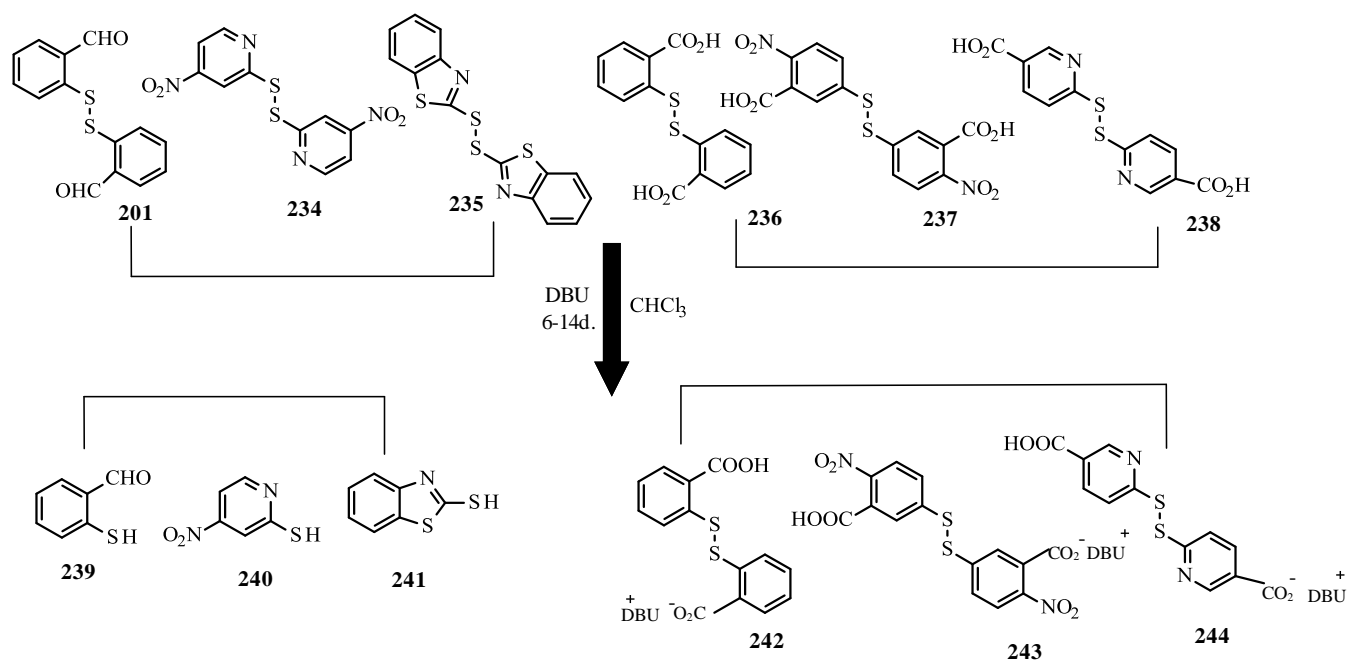
Scheme 51.
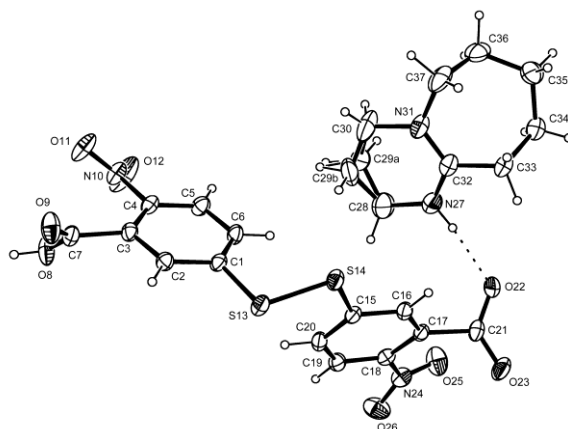
Figure 12. X-ray crystal structure of the mono-DBU-disulfide salt **243** showing the crystallographic numbering and thermal ellipsoids drawn at the 50% probability level.
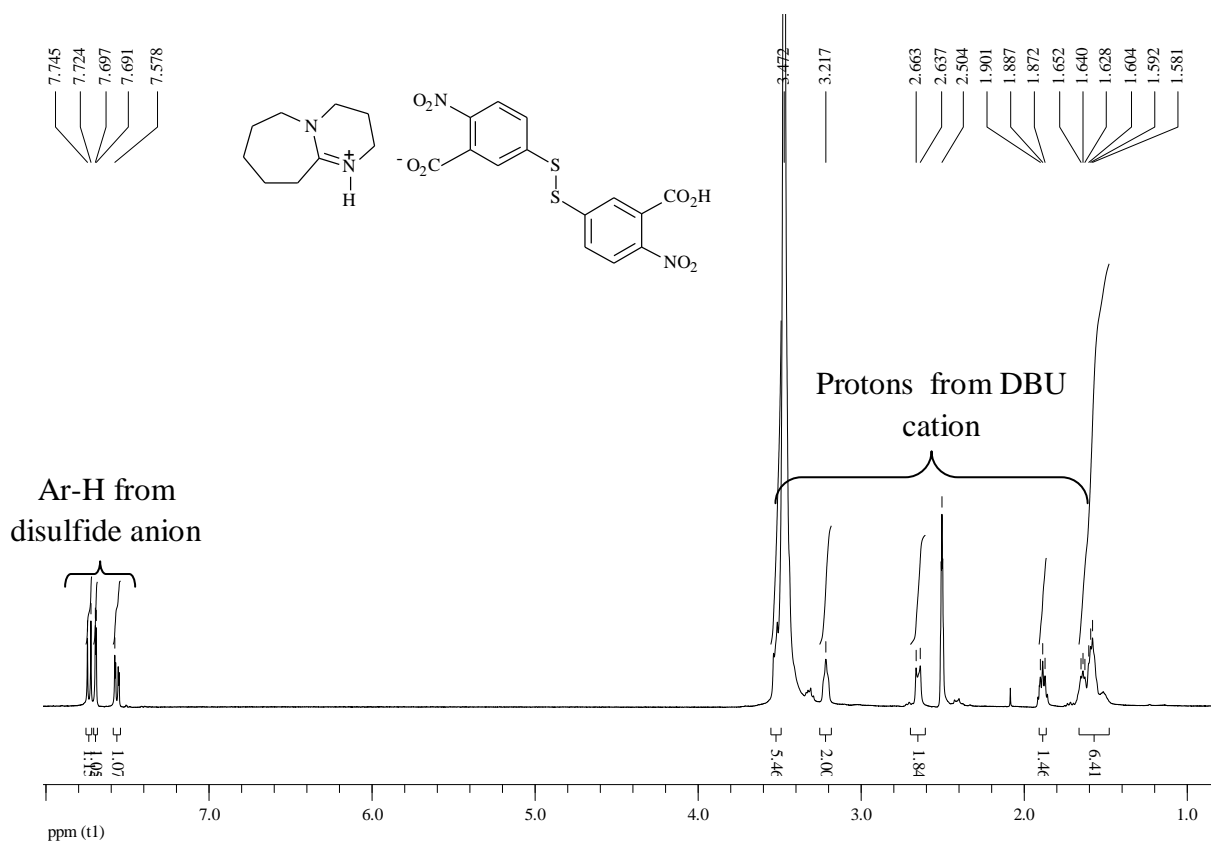
Figure 13. 400 MHz ^{1}H NMR spectrum of the mono-DBU-disulfide salt **243** in DMSO-d_6.
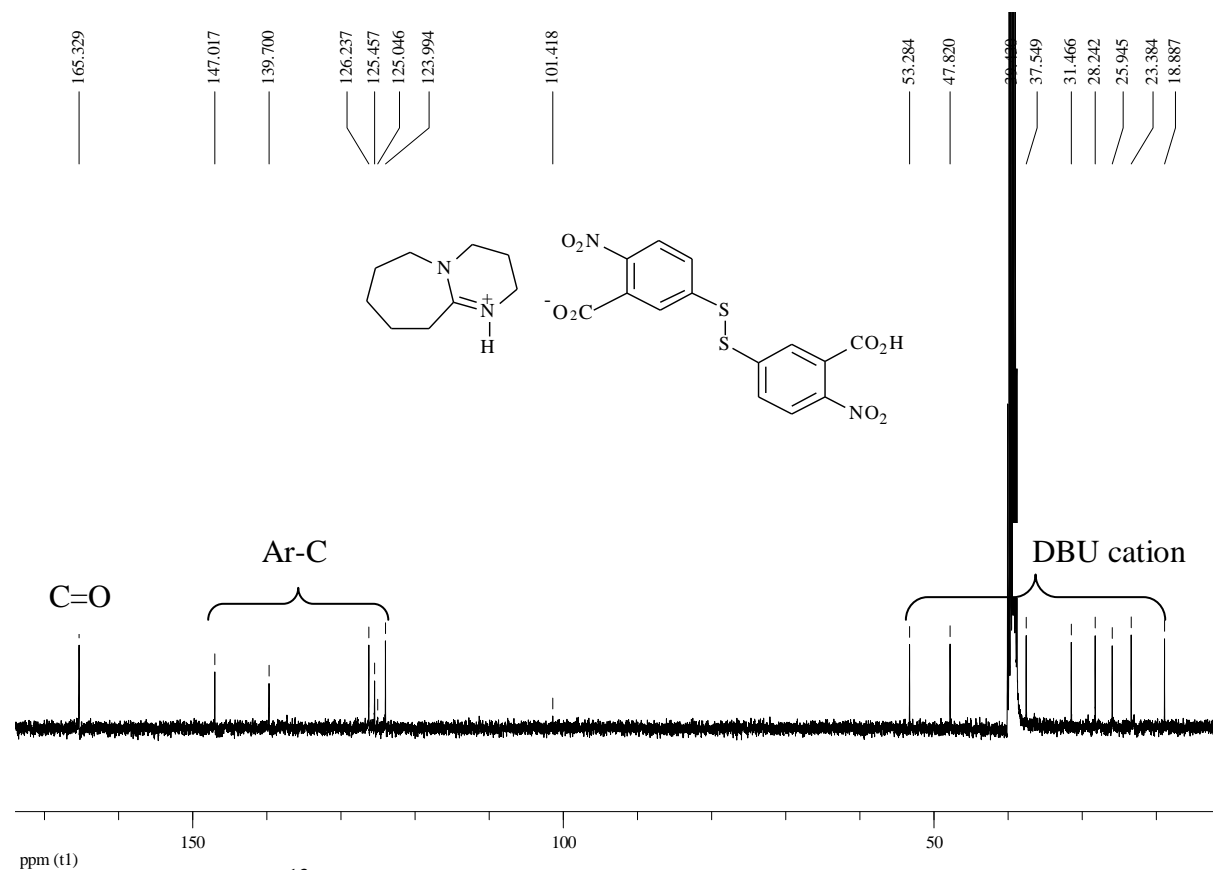
Figure 14. 100 MHz ^{13}C NMR spectrum of the mono-DBU-disulfide salt **243** in DMSO-d_6.

Figure 15 shows stacked plots reflecting the progress of the reaction between 2,2'-dithiodibenzaldehyde **201** and DBU **69** in CHCl$_3$. Quite evident in the spectra is the emergence of a new aldehydic signal at 10.14 ppm and a relative reduction in the intensity of the signal at 10.20 ppm corresponding to the disulfide substrate **201**. The signal at 10.14 ppm corresponds to the reduced product, 2-mercaptobenzaldehyde **239**, ^{1}H NMR analysis of which corresponds well with literature data.[137] After 9 days, there appeared to be no change in the intensities of the aldehyde signals in either the starting material or product.
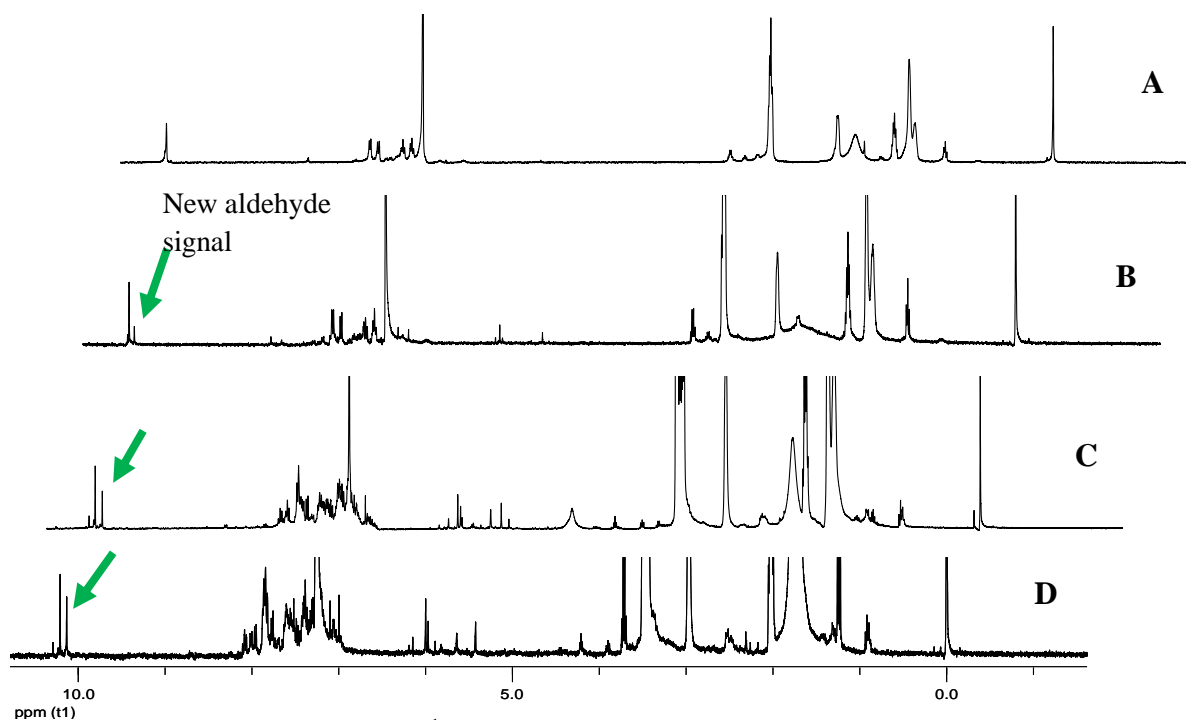
Figure 15. 400 MHz Stacked ^{1}H NMR spectra reflecting the progress of the reaction between 2,2'-dithiodibenzaldehyde and DBU in CHCl$_3$. **A:** Spectrum after 1 hour. **B:** Spectrum after 22 hours. **C:** Spectrum after 7 days. **D:** Spectrum after 9 days.

Formation of the DBU-disulfide salts **242-244** prompted synthesis of the corresponding methyl esters **245-247**, which were then treated with DBU in CHCl$_3$ as before, and the corresponding mercaptans **248-250** were isolated in low to moderate yields (30-53%) after long reaction times (6-14 days) (Scheme 52). Figures 16 and 17 show the ^{1}H NMR spectra of the methyl ester **245** and the reduced product, the mercaptan **248**, respectively. The methyl protons resonate at 3.98 ppm in both compounds while the mercaptan signal resonates at 3.84 ppm. While the low yields and long reaction times raised questions concerning the viability of DBU as an efficient disulfide reducing agent, its capacity to cleave disulfides had been clearly demonstrated.
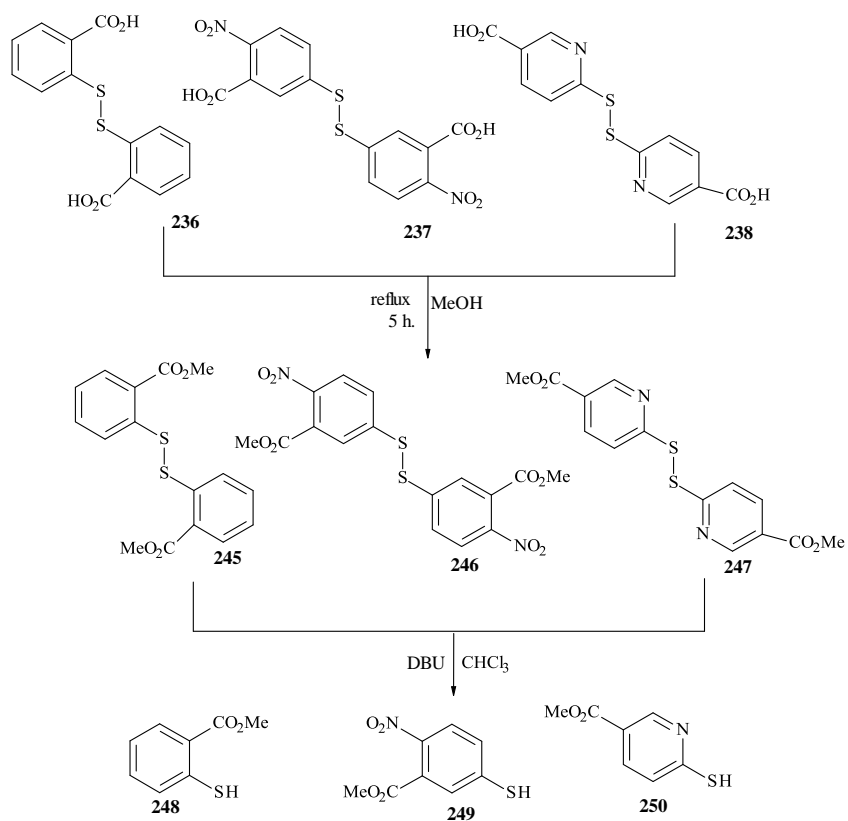
Scheme 52.
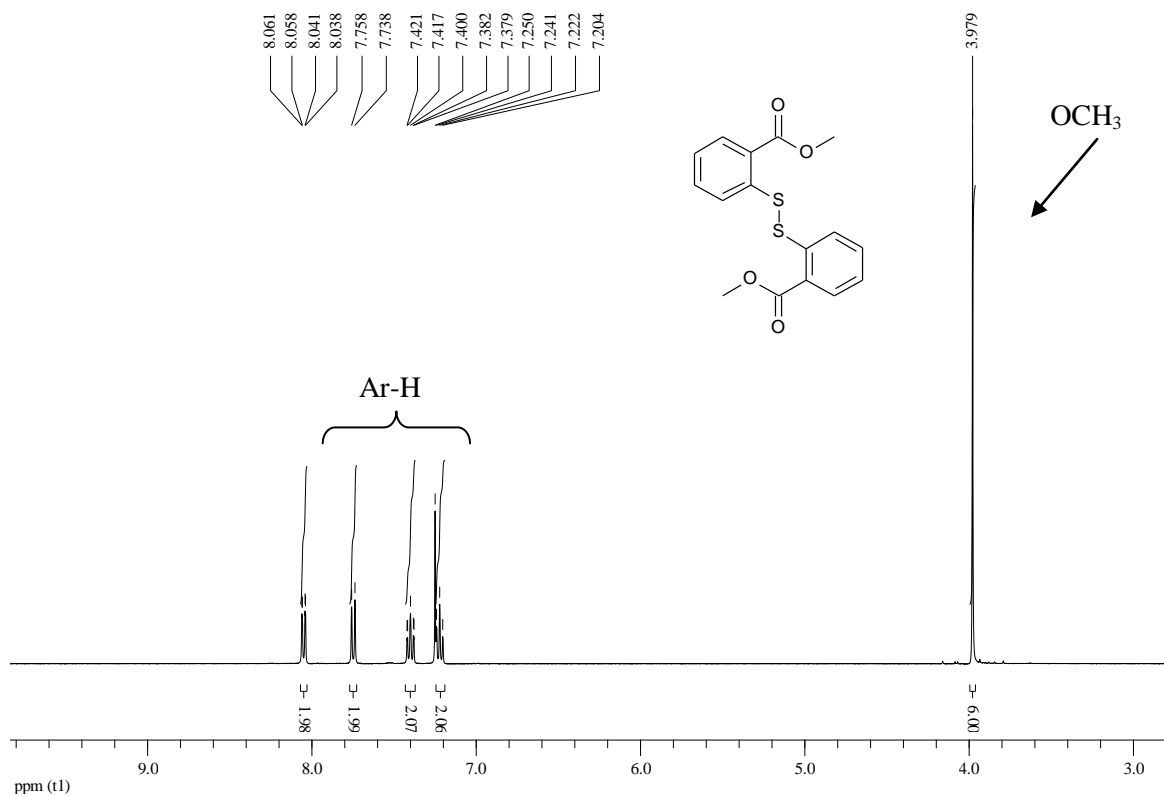
Figure 16. 400 MHz ^{1}H NMR spectrum of compound **245** in CDCl$_3$.
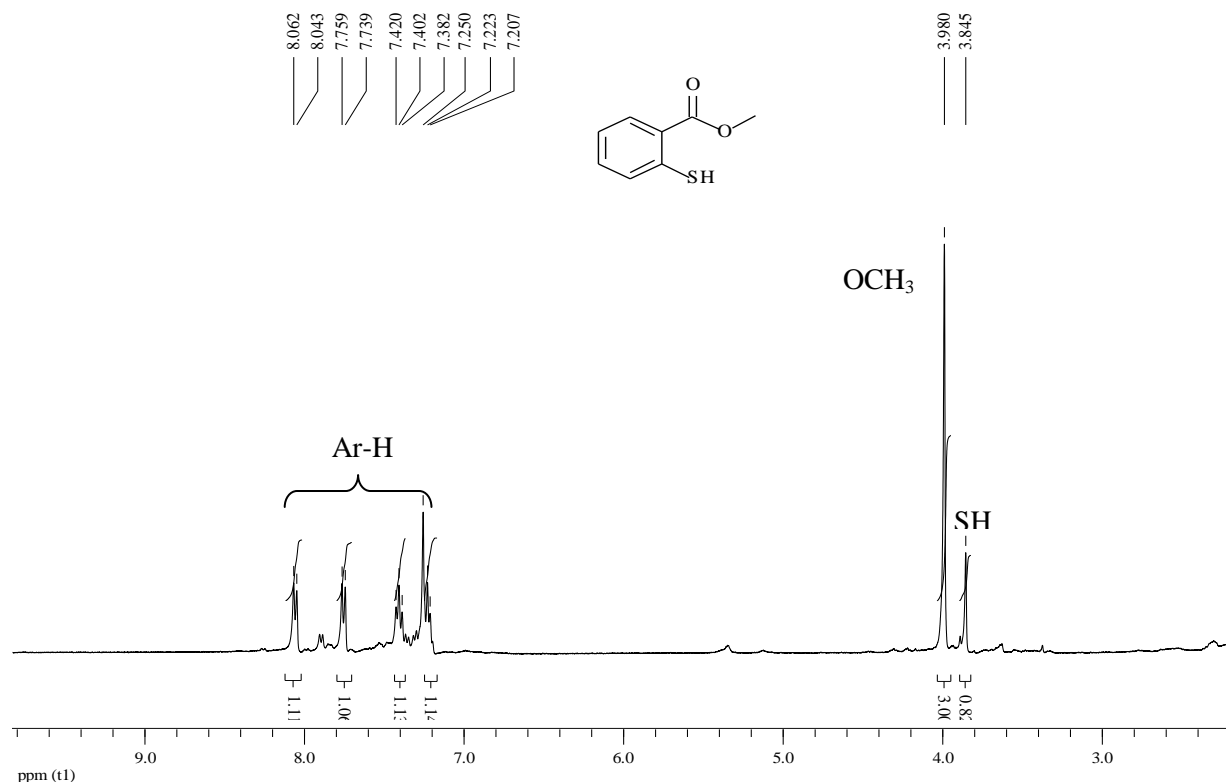
Figure 17. 400 MHz ^{1}H NMR spectrum of compound **248** in CDCl$_3$.

2.1.2.1 *Use of triphenylphosphine as catalyst in the MBH synthesis of thiochromenes*

Treatment of aromatic disulfides with triphenylphosphine (Ph$_3$P) in aqueous MeOH has been shown by Humphrey and Hawkins[138] to afford the corresponding mercaptans, while Morita's[1] use of Ph$_3$P pre-dates Baylis and Hillman's[2] patented use of tertiary amine catalysts. Following Humphrey and Hawkins' approach,[138] we sought to explore the MBH reaction of 2,2'-dithiodibenzaldehyde with MVK, using Ph$_3$P as an alternative catalyst to DBU. Two exploratory experiments were run, using CHCl$_3$ or aqueous MeOH as the solvent in each case. Both reactions were much slower than the DBU catalysed reaction in CHCl$_3$. Aqueous work-up of the reaction conducted in aqueous MeOH gave a yellow, foul smelling oil, typical of many sulfur containing compounds, ^{1}H NMR analysis of which showed a mixture of products which proved to be intractable. The reaction in CHCl$_3$, however, gave five products in low yields following flash chromatography, *viz.*, 3-acetyl-2*H*-1-benzothiopyran **202a**, 2-mercaptobenzaldehyde **239** and, as a mixture subsequently separated by HPLC, the hemi-thioketal **252**, the diastereomeric 4-hydroxythiochromans **217a** and the MVK dimer **251** (Scheme 53). Neither of the diastereomers **217a** nor the hemi-thioketal **252**, or their substituted analogues, had been detected previously in our

investigations. The MVK dimer **251** has been reported by Basavaiah[139] in reactions involving DABCO and by Molefe[79] in MBH reactions with 3-hydroxyquinuclidine (3-HQ) and DABCO. To the best of our knowledge, there have been no reports of the formation of the MVK dimer in reactions involving Ph_3P. A mechanism for the formation of the dimer **251** is illustrated in Scheme 54. The reaction is initiated by nucleophilic attack of Ph_3P on the vinylic carbon of MVK to form a zwitterion **of type 37**, which then reacts with a second molecule of MVK forming the dimer.
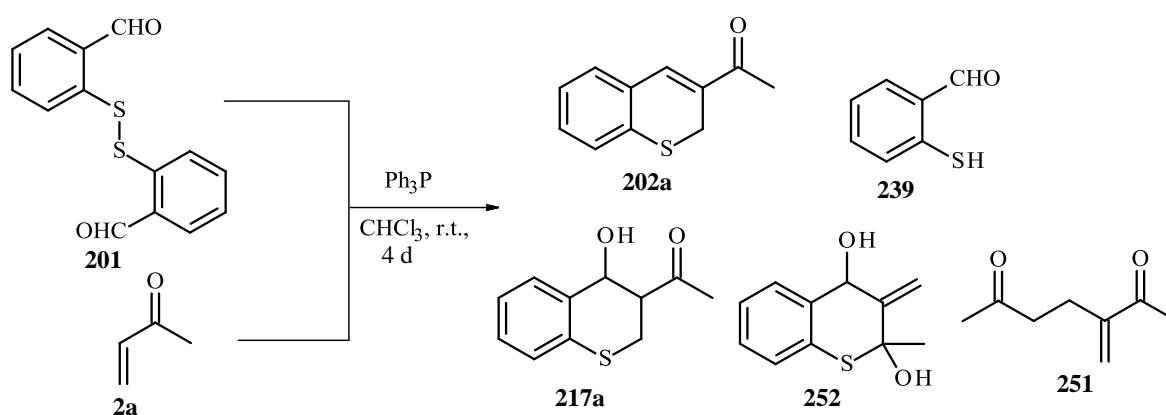
Scheme 53.
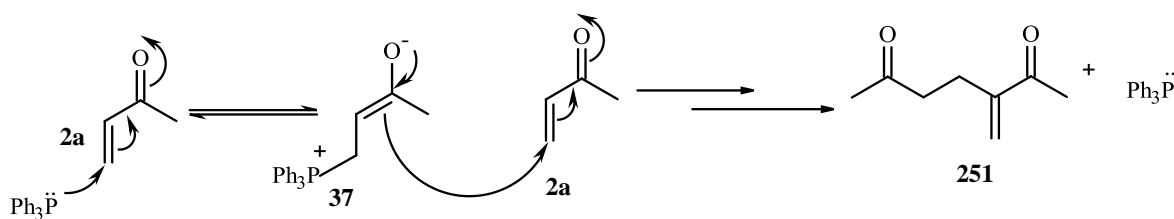
Scheme 54. Mechanism showing formation of the MVK dimer **251**.

Figure 18 (**1**) shows the ^{1}H NMR spectrum of the major diastereomer of 4-hydroxythiochroman (**217a₁**). The signal corresponding to the 4-H proton appears downfield at 5.12 ppm. One of the 2-methylene protons resonates at 3.40 ppm as a triplet, while the other 2-methylene proton signal overlaps with the 3-methine proton signal, resulting in a multiplet at *ca.* 3.0 ppm. The hydroxyl proton appears as a very broad signal at 2.72 ppm. Comparison of the ^{1}H NMR spectra of the two diastereomers **217a₁** and **217a₂** [Figure 18 (**1**)

and (**2**)], shows two significant differences:- i) the signals for both 2-methylene protons overlap with the 3-methine proton signal in the minor diastereomer, while the signal for only one of the 2-methylene protons overlaps with the 3-methine signal in the major diastereomer; and ii) the 4-methine proton in the major diastereomer resonates as a singlet, but as a doublet in the spectrum of the minor diastereomer. In the ^{13}C NMR spectrum of the major diastereomer **217a₁** (Figure 19), all of the expected 11 signals are present, with the methylene carbon (C-2) resonating at 21.9 ppm and the carbonyl carbon resonating downfield at 208.6 ppm. The DEPT 135 spectrum (Figure 20) confirms assignment of the methylene carbon at 21.9 ppm, the methyl carbon at 28.5 ppm and the C-3 and C-4 methine carbons at 51.8 and 67.3 ppm, respectively. Coupling of the 2-methylene protons with each other, and with the 3-methine proton is evident in the COSY spectrum (Figure 21). The HSQC spectrum, which is shown in Figure 22 was used, together with the HMBC spectrum to confirm the signal assignments.
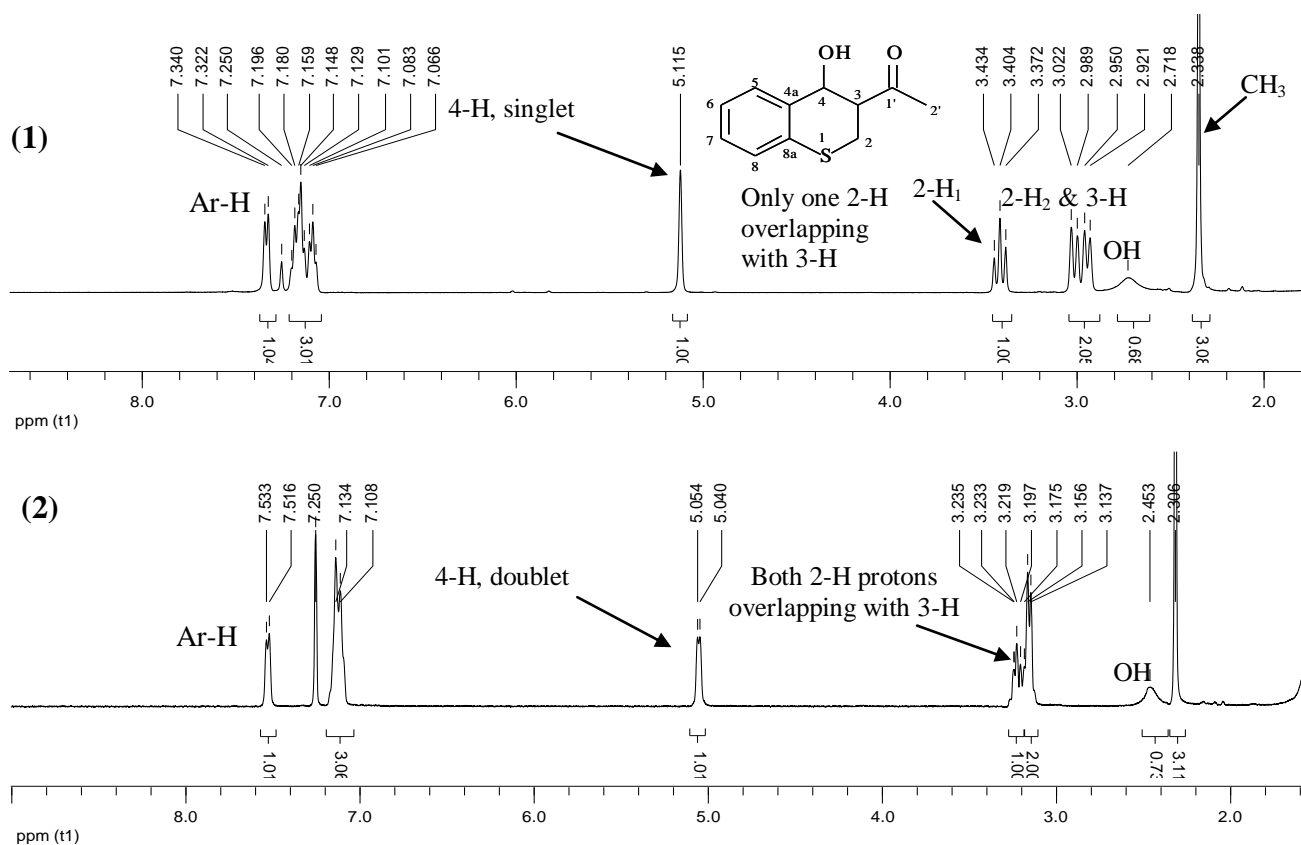
Figure 18. 400 MHz Stacked ^{1}H NMR spectra of the two hydroxythiochroman diastereomers, (**1**) **217a₁** and (**2**) **217a₂** in CDCl$_3$.
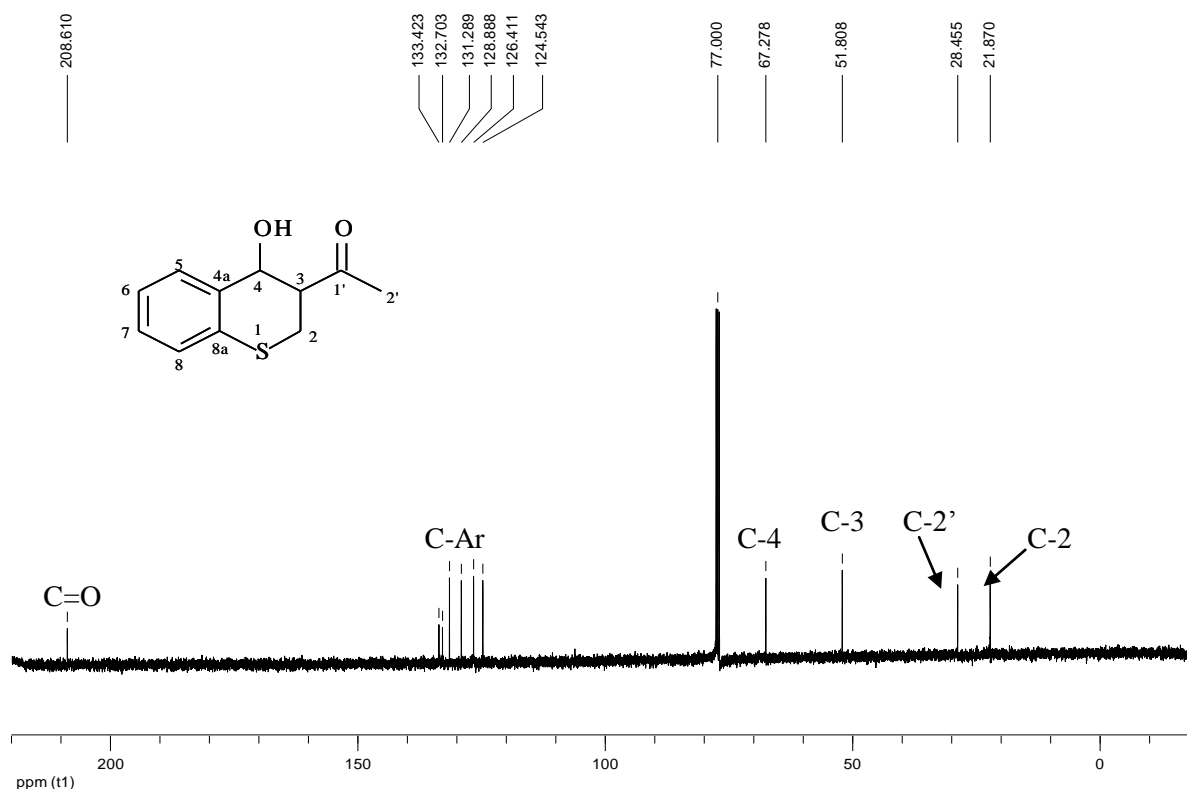
Figure 19. 100 MHz ^{13}C NMR spectrum of compound **217a$_1$** in CDCl$_3$.
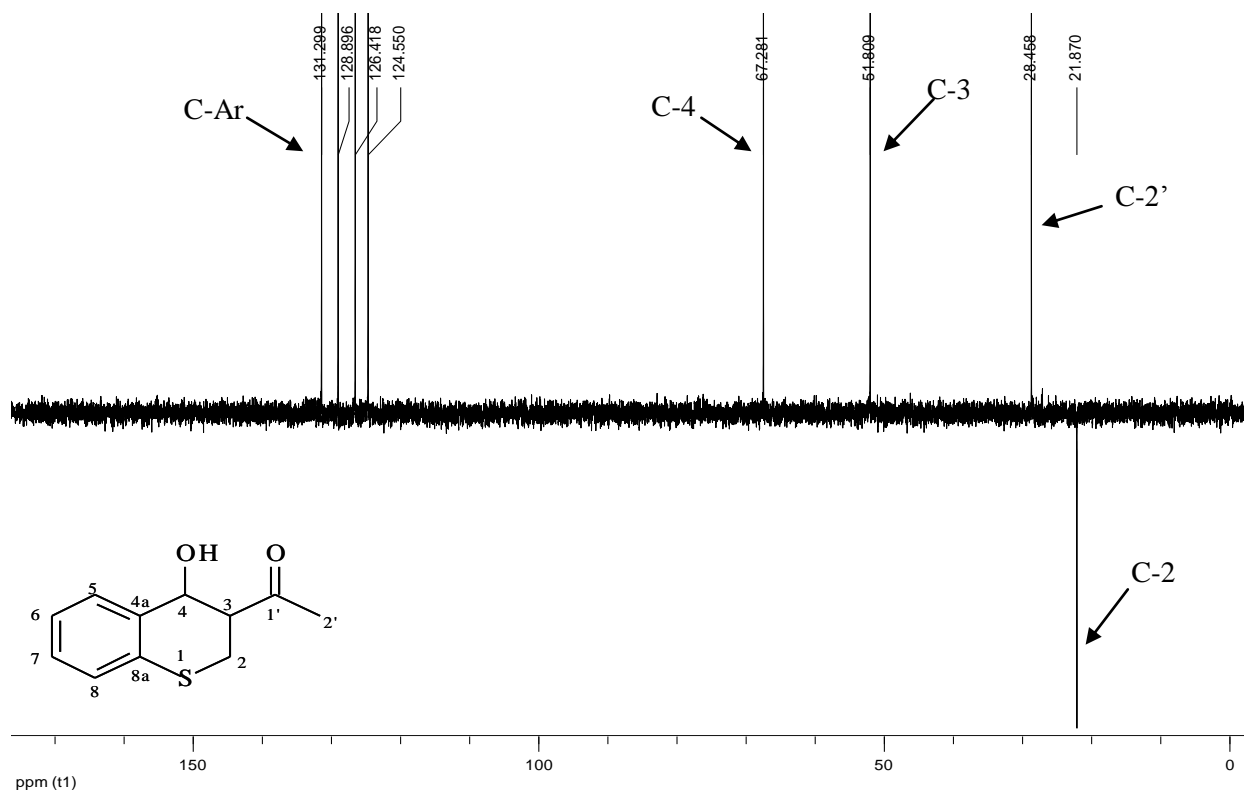
Figure 20. DEPT 135 spectrum of compound **217a$_1$** in CDCl$_3$.
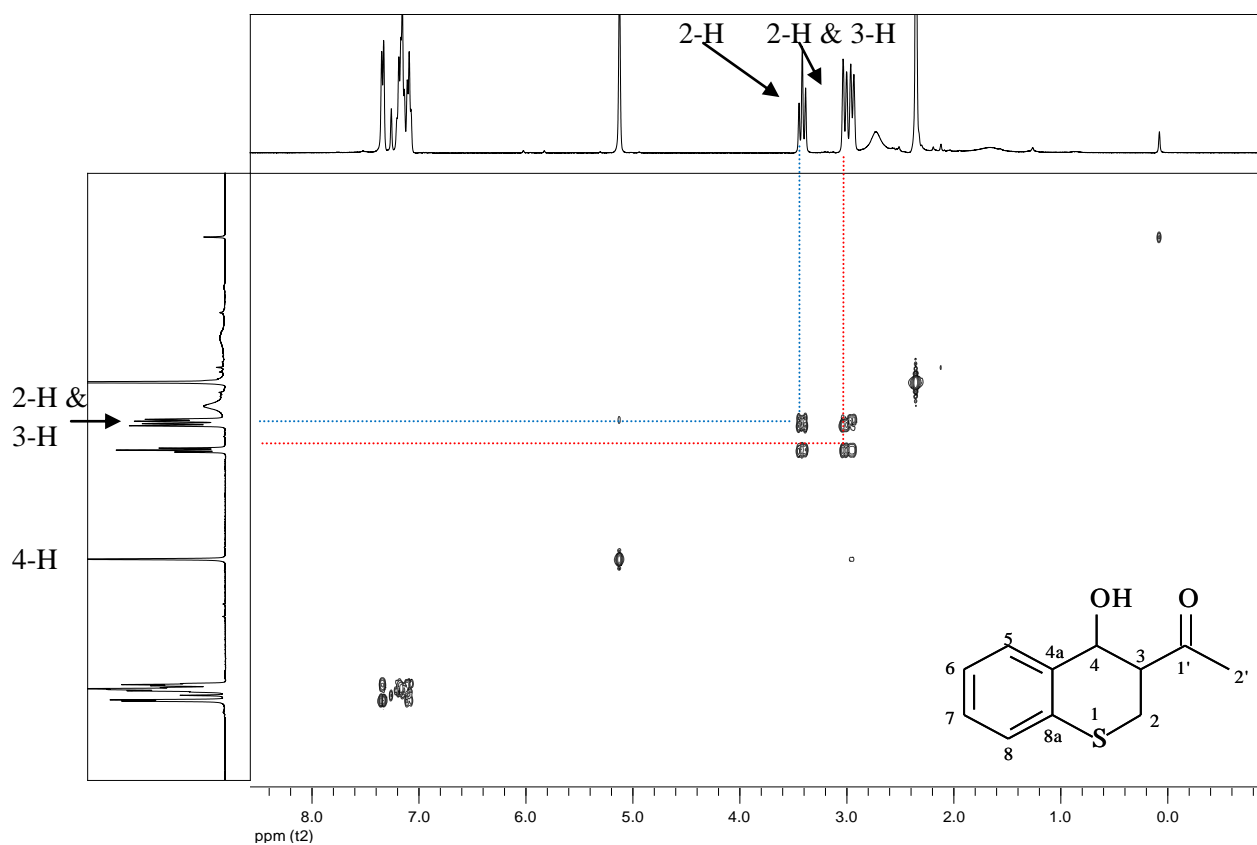
Figure 21. COSY NMR spectrum of compound **217a₁** in CDCl₃.
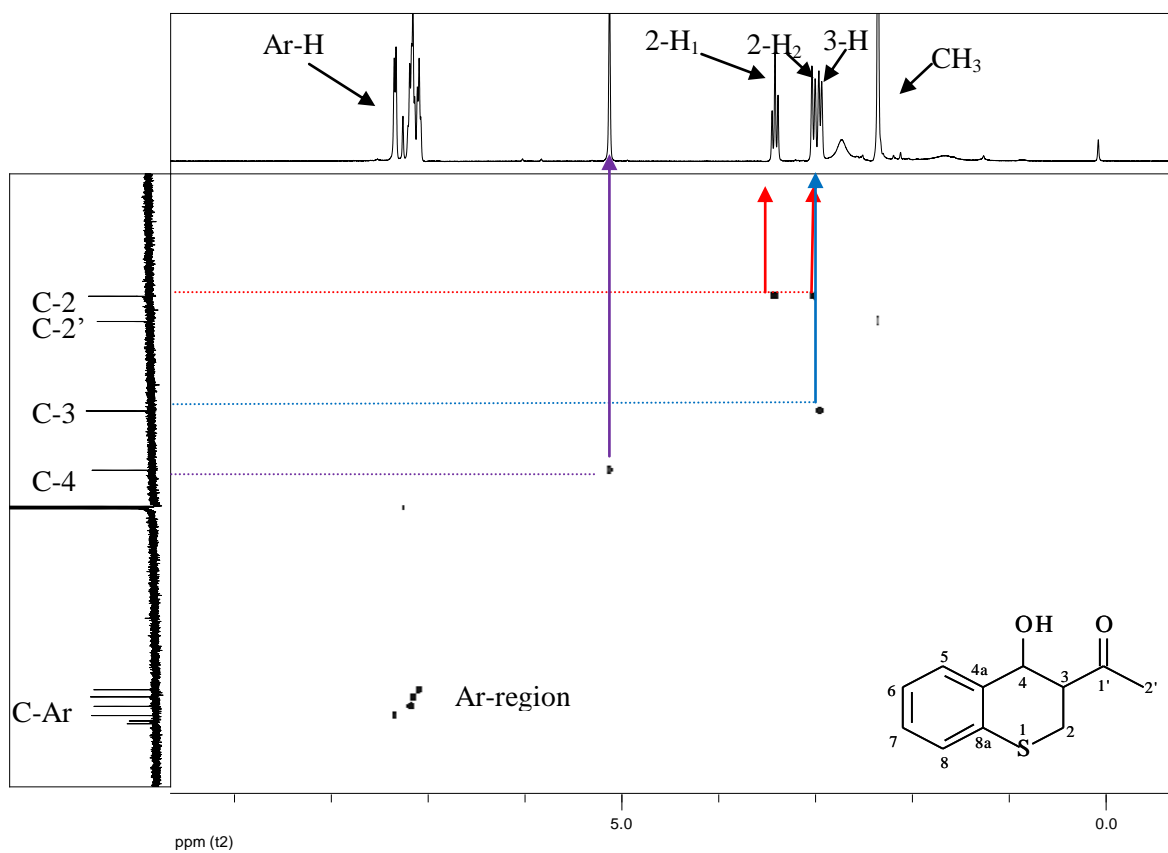
Figure 22. HSQC spectrum of compound **217a₁** in CDCl₃.

Initial attempts to assign relative configurations at the two stereogenic centers, C-3 and C-4, were made using NMR NOESY experiments of both diastereomers **217a$_1$** and **217a$_2$**. This however, failed to give any conclusive results and attention was then given to exploring the $^3J_{H,H}$ coupling constants and dihedral angles (Φ), between the 3-H and 4-H methine protons in both diastereomers. The Karplus equations[140] describe the relationship between the dihedral angle and the vicinal coupling constant ^3J. Knowledge of the 3-H-C-C-4-H dihedral angle in the diastereomers should provide useful information for assigning the relative configurations at the chiral centres. The structures of the two diastereomers **217a$_1$** and **217a$_2$** were subjected to geometry optimisation using Gaussian 03 and the hybrid density functional B3LYP, with the 6-31G(d) basis set. The optimised structures of the major (3*S**,4*S**) and minor (3*S**, 4*R**) diastereomers are shown in Figures 23 and 24 respectively. The dihedral angle between the 3-H and 4-H methine protons in the major diastereomer **217a$_1$** was found to be 62°, consistent with minimal coupling between the two protons and, hence, the 4-H proton is observed as a singlet in the ^{1}H NMR spectrum [Figure 18 (**1**)]. The dihedral angle in the minor diastereomer **217a$_2$** was found to be 179°, consistent with strong coupling between the 3-H and 4-H methine protons and, hence, the 4-H methine appears as a doublet in the ^{1}H NMR spectrum [Figure 18 (**2**)]. The relative configurations at the two stereogenic centres as shown in Figures 23 and 24 were assigned on this basis.
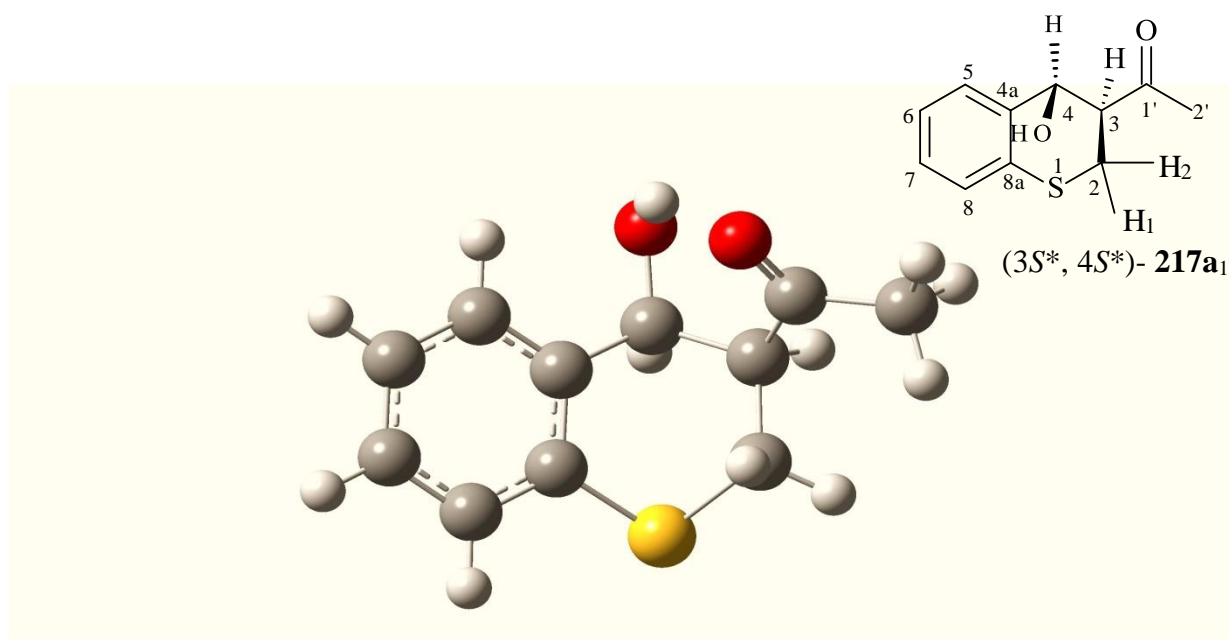
Figure 23. B3LYP/6-31G(d) energy-minimised structure of the (3*S**,4*S**)-diastereomer of compound **217a$_1$**,
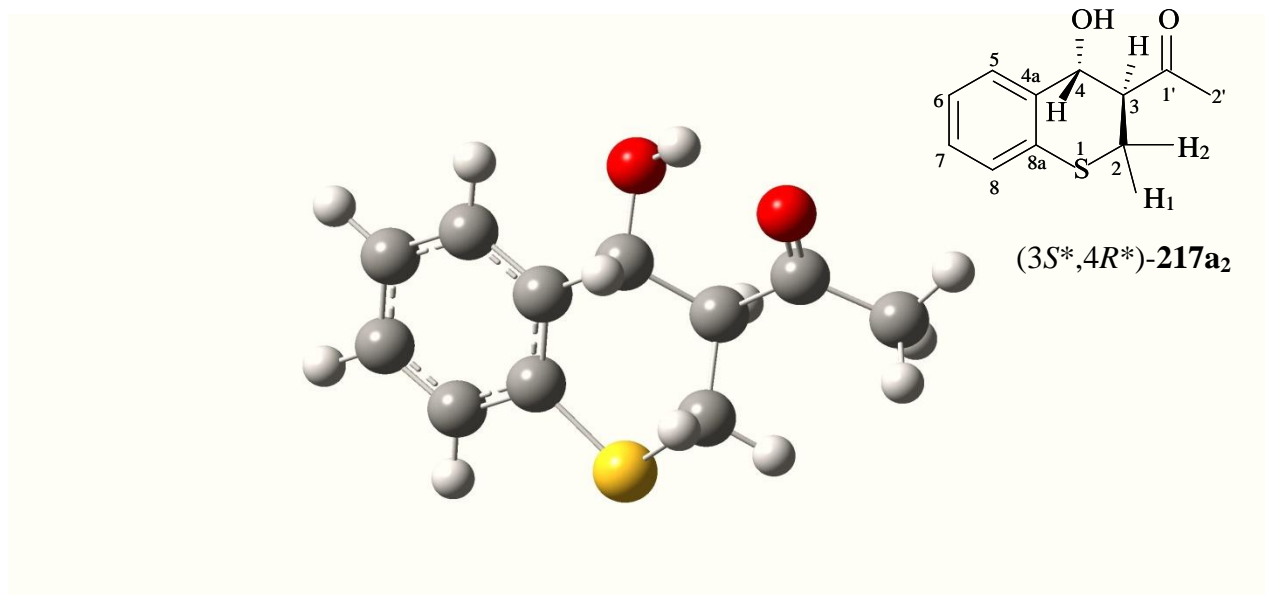
Figure 24. B3LYP/6-31G(d) energy-minimised structure of the (3*S**,4*R**)-diastereomer of compound **217a₂**,

Figure 25 shows the ^{1}H NMR spectrum of the diol **252**. Initially it was thought that this might be the MBH adduct, but the splitting of the vinylic protons indicated otherwise. The vinylic protons in MBH adducts normally appear as singlets, but doublets were observed in this case with a coupling constant $J = 13.46$ Hz. Careful examination of the spectroscopic and HRMS data confirmed that this was, in fact, the hemi-thioketal **252**. This observation prompted us to look at other possible products that could result from this reaction. Cyclisation of the MBH adduct could follow either conjugate addition/elimination to give the thiochromenes and 4-hydroxythiochromans, or direct nucleophilic addition, which would afford the hemi-thioketal (Scheme 55). However, in this particular MBH reaction cyclisation appeared to favour the conjugate addition pathway, hence isolation of the hemi-thioketal **252** in very low yield (7%). Isolation of 2-mercaptobenzaldehyde **239**, 4-hydroxythiochroman **217** and the hemi-thioketal **252** is consistent with the formation of a common intermediate **216** which may cyclise *via* either of the pathways illustrated in Scheme 55.
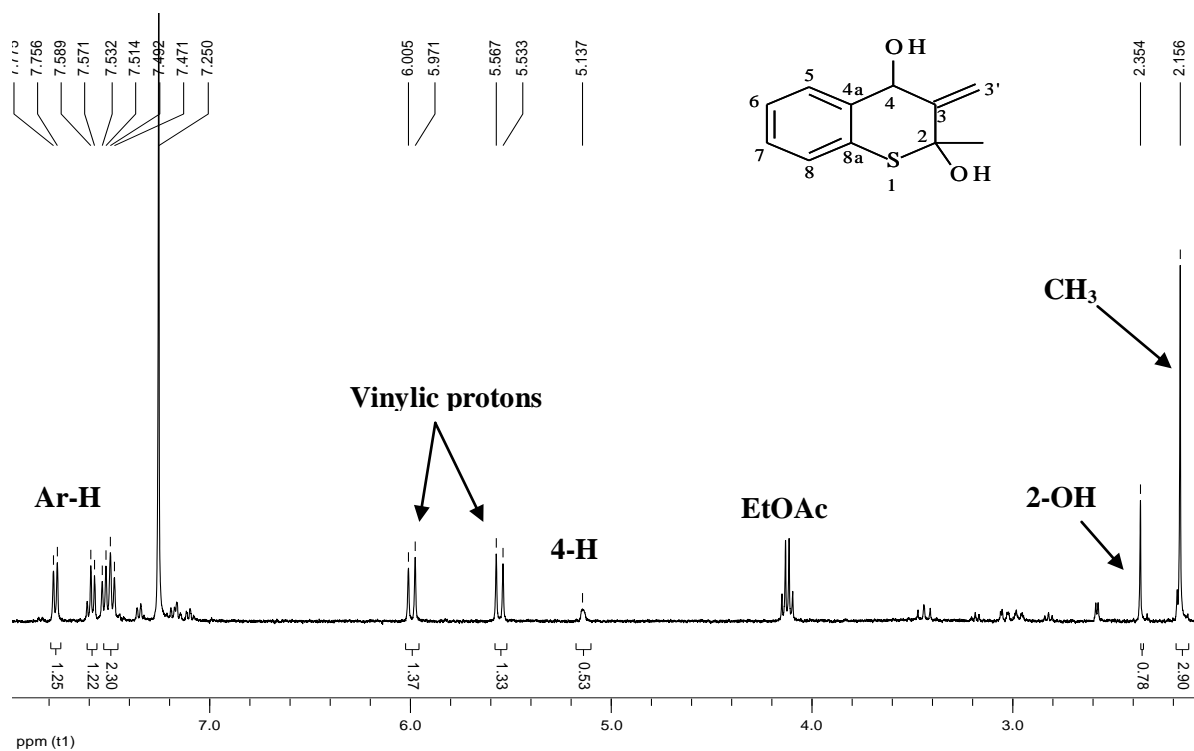
Figure 25. 400 MHz ^{1}H NMR spectrum of compound **252** in CDCl$_3$.
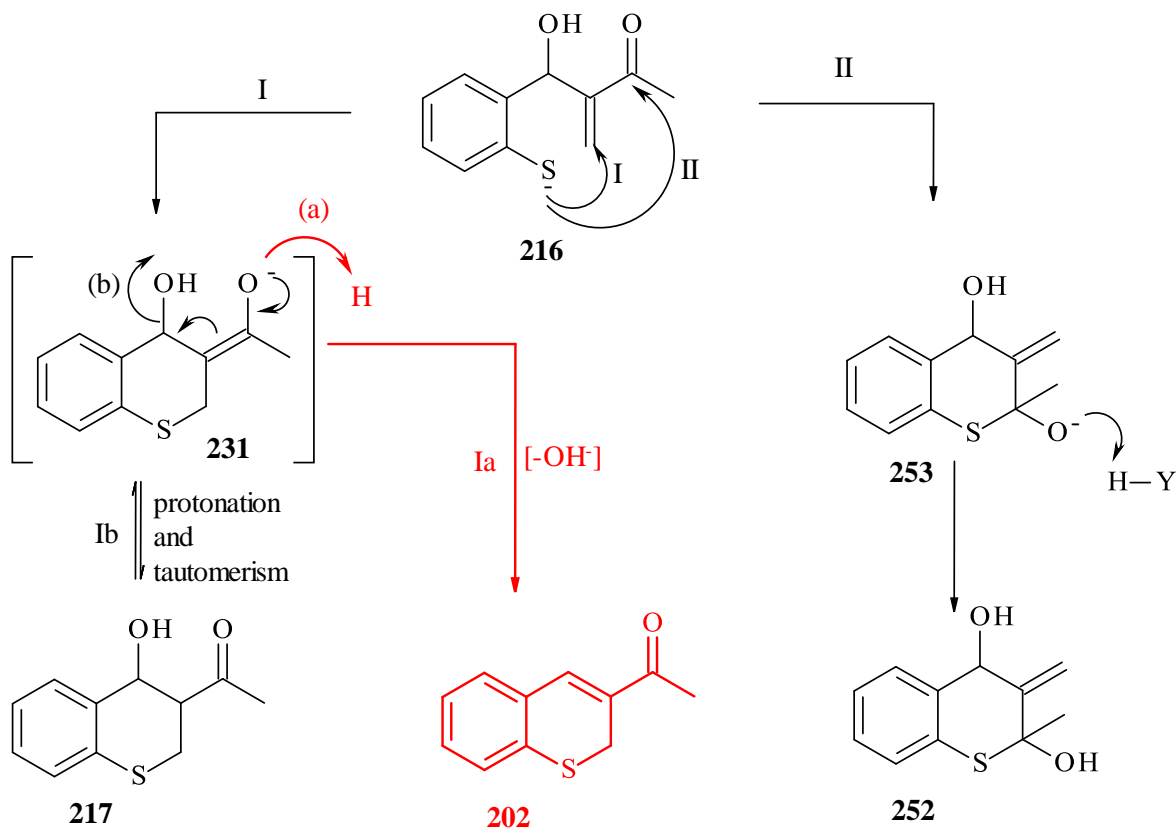
Scheme 55. Possible ways of cyclisation of the MBH adduct.

2.1.2.2 Use of the DBU-Ph₃P dual-catalyst system

The reaction between 2,2'-dithiodibenzaldehyde **201** and MVK **2a** was repeated using a combination of DBU and Ph₃P as a dual-catalyst system. The reaction afforded 3-acetyl-2*H*-1-benzothiopyran **202a** in 67% yield within two hours! Previously, the reaction using DBU as the sole catalyst had given the thiochromene in 59% yield after 24 hours. The dual-catalyst system (DBU/Ph₃P) was then used in reactions of 2,2'-dithiodibenzaldehyde with several other activated alkenes (Scheme 56), *viz.*, methyl acrylate, *tert*-butyl acrylate, acrylonitrile and EVK. From the results summarised in Table 1, it is apparent that the overall yields, all in excess of 60%, are significantly higher than those obtained using DBU alone. The reactions involving MVK, EVK and acrylonitrile gave only the corresponding thiochromene derivatives, whereas the acrylate esters gave the thiochromenes **202** together with their 4-hydroxy derivatives **217**.

	Z
a	COMe
c	CO₂Me
e	CO₂Buᵗ
f	CN
g	COEt
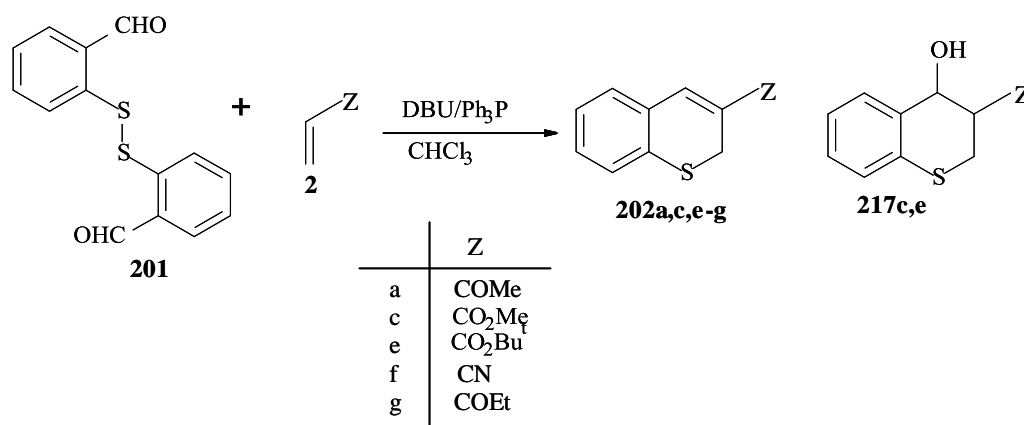
Scheme 56.

Table 1. Comparative yields of Morita-Baylis-Hillman products using DBU and DBU/Ph₃P in CHCl₃ (Scheme 56).

Activated Alkene	Product	%Yield using DBU [a]	%Yield using DBU/Ph₃P	Time/h [e]
MVK	**202a**	59	67	1.5-2
EVK	**202g**	67	71	1.5-2
Acrylonitrile	**202f**	52	60	2
Methyl acrylate	**202c**	40	34 [c] ⎤ 80[b]	2-3
	217c		46 [d] ⎦	2-3
t-Butyl acrylate	**202e**	-	35 [c] ⎤ 80[b]	2-3
	217e		45 [d] ⎦	2-3

[a] Yield of thiochromene after *ca.* 2 weeks- data as cited in reference 6. [b] Overall yield. [c] Yield of thiochromene. [d] Yield of 4-hydroxy derivative. [e] For dual-catalyst system.

2.1.3 Kinetic Studies of the Morita-Baylis-Hillman synthesis of 2*H*-1-benzothiopyrans

The progress of the reactions between 2,2'-dithiodibenzaldehyde **201** and MVK or methyl acrylate, catalysed by DBU or Ph₃P to form the corresponding thiochromenes **202** and 4-hydroxythiochromans **217**, were monitored using the ^{1}H NMR integral ratios of selected structure specific-signals. A computer programme developed by Lobb[141] was used to generate the integral data as text. In all cases, 1,3,5-trimethoxybenzene (TMB) was used as the internal standard. All kinetic experiments were carried out in CDCl₃, which was purified prior to use according to a literature procedure,[142] in which CDCl₃ is passed through neutral alumina and crushed 4Å molecular sieves under N₂ to remove any hydrochloric acid that may have formed. All kinetic runs were carried out in 1 mL graduated NMR tubes.

2.1.3.1 Reaction using DBU as sole catalyst
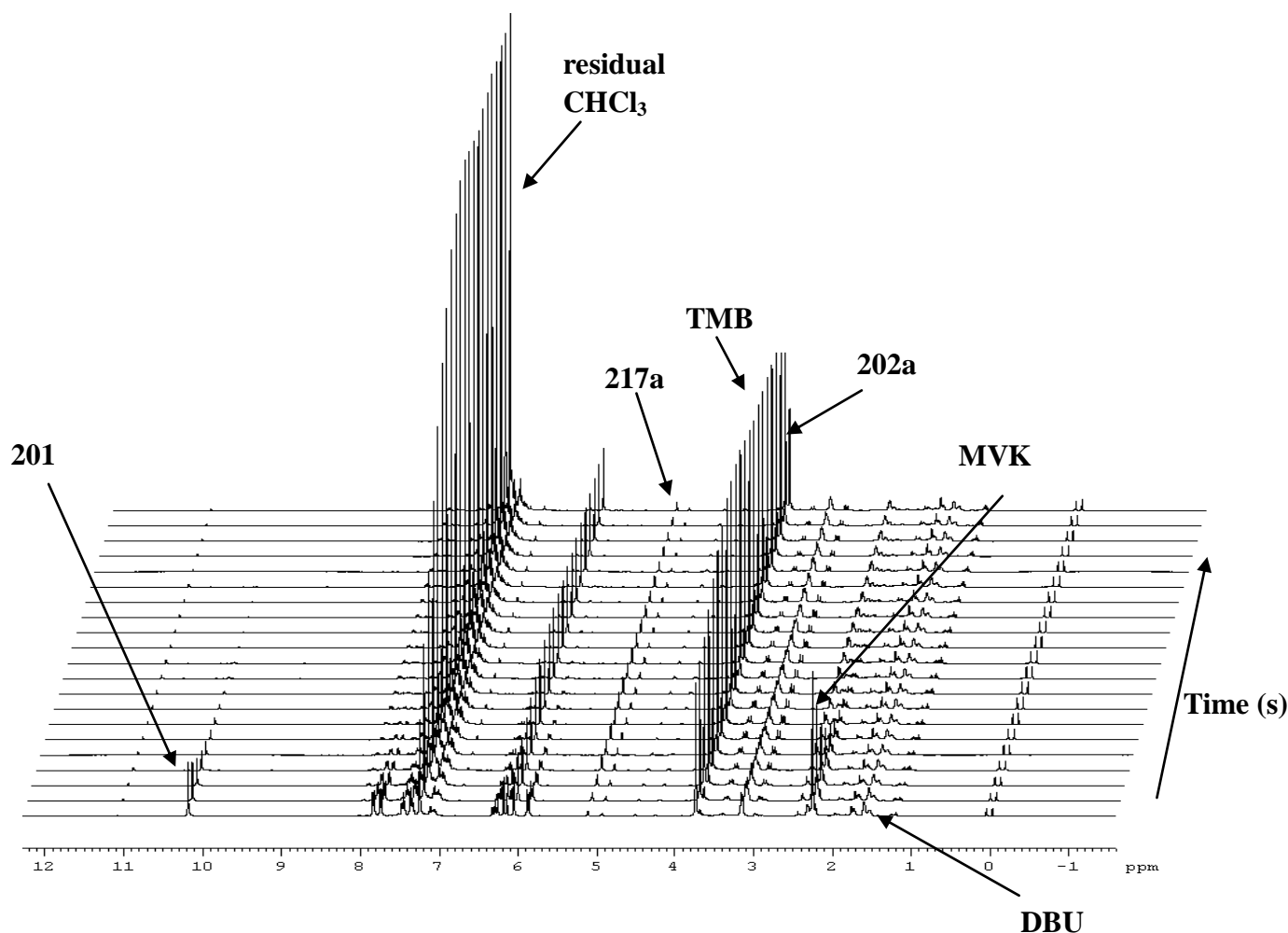
Figure 26. Stacked plots (time interval: 600 s) of ^{1}H NMR spectra showing the decay and evolution of signals during the DBU-catalysed reaction of 2,2'-dithiodibenzaldehyde **201** and MVK **2a** in CDCl₃ at 24 °C.

Figure 26 shows a stacked plot of the DBU-catalysed reaction of 2,2'-dithiodibenzaldehyde **201** and MVK in $CDCl_3$ at 24 ^{o}C. At *ca.* 5.0 ppm there are 2 signals, which are not due to the reactants and which appear to increase in intensity and then decrease as the reaction progresses, indicating the possibility of the formation of one or more intermediates. These signals, in fact, correspond to the 4-methine protons of the diastereomeric 4-hydroxy thiochromans **217a₁** and **217a₂** (Scheme 53) which we have isolated; their signals are evident in the ^{1}H NMR spectra shown in Figure 18. The TMB standard signal at 3.73 ppm remains constant throughout the reaction as expected. The ^{1}H NMR integral data were used to determine the rate of formation of product and the rate of consumption of the reactants. Using the formula below, integral data were converted into concentrations.

$$\left\{ \left(\frac{\text{Integral}}{\text{No. of protons}} \right) \div \left(\frac{\text{TMB integral}}{9} \right) \right\} \times \left[\text{TMB} \right]$$

Figure 27 shows a graph of concentration versus time for the reaction of 2,2'-dithiodibenzaldehyde **201** and MVK using DBU as catalyst. From the graph, the decrease in the concentration of 2,2'-dithiodibenzaldehyde **201** as well as that of MVK is evident. Product formation is also evident. The concentration of DBU appears to decrease slowly, while the aldehyde is consumed after about 8 000 s. The data for each run was corrected for zero-time error. When methyl acrylate was used as the activated alkene, in place of MVK, the results obtained showed that the reaction was much slower than with MVK (Figure 28). It is evident that after more than 35 000 s the dialdehyde **201** had still not been fully consumed. Drewes *et al.*[71] had earlier observed this slow reactivity of methyl acrylate and their results showed that MVK reacted 10-45 times faster than methyl acrylate.
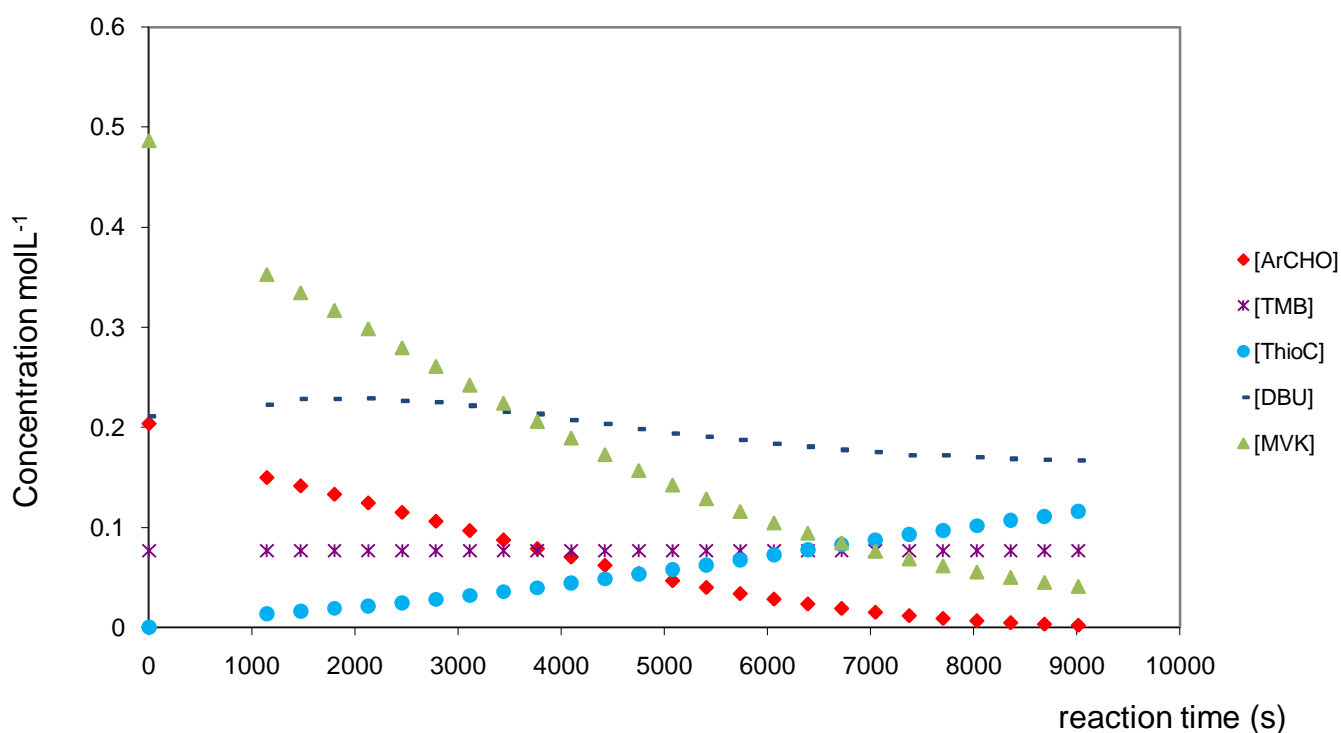
Figure 27. Graph of concentration *vs* time for the reaction of 2,2'-dithiodibenzaldehyde **201** with MVK using DBU as catalyst.
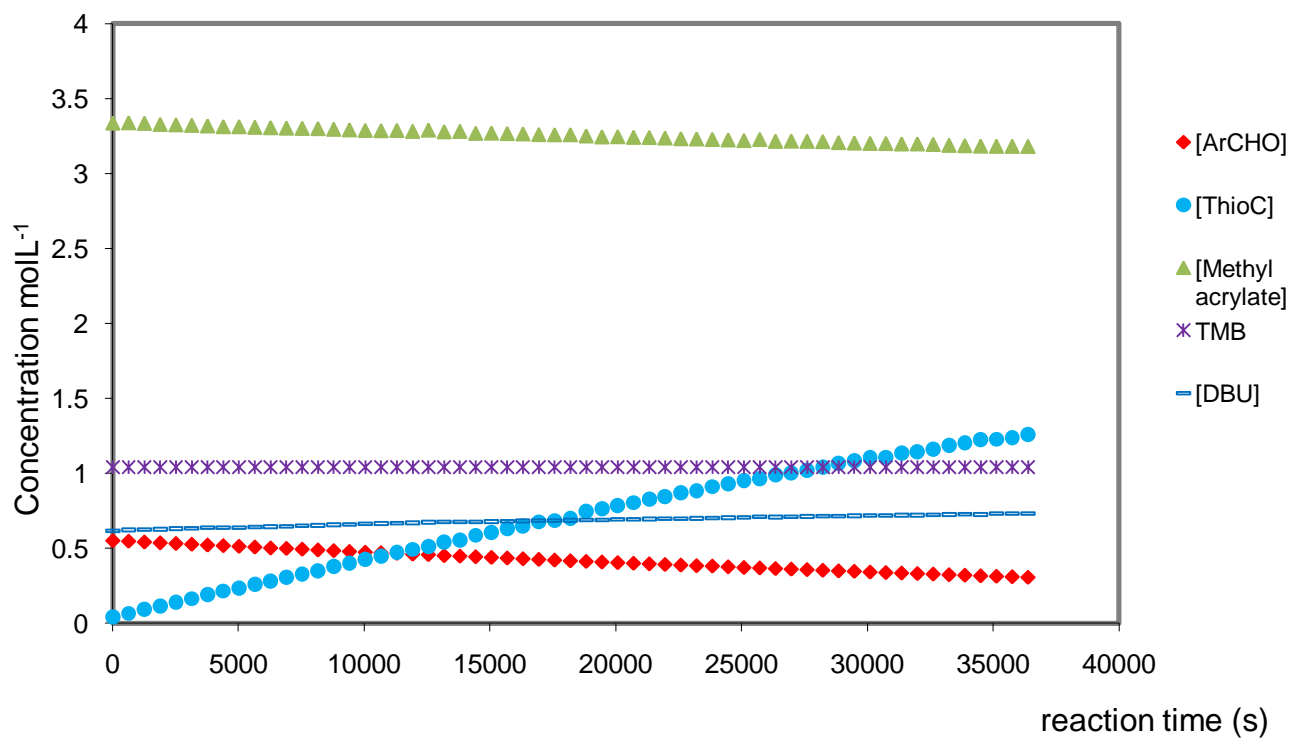
Figure 28. Graph of concentration vs time for the reaction of 2,2'-dithiodibenzaldehyde **201** with methyl acrylate using DBU as catalyst.

2.1.3.2 Reactions using Ph₃P as sole catalyst

When triphenylphosphine (Ph_3P) was used as the catalyst, the results obtained showed that the reaction with MVK was much slower than when DBU was used. Figure 29 shows a stacked plot of the progress of this reaction, and the signals observed at *ca* 5.0 ppm for the diastereomeric 4-hydroxythiochroman **217** in Figure 18 are also evident. The aldehyde signal remained almost constant. The even slower reactivity of the Ph_3P-catalysed reaction of methyl acrylate compared to MVK was also apparent. Figure 30 shows the progress of the reaction with methyl acrylate; after more than 25 000 s there is no evidence of the formation of any product. We were thus able to conclude that Ph_3P alone is not a suitable catalyst for these reactions.
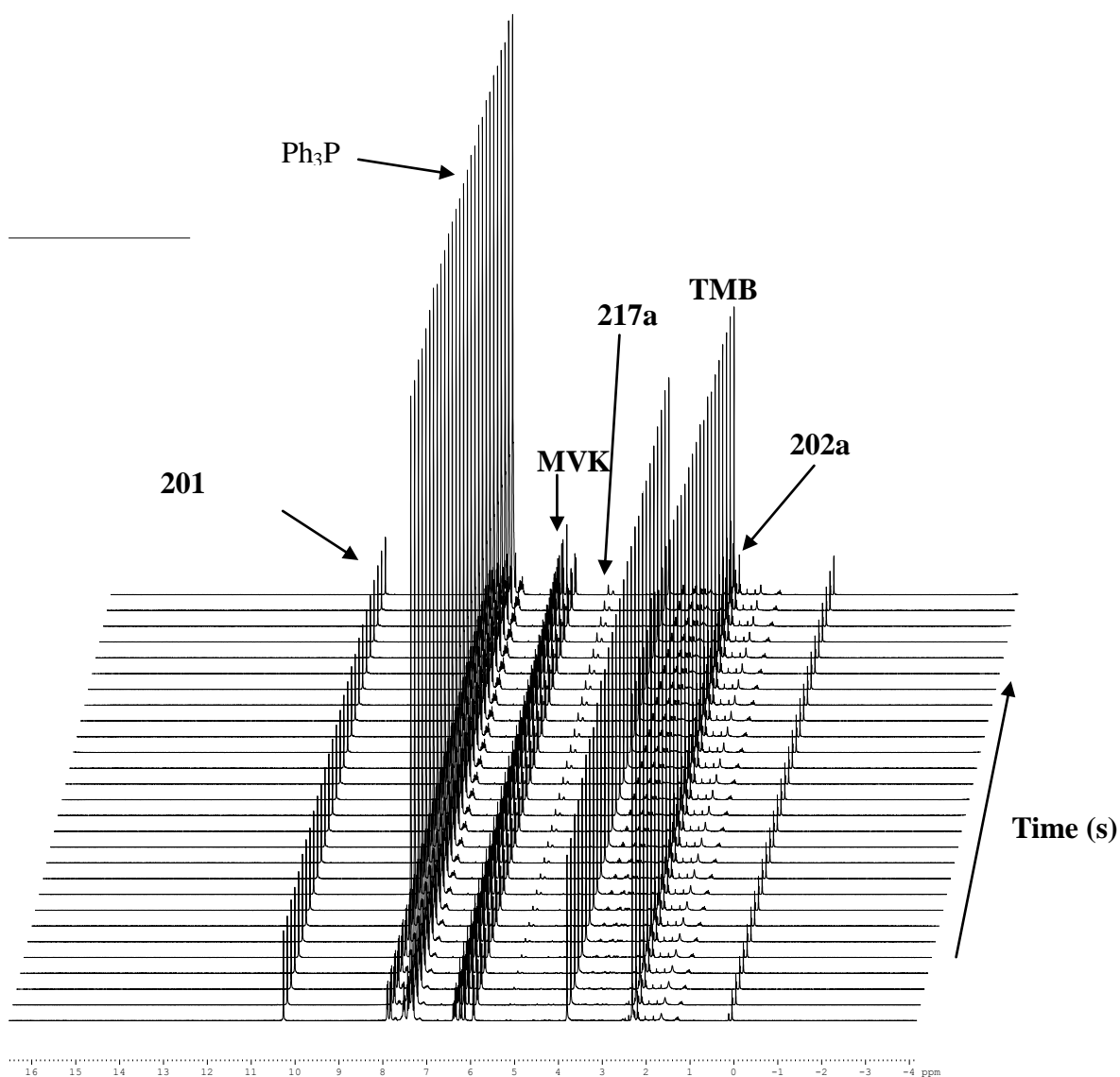
Figure 29. Stacked ^{1}H NMR plots of the reaction of 2,2'dithiodibenzaldehyde **201** with MVK using only Ph_3P as catalyst in place of DBU. Time interval: 600 s.
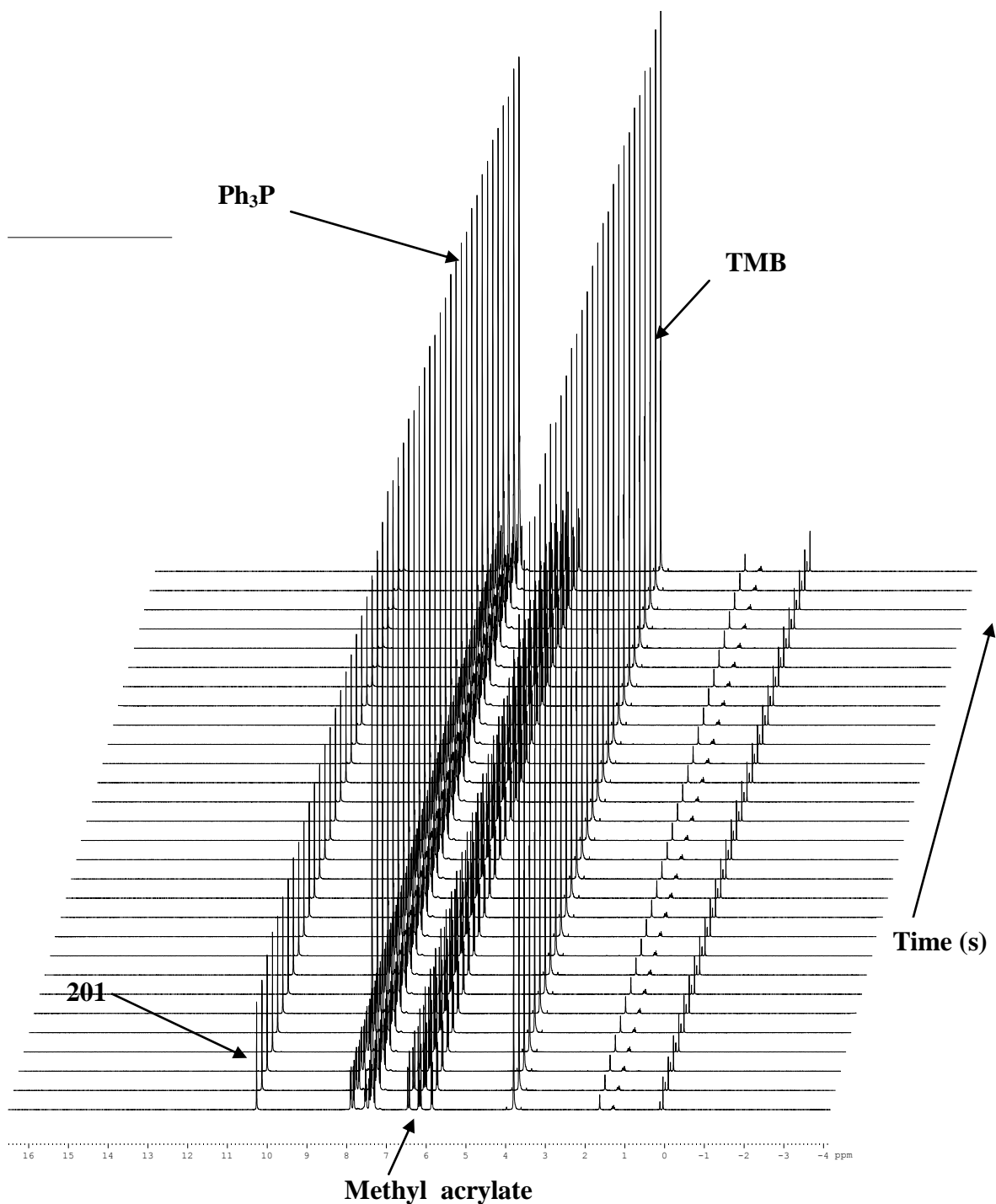
Figure 30. Stacked ¹H NMR plots of the reaction of 2,2'-dithiodibenzaldehyde **201** with methyl acrylate using only Ph₃P as catalyst in place of DBU. Time interval: 600 s.

2.1.3.3 Reactions using a combination of DBU and Ph₃P as a dual organocatalyst system

When both DBU and Ph$_3$P were used together for the MBH reactions with 2,2'-dithiodibenzaldehyde **201**, the reactions were significantly faster. When MVK was used as the activated alkene (Figures 31 and 32), the aldehyde was consumed in approximately 2 400 s, representing a rate acceleration of almost 330% compared to when only DBU was used and even greater than when only Ph$_3$P was used. The intermediate 4-hydroxythiochroman **217a** begins to form immediately the reactants are mixed. This is evident in the stacked plot of the reaction progress (Figure 31), in which the signals at *ca* 5.0 ppm are present right from the first spectrum, indicating that this product is being formed within the first few seconds of the reaction. The aldehyde signal at 10.2 ppm also disappears quickly. The reaction with methyl acryate was slightly slower than with MVK, but was still much faster than when either DBU or Ph$_3$P were used as sole catalysts. The stacked plot Figure 33 shows the aldehyde disappearing rapidly. Figure 34 shows the aldehyde being consumed within *ca.* 8000 s, a rate acceleration of more than 5 times that achieved with either DBU or Ph$_3$P alone.
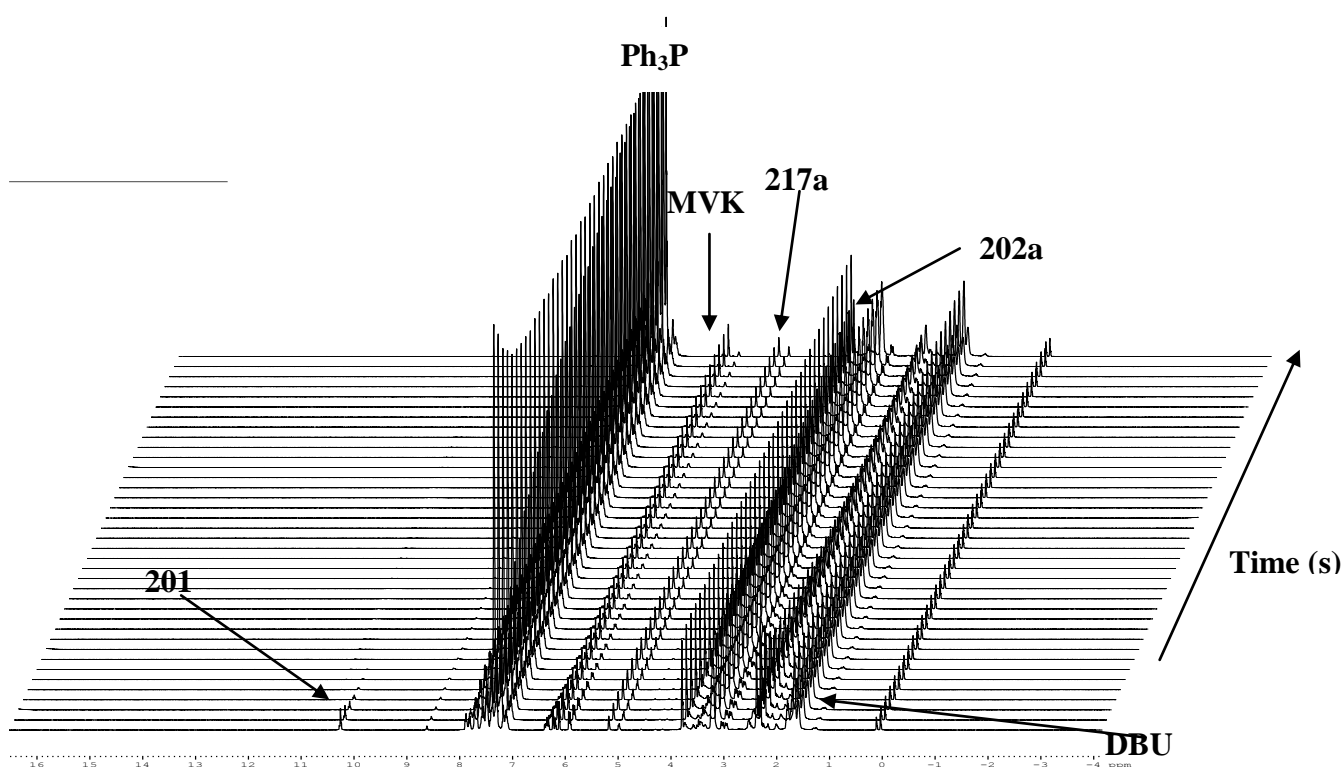
Figure 31. Stacked ^{1}H NMR plots of the reaction of 2,2'-dithiodibenzaldehyde **201** with MVK using both DBU and Ph$_3$P as catalysts (dual-catalyst).
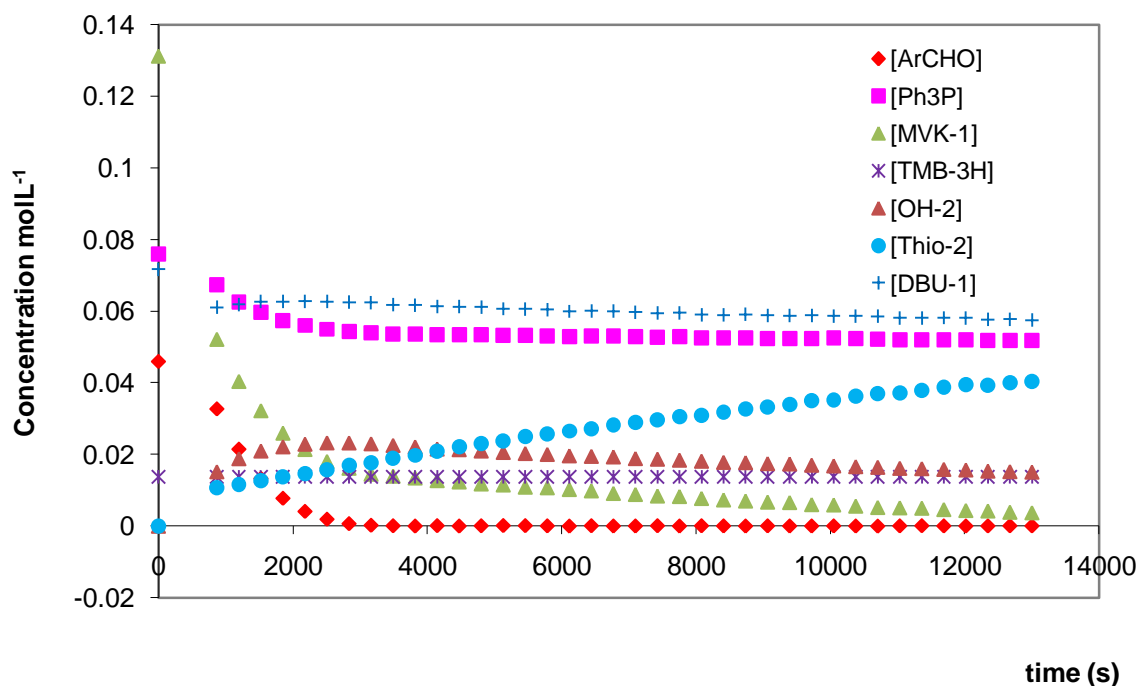
Figure 32. Graph of concentration vs time for the reaction of 2,2'-dithiodibenzaldehyde **201** (ArCHO) with MVK, using the dual-catalyst system, DBU-Ph$_3$P. Also shown are the thiochromene **202a** (Thio-2), the 4-hydroxythiochroman **217a$_1$** (OH-2) and the standard (TMB).
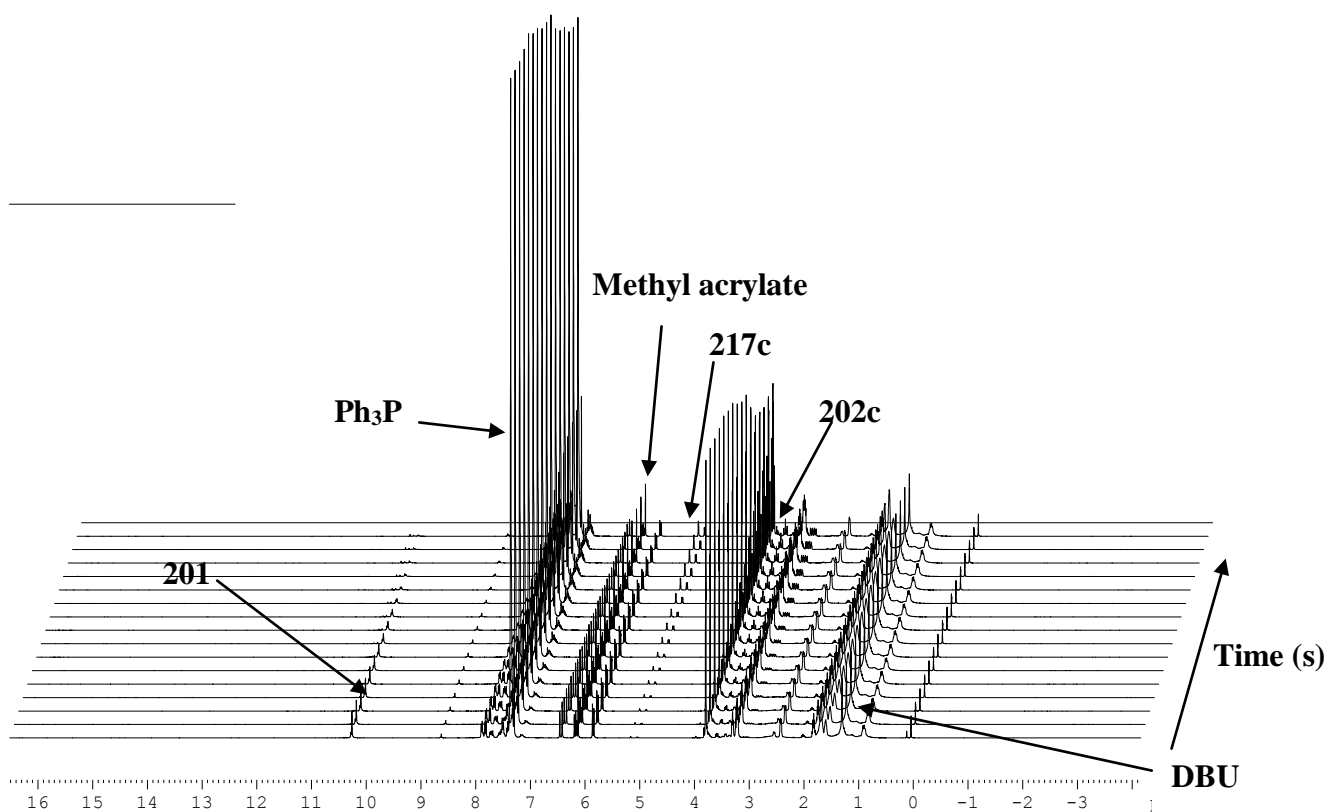
Figure 33. Stacked ^{1}H NMR plots of the reaction of 2,2'-dithiodibenzaldehyde with methyl acrylate using both DBU and Ph$_3$P as catalysts (dual-catalyst system).
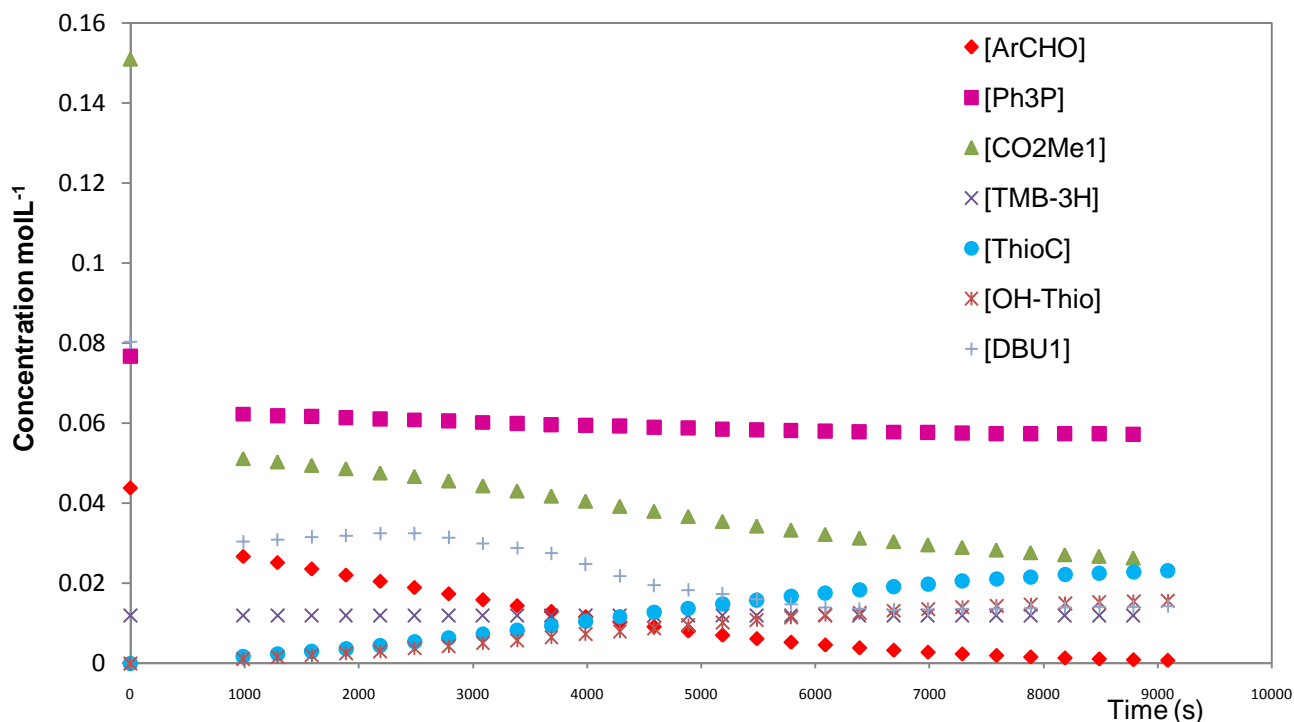
Figure 34. Graph of concentration vs time for the reaction of 2,2'-dithiodibenzaldehyde **201** (ArCHO) with methyl acrylate (CO2Me1), using the dual-catalyst system, DBU-Ph$_3$P. Also shown are the thiochromene **202c** (ThioC), the 4-hydroxythiochroman **217c** (OH-Thio) and the standard (TMB).

2.1.3.4 Phosphorus 31 Kinetics

A phosphorus-31 (^{31}P) NMR kinetics study was carried out on the MBH reaction of 2,2'-dithiodibenzaldehyde **201** with MVK, in the presence of the dual-catalyst system (DBU-Ph$_3$P). There is clear evidence of the emergence of a new phosphorus species (Ph$_3$PO), confirming what Humphrey and Hawkins[138] had reported earlier using analytical methods, *i.e* that Ph$_3$P acts as a disulfide reducing agent, and in the process is oxidised to its oxide Ph$_3$PO (Figure 35). Figure 36 shows depletion of Ph$_3$P with the formation of the oxide.
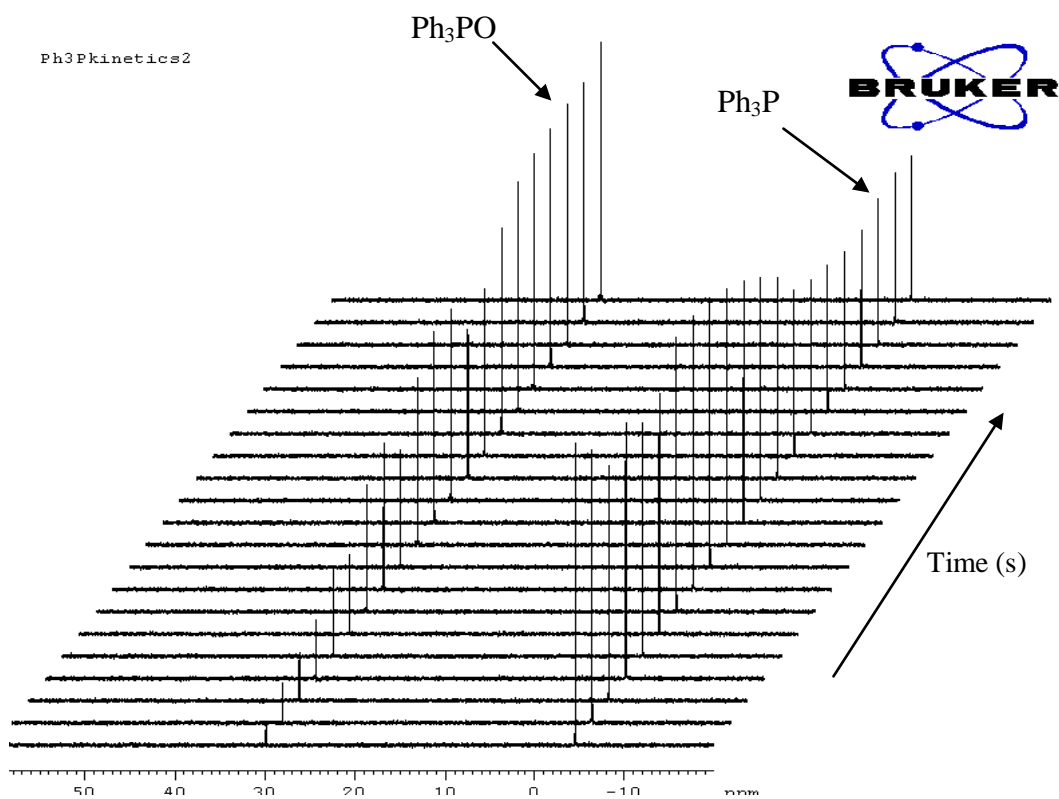
Figure 35. Stacked ^{31}P NMR plots showing depletion of Ph_3P and the formation of Ph_3PO in the MBH reaction of 2,2'-dithiodibenzaldehyde **201** with MVK using the dual-catalyst system (DBU-Ph_3P). Reaction temperature 24 ^oC and delay time 90 s.
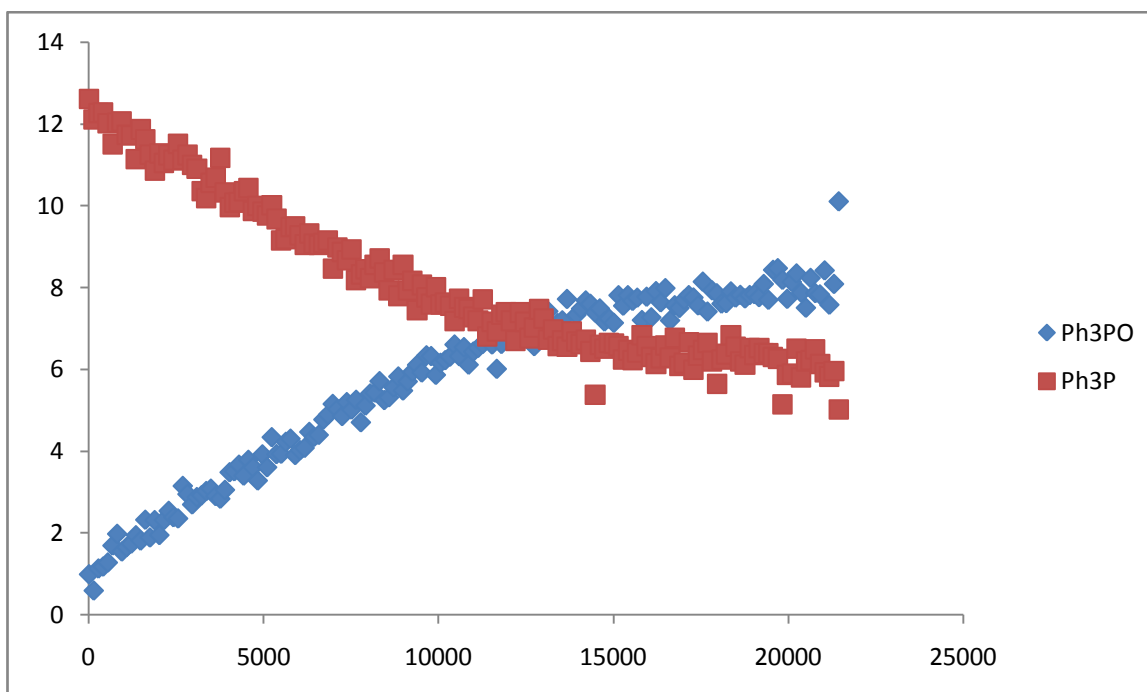
Figure 36. Graph showing depletion of Ph_3P and formation of Ph_3PO in the MBH reaction of 2,2'-dithiodibenzaldehyde **201** with MVK using the dual-catalyst system (DBU-Ph_3P). Reaction temperature 24 ^oC and delay time 90 s. Integral data was used for the plot.

2.1.4 Determination of the Rate Law for the Morita-Baylis-Hillman synthesis of 2*H*-1-benzothiopyrans from 2,2'-dithiodibenzaldehyde

In a preliminary kinetic study,[72] it was observed that both the aldehyde and alkene appeared to follow first-order kinetics in the initial stages of the reaction but deviated from linearity as the reaction progressed. This was an indication that the mechanism of the reaction was more complex than had been anticipated. In the current study, the isolation of the 4-hydroxy derivatives **217** (Schemes 53 and 56), which had been proposed as intermediates in the initial report by Kaye and Nocanda,[6] was an indication that aspects of the proposed mechanism had some merit. The isolation of the hemi-thioketal **252** is consistent with involvement of the MBH adduct **216** in the sequence of transformations involved, while DBU's ability to directly cleave aryl- and heteroaryl disulfides has been proved in the current work.

Based on these findings and the proposed mechanism, we decided to consider all of the possible transformation sequences that might be occurring in this reaction. Scheme 57 (Path 1) provides a summary of the likely transformations on the presumption that the MBH step precedes the cleavage of the sulfur-sulfur bond, while Scheme 58 (Path 2) provides a summary of the possible transformations when the cleavage of the sulfur-sulfur bond precedes the MBH reaction. For clarity, the compounds have been labelled using the letters **A**-**L**. Path 1 is, in fact, favoured since the kinetic data indicates that the MBH step precedes the cleavage of the disulfide; this is evidenced by the rapid, early and simultaneous consumption of both the aldehyde and activated alkene precursors (Figure 37). The summaries of transformations involved in both pathways shown in Schemes 57 and 58, illustrate twelve distinct steps, reflecting the inherent potential complexity of this reaction.
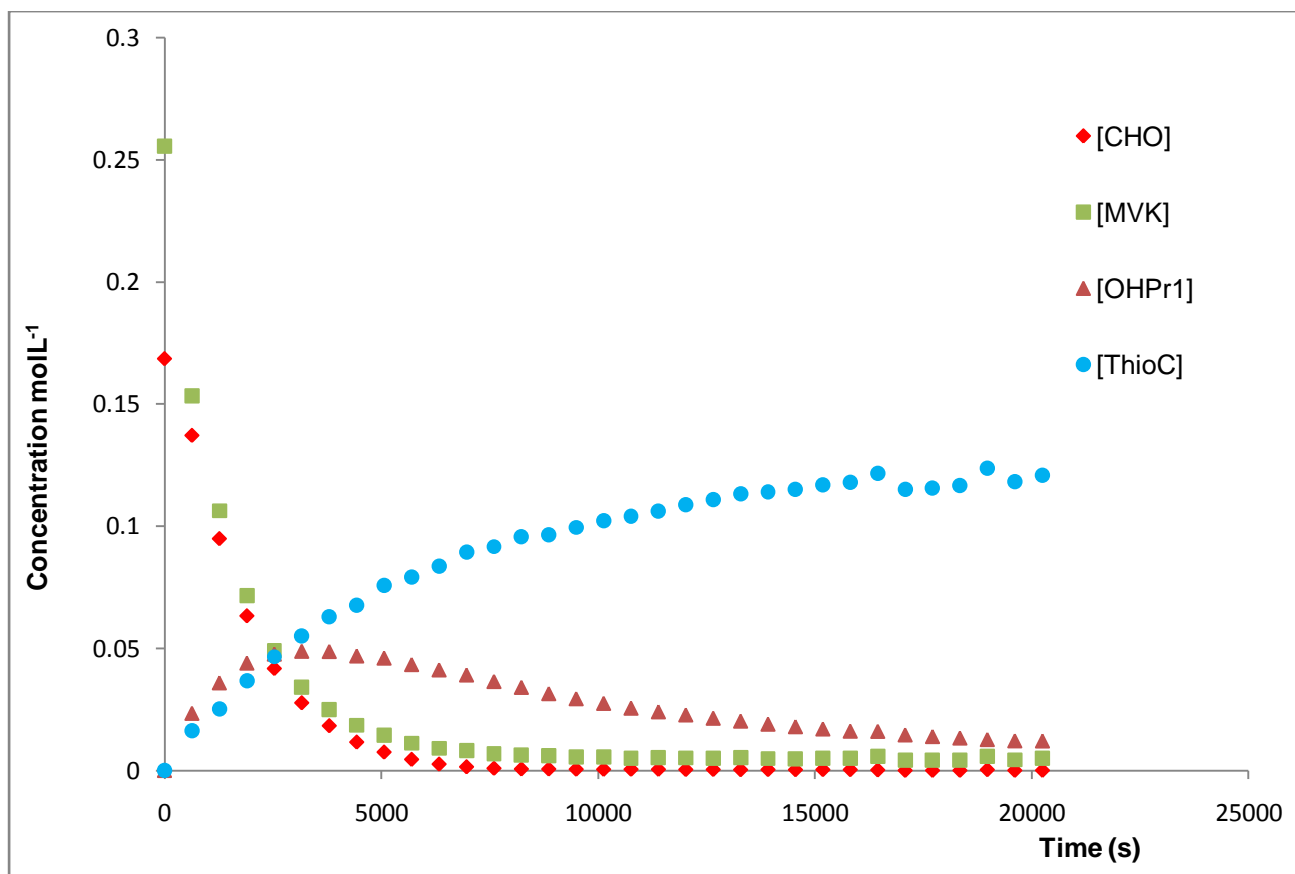
Figure 37. Experimental data: concentration *vs* time graphs for the reaction between 2,2'-dithiodibenzaldehyde **201** (CHO) and MVK. With the formation of the 4-hydroxy-thiochroman **217a** (OHPr1) and the thiochromene **202a** (ThioC).

Possible transformation sequences

$$A + B \longrightarrow C \ (k_1)$$

$$C + D \longrightarrow E + B \ (k_2)$$

$$E + C \longrightarrow F + B \ (k_3)$$

$$F + B \longrightarrow G + H \ (k_4)$$

$$H \longrightarrow I + B' \ (k_5)$$

$$G \longrightarrow I \ (k_6)$$

$$I \longrightarrow J + H_2O \ (k_7)$$
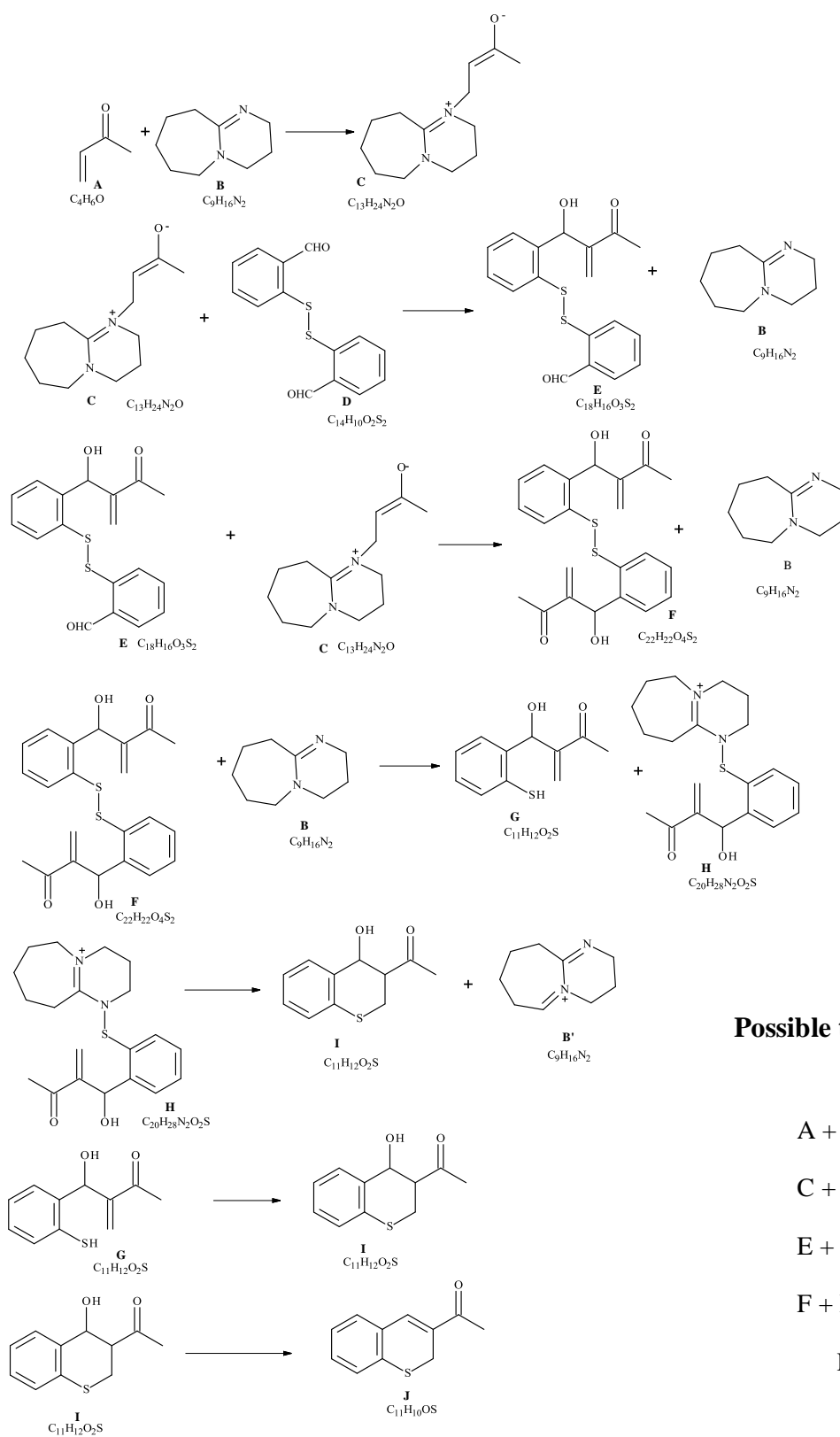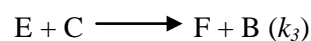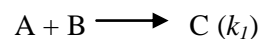
Scheme 57. Summary of favoured (path I) reaction sequences in the formation of thiochromene derivatives.

Possible transformations

$$D + B \longrightarrow K + L \; (k_8)$$

$$C + K \longrightarrow G + B \; (k_9)$$

$$L \longrightarrow K + B' \; (k_{10})$$

$$E + B \longrightarrow L + G \; (k_{11})$$

$$E + B \longrightarrow K + G \; (k_{12})$$
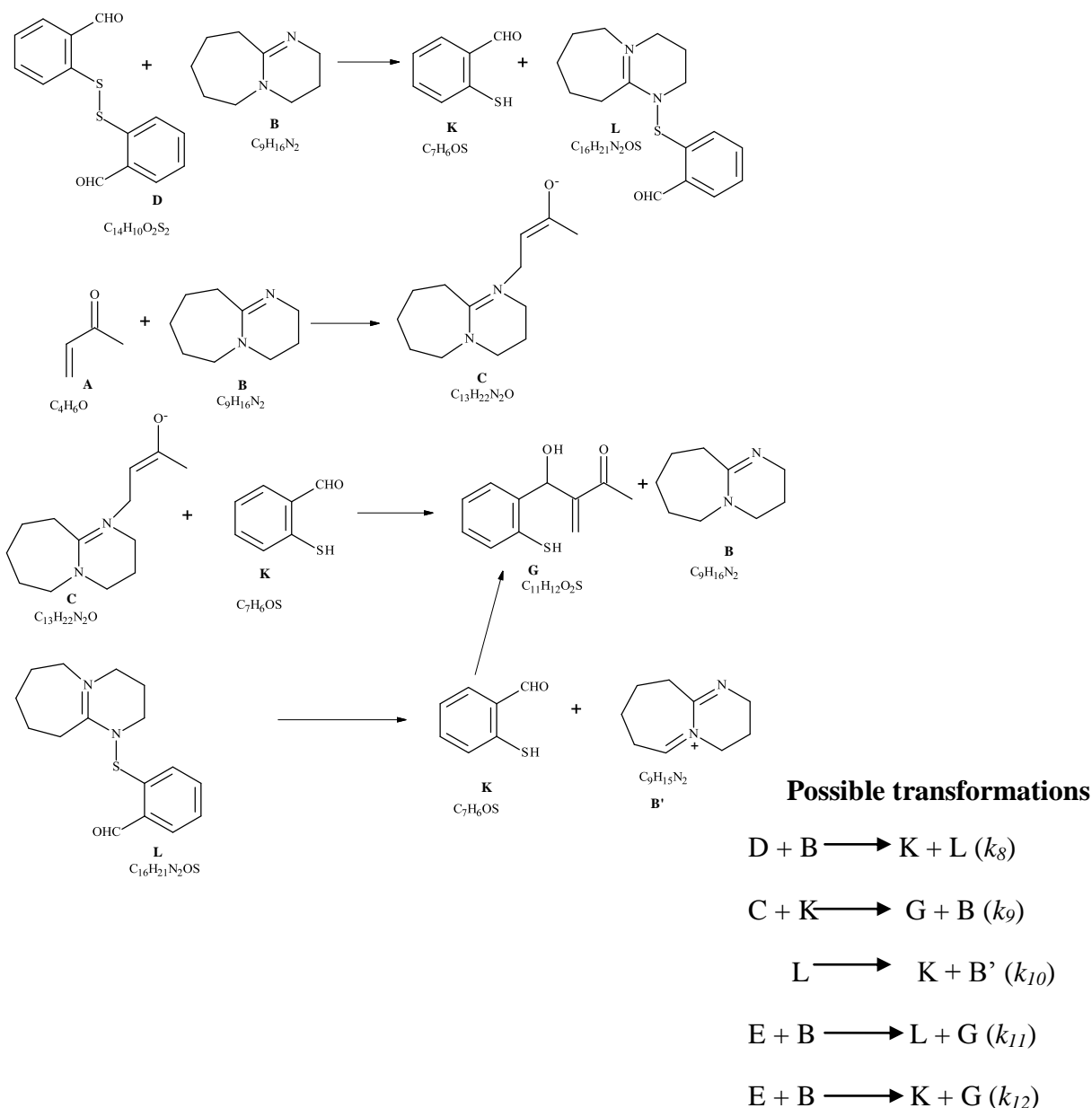
Scheme 58. A summary of possible reaction sequences in the alternative pathway (path 2) in the formation of thiochromene derivatives.

From Schemes 57 and 58, the following rate expressions (Equations 4-15) can be derived for the twelve identified steps. Using these rate expressions, and varying the values of the individual rate constants k_1-k_{12}, the change in concentration, with time, of each of the identified species was calculated. The theoretical concentration *vs* time graphs for the proposed model were then plotted as shown in Figure 38. The shapes of the curves for the reactants and products appears to follow similar patterns to those of the experimental kinetic data shown in Figure 37.

Rate 1 = k_1 [A] [B]   (4)

Rate 2 = k_2 [C] [D]   (5)

Rate 3 = k_3 [E] [C]   (6)

Rate 4 = k_4 [F] [B]   (7)

Rate 5 = k_5 [H]   (8)

Rate 6 = k_6 [G]   (9)

Rate 7 = k_7 [I]   (10)

Rate 8 = k_8 [D] [B]   (11)

Rate 9 = k_9 [C] [L]   (12)

Rate 10 = k_{10} [L]   (13)

Rate 11 = k_{11} [E] [B]   (14)

Rate 12 = k_{12} [E] [B]   (15)
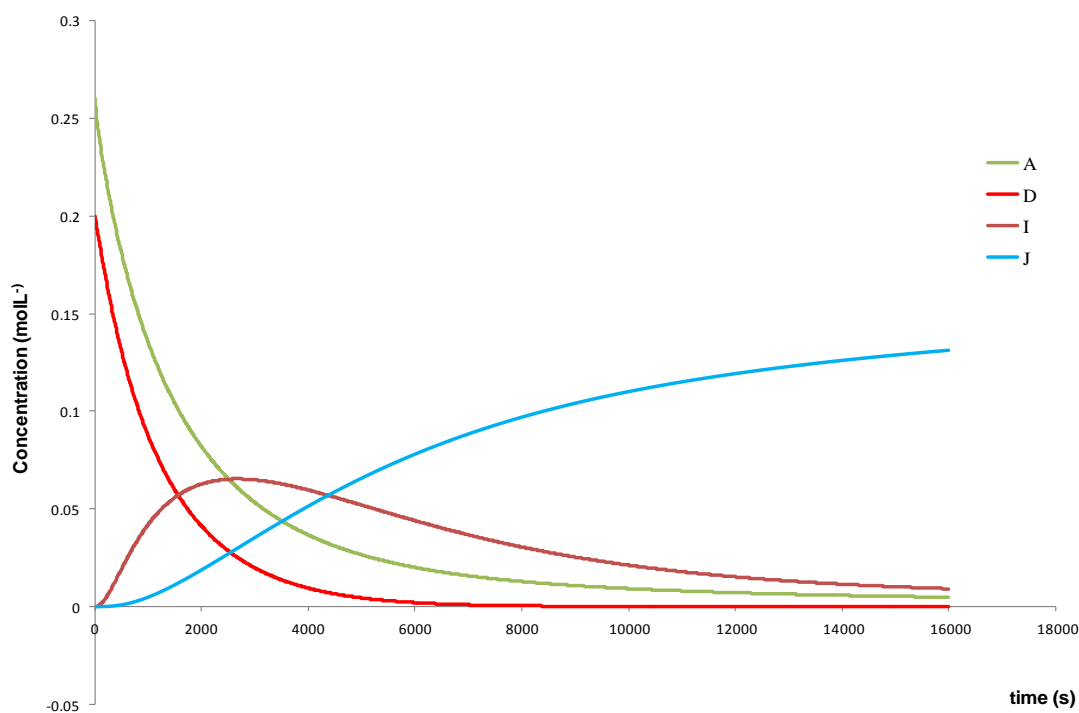
Figure 38. Theoretical model data: concentration *vs* time graphs for the reaction between 2,2'-dithiodibenzaldehyde (**201**; **D**) and MVK (**2a**; **A**); with the formation of the 4-hydroxythiochroman (**217a**; **I**) and the thiochromene (**202a**; **J**).

The two graphs were then superimposed on each other in order to determine how closely the theoretical data modelled the experimental data. Using the solver function in Excel to solve for the values of the constants k_1-k_{12} in the theoretical model, the best fit obtained was plotted and is shown in Figure 39. The theoretical data appears to model the consumption of MVK (**2a**; **A**), 2,2'-dithiodibenzaldehyde (**201**, **D**) and the formation of 4-hydroxythiochroman (**217a**; **I**) quite closely, but the theoretical data for the thiochromene (**202a**; **J**) deviates from the experimental data. Given the complexity of this reaction, such deviations are not surprising. It may be that the proposed model is not sufficiently comprehensive, but the fact that three of the four theoretical curves model the data reasonably well, suggests that the proposed model has some validity. The theoretical model does not take into account solvent effects which, in reality, may play a significant role on the mechanism. Moreover, while we have identified twelve possible steps for this reaction, it is possible that there could be more. These limitations in our theoretical model may have contributed to the observed deviations, and have, at this stage, precluded determination of the overall rate law for the reaction. Table 2, however details the values of the rate constants (k_1-k_{12}) used to obtain the theoretical graphs in Figure 39.

Table 2. Values of the rate constants k_1-k_{12} for the best fit shown in Figure 39.

Rate constant	Value
k_1	$0.0146 \ mol^{-1}Ls^{-1}$
k_2	$0.0196 \ mol^{-1}Ls^{-1}$
k_3	$1.6 \ mol^{-1}Ls^{-1}$
k_4	$0.04 \ mol^{-1}Ls^{-1}$
k_5	$0.00004 \ s^{-1}$
k_6	$0.001 \ s^{-1}$
k_7	$0.0003 \ s^{-1}$
k_8	$0.0099 \ mol^{-1}Ls^{-1}$
k_9	$0.5 \ mol^{-1}Ls^{-1}$
k_{10}	$0.006 \ s^{-1}$
k_{11}	$0.0000 \ mol^{-1}Ls^{-1}$
k_{12}	$0.07 \ mol^{-1}Ls^{-1}$
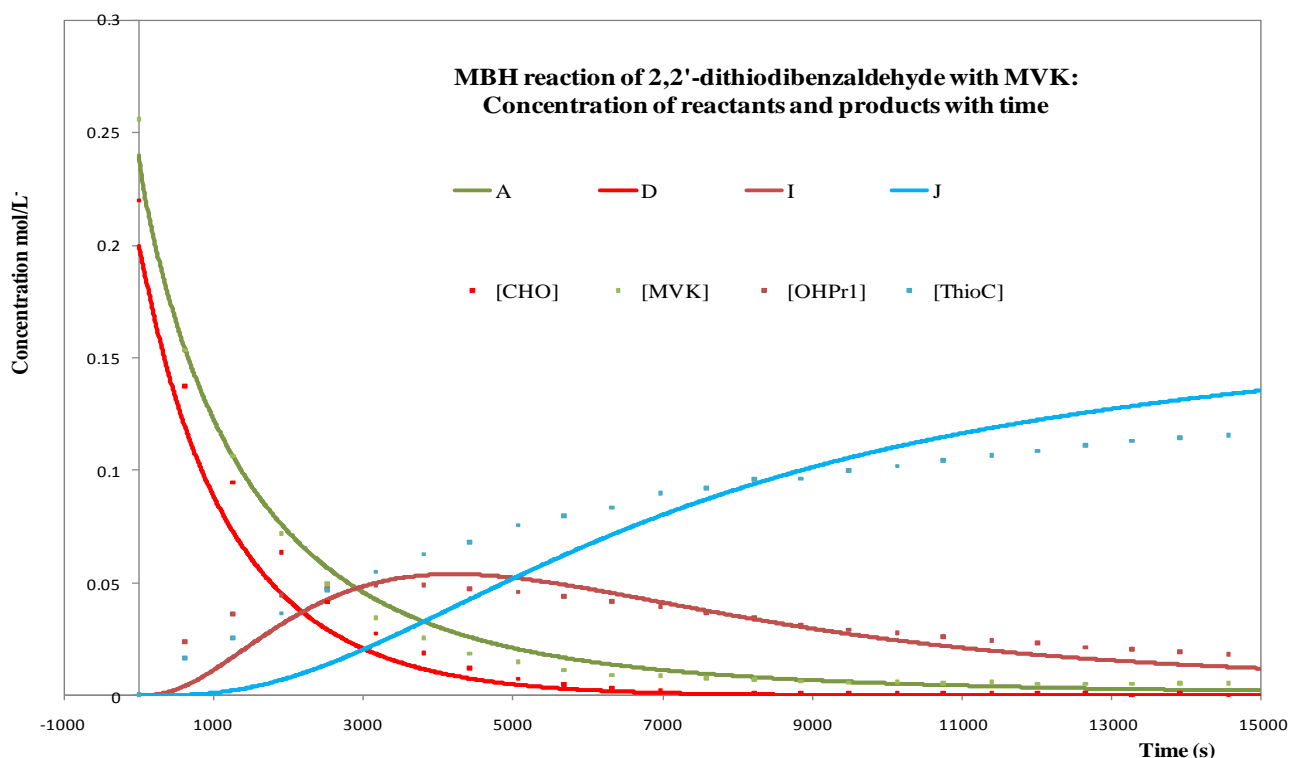
Figure 39. Concentration vs time graphs of the experimental (coloured symbols) and theoretical (solid lines) data; 2,2'-dithiodibenzaldehyde **201** (D; CHO) (red), MVK **2a** (A) (green), 4-hydroxythiochroman **217a** (I; OHPr1) (pink) and the thiochromene **202a** (J; ThioC) (blue).

2.1.5 Theoretical study of the MBH synthesis of 2*H*-1-benzothiopyrans

Theoretical studies were carried out based on the proposed mechanism[6] and on the sequence of steps outlined in Schemes 57 and 58. Geometry optimisation of the proposed intermediates and products was carried out using the Gaussian 03 programme. In some cases, conformational searches were carried out using the VEGA ZZ 2.4.0 programme[143] before optimisation with Gaussian. The hybrid density functional B3LYP with the 6-31G(d) basis set were used for the calculations. B3LYP combines exchange (Becke-3-Parameter)[144] and correlation functionals (Lee, Yang and Parr)[145] in computational results, and has been used widely in theoretical work involving the determination of reaction mechanisms giving results with acceptable levels of accuracy. The proposed mechanism[6] (Scheme 50), presumes that cleavage of the disulfide occurs after the MBH reaction − a presumption supported by the experimental kinetic data. Since theoretical mechanistic studies of the MBH reaction have received considerable attention in recent years (see Section 1.1.1.2),[40,41,42,44] the present study has focussed mainly on the post-MBH mechanistic sequences. Nonetheless, some attention

was given to exploring the structures of the initial DBU- and Ph$_3$P-MVK zwitterions. In earlier theoretical work by Lobb and Kaye,[146] it was found that the zwitterion formed in the inital step of the MBH reaction, between the catalyst and activated alkene (see Scheme 57: **A** + **B**-> **C**), failed to afford a minimised geometry. In their case, DABCO was being used as the catalyst and MVK as the activated alkene, and an energy surface scan showed that attempts to decrease the distance between the DABCO nitrogen and the MVK vinylic carbon to form the N-C bond in the zwitterions, resulted in an increase in energy causing the system to fall apart − in spite of the fact that a transition state could be located and optimised. Against this background, we sought to explore similar systems using DBU and Ph$_3$P as catalysts, and 2,2'-dithiodibenzaldehyde **201** and MVK as substrates. Energy surface scans of the N-C bond length and the torsion about this bond in both *cis-* and *trans*-configurations of the DBU and Ph$_3$P-derived zwitterionic enolates were carried out. The results obtained were similar to those observed by Lobb and Kaye,[146] with the *trans*-enolates at lower energies than the *cis*-enolates, a result that can be attributed to decreased steric crowding about the C=C bond in the former. Figure 40 illustrates the energy surface scan for the *cis*-enolate of the DBU-MVK zwitterion, while Figure 41 shows the results for the corresponding *trans*-enolate. The points marked **a-d** on the scan grid of the *cis*-DBU-MVK zwitterion (Figure 40), reveals an interesting pattern. Structure **a** shows the zwitterion during the first step of the scan, corresponding to point **a**; the N-C bond is intact with the system at a high energy. Structure **b,** corresponding to point **b**, shows an interesting feature: hydrogen-bonding interactions have developed between the electronegative oxygen and one of the protons on the carbon next to the reacting nitrogen in DBU, leading to the formation of a six-centered complex, which is at much lower energy than the initial structure **a**. Structure **b** was optimised at the B3LYP level to establish if it was a stable structure. The results showed it to be stable, optimising to a minimum without falling apart. Point **c**, corresponds to the zwitterionic system (Structure **c**) with the highest energy. However, while the desired enolate moiety is evident in the structure, the N-C bond has lengthened instead of shortening. Structure **d** exhibits the lowest energy attained for this system, but it is quite evident that the N-C separation has increased even further to 3.02Å, and the system simply disintegrates into the starting materials DBU and MVK. The *trans*-DBU-MVK zwitterion scan grid (Figure 41) on the other hand, failed to reveal any significant discontinuities, as observed with the *cis*-zwitterion. The zwitterion simply disintegrates to the reactants, DBU and MVK, at the lowest energy (Structure **f**). Structure **e** shows the structure of the zwitterion during the initial stages of the scan.

Structure **a**

Structure **b**

Structure **c**

Structure **d**
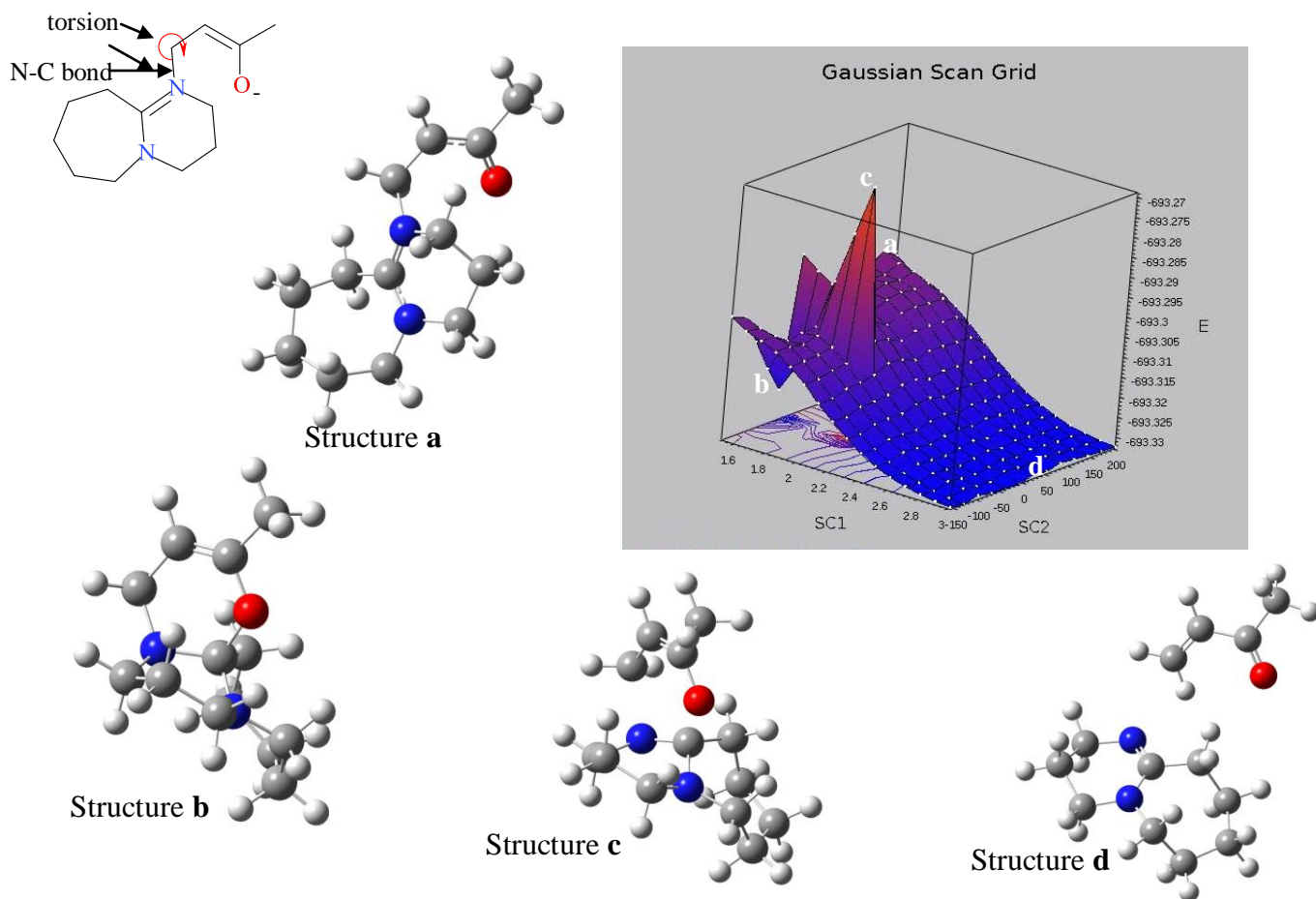
Figure 40. Energy surface scan grid for the *cis*-DBU-MVK zwitterion.

Structure **e**

Structure **f**
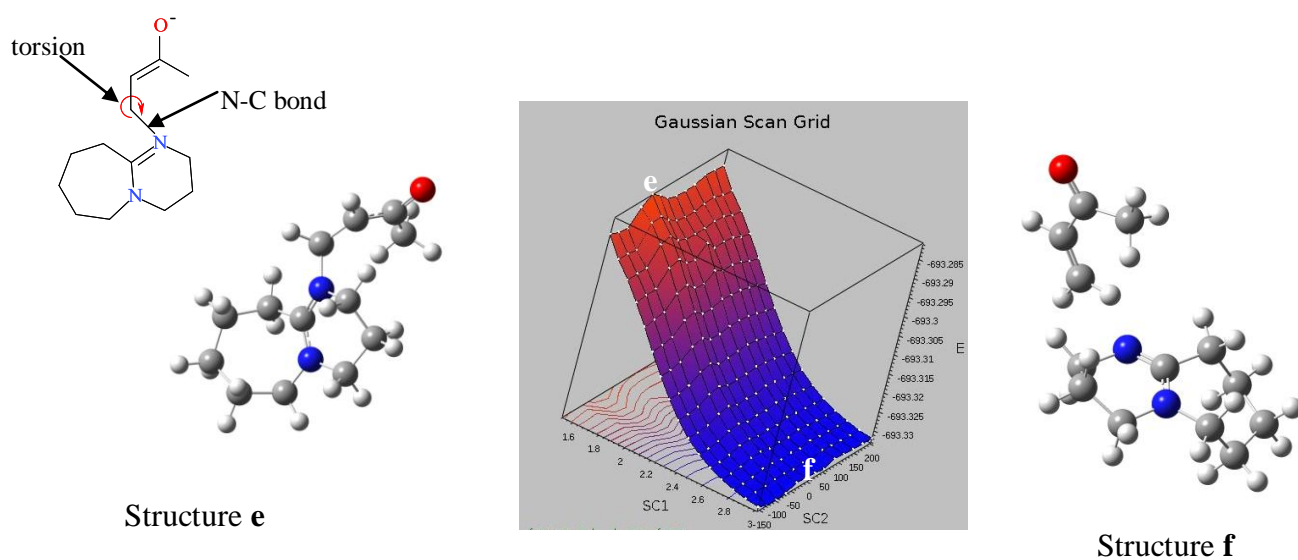
Figure 41. Energy surface scan grid for the *trans*-DBU-MVK zwitterion.

Figure 42 illustrates the energy surface scans for the *cis-* and *trans*-conformations of the Ph₃P-MVK zwitterionic enolate, neither of which minimises to a stable system; the systems disintegrate into Ph₃P and MVK, as observed with DBU.
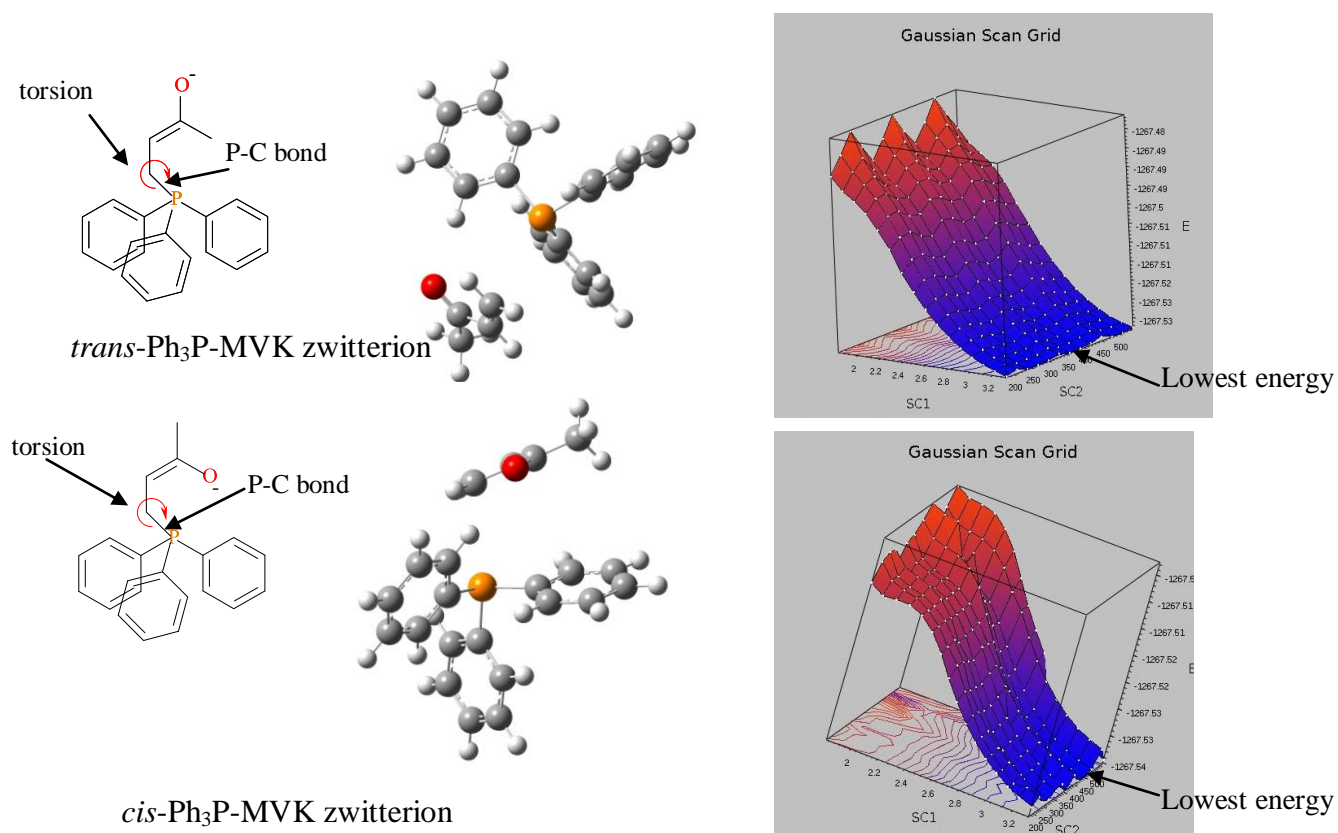
Figure 42. Energy surface scan grids for the *cis-* and *trans*-Ph₃P-MVK zwitterions and the structures corresponding to the lowest energy points.

The optimised structures for the intermediates and products in the proposed mechanism for the formation of the thiochromenes, illustrated in Scheme 50, are shown in Figure 43. The optimised structure for compound **215** shows the terminal vinylic carbon orientated in an arrangement that would favour nucleophilic attack by sulfur once cleavage of the S-S bond has occurred, leading to cyclisation to the 4-hydroxythiochroman **217** as proposed in Scheme 50. Interestingly, the optimised structure for intermediate **232** comprises two separate molecules, one being the 4-hydroxythiochroman **217** and the other DBU. This is an indication that loss of the catalyst and cyclisation, as proposed in Scheme 50 is likely to be a concerted process.
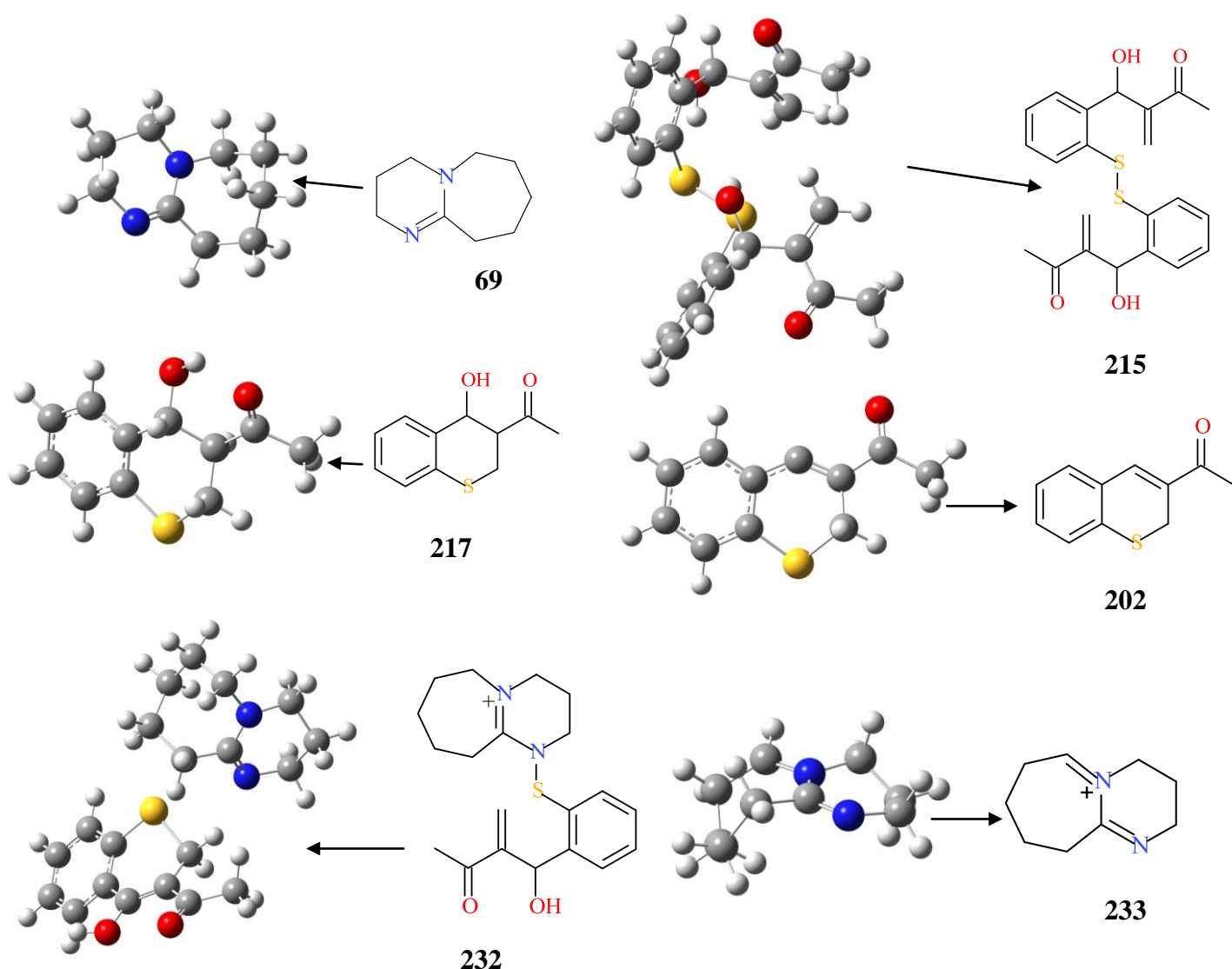
Figure 43. Optimised geometries for the species shown in the proposed mechanism for the formation of the thiochromenes when MVK is used as the activated alkene (Scheme 50).

2.1.5.1 Nucleophilic cleavage of the sulfur-sulfur bond

Phosphorus nucleophiles have been shown to reductively cleave the S-S bond in disulfides to afford the corresponding thiols under milder reaction conditions,[138,147-152] than those involved with the use of more powerful reducing agents, such as $NaBH_4$,[153] $LiAlH_4$[154] and Zn/acetic acid.[155] Overman and co-workers carried out a detailed kinetic study of the reduction of aryl disulfides with Ph_3P and H_2O (Scheme 59).[148,149,150] Their results showed that the cleavage mechanism involved two steps, with initial attack by Ph_3P on one of the sulfur atoms of the disulfide **254** to form a phosphonium ion intermediate **255** and a benzenethiolate anion **256** (Equation 16); hydrolysis of the phosphonium ion **255** then affords a second molecule of the

benzenethiolate anion **256** (Equation 17). They postulated that two different pathways were possible. Nucleophilic attack could occur at one of the sulfur atoms of the disulfide **254**, displacing the thiolate anion **256** in a concerted S_N2-type reaction *via* transition state **258** (Equation 18) or, alternatively, attack could occur at both sulfur atoms simultaneously in a pericyclic-type reaction involving a three-centred transition state complex **259**, which would lead to the formation of a penta-coordinated phosphorus intermediate **260** (Equation 19).

$$
\text{Ph}_3\text{P} + \text{ArS-SAr} \underset{k_{-1}}{\overset{k_1}{\rightleftharpoons}} \text{Ph}_3\overset{+}{\text{P}}\text{-SAr} + \text{ArS}^- \tag{16}
$$
$$
\qquad\qquad\text{254} \qquad\qquad\qquad\quad \text{255} \qquad \text{256}
$$

$$
\overset{+}{\text{Ph}_3}\text{P-SAr} + \text{H}_2\text{O} \xrightarrow{k_2} \text{Ph}_3\text{P=O} + \text{ArS}^- + 2\text{H}^+ \tag{17}
$$
$$
\text{255} \qquad\qquad\qquad\qquad \text{257} \qquad \text{256}
$$

(18)

(19)

Scheme 59.

In the present study, we have shown that the tertiary amine DBU can, like Ph_3P, cleave the S-S bond. However, we were not certain of the exact mechanism of such cleavage by a nitrogen nucleophile, such as DBU, in aryl and heteroaryl disulfides. The mechanistic sequence proposed for the reductive cleavage of the S-S bond (Scheme 50),[6] involves a concerted pathway, with the N-S bond forming as the S-S bond breaks − a pathway that is similar to that implied in Equation 18 (Scheme 59). When a relaxed surface energy scan was carried out with the aim of finding a transition state for such cleavage, it was observed that as the N-S bond length (**i**) was decreased, the S-S bond-length (**ii**) lengthened and the energy of the system increased without reaching a maximum, resulting in failure to find a transition state. Instead, the trial transition state **TS1**, disintegrated into three species shown as '**TS1scan**' in

Figure 44. The three species are a neutral mercaptobenzene, and an ion pair comprising a mercaptobenzene anion and a DBU cation. Although this approach failed to give the expected transition state, it showed clearly that the S-S bond could be cleaved in the presence of a nitrogen nucleophile. An optimisation and frequency calculation was carried out on the geometry **TS1**, in the triplet state to explore whether a free radical process might be involved in the cleavage of the S-S bond. The results revealed cleavage of the S-S bond to form two thiolate radicals without any involvement of DBU − a result that confirmed that free radicals were not involved since DBU had been shown experimentally to be involved in the cleavage. The absence of a photochemically induced pathway had also been excluded by demonstrating successful reaction in the dark in the presence of DBU.
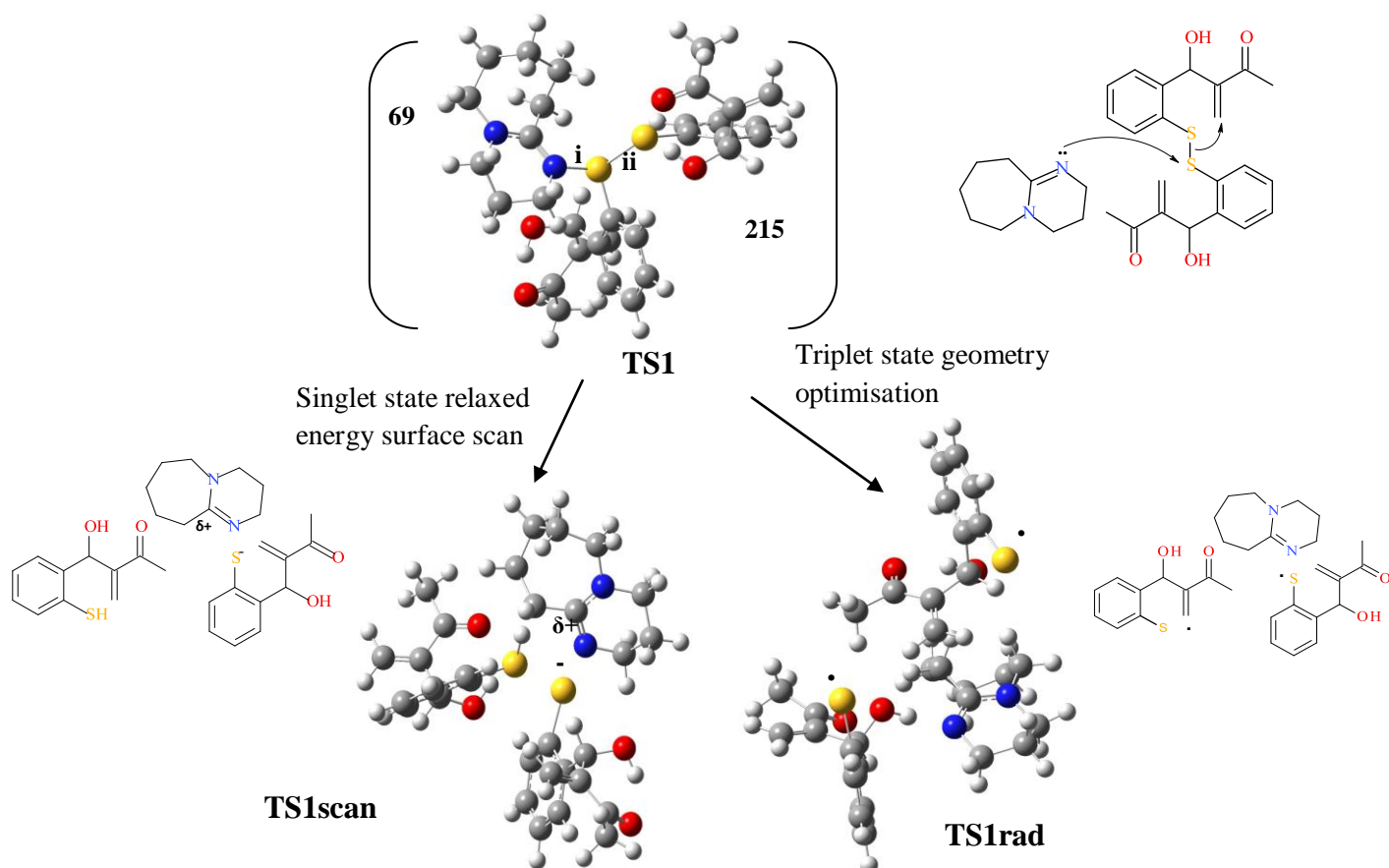
Figure 44. Trial transition state **TS1** showing nucleophilic attack by DBU **69** on the disulfide **215**. The N-S bond is marked as '**i**' and the S-S bond '**ii**'. **TS1scan** shows the result of a relaxed energy surface scan involving the N-S and S-S bonds, and **TS1rad** is the result following a geometry optimisation and frequency calculation, assuming an initial triplet state structure.

We then explored the possibility of a transition state involving a six-centered cyclic complex as shown in structure **TS2** (Figure 45). When the transition state optimisation was attempted on the structure **TS2**, the result observed is shown as **TS2opt**, with the N-S bond forming and the S-S bond breaking to form an ion pair, comprising a thiolate anion (ArS-), and a cationic nitrogen-sulfur complex with the positive charge delocalised between the sulfur atom and the DBU ring. In the DBU moiety, the positive charge is concentrated on the carbon atom located between the two nitrogen atoms, as shown in structure **TS2opt**. In fact, the cationic component in the ion pair corresponds to intermediate **232** in the proposed mechanism (Scheme 50). The stability of the ion pair formed resulted in **TS2** optimising to a minimum, *not to a transition state*. However, these results suggested that the transition state was likely to be found prior to the formation of the six-centered complex **TS2**. When Overmann *et al.*[145] carried out a kinetic study on the reaction of symmetrical aryl disulfides with Ph_3P in a 50% dioxane-H_2O mixture, they ruled out the direct formation of compound **260** *via* the three-centred transition state **259** (Equation 19; Scheme 59). In our study, however, the theoretical results point to a transition state leading *via* a 6-centred cyclic structure **TS2** to the cleaved ion pair system represented by **TS2opt**.
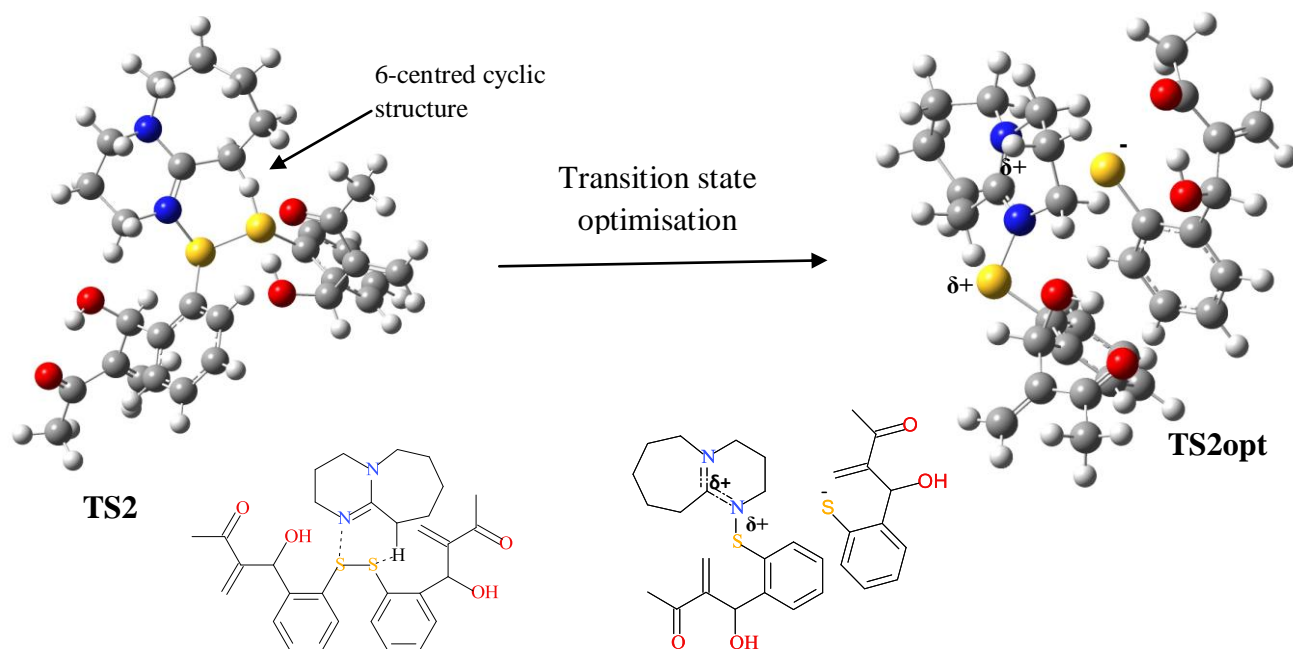
Figure 45. Structures of the proposed six-centered cyclic transition state **TS2** before optimisation and after optimisation **TS2opt**.

We then explored the transition state involved in the release of the catalyst DBU from intermediate **232** (Scheme 50). In the mechanism proposed, release of DBU could be effected when a base, such as the hydroxyl anion (released in the formation of the thiochromene **202**), picked up a proton from the DBU moiety in intermediate **232**, thus permitting a concerted reaction leading to cleavage of the N-S bond and release of a positively charged iminium ion **233**. Two possible cations *Iminium ion 1* and *Iminium ion 2* were likely to be formed depending on which proton reacted with the base. Figure 46 shows the structure of DBU with the highlighted protons likely to be removed by the base, and the resulting cation in each case. The two cations *Iminium ion 1* and *Iminium ion 2* were then optimised in order to determine the relative energies of each system and provide an indication as to which proton was most likely to react with a base. Interestingly, the energies of the two cations were found to be identical, indicating that, from energy considerations at least, either of the two protons was equally likely to react with a base.

-461.24 Ha   **Iminium ion 1**   **Iminium ion 2**   **-461.24 Ha**
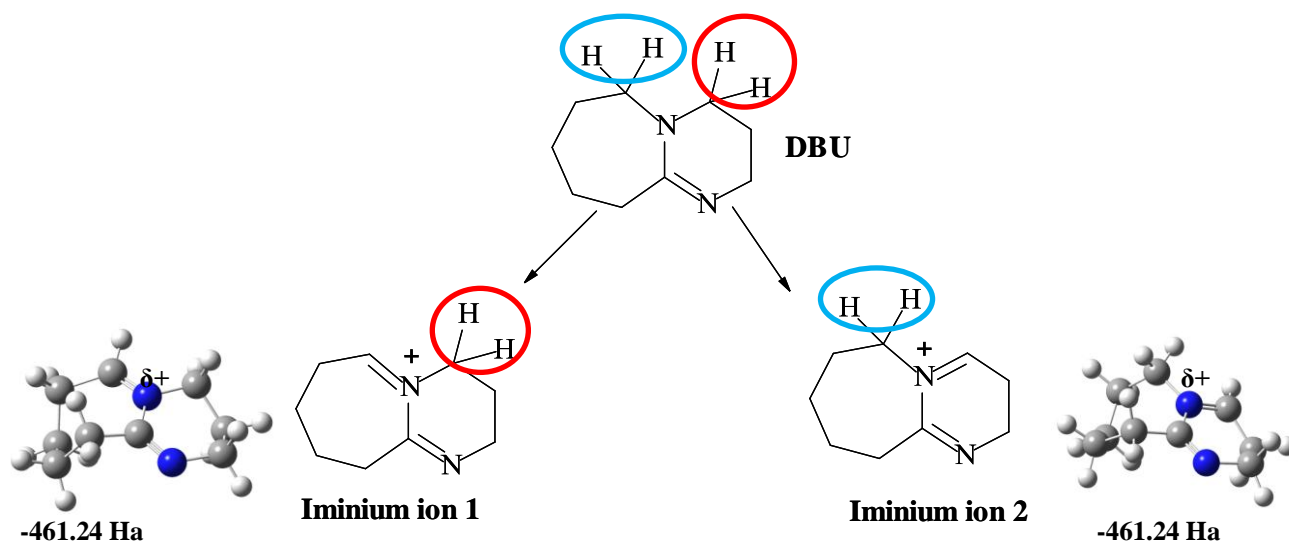
Figure 46. Structure of DBU and the two possible resonance-stabilised cationic species that could result following removal of a proton.

A relaxed surface energy scan was then carried out on the proposed transition state **TS3** involving OH⁻mediated deprotonation of the DBU moiety in the cationic component in the ion pair **TS2opt** (Figure 45) with the O-H bond (**i**) shortening and the N-S bond (**ii**) lengthening to facilitate release of the DBU (Figure 47). After 18 steps of the scan, the formation of H_2O and an ion-pair, comprising a mercaptobenzene anion and a DBU cation with the positive charge delocalised over the N-C-N bonds (**TS3scan1**), was observed. Interestingly after a further step, the formation of a bond between the positively charged carbon on the DBU moiety and the sulfur anion became apparent (**TS3scan2**), but no

transition state was observed. Geometry optimisation of **TS3scan2** showed that it was, in fact, a stable compound not an ion pair. Examination of structures **TS3scan1** and **TS3scan2** reveals that, in both cases, the sulfur atom is conveniently located to attack the terminal vinylic carbon, thus initiating cyclisation to the 4-hydroxythiochroman **217** (*via* conjugate addition) or to the thiochromene **202** (*via* conjugate addition-elimination or S_N' displacement of OH⁻). The HOMO and LUMO surfaces of **TS3scan2** shown in Figure 48 also show that the HOMO is poised in position with LUMO to form the thiochromene **202** with release of a DBU cation, a result that supports the mechanism proposed in Scheme 50.[6] While the transformation of the tight ion-pair **TS3scan1** to the thioether **TS3scan2** may be theoretically feasible, its formation is not supported by the experimental data, as such a product has yet to be isolated. Solvent separation of the tight ion-pair, however, should facilitate cyclisation of the mercaptobenzene anion.
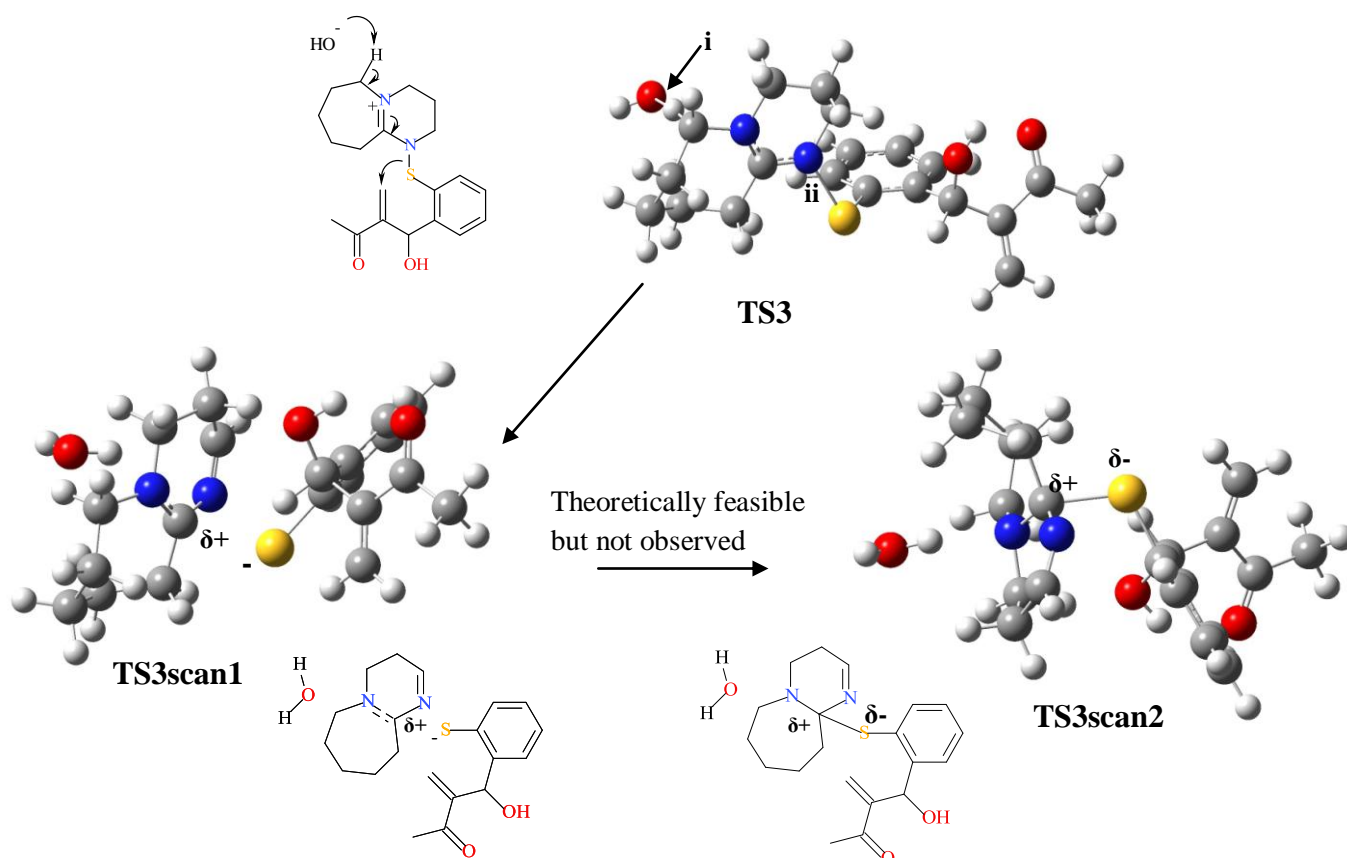
Figure 47. Structure of the proposed transition state **TS3**, showing the O-H (**i**) and N-S (**ii**) bonds scanned. **TS3scan1** shows the structure after 18 steps of a relaxed surface energy scan, while **TS3scan2** shows the structure after 19 steps.
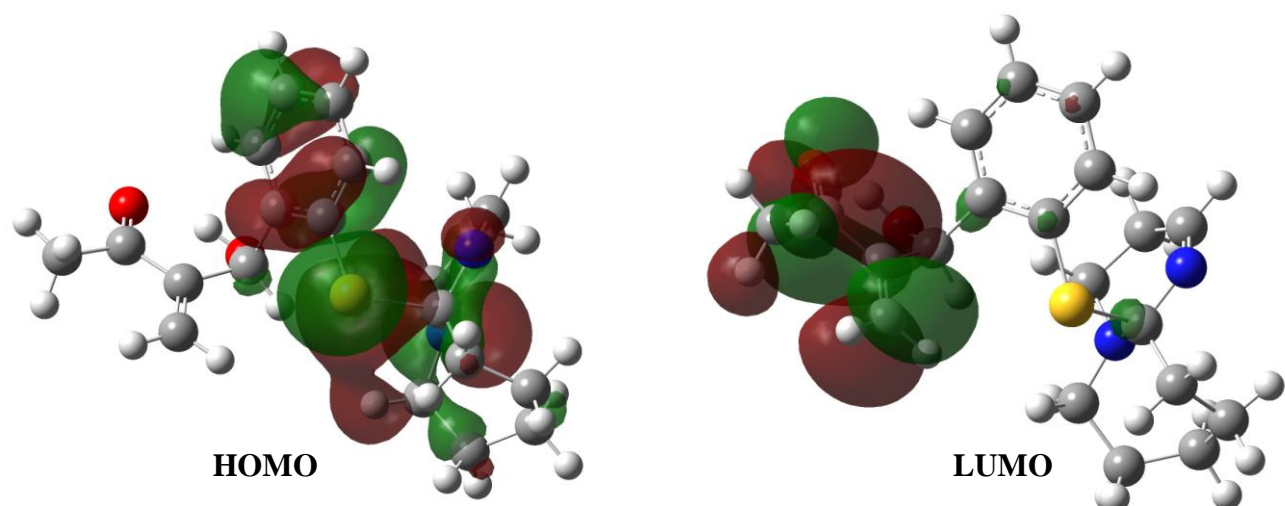
Figure 48. HOMO and LUMO surfaces for the **TS3scan2** structure.

2.1.5.2 Free energy profile for the MBH synthesis of 2H-1-benzothiopyrans

The calculated free-energy profile for the intermediates and products involved in the MBH reaction of 2,2'-dithiodibenzaldehyde with MVK, is illustrated in Figure 49. The transition states are not included at this point as attempts to locate them have, thus far, proved unsuccessful. The isolated products, thiochromene **202a** and the 4-hydroxythiochroman **217a**, are at lower energies than the starting material, 2,2'-dithiodibenzaldehyde **201**, as anticipated. From the experimental data (Figure 37), it seems that the 4-hydroxythiochroman **217**, while kinetically favoured is slowly converted to the thermodynamically more stable thiochromene **202** *via* the common precursor **231** (Scheme 55).
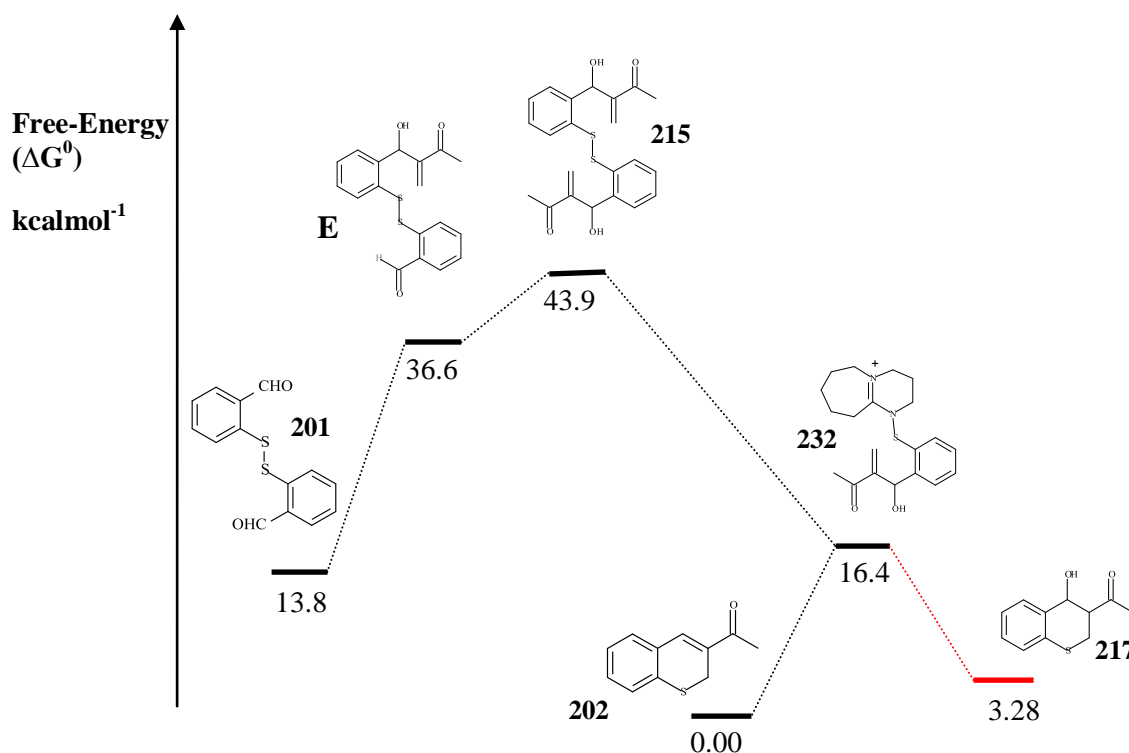
Figure 49. Effective mass balanced free-energy (ΔG^0) profile for intermediates and products in the reaction of 2,2'-dithiodibenzaldehyde **201** with MVK using DBU **69** as catalyst at the B3LYP/6-31G(d) level of theory.

The results from the kinetics experiments show that MVK is consumed at almost the same time as 2,2'-dithiodibenzaldehyde **201**. This is consistent with the MBH reaction occurring first, prior to cleavage of the S-S bond, which may well prove to be rate determining – an expectation consistent with the bis-MVK disulfide **215** being the highest energy species in the energy level diagram (Figure 49). This conclusion would account for the observed rate acceleration of the reaction when the dual-catalyst system (DBU/Ph$_3$P) is used. Ph$_3$P is known to effect cleavage of the S-S bond to the corresponding thiols in very good yields,[138,147-152] while, in the present study, DBU has been shown to be a much better MBH catalyst for this reaction. Hence, when the two catalysts are used together as a dual-catalyst system, a remarkable acceleration in the rate of the reaction is observed as the rate determining step involving S-S cleavage would be accelerated by the presence of Ph$_3$P, while MBH catalysis is efficiently carried out by DBU.

In summary, while key transition states have yet to be located, our study clearly supports the proposed mechanism[6] by demonstrating:-

i)   the capacity of DBU to cleave aryl and heteroaryl disulfides;

ii)   the sequence of major events, *i.e.* the MBH reactions precede disulfide cleavage;

iii) reasonable correspondence between the theoretical kinetic model and the experimental data;

iv)   the possibility of concerted cleavage and cyclisation processes; and

v)   the intrinsic thermodynamic stability of proposed intermediates.

2.2 Chromone derivatives: synthetic and mechanistic studies

Chromones are very interesting targets for organic chemists because they have been shown to possess a wide range of biological properties including anticancer,[156] antifungal,[157-159] antibacterial,[160,161] antitumor,[162,163] anti-inflammatory,[164] antallergic,[165] antimicrobial[166,167] and antiviral activities.[168] Chromones have been isolated from natural sources and examples include the styryl chromones, hormothamnione **261** and 6-desmethoxyhormothamnione **262**, isolated from the marine crytophyte *Chrysoplaeum taylori*.[162] These compounds possess antitumor activity against lymphocytic leukemia and HL-60 promyelocytic leukemia cell lines *in vitro*. Chromones are also effective metal ion chelators and play an important role in the initiation of free radical processes. Some drugs have been reported to show increased activity when administered as metal complexes rather than as organic compounds.[162,169-173] Examples of two chromone complexes **263** and **264** are shown below.[162]
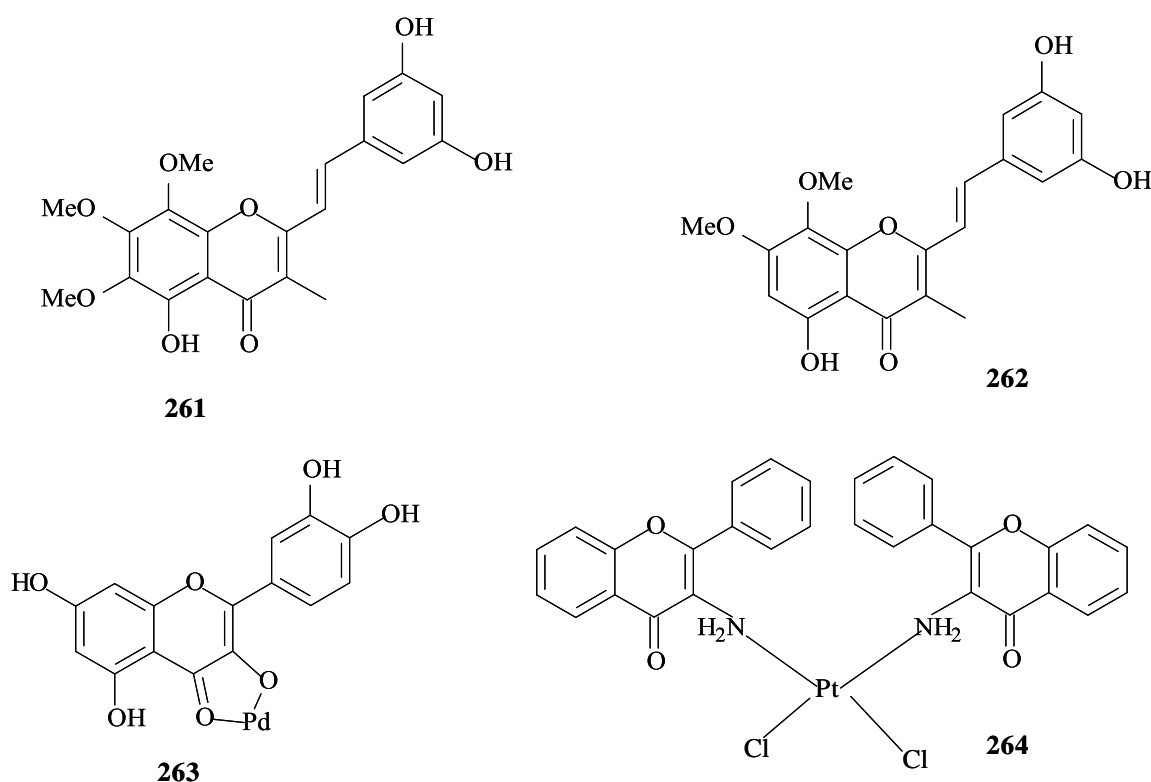
2.2.1. Vilsmeier-Haack synthesis of chromone-3-carbaldehydes

In this research, Vilsmeier-Haack methodology[174] has provided one-pot access to the substituted chromone-3-carbaldehydes **218a,b,e** in very good yields when the corresponding *o*-hydroxyacetophenones **265a-c** were treated with phosphorus oxychloride (POCl$_3$) in dry

DMF at -20 °C (Scheme 60).[174] The mechanism that has been proposed for this reaction is illustrated in Scheme 61. It is initiated by *in situ* reaction of POCl₃ with DMF to form the Vilsmeier-Haack "complex" **269**(**a-c**) with the tautomers **269b** and **269c** being predominant. Double formylation of the acetophenone enolate **270** by the Vielsmeier-Haack "complex" followed by hydrolysis affords the desired chromone-3-carbaldehydes **218a,b,e**.
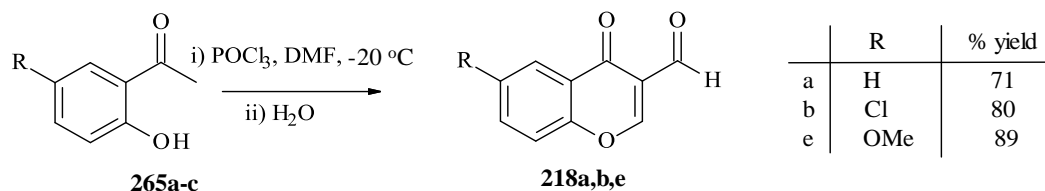
Scheme 60.
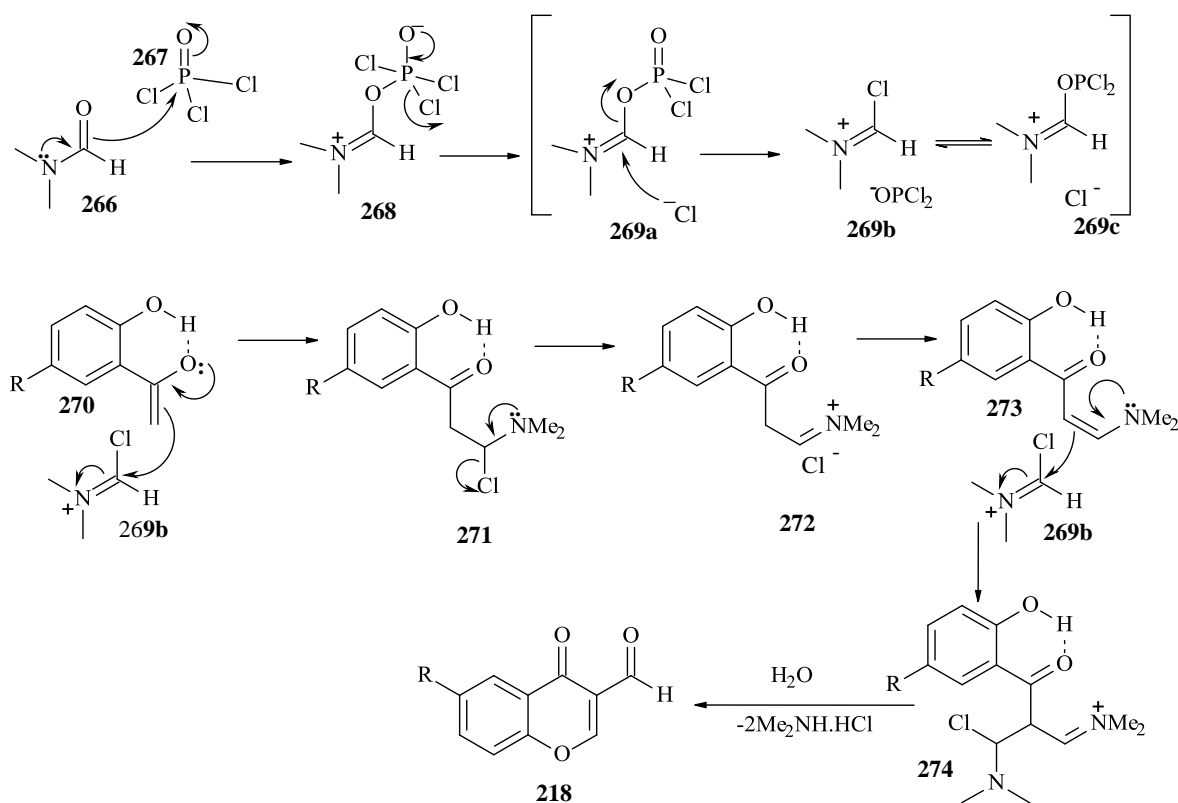
Scheme 61. Mechanism of the Vilsmeier-Haack methodology.[174]

Figures 50 and 51 show the ¹H NMR and ¹³C NMR spectra of compound **218a**, respectively. In the ¹H NMR spectrum the aldehyde proton resonates downfield at 10.33 ppm, the 2-methine proton as a singlet at 8.51 ppm, and the 6- and 8-methine protons as an overlapping doublet and triplet. In the ¹³C NMR spectrum all 10 of the expected carbon signals are accounted for, with the carbonyl signals at 175.8 and 188.5 ppm.
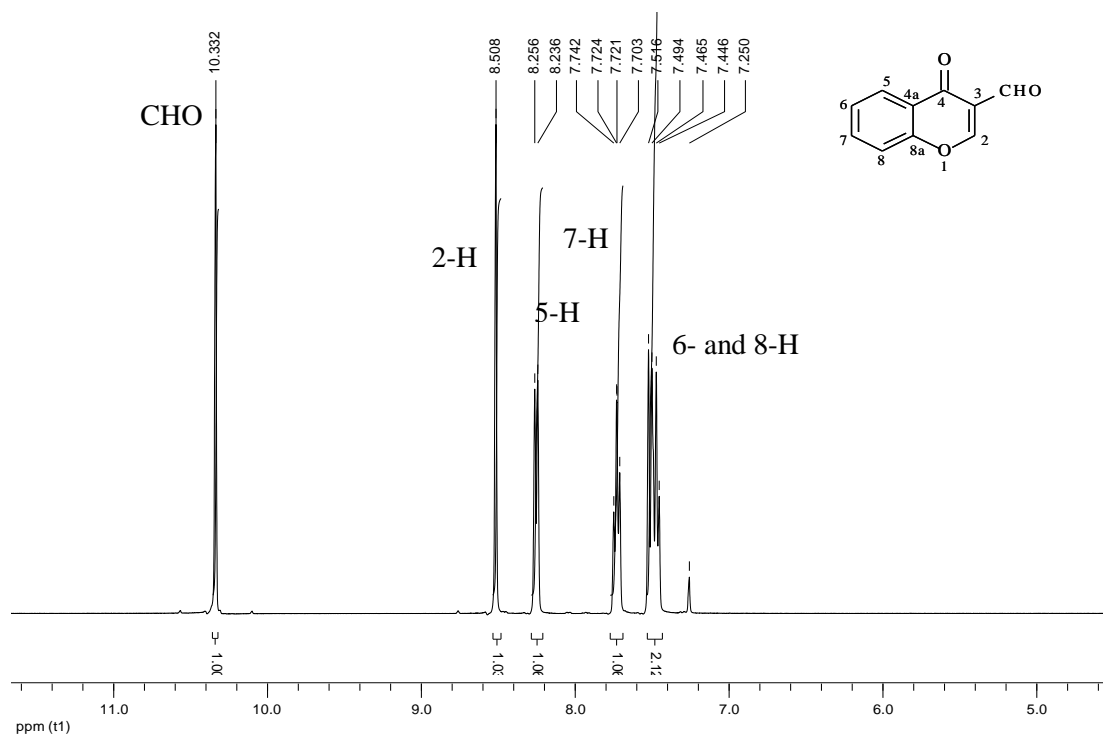
Figure 50. 400 MHz ^{1}H NMR spectrum of compound **218a** in CDCl$_3$.
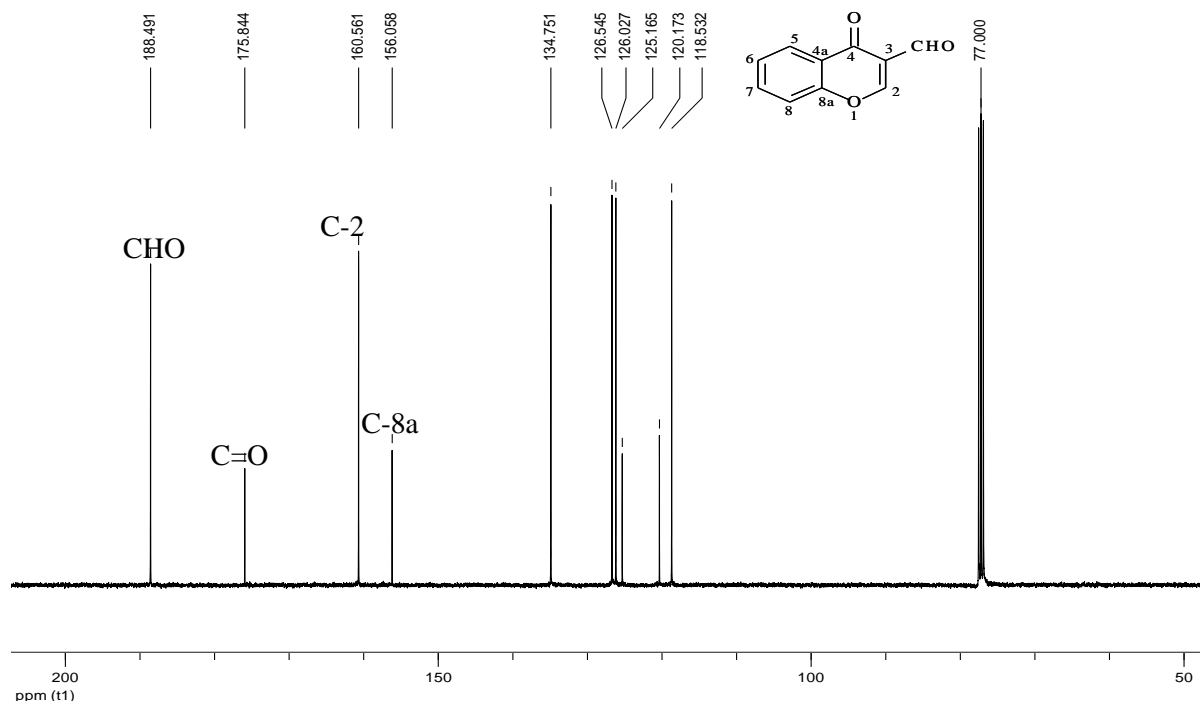
Figure 51. 100 MHz ^{13}C NMR spectrum of compound **218a** in CDCl$_3$.

2.2.2 Morita-Baylis-Hillman reactions of chromone-3-carbaldehydes with methyl vinyl ketone

In an earlier study, Molefe[79,80] had reacted substituted chromone-3-carbaldehydes with MVK and 3-HQ as catalyst in MBH-type reactions. Interestingly, as already mentioned in Section 1.2.1.2, work-up and column chromatography of the crude products failed to give the expected MBH adducts **219**. Instead, the chromone dimers **220** and the tricyclic derivatives **221** were obtained (Scheme 62). In order to explore the mechanistic sequences involved in the formation of these unexpected products, the reactions were repeated, using chromone-3-carbaldehyde **218a**, 6-chlorochromone-3-carbaldehyde **218b** and 6-methoxychromone-3-carbaldehyde **218e**. The corresponding chromone dimers **220a,b,e** and tricylic products **221a,b,e** were again obtained. The tricyclic derivatives were initially isolated as diastereomeric mixtures, which were subsequently separated using semi-preparative HPLC. Table 3 shows the yields of the isolated products.
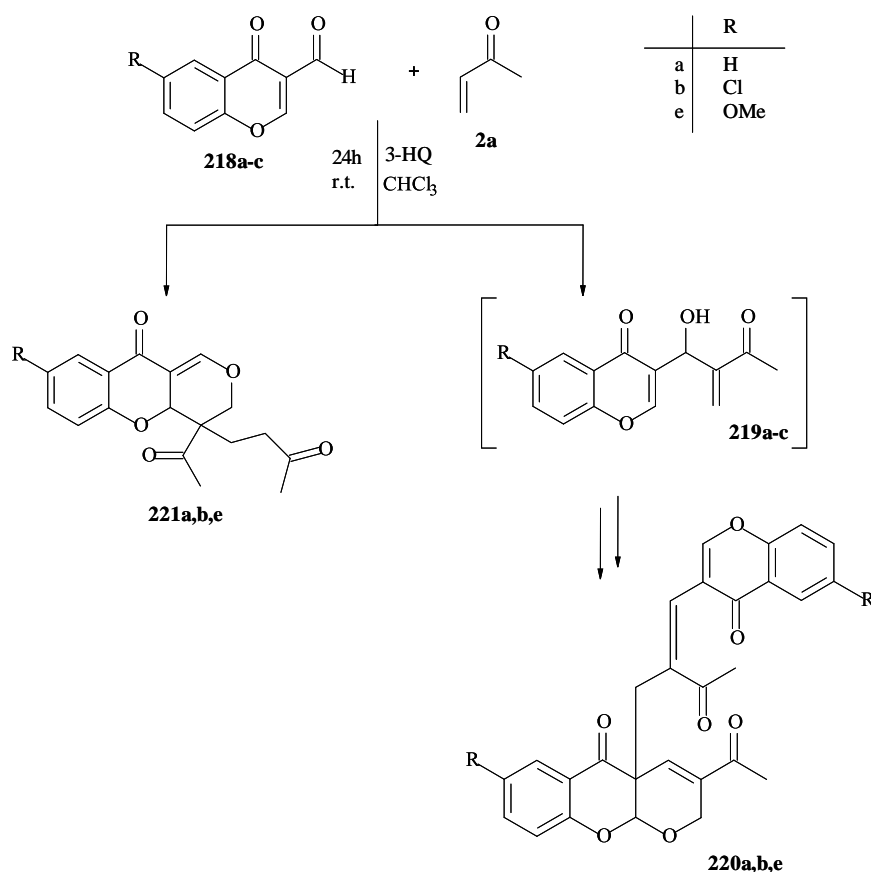
Scheme 62.

Table 3. Yields of the isolated chromone dimers and tricyclic products

Chromone-3-carbaldehyde	R	% Yield of dimer 220	% Yield of tricyclic product 221
218a	H	31	69 (3:1)[a]
218b	Cl	22	76 (4:1)[a]
218e	OMe	24	72 (3.5:1)[a]

[a] = Diastereomeric ratio

The dimers **220a,b,e** and the tricyclic adducts **221a,b,e** were fully characterised by IR, 1- and 2-dimensional NMR and HRMS analysis. The ^{1}H NMR spectrum of the chromone dimer **220a** (Figure 52) shows two singlets at 2.29 and 2.42 ppm corresponding to the 12- and 16-methyl protons. The 13-methylene protons resonate as a singlet at 3.23 ppm, and the 2-methylene protons as a doublet of doublets at 4.52 ppm. A singlet at 5.00 ppm corresponds to the 9a-methine proton, and all the aromatic protons are accounted for. The ^{13}C NMR spectrum (Figure 53) reveals all 28 expected carbon signals. The four carbonyl carbons appear downfield at 175.6, 191.5, 196.9 and 199.0 ppm, while the quaternary carbon (C-4a) resonates at 50.1 ppm and the 9a-methine carbon at 99.8 ppm. Signal assignments were facilitated using the DEPT 135, COSY, HSQC and HMBC spectra.
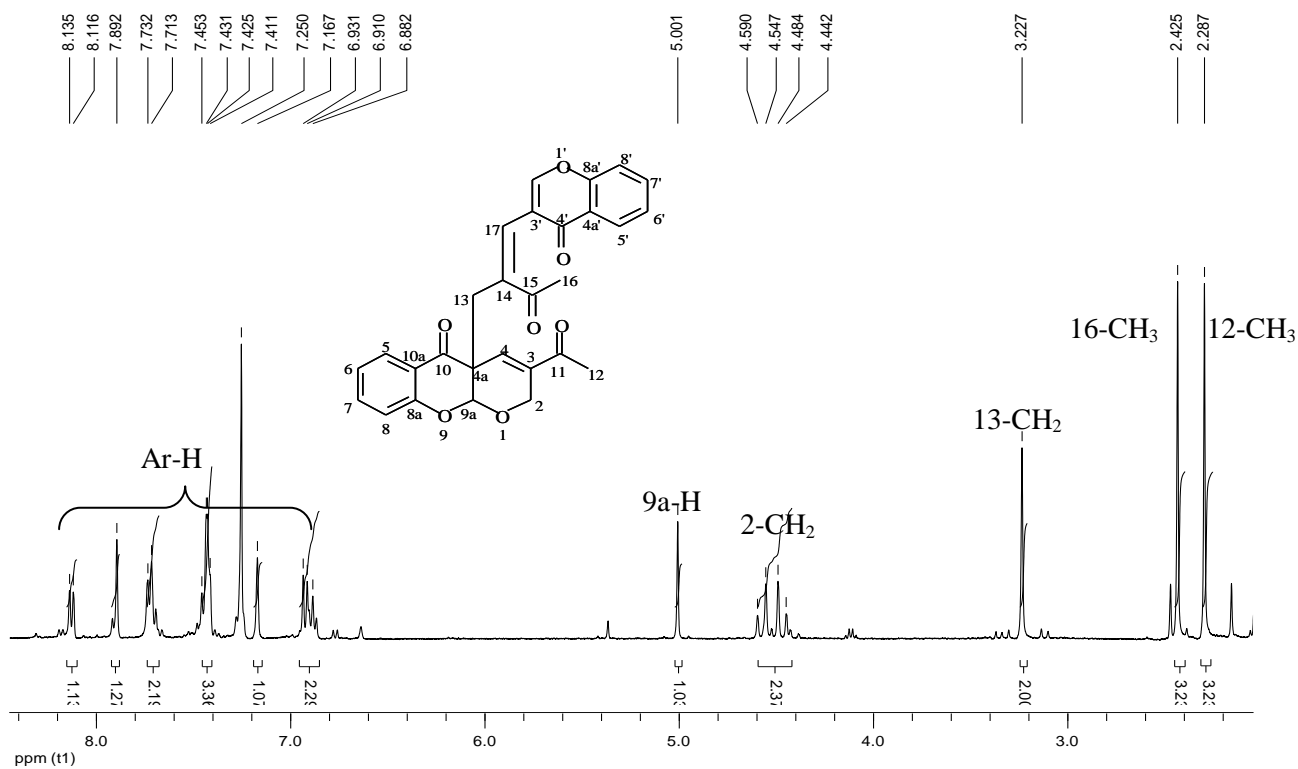
Figure 52. 400 MHz ^{1}H NMR spectrum of the chromone dimer **220a** in CDCl$_3$.
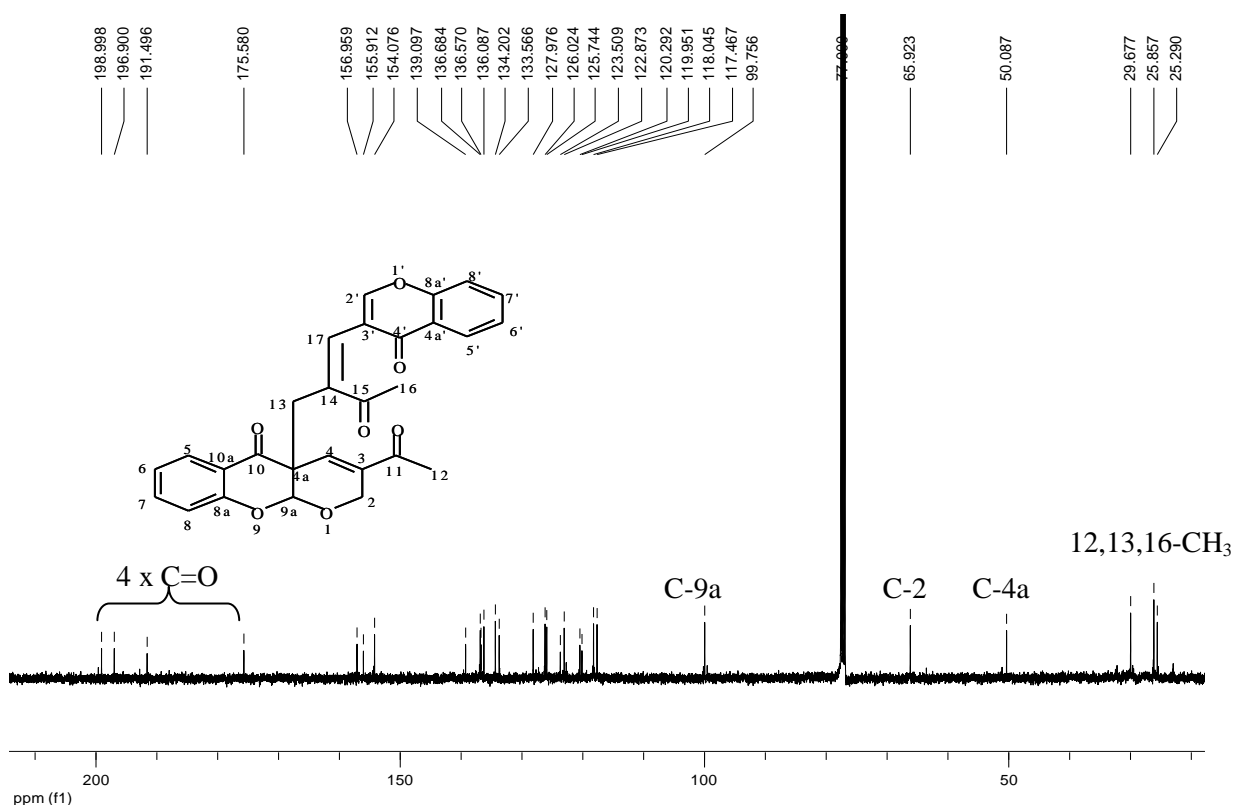
Figure 53. 100 MHz ^{13}C NMR spectrum of the chromone dimer **220a** in CDCl$_3$.

Figures 54 and 55 illustrate the ^{1}H NMR spectra of the major and minor diastereomers of the tricyclic products **221a$_1$** and **221a$_2$**, respectively. In Figure 54, the 12- and 16-methyl protons resonate as singlets at 2.07 and 2.39 ppm, the diastereotopic 13- and 14-methylene protons as multiplets at 1.98, 2.25, 2.40 and 2.60 ppm, the 10-methylene protons as a doublet of doublets at *ca.* 4.70 ppm, while the 8a-methine singlet appears at 5.14 ppm. Comparison of the ^{1}H NMR spectra of the two diastereomers reveals three main differences:- i) the splitting patterns of the 13- and 14-methylene protons suggest significant geminal coupling of diastereotopic protons in the major diastereomer (**221a$_1$**) but not in the minor diastereomer (**221a$_2$**); ii) the 8a-methine signal is further downfield at 5.42 ppm in compound **221a$_2$** compared to 5.14 ppm in **221a$_1$**; and iii) the 2-vinylic proton signal for **221a$_1$** is downfield (7.30 ppm) relative to the corresponding signal for **221a$_2$** (6.69 ppm). The relative stereochemical configurations at the stereogenic centres 8a and 9 are responsible for these observed differences. The ^{13}C NMR spectrum of the major diastereomer **221a$_1$** (Figure 56) shows 18 signals, accounting for all the expected nuclei. The 12- and 16-methyl carbons resonate at 25.5 and 30.0 ppm, while the 13- and 14-methylene carbons resonate at 24.9 and 37.8 ppm, the C-10 methylene nucleus at 65.9 ppm, the 8a-methine nucleus at 99.9 ppm and the three carbonyl carbons at 192.6, 196.6 and 206.7 ppm. The analytical data for the dimers **220** and the tricyclic adducts **221** prepared in the present study are consistent with those reported previously.[79,80,175] Formation of the chromone dimers **220a-c** has been presumed to proceed *via* the MBH adduct **219** (Scheme 63). Two molecules of the MBH adduct react with each other to give an intermediate **275**. Intramolecular cyclisation *via* an S$_N$2' or conjugate addition-elimination pathway resulting from attack of the hemi-acetal hydroxyl oxygen on the α,β-unsaturated carbonyl moiety, as illustrated in structure **275'**, affords the chromone dimers **220**. Formation of the tricyclic adducts **221** has been rationalised in terms of the mechanistic sequence outlined in Scheme 64. Thus, reaction of the catalyst with MVK results in the formation of the zwitterion **276**, which then attacks the chromone-3-carbaldehyde **218** at position 2 to afford the intermediate **277**; proton transfer and elimination of the catalyst then yields another intermediate **278**. Cyclisation of intermediate **278** *via* intramolecular conjugate addition and a tandem, intermolecular Michael reaction pathway, involving a second molecule of MVK, finally leads to the formation of the tricyclic products **221**.
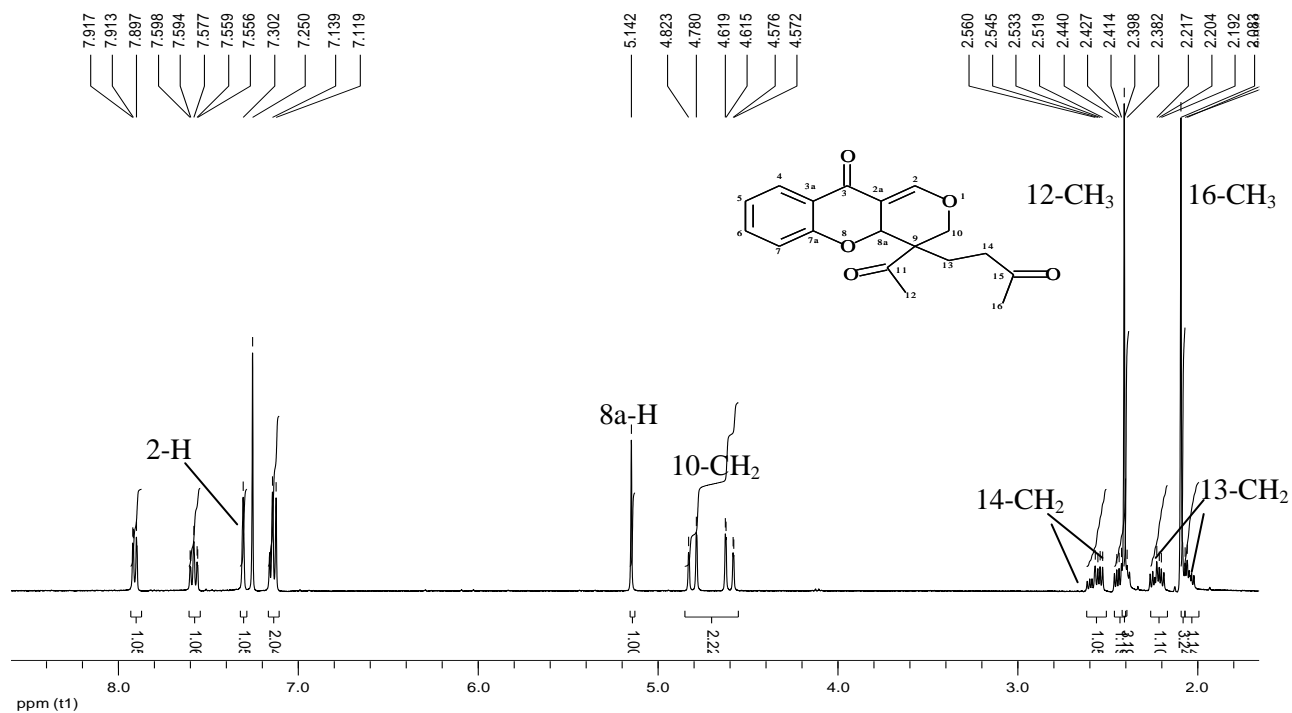
Figure 54. 400 MHz ^{1}H NMR spectrum of the tricyclic product **221a$_1$** in CDCl$_3$.
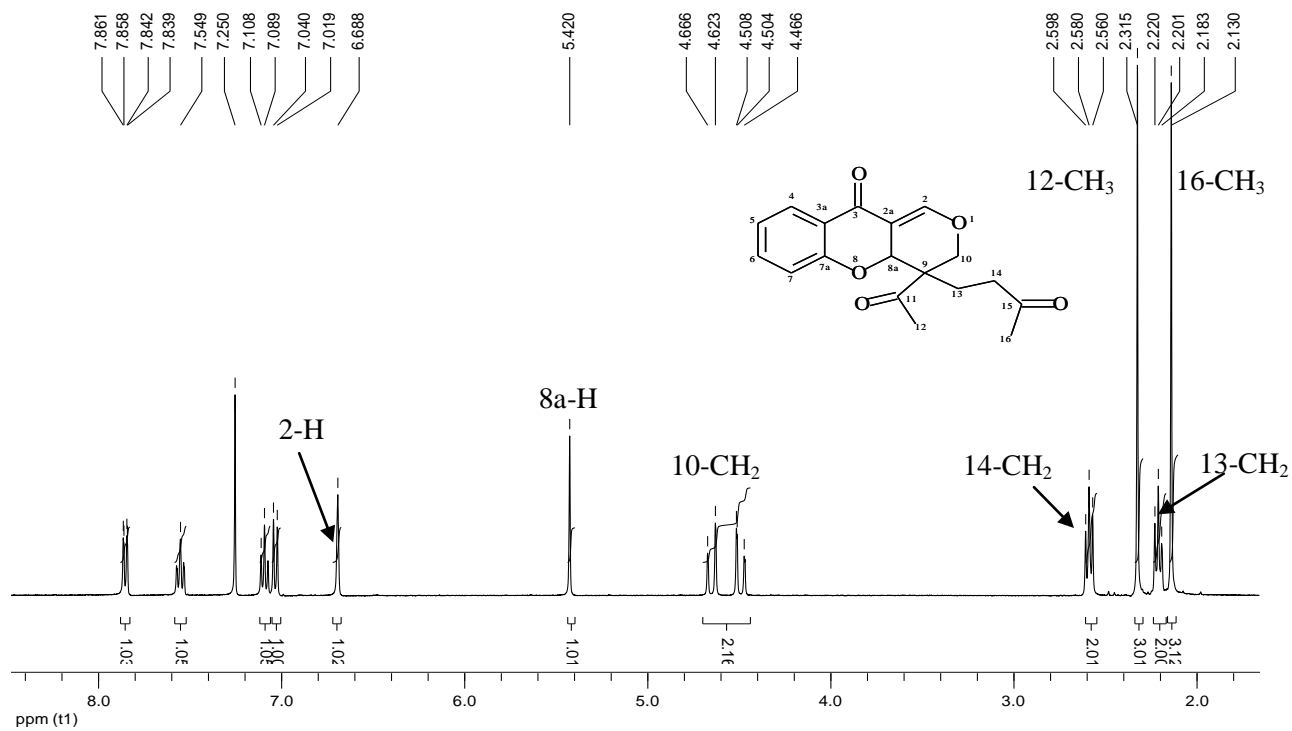
Figure 55. 400 MHz ^{1}H NMR spectrum of the tricyclic product **221a$_2$** in CDCl$_3$.
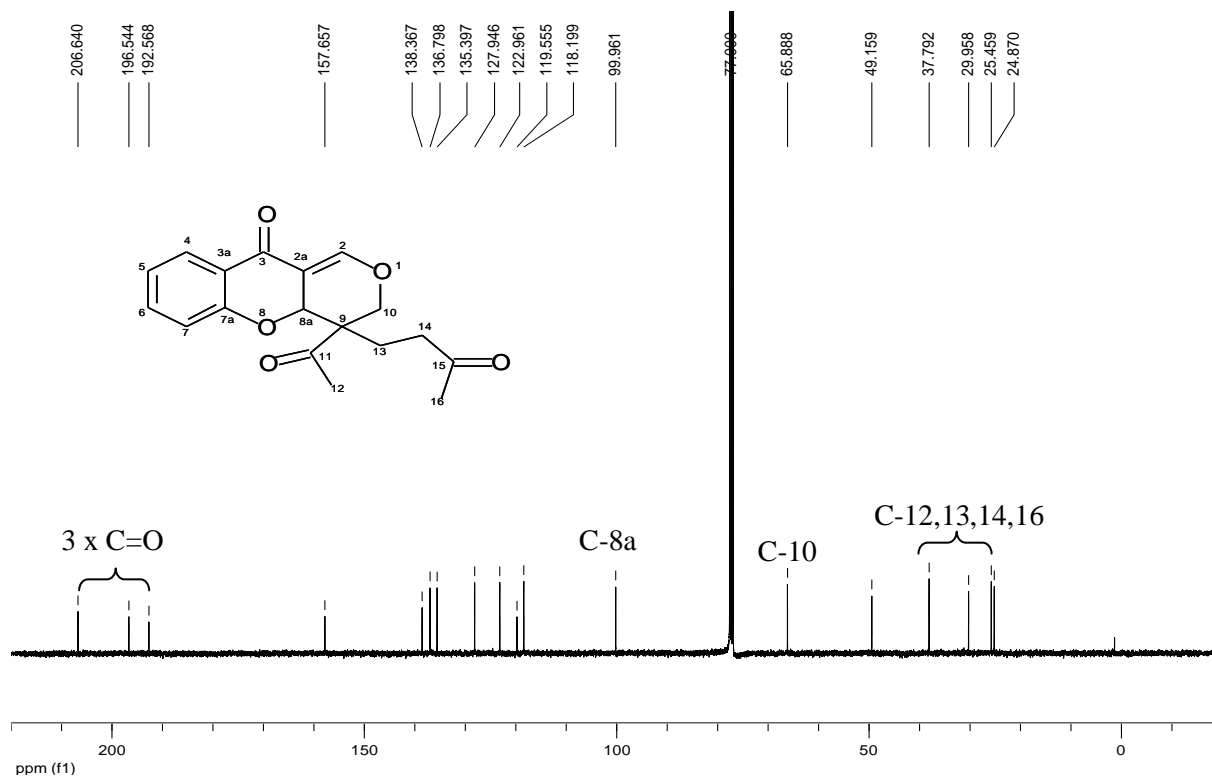
Figure 56. 100 MHz ^{13}C NMR spectrum of the tricyclic derivative **221a$_1$** in CDCl$_3$.
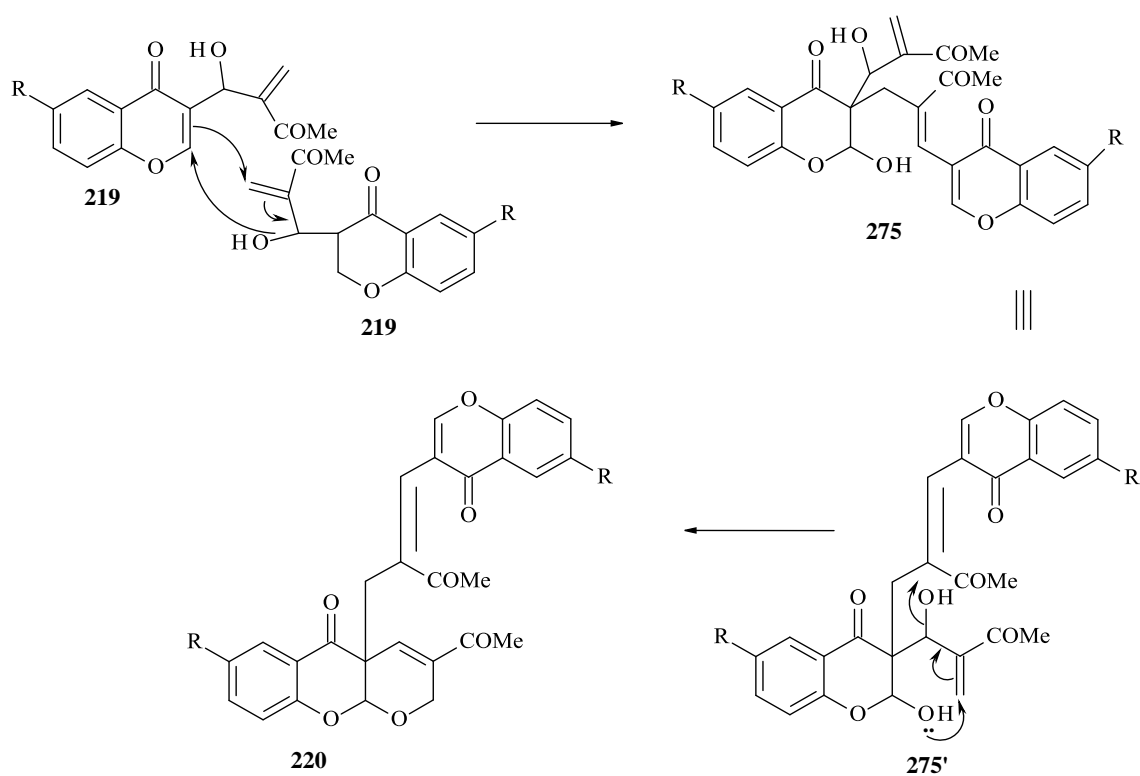
Scheme 63. Proposed mechanistic sequence for the formation of the chromone dimers **220a-c**.
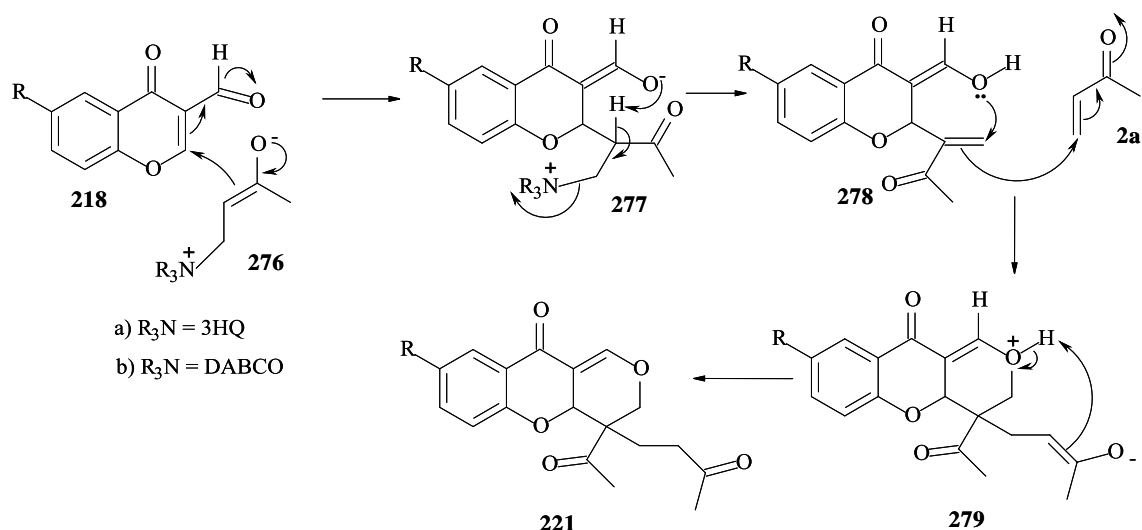
Scheme 64. Proposed mechanistic sequence for the formation of the tricyclic products **221a-c**.

2.2.3 Kinetic study of the Morita-Baylis-Hillman reactions of chromone-3-carbaldehydes with methyl vinyl ketone

Having prepared and characterised the reactants and products from these unusual reactions attention could be given to a detailed investigation of the reaction kinetics and mechanism.
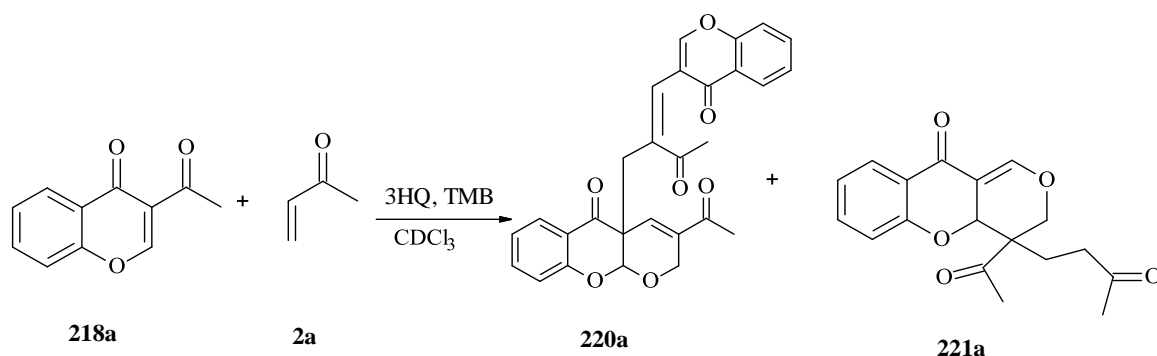
Scheme 65.

Kinetic experiments were set up for the MBH reaction of chromone-3-carbaldehyde **218a** with MVK as shown in Scheme 65. All kinetic runs were carried out in CDCl$_3$ with 1,3,5-trimethoxybenzene (TMB) as an internal standard. Proton integral ratios of the selected signals indicated in the stacked ^{1}H NMR plot of the progress of the reaction, were converted to concentrations using the formula shown earlier in Section 2.1. For the first experiment (Experiment 1), the molar ratios of the reactants, chromone-3-carbaldehyde:MVK:3HQ were

1:3:3, respectively. The results from Experiment 1 are illustrated in Figures 57 and 58. Figure 57 shows the stacked ^{1}H NMR spectra at 300 s intervals. Signals corresponding to chromone-3-carbaldehyde **218a**, MVK, the chromone dimer **220a**, the tricyclic product **221a**, 3-HQ and the internal standard TMB were followed. The concentration *vs* time graph of the reaction (Figure 58) shows clearly the depletion of the chromone-3-carbaldehyde (CHO-1) and MVK (MVK1), with the formation of the chromone dimer (C-Dimer) and the tricyclic product (Tri-2). Also evident is the presence of an intermediate species which is formed and consumed quite rapidly; it appears from Figure 58 that the concentration of this intermediate species reaches a maximum at *ca.* 2 500 s. With the aim of isolating this intermediate, the reaction of chromone-3-carbaldehyde with MVK was repeated for just 30 minutes. Work up and column chromatography followed by semi-preparative HPLC gave three products *viz.,* the chromone dimer **220a**, the tricyclic product **221a** and the novel MBH adduct **219a** in rather low yields. In the proposed mechanism for the formation of the chromone dimers outlined in Scheme 63, the MBH adduct **219** was presumed to be the precursor responsible for their formation, and its isolation confirms this presumption. The very low concentrations of the MBH adduct even at the expected maximum concentration seems to suggest its high reactivity in forming the dimeric products.
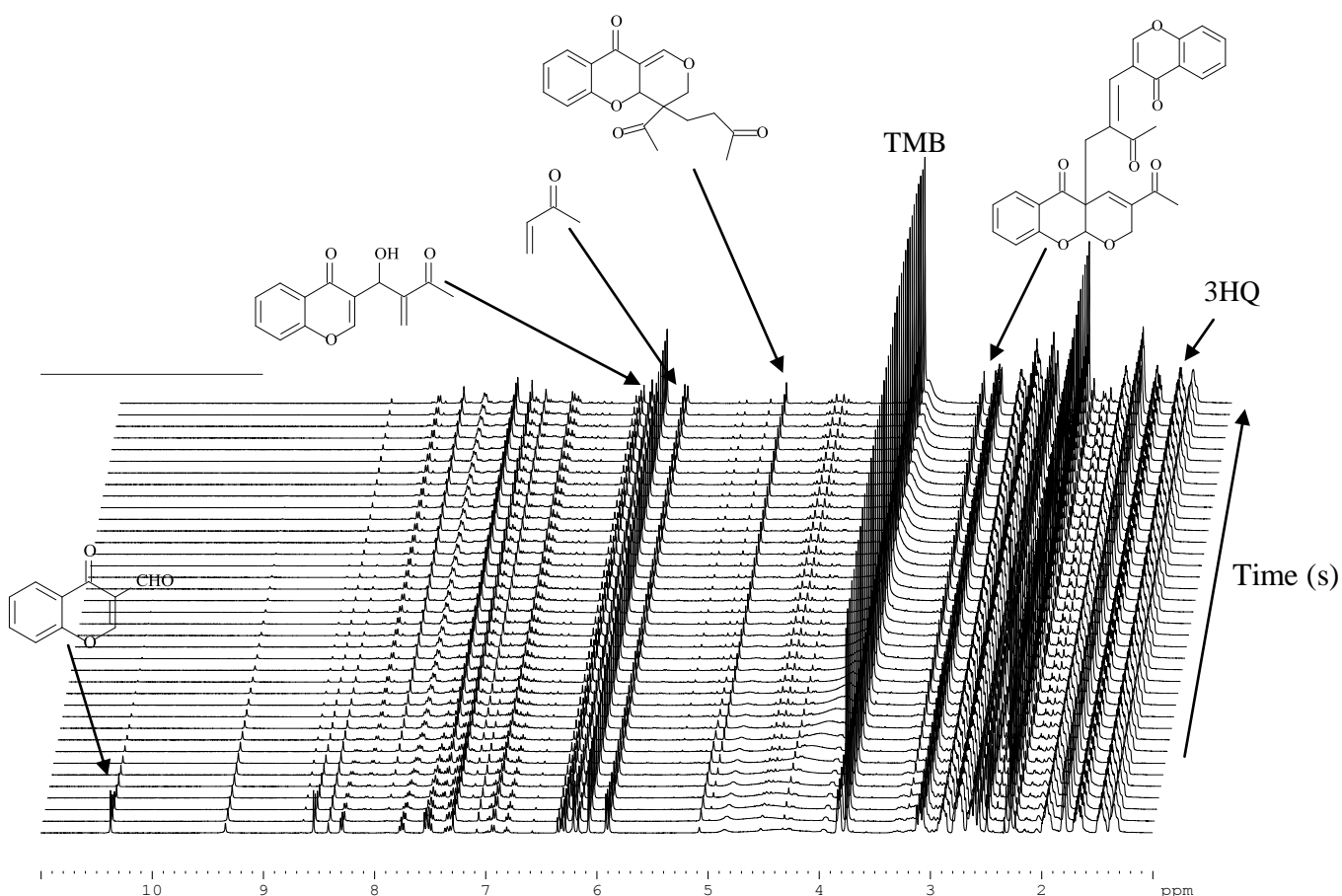
Figure 57. Stacked ¹H NMR spectra of the progress of the reaction between chromone-3-carbaldehyde **218a** and MVK. Shown are the selected signals and the corresponding species. Time interval: 300 s.
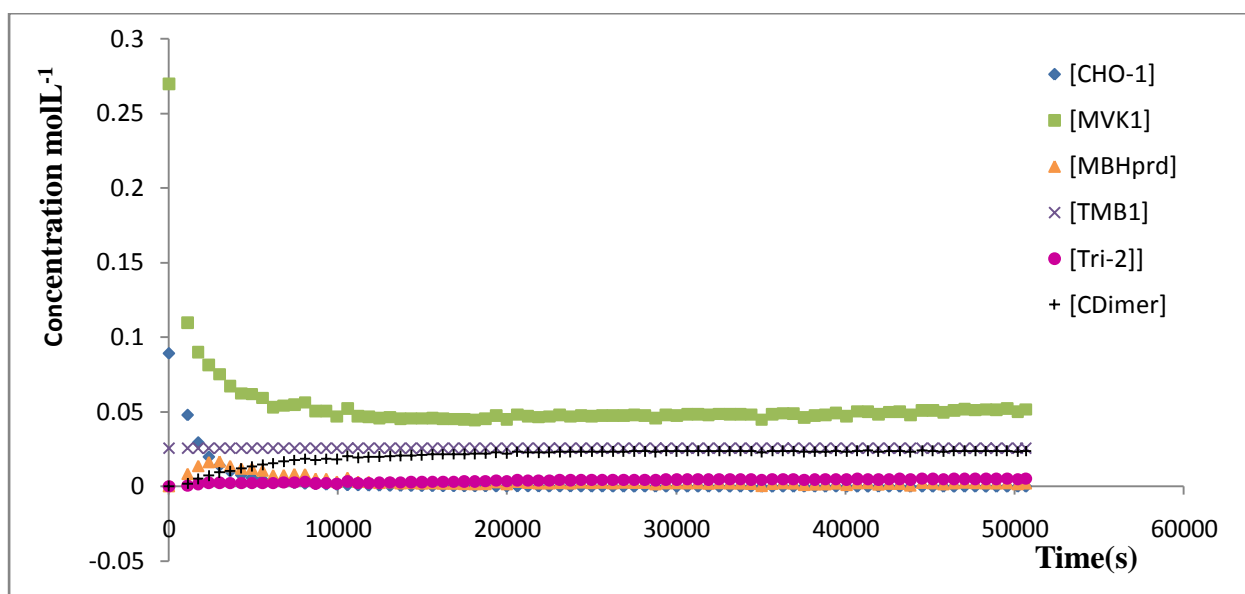
Figure 58. Concentration *vs* time graph showing progress of the reaction between chromone-3-carbaldehyde **218a** and MVK in Experiment 1, monitored using ¹H NMR integral data for selected signals corresponding to chromone-3-carbaldehyde **218a** (CHO-1), MVK (MVK1), tricyclic product **221a** (Tri-2), chromone dimer **220a** (C-Dimer) and the intermediate **219a** (MBHprd).

Figure 59 shows the ^{1}H NMR spectrum of the MBH adduct **219a**. The three characteristic MBH signals corresponding to the vinylic and 1'-H protons are quite evident at 5.85, 5.91 and 6.19 ppm and appear, as usual, as singlets. The methyl protons resonate at 2.35 ppm and all the aromatic protons are accounted for.
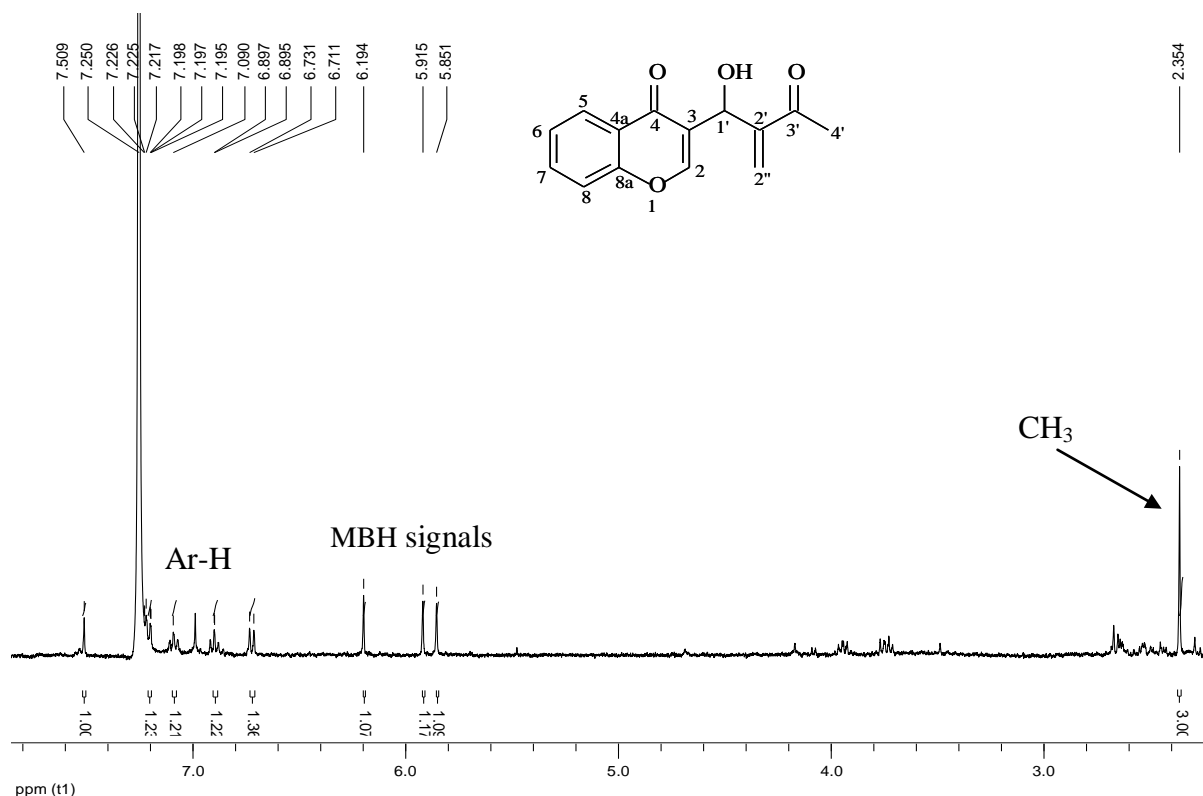
Figure 59. 400 MHz ^{1}H NMR spectrum of the MBH adduct **219a** in CDCl$_3$.

Experiments 2-4 were then set up with varying concentrations of MVK, and each experiment was conducted in duplicate. Table 4 shows the molar ratios of the reactants used in all four experiments.

Table 4: Molar ratios of reactants used in Experiments 1-4.

Expt#	Chromone-3-carbaldehyde **218a**	MVK	3HQ
Experiment 1	1	3	3
Experiment 2	1	1.5	3
Experiment 3	1	6	3
Experiment 4	1	9	3

The results obtained show that the concentration of MVK affects the rate of the overall reaction, with Experiment 2 being generally much slower than Experiment 1. Figure 60 shows the concentration *vs* time graph for the reaction when MVK concentration was halved (Experiment 2), and it is evident that the MVK has been consumed leaving some unreacted chromone-3-carbaldehyde **218a**. When the concentration of MVK was doubled (Experiment 3) (Figure 61), the consumption of the aldehyde was much faster than in both Experiments 1 and 2. The chromone-3-carbaldehyde **218a** was, in fact, fully consumed in just over 2 000 s, compared to over 7 000 s in Experiment 1 and incomplete consumption even after 50 000 s in Experiment 2. When the MVK concentration was trebled (Experiment 4), the reaction was even faster (Figure 62).

Two molecules of MVK were presumed to be required for the fomation of the tricyclic products **221**, while one molecule of MVK was required for formation of the chromone dimers **220**. In fact, MVK is involved in three separate transformations and, for complete consumption of the aldehyde **218a** would be required in at least a 3-fold molar excess. Hence when 1.5 equivalents of MVK are used (Experiment 2; Figure 60), the reaction does not go to completion, but when excess MVK is used the reaction is much much faster and the aldehyde is consumed almost instantly (Experiment 4; Figure 62); see Figure 63 for a more informative expansion of the low concentration data.
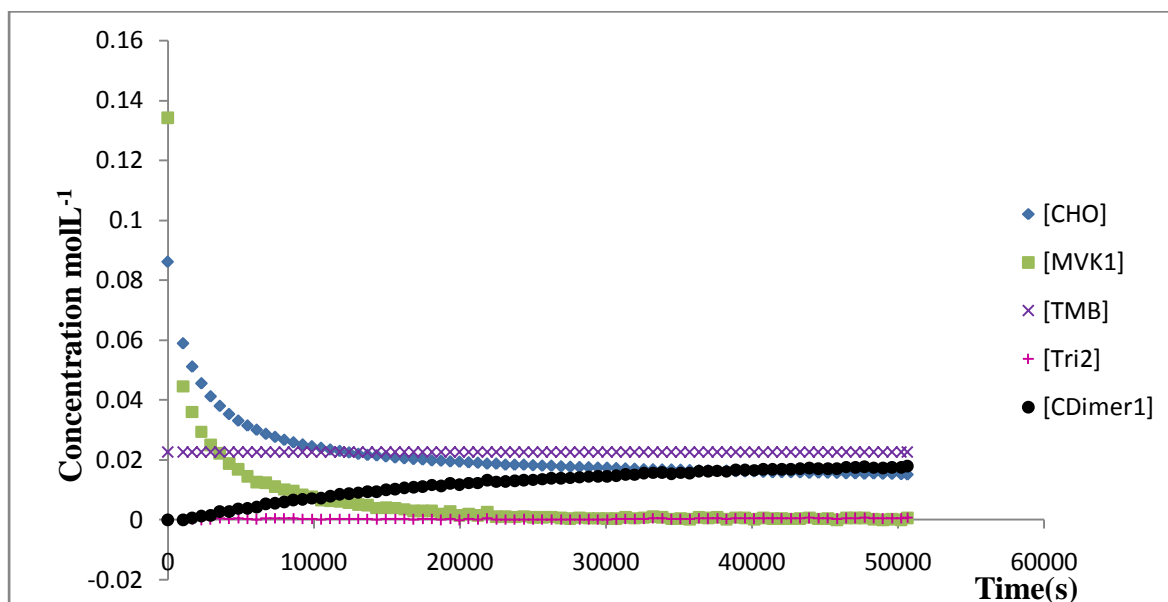
Figure 60. Graph showing progress of the reaction between chromone-3-carbaldehyde **218a** and MVK in Experiment 2, monitored using ^{1}H NMR integral data for selected signals corresponding to chromone-3-carbaldehyde **218a** (CHO), MVK (MVK1), tricyclic product **221a** (Tri2), chromone dimer **220a** (C-Dimer1) and the internal standard (TMB).
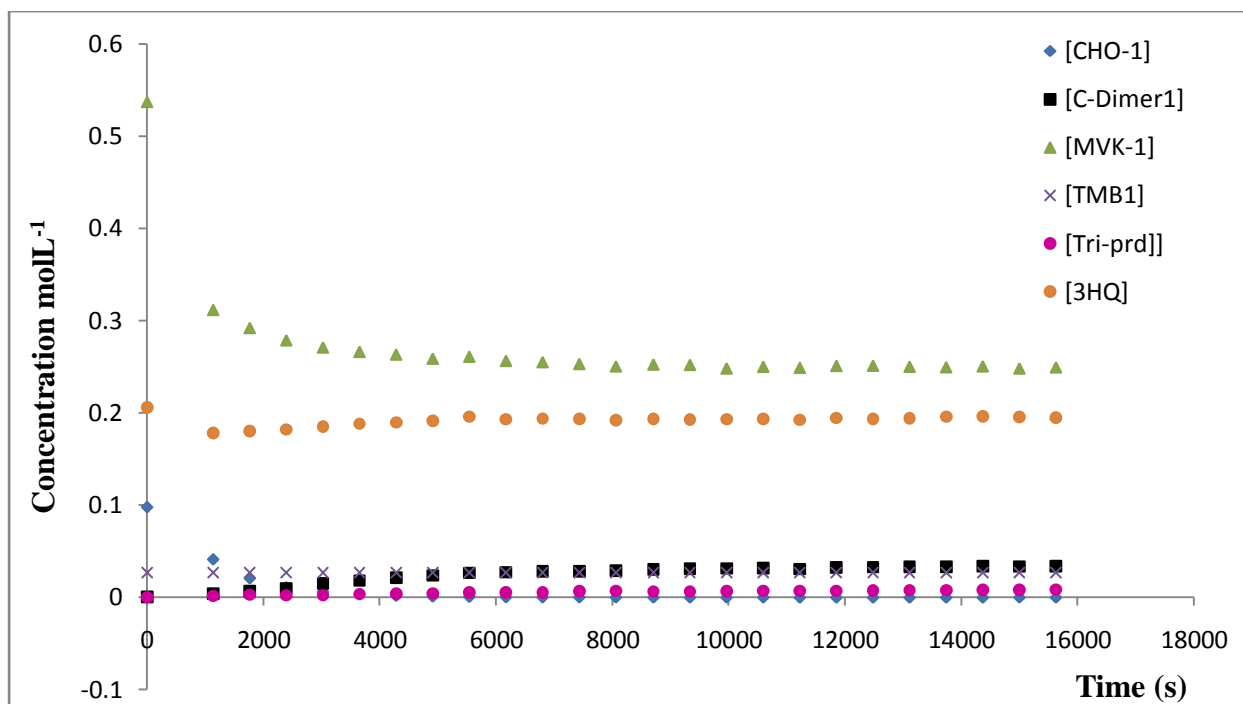
Figure 61. Graph showing progress of the reaction between chromone-3-carbaldehyde **218a** and MVK in Experiment 3, monitored using ^{1}H NMR integral data for selected signals corresponding to chromone-3-carbaldehyde **218a** (CHO-1), MVK (MVK-1), tricyclic product **221a** (Tri-prd), chromone dimer **220a** (C-Dimer1).
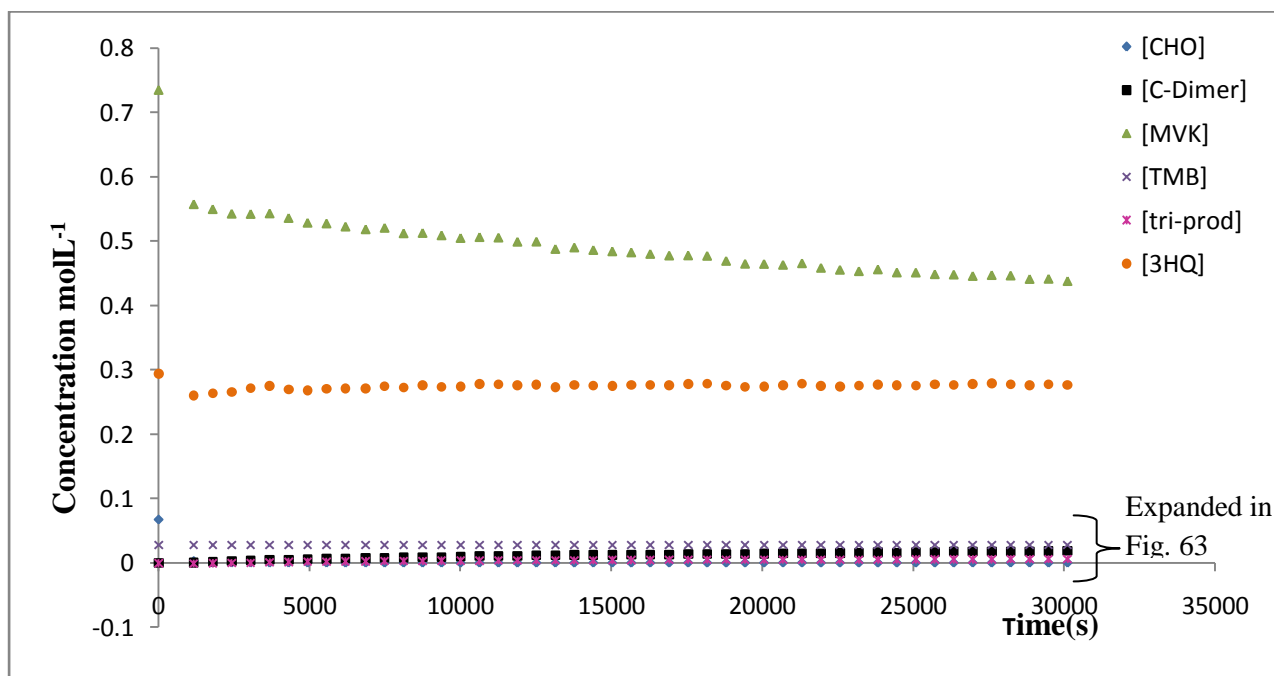
Figure 62. Graph showing progress of the reaction between chromone-3-carbaldehyde **218a** and MVK in Experiment 4, monitored using ^{1}H NMR integral data for selected signals corresponding to chromone-3-carbaldehyde **218a** (CHO), MVK, tricyclic product **221a** (tri-prod), chromone dimer **220a** (C-Dimer) and 3HQ.
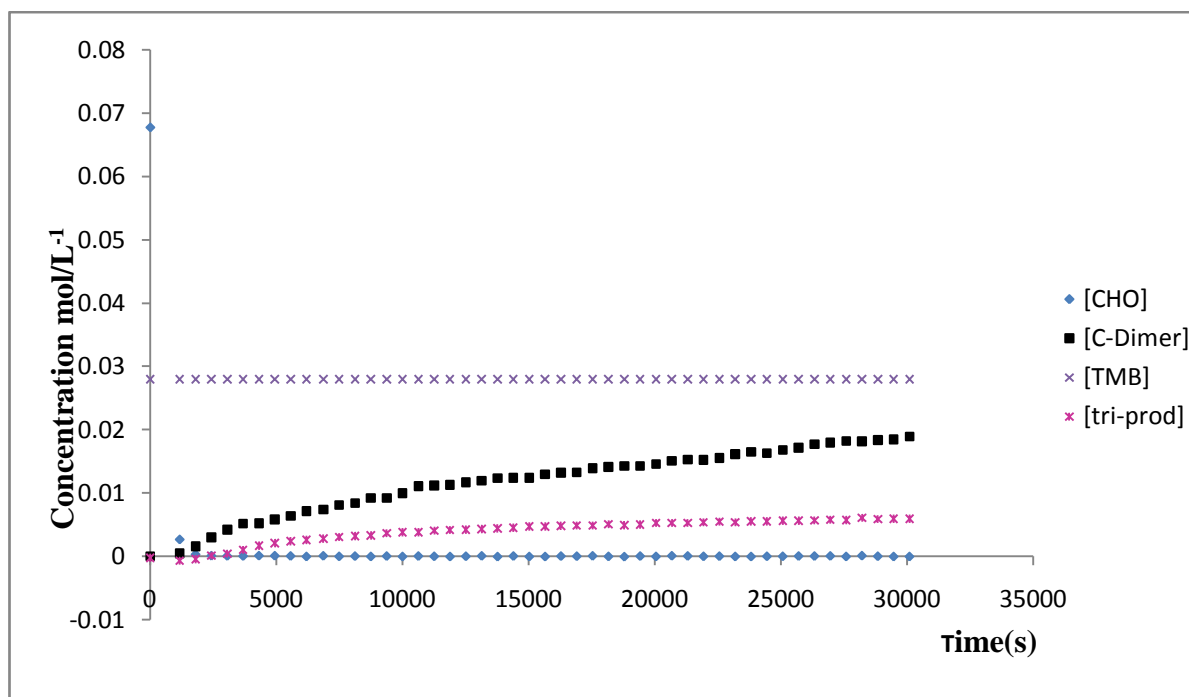
Figure 63. Expanded lower section of Figure 62. Shown are the curves for chromone-3-carbaldehyde **218a** (CHO), tricyclic product **221a** (tri-prod), chromone dimer **220a** (C-Dimer) and TMB.

For first-order reactions the rate expression is:

$$\text{Rate} = -\frac{d[\text{reactant}]}{dt} = k[\text{reactant}] \quad\quad\quad (20)$$

The simplified integrated rate equation becomes

$$\ln[\text{reactant}] = -akt + \ln[\text{reactant}]_o \quad\quad\quad (21)$$

A plot of ln[reactant] *vs* t should give a straight line with gradient −ak and y-intercept equal to the logarithm of the initial concentration of reactant ln[reactant]$_o$. The corresponding second-order rate expressions are shown in Equations 22 and 23, and a plot of 1/[reactant] *vs* t should give a straight line with a gradient equal to k and 1/[reactant]$_o$ as the y-intercept.

$$\text{Rate} = -\frac{d[\text{reactant }]}{dt} = k[\text{reactant}]^2 \quad\quad\quad (22)$$

$$\frac{1}{[\text{reactant }]} = akt + \frac{1}{[\text{reactant }]_0} \quad\quad\quad (23)$$

When first- and second-order graphs were plotted for the consumption of both the chromone-3-carbaldehyde **218a** and MVK for Experiments 1-4, it was evident that chromone-3-carbaldehyde follows first-order kinetics (Figure 64), while MVK follows second-order

kinetics, (Figure 65). However, because two competing reaction pathways are involved, these results could not be used to directly derive the rate expressions.
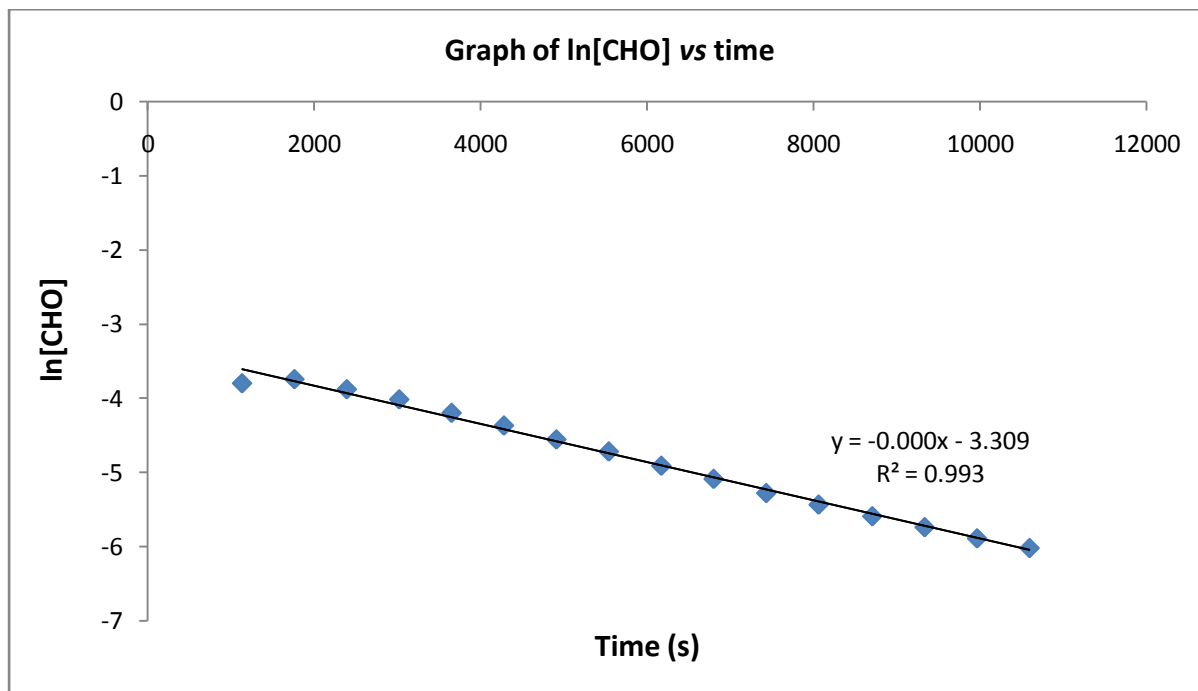
Figure 64. First-order plot for the consumption of chromone-3-carbaldehyde **218a** (CHO)
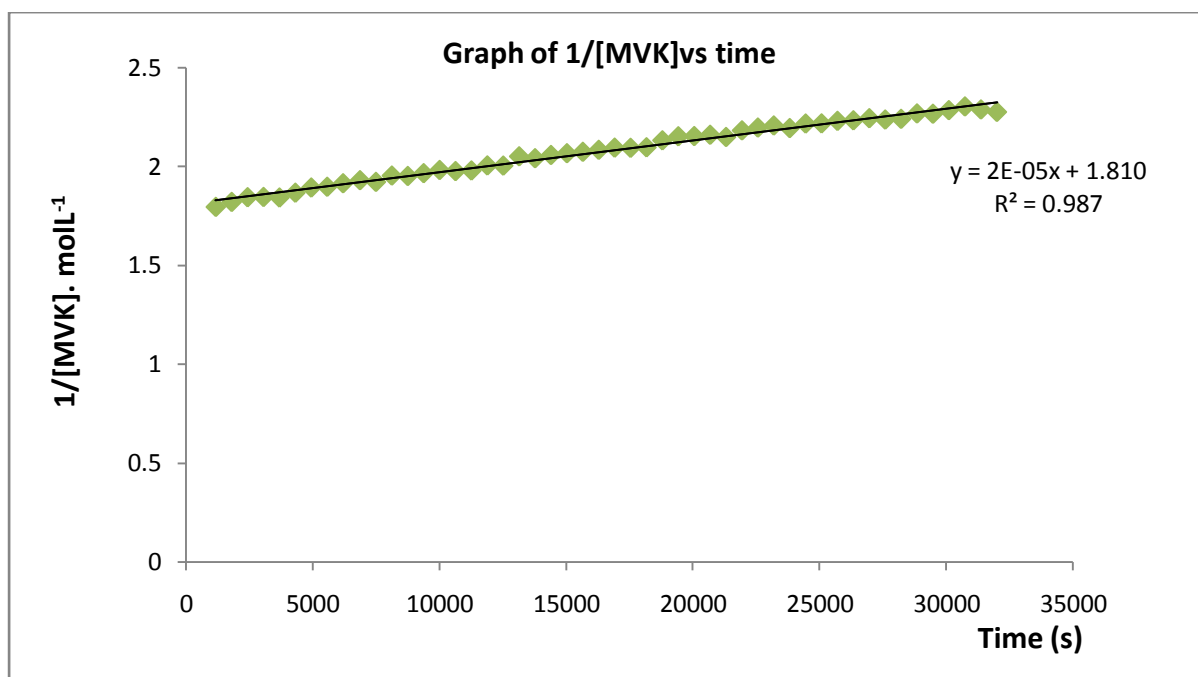
Figure 65. Second-order plot for the consumption of MVK.

Based on the experimental kinetic data and the proposed mechanisms for the formation of both the chromone dimers **220** and the tricyclic derivatives **221**, a theoretical model was proposed to model the transformations involved in the reaction of chromone-3-carbaldehyde **218a** with MVK. Scheme 66 summarises the theoretical model with the consecutive transformations (**ii**) and (**iii**) and the competing pathway (**i**). The reactants and products were assigned letters **A**-**E**, [chromone-3-carbaldehyde **218a** (**A**), MVK (**B**), tricyclic product **221a** (**C**), MBH adduct **219a** (**D**) and the chromone dimer **220a** (**E**)]. Rate expressions were derived for the proposed transformations (**i**) – (**iii**) and these are shown in equations 24, 26, and 28. The corresponding changes in concentration were calculated using equations 25, 27 and 29. Data from Experiment 1 provided the initial concentrations used in the theoretical model, and a programme was developed using Visual Basic in Excel to calculate the theoretical change in concentration of the reactants and products with time. The programme was run on Excel and generated theoretical concentrations using initial experimental concentrations for the reactants and an initial concentration of zero for the products − on the obvious assumption that no product would be present at the start of the reaction. The differences between the experimental and theoretical values (R) for the species **A**-**E** were calculated and their summations were squared ($\sum R^2$). The total $\sum R^2$ values were then calculated to give $\sum\sum R^2$ − a value used to solve for the values of the rate constants k_1, k_2 and k_3 corresponding to transformations (i), (ii) and (iii), respectively. The experimental and theoretical concentrations were then plotted on the same graph, and the solver function in Excel was used to solve for the rate constants k_1, k_2 and k_3.

Reaction Summary

Transformation (**i**): A + 2B = C

Transformation (**ii**): A + B = D

Transformation (**iii**): 2D = E
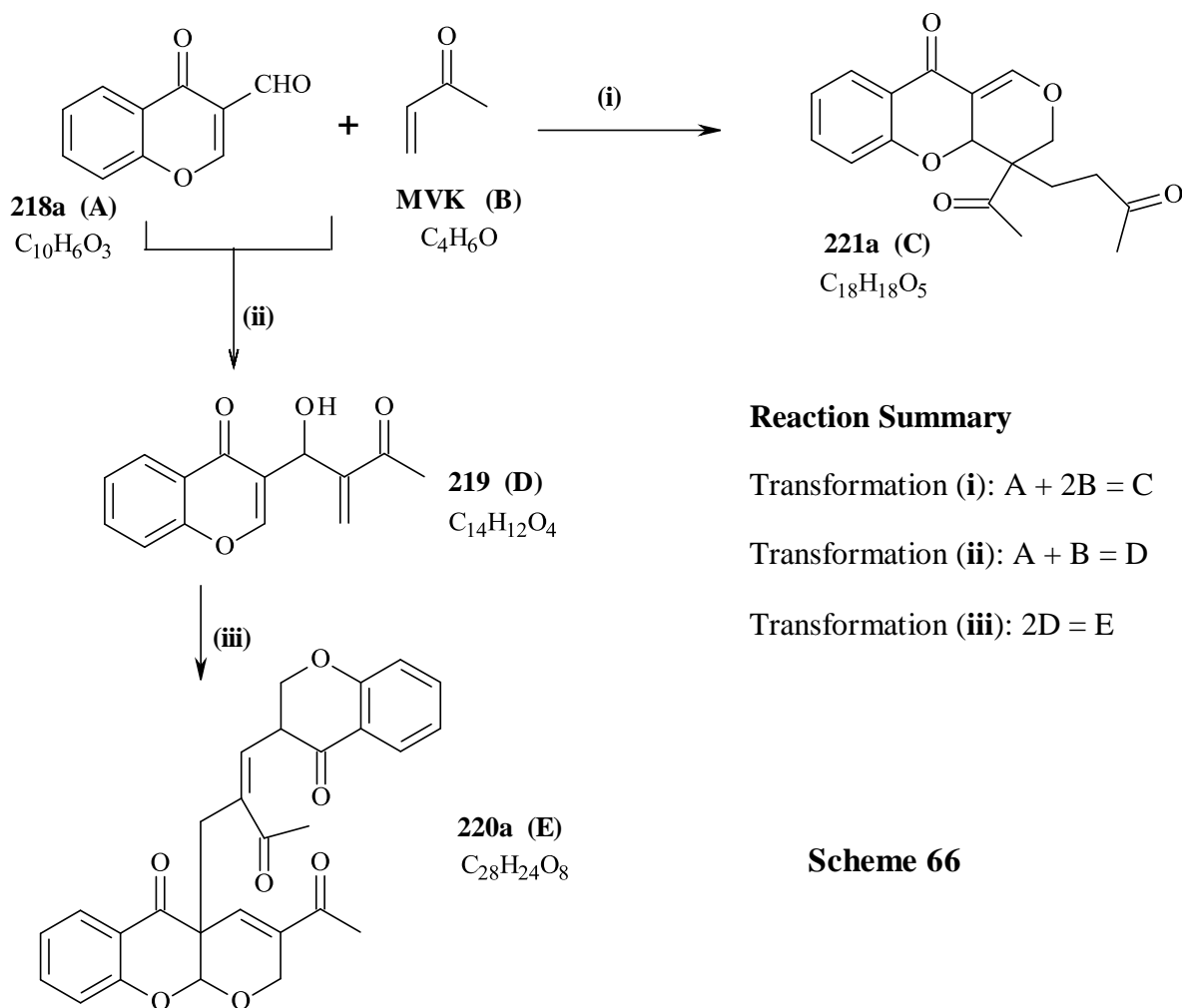
Scheme 66

Equations used in the theoretical kinetic model for the transformations (i), (ii) and (iii)

$$d[C]/dt = k_1[A][B]^2 \quad \text{(24)}$$
$$\Delta[C] \approx d[C]/dt * \Delta t \quad \text{(25)}$$

Transformation (**i**)

$$d[D]/dt = k_2[A][B] \quad \text{(26)}$$
$$\Delta[D] \approx d[D]/dt * \Delta t \quad \text{(27)}$$

Transformation (**ii**)

$$d[E]/dt = k_3[D]^2 \quad \text{(28)}$$
$$\Delta[E] \approx d[E]/dt * \Delta t \quad \text{(29)}$$

Transformation (**iii**)

Figure 66 shows plots of the experimental concentrations, as coloured symbols, and the theoretical concentrations, as solid lines as a function of time. With this fit, the values of the constants k_1, k_2 and k_3 were found to be 0.00448, 0.00398 and 0.0128, respectively. The

$\sum\sum R^2$ value of 0.0299 is small, corresponding to a good correlation between the experimental and theoretical data. In fact, the theoretical and experimental curves for chromone-3-carbaldehyde **218a** and MVK show almost perfect fits, although those of the chromone dimer **220**, the MBH adduct **219** and the tricyclic product **221** vary slightly. It should be noted, however, that, the theoretical initial concentrations for both MVK and chromone-3-carbaldehyde **218a** were lower than the experimental values.
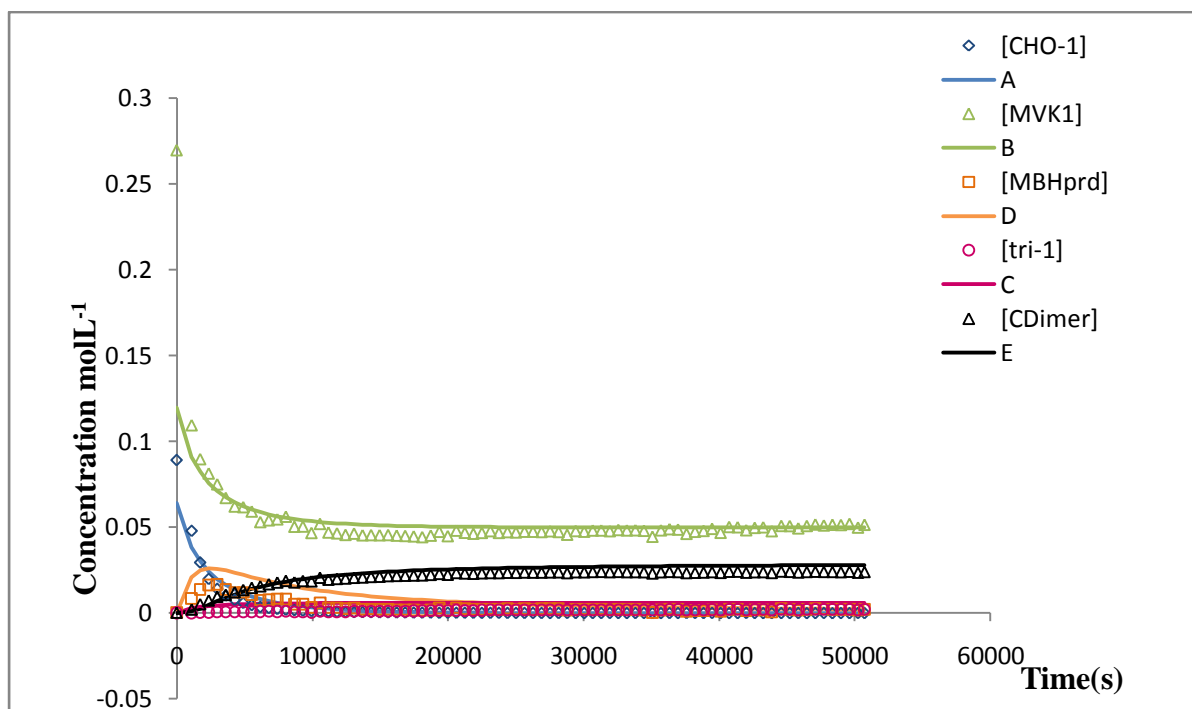
Figure 66. Concentration vs time graph of the experimental (symbols) and theoretical (solid lines) data, coloured to denote the chromone-3-carbaldehyde **218a** (blue), MVK (green), MBH adduct **219** (orange), tricyclic product **221a** (purple) and the chromone dimer **220a** (black). The resulting rate constants are: $k_1 = 0.004796$, $k_2 = 0.003981$ and $k_3 = 0.0128$, and $\sum\sum R^2 = 0.0299$.

While these initial results suggested that our theoretical model was very close to what was actually happening in the reaction, the deviations observed in the curves for the products indicated that we might have overlooked other transformations which may be involved in this reaction. This prompted re-examination of mechanisms proposed for the formation of compounds **220** and **221** (Schemes 63 and 64 respectively) and our theoretical model. More specifically, attention needed to be given to intermediates involved in the sequence of steps outlined earlier (Scheme 66, **i-iii**), which could contribute significantly to the overall kinetics and therefore needed to be included in the model in order to achieve a better fit. A revised model was then developed which accommodated additional possible intermediates and

equilibria. The new model assumes that formation of **C** (tricyclic derivative, **221**) proceeds through a putative intermediate 'W' (Equation 30) − an assumption consistent with the proposed mechanism for the formation of **C** (Scheme 64), which involves three possible intermediates (compounds **277**, **278** and **279**). An equilibrium is also proposed between the intermediate **W** and the tricyclic product **C** (Equations 31 and 32). The formation of **D** (the MBH adduct **219**) is also assumed to proceed through an intermediate 'V' (Equation 33), which is again consistent with the possible intermediates involved in the mechanism of the MBH reaction alluded to in Chapter 1, Section 1.1.1. An equilibrium is also assumed to exist between the MBH adduct **D** and **V** (Equations 34 and 35). The formation of **E** (the chromone dimer **220**) is proposed to proceed through an intermediate 'U' (Equation 36), which could correspond to the presence of intermediate **275** in the proposed mechanism (Scheme 63); an equilibrium is presumed to exist between **U** and **E** (Equations 37 and 38)

$$A + 2B \longrightarrow W \qquad k_1 \qquad (30)*$$

$$W \longrightarrow C \qquad k_8 \qquad (31)$$

$$C \longrightarrow W \qquad k_9 \qquad (32)$$

$$A + B \longrightarrow V \qquad k_2 \qquad (33)*$$

$$V \longrightarrow D \qquad k_6 \qquad (34)$$

$$D \longrightarrow V \qquad k_7 \qquad (35)$$

$$2D \longrightarrow U \qquad k_3 \qquad (36)*$$

$$U \longrightarrow E \qquad k_4 \qquad (37)$$

$$E \longrightarrow U \qquad k_5 \qquad (38)$$

Equations marked with an asterisk (*) were modified from the initial proposed sequence of steps (Scheme 66, **i-iii**), and the programme used earlier was changed to accommodate the new model based on Equations 30-38. The programme was run on Excel as before to obtain the rate constants k_1-k_9. The results obtained afforded a much better fit than the initial model. In fact, the theoretical curves fitted the experimental curves extremely well with a $\sum\sum R^2$ value of 0.00752, providing an excellent (albeit not necessarily unique) model of the reaction.

However, upon review it was observed that the equilibrium between W and C would not favour the formation of C, and so equation 32 was changed to be

$$W \longrightarrow A + 2B \qquad k_9 \qquad (32)$$

In this case k_9 was 0 (Table 5) and so this equation falls away.

The $\sum\sum R^2$ value is still good in this scenario at 0.0133. Figure 67 shows the fit between the experimental (symbols) and theoretical (solid lines) data.
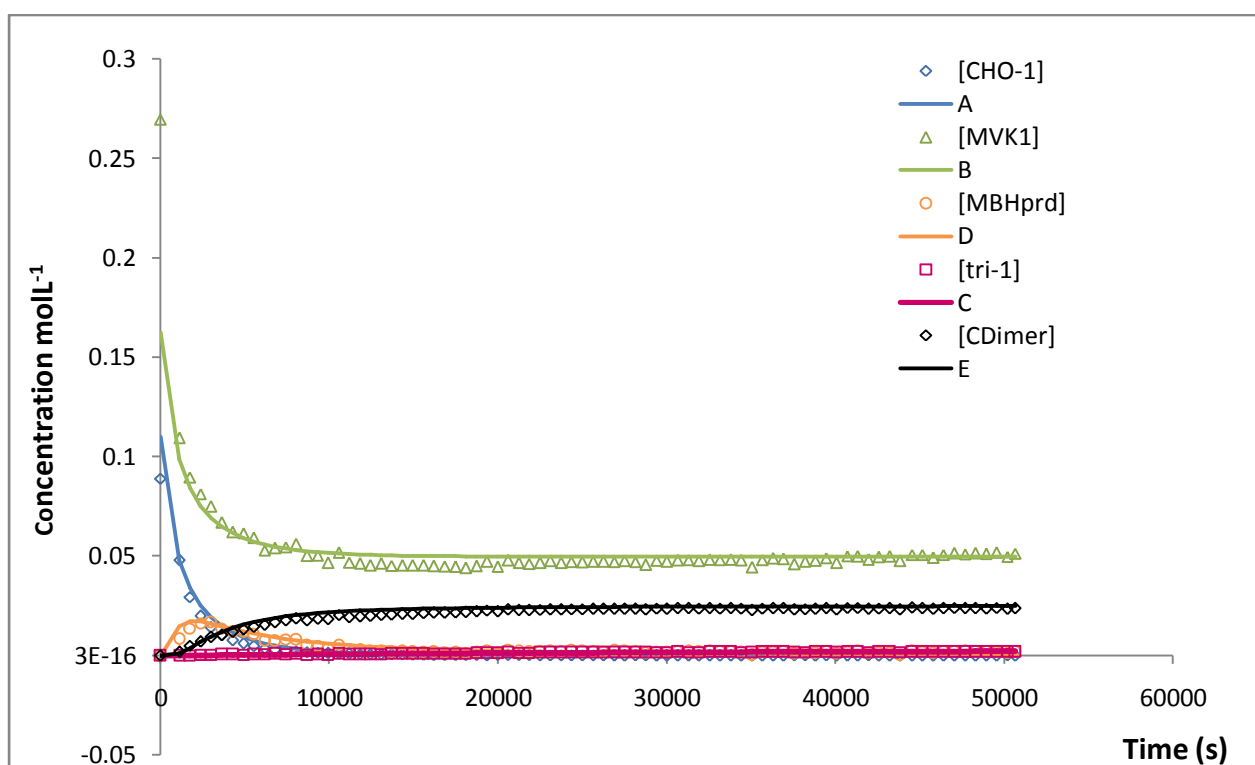
Figure 67. Concentration vs time graph of the experimental (symbols) and theoretical (solid lines) data using the revised model, coloured to denote the chromone-3-carbaldehyde **218a** (blue), MVK (green), MBH adduct **219** (orange), tricyclic product **221a** (purple) and the chromone dimer **220a** (black). $\sum\sum R^2 = 0.0133$.

2.2.3.1 Overall rate law for the reaction of chromone-3-carbaldehyde with MVK

The calculated rate constants $(k_1$-$k_9)$, corresponding to best fit between the experimental and theoretical data are presented in Table 5:

Table 5: Calculated rate constants at the best fit.

Rate constant	Value
k_1	$0.014 \text{ mol}^{-2}\text{L}^2\text{s}^{-1}$
k_2	$0.0059 \text{ mol}^{-1}\text{Ls}^{-1}$
k_3	$0.0335 \text{ mol}^{-1}\text{Ls}^{-1}$
k_4	0.0016 s^{-1}
k_5	0.0182 s^{-1}
k_6	0.0008 s^{-1}
k_7	0.0006 s^{-1}
k_8	0.00003 s^{-1}
k_9	0.0 s^{-1}

The rate determining step is therefore represented by Equation 31, in which intermediate **W** is converted to compound **221** (**C**), with the overall transformation being summarised by Equations 30 and 31.

$$A + 2B \longrightarrow W \qquad k_1 \qquad\qquad (30)$$

$$\mathbf{W \longrightarrow C} \qquad \mathbf{k_8} \quad \textit{slow} \qquad\qquad \mathbf{(31)}$$

Therefore the influence of the transformation W $\longrightarrow$ C in the mechanism is marked, however, formation of C is delayed, and this fits with the initial formation of W. The decay of the chromone-3-carbaldehyde **218a** (**A**) and MVK (**B**) follows first-order kinetics with respect to **A**, second order with respect to **B** and third order kinetic overall. The rate law for this decay is shown in Equation 39:

$$\text{Rate} = k_{\text{obs}} [\mathbf{A}] [\mathbf{B}]^2 \qquad\qquad (39)$$

2.2.4 Theoretical study of the reaction of chromone-3-carbaldehydes with MVK

Based on the proposed mechanisms for the formation of the chromone dimers **220** and the tricyclic analogues **221** (Schemes 63 and 64), respectively, a theoretical study was undertaken. Geometry optimisation of all the proposed products and intermediates was achieved using the hybrid density functional B3LYP at the 6-31G (d) level of theory in Gaussian 03.[144,145] The zwitterion **276b** formed between MVK and the tertiary amine catalyst DABCO failed to optimise to a minimum energy – a pattern already observed in Section 2.1.5.1, in reactions with DBU and Ph₃P. Energy surface scans were obtained for both the *s*-cis and *s*-trans-arrangements of the MVK-DABCO zwitterionic enolates by scanning the change in the N-C bond-length and the torsion indicated in the line structures in Figures 68 and 69. The results obtained are illustrated in Figures 68 and 69, where decreasing the N-C bond length, to facilitate formation of the zwitterions, resulted in an increase in energy causing the systems to fall apart, in spite of the fact that a transition state could be located. Structures **a** and **b** show the lowest energy arrangements in the respective enolates, and the disintegration of the zwitterions into DABCO and MVK from the starting arrangements in Figures 68 and 69 is quite evident.
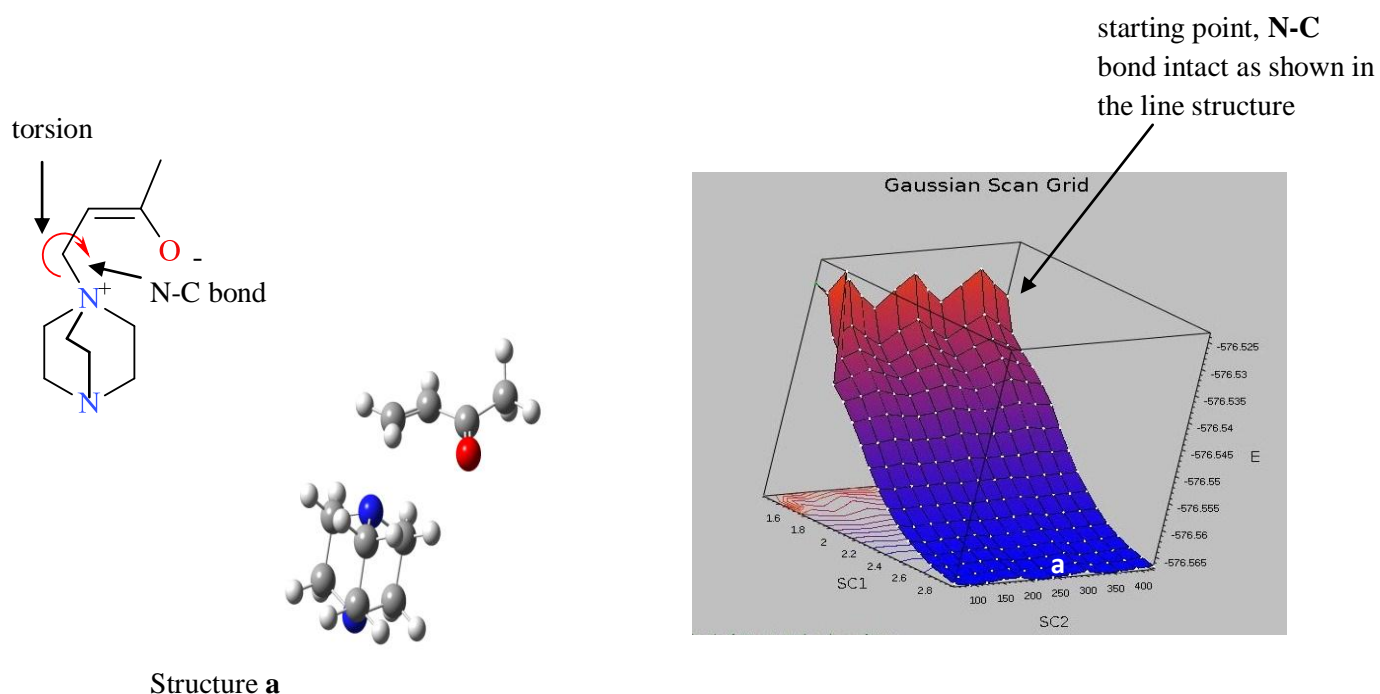
Structure **a**

Figure 68. Energy surface scan grid for the *s-cis*-MVK-DABCO zwitterion; the lowest possible energy is represented by point **a**. Indicated in the line structure are the relevant N-C bond and torsion varied in the scan.

torsion

N-C bond

starting point, **N-C** bond intact as shown in the line structure

Gaussian Scan Grid
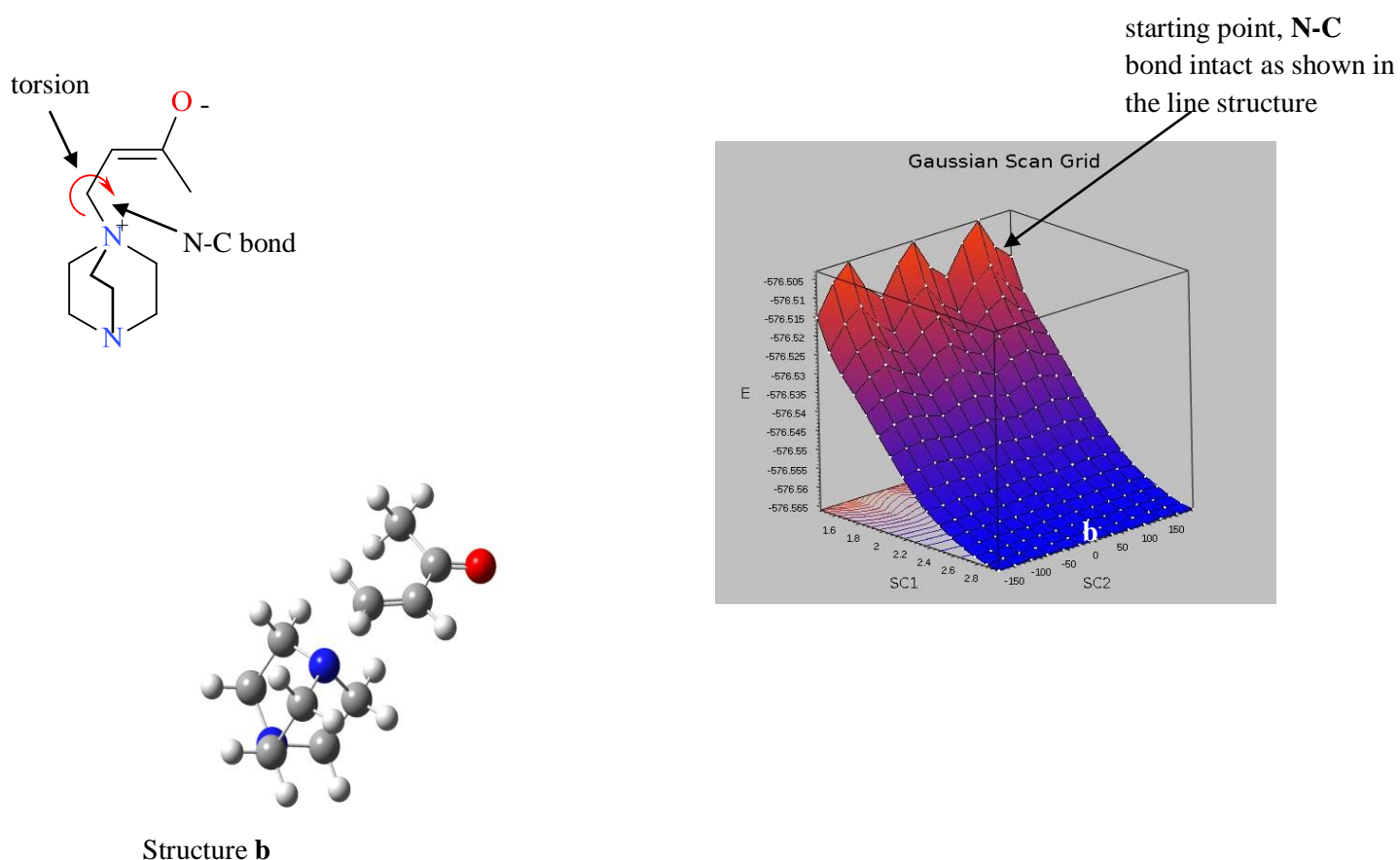
Structure **b**

Figure 69. Energy surface scan grid for the *s-trans*-MVK-DABCO zwitterion; the lowest possible energy is represented by point **b**. Indicated in the line structure are the relevant N-C bond and torsion varied in the scan.

Optimised geometries of the intermediates and the product involved in the formation of the chromone dimers **220**, as proposed by Molefe[79,80] (Scheme 63), are shown in Figure 70. An intramolecular cyclisation in structure **275** followed by dehydration was considered to afford the chromone dimer **220**. The close alignment of the nucleophilic hydroxyl group and the electrophilic vinylic carbon, highlighted in the optimised structure for compound **275**, agrees with the proposed mechanism. In the optimised structure of the dimer **220**, the bicyclic ring system lies in a plane perpendicular to the tricyclic ring system.
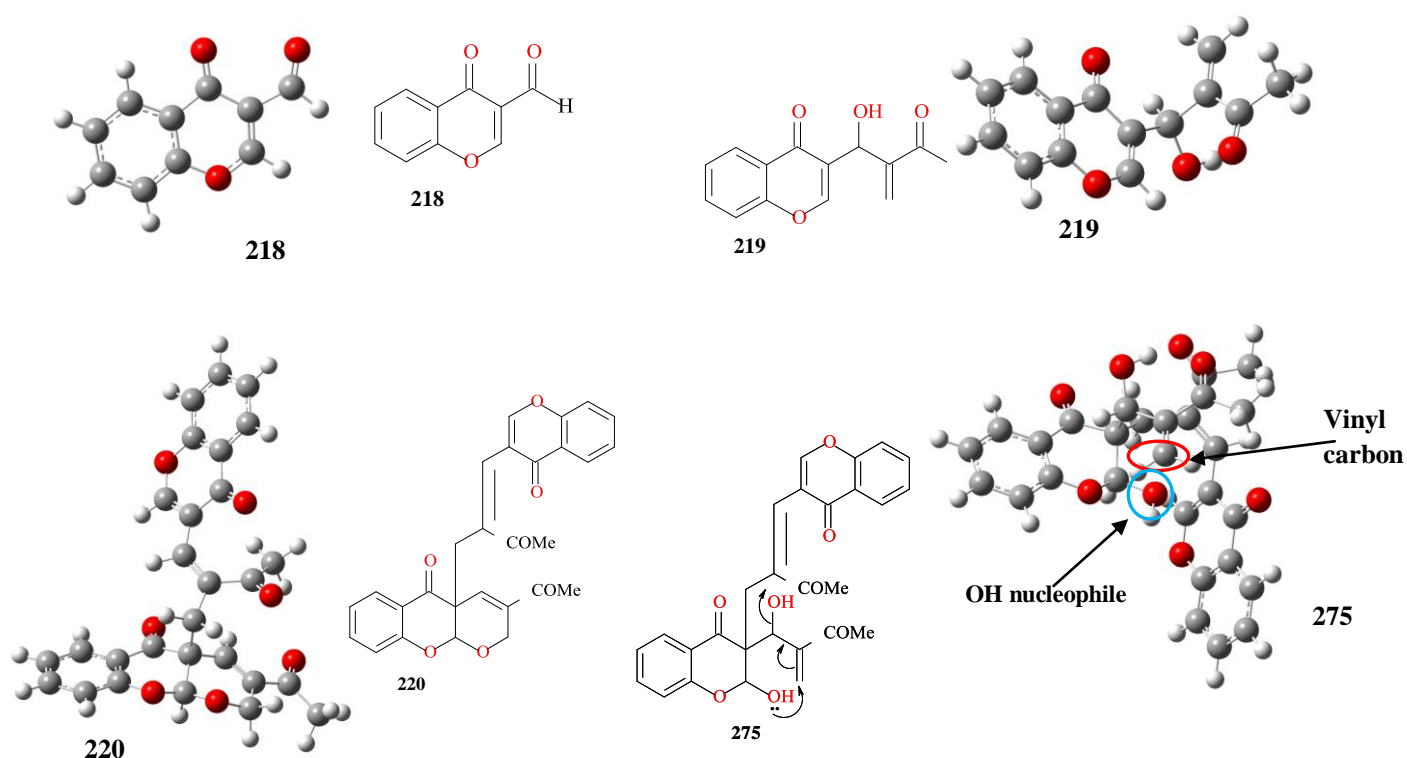
Figure 70. B3LYP/6-31G(d)-optimised geometries for structures in the proposed mechanism for the formation of the chromone dimers **220** (Scheme 63), and their line structures.

The optimised geometries of the compounds involved in the formation of the tricyclic products **221**, as proposed in Scheme 64, are shown in Figure 71. Release of the catalyst from compound **277** is common in MBH reactions and is likely to follow the sequence proposed. The orientation of the hydroxyl and vinyl groups required to form the third ring appears to be favoured and in fact, partial ring closure is already evident in the energy-minimised structure **278**. The transformation **277**→**278** suggests that loss of the catalyst, DABCO, is accompanied by spontaneous cyclisation. It is also interesting that, in the optimised structure for compound **279**, the protonated positively charged oxygen (in the line structure) has already given up the proton to the enolate oxygen, as shown by the arrow in the modelled structure **279**.
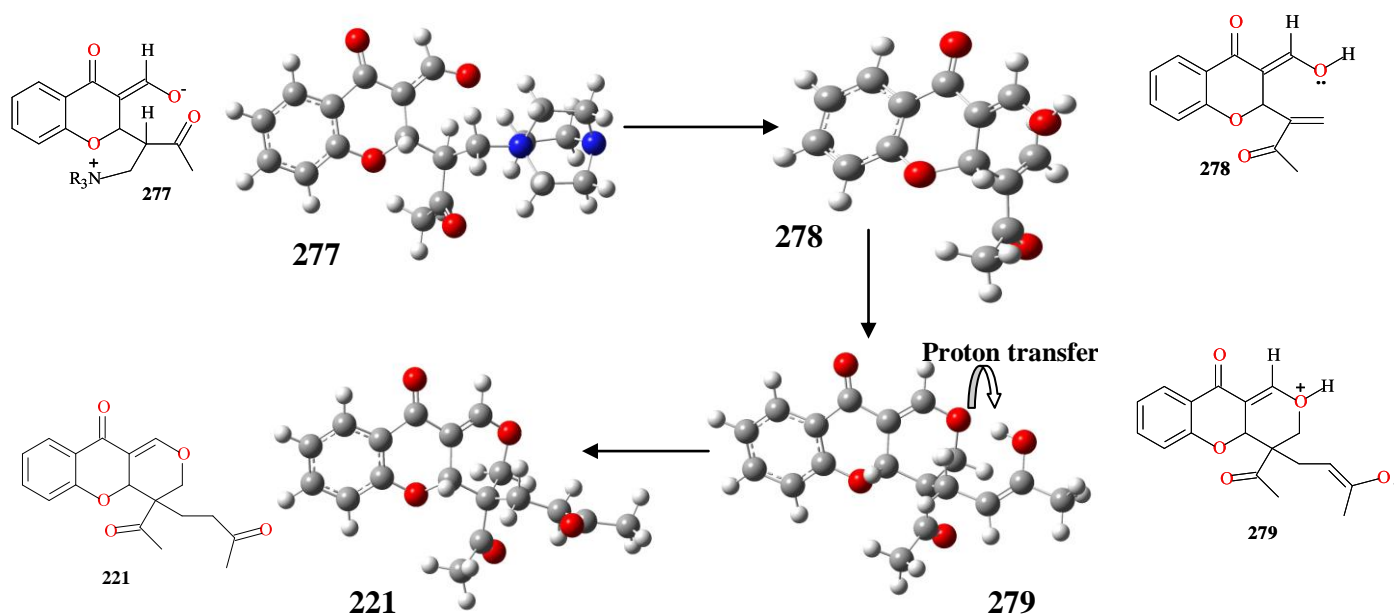
Figure 71. B3LYP/6-31G(d) optimised geometries for compounds in the proposed mechanism for the formation of the tricyclic products **221** (Scheme 64).

2.2.4.1 Thermodynamic free energy (ΔG^0) profile for the reaction of chromone-3-carbaldehyde with MVK

The free energy-level diagram in Figure 72, summarises the thermodynamic profile for the reaction, showing the two competing pathways. It is apparent that both pathways involve attack at the electrophilic centre C-3 of a chromone system. In the formation of the dimer **220**, the hydroxyl group of one molecule of the initial MBH product **219** attacks C-3 of another, while in the formation of the tricyclic systems, the reaction is initiated by attack of the MBH zwitterion **276** at C-3 of the chromone-3-carbaldehyde substrate **218**. The identification of all the structures in Figure 72 as stationary points (in fact as minima) support the proposed mechanistic pathways (Schemes 63 and 64). The tricyclic product is at a lower energy than the chromone dimer **220**, but there is no evidence from the experimental kinetic data of equilibration in favour of compound **221**. We therefore presume that the observed product distribution is kinetically rather than thermodynamically determined. Location of critical transition state complexes, which time has not permitted, would provide the information needed to calculate a full energy profile for this reaction.
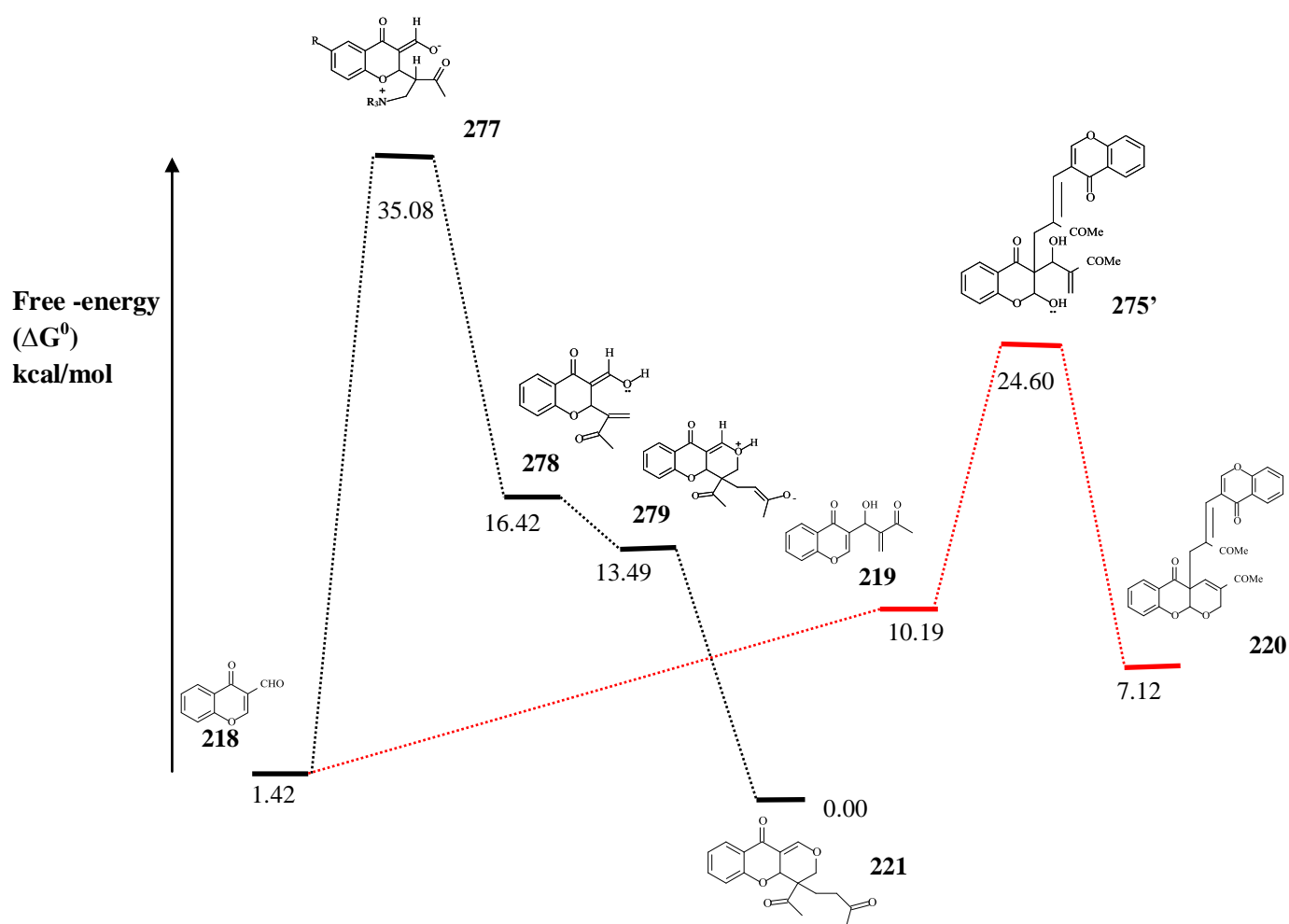
Figure 72. Thermodynamic free-energy (ΔG^0) profile diagram for the DABCO-catalysed MBH reaction of chromone-3-carbaldehyde **218a** with MVK. Shown are the free-energies of the reactants, intermediates and products involved. Structures were optimised at the DFT/B3LYP 6-31G(d) level of theory.

2.2.5 Kostanecki-Robinson synthesis of chromone-2-carbaldehydes

The synthesis of chromone-2-carbaldehydes **222a-e** was carried out in several steps from *o*-hydroxyacetophenones **265a-e** using the Kostanecki-Robinson method, as illustrated in **Scheme 67**. The first step involved base-catalysed condensation of the substituted *o*-hydroxyacetophenones **265a-e** with ethyl acetate. This was followed by acid-catalysed cyclisation of the intermediates **280a-e** to give the substituted 2-methylchromones **281a-e**. SeO_2 oxidation of the substituted 2-methylchromones then gave the corresponding chromone-2-carbaldehydes **222a-e**. The mechanism for the selenium dioxide oxidation, shown in Scheme 68, is considered to involve deprotonation of the methyl group to form a resonance stabilised enolate **282** (step i), which undergoes selenation at C-3 to form compound **283** (step ii). A [2,3]-sigmatropic rearrangement (step iii) followed by deselenation affords the chromone-2-carbaldehydes **222**. The ^1H NMR spectrum for 6-chloro-2-methylchromone **281d** is shown in Figure 73. The methyl protons resonate at 2.38 ppm and the 3-H proton at 6.16 ppm as a singlet, while the 5-H signal appears further downfield at 8.12 due to deshielding by the electron-withdrawing chlorine and the magnetic anisotropic effects of the carbonyl group. In the ^{13}C NMR spectrum (Figure 74), the methyl carbon resonates at 20.9 ppm and the carbonyl carbon much further downfield at 177.0 ppm. In the ^1H NMR spectrum (Figure 75) of the chromone-2-carbaldehyde **222d**, a new signal at 9.79 ppm corresponds to the aldehyde proton − its presence accompanied by the absence of the 2-methyl signal characteristic of the precursor **281d**. In the ^{13}C NMR spectrum (Figure 76), two carbonyl signals at 177.2 and 185.1 ppm are observed corresponding to the C-4 and aldehydic carbonyl carbons respectively.

	R
a	H
b	Br
c	OMe
d	Cl
e	F
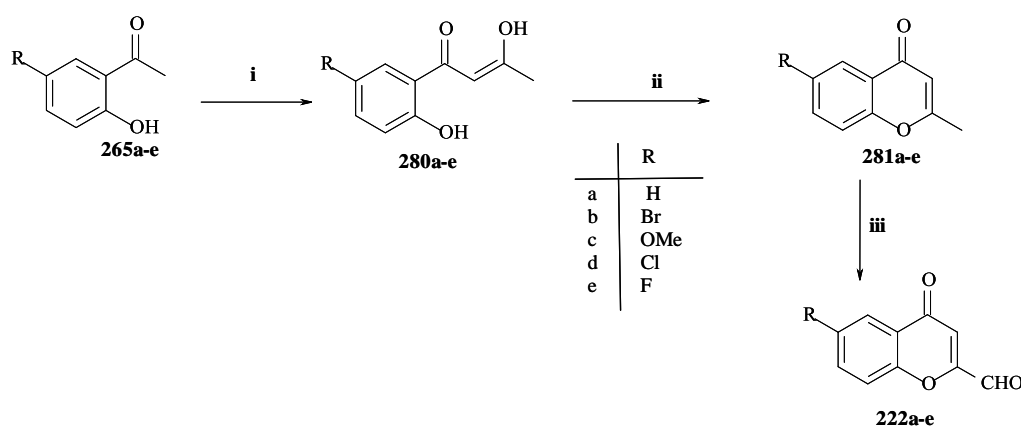
Scheme 67. *Reagents and conditions.* i) NaOEt (Na metal and EtOH), dry EtOAc, reflux; ii) acetic acid, conc. H_2SO_4, reflux; and iii) SeO_2, xylene, relux.
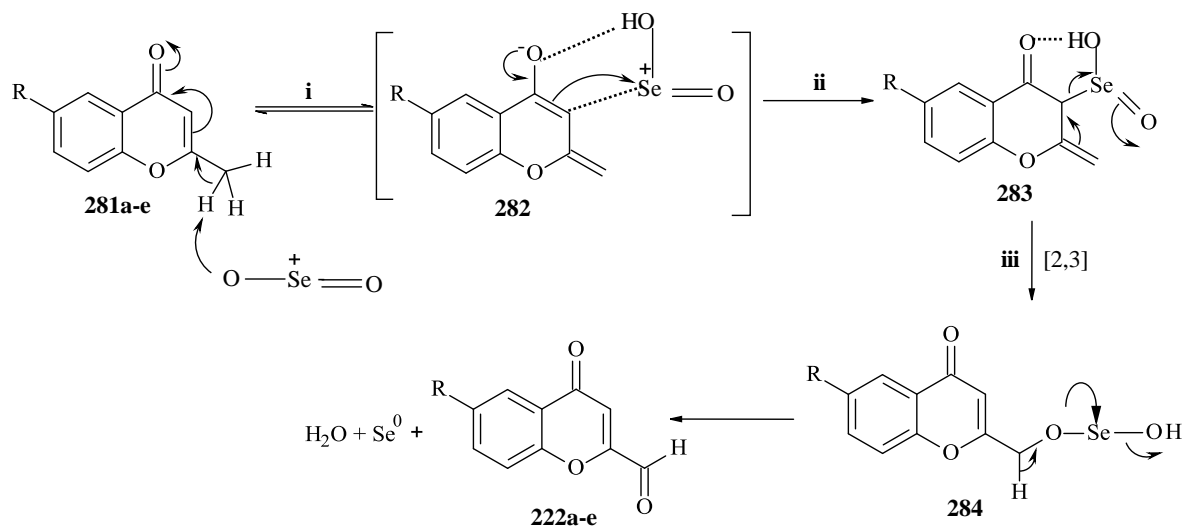
Scheme 68.
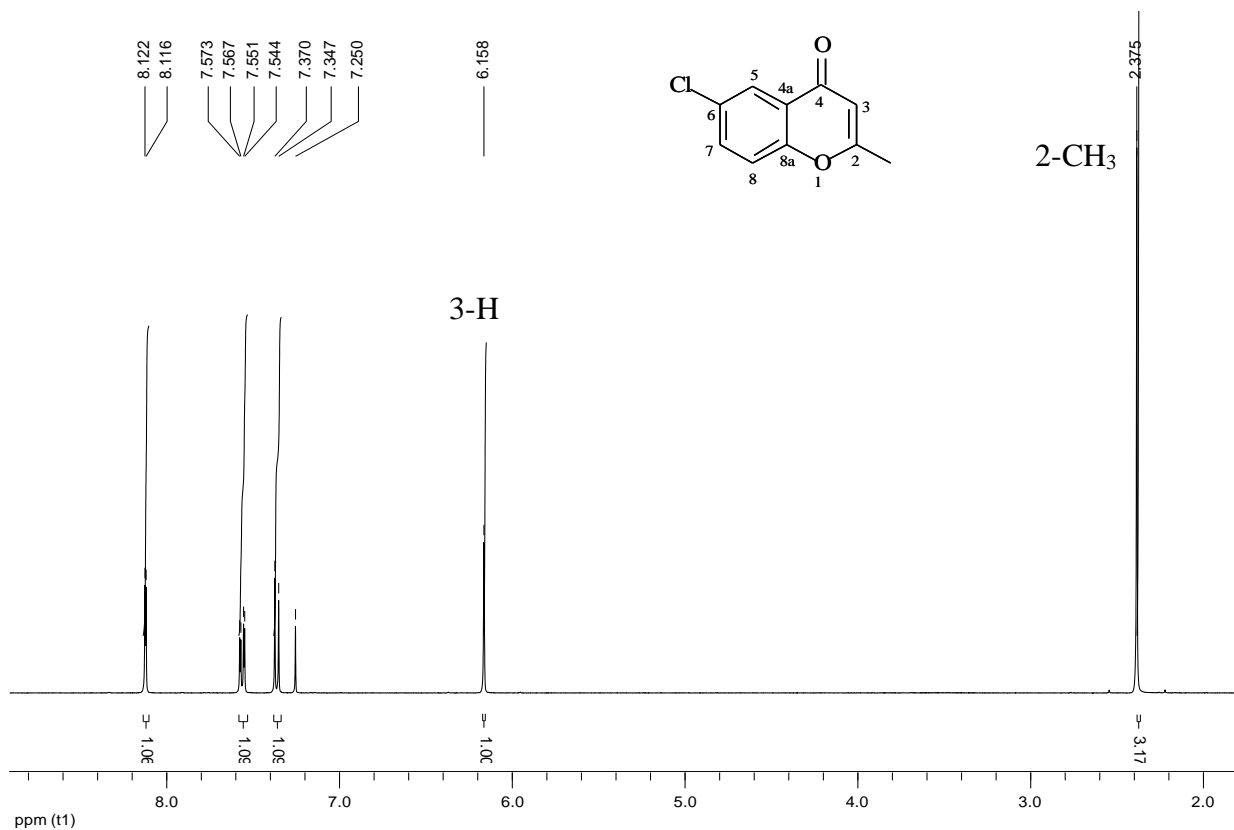
Figure 73. 400 MHz ^{1}H NMR spectrum of the 2-methylchromone **281d** in CDCl$_3$.
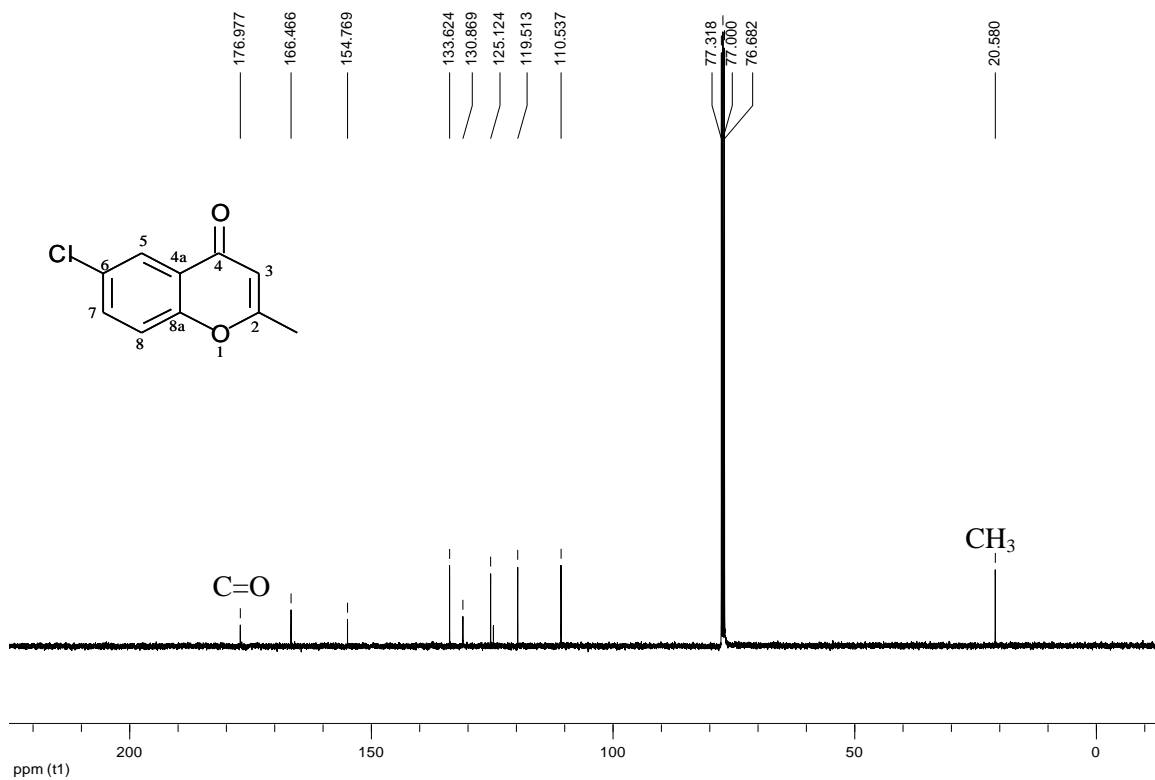
Figure 74. 100 MHz ^{13}C NMR spectrum of the 2-methylchromone **281d** in CDCl$_3$.
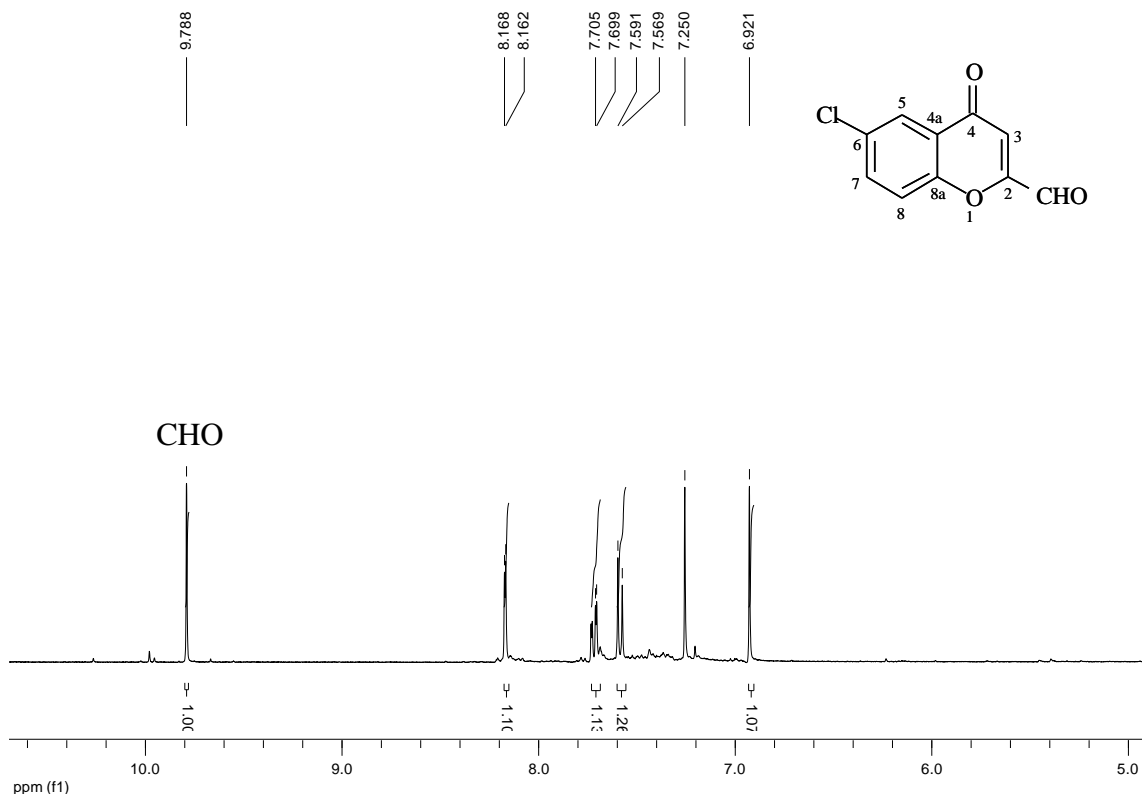
Figure 75. 400 MHz ^{1}H NMR spectrum of compound **222d** in CDCl$_3$.
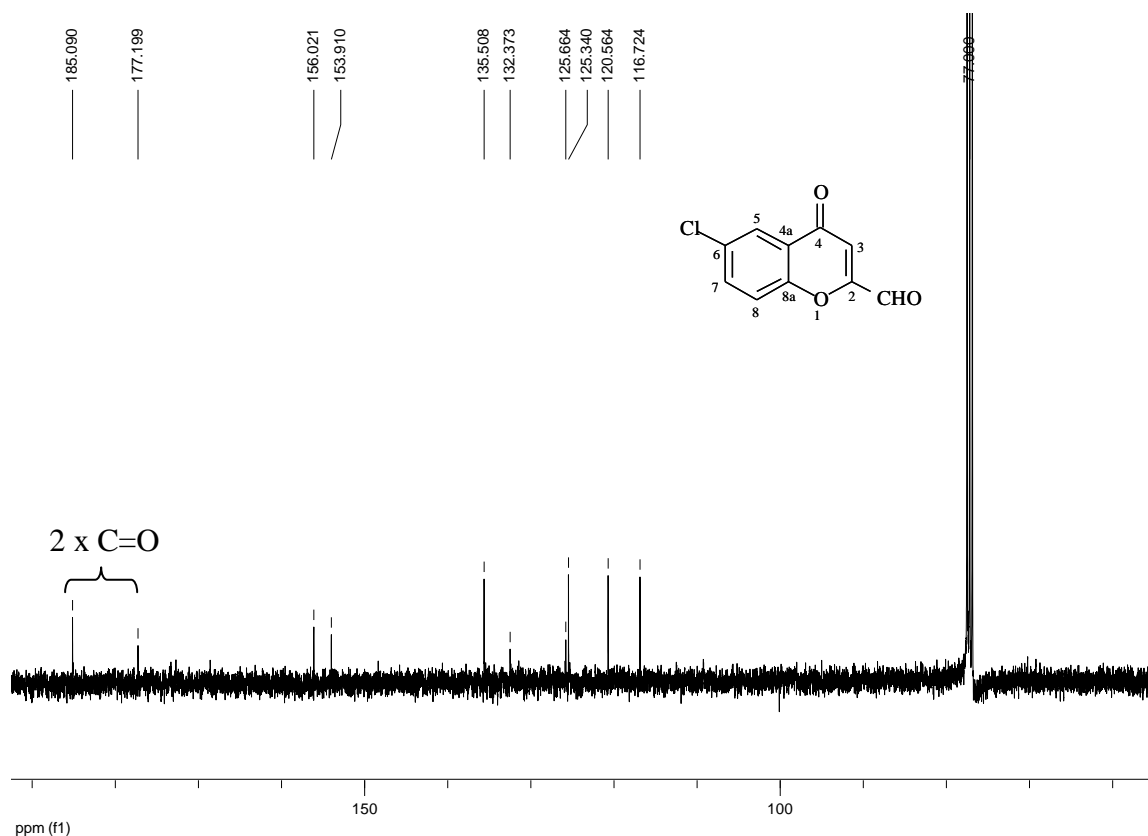
Figure 76. 100 MHz ^{13}C NMR spectrum of compound **222d** in CDCl$_3$.

2.2.6 Morita-Baylis-Hillman reactions of chromone-2-carbaldehydes with acrylonitrile

Previous work in the group has highlighted rather unusual reactivities of chromone-2-carbaldehydes **222** towards Michael acceptors under Morita-Baylis-Hillman conditions.[79] Thus, when the substituted chromone-2-carbaldehydes **222a-e** were reacted with acrylonitrile in MBH type reactions in both CHCl$_3$ and CH$_2$Cl$_2$, the expected MBH adducts **223a-e** were not obtained, and the isolated products were tentatively identified as the azetine derivatives **224a-c** on the basis of the 1- and 2-Dimensional NMR, HRMS and IR data (Scheme 69). The ^{1}H NMR spectrum of the proposed azetine **224a** is shown in Figure 77. Azetines are a rare class of heterocycles, which have been shown to be of biological importance,[193] and the apparently ready access to these systems *via* a simple reaction involving chromone-2-carbaldehydes **222a-e** and acrylonitrile under MBH reaction conditions prompted further investigation. The proposed mechanism to rationalise the formation of the azetines (Scheme 70) was considered to be initiated by the conjugate addition of the catalyst (R$_3$N) to the activated alkene to form a zwitterion **285**. The nucleophilic cyano nitrogen then attacks the electrophilic centre C-2, instead of the aldehydic carbonyl carbon to form intermediate **286**;

cyclisation and hydration then affords the azetine **224**, which was considered to be susceptible to dehydration to the resonance-stabilised system **288**.
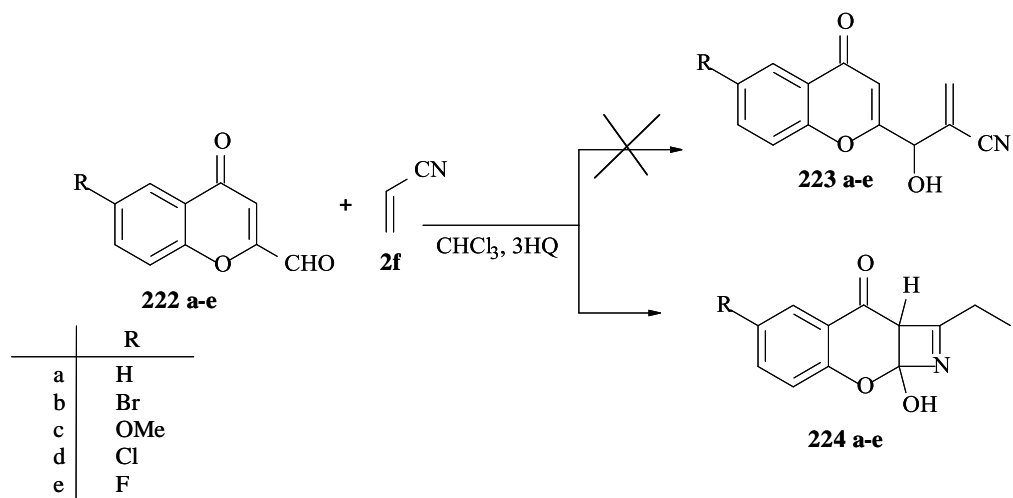
Scheme 69
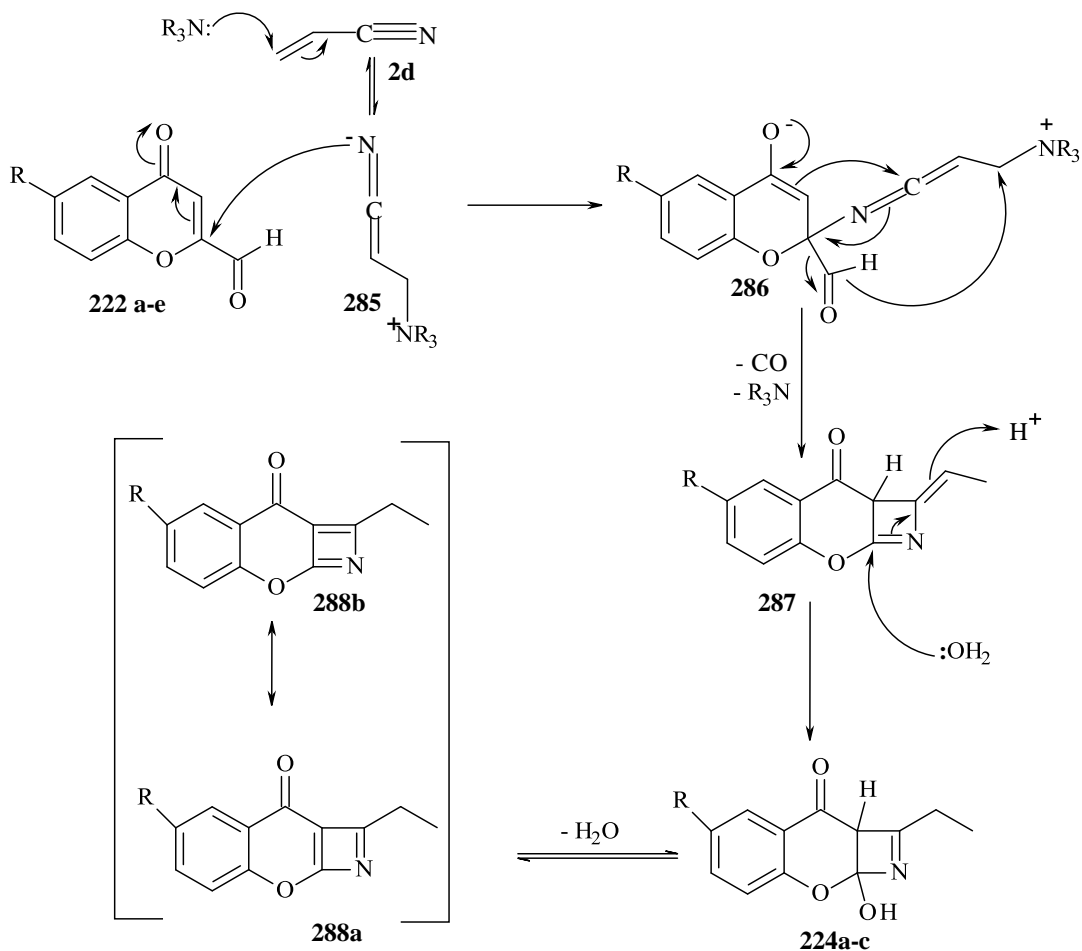
Scheme 70. Mechanism proposed previously for the formation of the azetine derivatives.[79]
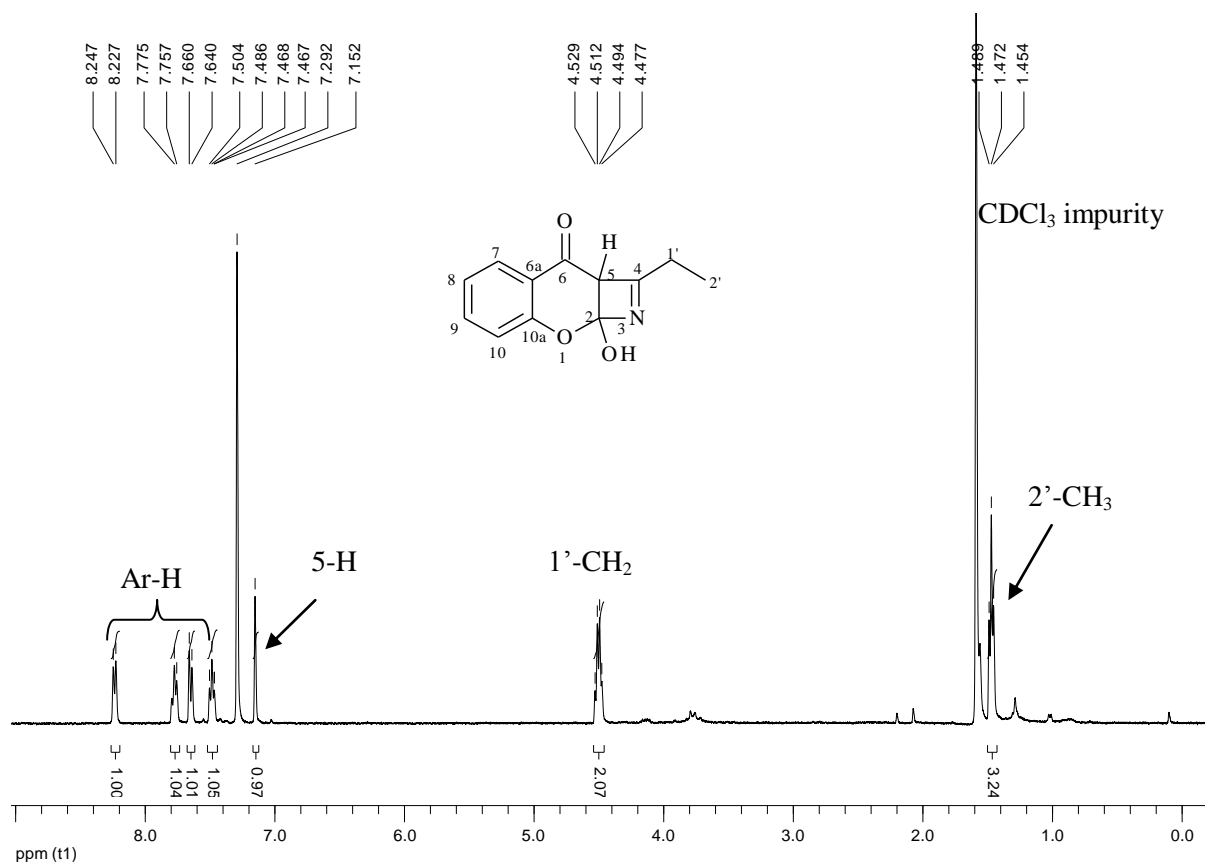
Figure 77. 400 MHz ^{1}H NMR spectrum of the proposed azetine **224a** in CDCl$_3$.

With the aim of confirming the identity of the isolated products and extending this reaction to other substrates, the reactions of various chromone-2-carbaldehydes **222** with acrylonitrile were repeated. Similar products were again isolated, and their ^{1}H NMR spectra were all characterised by typical ethyl group signals, *i.e.* a triplet at 1.45 ppm and a quartet at 4.50 ppm.

2.2.6.1 Solvent and catalyst effects on the reactions of chromone-2-carbaldehydes with acrylonitrile

Various solvents and catalysts have been used in MBH reactions.[6,43,45,51,56,59,79] In some cases, changing either the solvent or catalyst (or both) has been shown to affect the rate of the reaction or the type of products formed. Some catalysts work best with certain substrates, while others may not work at all. Against this background, we sought to explore the effect of changing both the catalyst and the solvent on this particular reaction. The catalyst 3-HQ was therefore replaced by DABCO, and EtOH was used as the solvent in place of CHCl$_3$. The chromone-2-carbaldehydes **222c** and **222e** were reacted with acrylonitrile in the same molar ratios as in the initial reaction. The product from the reaction using 5-methoxychromone-2-

carbaldehyde **222c** was obtained as an orange oil which slowly crystallised in 26% yield, while the compound derived from the fluoro analogue **222e** was obtained as an orange solid in 48% yield. However, both reactions proceeded much more slowly (4-6 days) than those conducted with 3-HQ and $CHCl_3$ (24 hours).

The effect of using DBU and TMPDA as catalysts was also explored. In the previous study,[79] use of DBU in $CHCl_3$ had proved unsuccessful; in the present study, reaction of 6-fluorochromone-2-carbaldehyde **222e** with DBU in EtOH resulted in consumption of the substrate, but ^{1}H NMR analysis of the crude material provided no evidence of the expected product. Use of TMPDA in EtOH, on the other hand, afforded the expected product as an orange solid, albeit in much lower yield than when DABCO was used. One advantage was that the products could be isolated as solids, and recrystallised.

While it was evident that the formation of these products could be reproduced under various conditions, further analysis began to raise doubts about the structural assignment, in particular, the presence of nitrogen (and the azetine moiety!). Given the expected involvement of acrylonitrile in the reaction, the MS peak at *m/z* 218.1632 obtained in the earlier study[79] was attributed to the **MH**[+] ion corresponding to the molecular formula of $C_{12}H_{12}NO_3$. However, the found and calculated values do not match particularly well, and combustion analysis as well as an ^{15}N HSQC NMR experiment, undertaken in the present study, failed to confirm the presence of nitrogen. We then aimed to prepare a naphthopyran analogue in expectation of obtaining crystals suitable for X-ray crystallographic analysis. The experimental procedure for the synthesis of the chromone-2-carbaldehydes **222a-e** was then extended to the synthesis of a naphthopyran analogue **292**, starting from *o*-1-acetyl-2-hydroxynaphthalene **289** (Scheme 71). Figure 78 shows the ^{1}H NMR spectrum of the resulting 2-methylchromone **291**. The methyl protons resonate at 2.41 ppm while the 3-methine proton signal is at 6.34 ppm. A rather interesting observation in this spectrum is the presence of a doublet at 10.01 ppm, a common region for aldehydic protons or hydrogen-bonded hydroxyl protons, but, in our case, there was no aldehyde or hydroxyl group in the expected product. The ^{13}C NMR spectrum (Figure 79) confirms the presence of only one carbonyl carbon at 180.3 ppm corresponding to C-4. 2-Dimensional NMR experiments (COSY, HSQC and HMBC) permitted assignment of the doublet to the 5-H proton. It appears that the magnetic anisotropic effects of the carbonyl group are greater in the naphthopyran-4-one derivatives compared to the chromone systems because the carbonyl group is positioned close to and in the same plane as the 5-H proton in the former system, resulting in increased

deshielding away from the expected aromatic region. The ^{1}H NMR spectrum of the aldehyde **292** is shown in Figure 80 and confirms the presence of an aldehyde signal at 9.82 ppm and the 5-H proton, again deshielded, at 9.96 ppm. Two carbonyl signals are present in the ^{13}C NMR spectrum (Figure 81) at 179.7 and 185.1 ppm, corresponding to the 4- and aldehydic carbonyl carbons, respectively.
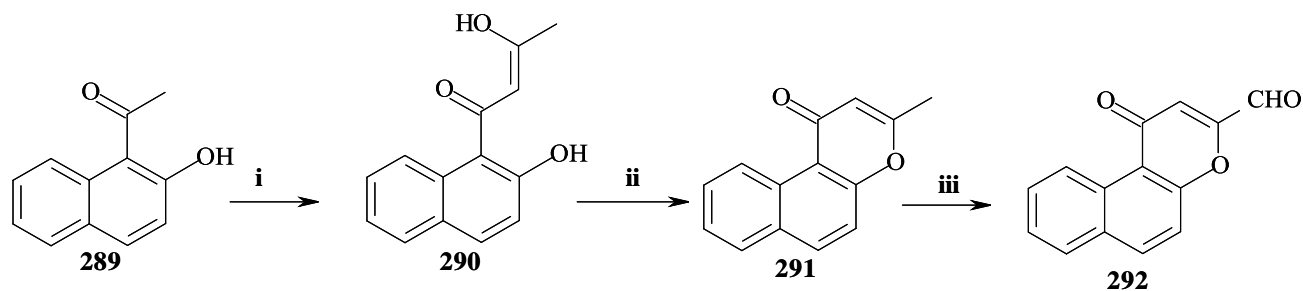
i) NaOEt, dry EtOAc, reflux, 8h
ii) glacial acetic acid, H_2SO_4 (98%), reflux, 4h
iii) SeO$_2$, xylene, reflux, 12h

Scheme 71.
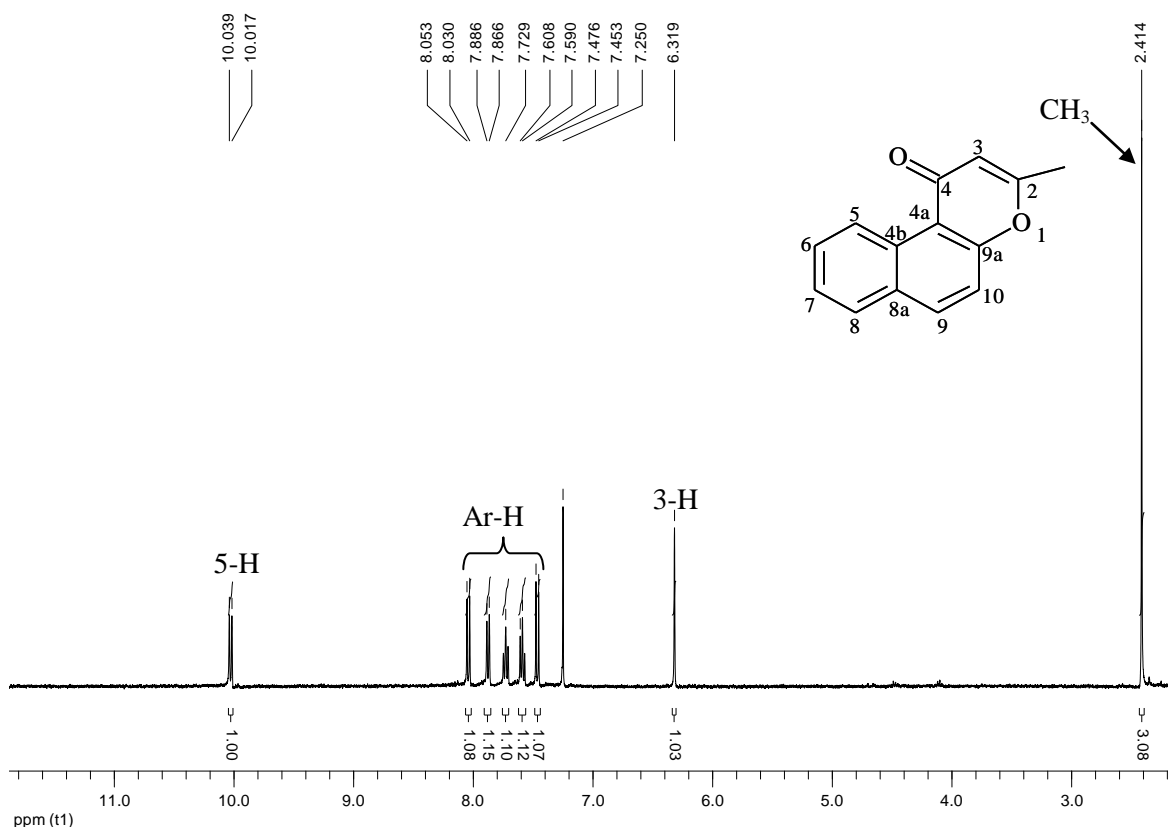
Figure 78. 400 MHz ^{1}H NMR spectrum of compound **291** in CDCl$_3$.
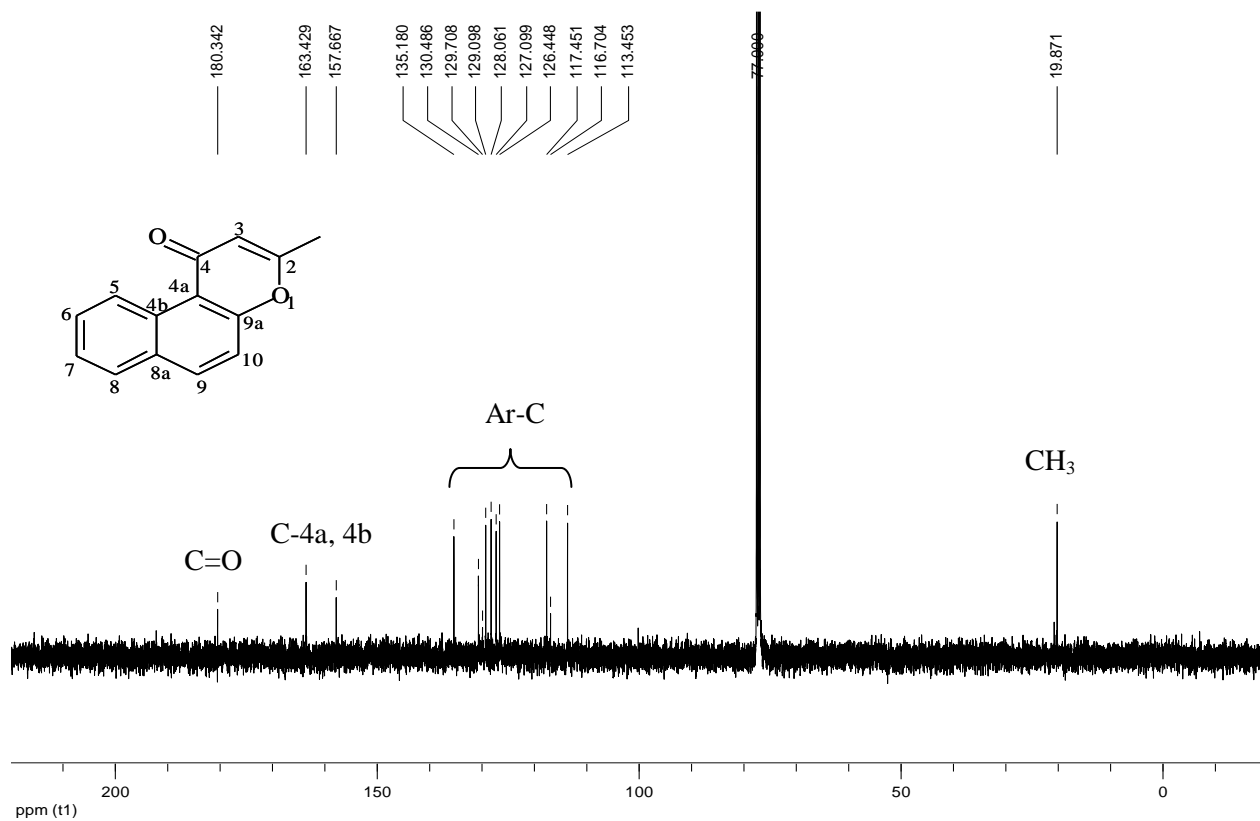
Figure 79. 100MHz ^{13}C NMR spectrum of compound **291** in CDCl$_3$.
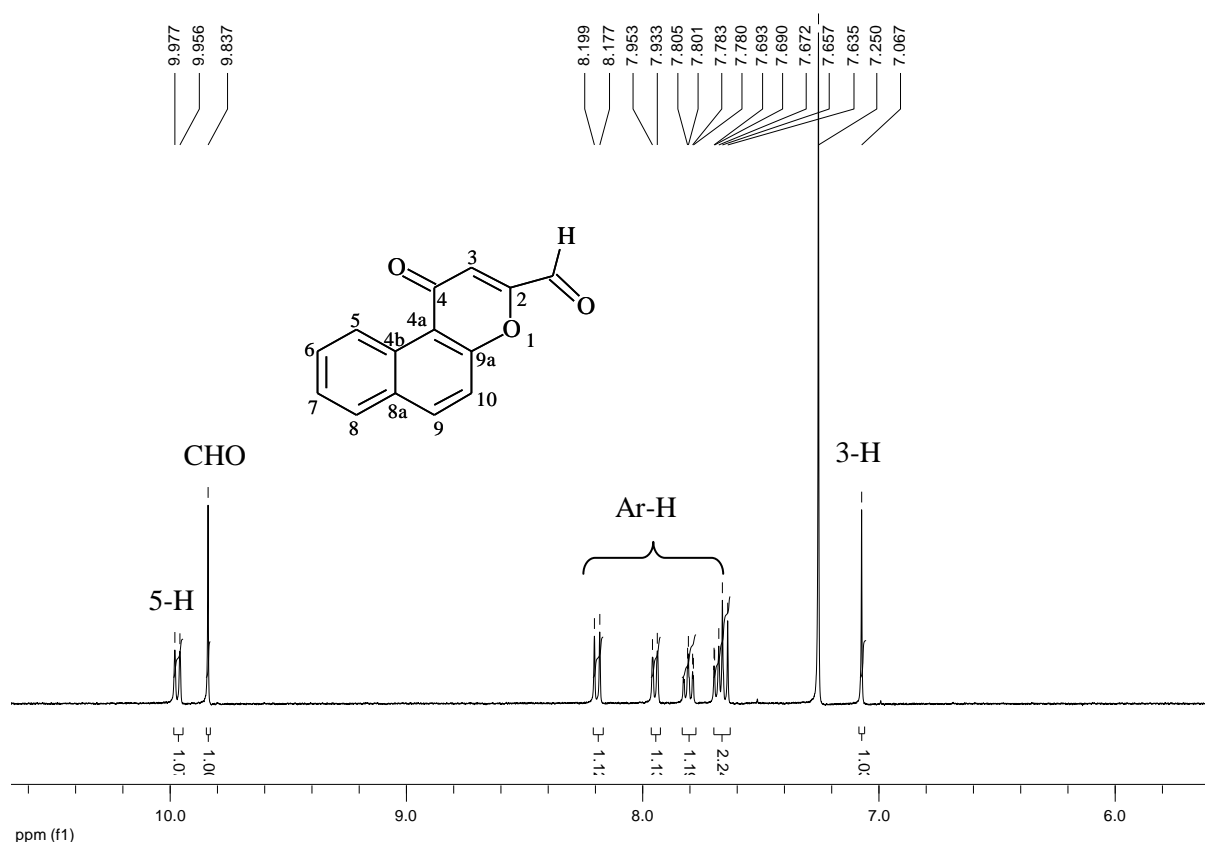
Figure 80. 400 MHz ^{1}H NMR spectrum of compound **292** in CDCl$_3$.
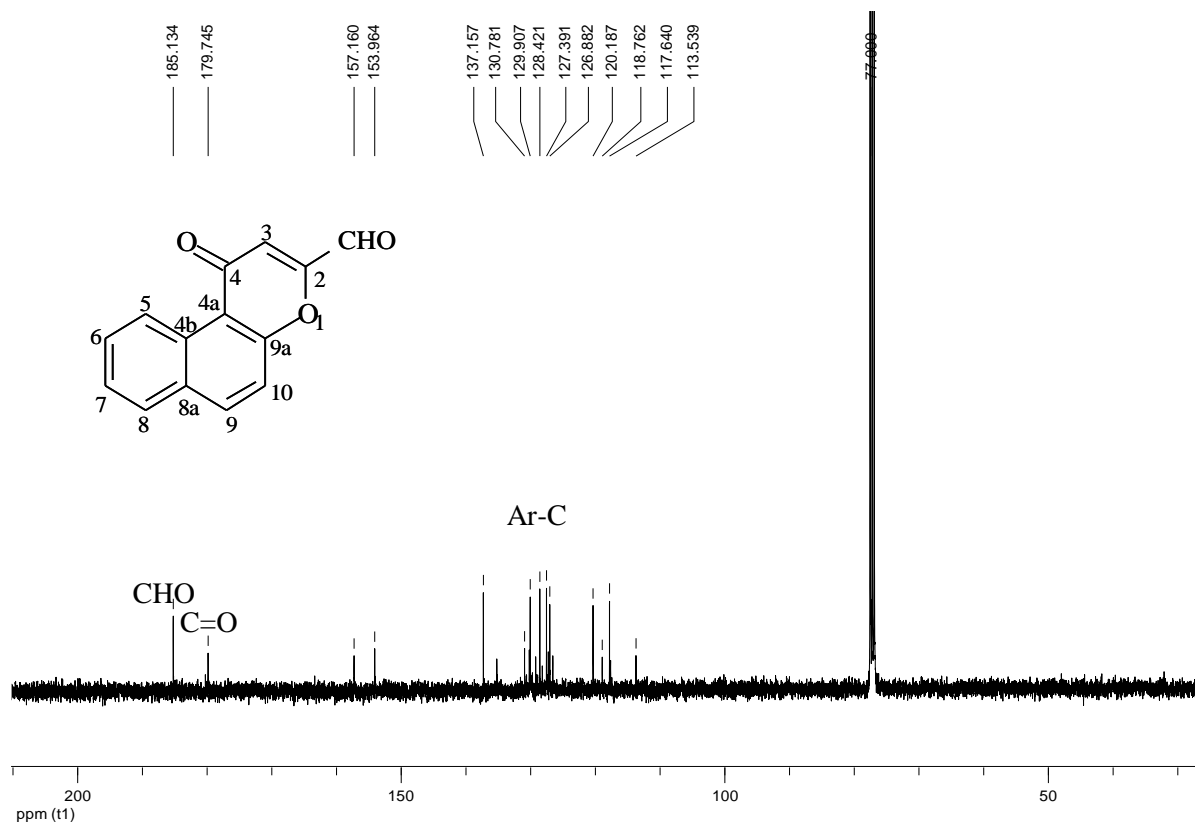
Figure 81. 100 MHz ^{13}C NMR spectrum of compound **292** in CDCl$_3$.

When the naphthopyranone-2-carbaldehyde **292** was reacted with acrylonitrile and 3-HQ, it afforded a product similar to those obtained for reactions of the chromone-2-carbaldehydes **222a-e**, characterised by a triplet at 1.45 ppm and a quartet at 4.50 ppm. This product was obtained as a yellow solid which was then recrystallised from a hexane-Et$_2$O mixture to give very fine yellow powdered crystals. The poor quality of these crystals prompted us to recrystallise the solid products obtained from the reactions of the 6-methoxy- and 6-fluoro-substituted chromone-2-carbaldehydes with DABCO in EtOH. A hexane-Et$_2$O solvent system was again used for the recrystallisation and the 6-methoxy-substituted product gave better crystals, which were subjected to single crystal X-ray analysis. The X-ray structure did not contain nitrogen (or an azetine ring!) as proposed initially. Instead the compound was shown (Figure 82) to be an ester derivative! Another interesting observation was the presence, in the asymmetric unit, of four different, independent conformations of the compound as shown in Figure 82. It became clear that the reaction of the chromone-2-carbaldehydes **222** with acrylonitrile afforded the ester derivatives **293a-e** and **294** (Scheme 72).
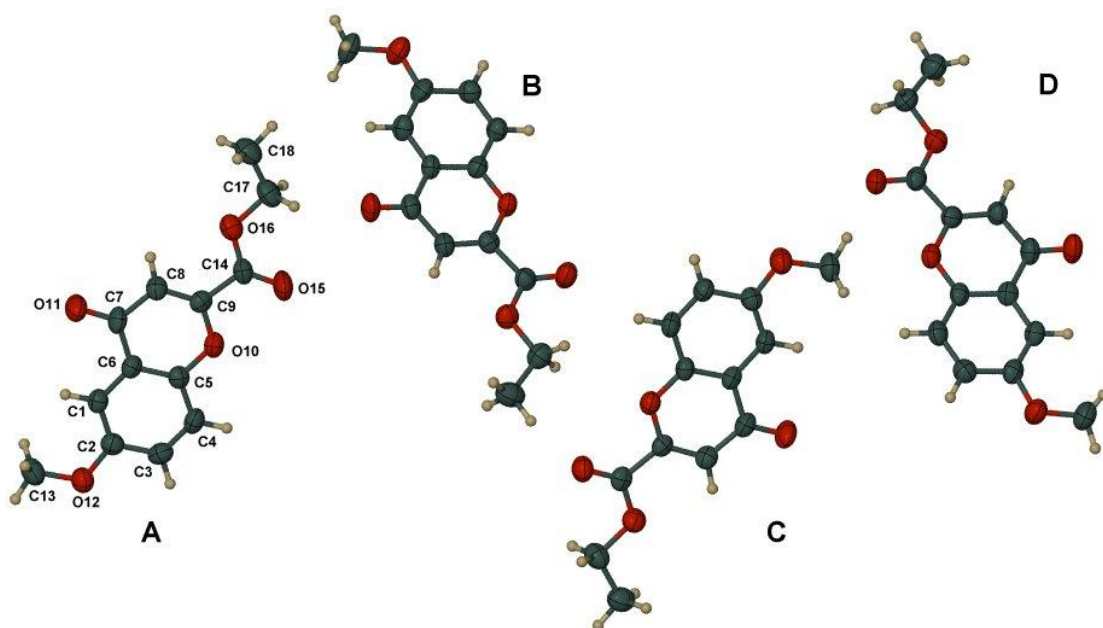
Figure 82. X-ray structure of the 6-methoxy substituted product **293c**. Shown are the four crystallographically independent molecules, with molecule **A** cystallographically numbered.

	R
222a	H
222b	Br
222c	OMe
222d	Cl
222e	F
292	Ph
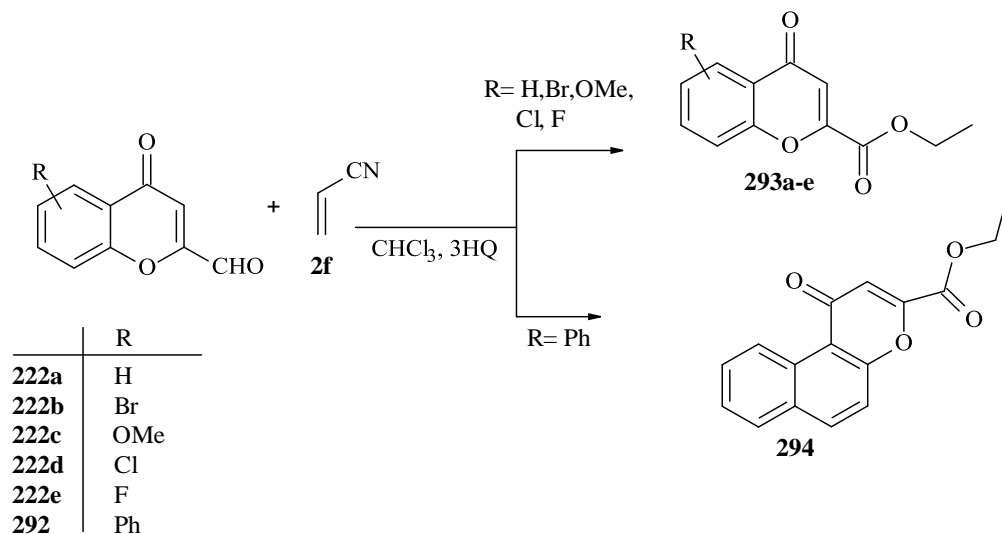
Scheme 72.

HRMS was used to further confirm the identity of the isolated compounds. Figure 83 shows the HRMS spectrum for the naphthopyrone derivative **294**. A peak at *m/z* 269.0819, corresponding to the molecular formula $C_{16}H_{13}O_4$ was observed, and is attributed to the **MH**$^+$ ion. The absence of nitrogen in the molecular formula of the observed protonated molecular ion is consistent with the X-ray structure of the 6-methoxy derivative **293c**.

Molecular formula: $C_{16}H_{12}O_4$;

Expected m/z: 268
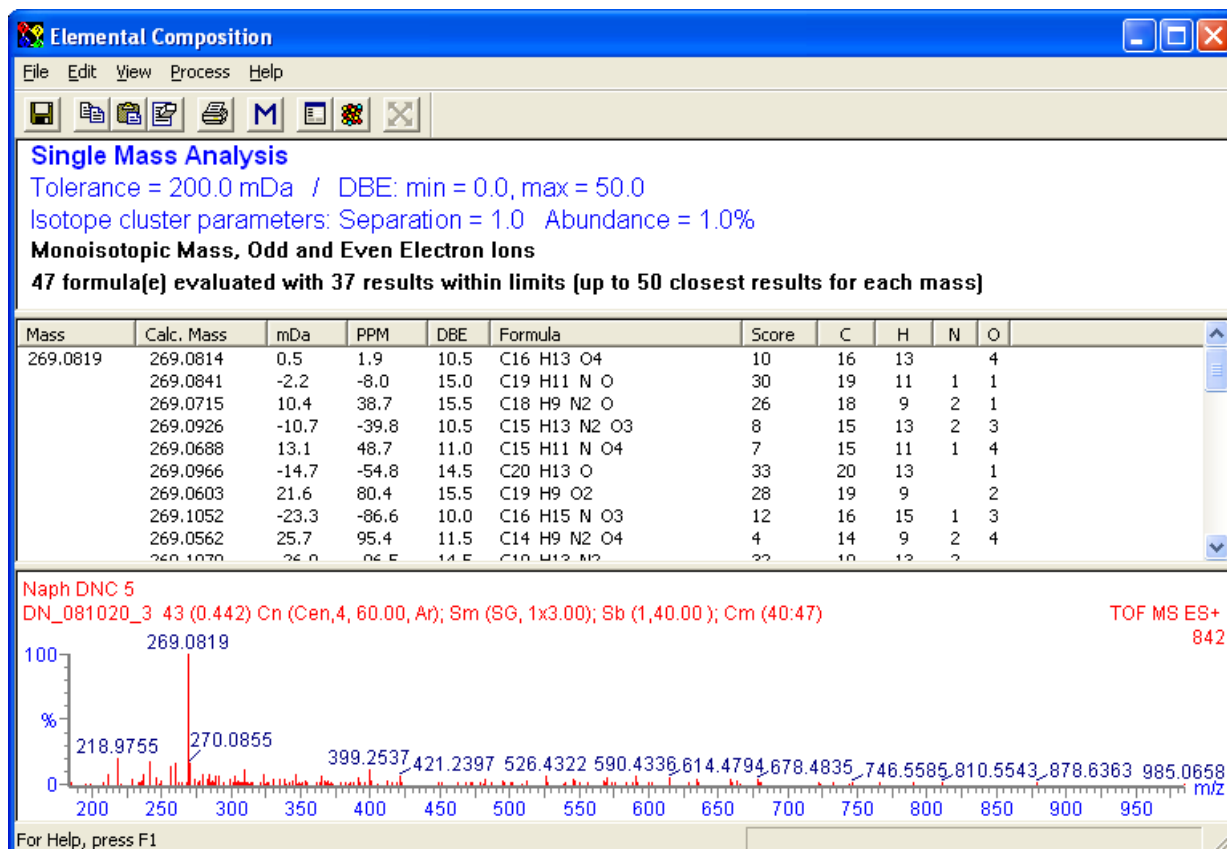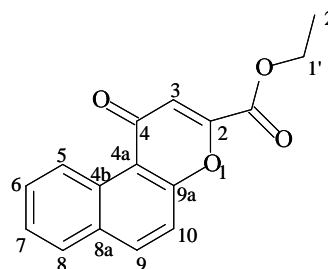
Figure 83. The HRMS spectrum and elemental composition of compound **294** using ESI.

The chromone analogues **293a-e** all gave satisfactory HRMS results and exhibited the expected NMR characteristics. The ^{1}H- and ^{13}C NMR spectra for compound **294** are shown in Figures 84 and 85 respectively. In the ^{1}H NMR spectrum, a triplet at c.a. 1.45 ppm is observed corresponding to the 3'-CH$_3$, while the 2'-CH$_2$ resonates as a quartet at *c.a.* 4.50 ppm. As observed with the precursors **291** and **292**, the 5-H aromatic proton appears further down field at 9.97 ppm due to the magnetic anisotropic effects of the carbonyl group. In the ^{13}C NMR spectrum the two carbonyl carbons C-1' and C-4 resonate at 160.5 and 179.9 ppm respectively.
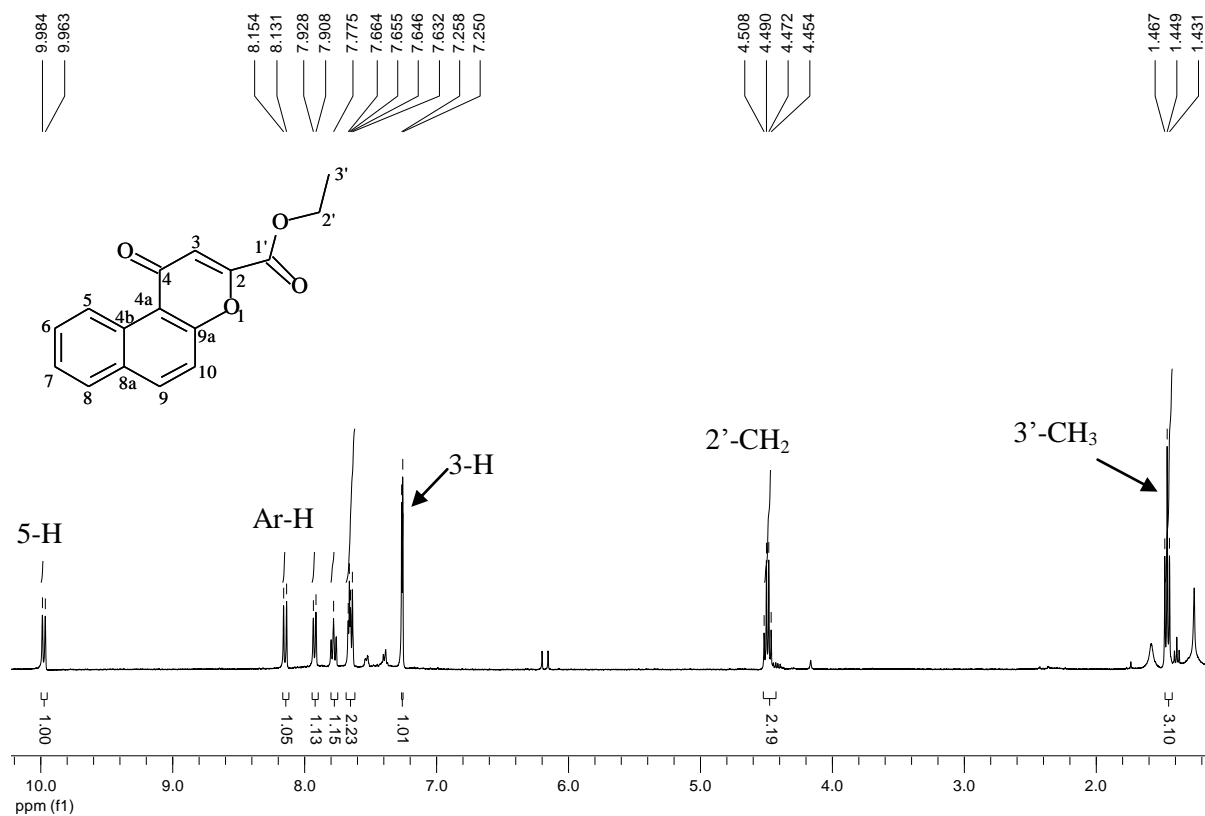
Figure 84. 400 MHz ^{1}H NMR spectrum of the naphthyl ester **294** derivative in CDCl$_3$.
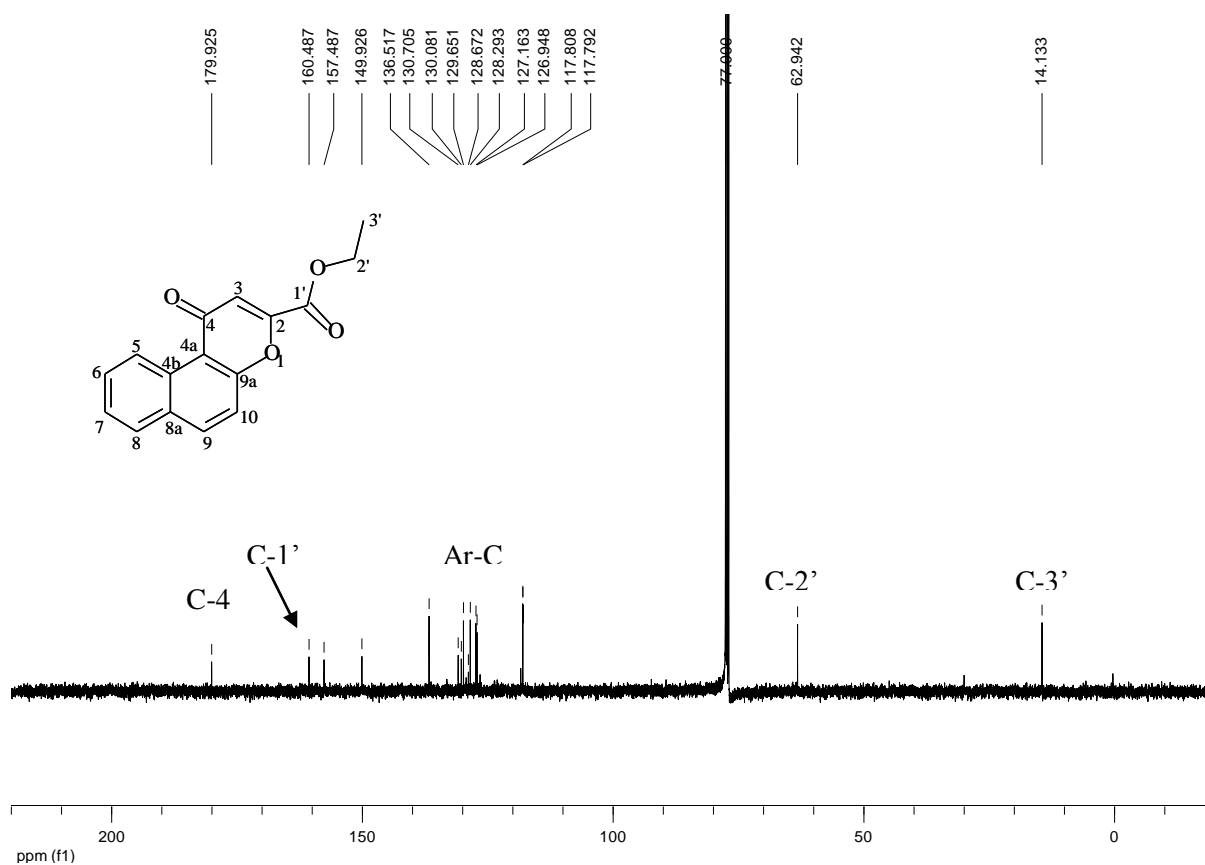
Figure 85. 100 MHz ^{13}C NMR spectrum of the naphtyl ester derivative **294** in CDCl$_3$.

2.2.6.2 *^{13}C NMR chemical shifts predictions*

NMR prediction programmes in ChemBioDraw[194] and MestreNova[195] were used to predict the ^{13}C NMR chemical shifts in compounds **293c** and **294**. A good correlation in most cases was observed between the predicted and experimental results, with slight deviations in a few cases. These results provided further confirmation that the isolated products were indeed the ester derivatives **293a-e** and **294**. Tables 6 and 7 show the predicted and experimental ^{13}C NMR chemical shifts for these compounds.
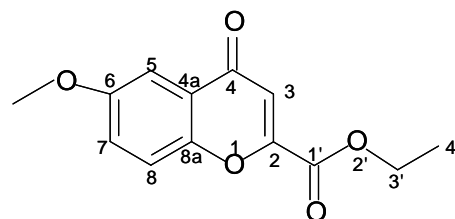
Table 6. Predicted and experimental ^{13}C NMR chemical shifts for compound **293c**.

Carbon Atom#	Experimental	ChemBioDraw	MestreNova
4'	14.1	14.2	14.7
3'	62.9	61.7	61.5
6-OMe	55.9	55.8	56.1
2	151.9	161.6	151.5
3	113.8	120.0	113.3
4	178.3	178.5	179.1
4a	125.2	123.8	123.6
5	104.6	105.6	108.3
6	157.5	155.3	156.4
7	125.0	124.7	122.3
8	120.2	120.7	119.6
8a	150.8	149.5	148.8
1'	160.6	162.1	162.4
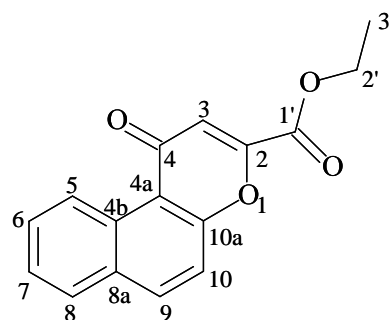
Table 7: Predicted and experimental ^{13}C NMR chemical shifts for compound **294**.

Carbon Atom#	Experimental	ChemBioDraw	MestreNova
3'	14.1	14.2	14.6
2'	62.9	61.7	61.5
2	149.9	161.6	153.6
3	117.7	120.0	114.3
4	179.9	182.1	179.9
4a	117.8	117.9	117.6
4b	130.1	131.0	133.3
5	128.3	126.9	126.0
6	130.7	135.0	127.3
7	127.2	124.9	126.3
8	128.7	131.6	128.5
8a	129.7	130.2	131.2
9	136.5	136.1	134.9
10	126.9	117.1	121.0
10a	157.5	156.9	161.5
1'	160.5	162.1	162.4

2.2.6.3 Origin of the unexpected ethyl chromone-2-carboxylates

The X-ray structure raised even more questions relating to the mechanism involved in the formation of the ester derivatives **293** and **294**, which contain no nitrogen in spite of forming in the presence of acrylonitrile. A possible explanation for the formation of the ester derivatives **293a-e** and **294** lay in the capacity of aldehydes to be readily oxidised in air to carboxylic acids, which could then react with EtOH to give the observed products, as outlined in Scheme 73. However, this explanation initially failed to explain the formation of the ester derivatives in the absence of EtOH, *i.e* when CHCl$_3$ is used as the solvent. We then realised that, in fact, EtOH is added in sufficiently high concentrations ($\approx$1%) to CHCl$_3$ as a stabiliser. Certain solvents such as CHCl$_3$ degrade with time on exposure to light, heat and oxygen, and stabilisers help to increase their shelf-life. It therefore seems that the EtOH added as a stabiliser was actually the source of EtOH when CHCl$_3$ is used in these reactions. The NMR

spectrum of the CHCl$_3$ used in these experiments is shown in Figure 86, and the presence of the EtOH signals is clearly evident. It would seem that acrylonitrile plays no role in these reactions!
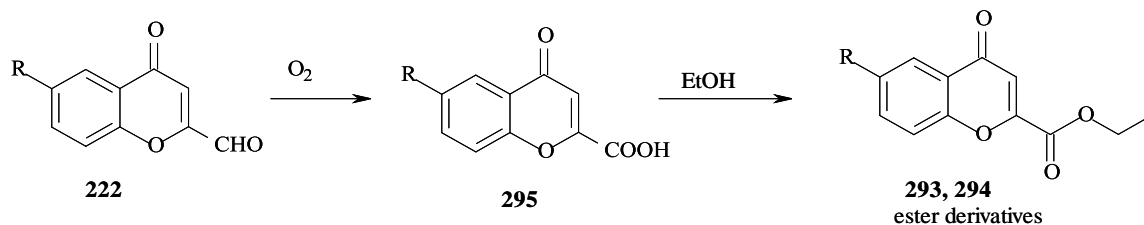
Scheme 73.
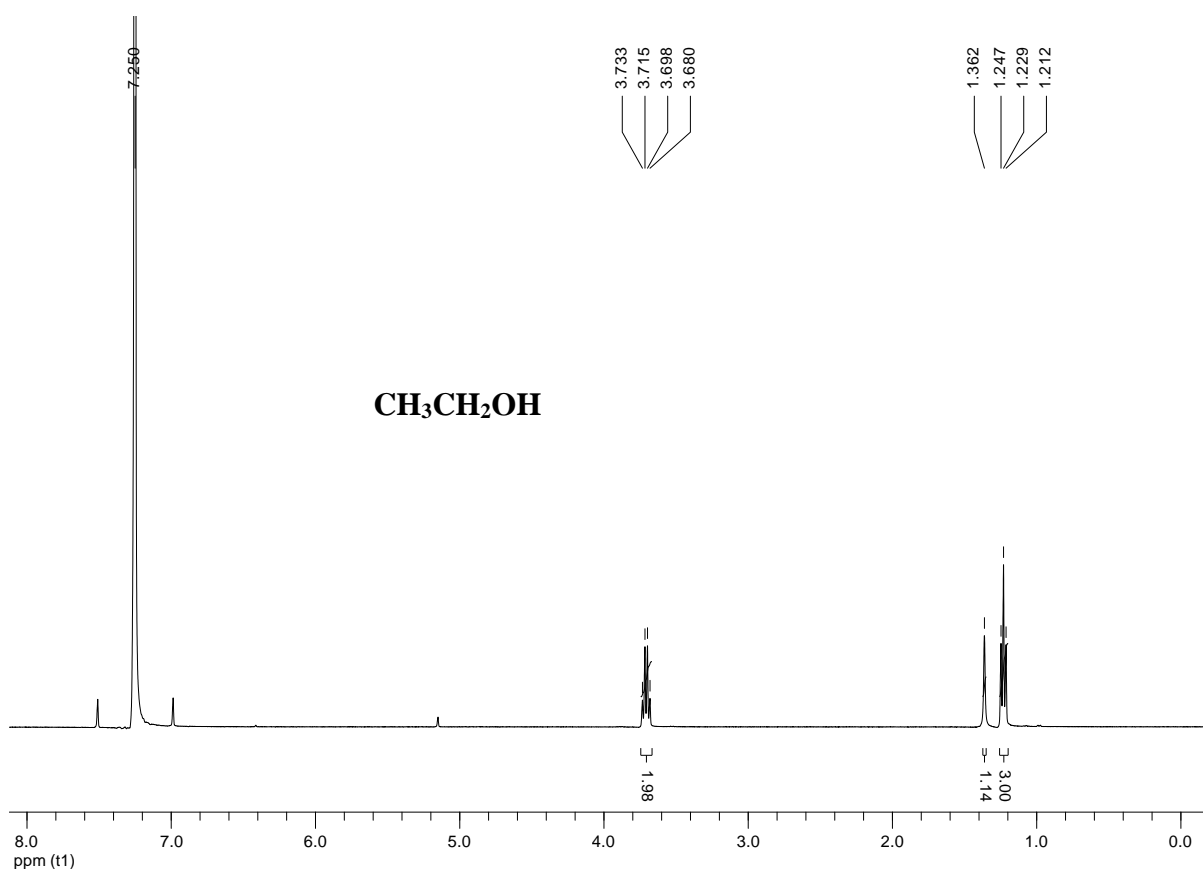
Figure 86. 400 MHz ^{1}H NMR spectrum, in CDCl$_3$, of the CHCl$_3$ solvent used in the reactions of chromone-2-carbaldehydes **222** with acrylonitrile.

2.2.7 Morita-Baylis-Hillman reactions of chromone-2-carbaldehydes with methyl acrylate

When the substituted chromone-2-carbaldehydes **222a-c** were reacted with methyl acrylate in the presence of 3-HQ as catalyst, different products were isolated depending on the substrate used. Scheme 74 shows the compounds isolated when the unsubstituted chromone-2-carbaldehyde **222a** was used. The three products **225a**, **293a** and **296** were all isolated in very low yields. Compound **225a** is the normal MBH adduct which had not been isolated in the previous study,[79] and its formation is directly linked to the formation of compound **296**. In the presence of excess methyl acrylate **2c**, more of the zwitterion **297** (Scheme 75) can be generated and react with the MBH adduct **225a**, acting as an electrophile, to give intermediate **298**. Elimination of the tertiary amine affords the product **296**. A similar product was isolated by Molefe in reactions of chromone-2-carbaldehyde **222a** with MVK.[79] The ester derivative **293a**, which had been isolated previously in the reaction with acrylonitrile in CHCl$_3$ was also interesting. The formation of this and of analogous products had been attributed to *in situ* oxidation of the aldehydes and reaction of the resulting carboxylic acids with ethanol present in CHCl$_3$ as a stabiliser (see Section 2.2.6.3). Figure 87 shows the ^{1}H NMR spectrum of the MBH adduct **225a** and the characteristic MBH signals are evident at 5.52, 5.85 and 6.38 ppm. The ^{1}H NMR spectrum of compound **296**, shown in Figure 88, reveals the presence of both the *syn* and *anti*-diastereomers.
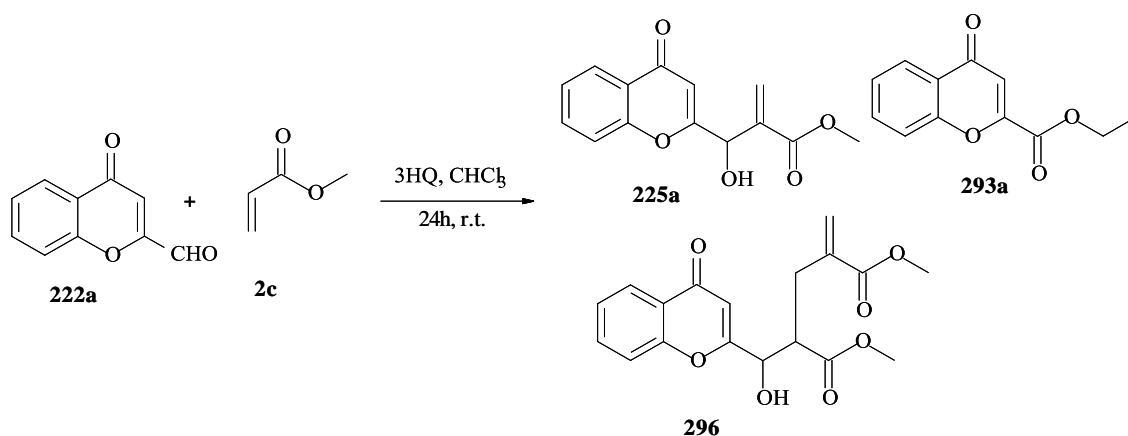
Scheme 74.
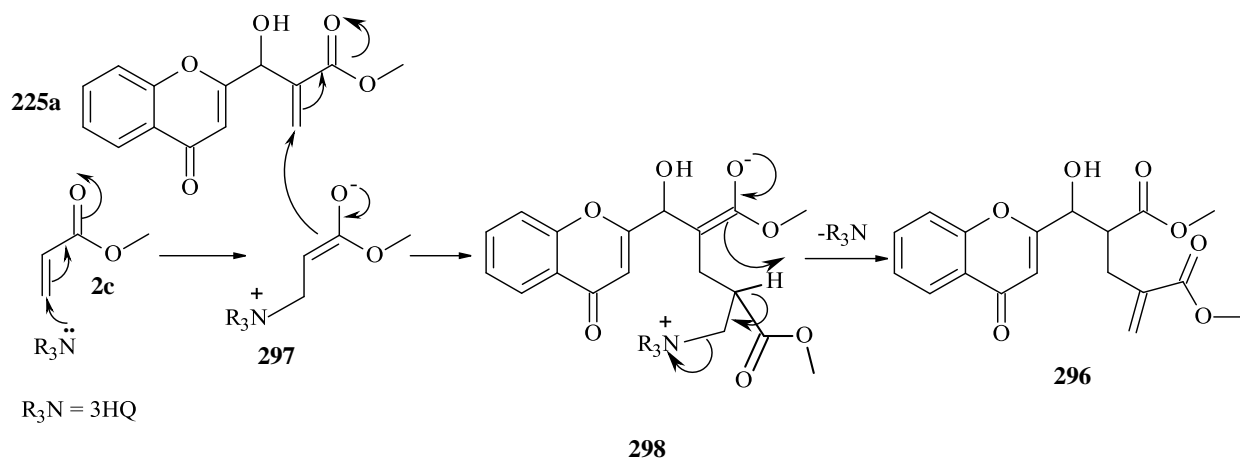
Scheme 75.
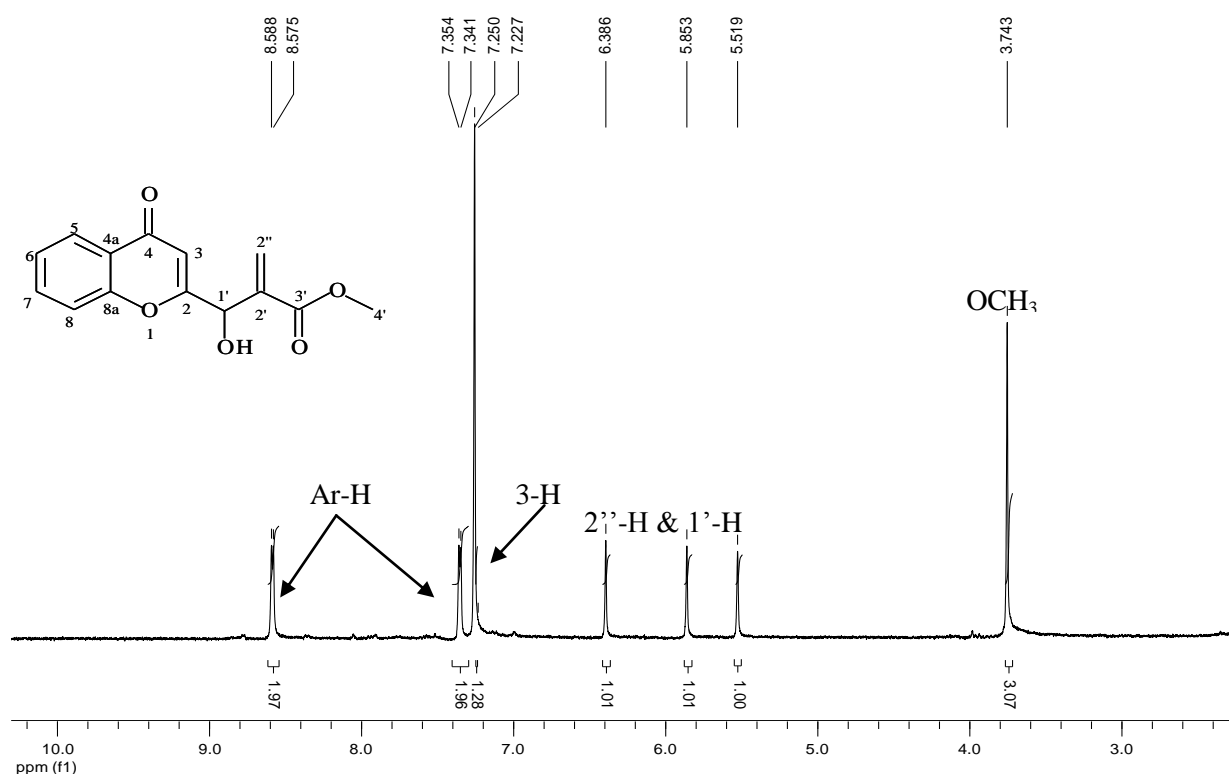
Figure 87. 400 MHz ^{1}H NMR spectrum of the MBH adduct **225a** in CDCl$_3$.
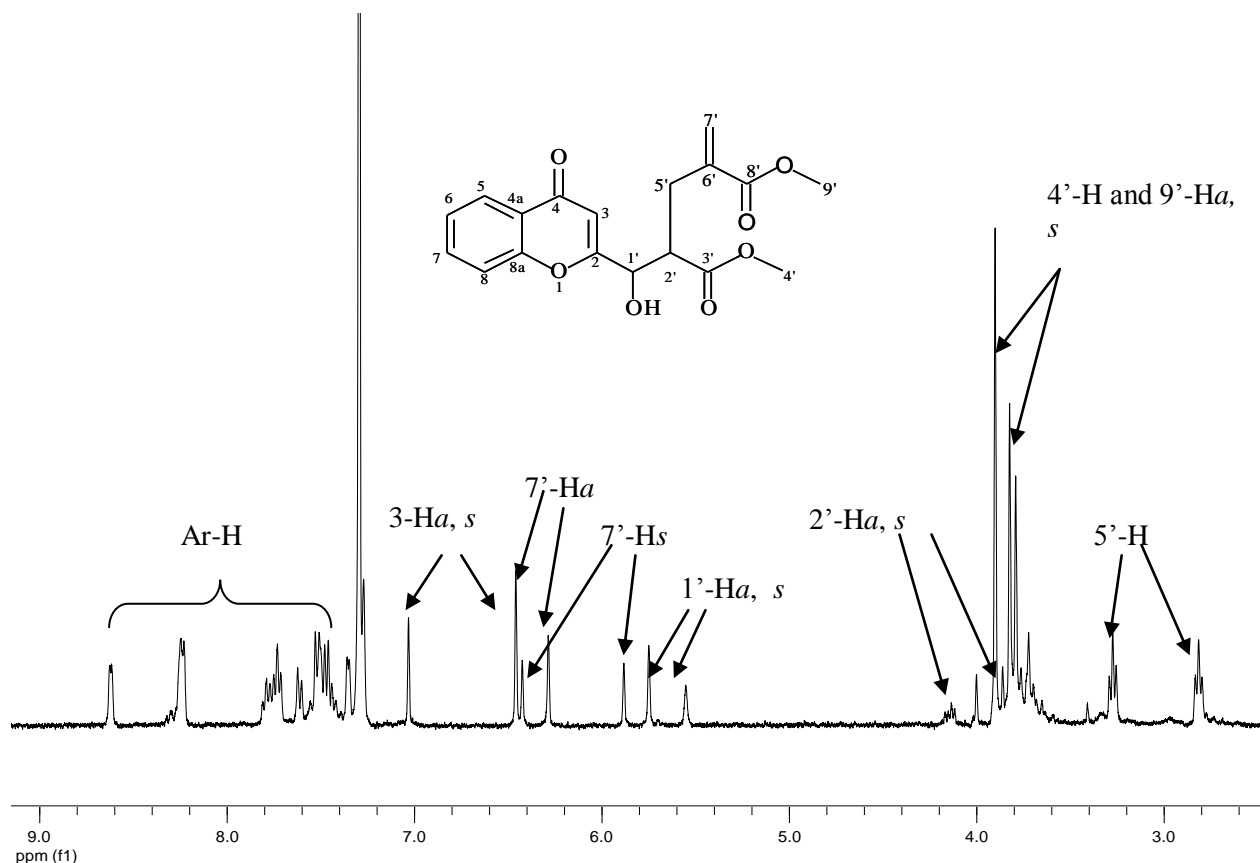
Figure 88. 400 MHz ^{1}H NMR spectrum of a mixture of the *syn* (s) and *anti* (a) diastereomers of compound **296** in CDCl$_3$.

The reaction of 6-methoxychromone-2-carbaldehyde **222c**, on the other hand, gave an unusual rearrangement product **226** as well as the ester derivative **293c** (Scheme 76). A proposed mechanism for the formation of compound **226** is illustrated in Scheme 77. This involves the displacement of the aldehyde group following attack of the zwitterionic enolate **297** at the electrophilic C-2 centre of the chromone system. A rearrangement leading to loss of carbon monoxide, an intramolecular hydride transfer and elimination of the catalyst in intermediate **299** affords the product **226**. When the chromone-2-carbaldehydes **222b** and **222d** were reacted with methyl acrylate intractable mixtures were obtained, ^{1}H NMR analysis of which indicated the presence of the ester derivatives **293**.
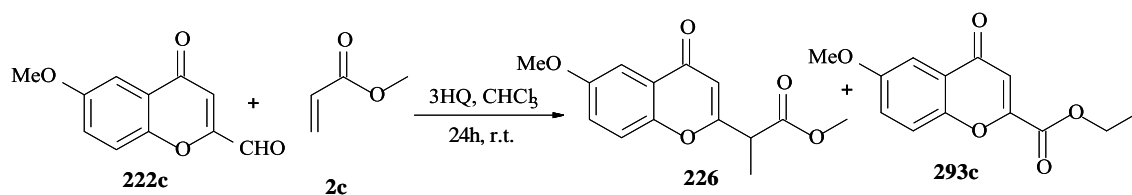
Scheme 76.
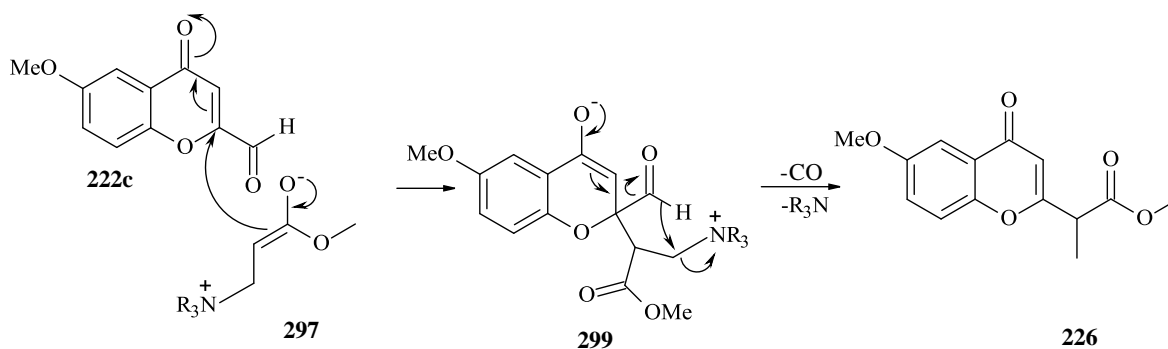
Scheme 77. Proposed mechanism for the formation of compound **226**.

The ^{1}H NMR spectrum of the unusual product **226** (Figure 89), reveals a doublet at 1.52 ppm corresponding to the 1''-methyl group and two singlets corresponding to the 4'- and 6-methoxy groups. The 1'-methine proton resonates as a quartet at 4.27 ppm, while the 3-methine proton resonates at 7.01 ppm. In the ^{13}C NMR spectrum (Figure 90), the fourteen expected carbon signals are evident. The 1''-methyl carbon resonates at 12.6 ppm and the 1'-methine carbon at 48.0 ppm. As expected, the two carbonyl carbons, C-2' and C-4 resonate much further downfield at 178.0 and 190.4 ppm, respectively. The assignments are supported by DEPT 135 and HSQC data.
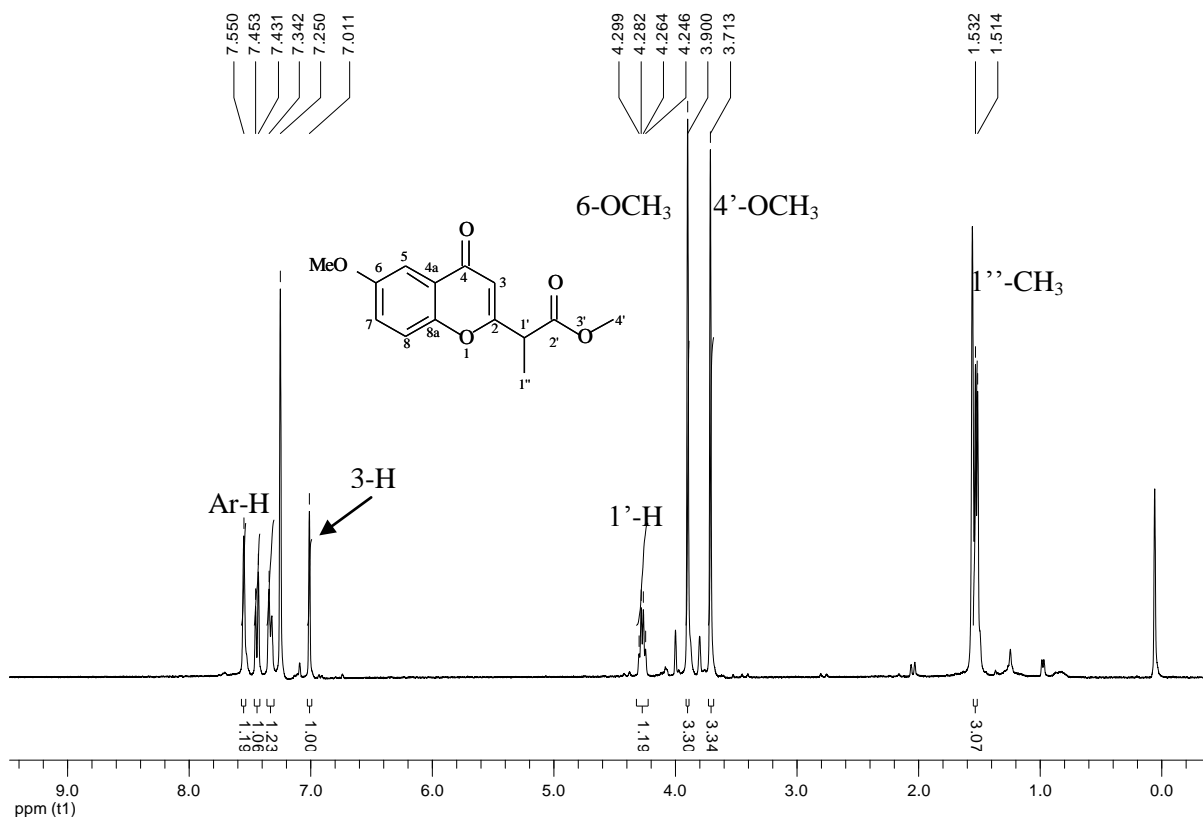
Figure 89. 400 MHz ^{1}H NMR spectrum of compound **226** in CDCl$_3$.
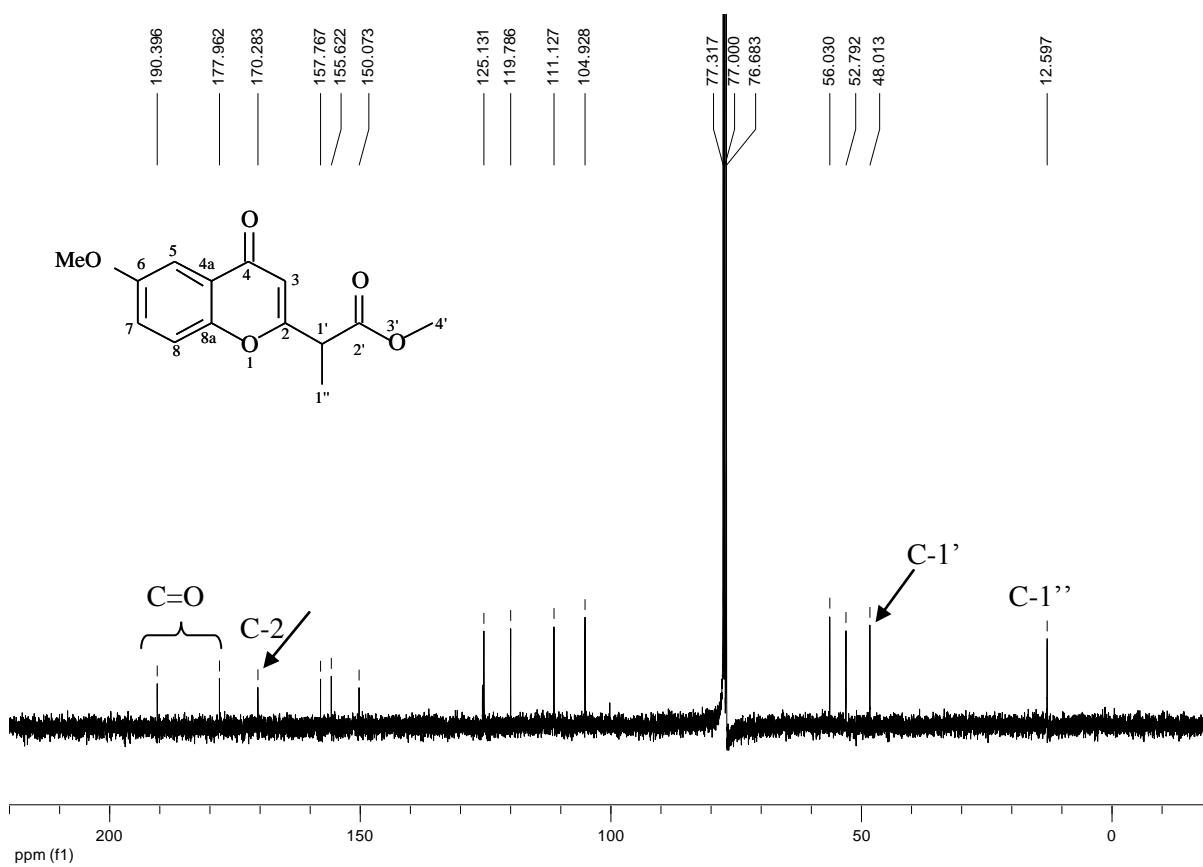
Figure 90. 100 MHz ^{13}C NMR spectrum of compound **226** in CDCl$_3$.

2.2.8 Kinetic studies of the Morita-Baylis-Hillman reactions of chromone-2-carbaldehydes with methyl acrylate

The progress of the reactions using chromone-2-carbaldehyde **222a** and 6-methoxychromone-2-carbaldehyde **222c** were followed by ^{1}H NMR spectroscopy, and the results obtained in both cases show the formation of several products and intermediates, indicating the operation of competing pathways. Figure 91 reflects the changes in the concentrations of the reactants and products with time when chromone-2-carbaldehyde **222a** was reacted with methyl acrylate in the presence of 3HQ as catalyst. The shape of the curve for the formation of compound **296** (**B**) indicates its dependency on the rate of formation of the MBH adduct **225a** (**A**). The formation of the MBH adduct **225a** (**A**) is initially quite rapid and reaches a maximum concentration at the same time at which the formation of compound **296** begins to increase rapidly, accompanied by a decrease in the concentration of the MBH adduct (**A**). These observations are consistent with the proposed mechanism (Scheme 75) for the formation of compound **296** (**B**) from attack of the zwitterion **297** on the MBH adduct **225a**.
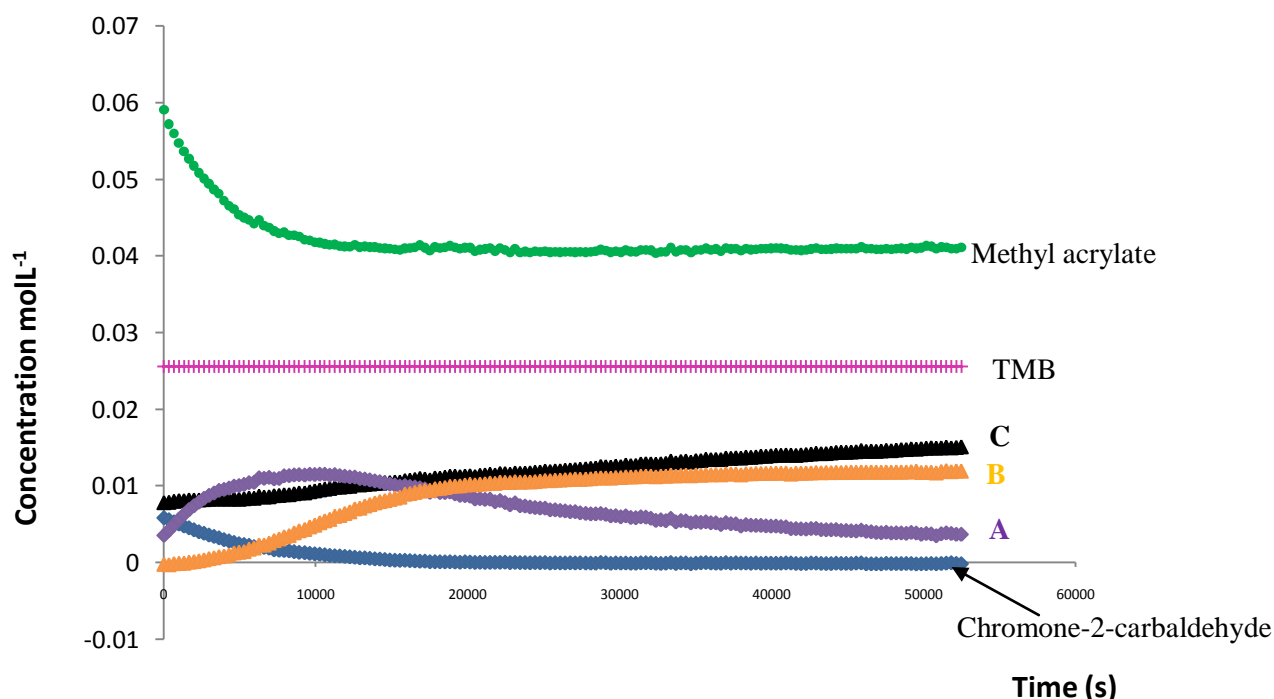
Figure 91. Graph of the progress of the reaction between the unsubstituted chromone-2-carbaldehyde **222a** with methyl acrylate, showing the three isolated products, the MBH adduct **225a** (**A**), adduct **296** (**B**) and ester derivative **293a** (**C**).

Figure 92, on the other hand, shows the changes in the concentrations of reactants and products in the reaction between 6-methoxychromone-2-carbaldehyde **222c** and methyl acrylate. Formation of compound **226** also appears to be dependent on the formation of an intermediate **B**. Thus, when there is a sufficient concentration of **B**, the rate of formation of compound **226c** begins to increase. The proposed mechanism for the formation of compound **226** is considered to proceed *via* the intermediate zwitterion **299** (Scheme 77). Assignment of the structure **299** to intermediate species (**B**), observed in the kinetic study but not isolated following work-up, is supported by the signals used to follow **B** which appear to correspond to compound **299**.

The kinetic plots (Figures 91 and 92) provide some confirmation of the proposed mechanisms (Schemes 75 and 77). Given the fact that the series of chromone-2-carbaldehyde substrates failed to exhibit consistent, general product distribution patterns, further investigation of the underlying mechanisms did not seem to be warranted at this stage.
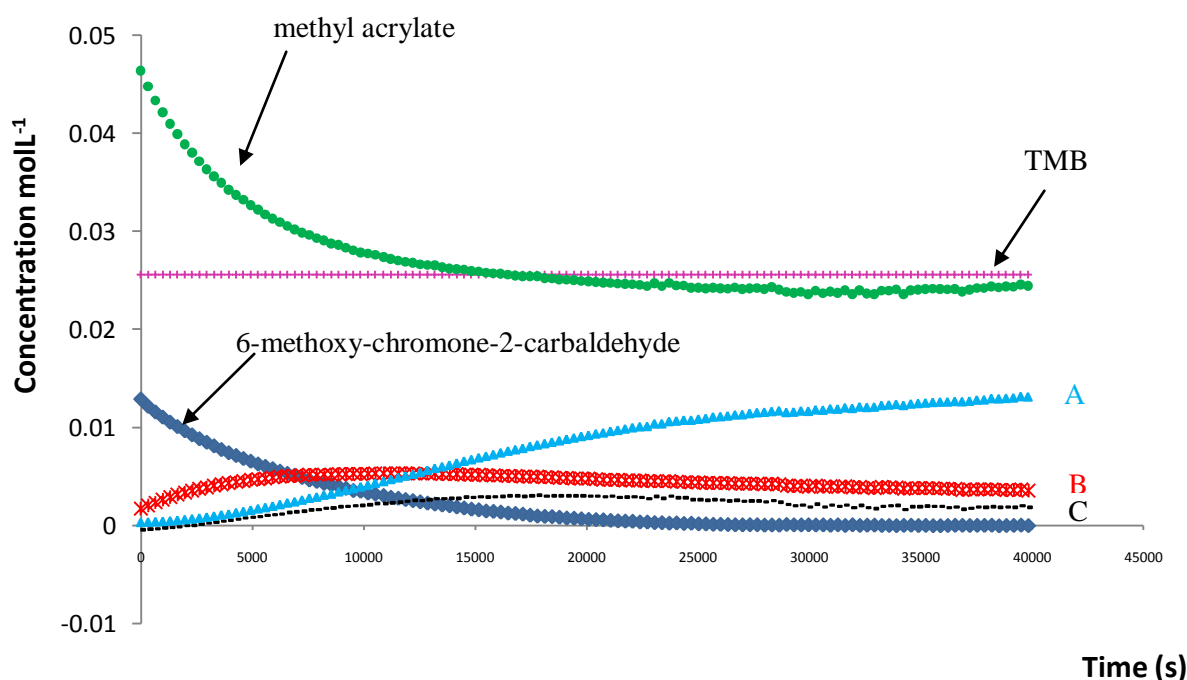
Figure 92. Graph of the progress of the reaction between 6-methoxychromone-2-carbaldehyde **222c** with methyl acrylate, showing the three isolated products, compound **226c** (**A**), the intermediate (**B**) and the ester derivative **293c** (**C**).

2.3 Synthesis and Michaelis-Arbuzov reactions of coumarin derivatives

Coumarins belong to the benzopyrone class of compounds and are found in many plants, such as tonka bean (*Dipteryx odoratal*), vanilla grass (*Anthoxanthum odoratum*) and cassia cinnamon (*Cinnamomum aromaticum*).[176-178]Coumarins have been shown to have a wide range of biological activity such as anti-HIV, anti-tumour, anti-hypertension, anti-osteoporosis, anti-septic, anti-arrhythmia, anti-inflammatory and analgesic. Reports have also been made on their use in the treatment of ashthma[176] and lymphedema.[177] As such their synthesis has received considerable attention.

2.3.1 Synthesis of salicylaldehyde-derived MBH adducts

Musa and Kaye[19,85] have reported that use of *tert*-butyl acrylate as the activated alkene in MBH reactions with substituted salicylaldehydes **72**, permits cyclisation of the corresponding MBH adducts to coumarins without the need to protect the phenolic hydroxyl group. Following their approach, the substituted salicylaldehydes **72a,c,e** were reacted with *tert*-butyl acrylate in the presence of DABCO in CHCl$_3$ (Scheme 78). Work-up and flash chromatography afforded the MBH adducts **83a,c,e** in yields ranging between 21 and 56%. Slow reaction times and low yields are often a draw-back in MBH reactions (see Section 1.1.2), as is the case in this particular reaction. Figure 93 shows the ^{1}H NMR spectrum of compound **83a**. The three characteristic MBH signals, due to the 2''-vinylic and 1'-methine protons, are present at 5.49, 5.69 and 6.23 ppm. The ^{13}C NMR spectrum (Figure 94) reveals the expected twelve signals with the *tert*-butyl methyl carbons resonating as an intense signal at 28.0 ppm, and the quartenary C-4' carbon at 82.6 ppm.

	R^1	R^2
a	H	H
c	H	OEt
e	Br	H
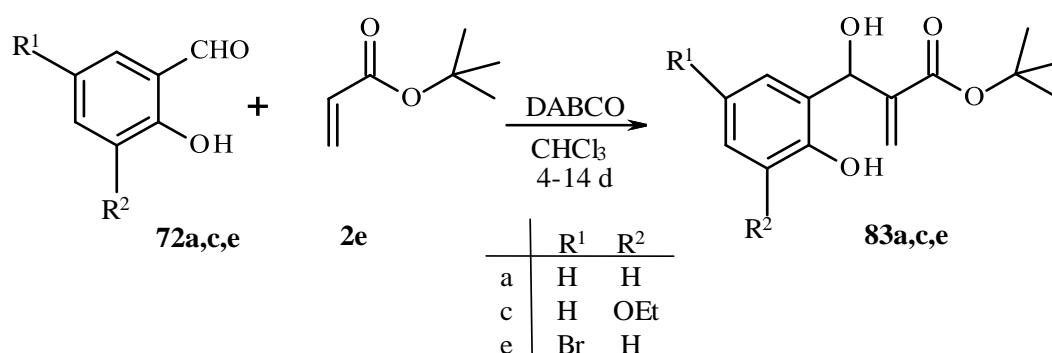
Scheme 78
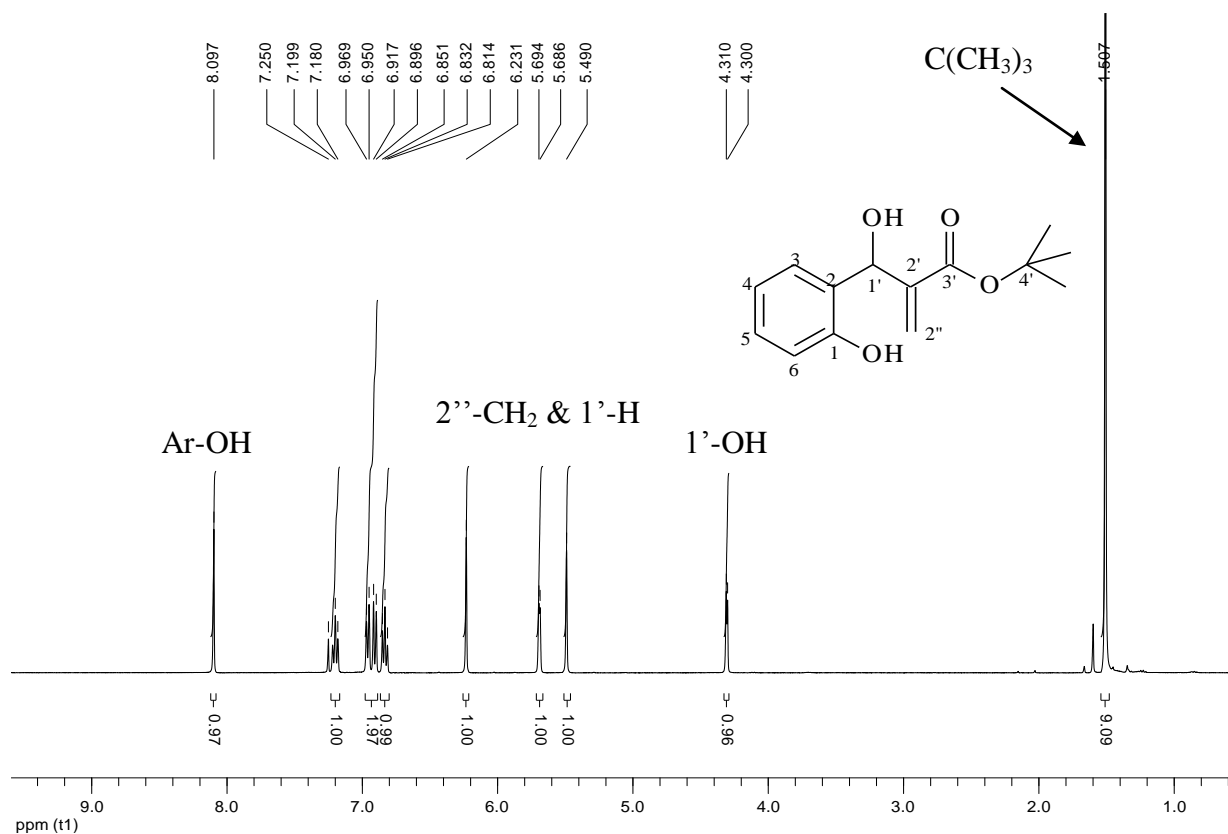
Figure 93. 400 MHz ^{1}H NMR spectrum of compound **83a** in CDCl$_3$.
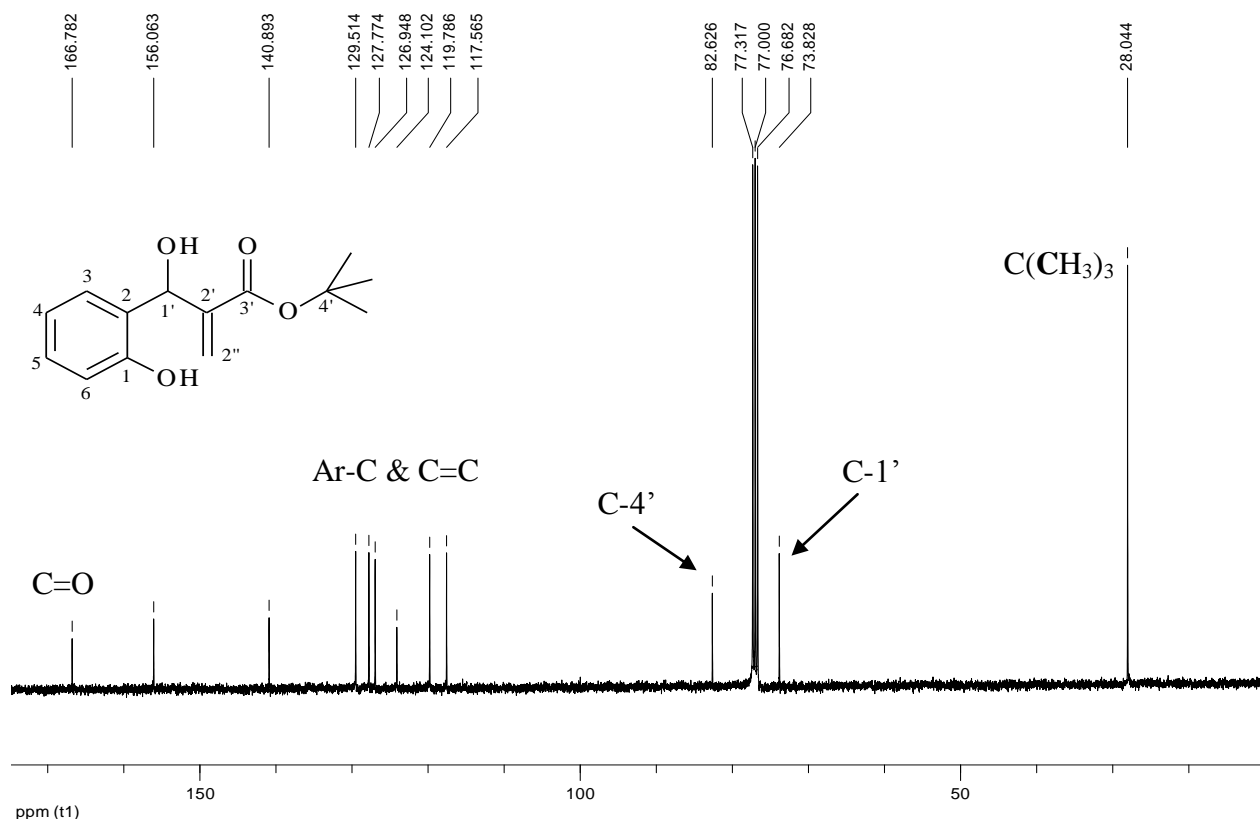
Figure 94. 100 MHz ^{13}C NMR spectrum of compound **83a** in CDCl$_3$.

2.3.2 Acid-catalysed cyclisation of salicylaldehyde-derived Morita-Baylis-Hillman adducts

Acid-catalysed cyclisation of the MBH adducts under reflux using either hydrochloric acid or hydroiodic acid in a mixture of acetic acid and acetic anhydride has been reported[19,85] to yield the 3-halomethyl coumarins **81** and **82**. In the present study when HCl was used, the expected 3-chloromethyl coumarins **82a,c,e** were isolated in very good yields (68-95%). However, in the case of compound **83a**, the 3-(hydroxymethyl)coumarin **300a** was isolated in a low yield of 1% together with the 3-(chloromethyl)coumarin **82a**. Figure 95 shows the ^{1}H NMR spectrum of the unsubstituted 3-(chloromethyl)coumarin **82a**. The methylene protons resonate as a singlet at 4.55 ppm and all the expected aromatic proton signals are present. The ^{13}C NMR spectrum (Figure 96) shows the methylene carbon resonating at 41.0 ppm, which is within the expected region for a methylene carbon bearing a chlorine atom. The carbonyl carbon resonates at 160.1 ppm, and the quartenary carbon C-6 is at 153.6 ppm. The ^{1}H- and ^{13}C-NMR spectra of the 3-(hydroxymethyl)coumarin **300a** are shown in Figures 97 and 98, respectively. The methylene protons resonate as a doublet at 4.62 ppm due to coupling with the neighbouring hydroxyl proton. In the ^{13}C NMR spectrum the methylene carbon resonates at 61.2 ppm, a downfield shift (compared to the chloromethylene carbon in compounds **82a,c-e**) which is due to the presence of the highly electronegative oxygen atom.
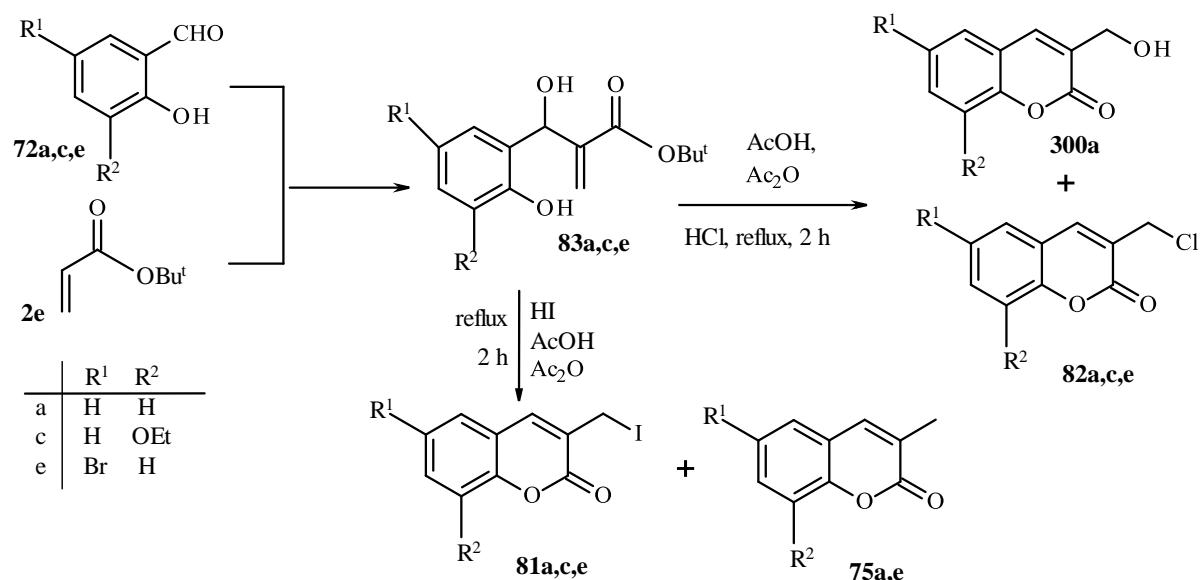
Scheme 79
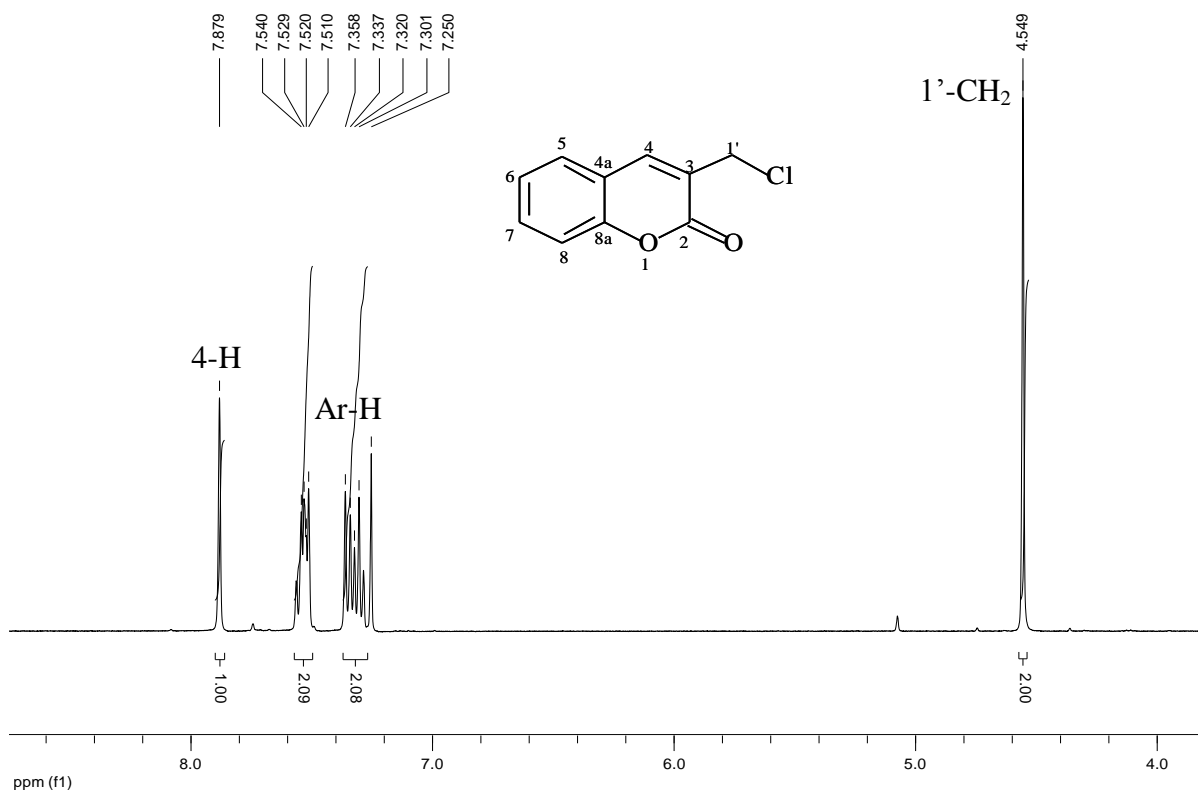
Figure 95. 400 MHz ^{1}H NMR spectrum of compound **82a** in CDCl$_3$.
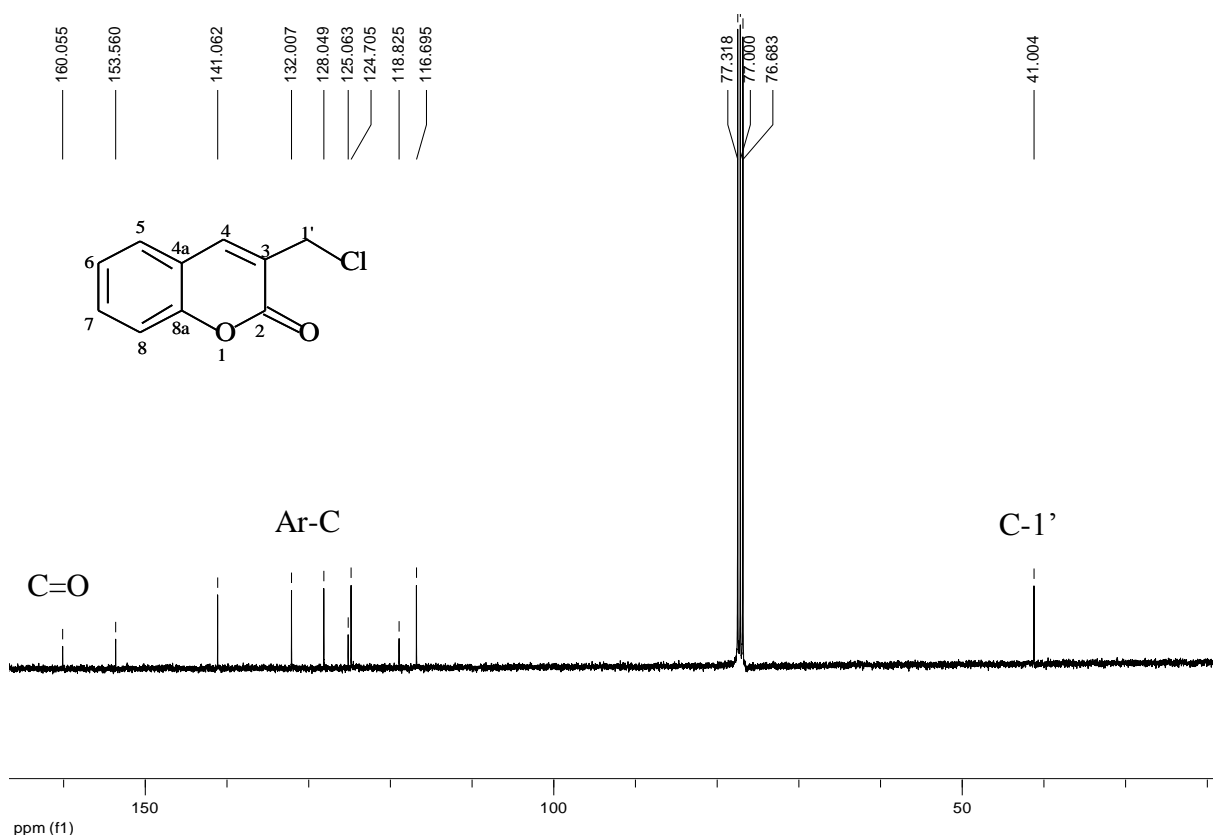
Figure 96. 100 MHz ^{13}C NMR spectrum of compound **82a** in CDCl$_3$.
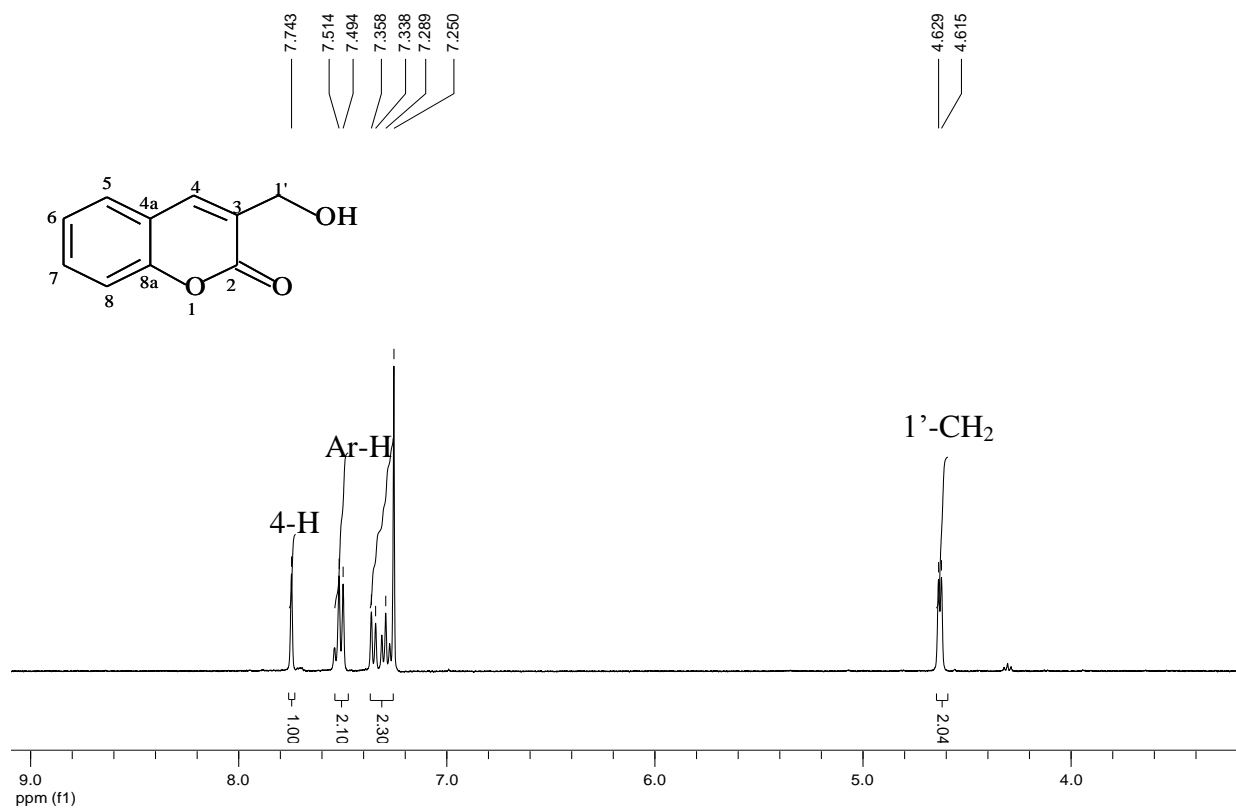
Figure 97. 400 MHz ^{1}H NMR spectrum of compound **300a** in CDCl$_3$.
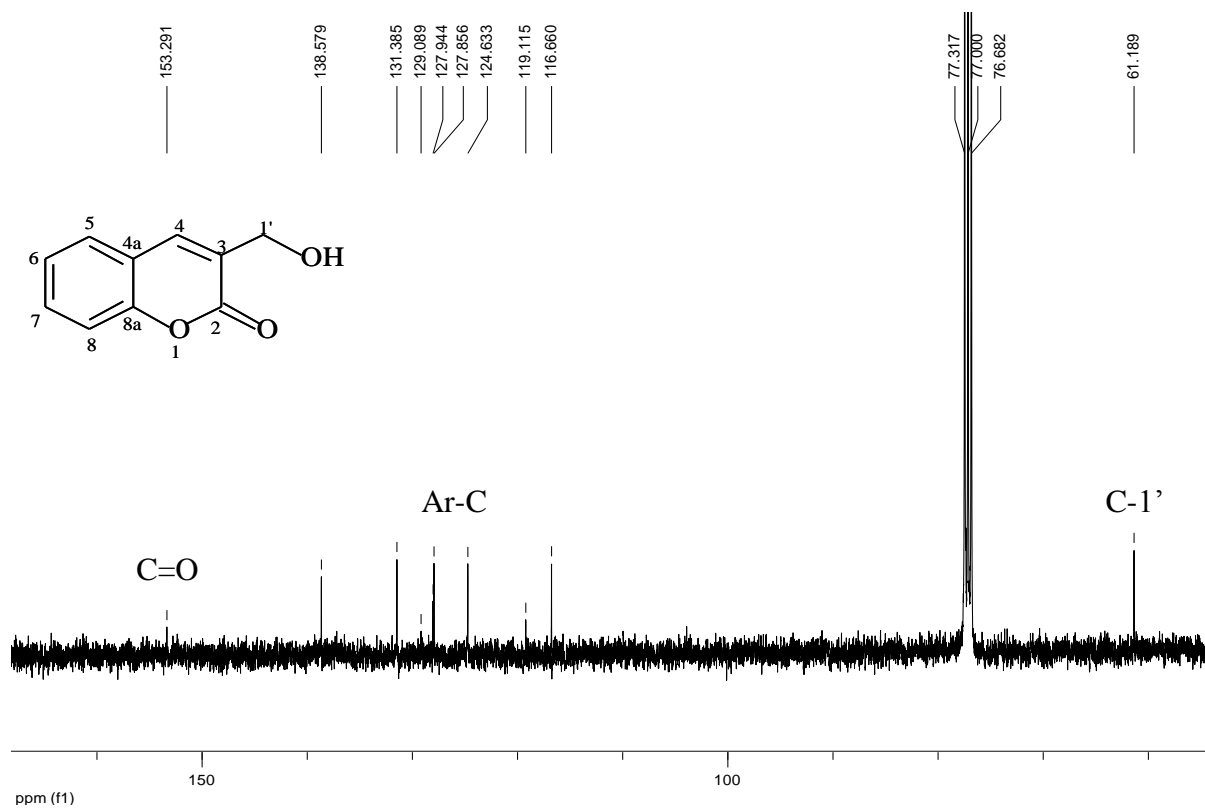
Figure 98. 100 MHz ^{13}C NMR spectrum of compound **300a** in CDCl$_3$.

When the MBH adducts **83** were reacted with hydroiodic acid (Scheme 79) at reflux temperature (*ca.* 140 °C) for 2 hours, the reduced methyl analogues **75a,e** were isolated exclusively, while the ethoxy-substituted adduct **83c** gave the expected 3-(iodomethyl)coumarin **81c**. These observations prompted us to explore the reaction conditions further. Firstly we looked at reducing the reaction time to 1 hour, on the assumption that formation of the 3-(iodomethyl)coumarins was occurring rapidly and that reducing the reaction time would stop their reduction to the methyl analogues. After 1 hour the methyl analogues were again isolated exclusively; a further reduction of the reaction time to 30 minutes gave the same results, suggesting that the length of time did not have a significant effect on the type of products produced. We then opted to use acetic acid alone (without acetic anhydride) but, again, the methyl analogues were isolated. The effect of temperature on the reaction was then explored. The oil bath temperature was reduced to *ca.* 120 °C and mixtures of the 3-(iodomethyl)coumarins **81a,e** and their reduced analogues **75a,e** were formed with the desired 3-(iodomethyl)coumarins **81a,e** being the major products. These observations suggested that the reaction was sensitive to the temperature; which was then reduced to 90 °C and then 40 °C but mixtures of the two products were still obtained, with more of the reduced methyl analogues! We further came to the conclusion that an optimum temperature *ca.* 120 °C was required and finally that the reaction time had little significance on the type of products isolated. Use of acetic anhydride did not appear to be really necessary as acetic acid alone gave the same products. It may be that the different product distributions obtained reflect changing concentrations on the hydroiodic acid.

The MBH adducts **83a,c,e** were all reacted with HI in acetic acid and at 120 °C. Flash chromatography on silica separated the mixtures although the unsubstituted derivatives proved rather difficult to isolate. Figure 99 shows the ^{1}H NMR spectrum of the mixture of compounds **81a** and **75a** before separation with the 1'-methylene and 3-methyl protons present at 4.36 and 2.22 ppm, respectively. The ^{1}H NMR spectrum of the 3-iodomethylcoumarin **81a** after separation is shown in Figure 100. The methylene protons resonate at 4.37 ppm as a singlet and the 4-methine proton as a singlet at 7.83 ppm. In the ^{13}C NMR spectrum (Figure 101) the methylene carbon resonates at -1.59 ppm, which is typical of methylene carbons bearing an iodine atom. The other expected carbon signals are all accounted for. Figure 102 shows the ^{1}H NMR spectrum of the reduced methyl analogue **75a**. The methyl protons resonate at 2.21 ppm and the 4-methine proton at 7.50 ppm, while the ^{13}C

NMR spectrum (Figure 103) reveals the expected ten carbon signals, with the methyl carbon resonating at 17.1 ppm and the carbonyl carbon at 162.2 ppm.
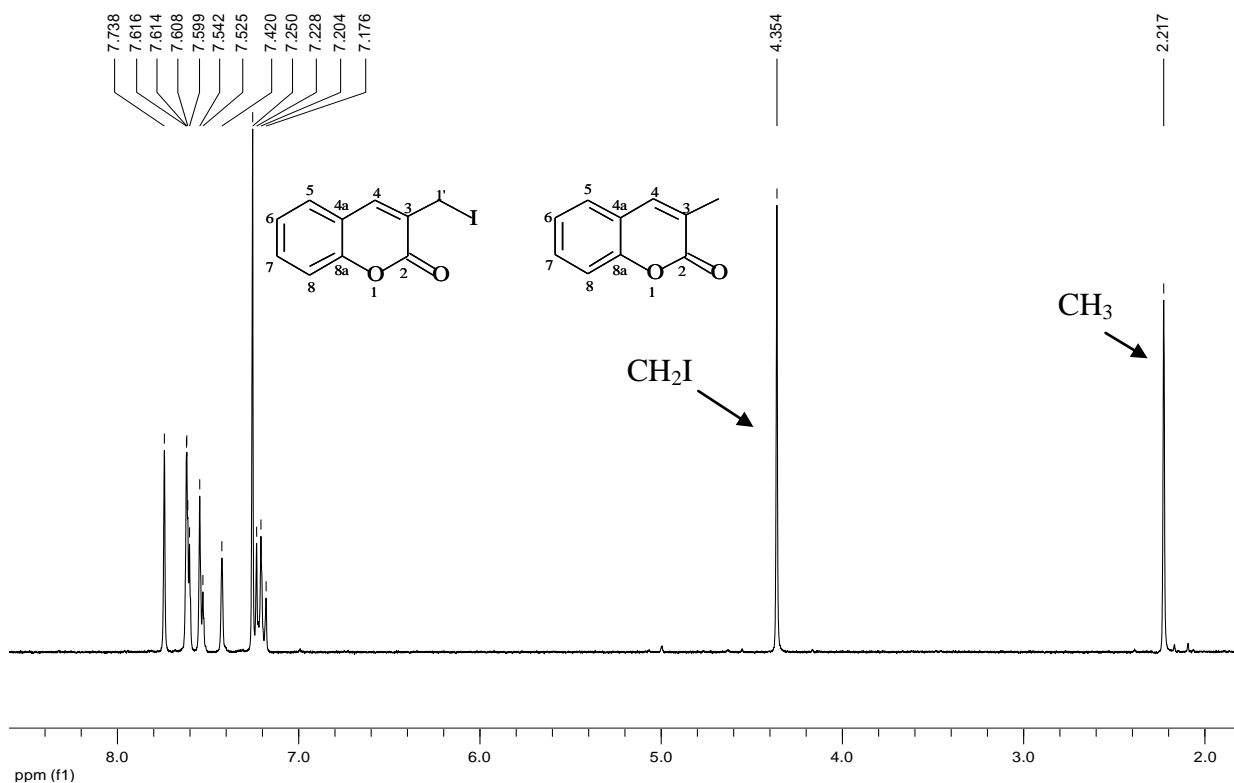
Figure 99. 400 MHz ^{1}H NMR spectrum of the mixture of compounds **81a** and **75a** in CDCl$_3$.
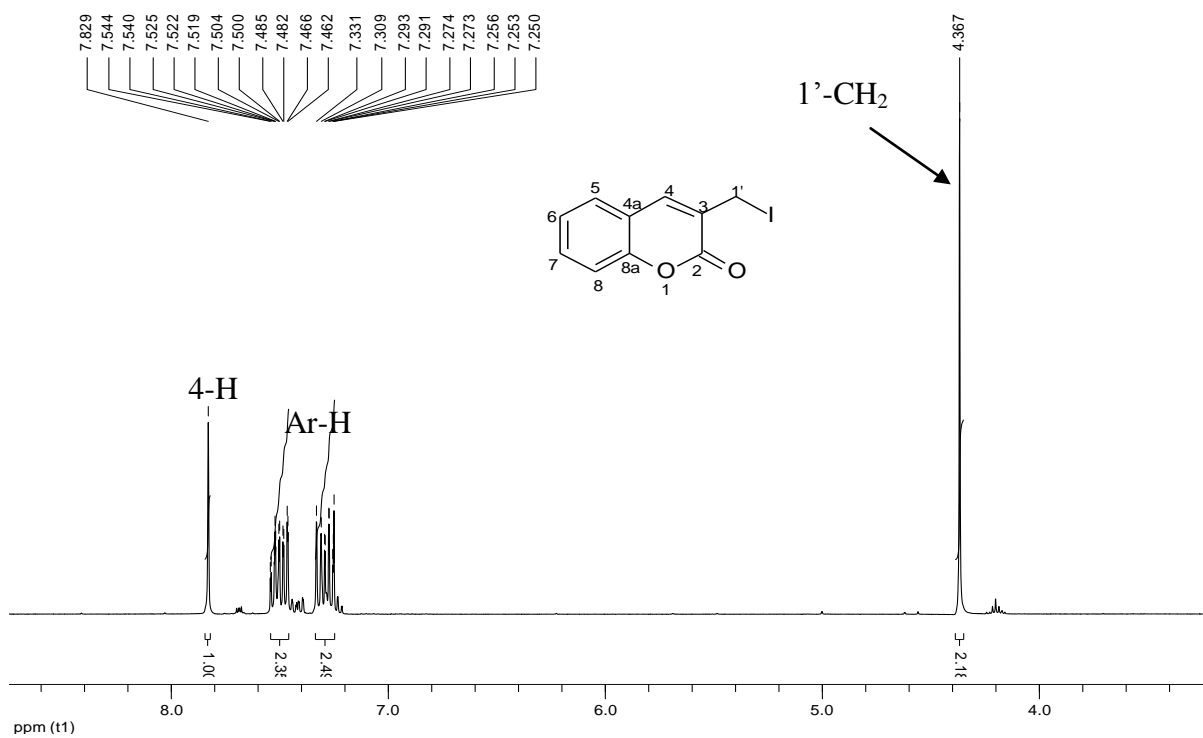
Figure 100. 400 MHz ^{1}H NMR spectrum of compound **81a** in CDCl$_3$.
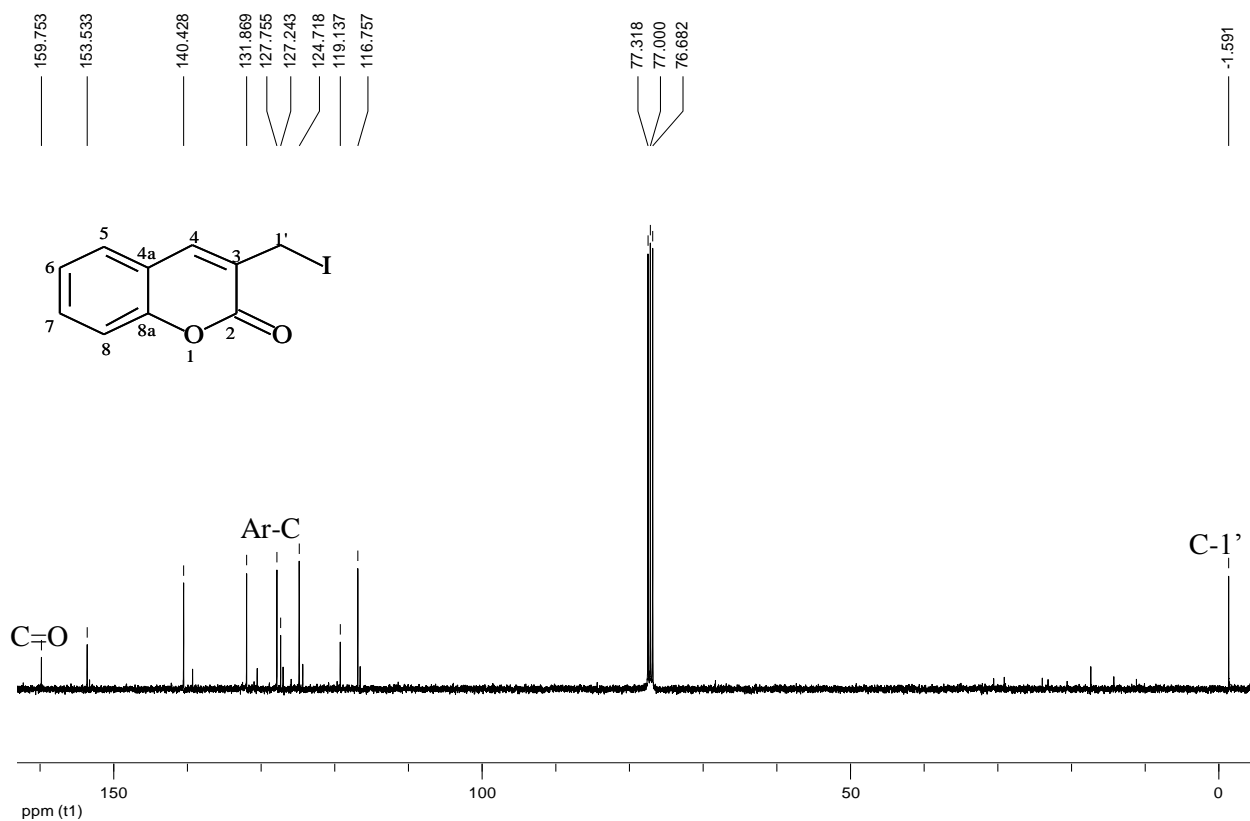
Figure 101. 100 MHz ^{13}C NMR spectrum of compound **81a** in CDCl$_3$.
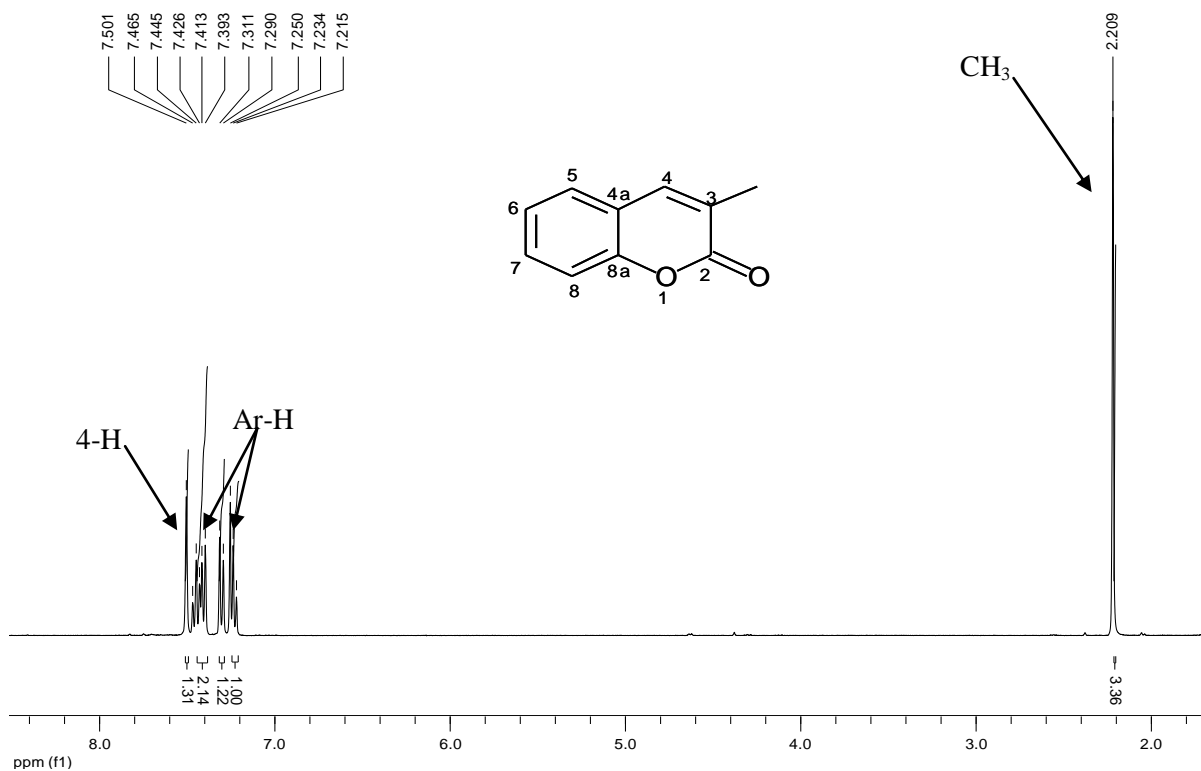
Figure 102. 400 MHz ^{1}H NMR spectrum of compound **75a** in CDCl$_3$.
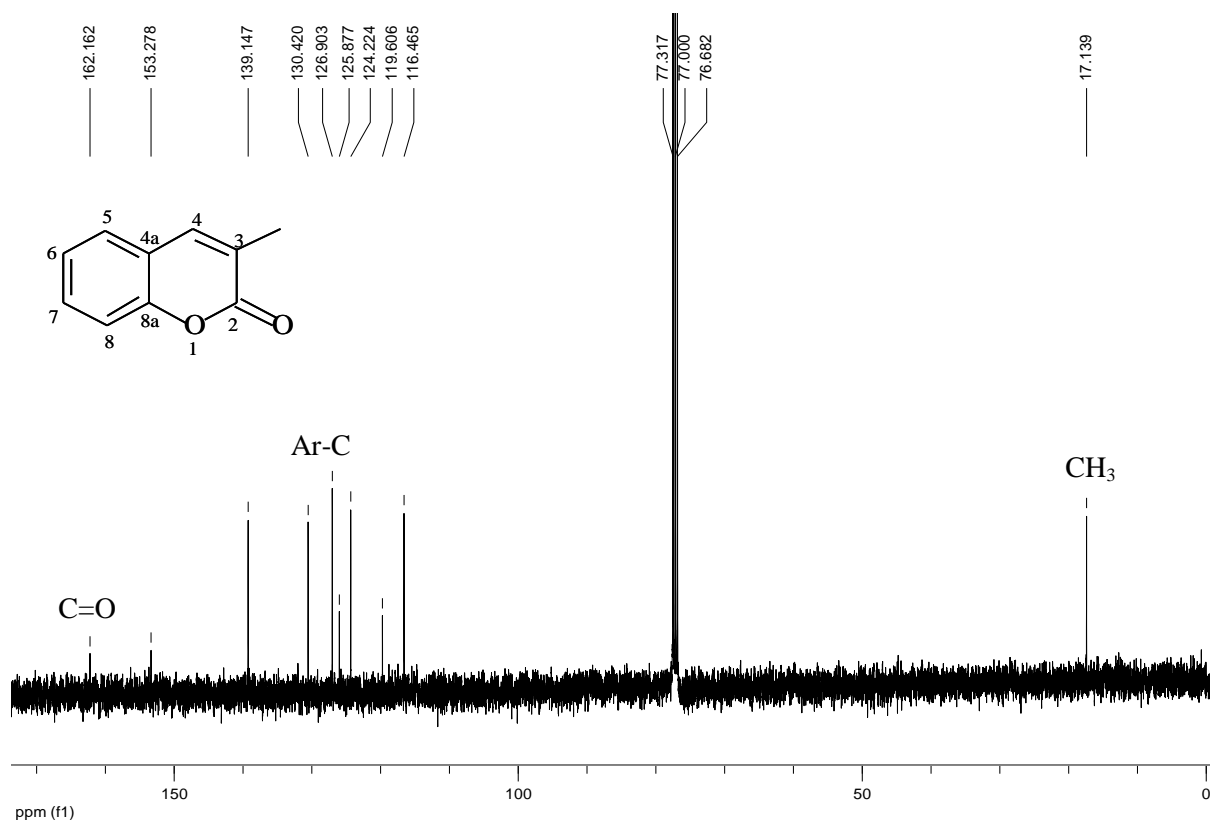
Figure 103. 100 MHz ^{13}C NMR spectrum of compound **75a** in CDCl$_3$.

2.3.3 Michaelis-Arbuzov reactions of the 3-(halomethyl)coumarins

The 3-(halomethyl)coumarin system could, in principle, undergo nucleophilic substitution reactions at three different carbon centres (C-2, C-4 and C-1'). As shown in Figure 104, attack at C-2 could result in acyl substitution and ring opening, while allylic substitution of the halide (S$_N$') or conjugate addition are possibilities following attack at C-4. Direct substitution (SN) at C-1 would also lead to displacement of the halide.
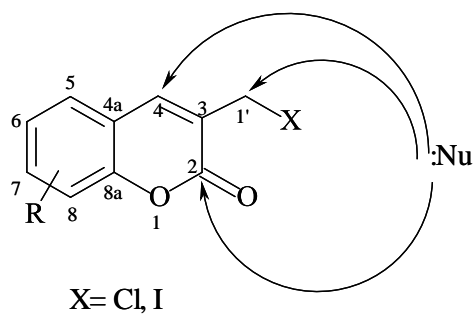
Figure 104. Possible modes of nucleophilic attack on the 3-(halomethyl)coumarins.

Previous work in our group by Rashamuse[86,121] involved reacting the 3-(halomethyl)coumarins with a trivalent phosphorus reagent in Michaelis-Arbuzov reactions, leading to the formation of phosphonated derivatives. The 3-(chloromethyl)coumarins **82** had been heated with two equivalents of triethyl phosphite at 120-130 ^{o}C in air (path I; Scheme 80). Work-up and column chromatography afforded the 4-phosphonated products **227a,c,e** exclusively. Following reports that substitution by phosphorus at C-1' can be achieved under nitrogen,[179,180] the reaction was repeated under nitrogen (path II), and a mixture of the expected 1'-phosphonated and 4-phosphonated products were isolated with the latter in low yields. However under similar conditions, the 3-(iodomethyl)coumarins **81** gave the 1'-phosphonated products **228a,c,e,** exclusively. These observations raised some questions regarding the influence of the halogen atom on nucleophilic substitution pathways in the 3-(halomethyl)coumarin system.

In order to understand these observations, the reactions outlined in Scheme 80 were repeated in the present study, and similar products were isolated.
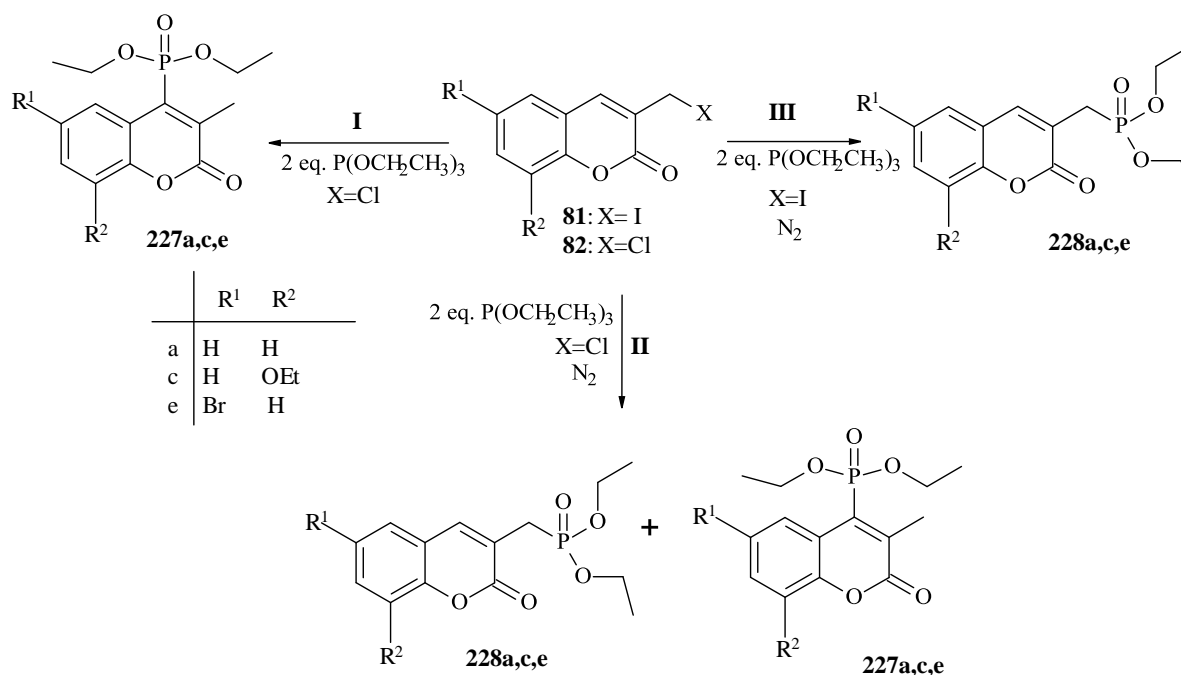
Scheme 80. Synthesis of phosphonated derivatives from 3-(halomethyl)coumarins.

Figure 105 shows the ^{1}H NMR spectrum of the 4-phosphonated product **227c**. The 3-methyl protons resonate as a doublet at 2.60 ppm due to coupling with phosphorus ($J_{P,H}$ = 3.2 Hz). The phosphonate methylene protons resonate as a multiplet at 4.15 ppm, and the aryl ethoxy

methylene protons as a quartet at 4.22 ppm. The ^{13}C NMR spectrum of compound **227c** (Figure 106), reveals four signals upfield of the CDCl$_3$ signals corresponding to the methylene and methyl carbons. The phosphonate and 3-methyl carbons resonate at *ca.* 16.0 ppm as doublets due to coupling with the phosphorus atom. The ^{1}H NMR spectrum (Figure 107) of the 1'-phosphonated isomer **228c** reveals a doublet at 3.14 ppm with a large coupling constant ($J_{P,H}$ = 22 Hz) corresponding to the methylene protons attached to phosphorus. The aromatic region has four signals, one more than those observed for the 4-phosphonated isomer **227c**, an indication that no substitution had occurred at C-4. The ^{13}C NMR spectrum (Figure 108) of compound **228c** reveals doublets corresponding to the methyl carbons at 16.3 and 16.5 ppm. The methylene carbon resonates at 62.3 and the carbonyl carbon at 160.8 ppm.
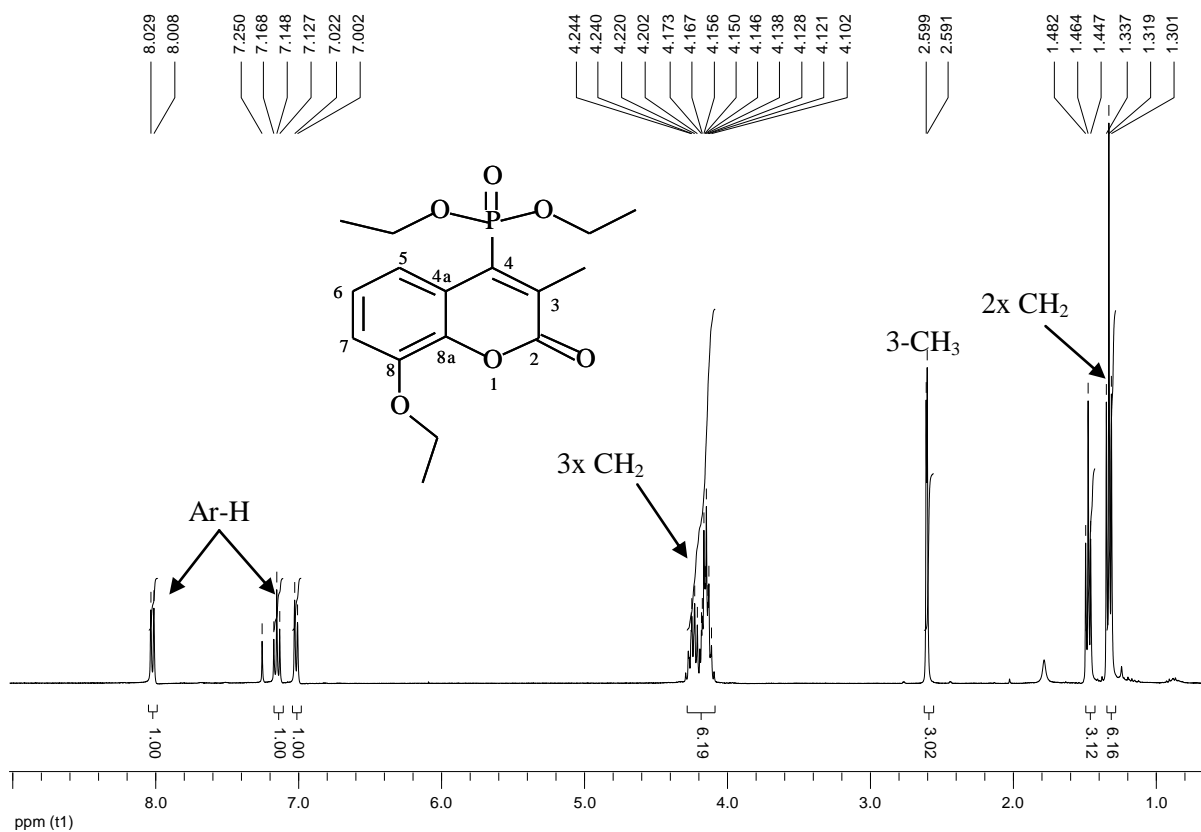
Figure 105. 400 MHz ^{1}H NMR spectrum of compound **227c** in CDCl$_3$.
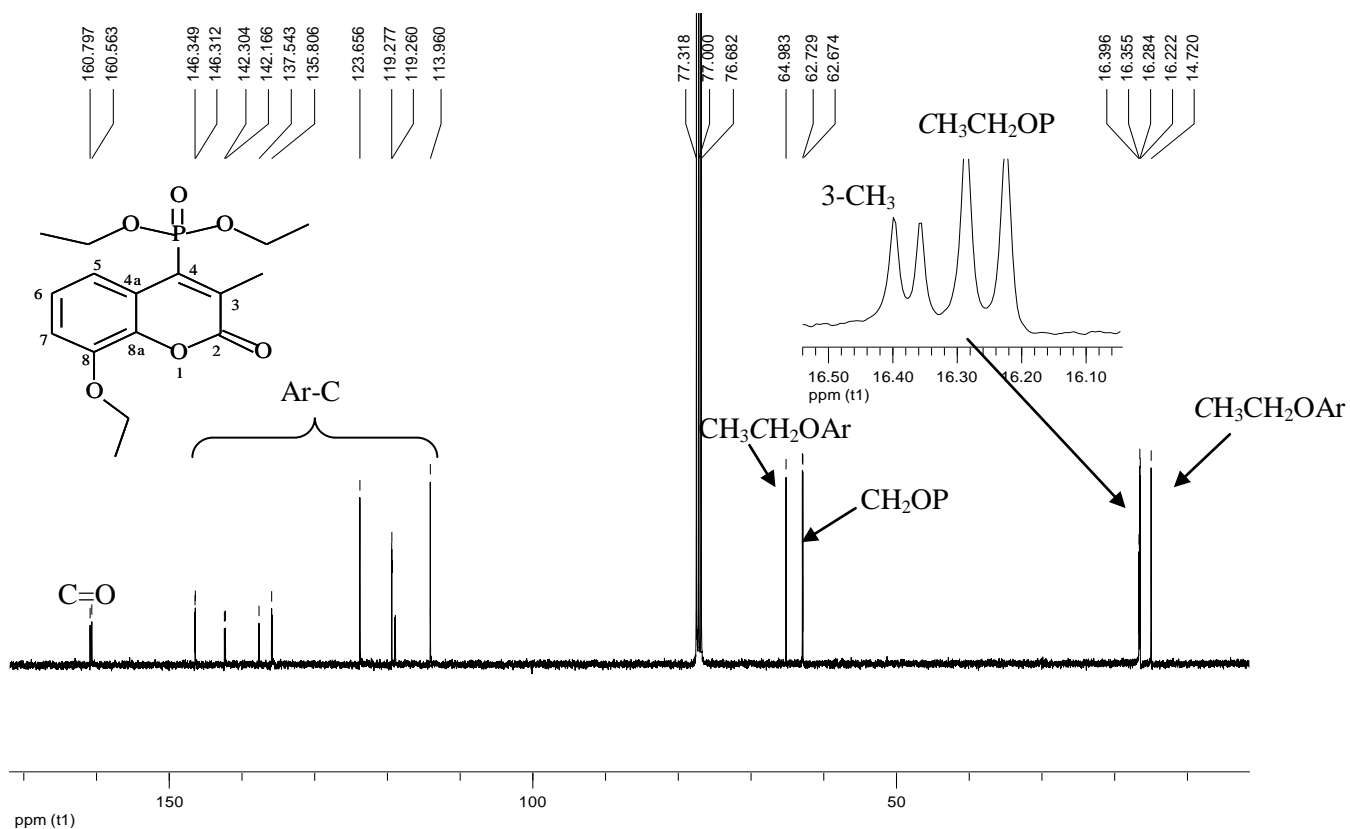
Figure 106. 100 MHz ^{13}C NMR spectrum of compound **227c** in CDCl$_3$.
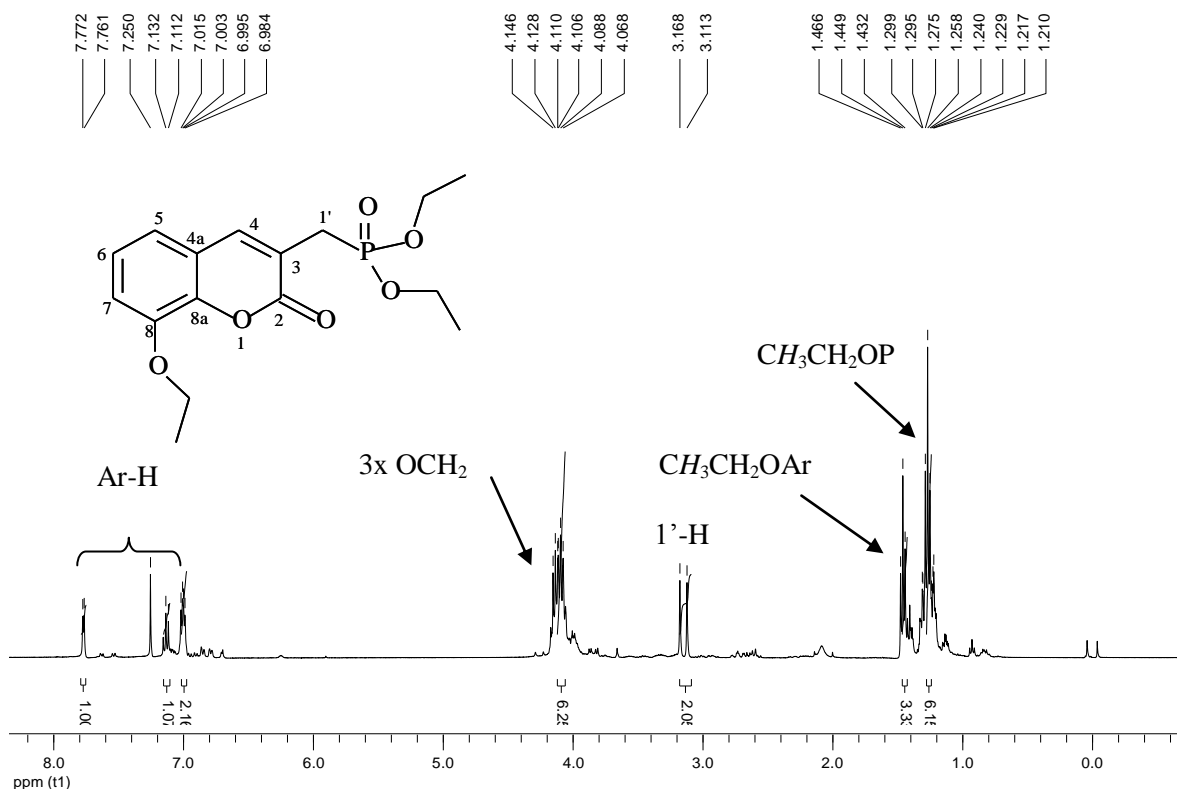
Figure 107. 400 MHz ^{1}H NMR spectrum of compound **228c** in CDCl$_3$.
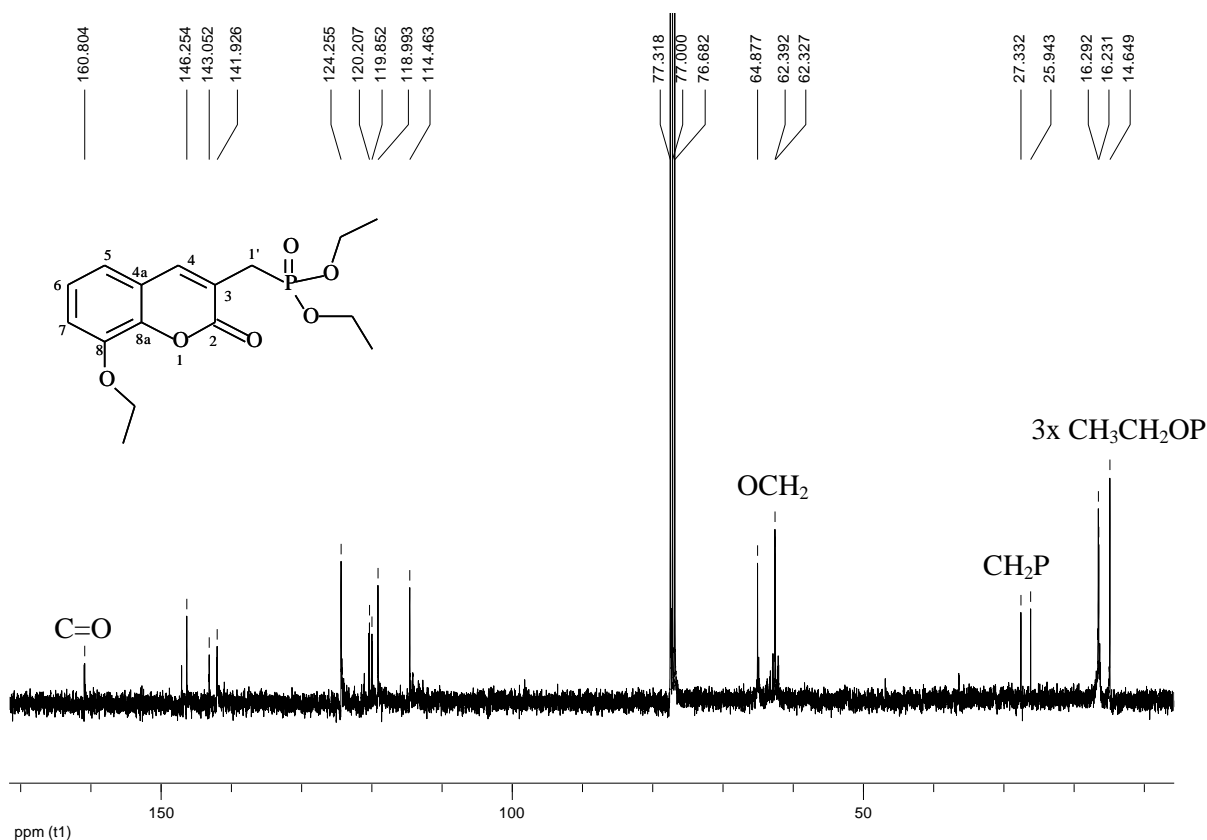
Figure 108. 100 MHz ^{13}C NMR spectrum of compound **228c** in CDCl$_3$.

Scheme 81 outlines the proposed mechanism for the formation of the 4-phosphonated products **227**. The initial step involves conjugate addition of P(OEt)$_3$ **301** to the α,β-unsaturated carbonyl system **82**, followed by displacement of the chlorine leading to the formation of a phosphonium intermediate **303**. Attack of chloride on one of the *O*-ethyl groups on the phosphonium intermediate **303** in a S$_N$ reaction, and rearrangement of the double bond affords the 3-methyl derivatives **227** in what can be called an allylic Arbuzov reaction.

Scheme 81.
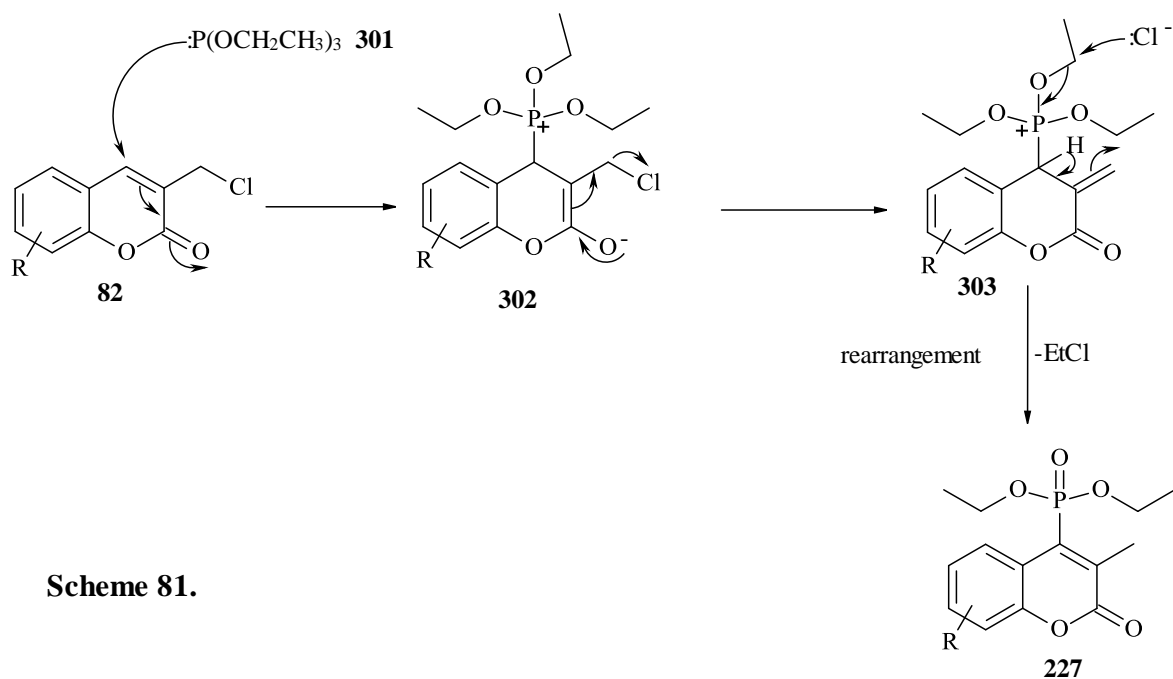
On the other hand, the formation of the 1'-phosphonated analogues involves an S_N mechanism in which the alkyl halide is attacked by the nucleophilic $P(OEt)_3$ **301** forming the intermediate **304**. Attack on one of the *O*-ethyl groups of the phosphonium intermediate **304** by the halide affords the 1'-phosphonated derivatives **228**.

Scheme 82.
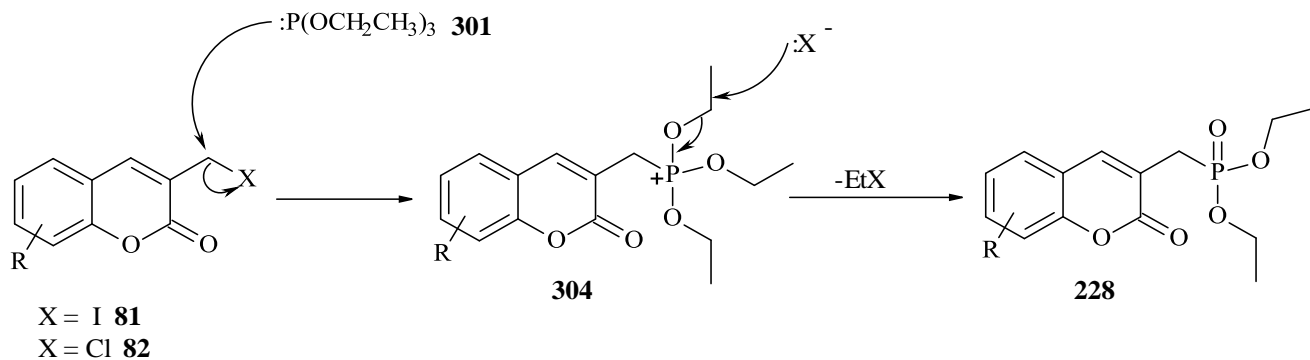
2.3.4 Preliminary experimental study of the Michaelis-Arbuzov reactions of 3-(halomethyl)coumarins

Following the progress of a reaction using NMR spectroscopy, as observed with reactions described in the previous sections, provides an understanding of what is actually happening in solution with regard to the consumption of reactants and the formation of intermediates and products. However, in the case of the Michaelis-Arbuzov reactions, which need to be carried out at elevated temperatures (120-130 $^{\circ}$C), it was not possible to monitor the reaction directly on the NMR spectrometer. The conventional laboratory set-up for the experiments was then used, and aliquots of the reaction mixture were collected periodically. The first aliquot was collected immediately after mixing the reactants, and, at 20 minute intervals over a 4 hour period; the aliquots were transferred to vials which were immediately cooled in ice to stop the reaction. The reactions using both 3-iodo- and 3-(chloromethyl)coumarins were conducted in duplicate. ^{1}H NMR spectra of the sampled aliquots were then run. The results are illustrated in the stacked ^{1}H NMR spectra (Figures 109 and 110), which show the progress of the reactions. The reaction of 3-(chloromethyl)coumarin **82a** with triethylphosphite (Figure 109), reveals the formation of both compounds **227a** and **228a**. The methylene signal for compound **228a**, which appears as a doublet due to coupling with the neighbouring phosphorus, and the methyl signal for compound **227a** were monitored. Judging from the signal intensities, it appears that the two products are present in almost equal concentrations. The reaction of the 3-(iodomethyl)coumarin **81a** with triethylphosphite (Figure 110) was quite interesting because in the synthetic study, only the 1'-phosphonated product **228a** was isolated, whereas the NMR data show that, in fact, both compounds **228a** and **227a** are formed. However, the 4-phosphonated product **227a** is formed at a much slower rate than the 1'-phosphonated product **228a**, and the small quantities of the former product could well have been lost in the isolation and purification of the major product. It is also quite evident from these results that 3-(iodomethyl)coumarin **81a** undergoes nucleophilic substitution at the 1'-position more readily than the chloro analogue **82a**, as formation of the 1'-phosphonated product is almost instantaneous. Nucleophilic substitution in the chloro analogue **82a** at both the 1'- and 4-positions appears to be much slower.
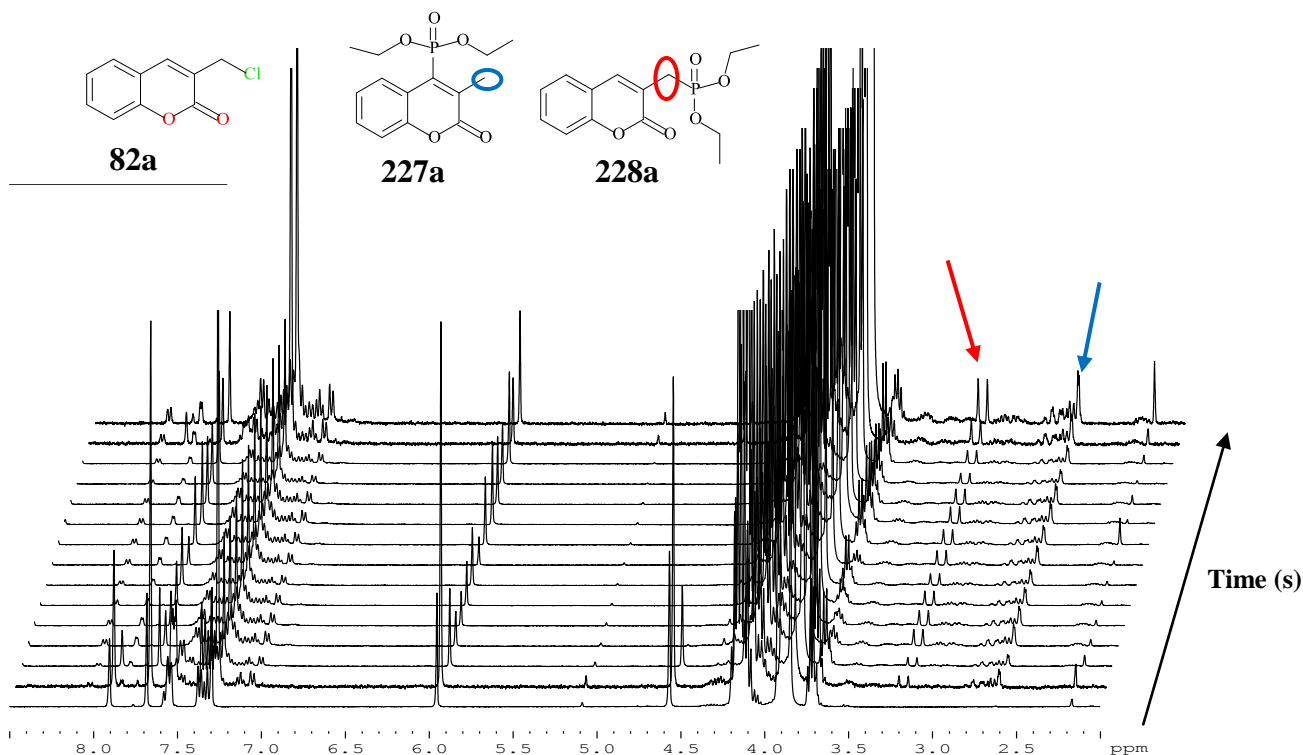
Figure 109. Stacked ^{1}H NMR spectra of the reaction between 3-(chloromethyl)coumarin **82a** and triethylphosphite. The methylene signal for **228a** (red) and the methyl signal for **227a** (blue) are highlighted.
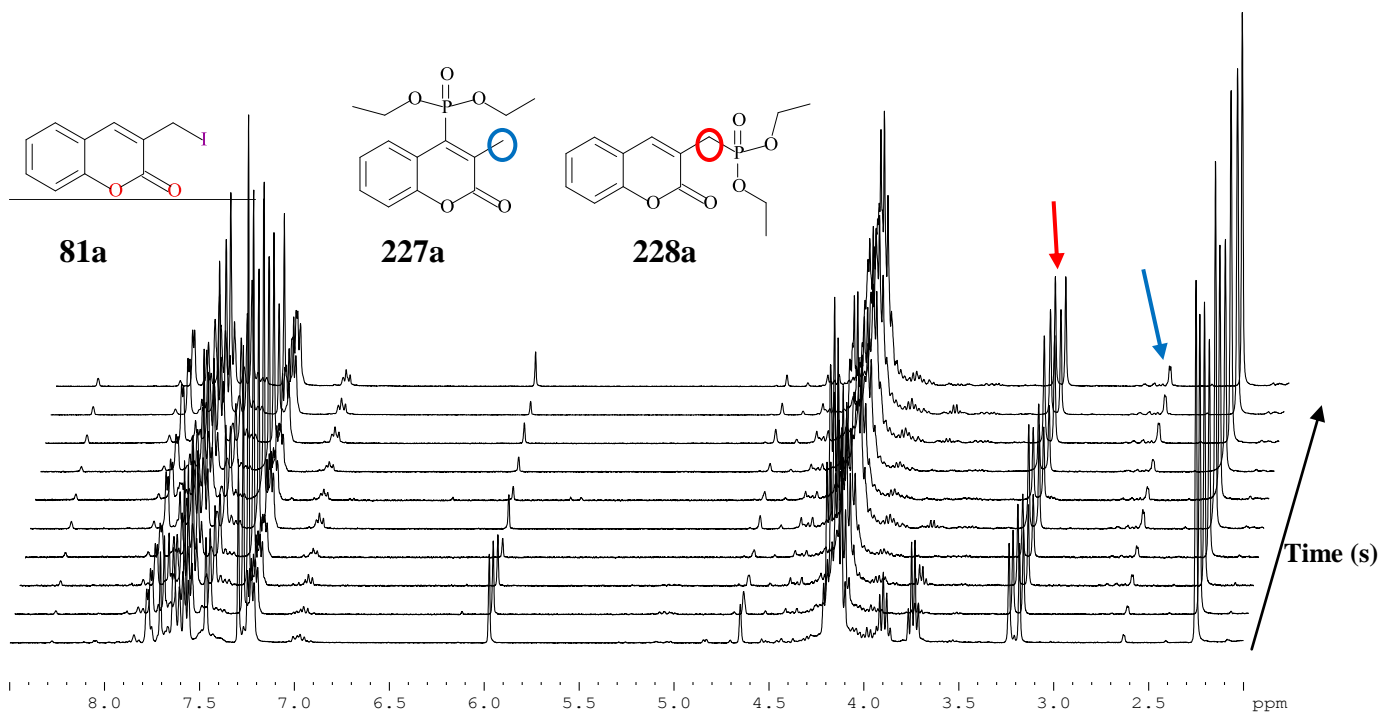
Figure 110. Stacked ^{1}H NMR spectra of the reaction between 3-(iodomethyl)coumarin **81a** and triethylphosphite. The methylene signal for **228a** (red) and the methyl signal for **227a** (blue) are highlighted.

2.3.5 Preliminary theoretical study of the Michaelis-Arbuzov reactions of 3-(halomethyl)coumarins

The different reactivities of the 3-chloro- and 3-(iodomethyl)coumarins towards the nucleophilic triethyl phosphite in the Michaelis-Arbuzov reactions was attributed to the fact that the iodide is a better leaving group than chloride.[121] As a result, the reaction rates of the chloro derivatives are lower, permitting attack of the nucleophile at both the C-1' and C-4 positions, presumably *via* S_N2 and S_N2' mechanisms, respectively. Increased electrophilicity of the C-4 centre *via* an electron-withdrawing inductive effect by the more electronegative Cl atom was also considered to be a likely factor facilitating attack at C-4.

In the present study, the first approach in exploring the validity of these explanations involved an investigation of charge densities on the centres of interest. Mulliken charges for the iodo- and chloro analogues **81a** and **82a** were calculated using Gaussian 03 at the B3LYP 6.31G(d) level of theory in order to check if there were any notable differences in charge density between the two compounds. The results failed to show any major differences (Figure 111) and, based on these data, both the iodo- and chloro-methyl derivatives should favour S_N2' reaction at C-4. The LUMOs of both compounds, shown in Figure 112, show similar patterns, indicating that, in principle, their reactivity towards nucleophiles should be similar.
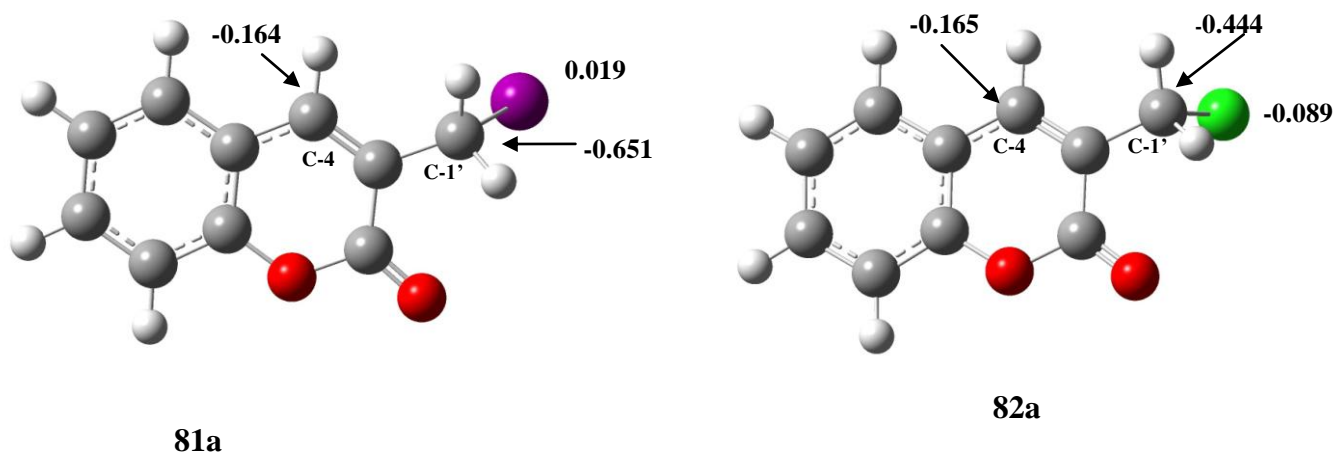
Figure 111. Gaussian-optimised structures of 3-(iodomethyl)coumarin **81a** and 3-(chloromethyl)coumarin **82a**. Shown are the calculated Mulliken charges on the C-4 and C-1' centres of interest and on the halogen atoms.

81a

82a
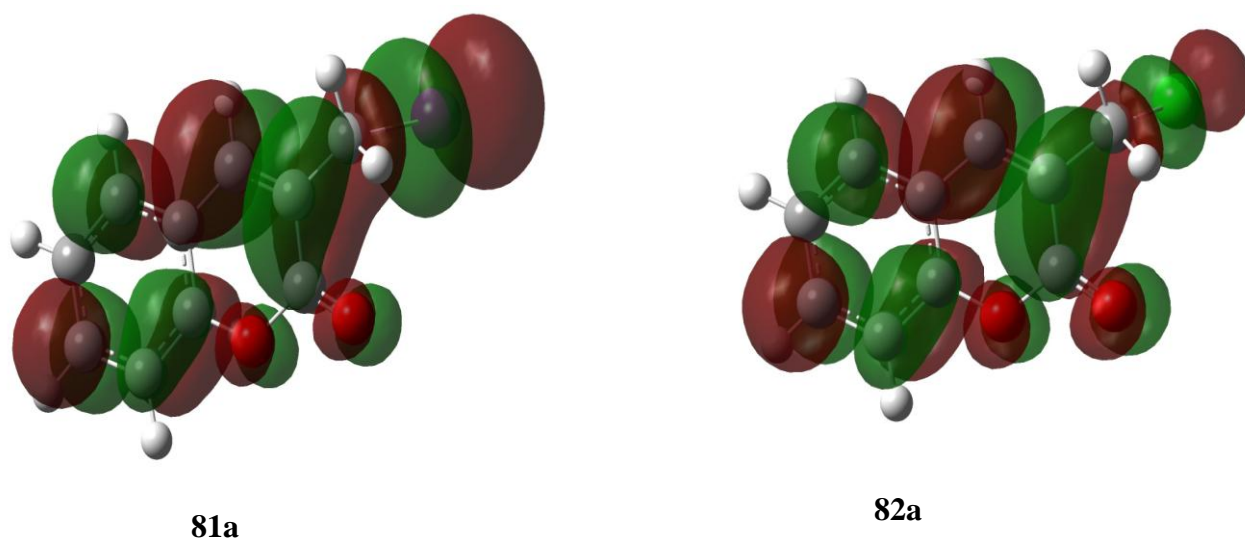
Figure 112. LUMO surfaces for the 3-(halomethyl)coumarins **81a** and **82a**.

The Fukui functions $[(f^-(r), f^+(r), f^0(r)]$, which are used to calculate the hardness or softness of a reaction centre towards electrophiles, nucleophiles and radicals, were then explored. The Dmol3 module in Materials Studio[181] was used initially for the calculations, but the results again failed to show any notable differences between compounds **81a** and **82a**. A more detailed analysis of the Fukui functions using Gaussian 03[182,183] was then undertaken. Following a procedure by Khene *et al.*,[182] the neutral (*N*), positive (*N*+1) and negative (*N*-1) electronic states of compounds **81a** and **82a** were optimised at the DFT B3LYP level using the 6.31G(d) basis set. Single-point energy calculations of the different electronic states gave the corresponding energy values $[(E_A(N), E_A(N+1)$ and $E_A(N-1)$] and the Mulliken charges on each atom (k) $[q_{Ak}(N), q_{Ak}(N+1)$ and $q_{Ak}(N-1)]$. In a series of steps following the reported approach,[182] these values were then used to calculate the condensed local softness of each of the atoms in molecules **81a** and **82a**. The respective, condensed local softness values (S^+_{Ak}, S^-_{Ak} and S^0_{Ak}) give an indication of the preferred reaction site when a nucleophile, electrophile or radical approaches a molecule. In our case, we were interested in S^+_{Ak} since we were looking at nucleophilic substitution reactions of the 3-(halomethyl)coumarins **81a** and **82a** when triethyl phosphite is used as a nucleophile. The more positive the value of S^+_{Ak}, the more susceptible the atom is to nucleophilic attack. Figure 113 shows the results for the two carbon centres of interest (C-4 and C-1') in each molecule. There is clearly a significant difference between the condensed local softness (S^+_{Ak}) values calculated for the 3-chloro- and (iodomethyl)coumarins **82a** and **81a**, respectively.
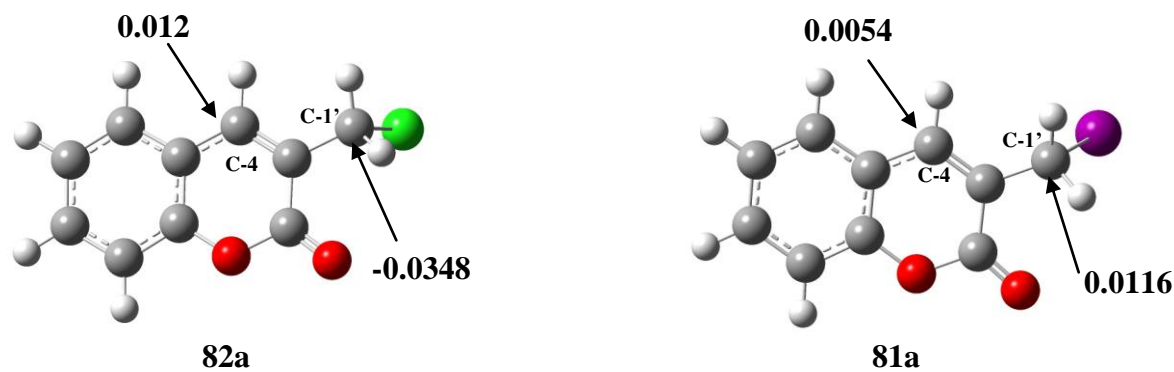
Figure 113. Local condensed softness (S^+_{Ak}) values for the C-4 and C-1' centres in compounds **82a** and **81a**, at the DFT B3LYP/6.31G(d) level using Gaussian 03.

It appears from these results that nucleophilic attack on the chloro analogue **82a** should favour the 4-position rather than the 1'-exocyclic centre. However, destabilisation of the S_N2' transition state complex **305** (Scheme 82) by loss of conjugation (and hence the overall aromaticity of the coumarin system) could account for the observed phosphonation at both C-1' and C-4 − the former *via* an S_N2 pathway.
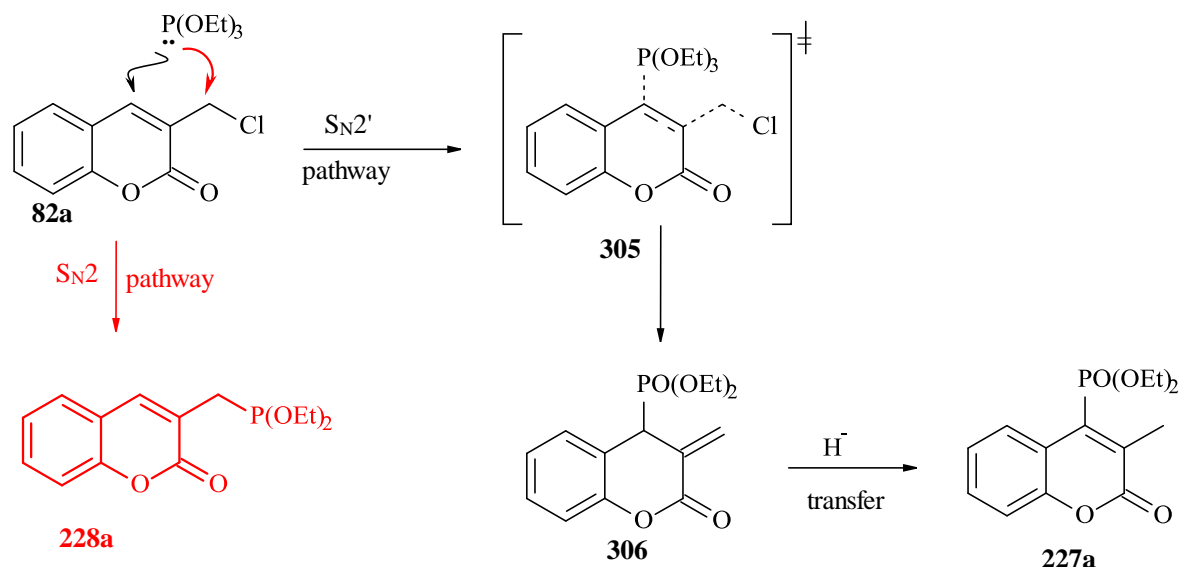
Scheme 83.

In the iodo compound **81a**, however, nucleophilic attack should favour the 1'-position, although the difference between the local softness at the two centres (1' and 4) is smaller than in the chloro analogue **82a**. In fact, the iodo analogue **81a** does exhibit dominant attack at the exocyclic centre C-1', but not exclusively so − as evidenced when the reactions were monitored using NMR spectroscopy (Figure 110). An alternative explanation may lie in an

S_N1 mechanism involving initial ionisation with loss of the iodide anion (a good leaving group[184]) to afford the resonance-stabilised allylic-benzylic carbocation **307** (Scheme 84). Subsequent attack by triethyl phosphite would then be favoured at the less hindered exocyclic centre C-1'. These observed theoretical and NMR analysis results, confirm the earlier proposal[121] that reactivity in the chloro analogue **81a** is lower due to chloride being a poorer leaving group than iodide and, hence, nucleophilic substitution reactions would be much slower, while the opposite is true for the iodo analogues.
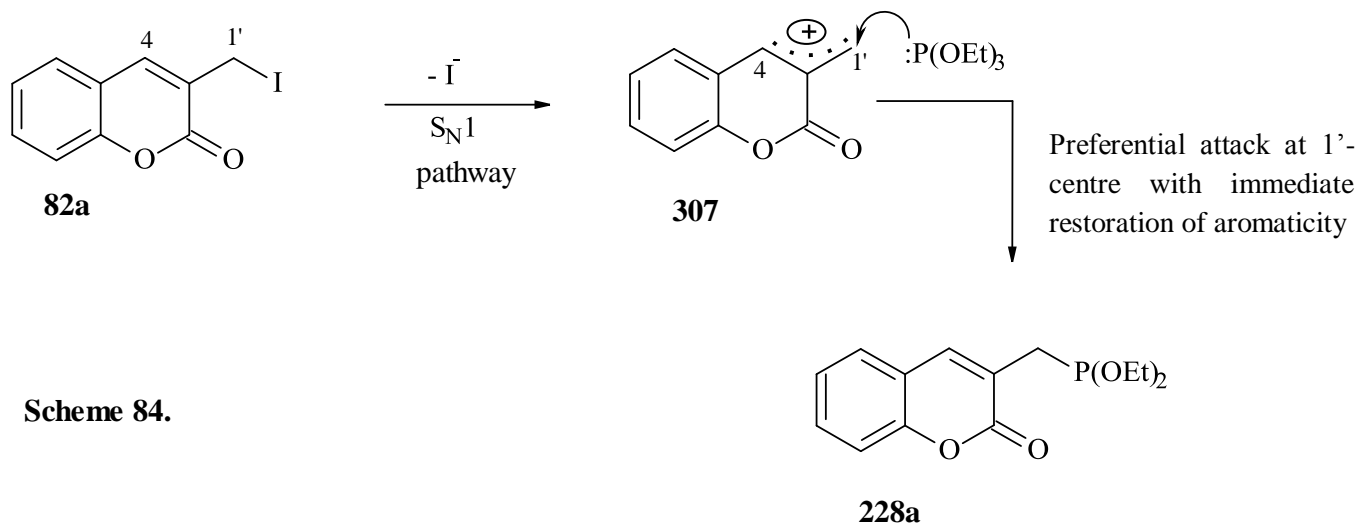
Scheme 84.

A better understanding of these reactions could be achieved by undertaking concentration effect studies which would establish the molecularity of the mechanistic pathways (S_N1 or S_N2). Location of critical transition-state complexes involved in the proposed pathways would also provide useful information on the thermodynamic and kinetic factors involved in these reactions. Future work in this area will be aimed at addressing these aspects.

2.4 Conclusions

This study has provided an opportunity of elucidating the mechanisms of four MBH-type reactions which had afforded unexpected and, in some cases, unusual products, *viz*, i) the reactions of the disulfide, 2,2'-dithiodibenzaldehyde with various activated alkenes; ii) the reactions of chromone-3-carbaldehydes with MVK; iii) the reactions of chromone-2-carbaldehydes with acrylonitrile and iv) the reactions of chromone-2-carbaldehydes with methyl acrylate. The opportunity has also been taken to explore the regioselectivity of nucleophilic substitutions of Michaelis-Arbuzov reactions of MBH-derived 3-(haolmethyl)coumarins.

The disulfide, 2,2'-dithiodibenzaldehyde was successfully synthesised in 54% yield, and the rate of its MBH reaction with various activated alkenes, has been dramatically accelerated by use of a novel, dual-catalyst system, comprising DBU and Ph_3P (DBU-Ph_3P); an increase in the yields of the thiochromenes was also observed; Use of Ph_3P as the sole catalyst for this reaction led to the isolation of key products, which have proved useful in understanding the mechanism, while the unprecedented cleavage of aryl and heteroaryl disufides by the nitrogen nucleophile DBU has been demonstrated; Detailed kinetic studies have been conducted on the reactions of 2,2'-dithiodibenzaldehyde with MVK and methyl acrylate, and a theoretical kinetic model has been developed. Computational studies, carried out at the hybrid DFT level [B3LYP/6-31G(d)], have permitted geometry optimisation of the structures in the proposed mechanism, and provided useful insights into this complex transformation.

Various chromone-3-carbaldehydes have been prepared using Vielsmeier-Haack methodology in yields ranging from 59 to 80%, while chromone-2-carbaldehydes have been obtained from Kostanecki-Robinson reactions in yields ranging from 46 to 70%. The reactions between chromone-3-carbaldehydes and MVK in the presence of the catalyst 3-HQ, have been successfully repeated affording dimeric MBH products together with tricyclic competition products, confirming earlier observations in our group. A theoretical model has been developed for the competing pathways and DFT calculations have proved particularly useful in supporting earlier mechanistic proposals. The structures of the unusual products obtained when chromone-2-carbaldehydes were reacted with acrylonitrile and with 3-HQ as catalyst, were confirmed using 1- and 2-dimensional NMR, HRMS and X-ray crystallographic methods. Reactions of chromone-2-carbaldehydes with methyl acrylate failed to exhibit consistent, product-distribution patterns, but explanations for the formation

of the unexpected products from these reactions of chromone-2- and chromone-3-carbaldehydes have been provided.

MBH-derived 3-chloro- and 3-(iodomethyl)coumarins have been prepared. Treatment of the 3-(halomethyl)coumarins with triethyl phosphite under Michaelis-Arbuzov reaction conditions, afforded both the 4- and 1'-phosphonated products in the case of the chloro analogue, but predominantly the 1'-phosphonated product in the case of the iodo analogue, confirming earlier observations in our group. Exploratory NMR-based kinetic studies of these phosphonation reactions confirmed the lack of regio-selectivity in reaction of 3-(chloromethyl)coumarin; in the case of the 3-iodomethyl analogue, phosphonation at the exocyclic 1'-position was clearly dominant but a very small amount of the 4-substituted isomer was, in fact, formed. Mulliken charges, LUMO surfaces and Fukui condensed local softness values have been calculated in attempts to rationalise the regioselectivity patterns.

It is clear that the objectives of this study have been largely achieved. Thus far, two papers on aspects of this research have been accepted for publication.[196,197] Future work in this area is expected to include the following.

i) Optimising the theoretical kinetic model proposed for the formation of thiochromenes.

ii) Locating critical transition-state complexes involved in the reactions in this study.

iii) Completing detailed kinetic and theoretical studies on the Michaelis-Arbuzov reactions of the 3-(halomethyl)coumarins to establish the molecularity of mechanistic pathways involved.

3. EXPERIMENTAL

3.1 General

NMR spectra and kinetic experiments were recorded on Bruker AMX 400 MHz and Biospin 600 MHz spectrometers and were referenced using solvent signals (δ_H: 7.25 ppm for $CDCl_3$, 2.50 ppm for DMSO-d_6; δ_C: 77.0 ppm for $CDCl_3$, 39.4 ppm for DMSO-d_6). IR spectra were recorded on a Perkin-Elmer FT-IR Spectrum 2000 spectrometer using nujol mulls or Perkin-Elmer FT-IR Spectrum 100 spectrometer (neat). Melting points were determined using a Reichert hot-stage apparatus and are uncorrected. High resolution mass spectra (HRMS) were recorded on a Waters API-Q-TOF Ultima spectrometer (University of Stellenbosch).

All chemical reagents were used as supplied by the manufacturers. Solvents were dried according to methods described by Perrin and Armarego,[185] hence, THF and Et_2O were dried over sodium wire and distilled from sodium, using benzophenone as indicator, under nitrogen; CH_2Cl_2 was pre-dried over $CaCl_2$ and distilled from CaH_2; *N,N*-dimethylformamide (DMF) was pre-dried and distilled from 3Å molecular sieves under reduced pressure. Ethanol and methanol were dried by reaction with Mg turnings and iodine and then distilled from the resulting magnesium alkoxide under nitrogen.

Flash chromatography was carried out using Merck silica gel 60 [230-400 mesh (particle size 0.040-0.063 mm)] and preparative layer chromatography was conducted using silica gel 60 PF_{254}. HPLC was conducted on a Partisil 10 Magnum 6 normal phase column using a Spectra-Physics P100 isocratic pump and a Waters K1410 differential refractometry detector. Thin layer chromatography (TLC) was carried out on pre-coated Merck silica gel F_{254} plates, visualisation being achieved by inspection under UV light (254/365nm) or following exposure to iodine.

Density functional theory (DFT) calculations were carried out using the Gaussian 03 programme running on an Intel/Linux cluster.

3.2 Synthesis of thiochromene derivatives
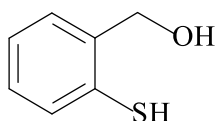
***2-Mercaptobenzyl alcohol* 230** [129]

A solution of 2-mercaptobenzoic acid **229** (4.36 g, 28.4 mmol) in dry THF was added dropwise to a stirred slurry of lithium aluminium hydride (2.0 g, 52 mmol) in THF (80 mL) under N_2, and the resulting mixture was stirred for 24 h. EtOAc (10 mL) and 10 % sulfuric acid (40 mL) were added dropwise. The resulting mixture was filtered and the aqueous layer extracted with EtOAc (2x 30 mL). The combined organic layers were washed with saturated brine and dried over anhydrous Na_2SO_4; the solvent was evaporated *in vacuo* to afford, as a light brown oil which crystallized after some time, 2-mercaptobenzyl alcohol **230** (3.28 g, 84 %); δ_H (400 MHz; $CDCl_3$) 2.03 (1H, br s, OH) 3.67 (1H, s, SH), 4.72 (2H, s, CH_2), 7.16-7.18 (2H, overlapping multiplets, ArH) and 7.32-7.35 (2H, overlapping multiplets, ArH); δ_C (100 MHz; $CDCl_3$) 64.4 (CH_2), 126.3 ,128.4, 128.6, 130.2, 131.4 and 138.8 (Ar-C).
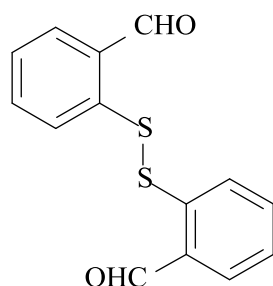
***2,2'-Dithiodibenzaldehyde* 201**[136]

In a 100 mL round-bottomed flask, fitted with a reflux condenser, pyridinium chlorochromate (12.0 g, 58 mmol) was dispersed in dry, deoxygenated dichloromethane (45 mL) under N_2. A solution of 2-mercaptobenzyl alcohol **230** (3.0 g, 22 mmol) in dry, deoxygenated dichloromethane (8.9 mL) was added, *via* a syringe through a septum, to the stirred mixture. After stirring the reaction mixture for 4 h at room temperature, dichloromethane (45 mL) was added and the supernatant liquid was decanted from the black gum which had formed. The black gum was washed with dichloromethane (3 x 15 mL) and dry diethyl ether (20 mL) and the combined washings were passed through a florisil pad. The solvent was evaporated *in vacuo* and the residual solid was recrystallised from ethanol to afford 2,2'-dithiodibenzaldehyde **201** as white crystals (1.33 g, 54 %), m.p. 156-157 °C (lit[114] 142-144

°C,); δ_H (400 MHz; CDCl$_3$) 7.38 (2H, t, J = 7.37 Hz, ArH), 7.48 (2H, t, J = 7.62 Hz, ArH), 7.77 (2H, d, J = 8.02 Hz, ArH), 7.85 (2H, d, J = 7.44 Hz, ArH) and 10.21 (2H, s, CHO); δ_C (100 MHz; CDCl$_3$) 126.3, 126.7, 133.8, 134.3, 134.6, 140.0 (Ar-C) and 191.8 (C=O).

3.2.1 Reaction of 2,2'-dithiodibenzaldehyde with MVK using triphenylphosphine (Ph$_3$P) as catalyst.
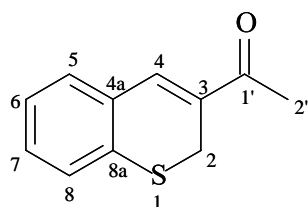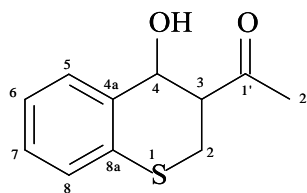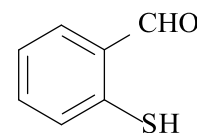
202a   **217a**   **239**

*3-Acetyl-2**H**-1-benzothiopyran*   *3-acetyl-4-hydroxythiochroman*   *2-mercaptobenzaldehyde*
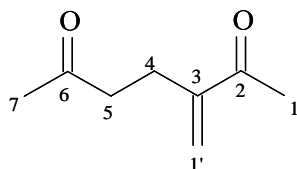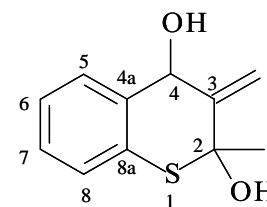
251   **252**

3-methyleneheptane-2,6-dione   *2-methyl-3-methylenethiochromene-2,4-diol*

To a solution of 2,2'-dithiodibenzaldehyde **201** (0.13 g, 0.46 mmol) and Ph$_3$P (0.20 g, 0.75 mmol) in CHCl$_3$ (0.6 mL), MVK (0.11 mL, 1.4 mmol) was added. The resultant mixture was stirred for 4 days. Evaporation of the solvent *in vacuo*, followed by flash chromatography on silica [elution with hexane-EtOAc (2:1)], followed by semi-preparative HPLC gave five fractions.

i)   3-Acetyl-2*H*-1-benzothiopyran **202a**, as a yellow oil (0.06 g, 34 %), v_{max}/cm^{-1} (neat) 1653 (C=O); δ_H (400 MHz; CDCl$_3$) 2.24 (3H, s, CH$_3$), 3.70 (2H, s, CH$_2$), 7.12-7.27 (4H, overlapping multiplets, ArH) and 7.38 (1H, s, 4-H); δ_C (100 MHz; CDCl$_3$) 22.8 (CH$_3$), 25.3 (CH$_2$), 125.7, 127.3, 130.5, 130.8, 131.4, 131.5, 135.5 and 137.8 (Ar-C, C-3 and C-4) and 196.6 (C=O).

ii)   *3-Acetyl-4-hydroxythiochroman* **217a** (0.04 g, 14 %); (Found **M$^+$**: 208.0539. C$_{11}$H$_{12}$O$_2$S requires: 208.0558); spectroscopic data for the major diastereomer **217a$_1$** isolated as a pale yellow oil: v_{max}/cm^{-1} (neat) 3411 (OH) and 1663 (C=O); δ_H (400 MHz; CDCl$_3$) 2.34 (1H, s, CH$_3$), 2.71 (1H, br s, OH), 2.93 (1H, br d, J

=11.01 Hz, 3-H), 3.00 (1H, br d, J = 12.98 Hz, 2-H_a) 3.40 (1H, t, J = 12.29 Hz, 2-H_b), 5.12 (1H, s, 4-H) and 7.08-7.34 (4H, m, Ar-H); δ_C (100 MHz; CDCl$_3$) 21.9 (CH$_2$), 28.5 (CH$_3$), 51.8 (C-3), 67.3 (C-4), 124.5, 126.4, 128.9, 131.3, 132.7 and 133.4 (Ar-C) and 208.6 (C=O).

Spectroscopic data for the minor diastereomer **217a$_2$** isolated as a white crystalline solid, m.p. 99-100 $^{\text{o}}$C: v_{max}/cm^{-1} (neat) 3415 (OH) and 1668 (C=O); δ_H (400 MHz; CDCl$_3$) 2.31 (1H, s, CH$_3$), 2.43 (1H, br s, OH), 3.12-3.27 (3H, overlapping multiplets, 2-CH$_2$ and 3-H), 5.05 (1H, d, J = 5.51 Hz, 4-H), 7.10-7.13 (3H, m, Ar-H) and 7.52 (1H, m, Ar-H); δ_C (100 MHz; CDCl$_3$) 25.5 (CH$_2$), 29.4 (CH$_3$), 53.1 (C-3), 68.5 (C-4), 125.0, 126.4, 128.0, 128.2, 131.8 and 135.0 (Ar-C) and 208.4 (C=O).

iii) 2-Mercaptobenzaldehyde **239** as a pale yellow oil (0.013 g, 9 %); v_{max}/cm^{-1} (neat) 2612 (SH); δ_H (400 MHz; CDCl$_3$) 5.96 (1H, d, J = 3.49 Hz, SH), 7.44-7.70 (2H, m, 5-H and 6-H), 7.82 (1H, t, J = 8.08 Hz, 4-H), 7.84 (1H, d, J = 7.97 Hz, 3-H) and 10.41 (1H, s, CHO); δ_C (100 MHz; CDCl$_3$) 127.4 (C-5), 128.2 (C-4), 129.3 (C-6), 130.4 (C-3), 134.1 (C-1), 134.8 (C-2) and 192.1 (CHO),

iv) *2-Methyl-3-methylenethiochroman-2,4-diol* **252**, as a pale yellow oil (0.01 g, 7 %); (Found **M$^+$**: 208.0573. C$_{11}$ H$_{12}$O$_2$S requires: 208.0558); v_{max}/cm^{-1} (neat) 3406 and 3358 (OH) δ_H (400 MHz; CDCl$_3$) 2.16 (3H, s, CH$_3$), 2.35 (1H, s, OH), 2.56 (1H, br s, OH), 5.14 (1H, s, C*H*OH), 5.55 and 5.99 (2H, d, J = 13.47 Hz, CH$_2$) and 7.51-7.82 (4H, m, ArH); δ_C (100 MHz; CDCl$_3$) 25.3 (CH$_3$), 67.3 (C-4), 78.2 (C-2), 122.5 (C-3''), 125.0 (C-6), 126.4 (C-5), 128.9 (C-7), 131.3 (C-8), 132.8 (C-8a), 133.5 (C-4a) and 147.8 (C-3); *m/z* 208 (**M$^+$**; 60 %) and 189 (100 %).

v) The MVK dimer, 2-methyleneheptane-2,6-dione **251** as a pale yellow oil (0.009 g, 4 %); δ_H (400 MHz; CDCl$_3$) 2.12 (3H, s, 7-CH$_3$), 2.32 (3H, s, 1-CH$_3$), 2.55 (4H, m, 4-H and 5-H), 5.83 and 6.02 (2H, 2x s, 1'-CH$_2$); δ_C (100 MHz; CDCl$_3$) 25.3 (C-4), 25.8 (C-7), 29.8 (C-1), 42.4 (C-5), 126.2 (C-1'), 147.7 (C-3), 199.5 and 207.8 (2x C=O).

3.2.2 Reactions of 2,2'-dithiodibenzaldehyde with various activated alkenes using the dual catalyst system of DBU and triphenylphosphine (DBU-Ph₃P).
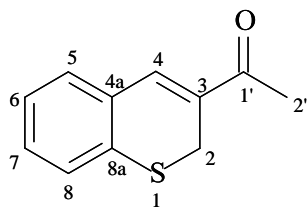
***3-Acetyl-2H-1-benzothiopyran* 202a**

To a solution of 2,2'-dithiodibenzaldehyde **201** (0.13 g, 0.46 mmol) and Ph₃P (0.20 g, 0.75 mmol) in CHCl₃ (0.6 mL), MVK (0.11 mL, 1.4 mmol) was added, followed by DBU (0.11 mL, 0.75 mmol). The resultant mixture was stirred for 2 h. Evaporation of the solvent *in vacuo*, followed by flash chromatography on silica [elution with hexane-EtOAc (2:1)] gave 3-acetyl-2*H*-1-benzothiopyran **202a**, as a yellow oil (0.12 g, 67 %),

Note: Use of DBU as sole catalyst afforded 3-acetyl-2*H*-1-benzothiopyran **202a** in 59 % yield after 24 h.[6,114]
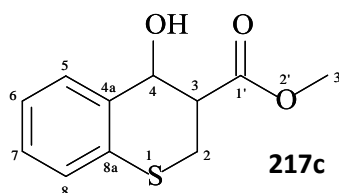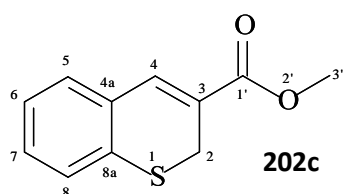
Methyl 2H-1-thiochromene-3-carboxylate and methyl 4-hydroxythiochroman-3-carboxylate

The procedure described for the synthesis of 3-acetyl-2*H*-1-benzothiopyran **202a** was followed using 2,2'-dithiodibenzaldehyde **201** (0.13 g, 0.46 mmol), Ph₃P (0.20 g, 0.75 mmol), CHCl₃ (0.6 mL), methyl acrylate (0.12 mL, 1.4 mmol) and DBU (0.11 mL, 0.75 mmol) and stirring for 3 h. Work-up afforded two products.

i) Methyl 2*H*-1-thiochromene-3-carboxylate **202c** as a yellow oil (0.07 g, 34 %); δ_H (400 MHz; CDCl₃) 3.75 (2H, s, 2-CH₂), 3.86 (3H, s, OCH₃), 7.09-7.25 (4H, m, ArH) and 7.54 (1H, s, 4-H); δ_C (100 MHz; CDCl₃) 24.0 (CH₂), 52.1 (CH₃), 123.0, 125.7, 127.1, 130.1, 130.6, 131.3, 134.0 and 137.3 (Ar-C, C-3 and C-4) and 166.3 (C=O).

ii) *Methyl 4-hydroxythiochroman-3-carboxylate* **217c**, a yellow oil, as a diastereomeric mixture (0.09 g, 46 %); (Found: $(\mathbf{M+1})^{+}$: 225.0585. $C_{11}H_{13}O_3S$ requires: $M+1$: 225.0585); v_{max}/cm^{-1} (neat) 3018 (OH) and 1639 (C=O); NMR data for the major diastereomer: δ_H (400 MHz; CDCl$_3$) 2.74 (1H, br s, OH), 2.99-3.06 (2H, overlapping multiplets, CH$_2$), 3.09 (1H, m, 3-H), 3.79 (3H, s, OCH$_3$), 5.11 (1H, s, 4-H), 7.08-7.17 (3H, m, Ar-H) and 7.34 (1H, d, J = 7.61 Hz, Ar-H); δ_C (100 MHz; CDCl$_3$) 22.2 (CH$_2$), 45.0 (C-3), 52.4 (CH$_3$), 67.3 (C-4), 124.5, 126.3, 128.8, 131.2, 133.4 and 133.6 (Ar-C) and 172.8 (C=O); m/z 225 $[(\mathbf{M+1})^{+}$, 60 %] and 209 (100 %).

Note: Use of DBU as sole catalyst afforded methyl 2*H*-1-thiochromene-3-carboxylate **202c** as the sole product in 40% yield after 24 h.[6,114]
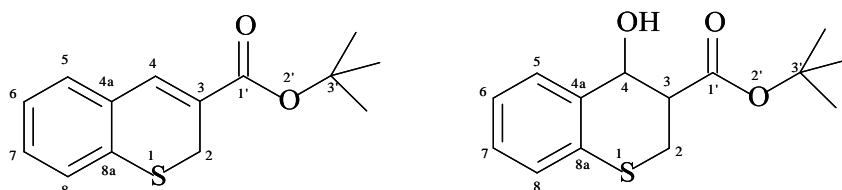
tert-*Butyl 2H-1-thiochromene-3-carboxylate* 202e *and* **tert-*butyl 4-hydroxythiochroman-3-carboxylate* 217e**

The procedure described for the synthesis of 3-acetyl-2*H*-1-benzothiopyran **202a** was followed using 2,2'-dithiodibenzaldehyde **201** (0.13 g, 0.46 mmol), Ph$_3$P (0.20 g, 0.75 mmol), CHCl$_3$ (0.5 mL), *tert*-butyl acrylate (0.20 mL, 1.35 mmol), DBU (0.11 mL, 0.75 mmol) and stirring for 3 h. Work-up afforded two products.

i) tert-*Butyl 2H-1-thiochromene-3-carboxylate* **202e** as a yellow oil (0.08 g, 35 %), (Found: **M-Bu^t:** 191.0000. $C_{10}H_7O_2S$ requires: 191.0172); v_{max}/cm^{-1} (neat) 1645 (C=O); δ_H (400 MHz; CDCl$_3$) 1.54 (9H, s, Bu^t), 3.68 (2H, s, CH$_2$), 7.10-7.26 (4H, series of multiplets, ArH) and 7.42 (1H, s, 4-H); δ_C (100 MHz; CDCl$_3$) 24.0 (3x CH$_3$), 28.1 (C-2), 81.3 (C-3'), 124.9, 125.7, 127.0, 129.9, 130.4, 131.6, 133.8 and 136.3 (Ar-C, C-3, C-4) and 165.0 (C=O); m/z 191 (**M-Bu^t**, 65%).

ii) ter*t-Butyl 4-hydroxythiochromane-3-carboxylate* as a diastereomeric mixtur*e* **217e** (0.11 g, 45 %), (Found: $[\mathbf{M+H}]^{+}$: 266.0989. $C_{14}H_{18}O_3S$ requires 266.0977); v_{max}/cm^{-1} (neat) 3042 (OH) and 1652 (C=O); NMR data for the major

diastereomer: δ_H (400 MHz; CDCl$_3$) 1.47 (9H, s, B^{ut}), 2.87 and 3.03 (2H, 2xm, C$_{H2}$), 3.45 (1H, dd, J = 11.29 and 12.50 Hz, 3-H), 5.04 (1H, s, 4-H), 7.05-7.14 (3H, m, ArH) and 7.35 (1H, d, J = 7.57 Hz, ArH); δ_C (100 MHz; CDCl$_3$) 23.3 (C$_{H2}$), 28.4 (3 x C$_{H3}$), 46.1 (C-3), 68.0 (C-4), 82.1 (C-3'), 124.8, 126.7, 128.3, 131.3, 132.2 and 134.2 (Ar-C) and 172.2 (C=O); m/z 266 ([M +H]$^+$, 100 %).
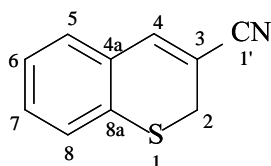
3-Cyano-2H-1-benzothiopyran 202f

The procedure described for the synthesis of 3-acetyl-2*H*-1-benzothiopyran **202a** was followed using 2,2'-dithiodibenzaldehyde **201** (0.13 g, 0.46 mmol), Ph$_3$P (0.20 g, 0.75 mmol), CHCl$_3$ (0.6 mL), acrylonitrile (0.12 mL, 1.4 mmol), DBU (0.11 mL, 0.75 mmol) and stirring for 2 h. Work-up afforded 3-cyano-2*H*-1-benzothiopyran **202f** as yellow crystals (0.10 g, 60 %), m.p. 74-77 °C (lit.[6,114] 78-80 °C); v_{max}/cm^{-1} (neat) 2214 (CN); δ_H (400 MHz; CDCl$_3$) 3.56 (2H, d, J = 1.2 Hz, CH$_2$) and 7.11-7.26 (5H, m, Ar-H and 4-H); δ_C (100 MHz; CDCl$_3$), 25.8 (C-2), 118.2 (CN), 103.8, 126.3, 127.5, 130.06, 130.1, 130.9, 132.7, 142.1 (Ar-C and C=CH).

Note: Use of DBU as sole catalyst afforded 3-cyano-2*H*-1-benzothiopyran **202f** in 52 % yield after 24 h.[6,114]
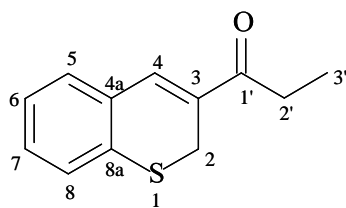
3-Propanoyl-2H-1-benzothiopyran 202g

The procedure described for the synthesis of 3-acetyl-2*H*-1-benzothiopyran **202a** was followed using 2,2'-dithiodibenzaldehyde **201** (0.13 g, 0.46 mmol), Ph$_3$P (0.20 g, 0.75 mmol), CHCl$_3$ (0.6 mL), ethyl vinyl ketone (0.12 mL, 1.4 mmol), DBU (0.11 mL, 0.75 mmol) and stirring for 2 h. Work-up afforded 3-propanoyl-2*H*-1-benzothiopyran **202g** as a yellow oil (0.13 g, 71 %); v_{max}/cm^{-1} (neat) 1672 (C=O); δ_H (400 MHz; CDCl$_3$) 1.18 (3H, t, J = 7.3 Hz, CH$_3$), 2.84 (2H, q, J = 7.2 Hz, 2'-CH$_2$), 3.72 (2H, d, J = 1.2 Hz, 2-CH$_2$), 7.11-7.27 (4H, m, Ar-H) and 7.39 (1H, s, 4-H); δ_C (100 MHz; CDCl$_3$) 8.7 (CH$_3$), 23.2 (C-2), 30.5 (C-

2'), 125.8, 127.4, 130.5, 130.8, 131.3, 131.5, 135.0 and 136.7 (Ar-C, C-3 and C-4) and 199.6 (C=O).

Note: Use of DBU as sole catalyst afforded 3-propanoyl-2*H*-1-benzothiopyran **202g** in 67 % yield after 48 h.[6,114]

3.2.3 Reactions of DBU with aryl and heteroaryl disulfides
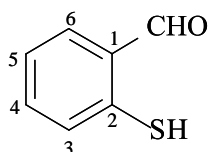
***2-Mercaptobenzaldehyde* 239**

DBU (0.11 mL, 0.75 mmol) was added slowly to a stirred solution of 2,2'-dithiodibenzaldehyde **201** (0.1 g, 0.46 mmol) in CHCl$_3$ (0.7 mL). The mixture was further stirred in a stoppered flask for 2 weeks. Flash chromatography followed by HPLC (elution with hexane-EtOAc (1:1) gave 2-mercaptobenzaldehyde **239** as a yellow oil (0.15 g, 49 %) (Found **M-H**: 137.0055. C$_7$H$_5$OS requires: 137.0061); v_{max}/cm^{-1} (neat) 2612 (S-H) and 1686 (C=O); δ_H (400 MHz; CDCl$_3$) 5.96 (1H, s, SH), 7.41 (1H, t, *J* = 7.45 Hz, 5-H), 7.58 (1H, d, *J* = 7.48 Hz, 3-H), 7.85 (1H, t, *J* = 8.08 Hz, 4-H), 7.93 (1H, d, *J* = 7.97 Hz, 6-H) and 10.14 (1H, s, CHO); δ_C (100 MHz; CDCl$_3$) 127.4 (C-5), 128.2 (C-4), 129.3 (C-6), 130.4 (C-3), 134.1 (C-1), 134.8 (C-2) and 192.1 (CHO); *m/z* 137 (**M-1**, 100 %).
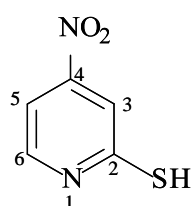
***2-Mercapto-4-nitropyridine* 240**

The procedure described for the synthesis of 2-mercaptobenzaldehyde **239** was followed using 2,2'-dithiobis[4-nitropyridine] **234** (0.1 g, 0.5 mmol), DBU (0.1 mL, 0.8 mmol) in CHCl$_3$ (0.7 mL). Flash chromatography on silica (elution with ethyl acetate) gave *2-mercapto-4-nitropyridine* **240** as a brown solid (0.06 g, 30 %), m.p. 96-98 ^{o}C (Found **M-H** 154.9900. C$_5$H$_3$N$_2$O$_2$S requires: 154.9915); v_{max}/cm^{-1} (neat) 2511 (S-H) and 1582 (C=N); δ_H (400 MHz; CDCl$_3$) 6.81 (1H, d, *J* = 9.63 Hz, 6-H) 8.33 (1H, dd, *J* = 9.53 and 1.99 Hz, 5-H) and 9.07 (1H, s, 3-H); δ_C (100 MHz; CDCl$_3$) 119.8, 132.1, 142.7, 145.3 and 165.0 (Ar-C); *m/z* 155 (**M-1**, 100 %).
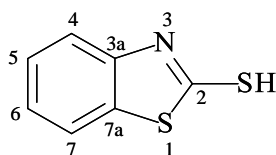
2-Mercapto-1,3-benzothiazole 241

The procedure described for the synthesis of 2-mercaptobenzaldehyde **239** was followed using 2,2'-dithiobis(benzothiazole) **235** (0.30 g, 0.91 mmol), DBU (0.22 mL, 1.5 mmol) in CHCl$_3$ (1.0 mL). The mixture was stirred in a stoppered flask for 8 days. The resulting solution was evaporated *in vacuo*. Flash chromatography on silica (elution with hexane-EtOAc: 1:1) gave 2-mercapto-1,3-benzothiazole **241** as a yellow crystalline solid (0.08 g, 53 %), m.p. 154-156 $^{\circ}$C (Found **M-1:** 165.9779. C$_7$H$_4$NS$_2$ requires: 165.9785); v_{max}/cm^{-1} (neat) 2572 (S-H) and 1464 (C=N); δ_H (400 MHz; CDCl$_3$) 3.52 (1H, s, SH), 7.28 (1H, m, 5-H), 7.37-7.39 (2H, m, 4-H and 7-H), 7.46 (1H, m, 6-H); δ_C (150MHz; CDCl$_3$) 112.4 (C-5), 121.8 (C-6), 125.1 (C-4), 127.6 (C-7), 130.5 (C-3a), 140.5 (C-7a) and 191.2 (C-2). *m/z* 166 (**M-1,** 100 %).

Formation of DBU-disulfide salts
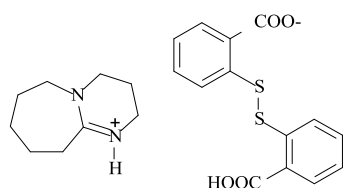
Mono-DBU-disulfide salt 242

The procedure described for the synthesis of 2-mercaptobenzaldehyde **239** was followed using 2,2'-dithiodibenzoic acid **236** (0.28 g, 0.91 mmol), DBU (0.22 mL, 1.5 mmol) in CHCl$_3$ (1.0 mL). The mixture was stirred in a stoppered flask for 6 days. The resulting solid which formed was filtered off to give the *mono-DBU-disulfide salt* **242** as a cream solid (0.39 g, 70 %), m.p. 213-216 $^{\circ}$C; v_{max}/cm^{-1} (neat) 1672 (C=O) and 1572 (C=N); δ_H (600 MHz; DMSO-d_6) 1.59 -1.66 (6H, m, DBU-CH$_2$), 1.88-1.91 (2H, m, DBU-CH$_2$), 2.75 (2H, m DBU-CH$_2$), 3.45-3.55 (6H, overlapping H$_2$O signal, DBU-CH$_2$), 7.06 (1H, t, *J* = 7.23 Hz, Ar-H), 7.13 (1H, t, *J* = 7.51 Hz, Ar-H), 7.45 (1H, d, *J* = 8.00 Hz, Ar-H), 7.80 (1H, d, *J* = 7.43 Hz, Ar-H) and 8.27 (1H, s, CO$_2$H); δ_C (150 MHz; DMSO-d_6) 18.7, 22.9, 25.7, 28.3, 31.6, 37.6, 47.7, 53.3 (DBU-C), 97.6 (C=N), 123.7, 123.7, 128.3, 129.9, 137.8 , 165.3 (Ar-C) and 168.8 (CO$_2$H).
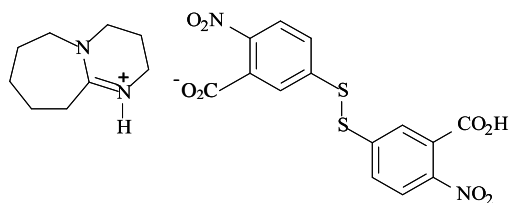
Mono-DBU-disulfide salt 243

The procedure outlined for the synthesis of 2-mercaptobenzaldeyde **239** was followed using 5,5'-dithiobis(2-nitrobenzoic acid) **237** (0.1 g, 0.9 mmol), DBU (0.10 mL, 1,5 mmol) and CHCl$_3$ (1.0 mL). Work-up afforded a yellow solid which was recrystallised from EtOH to give yellow crystals of the *mono-DBU-disulfide salt* **243** (0.12 g, 68 %), m.p. 217-220 °C; v_{max}/cm^{-1} (neat) 1689 (C=O) and 1592 (C=N); δ_H (600 MHz; DMSO-d_6) 1.63-1.71 (6H, m, DBU-CH$_2$), 1.89 (2H, m, DBU-CH$_2$), 2.65 (2H, m, DBU-CH$_2$), 3.22 (2H, br s, DBU-CH$_2$), 3.37-3.44 (4H, overlapping H$_2$O signal, DBU-CH$_2$), 7.48 (1H, dd, J = 8.46 and 2.20 Hz, Ar-H), 7.69 (1H, m, Ar-H), 7.73 (1H, s, Ar-H) and 10.15 (1H, s, CO$_2$H); δ_C (150 MHz; DMSO-d_6) 18.9, 23.4, 25.9, 28.2, 31.5, 37.5, 47.8 and 53.3 (DBU-C), 101.4 (C=N), 124.0, 125.0, 125.5, 126.2, 139.7 and 147.0 (Ar-C) and 165.3 (C=O).
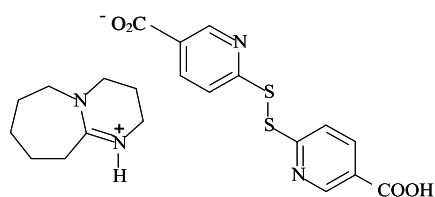
Mono-DBU-disulfide salt 244

The procedure described for the synthesis of 2-mercaptobenzaldehyde **239** was followed using 6,6'-dithiodinicotinic acid **238** (0.28 g, 0.91 mmol), DBU (0.22 mL, 1.5 mmol) and CHCl$_3$ (1 mL). The disulfide did not appear to dissolve completely in CHCl$_3$ and after stirring for 2 weeks, reaction was stopped. The solvent was evaporated *in vacuo* to give a yellow solid. This was further dried *in vacuo* to give the *mono-DBU-disulfide salt* **244** as a brown solid (0.33 g, 59 %), m.p. 207-209 °C; v_{max}/cm^{-1} (neat) 1662 (C=O) and 1606 (C=N); δ_H (400 MHz; DMSO-d_6) 1.64-1.72 (6H, m, DBU-CH$_2$), 1.98 (2H, m, DBU-CH$_2$), 2.86-2.87 (2H, m, DBU-CH$_2$), 3.38-3.45 (6H, overlapping H$_2$O signal, DBU-CH$_2$), 7.55 (1H, d, J = 8.31 Hz, Ar-H), 8.20 (1H, dd, J = 8.32 and 2.03 Hz, Ar-H), 8.84 (1H, s, Ar-H) and 9.04 (CO$_2$H); δ_C (150 MHz; DMSO-d_6) 18.9, 23.4, 26.0, 28.3, 31.5, 37.6, 47.8 and 53.3 (DBU-C), 108.7 (C=N), 118, 138.4, 150.5, 158.2 and 165.3 (Ar-C) and 166.3 (C=O).

Esterification of disulphides with carboxylic acid moieties
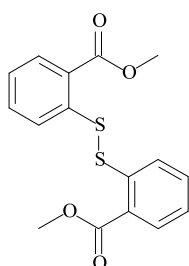
Methyl 2-[2-(methoxycarbonyl)phenyl]disulfanylbenzoate **245**

H_2SO_4 (0.4 mL) was added to MeOH (30 mL), followed by 2,2'-dithiodibenzoic acid **236** (6 g, 0.02 mol), and the resulting mixture was refluxed for 5 h. After cooling, H_2O (30 mL) was added and the mixture was stirred for several minutes, before adding further H_2O (30 mL) followed by saturated aqueous $NaHCO_3$ (15 mL). The precipitated solid was filtered off and washed with a little H_2O to give *methyl 2-[2-(methoxycarbony)lphenyl]disulfanylbenzoate* **245** as a cream powder (13.3 g, 49 %), m.p. 172-173 ^{o}C [Found **(M-CH$_3$O)$^+$**: 303.0676. $C_{14}H_7O_4S_2$ requires: 302.97857]; v_{max}/cm^{-1} (neat) 1661 (C=O); δ_H (400 MHz; CDCl$_3$) 3.98 (6H, s, OCH$_3$), 7.23 (2H, t, J = 7.57 Hz, ArH), 7.40 (2H, m, Ar-H), 7.75 (2H, d, J = 8.07 Hz, ArH) and 8.05 (2H, dd, J = 7.78 and 1.22 Hz, ArH); δ_C (100 MHz; CDCl$_3$) 52.3 (OCH$_3$), 125.4, 125.8, 127.2, 131.5, 133.3 and 139.9 (Ar-C) and 166.8 (C=O); *m/z* 303 [**(M- CH$_3$O)$^+$**, 30 %].
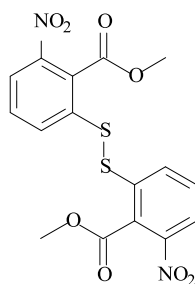
Methyl 2-[2-(methoxycarbonyl)-3-nitrophenyl]disulfanyl-6-nitrobenzoate **246**

The procedure described for the synthesis of methyl 2-[2-(methoxycarbonyl)phenyl]disulfanylbenzoate **245** was followed using 5,5'-dithiobis(2-nitrobenzoic acid) **237** (0.050 g, 0.13 mmol), MeOH (7 mL) and H_2SO_4 (0.1 mL). Work-up afforded *methyl 2-[2-(methoxycarbonyl)-3-nitrophenyl]disulfanyl-6-nitrobenzoate* **246** as a yellow oil (0.03 g, 57 %) (Found **M$^+$**: 425.0109. $C_{16}H_{13}N_2O_8S_2$ requires: 425.01132) v_{max}/cm^{-1} (neat) 1724 (C=O); δ_H (400 MHz; CDCl$_3$) 3.92 (6H, s, OCH$_3$), 7.87-7.94 (6H, series of

multiplets, Ar-H); δ_C (100 MHz; CDCl$_3$) 53.6 (OCH$_3$), 125.1, 126.8, 127.2, 128.4, 129.0 and 142.5 (Ar-C) and 167.7 (C=O); *m/z* 425 (**M$^+$**, 25 %) and 422 (100 %).
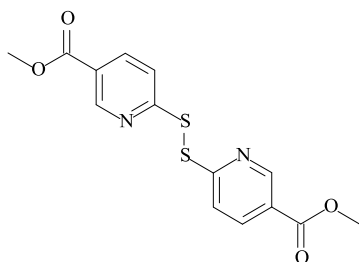
***Methyl 6-[(5-methoxycarbonyl-2-pyridyl)disulfanyl]pyridine-3-carboxylate* 247**

The procedure described for the synthesis of methyl 2-(2-methoxycarbonylphenyl)disulfanylbenzoate **245** was followed using 6,6'-dithiodinicotinic acid **238** (1.10 g, 3.57 mmol), MeOH (15 mL) and H$_2$SO$_4$ (0.3 mL). Work-up afforded *methyl 6-[(5-methoxycarbonyl-2-pyridyl)disulfanyl]pyridine-3-carboxylate* **247** as a cream solid (1.7 g, 70 %), m.p 149-151°C [Found (**M- CH$_3$O)$^+$**: 305.0059. C$_{12}$H$_6$N$_2$O$_4$S$_2$ requires: 304.9692]; v_{max}/cm^{-1} (neat) 1716 (C=O); δ_H (400 MHz; CDCl$_3$) 3.92 (6H, s, OCH$_3$), 7.64 (2H, d, *J* = 8.41 Hz, ArH), 8.18 (2H, d, *J* = 8.38 Hz, ArH) and 9.04 (2H, s, ArH); δ_C (100 MHz; CDCl$_3$) 52.6 (OCH$_3$), 124.1, 125.4, 138.1, 150.5 and 164.8 (Ar-C) and 165.8 (C=O); *m/z* 305 [(**M − CH$_3$O)$^+$**, 100 %]

Reaction of the disulfide esters with DBU
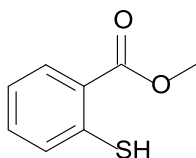
***Methyl 2-mercaptobenzoate* 248**

DBU (0.22 mL, 1.5 mmol) was added to a solution of methyl 2-[(2-methoxycarbonyl)phenyl]disulfanylbenzoate **245** (0.30 g, 0.91 mmol) in CHCl$_3$ (1.0 mL). The mixture was stirred for 24 h. The product was purified using flash chromatography [on silica; elution with hexane-EtOAc (1:1)]. The solvent was evaporated *in vacuo* to give methyl 2-mercaptobenzoate **248** as a yellow oil (0.03 g, 20 %) (Found **M$^+$**: 167.0167. C$_8$H$_7$O$_2$S requires: 167.0171); v_{max}/cm^{-1} (neat) 2556 (S-H) and 1704 (C=O); δ_H (400 MHz; CDCl$_3$) 3.84 (1H, s, SH), 3.97 (3H, s, OCH$_3$), 7.21 (1H, m, Ar-H), 7.40 (1H, t, *J* =7.73 Hz, Ar-H), 7.74 (1H, d, *J* = 8.17 Hz, Ar-H) and 8.05 (1H, d, *J* = 7.01 Hz, Ar-H); δ_C (100 MHz; CDCl$_3$)

52.4 (OCH$_3$), 125.5, 125.9, 127.3, 131.5, 133.1 and 140.4 (Ar-C) and 166.9 (C=O); *m/z* 167 (**M**$^+$, 100 %).
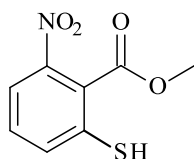
Methyl 2-mercapto-6-nitrobenzoate 249

The procedure described for the synthesis of methyl 2-mercaptobenzoate **248** was followed using methyl 2-[2-(methoxycarbonyl)-3-nitrophenyl]disulfanyl-6-nitro-benzoate **246** (0.03 g, 0.07 mmol), DBU (0.017 mL, 0.12 mmol) and CHCl$_3$ (1 mL). The product was purified using flash chromatography [on silica; elution with hexane-EtOAc (1:1)], to give *methyl 2-mercapto-6-nitrobenzoate* **249** as a yellow oil (0.017 g, 44 %) (Found **M-1**: 212.0018. C$_8$H$_6$NO$_4$S requires: 212.0022); v_{max}/cm^{-1} (neat) 2612 (S-H) and 1732 (C=O); δ_H (400 MHz; CDCl$_3$) 3.95 (3H, s, OCH$_3$), 7.45-7.47 (2H, m, Ar-H) and 7.83 (1H, m, Ar-H); δ_C (100 MHz; CDCl$_3$) 53.3 (OCH$_3$), 111.1, 124.9, 126.2, 128.3, 133.9 and 146.2 (Ar-C) and 171.1 (C=O); *m/z* 212 (**M-1**, 52 %).
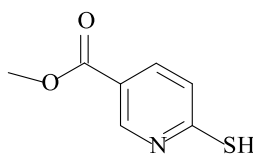
Methyl 6-mercaptopyridine-3-carboxylate 250

The procedure described for the synthesis of methyl 2-mercaptobenzoate was followed using methyl 6-[5-(methoxycarbonyl)-2-pyridyl]disulfanylpyridine-3-carboxylate **247** (0.30 g, 0.91 mmol), DBU (0.22 mL, 1.5 mmol) and CHCl$_3$ (2 mL). The product was purified using flash chromatography [on silica; elution with hexane-EtOAc (1:1)], to give *methyl 6-mercaptopyridine-3-carboxylate* **250** as a yellow oil (0.02 g, 13 %) (Found *M+1*: 170.0276. C$_7$H$_8$NO$_2$S requires: 170.0273); v_{max}/cm^{-1} (neat) 2541 (S-H) and 1714 (C=O); δ_H (400 MHz; CDCl$_3$) 3.92 (1H, s, SH), 3.95 (3H, s, OCH$_3$), 7.60 (1H, d, *J* = 8.32 Hz, Ar-H), 8.21 (1H, dd, *J* = 8.31 and 2.24 Hz, Ar-H) and 9.10 (1H, s, Ar-H); δ_C (100 MHz; CDCl$_3$) 52.9 (OCH$_3$), 125.4, 138.2, 138.3, 151.58 and 151.60 (Ar-C) and 165.7 (C=O); *m/z* 170 (**M+1**, 30 %).

3.3 Synthesis of chromone derivatives

3.3.1 Synthesis of chromone-3-carbaldehydes
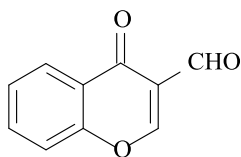
Chromone-3-carbaldehyde **218a**[174]

POCl$_3$ (9.4 mL, 0.10 mol) was added dropwise, during a period of 0.5 h., to a stirred solution of *o*-hydroxyacetophenone **265a** (3.0 mL, 25 mmol) in dry DMF (25 mL) under N$_2$, while maintaining the temperature at -23 $^{\circ}$C using a liquid nitrogen-carbon tetrachloride cooling bath. The resulting mixture was stirred overnight at room temperature and then poured into ice-water (50 mL). The resulting precipitate was filtered off, and washed successively with water and EtOH. Recrystallisation from acetone afforded chromone-3-carbaldehyde **218a** as colourless crystals (3.1g, 71 %), m.p. 151-153 $^{\circ}$C (lit.[174] 152-153 $^{\circ}$C); v_{max} (neat)/cm^{-1} 1690 and 1649 (2x C=O); δ_H (400 MHz; CDCl$_3$) 7.49 (1H, t, *J* = 7.1 Hz, 6-H), 7.53 (1H, d, *J* = 8.8 Hz, 8-H), 7.74 (1H, t, *J* = 7.8 Hz, 7-H), 8.23 (1H, d, *J* = 8.0 Hz, 5-H), 8.54 (1H, s, 2-H) and 10.38 (1H, s, CHO); δ_C (100 MHz; CDCl$_3$) 118.6 (C-8), 120.4 (C-3), 125.3 (C-4a), 126.2 (C-5), 126.6 (C-6), 134.8 (C-7), 156.2 (C-8a), 160.6 (C-2), 176.0 (C=O) and 188.6 (CHO); *m/z* 174 (**M**$^+$, 6 %) and 146 (100).
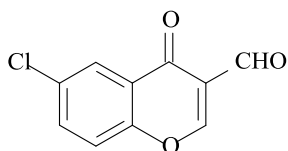
6-Chlorochromone-3-carbaldehyde **218b**[174]

The procedure described for the synthesis of chromone-3-carbaldehyde **218a** was followed using POCl$_3$ (9.4 mL, 0.10 mol), 5-chloro-2-hydroxyacetophenone **265b** (4.2 g, 25 mmol) and dry DMF (15 mL). Work-up afforded 6-chlorochromone-3-carbaldehyde **218b** as a yellow crystalline solid (4.13 g, 80 %), 164-166 $^{\circ}$C (lit. 164-166 $^{\circ}$C[186]); v_{max} (neat)/cm^{-1} 1690 and 1655 (2x C=O); δ_H (400 MHz; CDCl$_3$) 7.49 (1H, d, *J* = 8.9 Hz, 8-H), 7.68 (1H, dd, *J* = 2.6 and 8.9 Hz, 7-H), 8.25 (1H, d, *J* = 2.5 Hz, 5-H), 8.52 (1H, s, 2-H) and 10.36 (1H, s, CHO); δ_C (100 MHz; CDCl$_3$) 120.3 (C-8), 125.6 (C-5), 126.3 (C-4a), 132.8 (C-3 and C-6), 135.0 (C-7), 154.5 (C-8a), 160.6 (C-2), 174..8 (C=O) and 188.1 (CHO); *m/z* 208 (**M**$^+$, 4 %) and 180 (100 %).
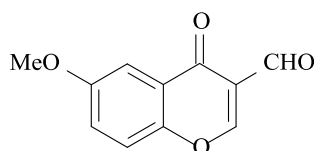
6-Methoxychromone-3-carbaldehyde 218c[174]

The procedure described for the synthesis of chromone-3-carbaldehyde **218a** was followed using POCl$_3$ (13.5 mL, 0.144 mmol), 2-hydroxy-6-methoxyacetophenone (6.0 g, 36 mmol) and dry DMF (25 mL). Work-up afforded 6-methoxychromone-3-carbaldehyde **218c** as yellow crystals (4.3 g, 59 %), m.p. 164-165 °C (lit.[79] 164-166 °C); ν_{max} (neat)/cm^{-1} 1701 and 1657 (2x C=O); δ_H (400 MHz; CDCl$_3$) 3.92 (3H, s, OMe), 7.31 (1H, dd, J = 3.1 and 9.2 Hz, 7-H), 7.46 (1H, d, J = 9.1 Hz, 8-H), 7.64 (1H, d, J = 3.1 Hz, 5-H), 8.51 (1H, s, 2-H) and 10.39 (1H, s, CHO); δ_C (100 MHz; CDCl$_3$) 56.1 (OCH$_3$), 105.5 (C-5), 119.6 (C-3), 120.0 (C-8), 124.4 (C-7), 126.1 (C-4a), 151.0 (C-6), 158.0 (C-8a), 160.2 (C-2), 175.9 (C=O) and 188.7 (CHO); m/z 204 (**M**$^+$, 1 %) and 176 (100 %).

3.3.2 Morita-Baylis-Hillman reactions of chromone-3-carbaldehydes with MVK
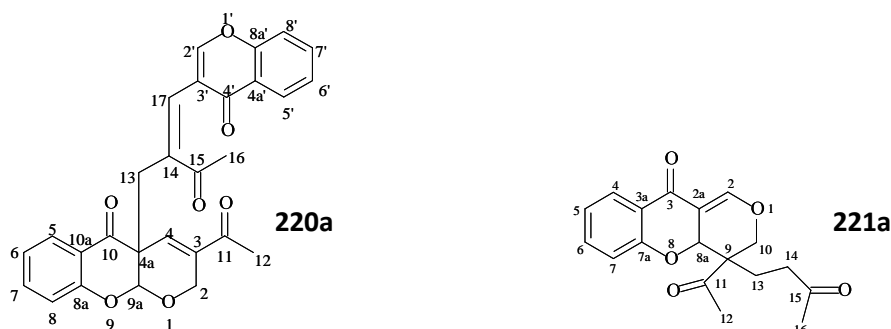
***Chromone dimer* 220a** and ***tricyclic product* 221a**

Chromone-3-carbaldehyde **218a** (0.25 g, 1.5 mmol) was dissolved in CHCl$_3$ (1.8 mL). MVK (0.2 mL, 3.8 mmol) and 3HQ (0.23 g, 1.8 mmol) were added, and the resulting mixture was stirred at room temperature for 24h, and then concentrated *in vacuo* to give a brown, oily residue which was purified by flash chromatography [on silica; elution with hexane-EtOAc (1:2)] to give two fractions.

Fraction 1. as a yellow viscous oil, the diastereomeric mixture of the tricyclic product **221a** (0.31 g, 69 %), further separation using HPLC afforded the two diastereomeric products.

Major diastereomer **221a$_1$,** as a yellow oil (Found **M**$^+$: 314.1131, C$_{18}$H$_{18}$O$_5$ requires 314.1154); ν_{max} (neat)/cm^{-1} 1700, 1665 and 1650 (3x C=O); δ_H (400 MHz; CDCl$_3$) 2.10 and

2.20 (2H, 2xm, 13-CH$_2$), 2.08 (3H, s, 16-CH$_3$), 2.39 (3H, s, 12-CH$_3$), 2.41 and 2.52 (2H, 2xm, 14-CH$_2$), 4.59 (1H, dd, J = 17.2 and 1.47 Hz, 10-H$_a$), 4.80 (1H, d, J = 17.17 Hz, 10-H$_b$), 5.14 (1H, s, 8a-H), 7.13 (2H, m, 5-H and 7-H), 7.30 (1H, s, 2-H), 7.57 (1H, t, J = 6.9 Hz, 6-H) and 7.91 (1H, d, J = 6.5 Hz, 4-H); δ_C (100 MHz; CDCl$_3$) 24.8 (C-13), 25.5 (C-14), 30.0 (C-12), 37.8 (C-16), 49.1 (C-9), 65.9 (C-10), 99.9 (C-8a), 118.2 (C-7), 119.5 (C-2a), 123.0 (C-4), 127.9 (C-5), 135.4 (C-6), 136.8 (C-2), 138.3 (C-3a), 157.6 (C-7a), 192.6 (3-C=O), 199.6 (15-C=O) and 206.7 (11- C=O); m/z 314 (**M**$^+$, 2 %) and 193 (100 %).

Minor diastereomer **221a$_2$**: as a yellow oil, δ_H (400 MHz; CDCl$_3$) 2.13 (3H, s, 16-CH$_3$), 2.20 (2H, t, J = 7.43 Hz, 13-CH$_2$), 2.31 (3H, s, 12-CH$_3$), 2.58 (2H, m, 14-CH$_2$), 4.49 (1H, dd, J = 17.0 and 1.67 Hz, 10-H$_a$), 4.65 (1H, d, J = 17.01 Hz, 10-H$_b$), 5.42 (1H, s, 8a-H), 6.69 (1H, s, 2-H), 7.03 (1H, d, J = 8.31 Hz, 7-H), 7.09 (1H, t, J = 7.51 Hz, 5-H), 7.55 (1H, t, J = 7.77 Hz, 6-H) and 7.85 (1H, dd, J = 7.80 and 1.21 Hz, 4-H); δ_C (100 MHz; CDCl$_3$) 25.2 (C-13), 27.7 (C-16), 29.9 (C-12), 37.7 (C-14), 49.7 (C-9), 62.5 (C-10), 99.4 (C-8a), 118.2 (C-7), 119.2 (C-2a), 122.6 (C-4), 127.2 (C-5), 135.9 (C-6), 137.1 (C-2), 138.0 (C-3a), 157.6 (C-7a), 193.1 (3-C=O), 196.3 (15-C=O) and 206.5 (11-C=O).

Fraction 2. The MVK chromone dimer **220a,** as a white solid, (0.24 g, 31 %) (Found **M**$^+$: 470.1364. C$_{28}$H$_{22}$O$_7$ requires 470.1366); m.p. 192-194 ^{o}C (lit.[79] 193-195 ^{o}C); ν_{max} (neat)/cm^{-1} 1695, 1665, 1642 and 1606 (4x C=O); δ_H (400 MHz; CDCl$_3$) 2.28 (3H, s, 12-H), 2.42 (3H, s, 16-H), 3.22 (2H, s, 13-CH$_2$), 4.51-4.59 (2H, m, 2-CH$_2$), 5.00 (1H, s, 9-Ha), 6.86-6.93 (2H, m, 5-H and 6-H), 7.16 (1H, s, 4-H), 7.26 (1H, m, 8-H), 7.40-7.45 (3H, m, 17-H, 7'-H and 8'-H), 7.69-7.73 (2H, m, 6'-H and 7-H), 7.89 (1H, s, 2'-H) and 8.12 (1H, dd, J = 7.8 and 1.2 Hz, 5'-H); δ_C (100 MHz; CDCl$_3$) 25.3 (C-12), 25.8 (C-16), 30.9 (C-13), 50.1 (C-4a), 65.9 (C-2), 99.9 (C-9a), 117.5 (C-5), 118.1 (C-7'), 120.0 (C-10a), 120.3 (C-4a'), 122.9 (C-6), 123.5 (C-8a'), 125.8 (C-8'), 126.1 (C-5'), 128.0 (C-7), 133.6 (C-17), 134.2 (C-6'), 136.1 (C-8), 136.6 (C-3), 136.7 (C-4), 139.1 (C-14), 154.1 (C-2'), 155.9 (C-3'), 157.0 (C-8a), 175.6 (C-4'), 191.5 (C-10), 196.9 (C-11) and 199.0 (C-15); m/z 470 (**M**$^+$, 24 %) and 185 (100 %).
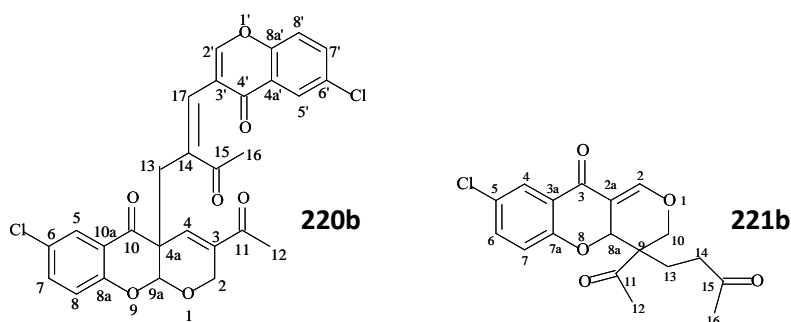
Chromone dimer 220b *and the tricyclic product* 221b

The procedure described for the synthesis of compounds **220a** and **221a** was followed, using 6-chloro-chromone-3-carbaldehyde **218b** (0.50 g, 2.4 mmol), MVK (0.24 mL, 2.6 mmol), 3HQ (1.5 g, 12 mmol) and CHCl$_3$ (3.0 mL). Work-up and flash chromatography [on silica; elution with hexane-EtOAc (2:1)] afforded two fractions.

Faction 1. The tricyclic product **221b** as a reddish-brown oil (0.65 g, 76 %) (Found **MH**$^+$: 349.0843. C$_{18}$H$_{17}$^{35}ClO$_5$ requires 349.0848); v_{max} (neat)/cm^{-1} 1713, 1699 and 1670 (3x C=O); δ_H (400 MHz; CDCl$_3$) 2.13 (3H, s, 16-CH$_3$), 2.15 and 2.25 (2H, 2xm, 13-CH$_2$), 2.31 (3H, s, 12-CH$_3$), 2.46 and 2.59 (2H, 2xm, 14-CH$_2$), 4.48 (1H, dd, J = 17.1 and 2.0 Hz, 10-H$_a$), 4.63 (1H, d, J = 17.0 Hz, 10-H$_b$), 5.40 (1H, s, 8a-H), 6.65 (1H, s, 2-H), 6.69 (1H, d, J = 8.8 Hz, 7-H), 7.48 (1H, dd, J = 8.8 and 2.7 Hz, 6-H) and 7.80 (1H, d, J = 2.7 Hz, 4-H); δ_C (100 MHz; CDCl$_3$) 25.2 (C-12), 27.6 (C-13), 30.0 (C-16), 37.6 (C-14), 48.8 (C-9), 62.7 (C-10), 99.6 (C-8a), 118.8 (C-2a), 120.0 (C-7), 126.6 (C-4), 135.4 (C-6), 136.9 (C-2), 139.4 (C-3a), 143.5 (C-5) 155.9 (C-7a), 192.0 (3-C=O), 196.4 (15- C=O) and 205.3 (11- C=O); *m/z* 349 (**MH**$^+$, 9 %) and 154 (100 %).

Fraction 2. The MVK chromone dimer **220b** as a yellow solid (0.42 g, 22 %), m.p. 118-121 °C (lit.[79] 112-114 °C); v_{max} (neat)/cm^{-1} 1695, 1665, 1642 and 1606 (4x C=O); δ_H (400 MHz; CDCl$_3$) 2.31 (3H, s, 12-CH$_3$), 2.44 (3H, s, 16-CH$_3$), 3.00 (2H, s, 13-CH$_2$), 5.16 (2H, dd, J = 17.0 and 1.7 Hz, 2-CH$_2$), 5.39 (1H, s, 9a-H), 6.93 (1H, s, 4-H), 7.12 (1H, d, J = 8.9 Hz, 8-H), 7.30 (1H, s, 17-H), 7.44 (1H, d, J = 8.9 Hz, 8'-H), 7.45 (1H, d, J = 8.9 Hz, 7'-H), 7.76 (1H, dd, J = 8.0 and 2.0 Hz, 7-H), 8.08 (1H, d, J = 2.0 Hz, 5-H), 8.66 (1H, s, 2'-H) and 9.18 (1H, d, J = 1.3 Hz, 5'-H); δ_C (100 MHz; CDCl$_3$) 25.4 (C-12), 25.9 (C-16), 31.3 (C-13), 50.5 (C-4a), 66.1 (C-2), 100.2 (C-9a), 116.6 (C-5), 118.0 (C-7'), 121.6 (C-10a), 122.2 (C-4a'), 124.4 (C-5'), 128.4 (C-8'), 128.5 (C-7), 133.6 (C-17), 134.0 (C-6), 136.6 (C-3), 136.7 (C-8), 139.3 (C-14), 141.4 (C-6'), 143.7 (C-4), 148.6 (C-8a'), 154.2 (C-2'), 156.2 (C-3'), 158.5 (C-8a),

174.8 (C-4'), 190.8 (C-10), 196.9 (C-11) and 199.0 (C-15); m/z 538 ($\mathbf{M}^+$, 40 %) and 164 (100 %).
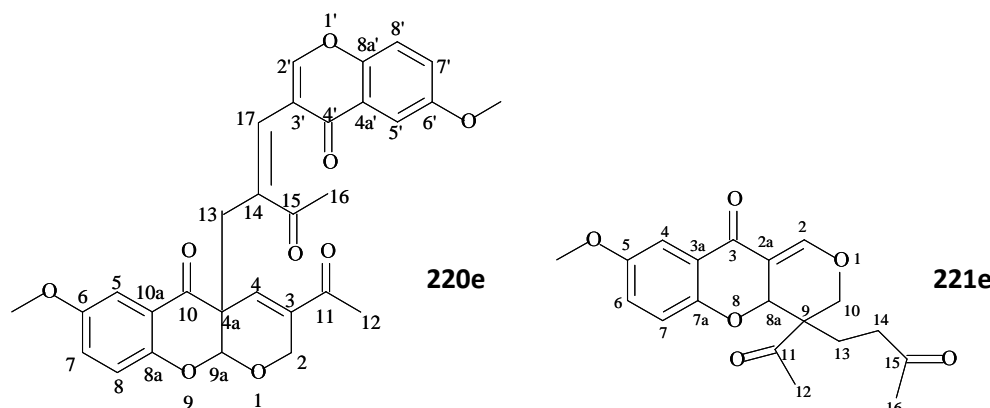
***Chromone dimer* 220e *and tricyclic product* 221e**

The procedure described for the synthesis of compounds **220a** and **221a** was followed, using 6-methoxychromone-3-carbaldehyde **218e** (0.254 g, 1.24 mmol), MVK (0.17 mL, 1.8 mmol), 3HQ (0.23 g, 1.8 mmol) and CHCl₃ (1.8 mL). Work-up and flash chromatography of the crude product [on silica; elution with hexane-EtOAc (2:1)] afforded two fractions.

Faction 1. The tricyclic product **221e** as a reddish oil (0.31 g, 72 %) Found $\mathbf{M}^+$: 344.1252. $C_{19}H_{20}O_6$ requires 344.1259); v_{max} (neat)/cm⁻¹ 1673, 1667 and 1654 (3x C=O); δ_H (400 MHz; CDCl₃) 2.09 and 2.23 (2H, 2xm, 13-CH₂), 2.15 (3H, s, 16-CH₃), 2.39 and 2.52 (2H, 2xm, 14-CH₂) 2.44 (3H, s, 12-CH₃), 3.91 (3H, s, 6-OCH₃), 4.55 (2H, dd, J = 17.15 and 1.9 Hz, 10-CH₂), 4.94 (1H, s, 8a-H), 6.69 (1H, s, 2-H), 7.08 (1H, d, J = 9.11 Hz, 7-H), 7.33 (1H, dd, J = 9.11 and 2.32 Hz, 6-H) and 7.85 (1H, d, J = 2.32 Hz, 4-H); δ_C (100 MHz; CDCl₃) 24.7 (C-13), 25.5 (C-16), 30.0 (C-12), 37.6 (C-14), 50.1 (C-9), 55.9 (OCH₃), 65.9 (C-10), 99.8 (C-8a), 118.5 (C-2a), 119.4 (C-7), 124.1 (C-4), 133.9 (C-6), 137.3 (C-2), 139.0 (C-3a), 143.5 (C-5) 154.8 (C-7a), 191.4 (3-C=O), 197.1 (15- C=O) and 199.2 (11- C=O); m/z 344 ($\mathbf{M}^+$, 33 %) and 193 (100 %).

Fraction 2. The MVK chromone dimer **220e** as a yellow oil (0.16 g, 24 %); v_{max} (neat)/cm⁻¹ 1701, 1677, 1674 and 1655 (4x C=O); δ_H (400 MHz; CDCl₃) 2.28 and 2.33 (6H, 2x s, 2xCH₃), 3.22 (2H, s, 13-CH₂), 3.72 and 3.92 (6H, 2x s, 2x OCH₃), 5.09 (2H, dd, J = 17.2 and 1.7 Hz, 2-CH₂), 5.25 (1H, s, 9a-H), 6.95 (1H, s, 4-C=CH), 6.99 (1H, d, J = 8.9 Hz, Ar-H), 7.27 (1H, s, C=CH), 7.44 (1H, d, J = 8.9 Hz, Ar-H), 7.64 (1H, d, J = 8.3 Hz, Ar-H), 7.73 (1H, dd, J = 8.0 and 2.0 Hz, Ar-H), 8.16 (1H, d, J = 1.3 Hz, Ar-H), 8.33 (1H, d, J = 2.0 Hz, Ar-H) and 8.70 (1H, s, Ar-H); δ_C (100 MHz; CDCl₃) 25.4 (C-12), 25.9 (C-13 and C-16), 50.1 (C-4a), 55.5 (6'-OMe), 55.9 (6-OMe), 66.9 (C-2), 99.7 (C-9a), 105.0 (C-5), 108.1 (C-8), 118.5

(C-6'), 119.2 (C-8'), 119.3 (C-7), 119.8 (C-3'), 124.0 (C-7'), 124.1 (C-4a'), 125.1 (C-10a), 133.9 (C-17), 136.0 (C-3), 137.3 (C-4), 139.0 (C-14), 150.6 (C-2'), 151.4 (C-8a'), 153.8 (C-8a), 154.7 (C-6), 157.2 (C-6'), 175.3 (C-4'), 191.4 (C-11), 197.1 (C-15) and 199.2 (C-10); *m/z* 530 (M^+, 21 %) and 487 (100 %).
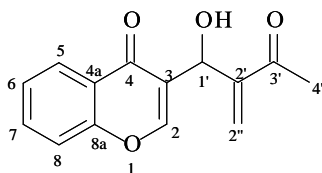
3-[2-Acetyl-1-hydroxy-2-propenyl]-4H-1-benzopyran-4-one 219

Chromone-3-carbaldehyde **218a** (0.25 g, 1.5 mmol) was dissolved in CHCl$_3$ (1.8 mL) and MVK (0.2 mL, 3.8mmol) and 3HQ (0.23 g, 1.8 mmol) were added. The resulting mixture was stirred at room temperature for 30 min., and concentrated *in vacuo* to give a brown, oily residue, which was purified by flash chromatography [on silica; elution with hexane-EtOAc (1:2)] to give three fractions. The dimer **220a**, the tricyclic product **221a** as a diastereomeric mixture, and compound **219**.

3-[2-Acetyl-1-hydroxy-2-propenyl]-4H-1-benzopyran-4-one **219** as a pale yellow oil (0.02 g, 6 %), v_{max} (neat)/cm^{-1} 3324 (OH), 1704 and 1654 (2x C=O); δ_H (400 MHz; CDCl$_3$) 2.35 (3H, s, 4'-CH$_3$), 5.85 (1H, s, 1'-H), 5.92 and 6.19 (2H, 2 x s, 2''-CH$_2$), 6.72 (1H, d, *J* = 8.10 Hz, 5-H), 6.90 (1H, t, *J* = 7.08 Hz, 6-H), 7.09 (1H, t, *J* = 7.10 Hz, 7-H), 7.20 (1H, d, *J* = 8.88 Hz, 8-H) and 7.51 (1H, s, 2-H); δ_C (100 MHz; CDCl$_3$) 25.2 (C-4'), 70.5 (C-1'), 113.9 (C-8), 122.4 (C-4a), 123.7 (C-3), 124.9 (C-6), 125.2 (C-2''), 125.7 (C-5), 132.5 (C-7), 143.2 (C-2'), 148.1 (C-2), 153.9 (C-8a), 183.1 (4-C=O) and 202.1 (3'-C=O).

3.3.3 Synthesis of chromone-2-carbaldehydes
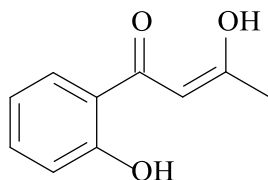
3-Hydroxy-1-(2-hydroxyphenyl)but-2-en-1-one 280a[79]

A solution of *o*-hydroxyacetophenone **265a** (10 mL, 83 mmol) in dry EtOAc (35 mL, 0.36 mmol) was added dropwise to a stirred suspension of NaOEt [generated *in situ* by adding Na metal pieces (8.0 g, 0.35 mmol) to dry EtOH (40 mL)]. The resulting yellow mixture was boiled gently under reflux for *ca.* 8 h, until a thick yellow slurry was formed. After cooling, the mixture was poured into Et$_2$O (200 mL) and allowed to stand for 1 h. The resulting

precipitate was filtered off, washed with Et₂O (200 mL) and dissolved in ice-cold water (100 mL). The solution was acidified with acetic acid and the resulting precipitate was filtered off and recrystallised from petroleum ether (b.p. 60-80 ^{o}C) to afford 3-hydroxy-1-(2-hydroxyphenyl)but-2-en-1-one **280a** as a yellow solid (8.1 g, 55 %), m.p. 83-85 ^{o}C, which was used immediately without further purification.
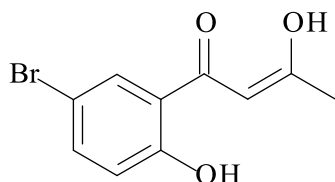
***1-(5-Bromo-2-hydroxyphenyl)-3-hydroxybut-2-en-1-one* 280b**[79]

The procedure described for the synthesis of 3-hydroxy-1-(2-hydroxyphenyl)but-2-en-1-one **280a** was followed, using 5-bromo-2-hydroxyacetophenone **265b** (10.0 g, 47 mmol), dry EtOAc (18.2 mL, 0.21 mmol) and NaOEt [generated *in situ* by adding Na metal (4.28 g, 186 mmol) to dry EtOH (45 mL)]. Work-up afforded 1-(5-bromo-2-hydroxyphenyl)-3-hydroxy-but-2-en-1-one **280b** as a yellow solid (4.8 g, 41 %), m.p. 116-119 ^{o}C, which was used immediately without further purification.
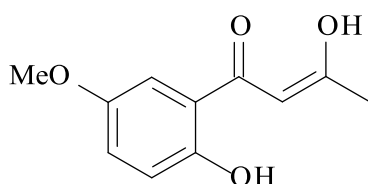
***3-Hydroxy-1-(2-hydroxy-5-methoxyphenyl)but-2-en-1-one* 280c**[79]

The procedure described for the synthesis of 3-hydroxy-1-(2-hydroxyphenyl)but-2-en-1-one **280a** was followed, using 2-hydroxy-5-methoxyacetophenone **265c** (10.0 g, 60 mmol), dry EtOAc (26 mL, 0.3 mmol) and NaOEt [generated *in situ* by adding Na metal (5.80 g, 252 mmol) to dry EtOH (29 mL)]. Work-up afforded 3-hydroxy-1-(2-hydroxy-5-methoxy-phenyl)but-2-en-1-one **280c** as a yellow solid (7.2 g, 75 %), m.p. 96-99 ^{o}C, which was used immediately without further purification.
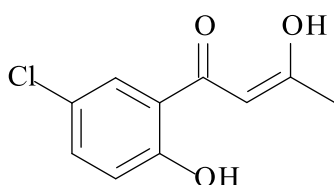
***1-(5-Chloro-2-hydroxyphenyl)-3-hydroxybut-2-en-1-one* 280d**[79]

The procedure described for the synthesis of 3-hydroxy-1-(2-hydroxyphenyl)but-2-en-1-one **280a** was followed, using 5-chloro-2-hydroxyacetophenone **265d** (3.0 g, 18 mmol), dry

EtOAc (7.0 mL, 70 mmol) and NaOEt [generated *in situ* by adding Na metal (1.6 g, 70 mmol) to dry EtOH (9.0 mL). Work-up afforded 1-(5-chloro-2-hydroxyphenyl)-3-hydroxy-but-2-en-1-one **280d** as a yellow solid (2.9 g, 77 %), m.p. 93-96 ^{o}C, which was used immediately without further purification.
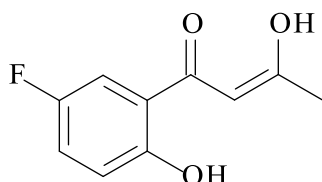
1-(5-Fluoro-2-hydroxyphenyl)-3-hydroxybut-2-en-1-one **280e**[79]

The procedure described for the synthesis of 3-hydroxy-1-(2-hydroxyphenyl)but-2-en-1-one **280a** was followed, using 5-fluoro-2-hydroxyacetophenone **265e** (3.0 g, 19.4 mmol), dry EtOAc (7.6 mL, 78 mmol) and NaOEt [generated *in situ* by adding Na metal (1.79 g, 78 mmol) to dry EtOH (29 mL)]. Work-up afforded 1-(5-fluoro-2-hydroxy-phenyl)-3-hydroxy-but-2-en-1-one **280e** as a yellow solid (1.56 g, 47 %), m.p. 81-83 ^{o}C, which was used immediately without further purification.
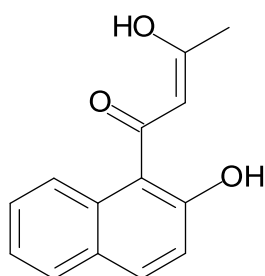
3-Hydroxy-1-(2-hydroxy-1-naphthyl)but-2-en-1-one **290**

The procedure described for the synthesis of 3-hydroxy-1-(2-hydroxyphenyl)but-2-en-1-one **280a** was followed, using 2'-hydroxy-1'-acetonaphthone **289** (3.0 g, 16 mmol), dry EtOAc (6.3 mL, 64 mmol) and NaOEt [generated *in situ* by adding Na metal pieces (1.48 g, 64.4 mmol) to dry EtOH (8.3 mL)]. Work-up afforded *3-hydroxy-1-(2-hydroxy-1-naphthyl)but-2-en-1-one* **290** as a yellow solid (1.64 g, 41.2 %) [m.p. 153-156 ^{o}C, (Found: **M+1** 229.0865, $C_{14}H_{13}O_3$ requires *M*: 229.0865); v_{max} (nujol)/cm^{-1} 3421 (OH) and 1676 (C=O)] which was used immediately without further purification.
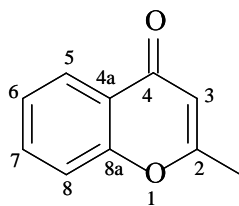
***2-Methylchromone* 281a**

A stirred solution of 3-hydroxy-1-(2-hydroxyphenyl)but-2-en-1-one **280a** (2.0 g, 11 mmol), glacial acetic acid (10 mL) and H_2SO_4 (95-98%; 0.4 mL) was boiled gently under reflux for 4 h. The resulting, hot, brick-red solution was poured into ice-cold water (50 mL) and basified with 10 % aq. $NaHCO_3$. The resulting precipitate was filtered, washed with ice-cold water, and recrystallised from hexane to afford 2-methylchromone **281a** as a yellow solid (1.2 g, 68 %), m.p. 69-71 ^{o}C (lit.[187] 69-70 ^{o}C); v_{max} (nujol)/cm^{-1} 1654 (C=O); δ_H (400 MHz; CDCl$_3$) 2.26 (3H, s, CH$_3$), 6.15 (1H, s, 3-H), 7.38 (1H, m, 8-H), 7.62 (1H, m, 7-H), and 8.16 (1H, dd, J = 8.0 and 1.6 Hz, 5-H); δ_C (100M Hz; CDCl$_3$) 20.5 (CH$_3$), 110.5 (C-3), 117.7 (C-8), 123.5 (C-4a), 124.9 (C-6), 125.6 (C-5), 133.4 (C-7), 156.5 (C-8a), 166.2 (C-2) and 178.2 (C=O).
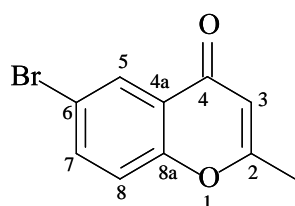
***6-Bromo-2-methylchromone* 281b**

The procedure described for the synthesis of 2-methylchromone **281a** was followed, using 1-(5-bromo-2-hydroxyphenyl)-3-hydroxybut-2-en-1-one **280b** (3.0 g, 12 mmol), glacial acetic acid (13 mL) and H_2SO_4 (95-98 %, 0.4 mL). Work-up afforded 6-bromo-2-methylchromone **281b** as a yellow solid (1.8 g, 68 %), m.p. 119-121 ^{o}C (lit.[79] 118-120 ^{o}C); v_{max} (nujol)/cm^{-1}, 1676 (C=O); δ_H (400 MHz; CDCl$_3$) 2.38 (3H, s, CH$_3$), 6.17 (1H, s, 3-H), 7.31 (1H, d, J = 8.9 Hz, 8-H), 7.71 (1H, dd, J = 8.9 and 2.5 Hz, 7-H), and 8.30 (1H, d, J = 2.5 Hz, 5-H); δ_C (100 MHz; CDCl$_3$) 20.6 (CH$_3$), 110.6 (C-3), 118.3 (C-5), 119.8 (C-7), 124.9 (C-6), 128.3 (C-8), 136.4 (C-4a), 155.2 (C-8a), 166.5 (C-2) and 176.8 (C=O).
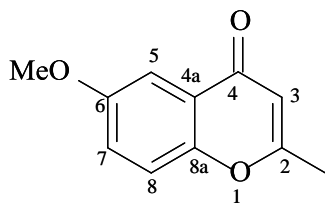
6-Methoxy-2-methylchromone 281c

The procedure employed for the synthesis of 2-methylchromone **281a** was followed, using 3-hydroxy-1-(2-hydroxy-5-methoxyphenyl)but-2-en-1-one **280c** (4.0 g, 20 mmol), glacial acetic acid (21.5 mL) and H_2SO_4 (95-98 %; 0.9 mL). Work-up afforded 6-methoxy-2-methylchromone **281c** as a yellow solid (2.6 g, 69 %), m.p. 107-108 $^{\circ}$C (lit.[79,188] 107-108 $^{\circ}$C); v_{max} (nujol)/cm^{-1} 1675 (C=O); δ_H (400 MHz; CDCl$_3$) 2.35 (3H, s, CH$_3$), 3.86 (3H, s, OCH$_3$), 6.14 (1H, s, 3-H), 7.20 (1H, m, 7-H), 7.53 (1H, d, J = 3.0 Hz, 5-H) and 7.72 (1H, d, J = 9.1 Hz, 8-H); δ_C (100 MHz; CDCl$_3$) 20.5 (CH$_3$), 55.9 (OCH$_3$), 104.9 (C-5), 109.8 (C-3), 119.1 (C-7), 123.4 (C-8), 124.1 (C-4a), 151.3 (C-6), 156.8 (C-8a), 165.9 (C-2), and 178.0 (C=O); m/z 190 (**M**$^+$, 100 %).
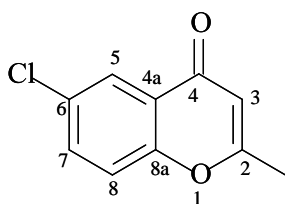
6-Chloro-2-methylchromone 281d

The procedure employed for the synthesis of 2-methylchromone **281a** was followed, using 1-(5-chloro-2-hydroxyphenyl)-3-hydroxybut-2-en-1-one **280d** (2.0 g, 9.4 mmol), glacial acetic acid (11 mL) and H_2SO_4 (95-98 %; 0.4 mL). Work-up afforded 6-chloro-2-methylchromone **281d** as a yellow solid (1.6 g, 86 %), m.p. 112-114 $^{\circ}$C (lit.[79] 112-114 $^{\circ}$C); v_{max} (nujol)/cm^{-1} 1674 (C=O); δ_H (400 MHz; CDCl$_3$) 2.38 (3H, s, CH$_3$), 6.16 (1H, s, 3-H), 7.36 (1H, d, J = 8.9 Hz, 8-H), 7.57 (1H, dd, J = 8.9 and 2.6 Hz, 7-H), and 8.12 (1H, d, J = 2.6 Hz, 5-H); δ_C (100 MHz; CDCl$_3$) 20.9 (CH$_3$), 110.5 (C-3), 119.5 (C-5), 124.5 (C-7), 125.1 (C-6), 130.9 (C-8), 133.6 (C-4a), 154.8 (C-8a), 166.5 (C-2) and 177.0 (C=O); m/z 194 (**M**$^+$, 100 %).
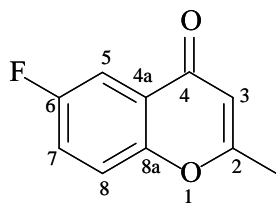
6-Fluoro-2-methylchromone 281e

The procedure employed for the synthesis of 2-methylchromone **281a** was followed, using 1-(5-fluoro-2-hydroxyphenyl)-3-hydroxybut-2-en-1-one **280e** (0.5 g, 2.6 mmol), glacial acetic acid (6.0 mL) and H_2SO_4 (95-98 %; 0.4 mL). Work-up afforded 6-fluoro-2-methylchromone **281e** as a yellow solid (0.4 g, 88 %), m.p. 101-102°C (lit.[189] 101-102°C); v_{max} (nujol)/cm^{-1} 1685 (C=O); δ_H (400 MHz; CDCl$_3$) 2.37 (3H, s, CH$_3$), 6.14 (1H, s, 3-H), 7.35-7.42 (2H, m, 5-H and 8-H), 7.78 (1H, dd, J = 8.4 and 3.3 Hz, 7-H); δ_C (100 MHz; CDCl$_3$) 20.5 (CH$_3$), 109.9 (C-3), 110.6 (C-5), 119.8 (C-7), 119.9 (C-6), 121.4 (C-8), 121.6 (C-4a), 160.6 (C-8a), 166.4 (C-2) and 177.3 (C=O); m/z 178 (**M**$^+$, 100 %).
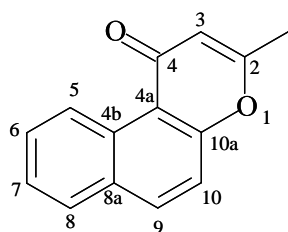
3-Methylbenzo[f]chromone 291

The procedure described for the synthesis of 2-methylchromone **281a** was followed, using 3-hydroxy-1-(2-hydroxy-1-naphthyl)but-2-en-1-one **290** (1.5 g, 6.6 mmol), glacial acetic acid (7 mL) and H_2SO_4 (95-98 %; 0.2 mL). Work-up afforded *3-methylbenzo[f]chromone* **291** as a yellow solid (0.96 g, 69.5 %), m.p. 162-165 ^{o}C; (Found **M+1**: 211.0756. C$_{14}$H$_{11}$O$_2$ requires *M*: 211.0759); v_{max} (nujol)/cm^{-1} 1676 (C=O); δ_H (400 MHz; CDCl$_3$) 2.41 (3H, s, CH$_3$), 6.31 (1H, s, 3-H), 7.45 (1H, d, J = 9.04 Hz, 8-H), 7.58 (1H, t, J = 7.48 Hz, 7-H), 7.72 (1H, t, J = 7.76 Hz, 6-H), 7.87 (1H, d, J = 8.04 Hz, 9-H), 8.03 (1H, d, J = 9.05 Hz, 10-H) and 10.02 (1H, d, J = 8.65 Hz, 5-H); δ_C (100 MHz; CDCl$_3$) 19.9 (CH$_3$), 113.4 (C-3), 116.7 (C-8a), 117.5 (C-7), 126.4 (C-6), 127.1 (C-4b), 128.1 (C-8), 129.1 (C-5), 130.5 (C-9), 135.2 (C-10), 157.7 (C-2), 160.9 (C-10a), 163.4 (C-4a) and 180.3 (C=O); m/z 211 (**M+1**, 100 %).
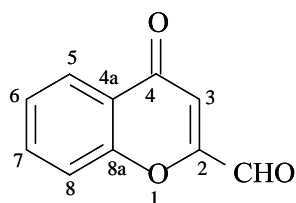
Chromone-2-carbaldehyde **222a**

A stirred mixture of 2-methylchromone **281a** (2.0 g, 11 mmol), SeO_2 (6.1 g, 31 mmol) and xylene (50 mL) was boiled under reflux for 20 h. The resulting mixture was filtered while hot to remove the black selenium, and the filtrate concentrated *in vacuo*. Flash chromatography of the residue [on silica; elution with $CHCl_3$] afforded chromone-2-carbaldehyde **222a** as a red-brown solid (1.3 g, 70 %), m.p 161-163 ^{o}C (lit.[190] 160-163 ^{o}C); v_{max} (nujol)/cm^{-1} 1700 and 1664 (2x C=O); δ_H (400 MHz; $CDCl_3$) 6.18 (1H, s, 3-H), 7.38 (1H, m, 6-H), 7.62 (1H, m, 8-H), 7.77 (1H, m, 7-H), 8.20 (1H, m, 5-H) and 9.79 (1H, s, CHO); δ_C (100 MHz; $CDCl_3$) 117.0 (C-3), 118.8 (C-8), 124.9 (C-4a), 125.9 (C-6), 126.2 (C-5), 135.2 (C-7), 155.6 (C-8a), 156.0 (C-2), 178.3 (C=O) and 185.5 (CHO); *m/z* 174 (**M^{+}**, 100 %).
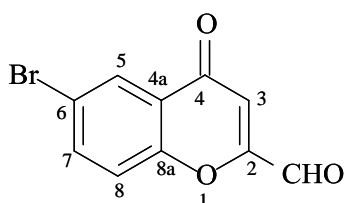
6-Bromochromone-2-carbaldehyde **222b**

The procedure described for the synthesis of chromone-2-carbaldehyde **222a** was followed using 6-bromo-2-methylchromone **281b** (2.0 g, 8.4 mmol), SeO_2 (4.6 g, 42 mmol) and xylene (30 mL). Work-up afforded 6-bromochromone-2-carbaldehyde **222b** as a yellow solid (1.0 g, 47 %), m.p. 171- 173 ^{o}C (lit.[79] 170-172 ^{o}C); v_{max} (nujol)/cm^{-1} 1705 and 1665 (2x C=O); δ_H (400 MHz; $CDCl_3$) 6.91 (1H, s, 3-H), 7.50 (1H, d, *J* = 8.9 Hz, 8-H), 7.84 (1H, dd, *J* = 8.9 and 2.5 Hz, 7-H), 8.31 (1H, d, *J* = 2.4 Hz, 5-H) and 9.78 (1H, s, CHO); δ_C (100 MHz; $CDCl_3$) 116.8 (C-3), 119.8 (C-5), 120.7 (C-7), 126.0 (C-6), 128.6 (C-8), 138.2 (C-4a), 154.4 (C-8a), 156.0 (C-2), 176.9 (C=O) and 185.0 (CHO).
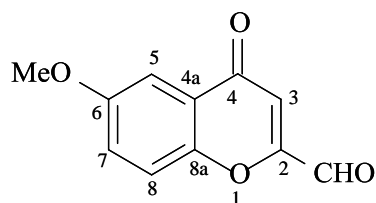
6-Methoxychromone-2-carbaldehyde 222c

The procedure described for the synthesis of chromone-2-carbaldehyde **222a** was followed using 6-methoxy-2-methylchromone **281c** (2.0 g, 11 mmol), SeO_2 (5.8 g, 53 mmol) and xylene (30 mL). Work-up afforded 6-methoxychromone-2-carbaldehyde **222c** as a yellow solid (1.4 g, 65 %), m.p. 173-175 ^{o}C (lit.[79] 174-176 ^{o}C); v_{max} (nujol)/cm^{-1} 1721 and 1675 (2x C=O); δ_H (400 MHz; CDCl$_3$) 3.91 (3H, s, OCH$_3$), 6.88 (1H, s, 3-H), 7.34 (1H, m, 8-H), 7.53-7.56 (2H, m, 5-H and 7-H), and 9.80 (1H, s, CHO); δ_C (100 MHz; CDCl$_3$) 56.0 (OCH$_3$), 104.9 (C-5), 115.8 (C-3), 120.2 (C-7), 124.5 (C-8), 125.7 (C-4a), 152.0 (C-6), 156.0 (C-8a), 157.8 (C-2), 178.1 (C=O) and 185.5 (CHO).
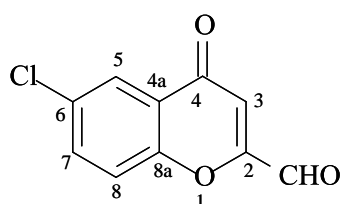
6-Chlorochromone-2-carbaldehyde 222d

The procedure described for the synthesis of chromone-2-carbaldehyde **222a** was followed using 6-chloro-2-methylchromone **281d** (2.00 g, 10.3 mmol), SeO_2 (5.70 g, 51.4 mmol) and xylene (25 mL). Work-up afforded 6-chlorochromone-2-carbaldehyde **222d** as a yellow solid (1.1 g, 51 %), m.p. 159-162 ^{o}C (lit.[79] 162-164 ^{o}C); v_{max} (nujol)/cm^{-1}, 1717 and 1674 (2x C=O); δ_H (400 MHz; CDCl$_3$) 6.90 (1H,s, 3-H), 7.57 (1H, d, J = 9.0 Hz, 8-H), 7.71 (1H, dd, J = 9.0 and 2.6 Hz, 7-H), 8.17 (1H, d, J = 2.6 Hz, 5-H) and 9.79 (1H, s, CHO); δ_C (100 MHz; CDCl$_3$) 116.6 (C-3), 120.5 (C-5), 125.3 (C-7), 125.7 (C-6), 132.3 (C-8), 135.4 (C-4a), 153.9 (C-8a), 156.0 (C-2), 177.1 (C=O) and 185.0 (CHO).
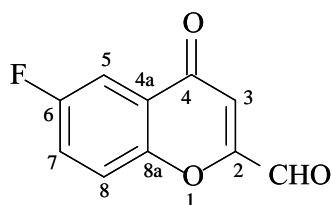
6-Fluorochromone-2-carbaldehyde 222e

The procedure described for the synthesis of chromone-2-carbaldehyde **222a** was followed using 6-fluoro-2-methylchromone **281e** (2.0 g, 11 mmol), SeO_2 (6.2 g, 56 mmol) and xylene (30 mL). Work-up afforded 6-fluorochromone-2-carbaldehyde **222e** as a yellow solid (1.1 g, 52 %), m.p 155-157 ^{o}C (lit.[79] 156-158 ^{o}C); v_{max} (nujol)/cm^{-1} 1707 and 1675 (2x C=O); δ_H (400 MHz; CDCl$_3$) 6.89 (1H,s, 3-H), 7.49 (1H, m, 7-H), 7.63 (1H, m, 8-H), 7.84 (1H, m, 5-H) and 9.79 (1H, s, CHO); δ_C (100 MHz; CDCl$_3$) 110.8 (C-3), 111.0 (C-5), 115.7 (C-7), 121.0 (C-6), 121.1 (C-8), 123.6 (C-4a), 156.1 (C-8a), 160.8 (C-2), 177.5 (C=O) and 185.1 (CHO); *m/z* 192 (**M**$^+$, 100 %).
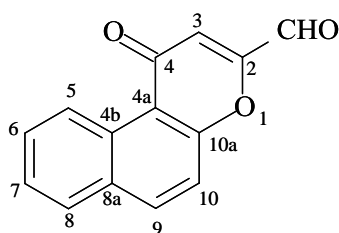
Benzo[f]chromone-3-carbaldehyde 292

The procedure described for the synthesis of chromone-2-carbaldehyde **222a** was followed using *3-methylbenzo[f]chromone* **291** (0.8 g, mmol), SeO_2 (2.0 g, 18 mmol) and xylene (12 mL). Work-up afforded *benzo[f]chromone-3-carbaldehyde* **292** as a yellow solid (0.39 g, 46 %), m.p 184-187 ^{o}C (Found **M+1**: 225.0552. C$_{14}$H$_9$O$_3$ requires *M*: 225.0552); v_{max} (nujol)/cm^{-1} 1723 and 1682 (2x C=O); δ_H (400 MHz; CDCl$_3$) 7.08 (1H, s, 3-H), 7.61 (1H, d, *J* = 9.08 Hz, 8-H), 7.68 (1H, m, 7-H), 7.80 (1H, t, *J* = 7.76 Hz, 6-H), 7.93 (1H, d, *J* = 8.14 Hz, 9-H), 8.16 (1H, d, *J* = 9.10 Hz, 10-H), 9.79 (1H, s, CHO) and 9.98 (1H, d, *J* = 6.57 Hz, 5-H); δ_C (100 MHz; CDCl$_3$) 19.9 (CH$_3$), 113.4 (C-3), 116.7 (C-8a), 117.5 (C-7), 126.4 (C-6), 127.1 (C-4b), 128.1 (C-8), 129.1 (C-5), 130.5 (C-9), 135.2 (C-10), 157.7 (C-2), 160.9 (C-10a), 163.4 (C-4a) and 180.3 (C=O); *m/z* 225 (**M**+1, 40 %), 257 (100 %).

3.3.4 Reactions of chromone-2-carbaldehydes with acrylonitrile
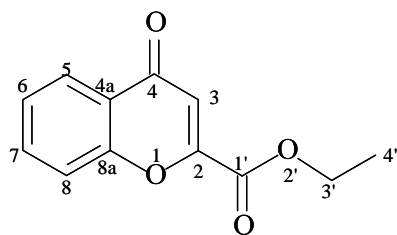
***Ethyl chromone-2-carboxylate* 293a**

Acrylonitrile (0.37 mL, 4.3 mmol) was added to a stirred solution of chromone-2-carbaldehyde **222a** (0.5 g, 3 mmol) and 3HQ (1.7 g, 14 mmol) in $CHCl_3$ (7.0 mL). The resulting mixture was stirred vigorously at room temperature for 24 h. Evaporation of the solvent *in vacuo* gave a brown, oily residue which was purified by flash chromatography [on silica; elution with hexane-EtOAc (1:2)] to afford *ethyl chromone-2-carboxylate* **293a** as a white oil (0.32 g, 50.3 %) (Found [**M+H**]$^+$: 219.0648. $C_{12}H_{10}O_4$ requires *M*: 219.0652); v_{max} (nujol)/cm^{-1} 1709 and 1658 (2x C=O); δ_H (400 MHz; $CDCl_3$) 1.42 (3H, t, *J* = 7.1 Hz, CH_3), 4.45 (2H, q, *J* = 7.1 Hz, CH_2), 7.10 (1H, s, 3-H), 7.43 (1H, t, *J* = 7.5 Hz, 6-H), 7.60 (1H, d, *J* = 8.6 Hz, 8-H), 7.73 (1H, t, *J* = 6.7 Hz, 7-H) and 8.80 (1H, d, *J* = 7.9 Hz, 5-H); δ_C (100 MHz; $CDCl_3$) 14.1 (C-4'), 63.0 (C-3'), 114.8 (C-3), 118.8 (C-5), 124.4 (C-7), 125.7 (C-6), 125.9 (C-4a), 134.7 (C-8), 152.2 (C-8a), 156.0 (C-2) and 160.5 and 178.4 (2x C=O); *m/z* 219 [(**M+H**)$^+$ 100 %].
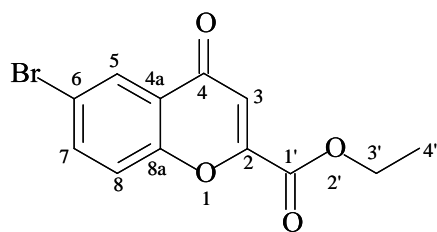
***Ethyl 6-bromochromone-2-carboxylate* 293b**

The experimental procedure employed for the synthesis of ethyl chromone-2-carboxylate **293a** was followed using 6-bromochromone-2-carbaldehyde **222b** (0.7 g, 3 mmol), acrylonitrile (0.37 mL, 4.3 mmol), 3-hydroxyquinuclidine (1.7 g, 14 mmol) and $CHCl_3$ (7.0 mL). Work-up and flash chromatography afforded ethyl 6-bromochromone-2-carboxylate **293b** as yellow oil (0.34 g, 40 %); [Found (**M+H**)$^+$: 296.9679. $C_{12}H_9{}^{79}BrO_4$ requires *M*: 296.9757]; v_{max} (nujol)/cm^{-1} 1709 and 1653 (2xC=O); δ_H (400 MHz; $CDCl_3$) 1.45 (3H, t, *J* = 7.1 Hz, CH_3), 4.49 (2H, q, *J* = 7.1 Hz, CH_2), 7.14 (1H, s, 3-H), 7.51 (1H, d, *J* = 8.9 Hz, 8-H), 7.82 (1H, dd, *J* = 8.9 and 2.5 Hz, 7-H) and 8.33 (1H, d, *J* = 2.4 Hz, 5-H); δ_C (100 MHz;

CDCl$_3$) 14.1 (CH$_3$), 63.2 (CH$_2$), 114.8 (C-3), 119.5 (C-5), 120.7 (C-8), 128.4 (C-4a), 129.4 (C-7), 137.7 (C-6), 152.4 (C-8a), 154.7 (C-2) and 163.9 and 177.0 (2x C=O); *m/z* 297 [(**M+H**)$^+$ 100 %].
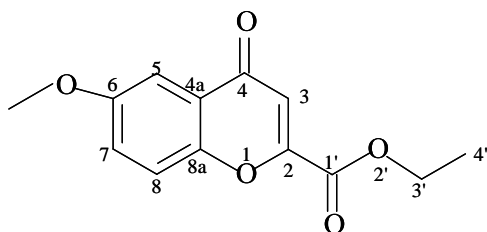
Ethyl 6-methoxychromone-2-carboxylate 293c

The procedure described for the synthesis of ethyl chromone-2-carboxylate **293a** was followed using 6-methoxychromone-2-carbaldehyde **222c** (0.59 g, 2.9 mmol), acrylonitrile (0.37 mL, 4.3 mmol) and 3-hydroxyquinuclidine (1.7 g, 14 mmol) in CHCl$_3$ (7.0 mL). Evaporation of the solvent *in vacuo* gave a brown oily residue which was purified by flash chromatography [on silica; elution with hexane-EtOAc (1:2)] to afford *ethyl 6-methoxychromone-2-carboxylate* **293c** as an orange oil (0.33 g, 46 %), which slowly crystallised.

Note: When this reaction was repeated using DABCO (1.6 g, 14 mmol) as catalyst and EtOH (7.0 mL) as solvent, the same product was obtained as orange crystals in 26 % yield after 4 days, m.p. 77-79 °C [Found (**M+H**)$^+$: 249.0771. C$_{13}$H$_{13}$O$_5$ requires, *M*: 249.0763]; v_{max} (nujol)/cm^{-1} 1715 and 1638 (2x C=O); δ_H (400 MHz; CDCl$_3$) 1.43 (3H, t, *J* = 7.1 Hz, CH$_3$), 3.89 (3H, s, OCH$_3$), 4.45 (2H, q, *J* = 7.1 Hz, CH$_2$), 7.09 (1H, s, 3-H), 7.46 (1H, dd, *J* = 9.1 and 3.2 Hz, 7-H) and 7.53-7.55 (2H, m, 5-H and 8-H); δ_C (100 MHz; CDCl$_3$) 14.1 (CH$_3$), 56.0 (OCH$_3$), 62.9 (CH$_2$), 104.6 (C-5), 113.8 (C-3), 120.2 (C-8), 125.0 (C-7), 125.2 (C-4a), 150.8 (C-8a), 151.9 (C-2), 157.5 (C-6) and 160.6 and 178.3 (2x C=O); *m/z* 249 [(**M+H**)$^+$ 100 %].
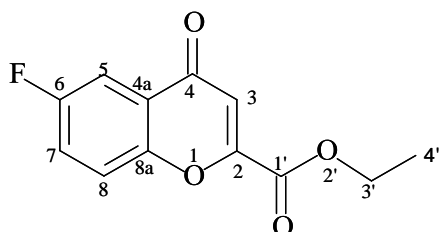
Ethyl 6-fluorochromone-2-carboxylate 293e

The procedure described for the synthesis of ethyl chromone-2-carboxylate **293a** was followed using 6-fluorochromone-2-carbaldehyde **222e** (0.56 g, 2.9 mmol), acrylonitrile

(0.37 mL, 4.3 mmol) and 3-hydroxyquinuclidine (1.7 g, 14 mmol) in $CHCl_3$ (7.0 mL). Evaporation of the solvent *in vacuo* gave a brown residue which was purified by flash chromatography [on silica; elution with hexane-EtOAc (1:2)] to afford *ethyl 6-fluorochromone-2-carboxylate* **293e** as an orange solid (0.29 g, 42 %), m.p. 178-182 $^{\circ}$C [Found (**M+H**)$^+$: 237.0564. $C_{12}H_9O_4F$ requires *M*: 237.0558]; ν_{max} (nujol)/cm^{-1} 1728 and 1652 (2x C=O); δ_H (400 MHz; $CDCl_3$) 1.43 (3H, t, *J* = 7.1 Hz, CH_3), 4.46 (2H, q, *J* = 7.1 Hz, CH_2), 7.10 (1H, s, 3-H), 7.46 (1H, ddd, *J* = 9.2, 7.6 and 3.1 Hz, 7-H), 7.63 (1H, dd, *J* = 9.2 and 4.2 Hz, 8-H) and 7.83 (1H, dd, *J* = 8.0 and 3.1 Hz, 5-H); δ_C (100 MHz; $CDCl_3$) 14.1 (CH_3), 63.1 (CH_2), 110.5 (C-3), 110.8 (C-5), 113.9 (C-8), 120.9 (C-4a), 121.9 (C-7), 123.2 (C-6), 152.2 (C-8a), 152.4 (C-2), 160.3 and 177.7 (2x C=O); *m/z* 237 [(**M+H**)$^+$ 100 %].

Notes:

i) When this reaction was repeated using DABCO (1.6 g, 14 mmol) as catalyst and EtOH (7.0 mL) as solvent, ethyl 6-fluorochromone-2-carboxylate **293e** was obtained as an orange solid (0.15 g, 22 %) after 6 days.

ii) When TMPDA (2.3 mL, 14 mmol) was used as catalyst in EtOH (7.0 mL), ethyl 6-fluorochromone-2-carboxylate **293e** was obtained in low yield (0.11 g, 16 %), after 6 days with some starting material still present.

iii) When DBU was used as catalyst in EtOH, no product was observed.
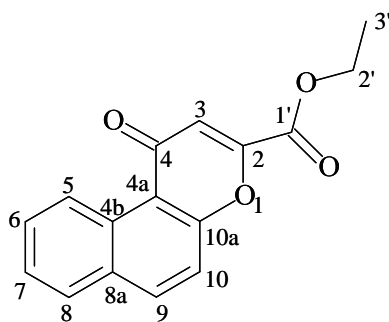
Ethyl benzo[f]chromone-3-carboxylate 294

The experimental procedure employed for the synthesis of ethyl chromone-2-carboxylate **293a** was followed using benzo[f]chromone-3-carbaldehyde **292** (0.43 g, 1.9 mmol), acrylonitrile (0.26 mL, 3.0 mmol), 3-hydroxyquinuclidine (0.70 g, 5.8 mmol) and $CHCl_3$ (5.0 mL). Work-up and flash chromatography afforded *ethyl benzo[f]chromone-3-carboxylate* **294** as a yellow crystalline solid (0.26 g, 51 %), m.p. 117-121 $^{\circ}$C [Found (**M+H**)$^+$: 269.0819. $C_{16}H_{12}O_4$ requires *M*: 269.0808]; ν_{max} (nujol)/cm^{-1} 1729 and 1643 (2x C=O); δ_H (400 MHz; $CDCl_3$) 1.44 (3H, t, *J* = 7.14 Hz, CH_3), 4.48 (2H, q, *J* = 7.14 Hz, CH_2), 7.26 (1H, s, 3-H),

7.63-7.67 (2H, m, 7-H and 9-H), 7.76 (1H, m, 10-H), 7.92 (1H, d, J = 7.99 Hz, 8-H), 8.14 (1H, d, J = 9.10 Hz, 6-H) and 9.98 (1H, d, J = 8.56 Hz, 5-H); δ_C (100 MHz; CDCl$_3$) 14.1 (CH$_3$), 62.9 (CH$_2$), 117.7 (C-3), 117.8 (C-4a), 126.9 (C-10), 127.2 (C-7), 128.3 (C-9), 128.7 (C-8), 129.7 (C-8a), 130.1 (C-4b), 130.7 (C-6), 136.5 (C-5), 149.9 (C-10a), 157.5 (C-2) and 160.5 and 179.9 (2x C=O); m/z 269 [(**M+H**)$^+$) 100 %].

3.3.5 Reactions of chromone-2-carbaldehydes with methyl acrylate
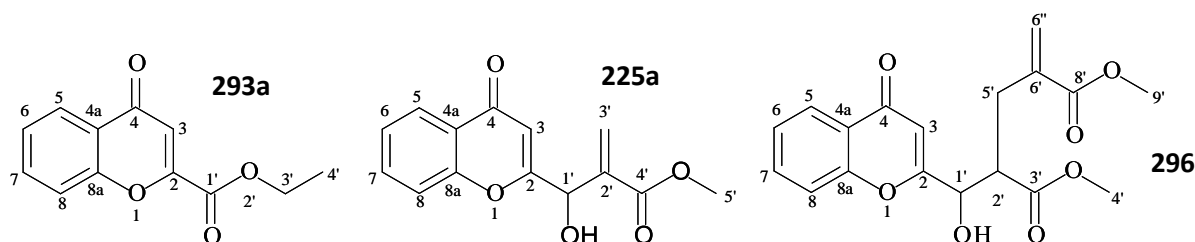
***Ethyl chromone-2-carboxylate* 293a**, ***methyl 3-(chromone-2-yl)-3-hydroxy-2-methylenepropanoate* 225a** and ***dimethyl 2-[hydroxy(4-oxochromen-2-yl)methyl]-4-methylenepentanedioate* 296**

Methyl acrylate (0.19 mL, 2.2 mmol) was added to a stirred solution of chromone-2-carbaldehyde **222a** (0.26 g, 1.5 mmol), and 3HQ (0.88 g, 7.3 mmol) in CHCl$_3$ (4.0 mL). The resulting mixture was stirred vigorously at room temperature for 24 h. Evaporation of the solvent *in vacuo* gave a brown, oily residue, which was purified by flash chromatography [on silica; elution with hexane:EtOAc (2:1)], followed by HPLC [hexane-EtOAc (3:1)] to afford three fractions.

Fraction 1. Ethyl chromone-2-carboxylate **293a** as a yellow crystalline solid (0.06 g, 18 %)

Fraction 2. *Methyl 3-(chromone-2-yl)-3-hydroxy-2-methylenepropanoate* **225a** as a yellow oil (0.11 g, 28 %), v_{max} (neat)/cm^{-1} 3471 (OH), 1729 and 1643 (2x C=O); δ_H (400 MHz; CDCl$_3$) 3.74 (3H, s, OCH$_3$), 5.52 (1H, s, 1'-H), 5.85 and 6.39 (2H, 2 x s, 2''-CH$_2$), 7.23 (1H, s, 3-H), 7.35 (2H, d, J = 5.12 Hz, 5-H and 6-H) and 8.58 (2H, d, J = 4.96 Hz, 7-H and 8-H); δ_C (100MHz; CDCl$_3$) 52.1 (OCH$_3$), 74.8 (C-1'), 110.0 (C-3), 115.9 (C-8), 123.4 (C-6), 123.7 (C-3'), 124.2 (C-4a), 126.1 (C-5), 135.1 (C-7), 144.2 (C-2'), 157.0 (C-8a), 167.5 (C-2), 170.5 and 178.2 (2x C=O).

Fraction 3. *Dimethyl 2-[hydroxy(chromon-2-yl)methyl]-4-methylenepentanedioate* **296** as a yellow oil (0.10 g, 19 %), Spectroscopic data for the *syn*-diastereomer: v_{max} (neat)/cm^{-1}, 3488 (OH), 1711, 1707 and 1652 (3 x C=O); δ_H (400 MHz; CDCl$_3$) 2.46-2.60 (2H, m, 5'-CH$_2$),

3.38 (1H, m, 2'-H), 3.74 and 3.85 (6H, 2x s, 4' and 9'-CH$_3$), 3.92 (1H, br s, OH), 4.56 (1H, d, C*H*OH), 5.79 and 5.99 (2H, 2x s, 6''-CH$_2$), 6.48 (1H, s, 3-H), 7.34-7.42 (2H, m, 6-H and 8-H), 7.64 (1H, t, *J* = 7.8 Hz, 7-H) and 8.15 (1H, m, 5-H); δ$_C$ (100 MHz; CDCl$_3$) 28.7 (C-5'), 38.2 (C-2'), 52.2 (C-4'), 52.3 (C-9'), 74.7 (C-1'), 109.4 (C-3), 116.2 (C-8), 122.3 (C-6''), 123.4 (C-6), 123.9 (C-4a), 125.5 (C-5), 135.2 (C-7), 136.1 (C-6'), 157.2 (C-8a), 167.2 (C-2) and 171.0, 189.3 and 191.0 (3x C=O).

***Methyl 2-(6-methoxychroman-2-yl)propanoate* 226** and ***Ethyl 6-methoxychromone-2-carboxylate* 293c**

The procedure described above was followed using methyl acrylate (0.19 mL, 2.2 mmol), 6-methoxychromone-2-carbaldehyde (0.30 g, 1.5 mmol), and 3-hydroxyquinuclidine (0.88 g, 7.3 mmol) in CHCl$_3$ (4.0 mL). Work up and flash chromatography gave two fractions:

Fraction 1: Ethyl 6-methoxychromone-2-carboxylate **293c** as an orange solid (0.04 g, 11 %).

Fraction 2: *Methyl 2-(6-methoxychromon-2-yl)propanoate* **226** as a pale yellow oil (0.12 g, 26 %), ν$_{max}$ (neat)/cm^{-1} 1674 and 1649 (2 x C=O); δ$_H$ (400 MHz; CDCl$_3$) 1.52 (3H, d, *J* = 7.1 Hz, *CH$_3$*CH), 3.71 (3H, s, ArOCH$_3$), 3.90 (3H, s, CO.OCH$_3$), 4.31 (1H, q, *J* = 7.1 Hz, 1'-H), 7.01 (1H, s, 3-H), 7.32 (1H, dd, *J* = 9.2 and 3.1 Hz, 7-H), 7.44 (1H, d, *J* = 9.2 Hz, 8-H) and 7.55 (1H, d, *J* = 3.1 Hz, 5-H); δ$_C$ (100 MHz; CDCl$_3$) 12.6 (*C*H$_3$CH), 48.0 (CH$_3$*C*H), 52.8 (ArO*C*H$_3$), 56.0 (CO.O*C*H$_3$), 104.9 (C-3), 111.1 (C-8), 119.8 (C-5), 125.1 (C-4a), 150.1 (C-7), 155.6 (C-6), 157.8 (C-8a), 170.3 (C-2), 178.3 (2'-C=O) and 190.4 (4-C=O).

Note: When the bromo- and chloro-substituted chromone-2-carbaldehydes (**222b** and **222d**, respectively) were used, the crude mixtures appeared to show the presence of more than one product; however, separation of these products proved difficult. The signals corresponding to the ester derivatives obtained earlier, in reactions with acrylonitrile, were also present.

3.4 Synthesis of coumarin derivatives

3.4.1 Synthesis of Morita-Baylis-Hillman adducts from reactions of salicylaldehydes with *tert*-butyl acrylate
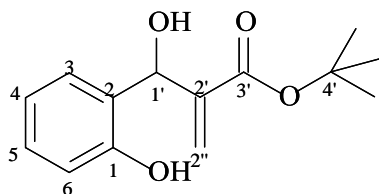
tert-*Butyl 3-hydroxy-3-(2-hydroxyphenyl)-2-methylenepropanoate* 83a

A mixture of salicylaldehyde **72a** (10 mL, 82 mmol), *tert*-butyl acrylate (10.5 mL, 115 mmol) and DABCO (6.5 g, 59 mmol) in CHCl$_3$ (15 mL) was stirred in a stoppered reaction flask for 15 days. The mixture was concentrated *in vacuo* to give a dark brown oil, which was purified using flash chromatography [on silica gel; elution with hexane-EtOAc (9:1)] to afford *tert*-butyl 3-hydroxy-3-(2-hydroxyphenyl)-2-methylenepropanoate **83a** as a white powder (4.9 g, 26 %); m.p. 107-109 $^{\circ}$C (lit.[86] 107-111 $^{\circ}$C); ν_{max} (neat)/cm^{-1} 3445 (OH) and 1722 (C=O); δ_H (400 MHz; CDCl$_3$) 1.50 (9H, s, Bu^t), 4.35 (1H, s, OH), 5.50 and 6.23 (2H, 2x s, CH$_2$), 5.69 (1H, s, C*H*OH), 6.81-7.21 (4H, series of multiplets, Ar-H) and 8.12 (1H, s, ArOH); δ_C (100 MHz; CDCl$_3$) 28.0 [C(*C*H$_3$)$_3$], 73.6 (CHOH), 82.6 (C-4'), 117.5, 119.8, 124.1, 124.2, 127.8, 129.5, 140.9 and 155.9 (C=CH$_2$ and Ar-C) and 166.7 (C=O).
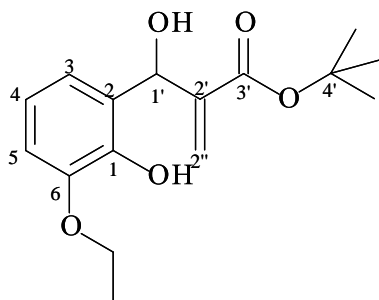
tert-*Butyl 3-hydroxy-3-(3-ethoxy-2-hydroxyphenyl)-2-methylenepropanoate* 83c

The procedure described for the synthesis of *tert*-butyl 3-hydroxy-3-(2-hydroxyphenyl)-2-methylenepropanoate **83a** was followed, using 3-ethoxysalicylaldehyde **72c** (5.0 g, 30 mmol), *tert*-butyl acrylate (6.25 mL, 68 mmol) and DABCO (2.15 g, 20.2 mmol) in CHCl$_3$ (7.5 mL). Work-up and chromatography [on silica gel; elution with EtOAc-hexane (1:8)] afforded *tert*-butyl 3-hydroxy-3-(3-ethoxy-2-hydroxyphenyl)-2-methylenepropanoate **83c** as a pale yellow oil (1.9 g, 21 %); ν_{max} (neat)/cm^{-1} 3491 (OH) and 1717 (C=O); δ_H (400 MHz; CDCl$_3$) 1.41 [12H, overlapping s and t, C(CH$_3$)$_3$ and CH$_2$C*H*$_3$], 3.60 (1H, d, *J* = 5.6 Hz, CHO*H*), 4.07 (2H,

q, *J* = 6.9 Hz, OCH$_2$), 5.66 and 6.22 (2H, 2 x s, C=CH$_2$), 5.81 (1H, d, *J* = 5.2 Hz, C*H*OH), 6.43 (1H, s, ArOH) and 6.78-6.84 (3H, series of overlapping signals, Ar-H); δ$_C$ (100 MHz; CDCl$_3$) 14.9 (CH$_2$*C*H$_3$), 28.0 [C(*C*H$_3$)$_3$], 64.6 (OCH$_2$), 69.4 (CHOH), 81.6 [*C*(CH$_3$)$_3$], 111.4, 119.5, 119.6, 125.1, 126.6, 142.2, 143.7 and 146.1(C=CH$_2$ and Ar-C) and 166.1 (C=O).
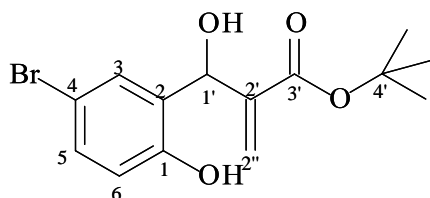
tert-*Butyl 3-(5-bromo-2-hydroxyphenyl)-3-hydroxy-2-methylenepropanoate* 83e

The procedure described for the synthesis of *tert*-butyl 3-hydroxy-3-(2-hydroxyphenyl)-2-methylenepropanoate **83a** was followed using 5-bromosalicyladehyde **72e** (5.0 g, 25 mmol), *tert*-butyl acrylate (5.3 mL, 57 mmol) and DABCO (2.15 g, 20.2 mmol) in CHCl$_3$ (7.5 mL) and stirring for 4 days. The reaction mixture was filtered through a layer of silica gel. Crystallization from CHCl$_3$ afforded *tert*-butyl 3-(5-bromo-2-hydroxyphenyl)-3-hydroxy-2-methylenepropanoate **83e** as white crystals (4.6 g, 56 %), m.p. 186-188 °C (lit.[19] 186-188 °C); *v*$_{max}$ (neat)/cm^{-1} 3324 (OH) and 1675 (C=O); δ$_H$ (400 MHz; DMSO-*d$_6$*) 1.32 (9H, s, Bu^t), 5.48 (1H, br s, OH), 5.65 and 6.05 (2H, 2 x s, C=CH$_2$), 5.66 (1H, s, C*H*OH), 6.74 (1H, d, *J* = 8.4Hz, Ar-H), 7.19 -7.22 (2H, m, Ar-H) and 9.70 (1H, br, ArOH); δ$_C$(100 MHz; DMSO-*d$_6$*) 27.4 [C(*C*H$_3$)$_3$], 64.5 (CHOH), 80.0 [*C*(CH$_3$)$_3$], 109.6, 117.1, 122.8, 129.7, 130.3, 131.8, 144.8 and 153.7 (C=CH$_2$ and Ar-C) and 164.9 (C=O).

3.4.2 Cyclisation of MBH adducts using hydrochloric acid
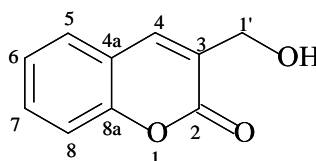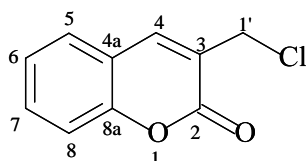
3-(Chloromethyl)coumarin **82a** and *3-(hydroxymethyl)coumarin* **301a**[31]

Conc. HCl (4 mL) was added to a solution of methyl 3-(2-benzyloxyphenyl)-3-hydroxy-2-methylenepropanoate **83a** (0.53 g, 2 mmol) in AcOH (2 mL). The mixture was boiled under reflux for 2 h, allowed to cool to room temperature and then poured into ice-cold water (20 mL). Stirring for *ca*. 30 min gave a precipitate, which was filtered off. The crude product was

then purified using flash chromatography [on silica; elution with hexane-EtOAc (2:1)] to afford two fractions.

Fraction 1. 3-(Chloromethyl)coumarin **82a** as a white solid (0.27 g, 66 %), m.p. 108-110 $^{\circ}$C (lit.[19,86] 108-110 $^{\circ}$C); v_{max} (neat)/cm^{-1} 1703 (C=O); δ_H (400 MHz; CDCl$_3$) 4.55 (2H, s, CH$_2$Cl), 7.28-7.55 (4H, series of multiplets, Ar-H) and 7.88 (1H, s, 4-H); δ_C (100 MHz; CDCl$_3$) 41.0 (CH$_2$), 116.7, 118.8, 124.7, 125.1, 128.0, 132.0, 141.1 and 159.6 (Ar-C) and 160.0 (C=O).

Fraction 2: 3-(Hydroxymethyl)coumarin **301a** as a cream solid (0.03 g, 8 %), m.p. 112-114 $^{\circ}$C (lit.[31] cited without m.p.); v_{max} (neat)/cm^{-1} 3342 (OH) and 1723 (C=O); δ_H (400 MHz; CDCl$_3$) 4.62 (2H, d, J = 5.52 Hz, CH_2OH), 7.29-7.51 (4H, series of multiplets, Ar-H) and 7.74 (1H, s, 4-H); δ_C (100 MHz; CDCl$_3$) 61.2 (CH$_2$), 116.7, 118.8, 124.6, 127.8, 127.9, 131.2, 138.6 and 158.3 (Ar-C) and 161.0 (C=O).
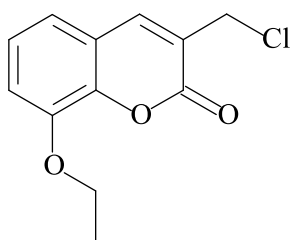
3-(Chloromethyl)-8-ethoxycoumarin 82c

The procedure described for the synthesis of 3-(chloromethyl)coumarin **82a** was followed, using conc. HCl (10 mL) and a solution of *tert*-butyl 3-(8-ethoxy-2-hydroxyphenyl)-3-hydroxy-2-methylenepropanoate **83c** (0.55 g, 2 mmol) in AcOH (5 mL). Work-up afforded, as a pale pink solid, 3-(chloromethyl)-8-ethoxycoumarin **82c** (0.33 g, 74 %), m.p. 122-124 $^{\circ}$C (lit.[86] 122-125 $^{\circ}$C); v_{max} (neat)/cm^{-1} 1717 (C=O); δ_H (400 MHz; CDCl$_3$) 1.46 (3H, t, J = 7Hz, CH$_2$CH_3), 4.14 (2H, q, J = 7 Hz, OCH_2CH$_3$), 4.53 (2H, s, CH$_2$Cl), 7.05-7.07 (2H, m, Ar-H), 7.17 (1H, t, J = 8 Hz Ar-H) and 7.83 (1H,s, 4-H); δ_C (100 MHz; CDCl$_3$) 14.7 (CH$_2$CH_3), 41.0 (CH$_2$Cl), 65.0 (OCH_2CH$_3$), 115.2, 119.3, 119.5, 124.5, 125.1, 141.3, 143.4 and 146.5 (Ar-C) and 159.7 (C=O).
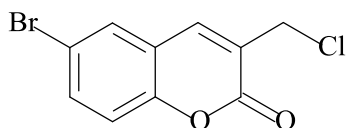
6-Bromo-3-(chloromethyl)coumarin **82e**

The procedure described for the synthesis of 3-(chloromethyl)coumarin **82a** was followed, using conc. HCl (10 mL) and a solution of *tert*-butyl 3-(5-bromo-2-hydroxyphenyl)-3-hydroxy-2-methylenepropanoate **83e** (1.5 g, 4.6 mmol) in AcOH (6 mL). Work-up afforded 6-bromo-3-(chloromethyl)coumarin **82e** as a pale brown solid (1.2g, 95%), m.p. 113-115 ^{o}C (lit.[86] 113-115 ^{o}C); v_{max} (neat)/cm^{-1} 1723 (C=O); δ_{H} (400 MHz; CDCl$_3$) 4.53 (2H, s, CH$_2$Cl), 7.21 (1H, m, Ar-H), 7.61-7.65 (2H, m, Ar-H) and 7.80 (1H, s, 4-H); δ_{C} (100 MHz; CDCl$_3$) 40.7 (CH$_2$), 117.2, 118.3, 120.24, 126.2, 130.2, 134.6, 139.5, and 152.3 (Ar-C) and 159.3 (C=O).

3.4.3 Cyclisation of Morita-Baylis-Hillman adducts using hydroiodic acid
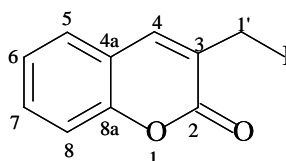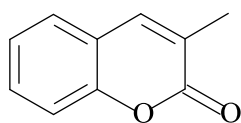
3-Methylcoumarin **75a** and *3-(iodomethyl)coumarin* **81a**

Conc. HI (10 mL) was added to a solution of methyl 3-(2-benzyloxyphenyl)-3-hydroxy-2-methylenepropanoate **83a** (0.5 g, 2 mmol) in a mixture of AcOH (5 mL) and Ac$_2$O (5 mL). The mixture was heated at 120 ^{o}C for 2 h, and allowed to cool to room temperature and then poured into ice cold water (10 mL). Stirring for *ca*. 30 min gave a precipitate, which was filtered off and washed with hexane. Purification of the precipitate using flash chromatography [elution with hexane-EtOAc (1:5)] afforded two fractions.

Fraction 1. 3-(Iodomethyl)coumarin **81a** as a grey solid (0.3 g, 52 %), m.p. 151-153 ^{o}C (lit.[191] 150-152 ^{o}C); v_{max} (neat)/cm^{-1} 1710 (C=O); δ_{H} (400 MHz; CDCl$_3$) 4.35 (2H, s, CH$_2$I), 7.28-7.53 (4H, series of overlapping multiplets, Ar-H) and 7.84 (1H, s, 4-H); δ_{C} (100 MHz; CDCl$_3$) −1.6 (CH$_2$I), 116.8, 119.1, 124.7, 127.2, 127.8, 131.9,140.3 and 153.5 (Ar -C) and 159.8 (C=O).

Fraction 2. 3-Methylcoumarin **75a** as a pale grey solid (0.12 g, 38 %), m.p, 91-94 (lit.[192] 92-94 ^{o}C); v_{max} (neat)/cm^{-1} 1685 (C=O); δ_{H} (400 MHz; CDCl$_3$) 2.21 (3H, s, CH$_3$), 7.23 (1H, d, *J*

= 7.47 Hz, 5-H), 7.30 (1H, d, *J* = 8.24 Hz, 8-H), 7.39-7.47 (2H, overlapping multiplets, 6-H and 7-H), 7.50 (1H, s, 4-H); δ_C (100 MHz; CDCl$_3$) 17.1 (CH$_3$), 116.5 (C-4), 119.6 (C-3), 124.2 (C-5), 125.9 (C-4a), 126.9 (C-6), 130.4 (C-7), 139.1 (C-8), 153.3 (C-8a) and 162.2 (C=O).

Note:

When the reflux was carried out at 140 °C (oil bath), the 3-methylcoumarin **75a** was isolated exclusively. Decreasing the reflux time to 30 mins at 140 °C still gave the 3-methylcoumarin **75a** and none of the desired 3-(iodomethyl)coumarin. When the temperature was decreased to 70 °C both **75a** and **81a** were isolated. Lowering the reaction temperature to 35 °C still gave a mixture of the two products. Use of AcOH alone as solvent also gave a mixture of products.
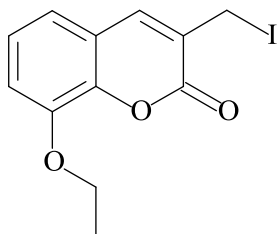
8-Ethoxy-3-(iodomethyl)coumarin 81c

The procedure described for the synthesis of 3-(iodomethyl)coumarin **81a** was followed, using conc. HI (10 mL) and *tert*-butyl 3-ethoxy-3(-2-hydroxyphenyl)-3-hydroxy-2-methylenepropanoate **83c** (0.6 g, 2 mmol) in a mixture of AcOH (5 mL) and Ac$_2$O (5 mL). Work-up afforded 3-(iodomethyl)-8-ethoxycoumarin **81c** as a pale yellow solid (0.37 g, 54 %), m.p. 119-121 °C (lit.[86] 120-123 °C); ν_{max} (neat)/cm^{-1} 1721 (C=O); δ_H (400 MHz; CDCl$_3$) 1.46 (3H, t, *J* = 6.8 Hz, CH$_2$C*H*$_3$), 4.14 (2H, q, *J* = 7.0 Hz, OC*H*$_2$CH$_3$), 4.36 (2H, s, CH$_2$I), 7.01-7.07 (2H, overlapping multiplets, Ar-H), 7.15 (1H, t, *J* = 7.94 Hz, Ar-H) and 7.80 (1H, s, 4-H); δ_C (100MHz; CDCl$_3$) -1.5 (CH$_2$I), 14.7 (CH$_2$*C*H$_3$), 65.1 (O*C*H$_2$CH$_3$), 115.1, 119.1, 119.9, 124.6, 127.4, 140.7, 143.4 and 146.6 (Ar-C) and 159.4 (C=O).
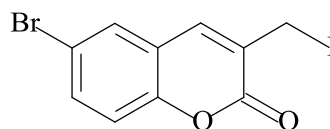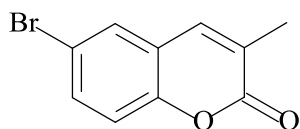
6-Bromo-3-methylcoumarin 75e and 6-bromo-3-(iodomethyl)coumarin 81e

The procedure described for the synthesis of 3-iodomethyl)coumarin **81a** was followed using conc. HI (10 mL), *tert*-butyl 3-(5-bromo-2-hydroxyphenyl)-2-methylenepropanoate **83e** (0.61

g, 1.9 mmol) in a mixture of AcOH (5 mL) and Ac$_2$O (5 mL). Work-up and flash chromatography [on silica; elution with hexane-EtOAc (1:5)] gave two fractions.

Fraction 1. 6-Bromo-3-(iodomethyl)coumarin **81e** as a grey solid (0.36 g, 52 %), m.p. 146-148 ^{o}C (lit.[86] 148-150 ^{o}C); v_{max} (neat)/cm^{-1} 1724 (C=O); δ_H (400 MHz; CDCl$_3$) 4.40 (2H, s, CH$_2$I), 7.27 (1H, s, Ar-H); 7.47-7.66 (2H, series of overlapping signals, Ar-H) and 7.80 (1H, s, 4-H); δ_C (100 MHz; CDCl$_3$) −2.2 (CH$_2$I), 117.3, 118.5, 120.6, 128.6, 130.0, 134.5, 139.9 and 152.3 (Ar-C) and 159.1 (C=O).

Faction 2: 6-Bromo-3-methylcoumarin **75e** as a grey solid (0.19 g, 42 %), m.p. 153-155 ^{o}C (lit.[86] 154-156 ^{o}C); v_{max} (neat)/cm^{-1} 1727 (C=O); δ_H (400 MHz; CDCl$_3$) 2.21 (3H, s, CH$_3$), 7.17 (1H, m, Ar-H), 7.53 (2H, m, Ar-H) and 7.51 (1H, s, 4-H); δ_C (100 MHz; CDCl$_3$) 17.3 (CH$_3$), 116.8, 118.2, 121.1, 127.2, 129.2, 133.2, 137.8 and 152.0 (Ar-C) and 161.5 (C=O).

3.4.4 Michaelis-Arbuzov reactions of 3-chloromethyl coumarins
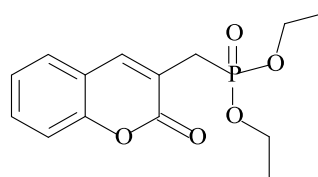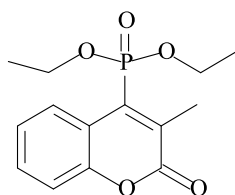
*Diethyl (3-methyl-2-oxo-2H-chromen-4-yl)phosphonate **227a** and diethyl [(2-oxo-2H-chromen-3-yl)methyl]phosphonate **228a**[86,121]*

To 3-(chloromethyl)coumarin **82a** (0.82 g, 4.2 mmol) was added triethyl phosphite (1.4 mL) and the mixture was refluxed under nitrogen for 4 hours. Upon completion of the reaction, as monitored by TLC, the mixture was flash chromatographed [on silica; elution with EtOAc-hexane (3:1)] to afford two fractions.

Fraction 1. Diethyl (3-methyl-2-oxo-2*H*-chromen-4-yl)phosphonate **227a** as a pale yellow solid (0.24 g, 19 %), m.p. 49-51 ^{o}C (lit.[86] 47-49 ^{o}C); v_{max} (neat)/cm^{-1} 1729 (C=O) and 1245 (P=O); δ_H (400 MHz; CDCl$_3$) 1.32 (6H, t, J = 7 Hz, 2x CH$_2$C*H$_3$*), 2.59 (3H, d, J = 3.2 Hz, CH$_3$), 4.13 and 4.25 (4H, 2 x m, 2 x CH$_2$OP), 7.25-7.28 (2H, m, Ar-H), 7.44 (1H, t, J = 8.4 Hz, Ar-H) and 8.46 (1H, dd, J = 8.21 and 1.05 Hz, Ar-H); δ_C (100 MHz; CDCl$_3$) 14.7 (OCH$_2$C*H$_3$*), 16.2 (Ar-CH$_3$), 16.3 (d, $J_{P,C}$ = 6.1 Hz, 2x CH$_2$CH$_3$), 62.8 (d, $J_{P,C}$ = 5.5 Hz, 2x CH$_2$OP), 116.7, 118.2, 124.2, 128.0, 137.4 and 152.0 (Ar-C), 135.6 (d, $J_{P,C}$ = 12 Hz, C-4) and 161.1 (C=O).

Fraction 2: Diethyl [(2-oxo-2*H*-chromen-3-yl)methyl]phosphonate **228a** as a pale brown oil (0.55 g, 44 %); v_{max}(neat)/cm^{-1} 1734 (C=O) and 1240 (P=O); δ_H (400 MHz; CDCl$_3$) 1.27 (6H, t, *J* = 7.0 Hz, 2 x OCH$_2$C*H$_3$*), 3.16 (2H, d, $J_{P,H}$ = 22 Hz, CH$_2$P), 4.09 (4H, q, *J* = 4.3 Hz, 2x CH$_2$OP), 7.21-7.48 (4H, series of multiplets, Ar-H) and 7.80 (1H, d, $J_{P,C}$ = 4.4 Hz, 4-H); δ_C (100 MHz;CDCl$_3$) 16.3 (d, $J_{P,C}$ = 6.2 Hz, 2x OCH$_2$C*H$_3$*), 26.7 (d, $J_{P,C}$ = 139 Hz, CH$_2$P), 62.4 (d, $J_{P,C}$ = 6.6 Hz, 2x CH$_2$OP), 116.4, 119.1, 120.2, 124.4, 127.6, 131.2, 141.7 and 153.2 (Ar-C) and 161.1 (C=O).
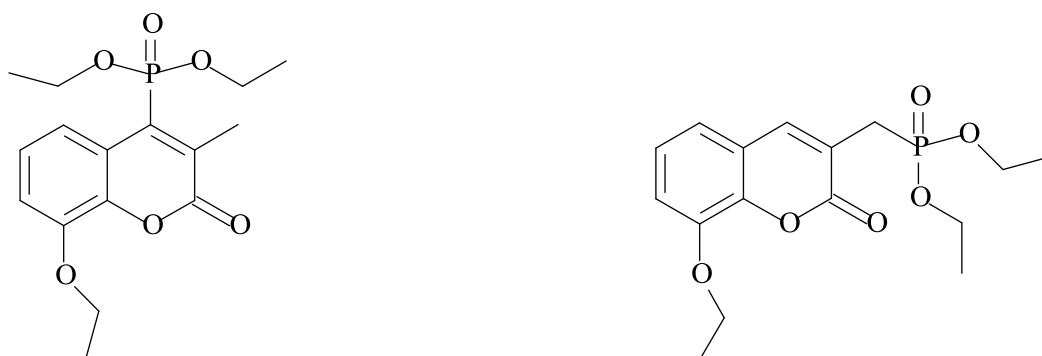
***Diethyl (8-ethoxy-3-methyl-2-oxo-2H-chromen-4-yl)phosphonate* 227c** and ***diethyl [(8-ethoxy-2-oxo-2H-chromen-3-yl)methyl]phosphonate* 228c**[86,121]

The procedure described for the synthesis of diethyl (3-methyl-2-oxo-2*H*-chromen-4-yl)phosphonate **227a** and diethyl [(2-oxo-2*H*-chromen-3-yl)methyl]phosphonate **228a** was followed using 8-ethoxy-3-(chloromethyl)coumarin **82c** (0.86 g, 3.6 mmol) and triethyl phosphite (1.2 mL). Work-up and chromatography [on silica gel; elution with EtOAc-hexane (1:3)] afforded two fractions.

Fraction 1. Diethyl (8-ethoxy-3-methyl-2-oxo-2*H*-chromen-4-yl)phosphonate **227c** as pale yellow crystals (0.24 g, 20 %), m.p. 44-46 °C (lit.[86] 42-45 °C); v_{max} (neat)/cm^{-1} 1715 (C=O) and 1261 (P=O); δ_H (400 MHz; CDCl$_3$) 1.31 (6H, t, *J* = 7.2 Hz, 2 x POCH$_2$C*H$_3$*), 1.46 (3H, t, *J* = 7.0 Hz, ArOCH$_2$C*H$_3$*), 2.59 (3H, d, *J* = 3.2 Hz, CH$_3$), 4.10-4.24 (6H, m, 2x CH$_2$OP and ArOC*H$_2$*CH$_3$), 7.00 (1H, d, *J* = 8.0 Hz, Ar-H), 7.13 (1H, t, *J* = 8.2 Hz, Ar-H) and 8.01 (1H, d, *J* = 8.4 Hz, Ar-H); δ_C (100 MHz; CDCl$_3$) 14.7 (ArOCH$_2$C*H$_3$*), 16.3 (CH$_3$), 16.4 (d, $J_{P,C}$ = 6.2 Hz, 2x OCH$_2$C*H$_3$*), 62.7 (d, $J_{P,C}$ = 5.5 Hz, 2x CH$_2$OP), 65.0 (ArOC*H$_2$*CH$_3$), 114.0, 118.8, 119.3, 123.6, 137.5, 142.2 and 146.3 (Ar-C), 135.8 (d, $J_{P,C}$ = 11.0 Hz, C4) and 160.8 (C=O).

Fraction 2. Diethyl [(8-ethoxy-2-oxo-2*H*-chromen-3-yl)methyl]phosphonate **228c** as a pale yellow solid (0.79 g, 65 %), m.p. 52-55 ^{o}C (lit.[86] 53-56 ^{o}C); v_{max} (neat)/cm^{-1} 1730 (C=O) and 1255 (P=O); δ_H (400 MHz; CDCl$_3$) 1.24 (6H, t, J = 7.0 Hz, 2 x POCH$_2$C*H*$_3$), 1.43 (3H, t, J = 6.8 Hz, ArOCH$_2$C*H*$_3$), 3.13 (2H, d, $J_{P,H}$ = 20 Hz, CH$_2$P), 4.06-4.14 (6H, m, 2x C*H*$_2$OP and Ar-OC*H*$_2$CH$_3$), 7.00 (2H, dd, J = 7.56 and 4.61 Hz, Ar-H), 7.12 (1H, t, J = 7.8 Hz, Ar-H) and 7.76 (1H, d, $J_{P,C}$ = 4.4 Hz, 4-H); δ_C (100 MHz; CDCl$_3$) 14.6 (ArOCH$_2$*C*H$_3$), 16.2 (d, $J_{P,C}$ = 6.1 Hz, 2x POCH$_2$*C*H$_3$), 26.6 (d, $J_{P,C}$ = 139 Hz, CH$_2$P), 62.3 (d, $J_{P,C}$ = 6.5 Hz, 2 x CH$_2$OP), 64.9 (ArO*C*H$_2$CH$_3$), 114.5, 119.0, 119.9, 120.3, 124.3, 142.0, 143.0 and 146.3 (Ar-C) and 160.8 (C=O).
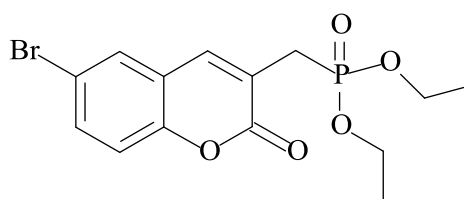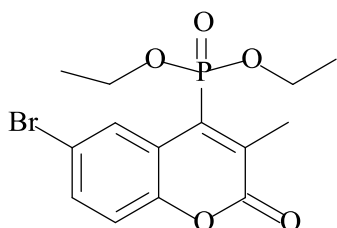
Diethyl (6-bromo-3-methyl-2-oxo-2H-chromen-4-yl)phosphonate *and* ***diethyl [((6-bromo-2-oxo-2H-chromen-3-yl)methyl]phosphonate***[86,121]

The procedure described for the synthesis of diethyl (3-methyl-2-oxo-2*H*-chromen-4-yl)phosphonate **227a** and diethyl [(2-oxo-2*H*-chromen-3-yl)methyl]phosphonate **228a** was followed using 6-bromo-3-(chloromethyl)coumarin **82e** (1.05 g, 3.8 mmol) and triethyl phosphite (1.3 mL). Work-up and chromatography [on silica gel; elution with EtOAc-hexane (1:3)] afforded two fractions.

Fraction1. Diethyl (6-bromo-3-methyl-2-oxo-2*H*-chromen-4-yl)phosphonate **227e** as a yellow solid (0.12 g, 8.3 %), m.p. 77-79 ^{o}C (lit.[86] 77-79 ^{o}C; v_{max}(neat)/cm^{-1} 1734 (C=O) and 1250 (P=O); δ_H (400 MHz; CDCl$_3$) 1.34 (6H, t, J = 7.2 Hz, 2x CH$_2$C*H*$_3$), 2.59 (3H, d, J = 3.2 Hz, CH$_3$), 4.16 and 4.26 (4H, 2 x m, 2x CH$_2$OP), 7.15 (1H, d, J = 8.8 Hz, Ar-H), 7.54 (1H, dd, J = 8.8 Hz, Ar-H) and 8.69 (1H, s, Ar-H); δ_C (100 MHz; CDCl$_3$) 16.3 (CH$_3$), 16.6 (d, $J_{P,C}$ = 6.1 Hz, 2 x OCH$_2$*C*H$_3$), 63.0 (d, $J_{P,C}$ = 5.5 Hz, 2 x C*H*$_2$OP), 117.2, 118.3, 119.6, 130.6, 133.5, 134.9 and 150.8 (Ar-C), 136.6 (d, $J_{P,C}$ = 10 Hz, C-4) and 160.3 (C=O).

Fraction 2. Diethyl [(6-bromo-2-oxo-2*H*-chromen-3-yl)methyl]phosphonate **228e** as a pale brown oil (0.8 g, 55 %); v_{max} (neat)/cm^{-1} 1725 (C=O) and 1265 (P=O); δ_H (400 MHz; CDCl$_3$) 1.28 (6H, t, *J* = 7.2 Hz, 2 x CH$_2$C*H*$_3$), 3.15 (2H, d, $J_{P,H}$ = 22 Hz, CH$_2$P), 4.14 (4H, q, *J* = 6.8 Hz, 2x CH$_2$OP), 7.15-7.49 (3H, series of multiplets, Ar-H) and 7.74 (1H, d, $J_{P,C}$ = 6.1 Hz, 4-H); δ_C (100 MHz; CDCl$_3$) 16.3 (d, $J_{P,C}$ = 6.1 Hz, 2 x OCH$_2$*C*H$_3$), 27.5 (d, $J_{P,C}$ = 139 Hz, CH$_2$P), 62.4 (d, $J_{P,C}$ = 6.1 Hz, 2x CH$_2$OP), 118.5, 120.8, 122.3, 127.5, 130.4, 131.9, 141.1 and 152.2 (Ar-C) and 161.0 (C=O).

Note: When the above reactions were repeated in the absence of N$_2$, only the 4-phosphonated products **227a,c,e** were isolated.

3.4.5 Michaelis-Arbuzov reactions of 3-(iodomethyl)coumarins
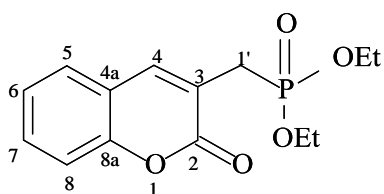
***Diethyl [(2-oxo-2*H*-chromen-3-yl)methyl]phosphonate* 228a**[86,121]

To 3-(iodomethyl)coumarin **81a** (0.34 g, 1.2 mmol) was added triethyl phosphite (0.40 mL) and the mixture was refluxed under nitrogen for 4 hours. Upon completion of the reaction, as monitored by TLC, the mixture was flash chromatographed [on silica gel; elution with EtOAc-hexane (3:1)] to afford diethyl [(2-oxo-2*H*-chromen-3-yl) methyl]phosphonate **228a** as a brown oil (0.21 g, 59 %).
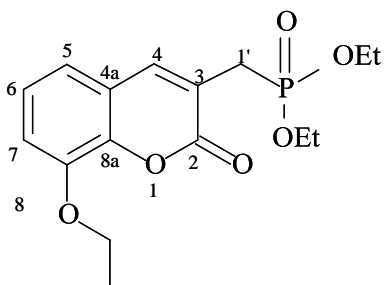
***Diethyl [(8-ethoxy-2-oxo-2*H*-chromen-3-yl)methyl]phosphonate* 228c**[86,121]

The procedure described for the synthesis of diethyl [(2-oxo-2*H*-chromen-3-yl)methyl]phosphonate **228a** was followed using 8-ethoxy-3-(iodomethyl)coumarin **81c** (0.40

g, 1.2 mmol) and triethyl phosphite (0.40 mL). Work-up and chromatography [on silica gel; elution with EtOAc-hexane (1:3)] afforded diethyl [(8-ethoxy-2-oxo-2*H*-chromen-3-yl)methyl]phosphonate **228c** as a yellow solid (0.16 g, 41 %).
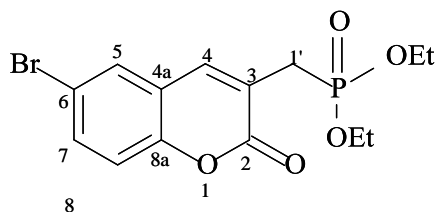
***Diethyl [(6-bromo-2-oxo-2H-chromen-3-yl)methyl]phosphonate* 228e**[86,121]

The procedure described for the synthesis of diethyl [(2-oxo-2*H*-chromen-3-yl)methyl]phosphonate **228a** was followed using 6-bromo-3-(iodomethyl)coumarin **81e** (0.42 g, 1.2 mmol) and triethyl phosphite (0.40 mL). Work-up and chromatography [on silica gel; elution with ethyl EtOAc-hexane (1:3)] afforded diethyl [(6-bromo-2-oxo-2*H*-chromen-3yl)methyl]phosphonate **228e** as a brown oil (0.18 g, 42 %).

3.5 Mechanistic Studies

3.5.1 Disulfide cleavage: Kinetic study

General procedure

The kinetic studies were carried out in $CDCl_3$ at 297 K. The $CDCl_3$ was cleaned prior to use by passing it through neutral alumina and crushed 4A molecular sieves in a dry Pasteur pipette under N_2.[142] All kinetic runs were carried out in 1 mL graduated NMR tubes. The reactants 2,2'-dithiodibenzaldehyde **201** and Ph_3P, as well as the internal standard trimethoxybenzene (TMB), were weighed directly into a graduated NMR tube. The liquid reactants, MVK, methyl acrylate and DBU, were measured using a micro syringe and weighed into a small vial, and a few drops of $CDCl_3$ added to each vial to allow for quantitative transfer into the graduated NMR tube. These were then transferred into the NMR tube. $CDCl_3$ was then added to the reactants and the solution made up to the mark. The mixture was quickly shaken. The timer was set as soon as the reactants were mixed, to allow for correction of zero-time error. The kinetic runs were carried out on either the Bruker 400 MHz spectrometer or the Bruker Biospin 600 MHz NMR spectrometer. All concentrations are in $molL^{-1}$.

3.5.1.1 Reactions of 2,2'-dithiodibenzaldehyde 201 with MVK using DBU as sole catalyst

Experiment 1.

The general procedure was followed using 2,2'-dithiodibenzaldehyde **201** (0.012 g), TMB (0.0023 g), DBU (0.011 mL, 0.0129 g) and MVK (0.012 mL, 0.0092 g). The experimental results are presented in Table 8.

Table 8. Data for Figure 32

Expt#	Time(s)	[ArCHO]	[MVK]	[DBU]	[Prod.CH$_2$]	[TMB]
100	0	0.203499	0.486232	0.210746	0.000001	0.076687
101	1143	0.149644	0.3526231	0.230586	0.013519	0.076687
102	1471	0.141333	0.3344392	0.230472	0.016172	0.076687
103	1799	0.13297	0.3167666	0.228585	0.018945	0.076687
104	2127	0.124353	0.2984462	0.228138	0.021163	0.076687
105	2455	0.11494	0.2794625	0.226685	0.024375	0.076687
106	2783	0.106083	0.2608752	0.226742	0.027885	0.076687
107	3111	0.096789	0.2421098	0.226079	0.031801	0.076687
108	3439	0.087494	0.2240849	0.224079	0.035604	0.076687
109	3767	0.078786	0.2058934	0.224116	0.039509	0.076687
110	4095	0.070434	0.189299	0.222957	0.04433	0.076687

111	4423	0.062177	0.1728169	0.222313	0.048454	0.076687
112	4751	0.054079	0.1569208	0.221035	0.053264	0.076687
113	5079	0.046851	0.1424509	0.220207	0.05777	0.076687
114	5407	0.040098	0.1287171	0.219726	0.062461	0.076687
115	5735	0.033958	0.1160222	0.219596	0.06756	0.076687
116	6063	0.028543	0.1046461	0.218899	0.072528	0.076687
117	6391	0.023668	0.0943042	0.218781	0.077715	0.076687
118	6719	0.019186	0.0847419	0.217781	0.082877	0.076687
119	7047	0.015399	0.0762429	0.217123	0.087518	0.076687
120	7375	0.012001	0.068629	0.215537	0.092944	0.076687
121	7703	0.009245	0.0617502	0.21744	0.096812	0.076687
122	8031	0.006927	0.0555679	0.216897	0.10161	0.076687
123	8359	0.004998	0.050219	0.216057	0.106973	0.076687
124	8687	0.003529	0.0452339	0.216006	0.111113	0.076687
125	9015	0.002415	0.0412154	0.215951	0.116101	0.076687

Experiment 2

The general procedure was followed using 2,2'-dithiodibenzaldehyde **201** (0.035 g), TMB (0.007 g), DBU (0.008 mL, 0.006 g) and MVK (0.020 mL, 0.032 g). The experimental results are presented in Table 9.

Table 9 . Data for Figure 43

Exp#	Time(s)	[ArCHO]	[MVK]	[OH-Thio]	[ThioC]	[DBU]	[TMB]
100	0	0.18	0.25566	0	0	0.05657	0.04162
101	633	0.13711	0.15351	0.02343	0.01633	0.05556	0.04162
102	1266	0.09485	0.10644	0.03593	0.02506	0.04884	0.04162
103	1901	0.06328	0.07166	0.04403	0.03666	0.04289	0.04162
104	2534	0.04172	0.04908	0.04772	0.04653	0.04043	0.04162
105	3166	0.02769	0.03425	0.04887	0.05498	0.03939	0.04162
106	3801	0.01830	0.02506	0.04878	0.06290	0.03921	0.04162
107	4434	0.01161	0.01867	0.04695	0.06759	0.0392	0.04162
108	5066	0.00753	0.01452	0.04608	0.07569	0.03989	0.04162
109	5701	0.00454	0.01134	0.04341	0.07921	0.03946	0.04162
110	6335	0.00261	0.00924	0.04123	0.08362	0.03925	0.04162
111	6968	0.00149	0.00824	0.03915	0.08942	0.03923	0.04162
112	7601	0.00089	0.00706	0.03647	0.09156	0.03791	0.04162
113	8233	0.00061	0.00650	0.03408	0.09567	0.03707	0.04162
114	8864	0.00059	0.00631	0.03149	0.09651	0.03542	0.04162
115	9497	0.00050	0.00575	0.02942	0.09943	0.03456	0.04162
116	10130	0.00046	0.00560	0.02752	0.10208	0.03372	0.04162
117	10762	0.00048	0.00515	0.02555	0.10395	0.03277	0.04162
118	11394	0.00046	0.00538	0.02405	0.10608	0.03205	0.04162
119	12025	0.00039	0.00528	0.02278	0.10883	0.03166	0.04162
120	12658	0.00039	0.00520	0.02143	0.11081	0.03105	0.04162
121	13290	0.00030	0.00535	0.02024	0.11322	0.03063	0.04162
122	13922	0.00036	0.00505	0.01899	0.11406	0.02971	0.04162

123	14555	0.00030	0.00493	0.01794	0.11507	0.02888	0.04162
124	15187	0.00035	0.00514	0.01703	0.11686	0.02831	0.04162
125	15819	0.00032	0.00524	0.01612	0.11799	0.02752	0.04162
126	16453	0.00020	0.00606	0.01604	0.12152	0.02785	0.04162
127	17085	1.8E-05	0.00437	0.01459	0.11509	0.02477	0.04162
128	17717	1.3E-05	0.00436	0.01391	0.11547	0.02401	0.04162
129	18349	3.3E-05	0.0044o	0.01331	0.11651	0.02353	0.04162
130	18981	0.00032	0.00586	0.01268	0.12368	0.02478	0.04162

3.5.1.2 Reaction of 2,2'-dithiodibenzaldehyde 201 and methyl acrylate using DBU as sole catalyst

The general procedure was followed using 2,2'-dithiodibenzaldehyde **201** (0.012 g), DBU (0.011 mL, 0.0129 g), methyl acrylate (0.012 mL, 0.0129 g) and TMB (0.0024 g). The experimental results are presented in Table 10.

Table 10. Data for Figure 33

Expt#	Time (s)	[ArCHO]	[Product]	[Methyl acrylate]	[TMB]	[DBU]
100	0	0.551714	0.03907	3.336196059	1.03897	0.617883
101	627	0.547651	0.06321	3.33822411	1.03897	0.623024
102	1255	0.542149	0.091016	3.334502855	1.03897	0.626602
103	1882	0.53662	0.113232	3.327127906	1.03897	0.628273
104	2508	0.53207	0.13793	3.3245799	1.03897	0.631501
105	3136	0.527195	0.161368	3.321306032	1.03897	0.633038
106	3763	0.521514	0.189604	3.317475238	1.03897	0.637079
107	4390	0.517669	0.212488	3.312252739	1.03897	0.638057
108	5016	0.5131	0.230547	3.312199496	1.03897	0.639055
109	5645	0.508212	0.259024	3.30805943	1.03897	0.643202
110	6272	0.502037	0.279782	3.305643216	1.03897	0.644444
111	6900	0.498948	0.303217	3.30267476	1.03897	0.647375
112	7526	0.494032	0.32728	3.300895141	1.03897	0.65109
113	8153	0.488795	0.347174	3.29952625	1.03897	0.653049
114	8780	0.484037	0.376719	3.295095096	1.03897	0.657003
115	9406	0.478684	0.398678	3.291197674	1.03897	0.658966
116	10033	0.473419	0.423414	3.287416918	1.03897	0.662277
117	10661	0.470099	0.446897	3.285667558	1.03897	0.665238
118	11291	0.465637	0.471883	3.2875491	1.03897	0.668684
119	11918	0.460791	0.491063	3.281133648	1.03897	0.668847
120	12544	0.457071	0.508595	3.289538533	1.03897	0.673154
121	13171	0.450513	0.540426	3.27852346	1.03897	0.67422
122	13797	0.447292	0.554494	3.281163153	1.03897	0.675987
123	14424	0.443073	0.585125	3.26815567	1.03897	0.676003
124	15051	0.438612	0.603557	3.269641611	1.03897	0.678235
125	15677	0.43455	0.630034	3.266593516	1.03897	0.679652
126	16304	0.429522	0.646977	3.264465371	1.03897	0.682051
127	16933	0.424949	0.674367	3.259777253	1.03897	0.682618
128	17560	0.420581	0.683606	3.258682898	1.03897	0.684177
129	18188	0.41566	0.699685	3.258873862	1.03897	0.685852
130	18816	0.411472	0.744336	3.250890391	1.03897	0.687408

131	19443	0.407575	0.764012	3.244354429	1.03897	0.688402
132	20071	0.403246	0.785095	3.245673386	1.03897	0.69145
133	20698	0.398998	0.802882	3.24156289	1.03897	0.691841
134	21324	0.395379	0.826001	3.240623813	1.03897	0.694007
135	21951	0.39117	0.843812	3.236984237	1.03897	0.695934
136	22579	0.386936	0.867908	3.232491928	1.03897	0.697894
137	23205	0.382895	0.881752	3.230911515	1.03897	0.698848
138	23832	0.380294	0.910253	3.227674798	1.03897	0.700899
139	24461	0.37528	0.928785	3.224681308	1.03897	0.702533
140	25088	0.370531	0.951439	3.220305531	1.03897	0.703587
141	25716	0.367606	0.964189	3.227423612	1.03897	0.707707
142	26342	0.363559	0.98772	3.215001042	1.03897	0.707012
143	26969	0.359752	1.001633	3.216383596	1.03897	0.709391
144	27596	0.356258	1.018517	3.215080069	1.03897	0.711021
145	28223	0.351978	1.041986	3.213364032	1.03897	0.713122
146	28849	0.347873	1.067896	3.206560619	1.03897	0.714605
147	29476	0.345011	1.08354	3.203537912	1.03897	0.715284
148	30103	0.339887	1.103012	3.201135819	1.03897	0.716563
149	30729	0.336551	1.106993	3.200605225	1.03897	0.716975
150	31356	0.333303	1.134869	3.197593878	1.03897	0.718851
151	31984	0.329883	1.144585	3.197667705	1.03897	0.719895
152	32612	0.326366	1.160094	3.194404609	1.03897	0.720853
153	33242	0.322006	1.184566	3.188402639	1.03897	0.723408
154	33869	0.318732	1.20451	3.186227742	1.03897	0.725635
155	34497	0.314637	1.223148	3.183314602	1.03897	0.7238
156	35125	0.311544	1.226363	3.181939924	1.03897	0.728799
157	35753	0.308618	1.237166	3.181761339	1.03897	0.728306
158	36380	0.304766	1.259148	3.180706593	1.03897	0.729247

3.5.1.3 MBH reaction of 2,2'-dithiodibenzaldehyde 201 with MVK using Ph₃P as sole catalyst

The general procedure was followed using 2,2'-dithiodibenzaldehyde **201** (0.012 g), Ph₃P (0.021 g). MVK (0.012 mL, 0.0129 g) and TMB (0.0023g). The experimental results are presented in Table 11.

Table 11. Data for Figure 34

Exp#	time	[ArCHO]	[Ph₃P]	[MVK1]	[TMB-3H]	[OH-prod1]
100	0	0.045985401	0.07519084	0.138393494	0.014285714	0.00001
101	808	0.037278857	0.07504505	0.085607283	0.014285714	0.001247329
102	1136	0.036363156	0.074259445	0.083977458	0.014285714	0.00178476
103	1464	0.035386311	0.073575049	0.082217536	0.014285714	0.002499011
104	1792	0.034414402	0.072946026	0.080696227	0.014285714	0.003150002
105	2120	0.033644642	0.07242766	0.079932195	0.014285714	0.003683699
106	2448	0.032605685	0.071741298	0.078059624	0.014285714	0.004163348
107	2776	0.031867317	0.071113355	0.076772398	0.014285714	0.004870848
108	3104	0.030977052	0.070376035	0.07510124	0.014285714	0.00537608
109	3432	0.030138804	0.069806893	0.073809791	0.014285714	0.005910556
110	3760	0.029301305	0.069147708	0.07246364	0.014285714	0.006425976
111	4088	0.028564471	0.068611824	0.07126276	0.014285714	0.006979644
112	4416	0.027852417	0.068091936	0.069954928	0.014285714	0.007491205
113	4744	0.027119399	0.067610586	0.068937125	0.014285714	0.007997128
114	5072	0.026485821	0.067095573	0.067749123	0.014285714	0.008443743
115	5400	0.025788975	0.066617627	0.066740119	0.014285714	0.008817269
116	5728	0.025101812	0.066027342	0.065732376	0.014285714	0.009370593
117	6056	0.024561871	0.065717435	0.064706484	0.014285714	0.00974765
118	6384	0.023867886	0.065091546	0.063559777	0.014285714	0.010223897
119	6712	0.023375678	0.064620506	0.062657865	0.014285714	0.010507488
120	7040	0.022775643	0.06429614	0.061795263	0.014285714	0.011039342
121	7368	0.022183334	0.063823626	0.060876691	0.014285714	0.01144164
122	7696	0.021640489	0.063366285	0.059899833	0.014285714	0.011904583
123	8024	0.021126193	0.062977223	0.05906592	0.014285714	0.01222576
124	8352	0.020644602	0.062459165	0.058277807	0.014285714	0.012513471
125	8680	0.02014515	0.062151343	0.057579997	0.014285714	0.012859567
126	9008	0.019736823	0.061871231	0.056907667	0.014285714	0.013302978
127	9336	0.019213402	0.061440665	0.055922683	0.014285714	0.013683579
128	9664	0.018740557	0.06097053	0.055155971	0.014285714	0.014024775

3.5.1.4 Reaction of 2,2'-dithiodibenzaldehyde 201 with methyl acrylate using Ph₃P as sole catalyst

The general procedure was followed using 2,2'-dithiodibenzaldehyde **201** (0.012 g), Ph$_3$P (0.021 g), methyl acrylate (0.012 mL, 0.013 g) and TMB (0.0024g). The experimental results are presented in Table 12.

Table 12. Data for Figure 35

Exp#	Time(s)	[ArCHO]	[Macrylate]	[Ph3P]	[OH-Thio]	[ThioC]	[TMB]
100	0	0.0425	0.1383	0.06836	-0.0001	-0.0001	0.0135
101	930	0.0329	0.0781	0.04972	-9.99E-05	-0.000137543	0.0135
102	1258	0.0327	0.0782	0.04951	-5.3E-05	-9.25192E-05	0.0135
103	1586	0.0325	0.078	0.04905	-3.44E-05	5.35138E-06	0.0135
104	1914	0.0323	0.078	0.04879	-1.73E-05	-6.63729E-05	0.0135
105	2242	0.032	0.0777	0.04846	-9.14E-06	-6.19347E-05	0.0135
106	2570	0.0319	0.0779	0.0484	6.351E-07	5.34726E-06	0.0135
107	2898	0.0316	0.0778	0.04814	1.416E-06	-6.73842E-05	0.0135
108	3226	0.0314	0.0778	0.04788	-5.72E-06	-8.06179E-05	0.0135
109	3554	0.0312	0.0777	0.04763	4.808E-05	4.56829E-05	0.0135
110	3882	0.031	0.0777	0.04743	7.775E-06	4.86192E-05	0.0135
111	4210	0.0308	0.0776	0.04715	5.96E-05	-2.58736E-05	0.0135
112	4538	0.0305	0.0775	0.04692	0.000134	8.46752E-05	0.0135
113	4866	0.0303	0.0774	0.04664	0.0001052	7.03276E-05	0.0135
114	5194	0.03	0.0772	0.04638	0.0001066	7.727E-05	0.0135
115	5522	0.0299	0.0773	0.04617	0.00016	8.23159E-05	0.0135
116	5850	0.0297	0.0773	0.04603	0.0001346	8.33129E-05	0.0135
117	6178	0.0294	0.0771	0.04572	0.0001637	0.000200634	0.0135
118	6506	0.0293	0.0771	0.04561	0.000198	0.00016884	0.0135
119	6834	0.0291	0.077	0.04534	0.0002649	0.000174565	0.0135
120	7162	0.0289	0.0769	0.04514	0.0002588	0.000181568	0.0135
121	7490	0.0286	0.0767	0.04485	0.0002938	0.000254853	0.0135
122	7818	0.0285	0.0769	0.04472	0.0002969	0.000178442	0.0135
123	8146	0.0284	0.077	0.04458	0.00034	0.000252341	0.0135
124	8474	0.0281	0.0767	0.04433	0.0003248	0.000292756	0.0135
125	8802	0.028	0.0768	0.04421	0.0003295	0.000301188	0.0135
126	9130	0.0278	0.0768	0.04397	0.000343	0.000304773	0.0135
127	9458	0.0277	0.0767	0.04379	0.0003441	0.000275712	0.0135
128	9786	0.0275	0.0766	0.0436	0.0003647	0.000321215	0.0135
129	10114	0.0273	0.0766	0.0434	0.0004108	0.000390959	0.0135
130	10442	0.0272	0.0768	0.04334	0.0004103	0.000421719	0.0135

3.5.1.5 Reaction of 2,2'-dithiodibenzaldehyde 201 with MVK using the dual-catalyst system (DBU-Ph₃P)

The general procedure was followed using 2,2'-dithiodibenzaldehyde **201** (0.012 g) Ph$_3$P (0.021 g). DBU (0.011 mL, 0.0129 g), MVK (0.012 mL, 0.0129 g) and TMB (0.0024 g). The experimental results are presented in Table 13.

Table 13. Concentration data for Figure 37

Exp#	Time(s)	[ArCHO]	[MVK]	[OH-Prod]	[ThioC]	[Ph₃P]	[DBU]	[TMB]
100	0	0.04598	0.13126	0.00000	0.00000	0.07595	0.07171	0.01369
101	870	0.03272	0.05218	0.02615	0.01068	0.06744	0.06113	0.01369
102	1198	0.02145	0.04042	0.03260	0.01169	0.06256	0.06192	0.01369
103	1526	0.01328	0.03225	0.03697	0.01279	0.05976	0.06274	0.01369
104	1854	0.00772	0.02598	0.03980	0.01374	0.05743	0.06276	0.01369
105	2182	0.00405	0.02143	0.04196	0.01471	0.05604	0.06282	0.01369
106	2510	0.00186	0.01808	0.04308	0.01576	0.05497	0.06274	0.01369
107	2838	0.00061	0.01619	0.04356	0.01696	0.05434	0.06258	0.01369
108	3166	0.00016	0.01452	0.04363	0.01766	0.05404	0.06242	0.01369
109	3494	3.05E-05	0.01397	0.04305	0.01897	0.05363	0.06183	0.01369
110	3822	4.9E-05	0.01347	0.04228	0.01979	0.05360	0.06172	0.01369
111	4150	6.04E-05	0.01273	0.04168	0.021	0.05346	0.06137	0.01369
112	4478	4.9E-05	0.01235	0.04101	0.02223	0.05347	0.06127	0.01369
113	4806	2.37E-05	0.01180	0.0403	0.02314	0.05351	0.06119	0.01369
114	5134	9.06E-05	0.01151	0.03953	0.02386	0.05321	0.06072	0.01369
115	5462	7.03E-05	0.01090	0.03904	0.02500	0.05322	0.06064	0.01369
116	5790	6.93E-06	0.01073	0.03843	0.02570	0.05317	0.06046	0.01369
117	6118	5.9E-05	0.01025	0.03776	0.02656	0.05285	0.06000	0.01369
118	6446	3.88E-05	0.00986	0.03728	0.02721	0.05311	0.06015	0.01369
119	6774	3.4E-05	0.00915	0.03682	0.02832	0.05309	0.06004	0.01369
120	7102	2.9E-05	0.00886	0.03622	0.02901	0.05287	0.05975	0.01369
121	7430	4.12E-05	0.00843	0.03550	0.02970	0.05281	0.05954	0.01369
122	7758	4.5E-05	0.00829	0.03513	0.03061	0.05287	0.05958	0.01369
123	8086	2.74E-05	0.00775	0.03443	0.03096	0.05253	0.05902	0.01369
124	8414	1.1E-05	0.00734	0.03405	0.03184	0.05250	0.059	0.01369
125	8742	4.6E-05	0.00703	0.03379	0.03280	0.05263	0.05913	0.01369
126	9070	6.52E-06	0.00672	0.03317	0.03327	0.05246	0.05888	0.01369
127	9398	3.3E-05	0.00660	0.03283	0.03406	0.05238	0.05882	0.01369
128	9726	3E-05	0.00603	0.03250	0.03505	0.05240	0.05884	0.01369
129	10054	7.6E-06	0.00593	0.03192	0.03531	0.05251	0.05872	0.01369
130	10382	3.7E-05	0.00560	0.03149	0.03634	0.05234	0.05868	0.01369
131	10710	7.4E-05	0.00523	0.03113	0.03709	0.05222	0.05864	0.01369
132	11038	2.1E-06	0.00513	0.03073	0.03723	0.05204	0.05814	0.01369
133	11366	4.39E-05	0.00503	0.03026	0.03801	0.05207	0.05816	0.01369
134	11694	1E-05	0.00465	0.02993	0.03878	0.05204	0.05822	0.01369
135	12022	3.5E-05	0.00439	0.02957	0.03953	0.05199	0.05814	0.01369
136	12350	1.2E-05	0.00425	0.02910	0.03932	0.05184	0.05769	0.01369
137	12678	1.98E-05	0.00390	0.02879	0.04013	0.05193	0.05779	0.01369
138	13006	6.9E-06	0.00375	0.02843	0.04046	0.05185	0.05757	0.01369

3.5.1.6 Reaction of 2,2'-dithiodibenzaldehyde 201 with methyl acrylate using the dual-catalyst system (DBU-Ph₃P)

The general procedure was followed using 2,2'-dithiodibenzaldehyde **201** (0.012 g) Ph$_3$P (0.021 g), DBU (0.011 mL, 0.0129 g), methyl acrylate (0.012 mL, 0.0127 g) and TMB (0.0024 g). The experimental results are presented in Table 14.

Table 14. Data for Figure 39

Exp#	Time(s)	[ArCHO]	[ThioC]	[Macrylate]	[OH-Thio]	[Ph₃P]	[DBU]	[TMB]
100	0	0.04379	0.00001	0.15100	0.00001	0.07677	0.08026	0.01190
101	989	0.02666	0.00338	0.05120	0.00172	0.06231	0.03037	0.01190
102	1289	0.02513	0.00406	0.05038	0.00234	0.06197	0.03090	0.01190
103	1589	0.02354	0.00469	0.04950	0.003	0.06177	0.03158	0.01190
104	1889	0.02200	0.00536	0.04867	0.00369	0.06137	0.03192	0.01190
105	2189	0.02044	0.00606	0.04760	0.00447	0.06104	0.03241	0.01190
106	2489	0.01889	0.00679	0.04673	0.00535	0.06086	0.03245	0.01190
107	2789	0.01731	0.00753	0.04561	0.00633	0.06056	0.03143	0.01190
108	3089	0.01584	0.00829	0.04439	0.00734	0.06023	0.02992	0.01190
109	3389	0.01434	0.00921	0.04311	0.00835	0.05997	0.02882	0.01190
110	3689	0.01291	0.01003	0.04182	0.00944	0.05971	0.02751	0.01190
111	3989	0.01158	0.01076	0.04056	0.01052	0.05947	0.02474	0.01190
112	4289	0.01030	0.01165	0.03926	0.01162	0.05932	0.02184	0.01190
113	4589	0.00910	0.01242	0.03803	0.01273	0.05898	0.01951	0.01190
114	4889	0.00803	0.01312	0.03674	0.01376	0.05882	0.01833	0.01190
115	5189	0.00697	0.01379	0.03549	0.01481	0.05859	0.01737	0.01190
116	5489	0.00609	0.01441	0.03433	0.01581	0.05837	0.01605	0.01190
117	5789	0.00522	0.01494	0.03333	0.01673	0.05818	0.0148	0.01190
118	6089	0.00453	0.01549	0.03226	0.01757	0.05811	0.01392	0.01190
119	6389	0.00382	0.01602	0.03132	0.01837	0.05797	0.01361	0.01190
120	6689	0.00323	0.01633	0.03046	0.01918	0.05784	0.01336	0.01190
121	6989	0.00271	0.01676	0.02965	0.01981	0.05772	0.01338	0.01190
122	7289	0.00228	0.01707	0.02901	0.02048	0.05759	0.01362	0.01190
123	7589	0.00190	0.01736	0.02834	0.02100	0.05749	0.01364	0.01190
124	7889	0.00153	0.01771	0.02769	0.02151	0.05745	0.01376	0.01190
125	8189	0.00128	0.01793	0.02719	0.02207	0.05744	0.01395	0.01190
126	8489	0.00104	0.01818	0.02678	0.02247	0.05737	0.01408	0.01190
127	8789	0.00084	0.01832	0.02636	0.02283	0.05726	0.01417	0.01190
128	9089	0.00068	0.01847	0.02590	0.02310	0.05721	0.01429	0.01190

3.5.1.7 Phosphorus-31 kinetic studies of the reaction of 2,2'-dithiodibenzaldehyde 201 with MVK using the dual-catalyst system (DBU-Ph₃P)

The general procedure was followed using 2,2'-dithiodibenzaldehyde **201** (0.012 g) Ph₃P (0.021 g), DBU (0.011 mL, 0.0129 g), MVK (0.012 mL, 0.0127 g) and TMB (0.0024 g). The experimental results are presented in Table 15.

Table 15. Data for Figure 41

Exp#	Time(s)	[Ph₃P]	[Ph₃PO]	Total [P]
101	0	0.91415	0.0572	0.97135
102	135	0.902477	0.044331	0.946808
103	269	0.889701	0.010918	0.900619
104	403	0.886068	0.007572	0.89364
105	537	0.882692	0.014828	0.89752
106	671	0.87578	8.31E-05	0.875863
107	805	0.873549	0.016396	0.889945
108	939	0.870398	0.015922	0.88632
109	1073	0.868184	0.015666	0.88385
110	1207	0.86059	0.016457	0.877046
111	1341	0.858707	0.024571	0.883278
112	1475	0.853285	0.010379	0.863664
113	1609	0.849696	0.017014	0.86671
114	1743	0.841285	0.018456	0.859741
115	1877	0.83774	0.021101	0.858841
116	2011	0.835378	0.023564	0.858942
117	2145	0.832802	0.023789	0.856591
118	2279	0.825735	0.022644	0.848379
119	2413	0.829574	0.024567	0.854141
120	2547	0.815157	0.025438	0.840595
121	2681	0.811904	0.026457	0.838361
122	2815	0.815065	0.028458	0.843523
123	2949	0.81182	0.028145	0.839965
124	3083	0.805547	0.049759	0.855306
125	3217	0.80052	0.019562	0.820082
126	3351	0.795496	0.044776	0.840272
127	3485	0.794739	0.039199	0.833938
128	3619	0.783955	0.032405	0.81636
129	3753	0.782369	0.033319	0.815688
130	3887	0.77756	0.048	0.82556
131	4021	0.775509	0.039372	0.814881
132	4155	0.769349	0.03373	0.803079
133	4289	0.769335	0.037754	0.807089
134	4423	0.759739	0.050319	0.810058
135	4557	0.754303	0.053454	0.807757
136	4691	0.744048	0.045689	0.789737

137	4825	0.746222	0.047722	0.793944
138	4959	0.746329	0.058764	0.805093
139	5093	0.738748	0.046722	0.78547
140	5226	0.739149	0.045108	0.784257

3.5.2 Kinetic study of the reaction of chromone-3-carbaldehyde 218a with MVK

3.5.2.1 Experiment 1

Chromone-3-carbaldehyde **218a** (0.016 g) was weighed directly into a graduated NMR tube, followed by 3HQ (0.038 g). MVK (0.019 g) was weighed into a vial using a microsyringe and *ca.* 5 drops of CDCl$_3$ were added to the vial. CDCl$_3$ (*ca.* 0.5 mL) was added to dissolve the chrome-3-carbaldehyde and 3-HQ in the graduated NMR tube. The MVK solution was then added to the NMR tube which was made up to the mark using CDCl$_3$. The mixture was shaken and the start of the reaction was timed to correct for zero-time error.

The procedure described for Experiment 1 was followed for Experiments 2-4 in the molar ratios given in Table 16. The experimental results for Experiment 1 are presented in Table 17.

Table 16. Molar ratios of reagents for Experiments 2-4

	Chromone-3-carbaldehyde **218a**	MVK	3HQ
Experiment 2	1	1.5	3
Experiment 3	1	6	3
Experiment 4	1	9	3

Table 17. Data for Experiment 1 (Figures 58, 66 and 67)

Exp#	Time(s)	[ArCHO]	[MVK]	[MBHprd]	[Tri-2]	[CDimer]	[3HQ]	[TMB]
100	0	0.089	0.2696	0.0001	0.0001	0.0001	0.2995	0.0255
101	1108	0.0479	0.1093	0.0086	0.0004	0.0018	0.2368	0.0255
102	1736	0.0294	0.0896	0.0136	0.0015	0.0049	0.2288	0.0255
103	2364	0.0199	0.0812	0.0162	0.0023	0.0071	0.2370	0.0255
104	2993	0.0141	0.0749	0.0166	0.0023	0.0093	0.2415	0.0255
105	3622	0.0102	0.0669	0.0136	0.0021	0.0104	0.2378	0.0255
106	4281	0.0076	0.0620	0.0119	0.0022	0.0119	0.2411	0.0255
107	4908	0.0059	0.0616	0.0118	0.0019	0.0132	0.2454	0.0255
108	5536	0.0046	0.0590	0.0105	0.0021	0.0144	0.2539	0.0255
109	6165	0.0035	0.0529	0.0073	0.0020	0.0153	0.2470	0.0255
110	6793	0.0029	0.0539	0.0075	0.0025	0.0166	0.2608	0.0255
111	7420	0.0024	0.0545	0.0082	0.0024	0.0179	0.2746	0.0255
112	8049	0.0019	0.0560	0.0081	0.0029	0.0185	0.2944	0.0255

113	8678	0.0017	0.0502	0.0050	0.0018	0.0176	0.2894	0.0255
114	9306	0.0014	0.0503	0.0049	0.0020	0.0184	0.3059	0.0255
115	9934	0.0012	0.0465	0.0031	0.0016	0.0182	0.3144	0.0255
116	10561	0.0010	0.0518	0.0056	0.0031	0.0203	0.3578	0.0255
117	11189	0.0009	0.0468	0.0029	0.0020	0.0192	0.3533	0.0255
118	11817	0.0007	0.0463	0.0029	0.0021	0.0196	0.3630	0.0255
119	12445	0.0007	0.0454	0.0022	0.0023	0.0199	0.3574	0.0255
120	13073	0.0005	0.0462	0.0027	0.0024	0.0203	0.3675	0.0255
121	13701	0.0005	0.0452	0.0019	0.0025	0.0205	0.3625	0.0255
122	14328	0.0005	0.0453	0.0021	0.0027	0.0208	0.3523	0.0255
123	14956	0.0004	0.0452	0.0018	0.0027	0.0209	0.3543	0.0255
124	15584	0.0004	0.0454	0.0020	0.0029	0.0213	0.3434	0.0255
125	16213	0.0003	0.0450	0.0018	0.0030	0.0214	0.3372	0.0255
126	16841	0.0003	0.0448	0.0017	0.0031	0.0215	0.3283	0.0255
127	17469	0.0003	0.0446	0.0014	0.0031	0.0216	0.3200	0.0255
128	18096	0.0003	0.0441	0.0013	0.0032	0.0217	0.3108	0.0255
129	18724	0.0003	0.0450	0.0014	0.0034	0.0220	0.3119	0.0255
130	19352	0.0002	0.0472	0.0027	0.0037	0.0226	0.3208	0.0255
131	19980	0.0002	0.0447	0.0014	0.0034	0.0221	0.3040	0.0255
132	20608	0.0002	0.0479	0.0029	0.0040	0.0231	0.3195	0.0255
133	21236	0.0002	0.0467	0.0023	0.0039	0.0228	0.3100	0.0255
134	21864	0.0001	0.0462	0.0019	0.0038	0.0227	0.3048	0.0255
135	22491	0.0001	0.0466	0.0019	0.0039	0.0229	0.3039	0.0255
136	23120	0.0001	0.0477	0.0022	0.0041	0.0231	0.3040	0.0255
137	23748	0.0001	0.0466	0.0019	0.0040	0.0230	0.3006	0.0255
138	24376	0.0001	0.0471	0.0025	0.0042	0.0233	0.3039	0.0255
139	25004	0.0001	0.0469	0.0022	0.0042	0.0232	0.3012	0.0255
140	25632	0.0001	0.0473	0.0024	0.0043	0.0234	0.2993	0.0255
141	26259	0.0001	0.0473	0.0020	0.0043	0.0233	0.3008	0.0255
142	26890	0.0001	0.0471	0.0024	0.0043	0.0234	0.3027	0.0255
143	27518	0.0001	0.0475	0.0023	0.0044	0.0235	0.3006	0.0255
144	28147	0.0001	0.0471	0.0023	0.0043	0.0235	0.2968	0.0255
145	28776	0.0001	0.0455	0.0014	0.0041	0.0230	0.2892	0.0255

3.5.2.2 Experiment 2

The procedure described for Experiment 1 was followed for Experiment 2 with the molar ratios of 1:1.5:3 (chromone-3-carbaldehyde: MVK: 3HQ). The experimental results are presented in Table 18.

Table 18. Data for Experiment 2 (Figure 60)

Exp#	Time(s)	[ArCHO]	[MVK]	[CDimer]	[Tri-prd]	[3HQ]	[TMB]
100	0	0.0861	0.1341	0	0	0.28618	0.022593
101	1054	0.0588	0.0444	8.912E-05	0.00023	0.26696	0.0225934
102	1683	0.0511	0.0359	0.0007413	0.00012	0.26333	0.0225934
103	2313	0.0455	0.0293	0.0013476	0.00019	0.26302	0.0225934
104	2942	0.0411	0.0250	0.0015794	0.00021	0.25852	0.0225934
105	3572	0.0380	0.0221	0.0027612	2.0E-05	0.25661	0.0225934
106	4201	0.0352	0.0187	0.0027638	0.00017	0.26178	0.0225934
107	4834	0.0330	0.0167	0.0037525	2.7E-06	0.25287	0.0225934
108	5464	0.0314	0.0144	0.0038733	0.00019	0.26179	0.0225934
109	6095	0.0300	0.0126	0.0042460	0.00022	0.25913	0.0225934
110	6724	0.0286	0.0124	0.0052742	6.8E-05	0.25967	0.0225934
111	7353	0.0276	0.0110	0.0056103	1.1E-05	0.26093	0.0225934
112	7983	0.0266	0.0101	0.0060430	7.2E-05	0.26086	0.0225934
113	8611	0.0258	0.0095	0.0066501	1.7E-05	0.26288	0.0225934
114	9241	0.0251	0.0082	0.0068516	0.00020	0.27043	0.0225934
115	9871	0.0245	0.0075	0.0071247	0.00020	0.26819	0.0225934
116	10501	0.0240	0.0065	0.0072749	0.00042	0.27060	0.0225934
117	11130	0.0234	0.0063	0.0079379	0.00022	0.27016	0.0225934
118	11781	0.0229	0.0061	0.0084656	0.00015	0.27407	0.0225934
119	12422	0.0224	0.0056	0.0088199	0.00020	0.27410	0.0225934
120	13051	0.0219	0.0051	0.0090504	0.00030	0.27515	0.0225934
121	13680	0.0216	0.0048	0.0094549	0.00026	0.27650	0.0225934
122	14310	0.0214	0.0039	0.0094374	0.00044	0.27529	0.0225934
123	14940	0.0211	0.0039	0.0099684	0.00030	0.27748	0.0225934
124	15570	0.0207	0.0039	0.0102912	0.00032	0.27786	0.0225934
125	16201	0.0205	0.0034	0.0106247	0.00036	0.27937	0.0225934
126	16829	0.0202	0.0030	0.0108058	0.00041	0.27878	0.0225934
127	17457	0.0201	0.0029	0.0110863	0.00030	0.27829	0.0225934
128	18086	0.0197	0.0029	0.0116061	0.00025	0.27286	0.0225934
129	18716	0.0197	0.0019	0.0112485	0.00059	0.27666	0.0225934
130	19349	0.0194	0.0026	0.0121347	0.00019	0.27426	0.0225934
131	19977	0.0193	0.0014	0.0116927	0.00062	0.27857	0.0225934
132	20606	0.0191	0.0018	0.0122672	0.00040	0.27950	0.0225934
133	21237	0.0190	0.0014	0.0122659	0.00055	0.27883	0.0225934
134	21867	0.0187	0.0024	0.0131817	6.7E-05	0.26917	0.0225934
135	22495	0.0187	0.0010	0.0126545	0.00057	0.28009	0.0225934

3.5.2.3 Experiment 3

The procedure described for Experiment 1 was followed for Experiment 3 with the molar ratios of 1:6:3 (chromone-3-carbaldehyde: MVK: 3HQ). The experimental results are presented in Table 19.

Table 19. Data for Experiment 3 (Figure 61)

Exp#	Time(s)	[ArCHO]	[MVK]	[CDimer]	[Tri-prd]	[3HQ]	[TMB]
100	0	0.09761	0.53697	0.0001	0.0001	0.20584	0.02702
101	1136	0.04122	0.31155	0.00534	0.00147	0.17786	0.02702
102	1765	0.02083	0.29197	0.01001	0.00268	0.18015	0.02702
103	2394	0.01085	0.27861	0.01127	0.00215	0.18179	0.02702
104	3024	0.00609	0.27085	0.01191	0.00201	0.18507	0.02702
105	3653	0.00327	0.26611	0.01519	0.00351	0.18805	0.02702
106	4282	0.00190	0.26319	0.01681	0.00397	0.18934	0.02702
107	4912	0.00109	0.25878	0.01788	0.00440	0.19120	0.02702
108	5541	0.00073	0.26082	0.01982	0.00534	0.19573	0.02702
109	6172	0.00040	0.25632	0.01987	0.00539	0.19279	0.02702
110	6801	0.00022	0.25495	0.01971	0.00530	0.19368	0.02702
111	7433	0.00021	0.25296	0.02187	0.00671	0.19309	0.02702
112	8062	0.00019	0.25037	0.02235	0.00706	0.19163	0.02702
113	8707	9.2E-05	0.25234	0.02069	0.00629	0.19325	0.02702
114	9336	6.6E-05	0.25194	0.02106	0.00645	0.19245	0.02702
115	9966	1.9E-05	0.24812	0.02098	0.00668	0.19286	0.02702
116	10596	8.9E-05	0.24995	0.02121	0.00695	0.19333	0.02702
117	11225	4.0E-05	0.24882	0.02100	0.00700	0.19228	0.02702
118	11854	2.4E-05	0.25089	0.02128	0.00723	0.19439	0.02702
119	12484	5.6E-07	0.25112	0.02156	0.00751	0.19309	0.02702
120	13113	2.8E-05	0.25000	0.02173	0.00770	0.19385	0.02702
121	13742	2.1E-07	0.24947	0.02203	0.00787	0.19556	0.02702
122	14371	4.4E-05	0.25041	0.02217	0.00816	0.19623	0.02702
123	15002	0.00011	0.24810	0.02177	0.00808	0.19526	0.02702
124	15630	3.0E-05	0.24935	0.02201	0.00834	0.19446	0.02702
125	16259	3.2E-05	0.24887	0.02202	0.00837	0.19617	0.02702
126	16889	1.8E-05	0.24897	0.02232	0.00854	0.19521	0.02702
127	17517	2.5E-05	0.24904	0.02219	0.00862	0.19524	0.02702
128	18146	9.3E-05	0.24949	0.02229	0.00869	0.19448	0.02702
129	18776	3.8E-05	0.24855	0.02239	0.00882	0.19543	0.02702
130	19405	5.7E-06	0.24817	0.02208	0.00873	0.19654	0.02702

3.5.2.4 Experiment 4

The procedure described for Experiment 1 was followed for Experiment 4 with the molar ratios of 1:9:3 (chromone-3-carbaldehyde: MVK: 3HQ). The experimental results are presented in Table 20.

Table 20. Data for Experiment 4 (Figures 62 and 63)

Exp#	Time(s)	[ArCHO]	[MVK]	[CDimer]	[Tri-prd]	[3HQ]	[TMB]
100	0	0.06775	0.73477	0	0	0.29404	0.02797
101	1164	0.00270	0.566255	0.00025	-0.00027	0.27725	0.02797
102	1792	0.00032	0.558389	0.00012	0.00016	0.27874	0.02797
103	2420	9.9E-05	0.54761	0.00027	0.00080	0.27902	0.02797
104	3048	3.9E-05	0.545565	0.00049	0.00122	0.28276	0.02797
105	3677	8.3E-05	0.544413	0.00063	0.00188	0.28524	0.02797
106	4305	0.00010	0.529018	0.00094	0.00237	0.27977	0.02797
107	4933	7.4E-05	0.525025	0.00115	0.00282	0.27939	0.02797
108	5561	6.4E-05	0.520892	0.00129	0.00312	0.28105	0.02797
109	6189	1.2E-05	0.525219	0.00138	0.00333	0.28096	0.02797
110	6857	6.4E-05	0.514288	0.00164	0.00361	0.28197	0.02797
111	7485	4.6E-05	0.514814	0.00191	0.00383	0.28483	0.02797
112	8114	4.3E-05	0.505404	0.00220	0.00401	0.28358	0.02797
113	8742	9.5E-06	0.511742	0.00245	0.00415	0.28720	0.02797
114	9370	3.6E-05	0.500101	0.00280	0.00446	0.28500	0.02797
115	9999	6.9E-07	0.502795	0.00314	0.00455	0.28634	0.02797
116	10627	6.6E-05	0.509662	0.00341	0.00462	0.28871	0.02797
117	11255	4.4E-05	0.505654	0.00361	0.00484	0.28872	0.02797
118	11883	3.8E-06	0.50032	0.00381	0.00492	0.28835	0.02797
119	12511	2E-05	0.501397	0.00404	0.00502	0.28910	0.02797
120	13139	7.3E-05	0.493295	0.00420	0.00510	0.28565	0.02797

3.5.2.5 *Determination of the order of reaction with respect to the chromone-3-carbaldehyde 218a and MVK.*

Table 21. First order data for Figure 64

Exp#	Time(s)	ln[ArCHO]
100	0	-2.6918717
101	1164	-4.7678565
102	1792	-5.05645927
103	2420	-5.30303612
104	3048	-5.54330737
105	3677	-5.78318534
106	4305	-6.09402961
107	4933	-6.40800047
108	5561	-6.59956759
109	6189	-6.83981411
110	6857	-7.20301429
111	7485	-7.42277082
112	8114	-7.78777263
113	8742	-8.03290246
114	9370	-9.0747951

Table 22. Second order data for Figure 65

Exp#	Time(s)	1/[MVK]
100	0	1.36097
101	1164	1.794771
102	1792	1.819909
103	2420	1.843717
104	3048	1.844976
105	3677	1.842157
106	4305	1.866596
107	4933	1.892772
108	5561	1.896649
109	6189	1.914383
110	6857	1.92992
111	7485	1.92144
112	8114	1.953393
113	8742	1.951284
114	9370	1.965544
115	9999	1.981704
116	10627	1.976171
117	11255	1.979129
118	11883	2.0047
119	12511	2.00385
120	13139	2.050899

121	13767	2.041278
122	14396	2.057727
123	15025	2.066594
124	15653	2.0737
125	16281	2.083743

3.5.2.6 Theoretical kinetic models

The data for the theoretical model of the reaction of chromone-3-carbaldehyde **218a** with MVK, proposed from the transformations summarised in Scheme 66, are presented in Table 23.

Table 23. Theoretical model data for Figure 66

Exp#	Time(s)	[A]	[B]	[C]	[D]	[E]
100	0	0.064125272	0.11984	0	0	0.00001
101	1108	0.038336435	0.09115	0.002905	0.02080	0.00105
102	1736	0.030185899	0.08223	0.003675	0.02481	0.00273
103	2364	0.024313755	0.07584	0.004186	0.02605	0.00479
104	2993	0.019900954	0.07107	0.004545	0.02584	0.00693
105	3622	0.016490943	0.06740	0.004807	0.02491	0.00896
106	4281	0.013681946	0.06438	0.005014	0.02362	0.01091
107	4908	0.011542194	0.06209	0.005165	0.0223	0.01257
108	5536	0.009792695	0.06022	0.005285	0.02098	0.01404
109	6165	0.008346865	0.05868	0.005382	0.01972	0.01535
110	6793	0.007144985	0.05740	0.00546	0.01854	0.01650
111	7420	0.00613813	0.05633	0.005525	0.01745	0.01751
112	8049	0.005285441	0.05542	0.005579	0.01644	0.01842
113	8678	0.004562029	0.05465	0.005624	0.01551	0.01922
114	9306	0.003946475	0.05400	0.005661	0.01466	0.01992
115	9934	0.003419827	0.05344	0.005693	0.01387	0.02058
116	10561	0.002968466	0.05296	0.005721	0.01315	0.02115
117	11189	0.002579334	0.05255	0.005744	0.01248	0.02167
118	11817	0.002243638	0.05219	0.005764	0.01186	0.02213
119	12445	0.001953454	0.05189	0.005781	0.01129	0.02255
120	13073	0.001702174	0.05162	0.005796	0.01077	0.02294
121	13701	0.001484252	0.05139	0.005808	0.01028	0.02329
122	14328	0.001295294	0.05119	0.005819	0.00982	0.02360
123	14956	0.001130741	0.05101	0.005829	0.00939	0.02389
124	15584	0.000987544	0.05086	0.005837	0.00899	0.02416
125	16213	0.000862639	0.05073	0.005844	0.00863	0.02440
126	16841	0.000753956	0.05062	0.005851	0.00828	0.02463
127	17469	0.000659164	0.05052	0.005856	0.00795	0.02483
128	18096	0.000576565	0.05043	0.005861	0.00765	0.02503
129	18724	0.000504325	0.05035	0.005865	0.00736	0.02520
130	19352	0.000441224	0.05029	0.005869	0.00709	0.02537

| 131 | 19980 | 0.000386086 | 0.05023 | 0.005872 | 0.00684 | 0.02552 |
| 132 | 20608 | 0.00033789 | 0.05018 | 0.005874 | 0.00660 | 0.02566 |

3.5.2.6.1 The modified theoretical model based on Equations 15-23

The data for the modified theoretical model of the reaction of chromone-3-carbaldehyde **218a** with MVK, proposed from the transformations summarised in Scheme 66, are presented in Table 24.

Table 24. Theoretical model data for Figure 67

Exp#	Time(s)	[A]	[B]	[C]	[D]	[E]
100	0	0.11	0.19	0	0	0
101	1108	0.038656197	0.093973	0.001192	0.012315	0.006458466
102	1736	0.026993186	0.079421	0.000894	0.014396	0.008464185
103	2364	0.019952127	0.070817	0.000623	0.014188	0.010342977
104	2993	0.015250464	0.06515	0.000423	0.013294	0.012010735
105	3622	0.011921199	0.061177	0.000286	0.012236	0.013434705
106	4281	0.00936612	0.058149	0.000191	0.011139	0.014681298
107	4908	0.007532347	0.055989	0.000132	0.010167	0.015681104
108	5536	0.006107444	0.054317	9.24E-05	0.009282	0.016525256
109	6165	0.004983282	0.053003	6.59E-05	0.008487	0.017238992
110	6793	0.004088469	0.051959	4.79E-05	0.007779	0.017842891
111	7420	0.003369179	0.051122	3.55E-05	0.00715	0.018356131
112	8049	0.002783914	0.050442	2.68E-05	0.006588	0.018796131
113	8678	0.002306487	0.049888	2.06E-05	0.006087	0.019173897
114	9306	0.001915672	0.049435	1.61E-05	0.005641	0.019499338
115	9934	0.001593912	0.049063	1.27E-05	0.005241	0.019781459
116	10561	0.001328522	0.048756	1.01E-05	0.004883	0.020026801
117	11189	0.001108336	0.048501	8.16E-06	0.00456	0.020241747
118	11817	0.000925568	0.04829	6.63E-06	0.004269	0.020430563
119	12445	0.00077358	0.048115	5.41E-06	0.004005	0.020597117
120	13073	0.000646996	0.047968	4.45E-06	0.003765	0.020744618
121	13701	0.000541436	0.047847	3.66E-06	0.003548	0.020875745
122	14328	0.000453442	0.047745	3.03E-06	0.003349	0.020992579
123	14956	0.000379794	0.04766	2.51E-06	0.003168	0.021097362
124	15584	0.000318214	0.047589	2.09E-06	0.003001	0.021191503
125	16213	0.000266617	0.04753	1.74E-06	0.002848	0.021276481
126	16841	0.000223502	0.04748	1.45E-06	0.002707	0.021353196
127	17469	0.000187396	0.047438	1.21E-06	0.002577	0.021422771
128	18096	0.000157192	0.047403	1.01E-06	0.002458	0.021485962
129	18724	0.000131837	0.047374	8.45E-07	0.002347	0.021543692
130	19352	0.000110585	0.04735	7.07E-07	0.002244	0.021596489
131	19980	9.27673E-05	0.047329	5.92E-07	0.002149	0.021644899
132	20608	7.78268E-05	0.047312	4.96E-07	0.00206	0.021689398

3.5.3 Preliminary kinetic study of the reactions of chromone-2-carbaldehydes with methyl acrylate

3.5.3.1 General procedure

Chromone-2-carbaldehyde **222a** (0.016 g) was weighed directly into a graduated NMR tube, followed by 3HQ (0.040 g) and TMB (0.0043 g). Methyl acrylate (0.012 mL, 0.015 g) was weighed into a vial using a microsyringe and *ca.* 5 drops of CDCl$_3$ were added to the vial. CDCl$_3$ (ca. 0.5 mL) was added to dissolve the chrome-2-carbaldehyde, 3HQ and TMB in the graduated NMR tube. The methyl acrylate solution was then added to the NMR tube and the solution was made up to the mark using CDCl$_3$. The mixture was shaken and the start of the reaction was timed to correct for zero-time error. The experimental results are presented in Table 25.

Table 25. Data for Figure 91

Exp#	Time(s)	[ArCHO]	[Macrylate]	[A]	[B]	[C]	[TMB]
100	0	0.00581056	0.05906	0.00352	-0.0003	0.00776	0.02556
101	329	0.00554528	0.05722	0.00418	-0.0003	0.00781	0.02556
102	658	0.00526249	0.05599	0.00492	-0.0002	0.00794	0.02556
103	988	0.00498463	0.05473	0.00562	-0.0001	0.00803	0.02556
104	1317	0.00472693	0.05363	0.00626	-0.0001	0.00802	0.02556
105	1647	0.00449379	0.05269	0.00688	3.5E-05	0.00813	0.02556
106	1976	0.00423414	0.05174	0.00739	0.00010	0.00812	0.02556
107	2305	0.00397524	0.05083	0.00785	0.00021	0.00812	0.02556
108	2635	0.00378321	0.05006	0.00834	0.00033	0.00816	0.02556
109	2964	0.00354451	0.04940	0.00873	0.00049	0.00821	0.02556
110	3294	0.00336779	0.04863	0.00904	0.0006	0.00825	0.02556
111	3623	0.00318268	0.04809	0.00939	0.00075	0.00825	0.02556
112	3953	0.00294754	0.04716	0.00951	0.00082	0.00823	0.02556
113	4282	0.00277974	0.04652	0.00969	0.00096	0.00823	0.02556
114	4612	0.00258093	0.04607	0.00994	0.00123	0.00826	0.02556
115	4941	0.00240991	0.04534	0.01001	0.00132	0.00821	0.02556
116	5271	0.00230764	0.04498	0.01016	0.00140	0.00828	0.02556
117	5601	0.00220411	0.04467	0.01039	0.00172	0.00837	0.02556
118	5930	0.00202882	0.04417	0.01043	0.00187	0.00834	0.02556
119	6260	0.00205128	0.04468	0.01103	0.00226	0.00861	0.02556
120	6589	0.00193634	0.04393	0.01096	0.00225	0.00849	0.02556
121	6919	0.00183480	0.04365	0.01108	0.00252	0.00853	0.02556
122	7249	0.00162305	0.04320	0.01089	0.00284	0.00868	0.02556
123	7579	0.00156044	0.04292	0.01094	0.00305	0.00871	0.02556
124	7908	0.00152580	0.04305	0.01129	0.00333	0.00880	0.02556
125	8238	0.00148235	0.04267	0.01131	0.00348	0.00881	0.02556

126	8567	0.00137862	0.04265	0.01140	0.00384	0.00894	0.02556
127	8897	0.00128167	0.04247	0.01144	0.00411	0.00903	0.02556
128	9265	0.00124417	0.04208	0.01138	0.00429	0.00904	0.02556
129	9596	0.00115160	0.04197	0.01149	0.00462	0.00919	0.02556
130	9925	0.00109161	0.04175	0.01145	0.00484	0.00931	0.02556
131	10254	0.00104020	0.04168	0.01150	0.00516	0.00944	0.02556
132	10583	0.00096695	0.04153	0.01149	0.00541	0.00953	0.02556
133	10913	0.00088549	0.04140	0.01137	0.00560	0.00963	0.02556
134	11243	0.00083074	0.04143	0.01144	0.00600	0.00978	0.02556
135	11572	0.00081053	0.04125	0.01131	0.00611	0.0098	0.02556

3.5.3.2 Reaction using 6-methoxychromone-2-carbaldehyde 222c

The general procedure was followed using 6-methoxychromone-2-carbaldehyde **222c** (0.0141 g), methyl acrylate (0.012 mL, 0.015 g), 3HQ (0.039 g) and TMB (0.0043 g). The results are presented in Table 26.

Table 26. Data for Figure 92

Exp#	Time(s)	[ArCHO]	[Macrylate]	[A]	[B]	[C]	[TMB]
100	0	0.0317	0.04639	0.00032	0.00171	-0.00046	0.02556
101	330	0.03114	0.04478	0.00034	0.00206	-0.00039	0.02556
102	659	0.03037	0.04333	0.00038	0.00234	-0.00034	0.02556
103	986	0.03004	0.04213	0.00041	0.00264	-0.00025	0.02556
104	1316	0.02954	0.04097	0.00047	0.00288	-0.00021	0.02556
105	1643	0.02924	0.03992	0.00053	0.00315	-0.00016	0.02556
106	1973	0.02860	0.03888	0.00059	0.00333	-2E-05	0.02556
107	2301	0.02837	0.03801	0.00067	0.00355	2.37E-05	0.02556
108	2629	0.02798	0.03716	0.00075	0.00374	0.00014	0.02556
109	2958	0.02757	0.03633	0.00085	0.00390	0.00024	0.02556
110	3287	0.02722	0.03561	0.00095	0.00404	0.00034	0.02556
111	3617	0.02697	0.03496	0.00107	0.00419	0.00041	0.02556
112	3946	0.02665	0.03424	0.00116	0.00432	0.00053	0.02556
113	4276	0.02632	0.03372	0.00130	0.00443	0.00062	0.02556
114	4604	0.02595	0.03322	0.00141	0.00453	0.00075	0.02556
115	4933	0.02566	0.03267	0.00156	0.00463	0.00083	0.02556
116	5262	0.02558	0.03221	0.00170	0.00474	0.00089	0.02556
117	5590	0.02511	0.03174	0.00182	0.00478	0.00102	0.02556
118	5920	0.02501	0.03131	0.00197	0.00488	0.00107	0.02556
119	6248	0.02486	0.03094	0.00213	0.00496	0.00114	0.02556
120	6578	0.02463	0.03056	0.00230	0.00502	0.00129	0.02556
121	6908	0.02406	0.03019	0.00241	0.00502	0.00135	0.02556
122	7238	0.02418	0.02988	0.00259	0.00512	0.00143	0.02556
123	7565	0.02402	0.02965	0.00278	0.00517	0.00156	0.02556

124	7894	0.02348	0.02931	0.00290	0.00515	0.00158	0.02556
125	8221	0.02349	0.02909	0.00310	0.00521	0.00171	0.02556
126	8551	0.02295	0.02877	0.00321	0.00519	0.00174	0.02556
127	8880	0.02302	0.02863	0.00344	0.00525	0.00189	0.02556
128	9209	0.02277	0.02834	0.00360	0.00526	0.00191	0.02556
129	9538	0.02261	0.02808	0.00375	0.00527	0.00197	0.02556
130	9866	0.02233	0.02786	0.00394	0.00527	0.00202	0.02556
131	10194	0.02216	0.02775	0.00410	0.00527	0.00207	0.02556
132	10524	0.02207	0.02762	0.00432	0.00529	0.0022	0.02556
133	10897	0.02191	0.02737	0.00448	0.0053	0.00222	0.02556
134	11224	0.02189	0.02719	0.00470	0.00531	0.00229	0.02556
135	11554	0.02162	0.02702	0.00487	0.00530	0.00234	0.02556
136	11882	0.02144	0.02689	0.00504	0.00528	0.00242	0.02556
137	12211	0.02139	0.02680	0.00523	0.00528	0.00252	0.02556
138	12539	0.02120	0.02664	0.00542	0.00527	0.00250	0.02556
139	12867	0.02114	0.02657	0.00562	0.00527	0.00259	0.02556
140	13196	0.02113	0.02652	0.00583	0.00527	0.00269	0.02556

3.6 Theoretical studies

All density functional theory (DFT) calculations were performed using the Gaussian 03 programme running on an Intel/Linux cluster. All calculations were done using the hybrid density functional B3LYP with the 6.31G(d) double zeta basis set with polarisation functionals. Geometry optimisations were subjected to convergence criteria of threshold values 1×10^{-7} Ha and 1×10^{-6} Ha for displacement and self-consistent field (SCF) density and energy, respectively. Scans were relaxed using the same criteria as for normal optimisation, and all optimisations were characterised with a vibrational analysis observing none or one imaginary frequency for intermediates and transition states, respectively.

3.6.1 Computational data for the reaction of 2,2'-dithiodibenzaldehyde 201 with MVK

Table 27. Total electronic and free energies, gas phase enthalpies and entropies for molecules depicted in Schemes 57 and 58 and Figure 49, calculated at the DFT level.

Compound	*G*/ Ha	*H*/Ha	ZPE/Ha	ZPEC/Ha	*S*
MVK	-231.173625	-231.138152	-231.234886	0.090036	74.1662
DBU	-461.877692	-461.831737	-462.089873	0.247396	96.721
C	-693.048141	-692.979223	-693.336187	0.338350	145.049
201	-1486.162391	-1486.097401	-1486.31777588	0.202948	136.783
E	-1717.296456	-1717.289762	-1717.55603192	0.263145	198.106
215	-1948.455307	-1948.363079	-1948.78468163	0.391940	194.110
216a	-974.831798	-974.773742	-974.789199	0.203209	122.188
H	-1435.531129	-1435.447240	-1435.90638814	0.433831	176.559
217a	-974.857390	-974.804015	-975.02670783	0.209063	112.338
202a	-897.784382	-897.733144	-897.91310800	0.167599	107.839
K	-743.679679	-743.637232	-743.75547142	0.109120	89.336
L	-1204.929759	-1204.855754	-1205.22485964	0.348601	155.758
M	-974.817076	-974.764871	-974.98630320	0.207710	109.873
B'	-461.241719	-461.194859	-461.43873026	0.232842	98.625
H_2O	-76.405452	-76.384006	-76.387785	0.021168	45.136

ZPE- zero-point energy

ZPEC- zero-point energy correction

3.6.2 Computational data for the reaction of chromone-3-carbaldehyde 218a with MVK

Table 28. Total electronic and free energies, gas phase enthalpies and entropies for molecules depicted in Schemes 63 and 64 and Figure 72, calculated at the DFT level.

Compound	*G*/Ha	H/Ha	ZPE/Ha	ZPEC/Ha	*S*
MVK	-231.173625	-231.138151	-231.234887	0.090036	74.166
DABCO	-345.175452	-345.138060	-345.329765	0.184516	78.700
3HQ	-404.351492	-404.310825	-404.519638	0.200211	85.591
218	-610.223565	-610.177155	-610.3250446	0.137207	97.680
16	-1186.519010	-1186.444049	-1186.890259	0.423048	157.770
17	-841.373281	-841.312271	-841.56091096	0.231780	128.406
18	-1072.551578	-1072.480991	-1072.83229619	0.329851	148.563
221	-1072.573081	-1072.501677	-1072.85158828	0.328712	150.282
219	-841.383220	-841.321941	-841.57056279	0.231683	128.972
15	-1682.749347	-1682.654039	-1683.15558394	0.468938	200.593
220	-1606.362376	-1606.269202	-1606.74195299	0.442142	196.100

ZPE- zero-point energy

ZPEC- zero-point energy correction

3.6.3 Calculation of the condensed Fukui functions

The condensed Fukui functions were calculated for both the 3-(iodomethyl)- and 3-(chloromethyl)-coumarins **81a** and **82a**, respectively) and the results are presented in Tables 29 and 30 respectively. The red high-lighted carbon atoms in Tables 29 and 30 were the carbons of interest in this study.

*3.6.3.1 Data used to calculate the condensed Fukui function for 3-(iodomethyl)coumarin **81a***

E(+) = -7381.55, E(-) = -7381.71, E(n) = -547.114
IP_A = -6834.6, EA_A = -6834.44
η_A = -0.078, S_A = -0.039

Table 29.

Atom#	Atom	Mulliken +ve	charges -ve	Neutral	F^{+}_{Ak}	F^{-}_{Ak}	S^{+}_{Ak}
1	C	0.15951	0.02112	-0.1055	0.26499	-0.1266	-0.01034
2	C	-0.1188	-0.1973	0.16580	-0.2846	0.36311	0.01110
3	C	-0.1617	0.33444	-0.2382	0.07652	-0.5727	-0.00298
4	C	0.23281	0.03630	0.36106	-0.1283	0.32476	0.005002
5	C	0.10144	0.21524	-0.2862	0.38770	-0.5015	-0.01512
6	C	0.26490	-0.3154	0.04606	0.21884	0.36145	-0.00853
7	H	0	0	0	0	0	0
8	H	0	0	0	0	0	0
9	H	0	0	0	0	0	0
10	H	0	0	0	0	0	0
11	**C**	**0.22853**	**-0.1605**	**0.36702**	**-0.1385**	0.52753	**0.00540**
12	C	0.06333	-0.7817	-0.3403	0.40367	0.44134	-0.01574
13	H	0	0	0	0	0	0
14	**C**	**0.19283**	**1.0309**	**0.48905**	**-0.2962**	-0.5419	**0.011552**
15	H	0	0	0	0	0	0
16	H	0	0	0	0	0	0
17	C	0.16325	0.8129	1.04664	-0.8834	0.23375	0.03445
18	O	-0.0259	-0.4721	-0.7653	0.73937	-0.2932	-0.02883
19	O	-0.0874	-0.5143	-0.6486	0.5612	-0.1343	-0.02189
20	I	-0.0128	-1.0096	-0.3491	0.33627	0.66052	-0.01311

3.6.3.2 Data used to calculate the condensed Fukui function for 3-(chloromethyl)coumarin 82a

E(+) = -995.63. E(-) = -995.972, E(n) = -995.935

IP_A = -0.0368, EA_A = 0.305297

η_A = -0.17105, S_A = -0.08553

Table 30.

Atom#	Atom	Mulliken	charges		F^+_{Ak}	F^-_{Ak}	S^+_{Ak}
		+ve	*-ve*	*neutral*			
1	C	0.1665	-0.0381	0.0117	0.1548	0.0497	-0.013240458
2	C	-0.1946	-0.1100	-0.0502	-0.1444	0.0598	0.012348683
3	C	0.1761	0.1625	0.1322	0.0439	-0.0303	-0.003754911
4	C	0.4370	0.2939	0.3150	0.1220	0.0211	-0.010431458
5	C	0.0377	-0.0657	-0.0063	0.0440	0.0594	-0.003766286
6	C	0.3298	-0.0588	0.0180	0.3119	0.0768	-0.026673177
7	H	0	0	0	0	0	0
8	H	0	0	0	0	0	0
9	H	0	0	0	0	0	0
10	H	0	0	0	0	0	0
11	**C**	**-0.1458**	**-0.1252**	**-0.0060**	**-0.1398**	**0.1192**	**0.011953214**
12	C	0.3739	0.1224	0.0711	0.3029	-0.0513	-0.025901737
13	H	0	0	0	0	0	0
14	**C**	**0.3888**	**0.0029**	**-0.0176**	**0.4065**	**-0.0205**	**-0.034763974**
15	H	0	0	0	0	0	0
16	H	0	0	0	0	0	0
17	C	0.4878	0.5396	0.5822	-0.0944	0.0426	0.008071639
18	O	-0.3217	-0.4877	-0.4544	0.1327	0.0332	-0.011347009
19	O	-0.3776	-0.5389	-0.5150	0.1374	0.0238	-0.011754452
20	Cl	-0.3579	-0.6968	-0.0804	-0.2775	0.6164	0.023734435

3.7 Excel Visual Basic Programmes

Visual Basic programmes were developed to calculate the theoretical data for the proposed theoretical models in Figure 66 and 67.

3.3.4.4.1 An excerpt of the Excel Visual Basic programme used to calculate the theoretical data for Figure 66

```vb
Function nextvalueA(timei As Double, timef As Double, concai As Double,
        concbi As Double, k1 As Double, k2 As Double) As Double

For i = timei To timef Step 1

Rate1 = k1 * concai * concbi * concbi
Rate2 = k2 * concai * concbi

dconc1 = Rate1 * 1
dconc2 = Rate2 * 1

Rem after one second!
dconca = -dconc1 - dconc2
dconcb = -dconc1 * 2 - dconc2

concai = concai + dconca
concbi = concbi + dconcb

Next i

nextvalueA = concai

End Function


Function nextvalueE(timei As Double, timef As Double, concai As Double, concbi As
        Double, concdi As Double, concei As Double, k1 As Double,k2 As Double,
        k3 As Double) As Double

For i = timei To timef Step 1

Rate1 = k1 * concai * concbi * concbi
Rate2 = k2 * concai * concbi
Rate3 = k3 * concdi * concdi

dconc1 = Rate1 * 1
dconc2 = Rate2 * 1
dconc3 = Rate3 * 1

Rem after one second!
dconca = -dconc1 - dconc2
dconcb = -dconc1 * 2 - dconc2
dconcd = dconc2 - dconc3 * 2
dconce = dconc3

concai = concai + dconca
concbi = concbi + dconcb
concdi = concdi + dconcd
concei = concei + dconce

Next i
nextvalueE = concei

End Function
```

3.3.4.4.2 An excerpt of the modified Visual Basic programme used to calculate the theoretical data for Figure 67

```
Function nextvalueA (timei As Double, timef As Double, concai As Double, concbi As
Double, concci As Double, concdi As Double, concei As Double, concui As Double,
concvi As Double, concwi As Double, k1 As Double, k2 As Double, k3 As Double, k4 As
Double, k5 As Double, k6 As Double, k7 As Double, k8 As Double, k9 As Double) As
Double

Rem  A+2B -> CxW    k1

Rem  A+B  -> DxV    k2

Rem  2D   -> U      k3

Rem  U    -> E      k4

Rem  E    -> U      k5

Rem ----------------

Rem  V    -> D      k6

Rem  D    -> V      k7

Rem  W    -> C      k8

Rem  W    -> A + 2B    k9


For i = timei To timef Step 1

If concai < 0 Then concai = 0

If concbi < 0 Then concbi = 0

If concci < 0 Then concci = 0

If concdi < 0 Then concdi = 0

If concei < 0 Then concei = 0

If concui < 0 Then concui = 0

If concvi < 0 Then concvi = 0

If concwi < 0 Then concwi = 0

Rate1 = k1 * concai * concbi * concbi

Rate2 = k2 * concai * concbi

Rate3 = k3 * concdi * concdi

Rate4 = k4 * concui

Rate5 = k5 * concei

Rate6 = k6 * concvi

Rate7 = k7 * concdi

Rate8 = k8 * concwi

Rate9 = k9 * concwi

dconc1 = Rate1 * 1

dconc2 = Rate2 * 1

dconc3 = Rate3 * 1

dconc4 = Rate4 * 1

dconc5 = Rate5 * 1

dconc6 = Rate6 * 1
```

```
dconc7 = Rate7 * 1
dconc8 = Rate8 * 1
dconc9 = Rate9 * 1
Rem after one second!
dconca = -dconc1 - dconc2 + dconc9
dconcb = -(dconc1 * 2) - dconc2 + (dconc9 * 2)
dconcc = dconc8
dconcd = -(dconc3 * 2) + dconc6 - dconc7
dconce = dconc4 - dconc5
dconcu = dconc3 - dconc4 + dconc5
dconcv = dconc2 - dconc6 + dconc7
dconcw = dconc1 - dconc8 + dconc9

concai = concai + dconca
concbi = concbi + dconcb
concci = concci + dconcc
concdi = concdi + dconcd
concei = concei + dconce
concui = concui + dconcu
concvi = concvi + dconcv
concwi = concwi + dconcw

If concai < 0 Then concai = 0
If concbi < 0 Then concbi = 0
If concci < 0 Then concci = 0
If concdi < 0 Then concdi = 0
If concei < 0 Then concei = 0
If concui < 0 Then concui = 0
If concvi < 0 Then concvi = 0
If concwi < 0 Then concwi = 0

Next i

nextvalueA = concai

End Function
```

3.8 Crystallographic data

3.8.1 X-ray crystallographic data for compound 243

Crystal data for the mono-{1,8-diazabicyclo[5.4.0]undec-7-ene} salt of 5,5'-dithiobis-(2-nitrobenzoic acid) **243**: $(C_{14}H_7N_2O_8S_2)^-$ $(C_9H_{17}N_2)^+$, M = 548.58, 0.18 x 0.16 x 0.13 mm^3, triclinic, space group P (-1) (No. 2), a = 10.1019(8), b = 10. 4227(8), c = 12.38059(9) Å, α = 77.899 (2), β = 74.919(2), γ = 80.698(2)^o, V = 1222.73(16) Å^3, Z = 2, D_c = 1.490 g/cm^3, F_{000} = 572, MoKα radiation, λ = 0.71073 Å, T = 173(2)K, $2\theta_{max}$ = 56.7^o, 48890 reflections collected, 6080 unique (R_{int} = 0.0435). Final *GooF* = 1.049, R_1 = 0.0361, $w R_2$ = 0.0912, R indices based on 5006 reflections with I >2σ(I) (refinement on F^2), 353 parameters, 2 restraints. Lp and absorption corrections applied, μ = 0.275 mm^{-1}. Primary dihedral angles in the disulphide ion include C1-S13-S14-C15 -90.40(7)^o, S13-S14-C15-C20 15.1(1)^o and S14-S13-C1-C6 21.0(1)^o. One of the methylene groups (C29) is statistically disordered over two positions (a, b).

Table 31. Atomic coordinates for atoms in the mono-DBU-disulfide salt 243

Atom	x	y	z	U(eq) [Ang^2]
S13	0.46911(4)	0.70836(4)	0.56792(3)	0.0251(1)
S14	0.49730(4)	0.78933(4)	0.40093(3)	0.0252(1)
O8	0.76092(13)	0.27780(13)	0.85174(10)	0.0385(4)
O9	0.55510(13)	0.23048(13)	0.84505(10)	0.0397(4)
O11	0.86832(14)	0.14441(11)	0.65660(13)	0.0452(4)
O12	1.02515(13)	0.27444(14)	0.58348(16)	0.0623(6)
O22	0.74572(14)	1.13747(11)	0.04133(10)	0.0374(4)
O23	0.65407(14)	1.30506(11)	0.13421(11)	0.0383(4)
O25	0.92654(14)	1.24358(14)	0.18130(11)	0.0450(4)
O26	0.92388(14)	1.23163(14)	0.35803(12)	0.0446(5)
N10	0.90538(14)	0.25338(13)	0.61678(13)	0.0312(4)
N24	0.88545(14)	1.19992(13)	0.28240(12)	0.0289(4)
C1	0.60145(15)	0.57471(13)	0.57484(12)	0.0205(4)
C2	0.58018(15)	0.48078(14)	0.67435(12)	0.0220(4)
C3	0.68005(15)	0.37539(14)	0.69104(12)	0.0218(4)
C4	0.79942(15)	0.36587(14)	0.60542(13)	0.0226(4)
C5	0.82246(16)	0.45839(14)	0.50651(13)	0.0252(4)
C6	0.72247(16)	0.56349(14)	0.49118(12)	0.0242(4)
C7	0.65872(17)	0.28380(14)	0.80444(13)	0.0258(4)
C15	0.60891(15)	0.91232(13)	0.37700(12)	0.0210(4)
C16	0.61839(15)	0.99776(14)	0.27276(12)	0.0221(4)
C17	0.70754(15)	1.09455(14)	0.23978(12)	0.0215(4)
C18	0.78717(15)	1.10193(14)	0.31439(12)	0.0219(4)
C19	0.77769(16)	1.01928(15)	0.41891(13)	0.0246(4)
C20	0.68761(16)	0.92403(14)	0.45063(13)	0.0242(4)
C21	0.70306(16)	1.19098(15)	0.12994(13)	0.0259(4)
N27	0.80431(16)	0.86095(15)	0.05674(13)	0.0373(5)
N31	0.74965(16)	0.67012(14)	0.02062(13)	0.0353(4)
C28	0.8940(2)	0.7934(2)	0.1319(2)	0.0499(7)

C29A	0.9384(4)	0.6605(3)	0.1175(4)	0.0375(11)
C30	0.8271(3)	0.5881(2)	0.1004(2)	0.0554(7)
C32	0.74116(17)	0.79970(16)	0.00494(14)	0.0293(5)
C33	0.66157(17)	0.88344(15)	-0.07599(14)	0.0299(4)
C34	0.73404(17)	0.87768(16)	-0.20044(14)	0.0310(5)
C35	0.7188(2)	0.75336(19)	-0.24091(17)	0.0392(6)
C36	0.7672(2)	0.62388(18)	-0.17162(18)	0.0432(6)
C37	0.6916(2)	0.60261(18)	-0.04687(19)	0.0450(7)
C29B	0.8522(7)	0.6550(5)	0.1748(4)	0.0515(18)
H2	0.49680	0.48910	0.73100	0.0260
H5	0.90580	0.44980	0.44990	0.0300
H6	0.73650	0.62780	0.42360	0.0290
H8	0.74430	0.23030	0.91640	0.0460
H16	0.56300	0.98950	0.22370	0.0270
H19	0.83250	1.02800	0.46820	0.0300
H20	0.67950	0.86700	0.52220	0.0290
H27	0.79170	0.94780	0.04530	0.0450
H28A	0.88170	0.84030	0.19620	0.0600
H29A	0.984(4)	0.609(4)	0.178(3)	0.058(12)
H29B	1.008(3)	0.660(4)	0.0445(18)	0.042(10)
H30A	0.77460	0.51380	0.14380	0.0660
H30B	0.91620	0.55030	0.05670	0.0660
H33A	0.64870	0.97610	-0.06420	0.0360
H33B	0.56910	0.85340	-0.05940	0.0360
H34A	0.69660	0.95560	-0.24910	0.0370
H34B	0.83350	0.88390	-0.21100	0.0370
H35A	0.62040	0.75320	-0.23960	0.0470
H35B	0.77150	0.75750	-0.32080	0.0470
H36A	0.75500	0.55000	-0.20570	0.0520
H36B	0.86700	0.62130	-0.17680	0.0520
H37A	0.59290	0.63620	-0.04020	0.0540
H37B	0.69770	0.50680	-0.01590	0.0540
H28B	0.99200	0.79000	0.08990	0.0600
H29C	0.92600	0.60090	0.20900	0.0610
H29D	0.76790	0.66030	0.23690	0.0610

Table 32. Bond lengths in the mono-DBU-disulfide salt 243

Atoms	Bond length (Å)	Atoms	Bond length (Å)
S13-S14	2.0267(5)	C15-C20	1.390(2)
S13-C1	1.7727(15)	C16-C17	1.388(2)
S14-C15	1.7710(15)	C17-C21	1.519(2)
O8-C7	1.300(2)	C17-C18	1.394(2)
O9-C7	1.206(2)	C18-C19	1.386(2)
O11-N10	1.2165(19)	C19-C20	1.382(2)
O12-N10	1.213(2)	C2-H2	0.9500
O22-C21	1.2779(19)	C5-H5	0.9500
O23-C21	1.218(2)	C6-H6	0.9500
O25-N24	1.2239(19)	C16-H16	0.9500
O26-N24	1.224(2)	C19-H19	0.9500
O8-H8	0.8400	C20-H20	0.9500
N10-C4	1.464(2)	C28-C29A	1.419(4)
N24-C18	1.463(2)	C28-C29B	1.517(6)
N27-C32	1.320(2)	C29A-C30	1.531(5)
N27-C28	1.463(3)	C29B-C30	1.359(6)
N31-C32	1.315(2)	C32-C33	1.496(2)
N31-C30	1.466(3)	C33-C34	1.533(2)
N31-C37	1.474(3)	C34-C35	1.527(3)

Atoms			
N27-H27	0.8800	C35-C36	1.522(3)
C1-C6	1.388(2)	C36-C37	1.522(3)
C1-C2	1.395(2)	C28-H28A	0.9900
C2-C3	1.386(2)	C28-H28B	0.9900
C3-C4	1.389(2)	C29A-H29B	1.00(4)
C3-C7	1.509(2)	C29B-H29D	0.99(2)
C4-C5	1.383(2)	C29B-H29C	0.9900
C5-C6	1.382(2)	C30-H30B	0.9900
C15-C16	1.396(2)	C35-H35A	0.9900
C30-H30A	0.9900	C36-H36A	0.9900
C33-H33A	0.9900	C36-H36B	0.9900
C33-H33B	0.9900	C37-H37B	0.9900
C34-H34B	0.9900	C37-H37A	0.9900
C35-H35B	0.9900		

Table 33. Bond angles between atoms in the mono-DBUdisulfide salt 243

Atoms	Bond angle (degrees)	Atoms	Bond angle (degrees)
S14 -S13 -C1	105.29(5)	O8 -C7 -C3	111.25(14)
S13 -S14 -C15	106.04(5)	O9 -C7 -C3	122.15(15)
C7 -O8 -H8	109.00	S14 -C15 -C16	114.52(11)
O11 -N10 -O12	123.99(15	S14 -C15 -C20	125.03(11)
O11 -N10 -C4	118.27(14)	C16 -C15 -C20	120.40(14)
O12 -N10 -C4	117.72(14)	C15 -C16 -C17	120.91(14)
O25 -N24 -O26	123.77(15)	C16 -C17 -C21	117.72(14)
O25 -N24 -C18	118.07(14)	C16 -C17 -C18	117.30(13)
O26 -N24 -C18	118.15(14)	C18 -C17 -C21	124.80(14)
C28 -N27 -C32	124.07(16)	N24 -C18 -C19	117.91(14)
C32 -N31 -C37	121.60(16)	N24 -C18 -C17	119.49(13)
C30 -N31 -C32	120.46(16)	C17 -C18 -C19	122.60(14)
C30 -N31 -C37	117.78(15)	C18 -C19 -C20	119.26(15)
C32 -N27 -H27	118.00	C15 -C20 -C19	119.50(14)
C28 -N27 -H27	118.00	O22 -C21 -O23	127.12(15)
S13 -C1 -C2	115.51(11)	O23 -C21 -C17	119.22(14)
S13 -C1 -C6	123.98(11)	O22 -C21 -C17	113.51(13)
C2 -C1 -C6	120.45(14)	C1 -C2 -H2	120.00
C1 -C2 -C3	120.35(14)	C3 -C2 -H2	120.00
C2 -C3 -C7	118.44(13)	C4 -C5 -H5	120.00
C2 -C3 -C4	117.96(13)	C6 -C5 -H5	120.00
C4 -C3 -C7	123.40(14)	C1 -C6 -H6	120.00
N10 -C4 -C3	120.08(13)	C5 -C6 -H6	120.00
C3 -C4 -C5	122.44(14)	C17 -C16 -H16	120.00
N10 -C4 -C5	117.47(14)	C15 -C16 -H16	120.00
C4 -C5 -C6	119.04(14)	C20 -C19 -H19	120.00
C1 -C6 -C5	119.75(13)	C18 -C19 -H19	120.00
O8 -C7 -O9	126.50(15)	C15 -C20 -H20	120.00
C19 -C20 -H20	120.00	C28 -C29B -H29C	108.00
N27 -C28 -C29A	112.2(2)	C28 -C29B -H29D	108.00
N27 -C28 -C29B	106.4(3)	C30 -C29B -H29D	108.00
C28 -C29A -C30	114.3(3)	H29C -C29B -H29D	107.00
C28 -C29B -C30	118.9(4)	N31 -C30 -H30A	109.00
N31 -C30 -C29A	111.8(2)	C29B -C30 -H30B	109.00
N31 -C30 -C29B	113.6(3)	C29B -C30 -H30A	109.00
N27 -C32 -N31	122.10(16)	C29A -C30 -H30A	136.00
N27 -C32 -C33	117.40(15)	C29A -C30 -H30B	74.00
N31 -C32 -C33	120.49(15)	N31 -C30 -H30B	109.00
C32 -C33 -C34	112.45(14)	H30A -C30 -H30B	108.00
C33 -C34 -C35	114.65(14)	C32 -C33 -H33B	109.00
C34 -C35 -C36	115.10(16)	C34 -C33 -H33A	109.00
C35 -C36 -C37	114.20(16)	C32 -C33 -H33A	109.00

N31	-C37	-C36	111.93(17)	H33A	-C33	-H33B	108.00
N27	-C28	-H28A	110.00	C34	-C33	-H33B	109.00
N27	-C28	-H28B	110.00	H34A	-C34	-H34B	108.00
C29A	-C28	-H28A	133.00	C35	-C34	-H34B	109.00
C29A	-C28	-H28B	73.00	C33	-C34	-H34A	109.00
H28A	-C28	-H28B	109.00	C33	-C34	-H34B	109.00
C29B	-C28	-H28A	110.00	C35	-C34	-H34A	109.00
C29B	-C28	-H28B	110.00	H35A	-C35	-H35B	107.00
C28	-C29A	-H29A	113(2)	C34	-C35	-H35B	109.00
C28	-C29A	-H29B	109(2)	C36	-C35	-H35A	108.00
C30	-C29A	-H29A	112(2)	C34	-C35	-H35A	109.00
C30	-C29A	-H29B	102(2)	C36	-C35	-H35B	109.00
H29A	-C29A	-H29B	107(3)	C35	-C36	-H36B	109.00
C30	-C29B	-H29C	108.00	C37	-C36	-H36A	109.00
C35	-C36	-H36A	109.00	C36	-C37	-H37B	109.00
H36A	-C36	-H36B	108.00	N31	-C37	-H37A	109.00
C37	-C36	-H36B	109.00	N31	-C37	-H37B	109.00
H37A	-C37	-H37B	108.00	C36	-C37	-H37A	109.00

3.8.2 X-ray crystallographic data for compound 293c

Formula, $C_{13} H_{12} O_5$; Formula Weight, 248.23; Crystal System, Triclinic; Space group P-1(No. 2); a, b, c [Angstrom] 7.4664(6) 18.6096(15) 19.0622(17); alpha, beta, gamma [deg] 65.079(4) 82.868(5) 83.110(5); V [Ang**3] 2376.7(4) Z8; D(calc) [g/cm**3] 1.387; Mu(MoKa) [/mm] 0.108; F(000) 1040; Crystal Size [mm] 0.10 x 0.13 x 0.20; Data Collection: Temperature (K) 173; Radiation [Angstrom] MoKa   0.71073; Theta Min-Max [Deg] 1.2, 24.8; Dataset -8: 8 ; -21: 21 ; -22: 22; Tot., Uniq. Data, R(int) 15938,   8107, 0.071 Observed data [I > 2.0 sigma(I)] 4202; Refinement Nref, Npar 8107, 658 R, wR2, S 0.0944, 0.3206, 1.03; w = 1/[\s^2^(Fo^2^) + (0.1569P)^2^+ 3.6455P] where P=(Fo^2^+2Fc^2^)/3; Max. and Av. Shift/Error 0.00, 0.00; Min. and Max. Resd. Dens. [e/Ang^3]-0.34,0.51.

Table 34. Atomic coordinates for atoms in compound 293c

Atom	x	y	z	U(eq) [Ang^2]
O10A	0.6949(5)	0.0828(2)	0.0233(2)	0.0537(16)
O11A	0.7208(7)	-0.0163(3)	-0.1326(3)	0.0722(19)
O12A	0.9775(6)	-0.2276(2)	0.1208(2)	0.0609(17)
O15A	0.5594(8)	0.2301(3)	-0.0109(3)	0.086(2)
O16A	0.5372(5)	0.2507(2)	-0.1339(3)	0.0595(17)
C1A	0.8434(7)	-0.1111(3)	0.0179(3)	0.046(2)
C2A	0.9029(8)	-0.1504(3)	0.0908(3)	0.050(2)
C3A	0.8889(8)	-0.1118(4)	0.1406(3)	0.055(2)
C4A	0.8187(8)	-0.0349(4)	0.1186(3)	0.054(2)
C5A	0.7615(7)	0.0045(3)	0.0439(3)	0.0441(19)
C6A	0.7727(7)	-0.0320(3)	-0.0062(3)	0.0438(19)
C7A	0.7147(8)	0.0123(4)	-0.0844(4)	0.051(2)
C8A	0.6467(7)	0.0941(3)	-0.1013(3)	0.049(2)
C9A	0.6411(7)	0.1240(3)	-0.0491(3)	0.046(2)
C13A	0.9935(10)	-0.2694(4)	0.0715(4)	0.068(3)
C14A	0.5742(8)	0.2068(4)	-0.0616(4)	0.053(2)
C17A	0.4830(9)	0.3344(4)	-0.1556(4)	0.064(3)
C18A	0.4089(10)	0.3648(4)	-0.2310(4)	0.073(3)
H1A	0.85000	-0.13720	-0.01580	0.0550
H3A	0.92950	-0.13980	0.19110	0.0660
H4A	0.80910	-0.00930	0.15280	0.0650
H8A	0.60530	0.12680	-0.15090	0.0580
H13A	0.87280	-0.27400	0.05950	0.1030
H13B	1.05280	-0.32250	0.09820	0.1030
H13C	1.06600	-0.24000	0.02330	0.1030
H17A	0.58860	0.36350	-0.15890	0.0770
H17B	0.39050	0.34110	-0.11640	0.0770
H18A	0.49730	0.35280	-0.26790	0.1090
H18B	0.38240	0.42240	-1/4	0.1090
H18C	0.29720	0.33950	-0.22580	0.1090

Table 35. Bond lengths in compound 293c

Atoms	Bond length (Å)	Atoms	Bond length (Å)
O10A -C5A	1.385(7)	C8A -C9A	1.324(8)
O10A -C9A	1.351(6)	C9A -C14A	1.489(10)
O11A -C7A	1.235(9)	C17A -C18A	1.459(10)
O12A -C2A	1.377(7)	C1A -H1A	0.9500
O12A -C13A	1.438(9)	C3A -H3A	0.9500
O15A -C14A	1.204(9)	C4A -H4A	0.9500
O16A -C14A	1.317(9)	C8A -H8A	0.9500
O16A -C17A	1.452(9)	C13A -H13B	0.9800
C1A -C2A	1.372(7)	C13A -H13A	0.9800
C1A -C6A	1.400(8)	C13A -H13C	0.9800
C2A -C3A	1.400(9)	C17A -H17B	0.9900
C3A -C4A	1.367(11)	C17A -H17A	0.9900
C4A -C5A	1.394(7)	C18A -H18A	0.9800
C5A -C6A	1.376(8)	C18A -H18B	0.9800
C6A -C7A	1.459(9)	C18A -H18C	0.9800
C7A -C8A	1.456(10)		

Table 36. Bond angles in compound 293c

Atoms	Bond angle (degrees)	Atoms	Bond angle (degrees)
C5A -O10A -C9A	117.8(4)	O15A -C14A -C9A	122.9(6)
C2A -O12A -C13A	117.0(4)	O16A -C14A -C9A	112.2(6)
C14A -O16A -C17A	118.1(6)	O15A -C14A -O16A	124.8(7)
C2A -C1A -C6A	119.2(5)	O16A -C17A -C18A	107.2(6)
O12A -C2A -C1A	124.8(5)	C6A -C1A -H1A	120.00
C1A -C2A -C3A	119.9(6)	C2A -C1A -H1A	120.00
O12A -C2A -C3A	115.3(5)	C4A -C3A -H3A	119.00
C2A -C3A -C4A	121.9(5)	C2A -C3A -H3A	119.00
C3A -C4A -C5A	117.4(6)	C3A -C4A -H4A	121.00
C4A -C5A -C6A	122.0(6)	C5A -C4A -H4A	121.00
O10A -C5A -C4A	115.6(5)	C9A -C8A -H8A	119.00
O10A -C5A -C6A	122.4(5)	C7A -C8A -H8A	119.00
C1A -C6A -C7A	120.5(5)	O12A -C13A -H13B	109.00
C1A -C6A -C5A	119.6(5)	O12A -C13A -H13A	109.00
C5A -C6A -C7A	119.9(6)	H13B -C13A -H13C	109.00
O11A -C7A -C8A	122.2(6)	H13A -C13A -H13B	110.00
C6A -C7A -C8A	114.1(6)	H13A -C13A -H13C	110.00
O11A -C7A -C6A	123.7(7)	O12A -C13A -H13C	109.00
C7A -C8A -C9A	121.5(5)	C18A -C17A -H17B	110.00
C17A -C18A -H18C	110.00	O16A -C17A -H17A	110.00
H18B -C18A -H18C	109.00	C18A -C17A -H17A	110.00
H18A -C18A -H18C	109.00	H17A -C17A -H17B	109.00
C17A -C18A -H18A	109.00	O16A -C17A -H17B	110.00
C8A -C9A -C14A	125.0(5)	H18A -C18A -H18B	110.00
O10A -C9A -C8A	124.2(5)	C17A -C18A -H18B	109.00
O10A -C9A -C14A	110.8(5)		

4. References

1. Morita, K.; Suzuki, Z.; Hirose, H. *Bull. Chem. Soc. Jpn.*, **1968**, 41, 2815-2815.

2. Baylis, A. B.; Hillman, M. E. D. German Patent 2155113, 1972. (*Chem. Abstr*. **1972**, 77, 34174q.)

3. Bassavaiah, D.; Rao, P. D.; Hyma, R. S., *Tetrahedron*, **1996**, 52(24), 8001-8062.

4. Brzezinski, L. J.; Rafel, S.; Leahy, J. W., *J. Am. Chem. Soc.*, **1997**, 119, 4317-4318.

5. Kaye, P. T.; Robinson, R, S., *Synth. Commun.*, **1996**, 26, 2085.

6. Kaye, P. T.; Nocanda, X. W. *Synthesis*, **2001**, 16, 2389-2392.

7. Lee, K. Y.; Kim, J. M.; Kim, J. N. *Bull. Korean Chem. Soc*., **2002**, 23(10), 1493-1495.

8. Kaye, P. T.; Nocanda, X. W., *J. Chem. Soc., Perkin Trans. 1*, **2002**, 1318-1323.

9. Lee, K. Y.; Lee, H. S.; Kim, J. N. *Bull. Korean Chem. Soc*., **2007**, 28(2), 333-335.

10. Brzezinski, L. J.; Rafel, S.; Leahy, J. W. *Tetrahedron*, **1997**, 53(48), 16423-16434.

11. Familoni, O. B.; Klaas, P. J.; Lobb, K. A.; Pakade, V. E.; Kaye, P.T. *Org. Biomol. Chem.*, **2006**, 4, 3960-3965.

12. Basavaiah, D.; Reddy, R. J.; Rao, J. S. *Tetrahedron Lett.*, **2006**, 47, 73-77.

13. Gong, H.; Cai, C-Q.; Yang, N-F.; Yang, L-N.; Zhang, J.; Fan. Q-H. *J Mol. Catal. A: Chem.*, **2006**, 249, 236-239.

14. Familoni, O. B.; Kaye, P. T.; Klaas, P. J., *Chem. Commun.*, **1998**, 2563-2564.

15. Basavaiah, D.; Reddy, R. M.; Kumaragurubaran, N.; Sharada, D. S., *Tetrahedron*, **2002**, 58, 3693-3697.

16. Basavaiah, D.; Rao, A. J.; Satyanarayana, T., *Chem. Rev*., **2003**, 103(3), 811-891.

17. Lee, K. Y.; Kim, J. N. *Bull. Korean Chem. Soc*., **2002**, 23(7), 939-940.

18. Yi, H-W.; Park, H. W.; Song, Y. S.; Lee, K-J., *Synthesis*, **2006**, (12), 1953-1960.

19. Kaye, P. T.; Musa, M. A., *Synthesis*. **2002**, (18), 2701-2706.

20. Kaye, P. T.; Musa, M. A.; Nocanda, X. W., *Synthesis*, **2003**, (4), 531-534.

21. Singh, V.; Batra, S., *Tetrahedron*, **2008**, 64, 4511-4574.

22. Basavaiah, D.; Reddy, B. S.; Badsara, S. S., *Chem. Rev*., **2010**, 110, 5447-5674.

23. Bode, M. L.; Kaye, P. T., *J. Chem. Soc., Perkin Trans. 1*, **1990**, 2612-2613.

24. Idahosa, K. C.; Lee, Y-C.; Nyoni, D.; Kaye, P. T.; Caira, M. R., *Tetrahedron Lett.*, **2011**, 52 (23), 2972-2976.

25. Bauer, T.; Tarasiuk, J., *Tetrahedron: Asymmetry*, **2001**, 12, 1741-1745.

26. Yang, K-S.; Chen, K., *Org. Lett*., **2002**, 2(6), 729-731.

27. Hayashi, Y.; Tamura, T.; Shoji, M., *Adv. Synth. Cat*., **2004**, 346, 1106-1110.

28. Ke, H. E.; Zhou, Z. H.; Tang, H. Y.; Zhao, G. F.; Tang, C. C., *Chin. Chem. Lett.*, **2005**, 16, 1427-1430.

29. Hayashi, Y.; Tamura, T.; Shoji, M., *Adv. Synth. Catal.*, **2004**, 346, 1106-1110.

30. Hill, J. S.; Isaacs, N. S. *J. Phys. Org. Chem.*, **1990**, 3, 285-290.

31. Drewes, S. E.; Njamela, O. L.; Emslie, N. D.; Ramesar, N.; Field, J. S., *Synth. Commun.*, **1993**, 23, 2807-2815.

32. Bode, M. L.; Kaye, P. T., *Tetrahedron Lett.*, **1991**, 32, 5611-5614.

33. Kaye, P. T., unpublished data.

34. Clayden, J.; Greeves, N.; Warren, S.; Wothers, P., *Organic Chemistry*, 1st ed., Oxford University Press, **2000**, pg 1124.

35. Santos, L. S.; Pavam, C. H.; Almeida, W. P.; Coelho, F.; Eberlin, M. N., *Angew. Chem. Int. Ed.*, **2004**, 43, 4330-4333.

36. Price, K. E.; Broadwater, S. J.; Jung, H. M.; McQuade, D. T., *Org. Lett.*, **2005**, 7, 147-150.

37. Price, K. E.; Broadwater, S. J.; Walker, D. J.; McQuade, D. T., *J. Org. Chem.*, **2005**, 70, 3980-3987.

38. Aggarwal, V. K.; Fulford, S. Y.; Lloyd-Jones, G. C., *Angew. Chem. Int. Ed.,* **2005**, 44, 1706-1708.

39. Amarante, G. W.; Milagre, H. M. S.; Vaz, B. G.; Vilacha Ferreira, B. R.; Eberlin, M. N.; Coelho, F., *J. Org. Chem.*, **2009**, 74, 3031-3037.

40. Xu, J., *THEOCHEM*, **2006**, 767, 61-66.

41. Roy, D.; Sunoj, R. B., *Org. Lett*., **2007**, 9(23), 4873-4876.

42. Robiette, R.; Aggarwal, V. K.; Harvey, J. N., *J. Am. Chem. Soc*., **2007**, 129, 15513-15525.

43. Cai, J.; Zhou, Z.; Zhao, G.; Tang, C. *Org. Lett*., **2002**, 4(26), 4723-4725.

44. Amarante, G. W.; Benassi, M.; Milagre, H. M. S.; Braga, A. A. C.; Maseras, F.; Eberlin, M. N.; Coehlo, F., *Chem. Eur. J*., **2009**, 15, 12460-12469.

45. Rafel, S.; Leahy, J. W., *J. Org. Chem*., **1997**, 62, 1521-1522.

46. Roos, G. H. P.; Rampersadh, P., *Synth. Commun.* **1993**, 23(9), 1261-1266.

47. Hill, J. S.; Isaacs, N.S., *J. Chem. Res.*, **1988**, 330.

48. van Rozendaal, E. L. M.; Voss, B. M. W.; Scheeren, H. W., *Tetrahedron*, **1993**, 49, 6931-6936.

49. Yu, C.; Liu, B.; Hu, L., *J. Org. Chem*., **2001**, 66, 5413-5418.

50. Luo, S.; Mi, X.; Hui, Xu.; Wang, P. G.; Cheng, J., *J. Org. Chem.*, **2004**, 69, 8413-8422.

51. Auge, J.; Lubin, N.; Lubineau, A., *Tetrahedron Lett.*, **1994**, 35(43), 7947-7948.

52. Zhao. S-H.; Zhang. H-R.; Feng. L-H.; Chen. Z-B., *J. Mol. Catal. A: Chem.*, **2006**, 258, 251-256.

53. Krishna, P. R.; Manjuvani, A.; Kannan, V.; Sharma. G. V. M., *Tetrahedron Lett.*, **2004**, 45, 1183-1185.

54. Aggarwal, V. K.; Dean, D. K.; Mereu, A.; Williams, R., *J. Org. Chem.*, **2002**, 67, 510-514.

55. Shi, M.; Zhang, W., *Tetrahedron*, **2005**, 61, 11887-11894.

56. Aggarwal, V. K.; Mereu, A.; Tarver, G. J.; McCague, R., *J. Org. Chem.*, **1998**, 63, 7183-7189.

57. Maher, D. J.; Connon, S. J., *Tetrahedron Lett.*, **2004**, 45, 1301-1305.

58. Luo, S.; Wang, P. G.; Cheng, J-P., *J. Org. Chem.*, **2004**, 69, 555-558.

59. Lee, K.Y.; GowriSankar, S.; Kim, J. N., *Tetrahedron Lett.*, **2004**, 45, 5485-5488.

60. de Souza, R. O. M. A.; Meireles, B. A.; Aguiar, L. C. S.; Vasconcellos, M. L. A. A., *Synthesis*, **2004**, (10), 1595-1600.

61. Leadbeater, N. E.; van der Pol, C., *J. Chem. Soc., Perkin Trans. 1*, **2001**, 2831-2835.

62. Luo, S.; Wang, P. G.; Cheng, J., *J. Org. Chem.*, **2004**, 69, 555-558.

63. Lin, Y.; Lin, C.; Liu, C.; Tsai, T. Y. R., *Tetrahedron*, **2006**, 62, 872-877.

64. Mi, X.; Luo, S.; Cheng, J., *J. Org. Chem.*, **2005**, 70, 2338-2341.

65. Balan, D.; Adolfsson, H., *Tetrahedron Lett.*, **2003**, 44, 2521-2524.

66. Yamada, Y. M. A.; Ikegemi, S., *Tetrahedron Lett.*, **2000**, 41, 2165-2169.

67. Frank, S. A.; Mergott, D. J.; Roush, W. R., *J. Am. Chem. Soc.*, **2002**, 124(11), 2404-2405.

68. Zhao, L-J.; Kwong, C. K-W.; Shi, M.; Toy, P. H., *Tetrahedron*, 2005, 61, 12026-12032.

69. Yi, H-W.; Park, H. W.; Song, Y. S.; Lee, K-J., *Synthesis*, **2006**, (12), 1953-1960.

70. Fort, Y.; Berthe, M. C.; Caubere, P., *Tetrahedron*, **1992**, 48(31), 6371-6384.

71. Drewes, S. E.; Freese, S. D.; Emslie, N. D.; Roos, G. H. P., *Synth. Commun.*, **1988**, 18 (13), 1573-1580.

72. Nyoni, D., MSc Thesis, Rhodes University, **2008**.

73. Lee, K. Y.; Gong, J. H.; Kim, J. N., *Bull. Korean Chem. Soc.*, **2002**, 23(5), 659-660.

74. Yu, C.; Liu, B.; Hu, L., *J. Org. Chem.*, **2001**, 66, 5413-5418.

75. Sa, M. M.; Ramos, M. D.; Fernandes, L., *Tetrahedron*, **2006**, 62, 11652-11656.

76. Caumul, P.; Hailes, H. C., *Tetrahedron Lett.*, **2005**, 46, 8125-8127.

77. Pakade, V. E., MSc Thesis, Rhodes University, **2006**.

78. Das, B.; Damodar, K.; Chowdhury, N.; Saritha, D.; Ravikanth, B.; Krishnaiah, M., *Tetrahedron*, **2008**, 64, 9396-9400.

79. Molefe, D. M., PhD Thesis, Rhodes University, **2008**.

80. Molefe, D. M.; Ganto, M. M.; Lobb, K. A.; Kaye, P. T., *J. Chem. Res.*, **2009**, 7, 452-456.

81. Han, X.; Wang, Y.; Zhong, F.; Lu, Y., *Org. Biomol. Chem.*, **2011**, 9(19), 6734-6740.

82. Shah, J.; Yacob, Z.; Bunge, A.; Liebscher, J., *Synlet*t, **2010**, 14, 2079-2082.

83. Dordonne, S.; Crousse, B.; Bonnet-Delpon, D.; Legros, J., *Chem. Commun.*, **2011**, 47, 5855-5857.

84. Robinson, R. S., PhD Thesis, Rhodes University, **1998**.

85. Musa, M. A., PhD Thesis, Rhodes University, **2002**.

86. Rashamuse, T. J., MSc Thesis, Rhodes University, **2008**.

87. Rashamuse, T. J.; Klein, R.; Kaye, P. T., *Synth. Commun.,* **2010**, 40, 3683-3690.

88. Olomola T. O.; Klein, R.; Lobb, K. A.; Sayed, Y.; Kaye, P. T., *Tetrahedron Lett.,* **2010**, 51, 6325-6328.

89. Ahn, S-H.; Jang, S. S.; Han, E-G.; Lee, K-J., *Synthesis*, **2011**, 3, 377-386.

90. Gowrisanker, S.; Lee, K. Y.; Kim, J. N., *Tetrahedron Lett.*, **2005**, 46, 4859-4863.

91. Amarante, G. W.; Coelho, F., *Tetrahedron*, **2010**, 66, 6749-6753.

92. Jayashankaran, J.; Manian, R. D. R. S.; Sivaguru, M.; Raghunathan, R., *Tetrahedron Lett.*, **2006**, 47, 5535-5538.

93. Bakthados, M.; Sivakumar, N.; Sivakumar, G.; Murugan, G., *Tetrahedron Lett.*, **2008**, 49, 820-823.

94. Ramesh, E.; Raghunathan, R., *Tetrahedron Lett.*, **2008**, 49, 1125-1128.

95. Basavaiah, D.; Rao, A. J., *Tetrahedron Lett.*, **2003**, 44, 4365-4368.

96. Ganto, M. M.; Lee, Y-C.; Kaye, P. T., *Synth. Commun.*, **2011**, 41, 1688-1702.

97. Zhong, W.; Liu, Y.; Wang, G.; Hong, L.; Chen, Y.; Chen, X.; Zheng, Y.; Zhang, W.; Wang, M.; Shen, Y.; Yao, Y., *Org. Prep. Proced. Int.*, **2011**, 43, 1-66.

98. Kim, J. N.; Lee, K. Y.; Kim, H. S.; Kim, T. Y., *Org. Lett.*, **2000**, 2, 343-345.

99. Kim, J. N.; Lee, H. J.; Lee, K. Y.; Kim, H. S., *Tetrahedron Lett.*, **2001**, 42, 3737-3740.

100. Kim, J. N.; Kim, H. S.; Gong, J. H.; Chung, Y. M., *Tetrahedron Lett.*, **2001**, 42, 8341-8344.

101. Lee, C. G.; Lee, K. Y.; Gowrisanker, S.; Kim, J. N., *Tetrahedron Lett.*, **2004**, 45, 7409-7413.

102. Singh, V.; Singh, V.; Batra, S., *Eur. J. Org. Chem.*, **2008**, (32), 5446-5460.

103. Bode, M. L., PhD Thesis, Rhodes University, **1994**.

104. Bode, M. L.; Kaye, P. T., *J. Chem. Soc., Perkin Trans. 1*, **1993**, 1809-1815.

105. Bode, M. L.; Kaye, P. T.; George, R., *J. Chem. Soc., Perkin Trans. 1*, **1994**, 3023-3027.

106. Tukulula, M., MSc Thesis, Rhodes University, **2009**.

107. Tukulula, M.; Klein, R.; Kaye, P. T., *Synth. Commun.*, **2010**, 40, 2018-2028.

108. Gowrisanker, S.; Lee, H. S.; Lee, K. Y.; Lee, J-E.; Kim, J. N., *Tetrahedron Lett.*, **2007**, 48, 8619-8622.

109. Lee, H. S.; Kim, S. H.; Kim, T. H.; Kim, J. N., *Tetrahedron Lett.*, **2008**, 49, 1773-1776.

110. Kim, J. M.; Lee, S.; Kim, S. H.; Lee. H. S.; Kim, J. N., *Bull. Korean Chem. Soc.*, **2008**, 29(11), 2215-2220.

111. Cao, H.; Vieira, T. O.; Alper, H., *Org. Lett.*, **2011**, 13, 11-13.

112. Galeazzi, R.; Martelli, G.; Mobbili, G.; Orena, M.; Rinaldi, S., *Tetrahedron: Asymmetry*, **2004**, 15, 3249-3256.

113. Basavaiah, D.; Devendar, B.; Aravindu, K.; Veerendhar, A., *Chem. Eur. J.*, **2010**, 16, 2031-2035.

114. Nocanda, X. W., PhD Thesis, Rhodes University, **2001**.

115. Zhong, W.; Ma, W.; Liu, Y., *Tetrahedron*, **2011**, 67, 3509-3518.

116. Vasudevan, A.; Tseng, P-S.; Djuric, S. W., *Tetrahedron Lett.*, **2006**, 47, 8591-8593.

117. Sabbagh, L. V., PhD Thesis, Rhodes University, **2000**.

118. Molefe, D. M.; Kaye, P. T., *Synth. Commun.* **2009**, 39, 3586-3600.

119. Kaye, P. T.; Nchinda, A. T.; Sabbagh, L. V.; Bacsa, J., *J. Chem. Res. (S)*, **2003**, 111-113.

120. Kaye, P. T.; Molefe, D. M.; Nchinda, A. T.; Sabbagh, L. V., *J. Chem. Res.*, **2004**, 303-306.

121. Rashamuse, T. J.; Musa, M. A.; Klein, R.; Kaye, P. T., *J. Chem. Res.*, **2009**, 302-305.

122. Geissler, J. F.; Roesel, J. L.; Meyer, T.; Trinks, U. P.; Traxler, P.; Lydon, N. B., *Cancer Res.*, **1992**, 52, 4492-4498.

123. Bargagna, A.; Longobardi, M.; Mariani, E.; Schenone, P.;Losasso, C.; Esposito, G.; Falzarano, C.; Marmo, E., *Farmaco*, **1990**, 45, 405-413.

124. Arnoldi, A.; Bonsignori, A.; Melloni, P.; Merlini, L.; Quadri, M. L.; Rossi, A.C.; Valsecchi, M., *J. Med. Chem.*, **1990,** 33, 2865-2869.

125. Brown, M. J.; Carter, P. S.; Fenwick, A. E.; Fosberry, A. P.; Hamprecht, D. W.; Hibbs, M. J.; Jaevest, R. L.; Mensah, L.; Milner, P. H.; O'Hanlon, P. J.; Pope, A.J.; Richardson, C. M.; Ewst, A.; Witty, D. R., *Bioorg. Med. Chem. Lett.,* **2002**, 12(21), 3171-3174.

126. Quaglia, W.; Pigini, M.; Piergentili, A.; Giannella, M.; Gentili, F.; Marucci, G.; Carrieri, A.; Carotti, A.; Poggesi, E.; Leonardi, A.; Melchiorre, C., *J. Med. Chem.,* **2002**, 45(8), 1633-1643.

127. Ingall, A. H, in: *Comprehensive Heterocyclic Chemistry*, Vol. 3, Boulton, A. J.; McKillop, A. (eds.), Pergamon Press, Oxford, **1984**, p. 934.

128. Tercio, J.; Ferreira, B.; Catani, V.; Comasseto, J. V., *Synthesis*, **1987**, 149-153.

129. Arnoldi, A.; Carughi, M., *Synthesis*, **1988**, 155-157.

130. Kobayashi, K.; Nakahashi, R.; Shimizu, A., Kitamura, T.; Morikawa, O.; Konishi, H., *J. Chem. Soc., Perkin Trans. 1*, **1999**, 1547-1552.

131. Rios, R.; Sundén, H.; Ibrahem, S.; Zhao, G-L.; Eriksson, L.; Córdova, A., *Tettrahedron Lett.*, **2006**, 47, 8547-8551.

132. Rios, R.; Sundén, H.; Ibrahem, S.; Zhao, G-L.; Córdova, A., *Tettrahedron Lett.*, **2006**, 47, 8679-8682.

133. Zhao, G-L.; Vesely, J.; Rios, R.; Ibrahem, I.; Sundén, H.; Córdova, A., *Adv. Synth. Catal.*, **2008**, 350, 237-242.

134. Cha, M. J.; Song, Y. S.; Lee, K-J., *Bull. Korean Chem. Soc.*, **2006**, 27 (11), 1900-1902.

135. Li, H.; Wang, J.; Zu, L.; Wang, W., *J. Am. Chem. Soc.*, **2006**, 128, 10354-10355.

136. Kasmai, H. S.; Mischke, S. G., *Synthesis*, **1989**, 763-765.

137. Gallagher, T.; Pardoe, D. A.; Porter, R. A., *Tetrahedron Lett.*, **2000**, 41, 5415-5418.

138. Humphrey, R. E.; Hawkins, J. M., *Anal. Chem.*, **1964**, 36 (9), 1812-1814.

139. Basavaiah, D.; Gowriswari, V. V. L.; Bharathi, T. K., *Tetrahedron Lett.*, **1987**, 28 (39), 4591-4592.

140. Karplus, M., *J. Am. Chem. Soc.*, **1963**, 85 (18), 2870-2871.

141. Lobb, K. A., unpublished data.

142.   Duggan, A., PhD Thesis, Rhodes University, **2006**.

143.   http://nova.colombo58.unimi.it/cms/index.php?Software_projects:VEGA_ZZ

144.   Becke, A. D., *J. Chem.Phys.,* **1993,** 98, 5648-5652.

145.   Lee, C.; Yang, W.; Parr, R.G., *Phys. Rev. B,* **1988**, (37) 785-789.

146.   Lobb, K. A.; Kaye, P. T., unpublished data.

147.   Amos, R. A.; Fawcett, S. M., *J. Org. Chem.*, **1984**, 49(14), 2637-2639.

148.   Overman, L. E.; Matzinger, D.; O'Connor, E. M.; Overman, J. D., *J. Am. Chem. Soc.*, **1974**, 96(19), 6081-6089.

149.   Overman, L. E.; Petty, S. T., *J. Org. Chem.*, **1975**, 40(19), 2779-2782.

150.   Overman, L. E.; O'Connor, E. M., *J. Am. Chem. Soc.,* **1976**, 98, 771-775.

151.   Schönberg, A., *Chem. Ber.*, **1935**, 68B, 163.

152.   Schönberg, A.; Barakat, M. Z., *J. Chem. Soc.*, **1949**, 892-894.

153.   Stahl, C. R.; Siggia, S., *Anal. Chem.*, 1**957**, 29, 154-155.

154.   Brown, H. C.; Weismann, P. M.; Yoon, N. M., *J. Am. Chem. Soc.*, **1966**, 88(7), 1458-1463.

155.   Allen, C. F. H.; MacKay, D. D., "Organic Syntheses"; Wiley; New York; Coll., Vol. II, **1943**, pg. 580.

156.   Denis, L.; Morton, M. S.; Griffith, K., *Eur. Urol.,* **1999**, 35(5-6), 377-387.

157.   Ali, T. E; Ghfaar, S. A.; El-Shaaer, H. M.; Hanafy, F. I.; El-Fauomy, A.Z., *Turk. J. Chem.*, **2008**, 32(3), 365-374.

158.   Uher, M.; Konecny, V.; Rajniakova, O., *Chem. Papers*, **1994**, 48(4), 282-284.

159.   Ali, T. E., *Phosphorous, Sulfur, and Silicon*, **2007**, 182(8), 1717-1726.

160.   Harborne, J. B.; Williams, C. A., *Photochemistry*, **2000**, 55(6), 481-504.

161.   Guz, N. R.; Stermitz, F. R.; Johnson, J. B.; Beeson, T. D.; Willen, S.; Hastang, J. F.; Lewis, K., *J. Med. Chem.*, **2001**, 44(2), 261-268.

162.   Grazul, M.; Budzisz, E., *Coordination Chemistry Review*, **2009**, 253, 2588-2598.

163.   Yakout, E.A., *Egypt. J. Chem.*, **2004**, 45(6), 1029-1042.

164.   Jerzy, K.; Teodor, Z., (*Chem. Abstr.*, **1995**, 123, 339629).

165.   Ohata, M.; Watanabe, K.; Kumata, K.; Hisamichi, K.; Suzuki, S.; Ito, H., *Annu. Rep. Tohoku Coll. Pharm.*, **1991**, 38, 35.

166.   Goker, H.; Boykin, D.W.; Yildiz, S., *Bioorg. Med. Chem.*, **2005**, 13(5), 1707-1714.

167.   Nawort, M. J.; Nawrot, E.; Graczyk, J., *Eur. J. Med. Chem.*, **2006**, 41(11), 1301-1309.

168.   Desideri, N.; Mastromarino, P.; Conti, C., *Antiviral Chem. Chemother., (Chem. Abstr.*), **2003**, 14(4), 195-203.

169. Wang, B. O.; Yang, Z. Y.; Li, T. R., *Bioorg. Med. Chem.*, **2006**, 14(17), 6012-6021.

170. Wang, Q.; Yang, Z-Y.; Qi, G-F; Qin, D-D., *Biometals*, **2009**, 22, 927-940.

171. Prasanthi, Y.; Kiranmai, K.; Subhashini, N.J.P.; Shivaraj, *Spectrochimica Acta,* Part A., **2008**, 70(1), 30-35.

172. Hodnett, E. M.; Mooney, P. D., *J. Med. Chem.*, **1970**, 13(4), 786.

173. Hodnett, E. M.; Dunn, W. J., *J. Med. Chem.*, **1972**, 15(3), 339.

174. Nohara, A.; Umetani, T.; Sanno, Y., *Tetrahedron*, 1974, **30**, 3353-3361.

175. Ganto, M. M., PhD thesis, Rhodes University, **2009**.

176. Liu, H-W.; in *Traditional Herbal Medicine Research Methods: Identification, Analysis,Bioassay and Pharmaceutical and Clinical Studies*, (ed. by Willow, J. H.), John Wiley & Sons, Inc., **2011**.

177. Farinola, N.; Piller, N., *Lymphat. Res. Biol.*, **2005**, 3(2), 81-86.

178. Lewis, W. H.; Elvin-Lewis, M. P.; in *Medical Botany: Plants Affecting Man's Health*, New York, NY; John Wiley and Sons: **1977**.

179. Goodman, S.N.; Jacobsen, E.N.; *Adv. Catal.*, **2002**, *344*, 953-956.

180. Fall, Y.; Teran, C.; Teijeira, M.; Satana, L.; Uriarte, E., *Synthesis,* **2000**, 643-645.

181. Oxford, G. A. E.; Chaka, A. M., *J. Phys. Chem.*, **2011**, 115, 16992-17008.

182. Khene, S.; Lobb, K.; Nyokong, T., *Electrochimica Acta*, **2010**, 56, 706-716.

183. Torrent-Sucarrat, M.; De Proft, F.; Ayers, P. W.; Geerlings, P., *Phys. Chem. Chem. Phys.*, **2010**, 12, 1072–1080.

184. Clayden, J.; Greeves, N.; Warren, S.; Wothers, P., *Organic Chemistry*, 1st ed., Oxford University Press, **2000**, pg 430.

185. Perrin, D. D. and Armarego, W. L. F., *Purification of Laboratory Chemicals*, 3rd ed., Pergamon Press, Oxford, **1988**.

186. Klutchko, S.; Cohen, M. P.; Sharel Jr., J.; von Strandtmann, M., *J. Heterocycl. Chem.*, **1974,** 11, 183-188.

187. Hirao, I.; Yamaguchi, M.; Hamada, M., *Synthesis*, **1984**, 1076-1078.

188. Nakazumi, H.; Ueyama, T.; Kitao, T., *J. Heterocycl. Chem.*, **1984**, 21(1), 193-196.

189. Abdel-Megeld, F. M. E.; El-Kaschef, M. A. F.; Ghattas, A. A. G., *Egypt J. Chem.*, **1977**, 20, 453.

190. Wolfenden, R., *Bioorg. Med. Chem. Lett.*, **1999**, 7, 647-652.

191. Kaye, P. T., *S. Afr. J. Sci*, **2004**, 100, 545-547.

192. Olomola, T. O.; Klein, R.; Kaye, P. T., *Synth. Commun.,* **2012**, 42(2), 251-257.

193. Fenoglio, I.; Nano, G. M.; Vander Velde, D. G.; Appendino, G., *Tetrahedron Lett.*, **1996**, 37(18), 3203-3206.

194. www.intellogist.com/wiki/ChemBioDraw.

195. http://mestrelab.com/software/mnova-nmrpredict-desktop/

196. Nyoni, D.; Lobb, K. A.; Kaye, P. T., *Synth. Commun*., in press (LSYC-2011-6621).

197. Nyoni, D.; Lobb, K. A.; Kaye, P. T.; Caira, M. R., *ARKIVOC,* accepted subject to minor revision (12-7066QP).